

Novel quantitative push gravity/electricity theory poised for verification

Gerasimos D Danilatos

(Version 1: 1 January 2020)

Version 15: 21 May 2023

DOI [10.5281/zenodo.3596184](https://doi.org/10.5281/zenodo.3596184)

ESEM Research Laboratory
28 Wallis Parade
North Bondi, NSW 2026
Australia
gerry@danilatos.com

*In memory of my father,
who inspired me with truth and honesty,
the science ethics,
I dedicate this to all independent science workers.*

Abstract

[Note: The edits of this version_15 are typed in blue font]

New work provides compelling evidence for a genuine re-appraisal of an old way to explain gravity, which has been sidelined in the periphery of science for a long time. A novel quantitative push gravity theory has been advanced on the basis of a set of primary principles (postulates), from which the derivation of classical acceleration and force by stationary massive bodies in the steady state is possible. In contrast to prior conceptions, it is shown that the absorption of gravity particles by matter need not be extremely weak and linear, in order to derive and explain the observed classical laws of gravity. Any value of the absorption coefficient by a uniform spherical mass produces a gravitational field obeying the inverse square of distance law. The gravitational constant (big G), is itself a function of the ratio of the absorption coefficient over the density of matter. The latter ratio (mass attenuation coefficient) now becomes the new universal gravitational constant of the cosmos, whilst G can vary in different locations of the universe; it remains invariable inside material bodies. The measured mass of planets and stars is only an effective or apparent mass actually smaller than the real mass due to a self-shadowing or shielding effect of the absorption of gravitational particles. Any given mass appears quantitatively different depending on its spatial distribution. We now find that Newton's gravitational law uses only the apparent (or effective) masses with a potentially variable G , but the inverse square distance relationship is locally preserved in the cosmos. The radiant flux of energetic particles being uniform over a region of space creates a maximum acceleration of gravity for all material bodies in that region, so that any further mass accretion over a certain upper limit does not create additional acceleration; this limit is reached when practically all gravitational particles are absorbed (saturation state) by the massive body above a saturation mass. The latter limit should be measurable, for which some tentative situations and experiments are proposed for prospective experiments and tests. The internal field of a spherical mass and the external field of a two layered sphere have been derived. The superposition principle of gravity fields has been reformulated and the Allais effect explained and calculated. The equivalence principle can now be properly understood and explained in a way that the principle per se becomes redundant under the theory being self-consistent. Matter, inertia and mass can be properly defined and understood. For moving bodies, the established relationships from special and general relativity may continue to operate within the gravitational fields created by push particles, but may need to be adapted and re-aligned within the greater framework of push gravity principles operating at any distance. These advances constitute the main part of this report purported to become a valid mathematical formulation for a basic physical interpretation or embodiment of gravity poised for verification. An attempt is made to overcome the main remaining objection of presumed catastrophic thermal accretion of absorbed particles. A further attempt is made also for the push-gravity principles to explain the vastly higher intensity gravitational fields of white dwarfs, neutron stars and black holes. It is proposed that the field of white dwarf stars is created also by push particles but of a different kind, namely, by those responsible for mediating the electric field. In the same way, the field of neutron stars is created by yet a third kind of push particles, namely, those responsible for mediating the nuclear field. The effective mass attenuation

coefficient is variable around those massive bodies. In general, push particles may exist with different energy (or mass) having different mean free paths as they traverse different concentrations of masses like black holes, neutron stars, dwarfs, stars, planets, ordinary masses, atoms, nuclei, protons and all the known or unknown sub-nuclear particles. The invariable principle of momentum transfer (push) by particles directly relating to their absorption rate by the various concentrations (density) of masses could be the basis and the starting principle for a prospective unification theory of everything. Further work seems to explain a common underlying mechanism manifesting itself as effective mass and force, both of which are caused by the rate of push particles absorption. Intrinsic effective mass of lone bodies and variable effective mass of interacting bodies are liaised with a force always obeying the inverse square distance law. The general constitutional equations of push gravity are now provided. The electron radius can be found by this theory. A push electricity theory is initiated providing the general framework for a unification of gravitational and electric fields. Action, reaction, mass accretion during acceleration and mass dependence on velocity are investigated for a rocket system and for falling spheres system. Vortex fluid mechanics is introduced for improved electron/positron modeling. The speed of falling bodies is investigated. The relationships between internal versus external properties are established. [The Python codes used for computations of results have now been published.](#)

1 Introduction

Scientific theories are built from concepts and discoveries that have come before, and are constantly evolving and being refined. When it comes to the theory of gravity, there should be no difference. While maintaining established laws, e.g. in relativity, re-assessing sidelined theories of push gravity may help fill-in gaps of our understanding. This paper humbly seeks to re-assess what this author views as compelling evidence for push gravity and its only goal is to have related theories re-evaluated and ultimately incorporated into more extensive scientific writings.

The push (or shadow) gravity theory (PG) is not generally widely known, by and large, despite of it dating back since Newton's time. It remains outside the mainstream of established theories of gravity and is not generally accepted or introduced, even in a negative way, to primary, secondary or tertiary schooling systems. Whilst fully acknowledging its shortcomings and reasons for which it continues to receive little attention, the present paper reports new advances of this theory, which should provoke a renewed consideration beyond prior attempts to break out of the hitherto impasses in science. Push gravity is now developed on a new basis thought to overcome at least most, if not all, of the prevailing objections.

It would be helpful and productive, if we initially avoid the existing stalemate imposed by the existing criticisms and objections against the push gravity theory by patiently examining the mathematical or quantitative relationships newly derived in this work. The results and conclusions produced are important in their own right. We have opted to work out (or rework) a number of significant derivations of fundamental importance first and then follow with appropriate discussion here and elsewhere. Afterwards, we can re-visit all known arguments and objections to PG, most of which may be shown to be invalid, redundant, or not necessarily valid. Triggering a protracted series of arguments and counter-arguments from the outset could be counter-productive for the ordinary reader to proceed and appreciate the main findings and purpose of this report.

In the above sense, we initially assume the validity of a set of PG principles or postulates, which allow a novel derivation of the laws of gravity in the steady state of initially stationary (or slow moving) material bodies. In particular and based on these principles, Newton's law of gravity can be easily derived but with a new understanding of the universal constant of gravity. This is followed by the general case, where the same principles are used to derive some novel relationships beyond Newtonian mechanics, from whereby it is shown that Newton is the limiting case for very weak absorption of the push particles. A universal law for the acceleration of gravity is produced, which reveals the most fundamental physical quantities involved. Both the gravitational field around a material sphere and the force between two material spheres is established. An attempt is then made to use and propose tests, observations and experiments to verify the new physics. By this methodology, we will provide completely independent means of describing some fundamental physics and phenomena providing better explanations than hitherto existing theories.

This approach then, overall, will further assist towards invalidating most of the objections and at least neutralizing the others, or placing them on a rational speculation for an interim period. This will allow experts in the areas of particle physics, theoretical physics, astrophysics and mathematics to find new and fruitful ground for further progress to both use and advance the presented theory to its logical conclusions. Ultimately, work can include general relativity, a generalized theory of fields and a unified theory of everything.

In setting out such an ambitious goal, it should be clarified from the outset that the presented PG theory is thought to by no means be in conflict with the theories of relativity, by and large. The mathematical

tools of the general relativity may still be applicable and useful to PG in the case of moving bodies close to the speed of light, but this is left for later works, i.e. when the time dependence phenomena are considered under PG. For the present work, we start only with the steady state condition of push particle flows around stationary bodies, which is sufficient to reveal some important misses of existing theories in general and, perhaps, of the general relativity in particular.

Unavoidably, we include a certain amount of speculation and heuristic findings, which should be separated out from the fundamental derivations of PG. For this purpose, we divide this report in two parts, the first of which concentrates on the definite new mathematical derivations of PG, whilst the second part expands the first to include possible applications under certain conditions and speculations.

For the above purposes, there is no extensive literature relating to the novel developments of PG in the first part. However, by attempting in the second part to apply the new findings to existing data and theories, the task overwhelms the expertise of this author who takes a great risk in possible misapplication of what otherwise can be a valid PG theory. Therefore, this report does not contain an exhaustive search of literature on all aspects touched upon, but only a limited reference to prior works as needed or known to the present author, who also resorts and refers to Wikipedia to indirectly provide a more extensive list of references. These misses may be excused, whilst they could also be rectified by others in the spirit of further progress along the path ushered by the following work.

In relation to our "method", we quote from Feyerabend (2010): *"No theory ever agrees with all the facts in its domain, yet it is not always the theory that is to blame. Facts are constituted by older ideologies, and a clash between facts and theories may be proof of progress. It is also a first step in our attempt to find the principles implicit in familiar observational notions"*.

Part One (1)

2 Early push gravity theory

Nicolas Fatio de Duillier is considered to be the first who proposed an explanation of the phenomenon of gravity. That subject was one among many and various interests that he worked on around the same time that Newton developed his own laws of gravity. Fatio's works are not readily available in present journals for direct accessibility and reference, but can be found in a Wikipedia article (Wikipedia contributors, 2018b) containing numerous references (de Duillier, 1929; Gagnebin, 1949) and further reading on push gravity. His theory is *"based on minute particles streaming through space and pushing upon gross bodies..."* via collisions between ordinary matter and ethereal corpuscles, which was thought to be his greatest work. This theory was later reworked and presented also by Le Sage (Wikipedia contributors, 2018a). However, Fatio's mechanical theory of gravity soon fell into oblivion, chiefly because no drag by the aether on the motion of the planets could be detected in celestial motions; it was finally abandoned on account of a number of serious objections by renowned scientists around the beginning of the 20th century. As we know, Special Relativity (SR) and General Relativity (GR) have become the prevailing or established theories for over a century to date.

A few works have appeared from time to time attempting to revive PG. However, the latter still remains outside the mainstream physics.

3 Push Gravity (PG) principles

The fundamental principle or assumption of push gravity (PG) as understood or proposed in this report is that the forces we experience by an assumed gravitational field attached to material bodies is actually generated by the flow and absorption of a radiation energy in the form of elementary particles or waves, or both, traveling randomly but homogeneously in all directions in the interstellar/interplanetary space, or at least in regions of the order of magnitude of solar systems. This is a form of radiant flux, the nature of which need not be specified at the outset, but which, for convenience, we can initially assume that it consists of elementary particles to be called **gravions** (gravity + ion (from "ίόν" meaning "going") and are characterized by the following postulated properties:

1. They rarely interact (or collide) between themselves resulting in relatively very long mean free paths as compared with planetary size orbits.
2. They interact with material objects at any point at a rate in direct proportion to the density of the matter they traverse around the point in the object.

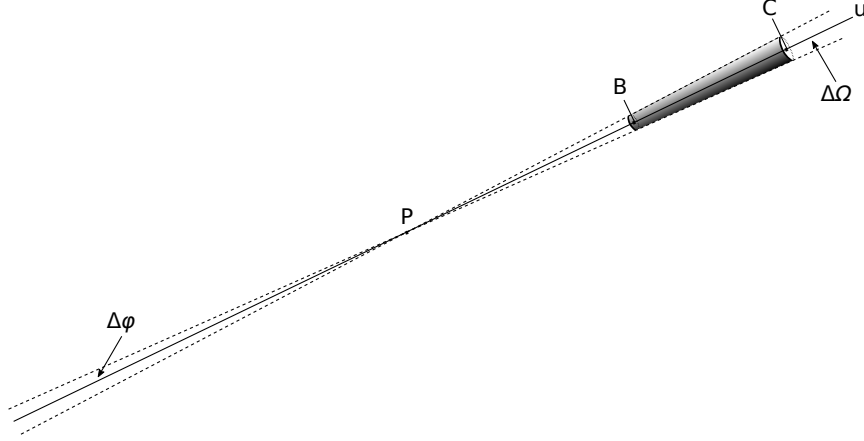


Figure 1: *Push Gravity principle.*

3. During their interaction with matter, they become partially or totally absorbed but re-emitted in a different form of particles (energy) with much shorter mean free path so as not to pertain (mediate) further to gravitational force, but likely to pertain to other types of forces or reactions.
4. Conservation of momentum: During their interaction with matter, they transfer momentum to the material body, a process that appears as a force acted upon the material body.

We further use two complementary provisional assumptions to connect the theory with existing theories, namely:

- 5 The gravions are relativistic.
- 6 The speed of gravions is the speed of light (photons).

The third principle (#3) is analyzed and discussed in considerable detail in Part 2.

The sum total of all gravion absorption by a material body results in a depletion zone around the said body, a process that appears as a gravitational field acting on any other material body inside the said field.

The nature of gravions and the nature of their interaction with matter remains to be found, so that “particle” and “matter” are as yet undefined entities, as they may pertain to energy or mass in particle or waveform according to established ideas and principles in physics.

Dibrov (2011) called the particles fations, or other names may be found, but we opted to use a fresh term for good reasons, such as to dissociate, not critically, the presented theory here from previous ones on this subject. The gravions may be identical to the known gravitons from elsewhere, but a new term aims to avoid possible conflicts or transferring properties from existing theories not necessarily needed or assumed by the PG as presented here. After all, gravions and gravitons might be the same thing, except that we attempt to start afresh (i.e. be independent) in this work. The term gravion has been coined by incorporating the root word “ion” meaning “going” or “traveling” from ancient Greek “ίόν” (hence, by denoting particles or energy that is flowing).

3.1 Formulation of principle

The preceding principles can be formulated as follows:

Let us denote the radiant flux of gravions (energy) by Φ_0 , which is the radiant energy emitted, transmitted or received anywhere per unit time (in Watts), i.e. the rate of flow of particles/energy by gravions. The radiant flux received by a surface, per unit solid angle Ω , per unit area S in a particular direction defines the radiance L_0 by:

$$L_0 = \frac{\partial^2 \Phi_0}{\partial \Omega \partial S} \quad (1)$$

At any point in space, we will need to find and use the flux density J_0 (also called intensity), namely, the flux per unit area received within a solid angle $\Delta \Omega$

$$J_{0\Delta\Omega} = L_0 \Delta \Omega \quad (2)$$

If within this solid angle there is a finite material body, the received flux will be diminished due to absorption. Referring to Fig. 1, the radiance and the flux density at any point in free space is initially the same from all directions resulting in zero force, except when at a point P the flux density is affected by the presence of matter in the direction u within a cone with small semi-angle $\Delta\varphi$ subtending a small solid angle $\Delta\Omega$. Due to the absorption of gravions by matter contained in the distance BC, there is a deficiency from that direction and hence an excess flux from the opposite direction within the same angle.

We can treat the problem as we use the general case of any radiation absorption by matter and write the well known equations of absorption. In the general case, the flux density (intensity) $J(u)$ at any point u along the line u diminishes in proportion to product $J(u)du$

$$dJ_{\Delta\Omega} = -kJ_{\Delta\Omega}(u)du \quad (3)$$

where the constant of proportionality k is the coefficient of absorption for gravions (or attenuation coefficient in the Beer-Lambert law). Upon integration, we obtain the classical exponential transmission equation

$$J_{\Delta\Omega} = J_{0\Delta\Omega} \exp(-ku) \quad (4)$$

where $J_{0\Delta\Omega}$ is the incident (initial) intensity per above. The absorbed intensity $J_{a\Delta\Omega}$ is simply the difference

$$J_{a\Delta\Omega} = J_{0\Delta\Omega} - J_{\Delta\Omega} \quad (5)$$

and the corresponding absorption fraction $f_{a\Delta\Omega}$ in the small solid angle $\Delta\Omega$ is:

$$f_{a\Delta\Omega} = \frac{J_{0\Delta\Omega} - J_{\Delta\Omega}}{J_{0\Delta\Omega}} = 1 - \exp(-ku) \quad (6)$$

For the case in Fig. 1, by setting $BC = \ell$ we simply write

$$f_{a\Delta\Omega} = 1 - \exp(-k\ell) \quad (7)$$

where k is constant if the density is uniform.

We note that for very small values of $k \ll 1$, Eq. 4 reduces to

$$J_{\Delta\Omega} = J_{0\Delta\Omega}(1 - k\ell) \quad (8)$$

and

$$J_{a\Delta\Omega} = J_{0\Delta\Omega} - J_{\Delta\Omega} = J_{0\Delta\Omega}k\ell \quad (9)$$

and

$$f_{a\Delta\Omega} = k\ell \quad (10)$$

The above equation is the basic assumption of Fatio's theory and all subsequent theories of push gravity, i.e. the absorption of gravions by a planet is very weak and linear, because only then could they reproduce Newton's equation of gravity.

In the above and subsequent notation, we use the subscript "a" to denote the presence of absorption so that f_a is a shorthand notation for the absorption fraction of gravions per unit area inside a finite solid angle:

$$f_a = \int f_{ad\Omega} d\Omega \quad (11)$$

This fraction will be used later for finding the total energy absorbed by a sphere.

4 Newton's gravity law

Based on the given PG principle, we can derive Newton's equation of gravity in a simple way as follows:

Referring to Fig. 2, let us consider a point O at distance r from the center of a sphere at point P with radius R . We draw a straight line u from point O traversing the sphere along the chord AB, the length $\ell(\varphi)$ of which is given by:

$$AB = 2(AM) = 2\sqrt{R^2 - r^2 \sin^2 \varphi} = 2r\sqrt{a^2 - \sin^2 \varphi} \equiv \ell(\varphi) \quad (12)$$

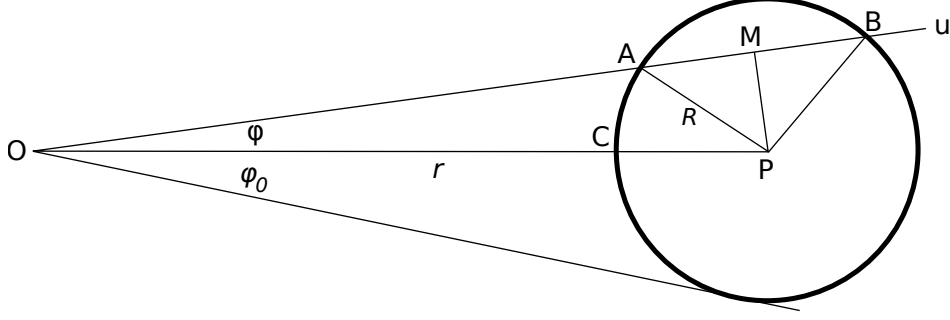


Figure 2: Derivation of push gravity around a sphere.

since

$$OM = r \sin \varphi \quad (13)$$

and

$$a = \frac{R}{r} = \sin \varphi_0 \quad (14)$$

while we want these quantities expressed as a function of the angle φ in the range

$$0 \leq \varphi \leq \varphi_0 \quad (15)$$

We also need the initial $u_1 = OA$ and final $u_2 = OB$ lengths on the line OAB along u corresponding to points A and B

$$u_1(\varphi) = r \cos \varphi - \sqrt{R^2 - r^2 \sin^2 \varphi} = r \left(\cos \varphi - \sqrt{a^2 - \sin^2 \varphi} \right) \quad (16)$$

and

$$u_2(\varphi) = r \cos \varphi + \sqrt{R^2 - r^2 \sin^2 \varphi} = r \left(\cos \varphi + \sqrt{a^2 - \sin^2 \varphi} \right) \quad (17)$$

We note that the above equations describe the given circle in polar coordinates, when the origin O lies away from the circle, which then it is simplified to just the chord length, when the origin lies on the surface ($r = R$) by the well known cosine equation:

$$\ell(\varphi) = 2r \cos \varphi \quad (18)$$

The elementary annular solid angle $d\Omega$ at angle φ around the axis OP is

$$d\Omega = 2\pi \sin \varphi d\varphi \quad (19)$$

Gravions arrive at point P from all directions uniformly in the absence of any mass around. However, if the sphere contains a uniform mass we can initially assume that some gravions are absorbed by the mass in direct proportion to the elementary solid angle and the length of the chord AB at angle φ . This creates a depletion of gravions from that direction, from which the total depletion (fractional absorption) of gravions is found by the double integral

$$f_a = \int_0^{\varphi_0} \int_{u_1}^{u_2} 2\pi \sin \varphi d\varphi k du \quad (20)$$

where we use the previously defined absorption coefficient being $k \ll 1$ along the length $\ell(\varphi)$. Integrating with u along the $\ell(\varphi)$, we get

$$f_a = \int_0^{\varphi_0} 2\pi \sin \varphi d\varphi \cdot k(u_2 - u_1) = 2\pi \int_0^{\varphi_0} \sin \varphi k \ell(\varphi) d\varphi \quad (21)$$

or

$$f_a = 4\pi kr \int_0^{\varphi_0} \sin \varphi \sqrt{a^2 - \sin^2 \varphi} d\varphi \quad (22)$$

Now, since the flux of gravions is a directional quantity (vector) at the test point O, the components normal to direction OP cancel out and only the components along OP add to a total directional flux for the generation of an acceleration of gravity g . The latter components are integrated by multiplying the above integrand by $\cos \varphi$:

$$f_g = 4\pi kr \int_0^{\varphi_0} \sin \varphi \cos \varphi \sqrt{a^2 - \sin^2 \varphi} d\varphi \quad (23)$$

to find the total component of accelerating fraction f_g below:

$$f_g = \left[-\frac{4\pi kr}{3} (a^2 - \sin^2 \varphi)^{3/2} \right]_0^{\varphi_0} \quad (24)$$

By substituting the integration limits on account of the above relationships, we finally get:

$$f_g = \frac{4\pi kr}{3} a^3 = \frac{4\pi k R^3}{3r^2} \quad (25)$$

By introducing an average density ρ of the spherical mass, the last result becomes :

$$f_g = \frac{k}{\rho} \frac{4\pi \rho R^3}{3r^2} = \frac{k M}{\rho r^2} \quad (26)$$

where M is the total mass of the sphere. This is essentially Newton's law of gravity subject to a proportionality constant to yield the force of the gravions on a test unitary mass, which is the acceleration at point O.

In the above and subsequent notation, we use the subscript "g" to mean the component of absorption responsible for the generation of acceleration g .

It should be noted that the ratio $\Lambda = \frac{k}{\rho}$ is the mass attenuation coefficient of the Beer-Lambert law in any absorption situation written in alternative form as a function of the area density (or mass thickness) $\lambda = \rho \ell$, that applies also in flux density attenuation in PG, i.e.

$$J = J_0 \exp\left(-\frac{k}{\rho} \rho \ell\right) \equiv J_0 \exp(-\Lambda \lambda) \quad (27)$$

The fraction f_g as initially derived above is a pure (dimensionless) parameter involving only geometrical parameters (Euclidean geometry) that appears to be a fundamental property of nature. The inverse square of distance law appears from the outset together with the sphere diameter and the absorption co-efficient k , which implies an absorbing entity like the mass, or density of the mass to appear in the next step.

This fraction was obtained by integrating over all absorption possible around the axis of symmetry defined by points O and P and yielding the simplest solution for a sphere. However, for any other shape, we should integrate around three normal independent axes (x,y,z) and add the corresponding acceleration fractions vectorially, as is shown in Appendix B.

5 Beyond Newton

Next, we obtain the expected acceleration from the previous derivation, as a consequence of the push gravity principle.

5.1 Universal gravitational constant in weak absorption regime

The simple derivations above can already lead to a better understanding of the universal constant G (or bigG).

From the absorption and acceleration fractions f_a and f_g introduced in the previous section, we convert to the corresponding fractions of absorption and acceleration for the flux density J_a and J_g below:

$$J_a = J_0 f_a \quad (28)$$

$$J_g = J_0 f_g \quad (29)$$

where J_a is the flux density absorbed by the presence of a mass (here spherical uniform mass) and J_g is the component of J_a in the direction of the axis of symmetry responsible for the generation of acceleration.

We now proceed to find the constant of proportionality to reproduce Newton's gravitational law from Eq. 26 by

$$J_g = J_0 \frac{k M}{\rho r^2} = J_0 \Lambda \frac{M}{r^2} \quad (30)$$

using the newly introduced constant Λ .

The physical meaning of this constant is the number of absorption events per unit density of matter in units of inverse mass-thickness (m^2/kg). In other words, it is the number of absorption events per kilogram per square meter. The inverse ($1/\Lambda$) is the mass-thickness (or area density) per absorption event. This is a new cosmic constant the magnitude of which remains to be found.

It is generally known in flow problems that the product of pressure times the velocity of the flow yields the flux intensity. Thus, if we divide J_g by the velocity c of the radiant flux (gravions), we obtain the pressure p_g exerted by the gravions at O:

$$p_g = \frac{J_g}{c} \quad (31)$$

An elementary test mass dm is located at point O with a surface area dS and thickness x having a density ρ' with corresponding absorption coefficient k' . The force dF on this test mass is then given by:

$$dF = p_g dS \cdot k' x = \frac{J_g}{c} dS \cdot k' x \quad (32)$$

where we multiply by $k' x$ to allow only for the fraction of gravions absorbed by the test mass, considering that k' , in general, is the number of absorption events per unit length. The force per unit mass, i.e. the acceleration g is then

$$g = \frac{dF}{dm} = \frac{\frac{J_g}{c} dS \cdot k' x}{\rho' dS \cdot x} = \frac{J_0 k M k'}{c \rho r^2} = \frac{J_0}{c} \Lambda^2 \frac{M}{r^2} \quad (33)$$

The above equation is exactly Newton's law, where the factors of proportionality between g and M/r^2 must correspond to the universal constant G :

$$G = \frac{J_0}{c} \Lambda^2 \quad (34)$$

The above is already an important derivation for the universal gravitational constant in terms of other constants, namely, the gravion speed and intensity of the neighboring universe, and the mass attenuation coefficient (new universal constant). Eqs. 33 and 34 are thought to be new fundamental derivations beyond Newton even within the realm of Newtonian mechanics for weak absorption.

5.2 General gravitation law in any absorption regime

Having considered the case of weak absorption, we now proceed to investigate what happens if absorption is strong, or to any arbitrary degree, i.e. the absorption coefficient can take any value. This actually means that we allow gravitational shielding inside a material body and between bodies. We may also refer to this condition as self-shadowing within the bulk of a massive body. In other words, we allow "gravitational shielding" as a core condition of a general push gravity theory, as opposed to considering it a case for rejecting PG, as has been done by the hitherto critics. This ushers a novel approach to push gravity.

In the general case, where self-shadowing (shielding) is caused by a significant k , we follow the same initial procedure as previously with reference to Fig. 2: The force is proportional again to the elementary annular solid angle $2\pi \sin \varphi$, but now multiplied by the absorption fraction of the flux intensity along the length AB (Fig. 2) provided by Eq. 6; we also multiply by $\cos \varphi$ to allow, as previously, only for the component of force along the direction OP, so that we only need to integrate with respect to angle as follows:

$$f_g = \int_0^{\varphi_0} 2\pi \sin \varphi \cos \varphi d\varphi \cdot [1 - \exp(-k\ell(\varphi))] \quad (35)$$

and

$$f_g = 2\pi \int_0^{\varphi_0} \sin \varphi \cos \varphi \left[1 - \exp\left(-2kr\sqrt{a^2 - \sin^2 \varphi}\right) \right] d\varphi \quad (36)$$

The final integration of the above expression in the given subtended angle φ_0 by the sphere is fortunately an analytical expression of the form:

$$f_g = 2\pi \left[\frac{\sin^2 \varphi}{2} - \frac{\exp\left(-2kr\sqrt{a^2 - \sin^2 \varphi}\right) \left(2kr\sqrt{a^2 - \sin^2 \varphi} + 1\right)}{4k^2 r^2} \right]_0^{\varphi_0} \quad (37)$$

and with the given values of integration from 0 to φ_0 , we finally obtain

$$f_g = \pi \left[R^2 - \frac{1}{2k^2} + \frac{\exp(-2kR)(2kR + 1)}{2k^2} \right] \frac{1}{r^2} \equiv \frac{\pi A}{r^2} \quad (38)$$

where we have now a new parameter A , which is a function of k and R only (i.e. independent of r):

$$A = \left[R^2 - \frac{1}{2k^2} + \frac{\exp(-2kR)(2kR + 1)}{2k^2} \right] \quad (39)$$

Like in Eq. 25, we find that the fraction f_g derived in the general case of strong absorption is again a dimensionless parameter (quantity) that appears to be a fundamental property of nature and that the inverse square of distance law is preserved. This law is a consequence of the geometry alone (Euclidean) by any uniform flux propagated and absorbed in space. It is the law in the steady state around any absorbing medium (mass), whilst the time dependence remains to be introduced at a later stage of PG development.

Now, we follow the same procedure, as previously, to obtain the acceleration: For the test mass acted upon by a pressure p_g , Eq. 29 now becomes

$$J_g = J_0 \frac{\pi A}{r^2} \quad (40)$$

In view of above, Eq. 33 is modified to become:

$$g = \frac{dF}{dm} = \frac{J_g dS \cdot k'x}{\rho' dS \cdot x} = \frac{J_0 k' \pi A}{c \rho' r^2} = \frac{J_0}{c} \Lambda \frac{\pi A}{r^2} \quad (41)$$

The above provides the equation of acceleration in PG, which again preserves the inverse square of distance law. However, the factor(s) of proportionality between g and M/r^2 is different from the corresponding PG derivation in Newton's equation, the significance of which will be described later. To understand the difference, we need to first investigate the properties of the newly derived parameter A .

6 Investigation, consequences and new physics with parameter A

6.1 PG versus Newton

From from Eqs. 25 and 38, we see that the corresponding f_g (or g , or force) is always proportional to $1/r^2$ regardless of the values of k and R . The general assumption by previous proponents of PG that the graviton absorption should be very weak (in order to produce Newton's Law), is now found to be redundant together with the allegation that the "gravitational shielding" is a reason to reject PG. On the contrary, this is now found to be a fundamental underlying mechanism of PG. This is already an important finding.

It is helpful and instructive to normalize the distance r over the radius of the sphere R :

$$n_R = \frac{r}{R} \quad (42)$$

whereby we re-write the newly found expression as

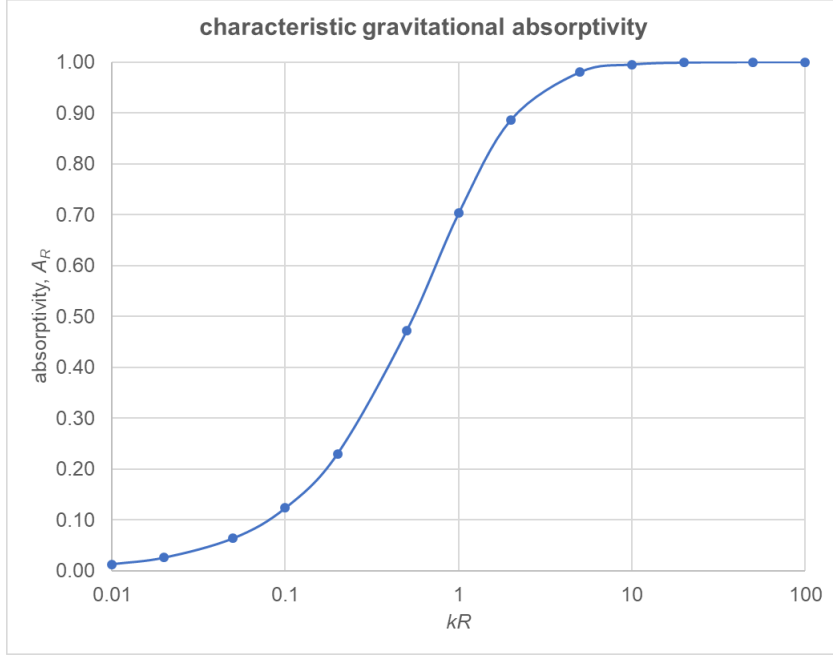


Figure 3: *Dependence of characteristic gravitational absorptivity A_R on kR .*

$$\frac{f_g}{\pi} = \left[1^2 - \frac{1}{2k^2 R^2} + \frac{\exp(-2kR)(2kR + 1)}{2k^2 R^2} \right] \frac{1}{n_R^2} = \frac{A_R}{n_R^2} \quad (43)$$

by introducing the characteristic parameter A_R :

$$A_R = 1 - \frac{1}{2k^2 R^2} + \frac{\exp(-2kR) \cdot (2kR + 1)}{2k^2 R^2} \quad (44)$$

The latter parameter depends only on the product kR and it is plotted in Fig. 3. This shows that A_R is monotonically (absolutely) increasing, as it should, but it reaches a saturation limit at very high values of kR . For simplicity, we may also set $R = 1$ and plot against k , or set $k = 1$ and plot against R , in either case reproducing the same curve. The important observation is that most of the change in value of A_R takes place over the span of about four orders of magnitude of k , or R , or kR . Overall, the magnitude varies from near zero to unity. This means that increasing the radius of a sphere, the shadowing parameter f_g (and acceleration) at the surface will reach a saturation value as opposed to infinity predicted by Newton. Likewise, by increasing the absorption capacity (density, or k) of a constant radius sphere, the shadowing parameter f_g (and acceleration) at the surface will again reach a saturation value, not the infinity provided by Newton. This new parameter A_R characterizes the absorbing ability of a spherical mass or planet and may be referred to as *characteristic gravitational absorptivity*, or absorptivity, for short.

For a direct comparison, we plot simultaneously f_g against normalized distance r_R for $r_R > 1$, i.e. by setting $R = 1$ au (arbitrary unit) in Eqs. 25 and 38 as shown in Fig. 4 for three fixed values of k in a range spanning three orders of magnitude. Initially, we may avoid the involvement of mass M and density ρ by investigating only the quantity f_g . For very low values of k , the pair of curves are indistinguishable. We note that as we increase k , the shadowing derived from PG is increased **absolutely** (see actual values), as it should, because more absorption by the gravitating mass means more **net** push by gravions. However, the curve lies below the corresponding expected Newtonian force, as it should. This is to be expected from the general absorption Eqs. 6 and 10, whereby the second equation is a straight line tangent to the first near (or at) the origin (at very short distance, or very low k), always yielding a higher value above the downward concave line of PG absorption. The latter is a consequence of the self-shadowing (gravitational shielding) effectively creating a hidden mass, which, if it could exert an “attractive” force (per Newton), it would be greater than the corresponding PG force found.

The above analysis is also consistent with a comparison between Newton and PG as provided in Fig. 5 by plotting the ratio of $f_{gPG}/f_{gNewton}$ from (Eq. 38)/(Eq. 25) vs. k for a constant sphere radius $R = 1$ au. The absorption ratios by PG/Newton approaches unity for very small values of k ($k < 0.01$), as it should, but vanishes for very large values of k , which means that f_g becomes infinity in Newton, whilst it reaches a saturation value in PG. This is reasonable and helpful in understanding the mechanism of shielding. Noted

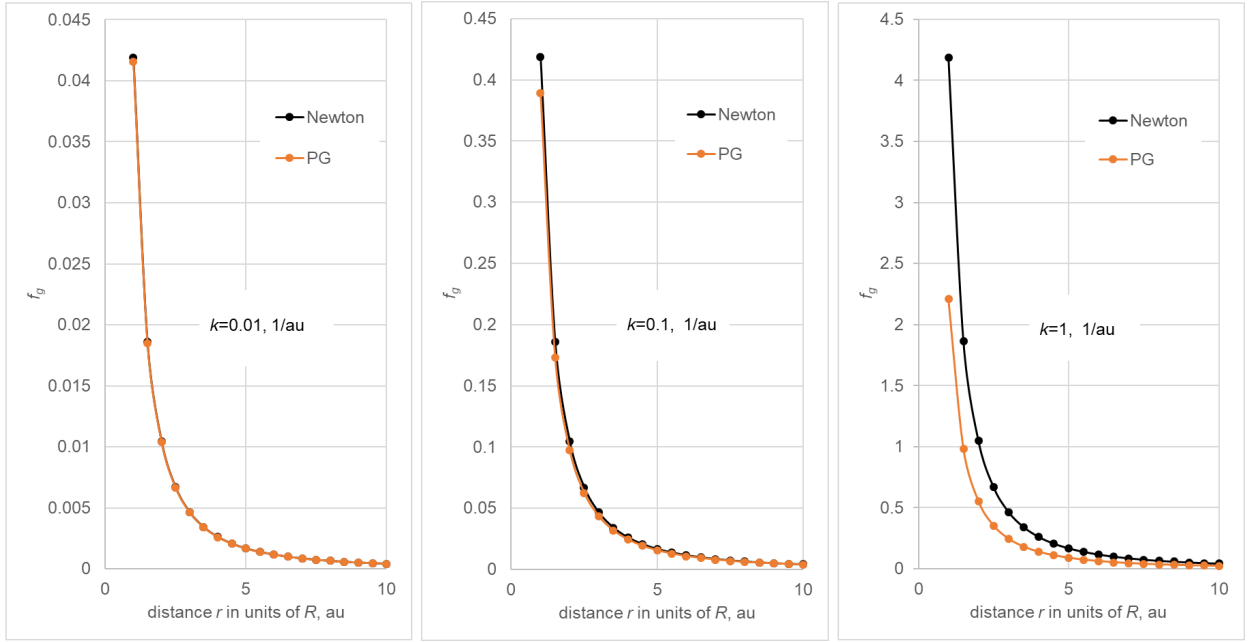


Figure 4: Gravity acceleration factor f_g vs. distance r in units of radius R for three different absorption coefficients k using linear (Newton) and exponential (PG) absorption.

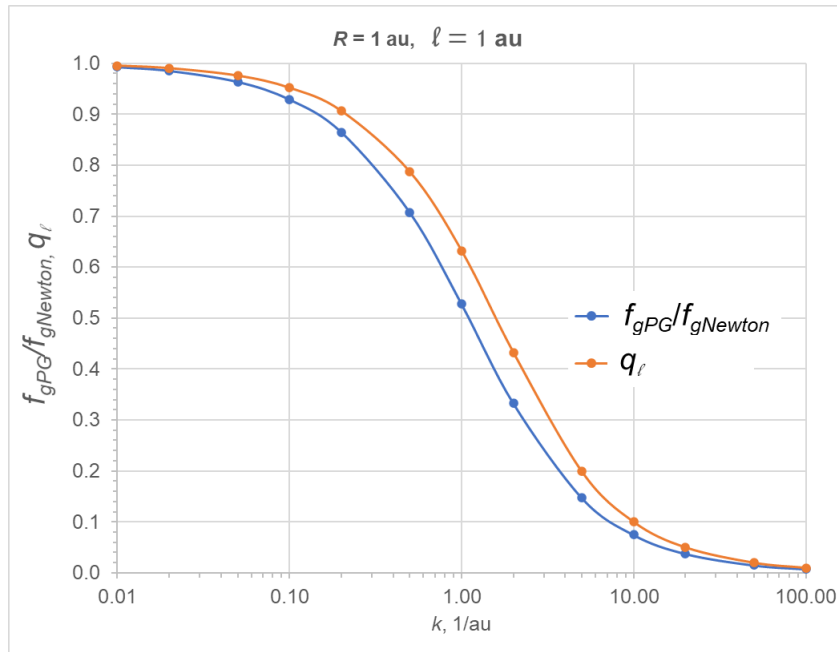


Figure 5: Dependence of ratio $f_{gPG}/f_{gNewton}$ and q_l on k

that the horizontal axis is logarithmic tending to uplift (concave up) the initial straight line (Newtonian) but eventually tending to reach a saturation value asymptotically (concave down). PG is the overriding physics in all cases, whilst Newtonian physics is an approximation in the limiting case of very low values of k . The above ratios are given by:

$$q = \frac{f_{gPG}}{f_{gNewton}} = \frac{g_{PG}}{g_{Newton}} = \frac{3A_R}{4kR} \quad (45)$$

which will be referred to as contraction factor, or factor q . The significance and use of this factor will become apparent in further development of PG theory.

If we also take the ratio from the integrands of Eqs. 23 and 36, i.e. the ratio of the differential accelerations (or factors df_g) inside an elementary solid angle $d\Omega$, we obtain another factor q_ℓ , to be referred to as length contraction factor:

$$q_\ell = \frac{df_{gPG}}{df_{gNewton}} = \frac{1 - \exp\left(-2kr\sqrt{a^2 - \sin^2\varphi}\right)}{2kr\sqrt{a^2 - \sin^2\varphi}} = \frac{1 - \exp(-k\ell)}{k\ell} \quad (46)$$

and is plotted on the same Fig. 5.

This is the ratio of an effective length $\ell_e(\varphi)$ in PG divided by the real length in Eq. 12 of the chord traversing the sphere at angle φ from the origin O in Fig. 2:

$$\ell_e(\varphi) = \frac{1}{k} \left[1 - \exp\left(-2kr\sqrt{a^2 - \sin^2\varphi}\right) \right] \quad (47)$$

It is a contracted or compressed length, with which we may construct a virtual volume (body) by replacing the points defined by Eq. 17 with new ones defined by

$$u_{e2} = u_1 + \ell_e \quad (48)$$

or correspondingly replacing the points by Eq. 16 with new ones defined by

$$u_{e1} = u_2 - \ell_e \quad (49)$$

We may refer to these shapes as *gravitoids*, which are helpful for our theoretical understanding of the underlying workings of PG. Further details and analysis are provided in Appendix A.

Note 1: The current practice to find the mass of a planet is to place an artificial satellite around it and measure the period and radius of orbit. However, we now find that the actual mass still remains unknown by such measurements. This is not a trivial finding.

Note 2: For small values of k or R , we revert to Newtonian mechanics, which can also be seen by expanding the exponential to a Taylor series $e^x = 1 + x + \frac{x^2}{2} + \frac{x^3}{6}$.

$$A_{R_{kR \rightarrow 0}} = \frac{4}{3}kR(1 - kR)_{kR \rightarrow 0} \approx \frac{4}{3}kR \quad (50)$$

$$\text{i.e. for very small } kR: \pi A_R = \frac{4}{3}\pi kR = f_{gNewton} \quad (51)$$

the latter reproducing Eq. 25 for f_g in Newton derivation at $r = R$.

6.2 Universal gravitational “constant” in any absorption regime vs. a new cosmic constant

We note that in Eq. 25 the multiplier preceding the factor $1/r^2$ divided by k provides the volume V of the gravitating sphere. Likewise, in Eq. 38, the multiplier preceding $1/r^2$ divided by k also provides an *effective* sphere volume V_e with the same center:

$$V_e \equiv \frac{\pi A}{k} \quad (52)$$

The real volume, real density and real mass are designated by V , ρ , and M . The measured (effective, measured, or apparent) density ρ_e is the effective mass M_e divided by the real volume

$$\rho_e = \frac{M_e}{V} = \frac{\rho V_e}{V} \quad (53)$$

and

$$\rho_e V = \rho V_e = M_e \quad (54)$$

also

$$\frac{\rho}{\rho_e} = \frac{V}{V_e} = \frac{M}{M_e} \quad (55)$$

We can now continue from Eq. 38 by multiplying with $V\rho_e$ both numerator and denominator as follows:

$$f_g = \frac{\pi A}{V\rho_e} \frac{V\rho_e}{r^2} = \frac{kV_e}{V\rho_e} \frac{M_e}{r^2} = \frac{kV_e}{V_e\rho} \frac{M_e}{r^2} = \frac{k}{\rho} \frac{M_e}{r^2} \quad (56)$$

which is identical to Eq. 26, except that we use the real density and not the effective (fictitious) one used (or implied) in Newton's equation. Based on this, we can repeat the same steps to establish the force on a testing mass and derive an identical form of equation as in 33

$$g = \frac{dF}{dm} = \frac{\frac{J_g}{c} dS \cdot k'x}{\rho' dS \cdot x} = \frac{J_0}{c} \frac{k}{\rho} \frac{M_e}{r^2} \frac{k'}{\rho'} = \frac{J_0}{c} \Lambda^2 \frac{M_e}{r^2} \quad (57)$$

but where again we use the real density of the gravitating body in Λ . We repeat the same equations in order to stress that they are different in the meaning of ρ and Λ , whereby we derive the same expression for the universal gravitational constant:

$$G = \frac{J_0}{c} \Lambda^2 \quad (58)$$

This is the same equation arrived at for weak graviton absorption, so that Λ is the new universal constant for the cosmos. From this and the known density of a given mass, we derive the absorption coefficient k . The universal constant G is proportional to the ratio of k/ρ squared, where ρ is the real density. For very low values of k the real density becomes very close to or is indistinguishable from the measured (effective) density. From this, we learn that G is constant only to the extent that J_0/c is constant in the neighboring universe. As pointed out earlier, Λ expresses the number of scattering events per unit length per unit mass density anywhere and provides a more tangible constant parameter to have. Thus, G may be found to be relatively more variable than previously suspected, according to further investigations by PG.

The effective volume introduced above is plotted in Fig. 6 against k after it is normalized over the real volume. As expected, it coincides with the real volume (at very low k), but then monotonically decreases to a vanishing value at very large k .

6.3 Maximum universal acceleration

We can try to use known values of planet parameters to derive the Λ , k , ρ and J_0 . Basically, we need to know the flux intensity J_0 , or the absorption coefficient k , on which all other parameters depend. Conversely, from the known physical parameters of a planet, we may assume values for J_0 in any given range and derive the other new parameters of Λ , k and ρ as a function of J_0 . In practice, we may proceed as follows:

The acceleration of gravity g_R at the surface of a sphere, i.e. at $r = R$, is given by Eq. 41 as:

$$g_R = \frac{J_0}{c} \Lambda \frac{\pi A}{R^2} = \frac{\pi J_0}{c} \Lambda A_R = \frac{\pi G}{\Lambda} A_R \quad (59)$$

From Eqs. 41, 44 and Fig. 3, there is a maximum possible acceleration $g_{maximum} \equiv g_0$ in the surrounding universe to be manifested on the surface of a star (sphere) with sufficiently large product kR , i.e. with $A_R = 1$, given by any of the following equations:

$$g_0 = \pi \frac{J_0}{c} \Lambda = \frac{\pi G}{\Lambda} = \frac{\pi \rho G}{k} \quad (60)$$

In subsequent work, we will be using values of g_0 in a tentative range to obtain an idea of the expected magnitude of various parameters and anticipated measurements. That is, until we establish the actual value

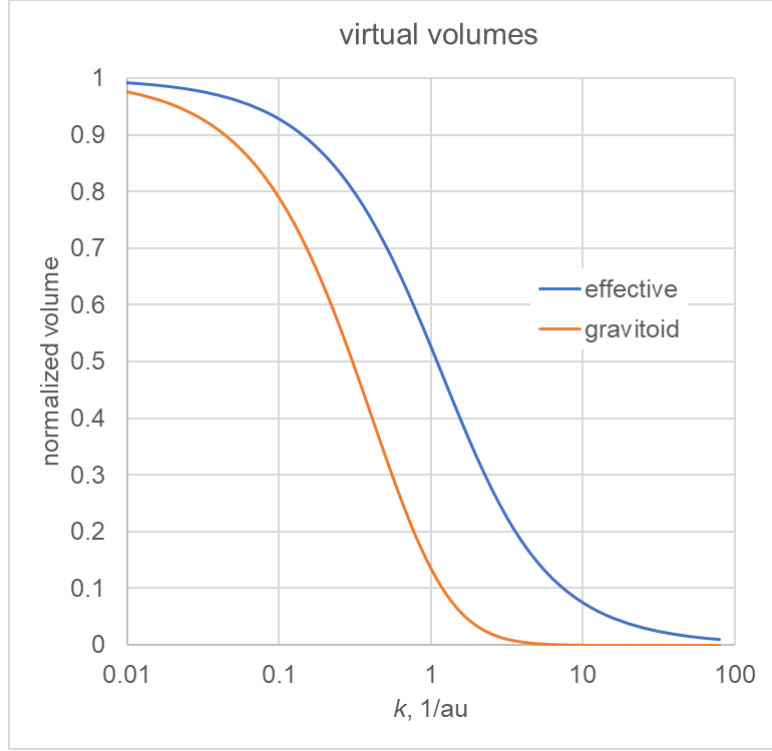


Figure 6: *Virtual volumes, gravitoid and effective, normalized over the real spherical volume.*

of g_0 , we may obtain the new constant Λ and hence k from the known density of a mass, for any given value g_0 .

It is useful to write Eqs. 57 and 59 correspondingly as:

$$g = G \frac{M_e}{r^2} = \frac{G \pi A}{\Lambda r^2} = g_0 \frac{A}{r^2} \quad (61)$$

$$g_R = g_0 A_R \quad (62)$$

Now, given the measured acceleration g_R on the surface of a spherical body, we can find k by solving the equation below:

$$g_0 A_R - g_R = g_0 \left[1 - \frac{1}{2k^2 R^2} + \frac{\exp(-2kR)(2kR + 1)}{2k^2 R^2} \right] - g_R = 0 \quad (63)$$

as a function of g_0 . Then, for any given g_0 , we can find in turn ρ , Λ and J_0 from Eq. 60. We will return to the question of g_0 in a subsequent section

6.4 Commonality and departure between Newton and PG

It is not fortuitous that both Newtonian and PG mechanics share a common limiting case but depart thereafter. Let us start from the derivation of the volume of the sphere as seen from point O in Fig. 2. For the elementary volume we have

$$dV = d\Omega u^2 du \quad (64)$$

which multiplied by the density ρ gives the elementary mass and, divided by the inverse square distance, yields the Newtonian acceleration:

$$dg_{Newton} = \frac{d\Omega u^2 du}{u^2} \rho \quad (65)$$

In PG, we use the factor f_g from which we obtain the same elementary acceleration by :

$$dg_{PG} = \frac{g_0}{\pi} d\Omega k du \quad (66)$$

which is identical to Newton above except for the proportionality constants. This initial similarity is not trivial, because it explains the fundamental difference at the root of the two theories (approaches), as we increase the absorption coefficient: In Newton, it is given that the acceleration is inversely proportional to the square of distance, whilst in PG this is a consequence of the solid angle (geometry) incorporating the inverse square distance relationship. In Newton, this is the result of an assumed radiance (of gravity) emanating from the elementary mass, whilst in PG the same field emanates from the radiance of the surrounding universe. Whilst the analogy might seem trivial simply shifting the problem of origin of the elusive gravity from the inside to the outside of a given mass, the consequences diverge from the two approaches as we increase the absorption coefficient to any level. That is, when considering very large masses or densities, Newton and PG provide very different solutions and outcomes: Newton provides a linear cumulative radiance of gravity by simple summation of all the constituent masses/volumes, whilst PG allows for shadowing (shielding) of the universal radiance traversing the mass, which, in turn, results in an asymptotic limit to the total shielding and hence to the total acceleration or force. We may think of this limit as effectively integrating the Newtonian law linearly but within contracting upper limits of a volume per Eq. 66, which defines the said gravitoid. This shape would produce the same Newtonian force with a mass having the actual (real) density. The above integration has been performed numerically and potted against k in Fig. 6 after it is normalized by dividing by the sphere volume, as was done for the effective spherical volume defined by Eq. 52. For comparison, this is also plotted against k in Fig. 6. We note that it is generally lying above the gravitoid, as it should, because it is further away from the gravitoid. They both have the same real density and both yield the correct value of acceleration for the real gravitating sphere.

Hence, these are important findings for cosmological considerations in relation to what happens as we keep adding mass (accretion) to a star (dwarfs, black holes, etc.). We will discuss this again later.

An important conclusion here is that there is more mass in the universe than Newton's Law measures. This is a form of dark matter but not exactly in the sense considered by existing theories to date, in accounting for the observed celestial motions. We now find weaker forces, not greater. However, the greater forces, if needed, may be accounted for by forces originating from the outside now predicted from PG theory, not from the inside anticipated by Newton. At very large distances, forces are exerted by the gravions in the universe, so there is no need to attribute them to an attraction by dark matter. However, dark matter should assume a different meaning now by the shadowing effect (gravitational shielding) in PG. Thus, breaking up a planet to dust would appear to create new matter (out of shadow - see redistribution of density in later Section 10), which gives a kind of credence to the creationist theory of matter, except that no new matter actually is created other than new matter coming out of the shadows (literally). All this and more creates new understanding and new physics that will become clearer as we develop and prove the novel PG presented in this work. As we investigate next, the bigG is a function of the gravion density in the universe, which should vary between regions inside a galaxy and in intergalactic regions. So, if we need extra forces, these may arise from the variation of bigG alone. The sum total of the effects caused by hidden masses and the variation of bigG might explain or replace the hypothesized dark matter and dark energy of current theories. PG may offer the new physics needed.

6.5 Summary of new parameters and relationships

We have already expressed various relationships in alternative forms, which we may further re-arrange for easy reference in later derivations here or elsewhere as follows: By combining Eqs. 41 and 57 we derive:

$$\pi A = \Lambda M_e \quad (67)$$

and

$$\Lambda = \frac{\pi A}{M_e} = \frac{\pi}{M_e} \left[R^2 - \frac{1}{2k^2} + \frac{\exp(-2kR)(2kR + 1)}{2k^2} \right] = \frac{\pi R^2 A_R}{M_e} \quad (68)$$

We obtain a further insight of the above parameters by re-writing the above as

$$A_R = \Lambda \frac{M_e}{\pi R^2} = \Lambda \lambda_e \quad (69)$$

by defining an effective mass-thickness λ_e (or area-density) with

$$\lambda_e = \frac{M_e}{\pi R^2} \quad (70)$$

The neighborhood prevailing gravion pressure p_g should be handy to have (per Eq. 58) as

$$p_g = \frac{J_0}{c} = \frac{G}{\Lambda^2} \quad (71)$$

If two spheres (planets) 1 and 2 have equal surface acceleration g_R , it follows from Eq. 59 that the product kR for both spheres is the same

$$k_1 R_1 = k_2 R_2 \quad (72)$$

Also we have the universal (cosmic) constancy for Λ giving:

$$\Lambda = \frac{k_1}{\rho_1} = \frac{k_2}{\rho_2} = \frac{\pi G}{g_0} = \frac{c g_0}{\pi J_0} = \text{constant} \quad (73)$$

so that we obtain

$$\rho_1 R_1 = \rho_2 R_2 \quad (74)$$

The above equations apply in PG theory with real densities ρ_1 and ρ_2 . In Newtonian mechanics, we similarly obtain for the effective (apparent) densities ρ_{e1} and ρ_{e2} , i.e. if the g_R is equal for both spheres (at their surface):

$$g_R = \frac{4}{3} G R_1 \rho_{e1} = \frac{4}{3} G R_2 \rho_{e2} \quad (75)$$

$$\rho_{e1} R_1 = \rho_{e2} R_2 \quad (76)$$

We obtain the ratios of real to effective densities as

$$\frac{\rho_1}{\rho_{e1}} = \frac{\rho_2}{\rho_{e2}} \quad (77)$$

From a given value for g_0 , we find the corresponding k from Eq. 63 and then ρ from Eqs. 60:

$$\rho = g_0 \frac{k}{\pi G} \quad (78)$$

and then the ratio ρ/ρ_e from the known effective (measured) density. This ratio is also provided directly from:

$$\frac{\rho}{\rho_e} = \frac{4}{3} k R \frac{g_0}{g_R} \quad (79)$$

We also derive relationships including the frequently encountered factor A_R :

$$M_e = \frac{\pi \rho R^2}{k} A_R = \frac{3 A_R}{4 k R} M = \frac{g_0}{G} R^2 A_R \quad (80)$$

$$V_e = \frac{\pi R^2}{k} A_R \quad (81)$$

Finally, it is important to note that the parameter g_0 or the factor f_g yield the acceleration g , via Eqs. 43, 60 and 61 in a simple form by a summary of equations:

$$g = f_g \frac{g_0}{\pi} = f_g \frac{J_0}{c} \Lambda = f_g \frac{G}{\Lambda} = g_0 \frac{A}{r^2} = g_0 \frac{A_R}{n_R^2} \quad (82)$$

The maximum (or limiting) universal constant g_0 now takes on a tangible significance in establishing the quantitative relationships in PG, and it may substitute the constant G accordingly. We should stress that new universal constant of the cosmos Λ is given by Eq. 68, which in words states that the hitherto universal constant G is proportional to the new universal constant (maximum acceleration) g_0 both with reference to a region of the universe, so that together they yield the cosmic (overall universal) constant Λ . It should be noted that we attempt to distinguish the term “universal” from the term “cosmic” with reference to the neighboring universe or to the “entire” universe (=cosmos).

With the new parameters now introduced, it is useful to re-write Eq. 45 of the ratio of accelerations as a function of tentative values for g_0 :

$$q = \frac{g_{PG}}{g_{Newton}} = \frac{3 A_R}{4 k R} = \frac{3 A_R}{4 \pi G \rho R} g_0 \quad (83)$$

This factor characterizes a multitude of parameters, not only the acceleration, with reference to PG and Newton. For example we can write

$$q = \frac{\rho_e}{\rho} = \frac{M_e}{M} = \frac{V_e}{V} \quad (84)$$

7 Force between two spherical masses

For the force between two spherical masses, we can formulate the problem entirely from gravion absorption considerations, carry out four integrations and produce the force law, as we did for the acceleration at a point for a single sphere. This would be an independent way, from first principles, to derive the required relationship. However, we can still arrive at the same desired result in a much simpler way as follows:

Since we already have established the relationships between all the parameters needed for the PG force equations, we can apply a “reverse engineering” approach. Now, in the knowledge that Newton is correct except for the masses used, we can start with the Newtonian law of force by using the effective masses provided by PG theory together with preceding equations between various parameters:

$$F = G \frac{M_{e1} M_{e2}}{r^2} = G \frac{\pi A_1}{\Lambda} \frac{\pi A_2}{\Lambda} \frac{1}{r^2} = \frac{J_0}{c} \frac{\pi A_1 \pi A_2}{r^2} = \frac{g_0}{\Lambda} \frac{\pi A_1 A_2}{r^2} \quad (85)$$

This is consistent with our hitherto understanding of the meaning of the parameters involved. The importance is that Newton’s law now involves the effective masses M_{e1} and M_{e2} , not the real masses assumed, but not used, in prior mechanics. The above equations is a far reaching conclusion. Now we can write, or start with the PG force law as

$$F = \pi \frac{g_0}{\Lambda} \frac{A_1 A_2}{r^2} \quad (86)$$

where we do not need the masses, but equivalently we need the more intrinsic parameter of absorption coefficients (relating to mass), the radii (geometry), the new cosmic constant Λ and the prevailing maximum acceleration g_0 in the neighboring universe, or equivalently the pressure J_0/c exerted by the radiant energy in our neighborhood. We may further rearrange the above to provide a more tangible idea of how the force is derived by

$$F = p_g A_{R_1} A_{R_2} \frac{\pi R_1^2 \pi R_2^2}{r^2} \quad (87)$$

which states that the force is proportional to the pressure exerted by the gravions times the absorptivities times the cross-sections of the spheres while still being inversely proportional to the square of the distance. It seems like we can separate one group of factors pertaining to geometry alone and another group of factors pertaining to matter (energy) and its interactions involving the local system of two masses interacting with the universal pressure of gravions. The two masses do nothing by themselves except for the mediating flow of gravions.

Therefore, the above equations provide variant expressions of the law of gravitational force in the new physics of PG. They are particularly appealing by their consistency and symmetry of parameters beyond Newtonian physics.

The mathematical derivation from first principles of the radiant intensity absorption involving multiple integrations involves a number of simplifications and cancellation of terms by appropriate choice of a reference system of co-ordinates. The multiple integrations may also be done by numerical means via relatively simple Python codes run in parallel to shorten the computation times. Integrals involving absorption along lines crossing a single sphere cancel out leaving only integrals crossing both spheres simultaneously. This work has been omitted from this Section to avoid needless congestion that could potentially distract from the important finding above and beyond. This section may be expanded to form a self contained chapter with sufficient detail to qualify for publication, which, however, can await at least for an initial response by the established scientific community on the current report as is. In the meantime, we have added more details by presenting the constitutional equations of the interaction of two material spheres in Appendix C, etc. Numerical integration of those equations has lead to important results and conclusions.

Some concern might arise by a later proposal in Section 14.5, namely, that the effective mass being involved in the generation of force may be variable with its distance from another mass due to the perturbation of the surrounding gravion flux. However, these concerns have been eased by finding that the above presented

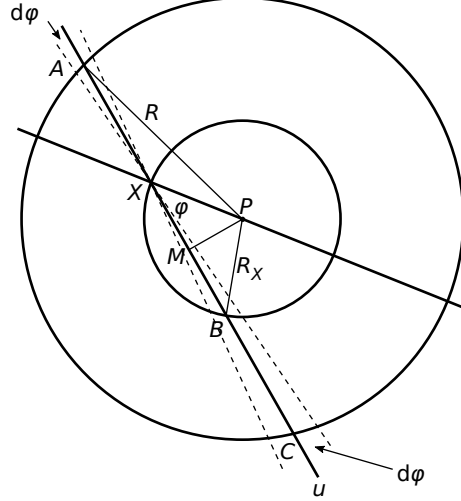


Figure 7: Derivation of the internal field of a uniform density sphere.

fundamental equation is still valid. The envisaged variation of mass is coordinated by the mathematics of absorption in a way that the inverse square of distance law is always preserved at any absorption regime. We have tested ordinary solar system bodies (near Newtonian) as well as “artificial” ones with extremely dense and massive bodies. These outcomes are better presented together with a new analysis of effective mass generation and variation with distance in Sections 15.7 and 16.

IMPORTANT: The new gravitational law in PG expressed by Eq. 87 has far more repercussions than being a simple substitution of old parameters with new. It states that the force between two masses is not simply proportional to the effective masses but proportional to the associated absorptivities of the masses. This means that non-spherical masses exert a different force for different relative orientation of the same masses (bodies). If, as they move towards or away from each other they change orientation, they also change gravitational absorptivity and hence the trajectories would not be as expected from Newtonian mechanics. The dependence of acceleration on the density distribution will become more clear in Section 10. Further analysis is presented under the Equivalence Principle in Section 14.3.

8 Internal spherical field

So far, we have examined the field generated externally to a spherical body, but we now proceed to find the field also inside the sphere. With reference to Fig. 7, the acceleration at any point X inside a sphere with radius $AP = R$ is provided by integrating the absorption along the lengths of mass inside the differential solid angles indicated on either side of the point X along any direction of the line u . We note that the absorption length $XA = BC$ leaving only the length XB to yield a net force absorption, which is the same as that of the sphere with radius R_X crossing the point X. Therefore, we have the same situation as that experienced by Newtonian mechanics, in that a hollow sphere would exert zero force inside its cavity. Now, the acceleration at this internal point is given by (see Eq. 82)

$$g_X = g_{0X} \left(1 - \frac{1}{2k_X^2 R_X^2} + \frac{\exp(-2k_X R_X) \cdot (2k_X R_X + 1)}{2k_X^2 R_X^2} \right) \equiv g_{0X} A_{R_X} \quad (88)$$

where A_{R_X} is the familiar A_R factor at the surface of the internal sphere with radius $PB = R_X$ and $g_{0X} < g_0$ due to the shielding of the outer layer from X (more on this can be found in Section 24).

We can find g_{0X} by resorting to the usual absorption factor f_{g_X} at point X by the following steps:

The exponential absorption factor in the direction XBC is

$$1 - \exp(-k \cdot XB(\varphi) - k \cdot BC(\varphi))$$

and in the direction XA is

$$1 - \exp(-k \cdot XA(\varphi))$$

so that we take their difference in the integral:

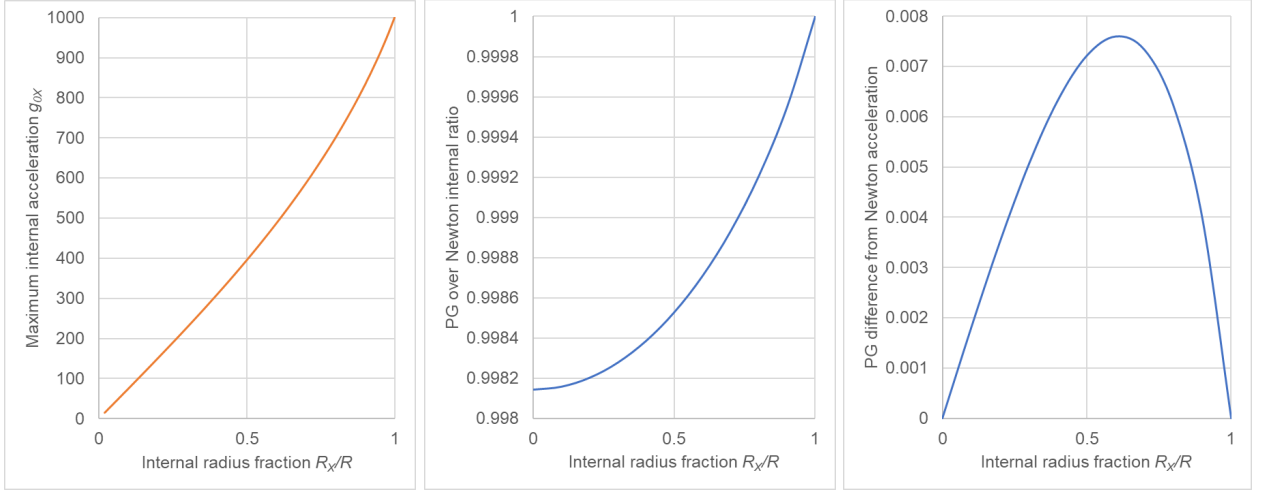


Figure 8: *Internal maximum acceleration g_{0X} , internal ratio of PG over Newton accelerations and internal difference of PG from Newton acceleration in Earth.*

$$f_{gX} = \int_0^{\pi/2} 2\pi \sin \varphi \cos \varphi d\varphi \cdot [\exp(-k \cdot XA(\varphi)) - \exp(-k \cdot XB(\varphi) - k \cdot BC(\varphi))] \quad (89)$$

and integrate with respect to angle φ from 0 to $\pi/2$ as can be seen in the referenced diagram.

From the geometry shown and M being the mid-point of the chord AC, we find and replace the lengths accordingly with:

$$XB(\varphi) = 2R_X \cos \varphi$$

$$XA(\varphi) = BC(\varphi) = \sqrt{R^2 - (R_X \sin \varphi)^2} - R_X \cos \varphi$$

to obtain the integral formula:

$$f_{gX} = \int_0^{\pi/2} 2\pi \sin \varphi \cos \varphi d\varphi \cdot \left[\exp\left(-k\sqrt{R^2 - (R_X \sin \varphi)^2} + kR_X \cos \varphi\right) - \exp\left(-k\sqrt{R^2 - (R_X \sin \varphi)^2} - kR_X \cos \varphi\right) \right] \quad (90)$$

From this found, we can derive the acceleration at X by the factor g_0/π and equate it to its value given above by Eq. 88:

$$g_X = \frac{g_0}{\pi} f_{gX} = g_{0X} A_{R_X} \quad (91)$$

from which we can find the relationship between the internal g_{0X} and external g_0 .

$$g_{0X} = \frac{g_0 f_{gX}}{\pi A_{R_X}} \quad (92)$$

The expected Newtonian acceleration at X is given by:

$$g_{XN} = \frac{4}{3} \pi G \rho_e R_X \quad (93)$$

No analytical relationship was found for f_{gX} , so that we may resort to numerical means for this parameter. For practical application, we also need to see the difference of PG from Newton acceleration against various depths from the surface of the Earth by replacing the internal radius as a function of depth.

$$R_X = R - \text{depth} \quad (94)$$

<i>depth</i> =	2500	5000	7500	10000	12500
g_N =	9.816404	9.812551	9.808697	9.804844	9.800990
g_0	Δg_X	Δg_X	Δg_X	Δg_X	Δg_X
300	7.29E-05	1.45E-04	2.18E-04	2.90E-04	3.61E-04
500	4.32E-05	8.62E-05	1.29E-04	1.72E-04	2.14E-04
1000	2.14E-05	4.27E-05	6.39E-05	8.50E-05	1.06E-04
2000	1.07E-05	2.13E-05	3.18E-05	4.23E-05	5.28E-05
5000	4.25E-06	8.48E-06	1.27E-05	1.69E-05	2.11E-05
10000	2.12E-06	4.24E-06	6.34E-06	8.43E-06	1.05E-05
20000	1.06E-06	2.12E-06	3.17E-06	4.21E-06	5.26E-06
30000	7.08E-07	1.41E-06	2.11E-06	2.81E-06	3.50E-06
50000	4.24E-07	8.47E-07	1.27E-06	1.69E-06	2.10E-06

Table 1: *Difference of acceleration Δg between Newton and PG at various depths in Earth.*

We present some values as in Table 1 for Earth by using average values for density and absorption coefficient taken from the Table 3 as used for various planets in the following section. Tentatively, we initially use the value $g_0 = 1000 \text{ m/s}^2$. The results provide the expected deviation of measurements from Newtonian physics at various depths, if the Earth’s crust had uniform density and a spherical shape. We can do measurements in a very deep mine or in a deep ocean, however, we would need to re-calculate the local acceleration in both Newton and PG cases. In practice, measurements of this kind would be complicated by influences of the local variations of density and time dependent fluctuations of the local acceleration, but the given table provides a first idea of the order of magnitude of expected deviation from Newton for a prospective careful experiment. It seems that these deviations should be measurable by a sensitive gravimeter with sufficient confidence if g_0 has a sufficiently low value. In turn, by establishing true measurements of the acceleration at various depths, we can deduce the unknown parameter g_0 .

For theoretical considerations, we can also see the variation of maximum internal acceleration g_{0X} , the ratio of g_X/g_{NX} (PG/Newton) and the difference of PG from Newton acceleration in Fig. 8 at any depth (fractional radius) again for a tentative external $g_0 = 1000 \text{ m/s}^2$ in the case of planet Earth using the same parameters. For further analysis, reference should be made to Section 24, especially noting that the internal Newton-acceleration is derived from the actual Newton-acceleration at the surface of the sphere.

Establishing the variation of the maximum acceleration factor g_0 inside a planet, it also suggests that this parameter may not be so constant even in our relatively “small” area of the universe even inside the heliosphere, since there is a significant mass within the heliosphere itself, whilst our planets are just internal points within this sphere. This might explain the Pioneer anomaly for the deviation of gravity measurements from expected values from Newtonian mechanics. This then points also to the alternative possibility of purposefully sending a spacecraft to more accurately measure the same effect while eliminating (preventing) other already proposed causes and explanations.

8.1 The Greenland experiment anomaly

Shortly before publication of the manuscript of this work, it has been accidentally found a report on “*The Greenland Gravitational Constant Experiment*” Zumberge *et al.* (1990) dealing exactly with the measurement of gravity in a bore hole in the ice-sheet. A deviation (shortfall) from Newton has been found in the range

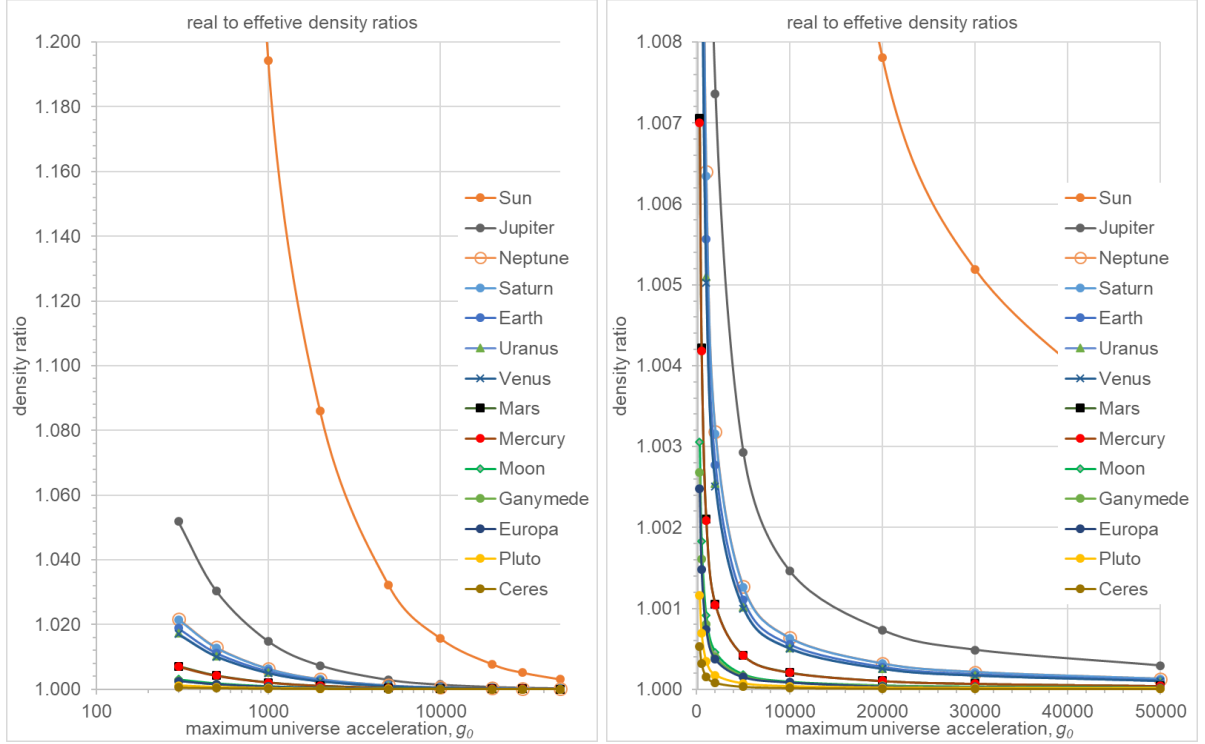


Figure 9: *Ratio of real to effective (measured) densities for planets, moons and the Sun.*

of between 1-4 mGal. This report appears particularly comprehensive in dealing with all possible sources of error and still found to establish a gravitational anomaly that cannot be explained by known theory stating in the abstract that: “*An anomalous variation in gravity totaling 3.87 mGal ($3.87 \times 10^{-5} \text{ m/s}^2$) in a depth interval of 1460 m was observed. This may be attributed either to a breakdown of Newtonian gravity or to unexpected density variations in the rock below the ice*”. Although these measurements cannot be used “as is” to do any quantitative connection to the PG predictions in this Section, we do note that the order of magnitudes match well with those of Table 8. This is particularly encouraging to organize a similar experiment, perhaps, best suited in an ocean, where the local variations of gravity may be less or more easily predictable and the depth measurements about one order of magnitude greater.

However, variant reports by Zumberge and coworkers have failed to reproduce this anomaly at various oceanic depths, which might be attributed to either (a) the experimental error involved overwhelms the anticipated effect, which is of the order of magnitude tentatively deduced from the Allais effect per following Section 12.4, or (b) the mathematical treatment used for the Newtonian derivation may need reworking, else the direct method used in PG computations needs to be applied for the specific mass distribution at the location tested and integrated with the whole planet.

9 Application to the solar system

We can tentatively apply the equations of PG so far, like in Sections 6.3 and 6.5, to the solar system by assuming values of the maximum prevailing acceleration g_0 in our area of the universe.

We first plot the density ratios for many bodies of the solar system in Fig. 9 in the given hypothetical range of values for g_0 between 300-50000 m/s^2 . These graphs show that we get practically identical curves for Mercury and Mars having close to same surface accelerations, whilst all else are proportionally separated in accordance to their surface gravity. The graphs indicate the degree of departure from real densities depending on the chosen value of g_0

For better appreciation of the magnitudes involved, numerical results are also presented, as example, for three bodies (Sun, Earth and Moon) in Table 2 in the same range of g_0 . Some typical values of Λ for the same range of g_0 are also given being universal for all bodies per Eq. 73.

For any given set of mass and radius of each planet, we have derived the corresponding surface acceleration and effective density rather than using random (published) values from different sources. This is necessitated by the need to be consistent and accurate in these calculations and avoid discrepancies. These parameters are sensitive to very small changes of the input data. Small bodies are even more sensitive and round-off errors

	Sun		Earth		Moon		
g_0 , m/s ²	k, 1/m,	ρ/ρ_e	k, 1/m	ρ/ρ_e	k, 1/m	ρ/ρ_e	Λ , m ² /kg
300	3.4245E-09	3.4640	3.9262E-09	1.01886	2.3464E-09	1.003060	6.99E-13
500	9.1141E-10	1.5366	2.3380E-09	1.01121	1.4061E-09	1.001833	4.19E-13
1000	3.5419E-10	1.1943	1.1625E-09	1.00556	7.0242E-10	1.000915	2.10E-13
2000	1.6103E-10	1.0860	5.7963E-10	1.00277	3.5105E-10	1.000457	1.05E-13
5000	6.1225E-11	1.0322	2.3146E-10	1.00111	1.4038E-10	1.000183	4.19E-14
10000	3.0125E-11	1.0158	1.1567E-10	1.00055	7.0185E-11	1.000091	2.10E-14
20000	1.4944E-11	1.0078	5.7818E-11	1.00028	3.5091E-11	1.000046	1.05E-14
30000	9.9371E-12	1.0052	3.8542E-11	1.00018	2.3393E-11	1.000030	6.99E-15
50000	5.9499E-12	1.0031	2.3123E-11	1.00011	1.4036E-11	1.000018	4.19E-15

Table 2: Calculated absorption coefficient k and ratio of real ρ over effective ρ_e density for the Sun, Earth and Moon in an assumed range of g_0 values.

in the calculations are significant. Excel sheets were used for formatting the plotted figures, which initially necessitated the use of an “Add-in” (xlPrecision) to increase accuracy beyond 15 decimal places. Likewise, in a later use of Python code to reproduce the same output, we had to use increased computational precision to avoid serious round-off errors. In Table 3, we provide the initial data used for various bodies here and in all calculations elsewhere in this report. We also quote in parenthesis some variant values of the surface acceleration that were found from different sources for comparison, but not applied.

In all above, the derived and used parameters are based on the average density of the chosen bodies, which strictly speaking cannot produce the correct (actual) PG result, unless we knew in advance the radial density distribution for any given body. However, we obtain some first order of magnitude idea of the new important parameters introduced in this work. It should be noted that the density ratios approach unity as we increase g_0 .

9.1 Further analysis

To better understand the meaning of the real density expected for a planet, we can plot what the acceleration on the surface would be if the measured (effective) density were used as the real density. Let’s use the data for the Sun given by Table 3 and plot g_R against g_0 in Fig. 10 using Eqs. 59 and 60. We note that the Sun’s real acceleration is approached asymptotically at very high values of g_0 . The latter is as expected, because increasing g_0 decreases k , which makes the PG value to become Newtonian, i.e. to reduce to $g_R = 274.825$ m/s² as given in Table 3. The same can be deduced by taking the limit of Eq. 59 as $k \rightarrow 0$.

We have already found that by increasing the radius of a planet by adding mass at constant density, the surface acceleration reaches a saturation limiting value, namely, g_0 , i.e. when A_R becomes unity. This is at variance with Newtonian prediction of infinity by Eq. 75.

Likewise, with increasing the density by keeping the radius constant, the Newtonian prediction is infinity. However, in PG the factor A_R being a function of the product kR becomes a product also of $\Lambda\rho R$ meaning that $A_R \rightarrow 1$ by increasing ρ with constant R and Λ . Similarly, by shrinking a star (sphere) with constant mass, we obtain unity for A_R as the density becomes fast very large (the density being inversely proportional to the third power of radius). In other words, the eventual surface acceleration reaches the saturation value of g_0 in clear distinction from Newtonian mechanics.

Last in this connection, we should also consider what happens at a fixed point in space away from a sphere (star), when the sphere shrinks with constant mass. By Newton, the acceleration remains constant at that point, but by PG this is not the case: The acceleration monotonically becomes smaller, due to self shadowing (k increases much faster than the radius) by

$$g_{fixed_r} = g_0 \frac{\pi A}{r^2} \quad (95)$$

noting that A varies as:

planet	radius R	mass M_e	density ρ_e	g_R (other)
Sun	6.95E+08	1.989E+30	1.41446E03	274.825 (273.7)
Jupiter	6.9911E7	1.8982E27	1.326E3	25.9204 (24.79)
Neptune	2.4622E7	1.02413E26	1.6379344E3	11.27456624 (11.15)
Saturn	5.8232E7	5.6834E26	6.87123E2	11.1860(10.44)
Earth	6.371E6	5.97237E24	5.5136E03	9.82026 (9.807)
Uranus	2.5362E7	8.6810E25	1.27037E3	9.00729 (8.69)
Venus	6.0518E6	4.8675E24	5.243E3	8.87009 (8.87)
Mars	3.3895E6	6.4171E23	3.93408E03	3.727854(3.720)
Mercury	2.4397E6	3.3011E23	5.42701E3	3.70150 (3.7)
Moon	1.73700E06	7.34767E22	3.34705E03	1.62533 (1.625)
Ganymede	2.634E6	1.4819E23	1.93590E3	1.42554 (1.428)
Europa	1.560E6	4.799844E22	3.01832E03	1.316343805 (1.315)
Pluto	1.1883E6	1.303E22	1.85386E03	0.615862 (0.62)
Ceres	4.730E05	9.393E20	2.161E3	0.280203 (0.28)
Callisto	2.4103E6	1.075938E23	1.8344	1.235

Table 3: Numerical constants of planets, moons, and the Sun used in calculations of preceding tables and graphs.

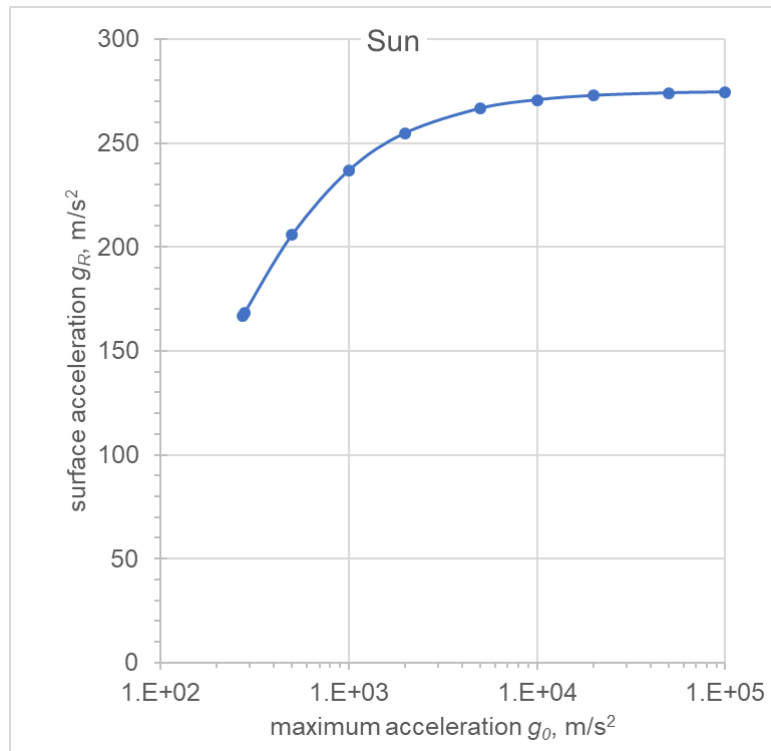


Figure 10: Expected surface acceleration on the surface of the Sun against maximum g_0 using the measured density as real density.

$$A = R^2 \left[1 - \frac{R^4}{2C^2} + \frac{R^4}{2C^2} \exp(-2C/R^2) \cdot (2C/R^2 + 1) \right] \quad (96)$$

where the constant C is defined during the k substitution below:

$$k = \frac{3GM}{4g_0R^3} \equiv \frac{C}{R^3} \quad (97)$$

Noted also that the PG equation of acceleration reduces to Newton's equation, as expected, for very small values of k :

$$g_A = g_0 A_{A_{k \rightarrow 0}} = g_0 \frac{4}{3} k R = \frac{4}{3} \pi G \rho R = G \frac{M}{R^2} \quad (98)$$

Furthermore, we can substitute k accordingly and find g_A for a white dwarf and a neutron star. The extreme accelerations reported for these bodies pose for now a serious question on whether PG could ever be directly measurable or detectable if g_0 needs to be too high. This would constitute a new serious challenge for PG by not being able to detect it experimentally, unless those extremely high values of acceleration are generated by yet another type of push particle. We will discuss this issue again in Part 2 of this report.

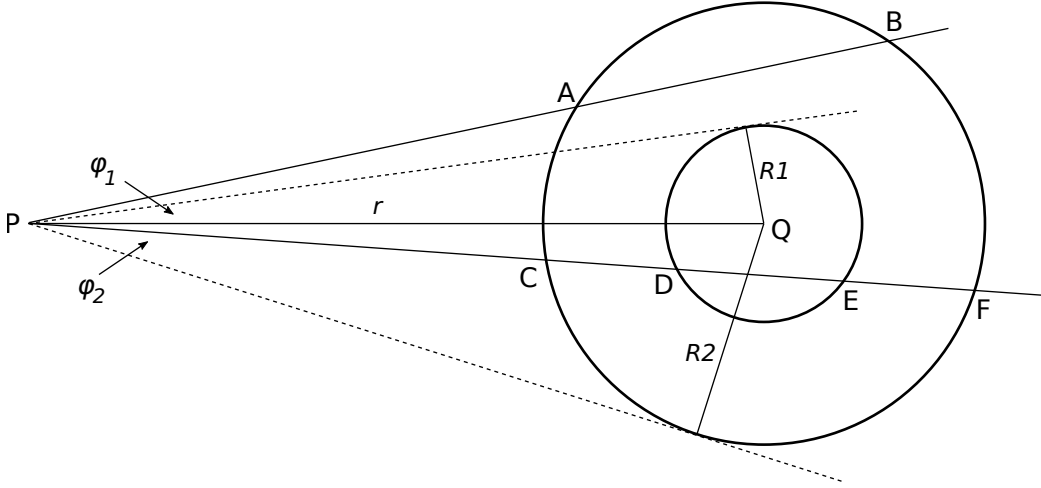


Figure 11: *Derivation of acceleration from concentric spheres with different densities.*

10 Concentric spheres with different densities

We now consider the case of two concentric spheres of different density as depicted in Fig. 11. The inner sphere has a radius R_1 with density ρ_1 , mass M_1 and absorption coefficient k_1 , and the outer sphere has a radius R_2 with density ρ_2 , mass M_2 , and absorption coefficient k_2 . There are two cases of PG absorption, namely, one along a typical chord AB traversing only the outer sphere, and another traversing segment CD of the outer sphere then a chord DE of the inner sphere and then segment EF of the outer sphere again.

To find the acceleration at point P being at a distance $r = PQ$, we follow the integration steps as in the first place for PG (Eq. 37), but for the two parts described above:

Part one involves integration in the angle between φ_1 and φ_2 for the outer spherical layer.

$$f_{g2} = 2\pi \left[\frac{\sin^2 \varphi}{2} - \frac{\exp\left(-2kr\sqrt{a^2 - \sin^2 \varphi}\right) \left(2kr\sqrt{a^2 - \sin^2 \varphi} + 1\right)}{4k_2^2 r^2} \right]_{\varphi_1}^{\varphi_2} \quad (99)$$

where

$$a = \frac{R_2}{r} = \sin \varphi_2 \quad (100)$$

After substituting the integration limits, we get a familiar relationship as follows:

$$f_{g2} = \pi \left[R_2^2 - R_1^2 - \frac{1}{2k_2^2} + \frac{\exp\left(-2k_2\sqrt{R_2^2 - R_1^2}\right) \left(2k_2\sqrt{R_2^2 - R_1^2} + 1\right)}{2k_2^2} \right] \frac{1}{r^2} \quad (101)$$

Part two then involves the following steps starting with the general PG Eq. 37, where we have for the inner sphere

$$a = \frac{R_1}{r} = \sin \varphi_1 \quad (102)$$

and need to replace the exponential having length ℓ in the exponent with three exponential factors corresponding to the three consecutive absorption layers (lengths) in EF, DE and CD:

$$f_{g1} = \int_0^{\varphi_0} 2\pi \sin \varphi \cos \varphi d\varphi \cdot [1 - \exp(-k_2 \cdot EF(\varphi)) \cdot \exp(-k_1 \cdot DE(\varphi)) \cdot \exp(-k_2 \cdot CD(\varphi))] \quad (103)$$

That is

$$f_{g1} = \int_0^{\varphi_0} 2\pi \sin \varphi \cos \varphi d\varphi \cdot [1 - \exp(-2k_2 \cdot EF(\varphi) - k_1 \cdot DE(\varphi))] \quad (104)$$

Because

$$2EF = CF - DE \quad (105)$$

and using Eq. 12 for each of the spheres, we can easily replace with:

$$f_{g1} = \int_0^{\varphi_0} 2\pi \sin \varphi \cos \varphi d\varphi \cdot \left[1 - \exp\left(-2k_2 r \sqrt{a_2^2 - \sin^2 \varphi} - 2(k_1 - k_2) r \sqrt{a_1^2 - \sin^2 \varphi}\right) \right] \quad (106)$$

for which unfortunately the anti-derivative could not be found analytically. The total acceleration is given by the usual factor as:

$$g = g_0(f_{g1} + f_{g2})/\pi \quad (107)$$

As usual, we equate $r = R_2$, when we need to find the acceleration g_R at the surface of a sphere.

We may appreciate the relative magnitudes involved, if we were to take, for example, Jupiter as consisting of two concentric spheres with the tentative (arbitrary) parameters provided in Table 4. Jupiter's core constitution is uncertain, so that the values are only indicative for the present purposes and chosen among various values in the literature (<https://sciencing.com/jupiters-core-vs-earths-core-21848.html>). The Jupiter mass is actually layered with variable densities, but the best we can demonstrate at this stage is to start with a uniform mass equal to the total one actually measured (M_e) from its corresponding acceleration $g_R = 25.92 \text{ m/s}^2$ (already used here). We then find the real mass M , as we did for various planets before, by first solving the equation of the parameter A_R for k with any given g_0 , from which we establish the real density ρ and density ratio ρ/ρ_e . Next, we redistribute this mass in the two spheres in the same proportion as initially provided in this table, namely 0.2259599008534 fraction of the total is compressed inside the inner sphere (core) and the remainder fraction is contained by the outer spherical layer. The real densities ρ_1 and ρ_2 in the two layers are readily found, from which the corresponding parameters k_1 and k_2 are calculated and used in Eq. 11. The results for the acceleration on the surface of the planet are given in numerical form in Table 4 again as a function in the typical range of g_0 .

In Newtonian mechanics, the redistribution would have no effect on the surface acceleration g_R , but in PG the surface acceleration g_{RPG} is very different, as we can see it is significant. The lower values obtained from PG indicate that the final actual densities should be increased in order to yield the real measured surface acceleration. In other words, there is a significant amount of hidden mass by the mere fact of having a dense core over and above (in addition to) the hidden mass also present in a uniform distribution. This is important, which means that any attempt to redistribute the mass of Jupiter along the radius should take into account the new physics revealed by PG. This also means that all previous calculations assuming an average constant density for the planets produces only approximate results. The difference becomes more important with the increase of the planet or star size. Noted also that the main (dominant) component

Jupiter	radius R	mass M_e	density ρ_e
whole planet	6.9911E7	1.8982E27	1326
core	1.6E7	4.289E26	25000
outer	6.9911E7	1.4693E27	1039
g_0	g_{RPG}	$g_R - g_{RPG}$	ρ/ρ_e
300	18.97555828	6.944841717	1.051873063
500	18.87716456	7.043235439	1.030304147
1000	18.80444874	7.115951257	1.014860051
2000	18.76839103	7.152008972	1.007359332
5000	18.74684295	7.17355705	1.002927051
10000	18.73967389	7.180726112	1.001460768
20000	18.73609184	7.184308161	1.000729697
30000	18.73489819	7.185501814	1.000486312
50000	18.73394339	7.186456606	1.000291714

Table 4: A two-layered sphere model of Jupiter with same real mass redistributed to the corresponding radii provided; Surface accelerations with PG and difference from Newton in a range of g_0 values.

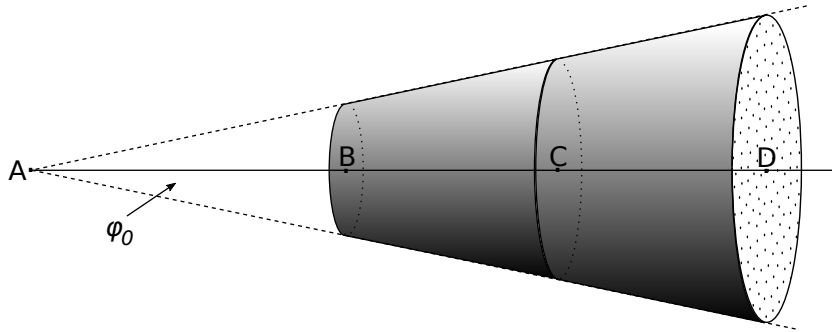


Figure 12: Coaxial truncated spherical cones (sections) with fixed and equal height.

of the PG acceleration comes from the diluted outer layer mass for the chosen mass redistribution - if the two components are considered separately. Hence in general, all prior attempts dealing with assumed mass and mass distributions should be re-appraised accordingly. In fact, artificial satellites orbiting Jupiter have reported anomalous orbits with a noticeable wobble, which may be attributed to Moons of Jupiter being shadowed by a different core density from the outer planet. We now have a new basis to re-evaluate and explain many phenomena already on record.

We may generalize and conclude that the radial distribution of density in a spherical body is critical in the generation of acceleration at the surface of the sphere and beyond according to PG, whereas this distribution makes no difference in the Newtonian acceleration lumping the mass at the center of gravity (i.e. center of the sphere). In an arbitrary shape with an arbitrary density distribution then, the only correct way is to derive the acceleration and force by integration of the graviton absorption around three coordinate axes yielding the three components of the vector of acceleration.

11 The superposition principle revisited and revised

The superposition principle, also known as superposition property, states that, for all linear systems, the net response caused by two or more stimuli is the sum of the responses that would have been caused by each stimulus individually. This applies to Newtonian gravity. However, this is not valid in general PG, unless the absorption coefficient k is relatively small.

Let us now consider Fig. 12, where we draw two co-axial truncated cones subtending the same solid angle

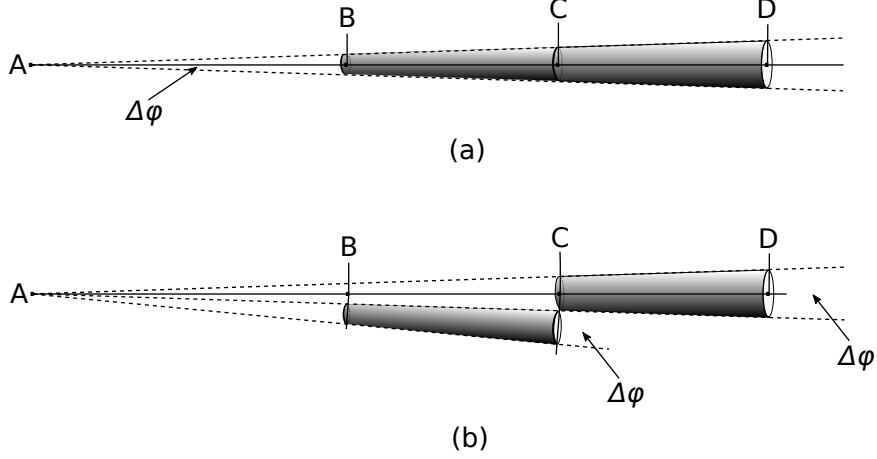


Figure 13: *Elementary truncated cones of equal height in series (a) and in parallel (b).*

at point A with semi-angle φ_0 and with equal height, namely, $BC = CD = \ell$. Each material cone creates the same amount of gravion shadowing, if considered separately, i.e. without the presence of the other. In other words, PG provides an insight first with an immediate result that all truncated cones of constant angle and equal height will produce the same acceleration of gravity regardless of their distance from a common convergence point; this result can be derived without any computation or integration of the elementary masses constituting these shapes.

However, when they act in series as depicted, the inner (nearest to A) cone is shadowed by the outer one and absorbs a lesser amount from the decreased output of gravion intensity by the outer cone. In the special case where the absorption is linear, which is the case when k is sufficiently small, then we can superpose their separate absorption like in Newtonian superposition of gravity.

Now, we consider the general case of PG again in Fig. 13(a), which is essentially the same as the previous figure but the truncated cones subtend a very small angle $\Delta\varphi$, which allows the shifting of the inner cone as in 13(b) by the same small angle without practically changing the direction of the vector of shadowing (acceleration), i.e. both are considered to retain the same direction at point A. By this, we get a simplified derivation in the case of exponential absorption of gravions (i.e. general PG) below.

Each truncated cone constitutes a material layer with thickness ℓ and absorption coefficient k , so that the transmitted intensity is given by Eq. 6. When the layers are in series as shown in (a), the total absorption through the double thickness is

$$\Delta J_{series} = \Delta J_0 (1 - \exp(-k2\ell)) \quad (108)$$

However, if the inner cone is shifted as in (b) with the vectors of acceleration practically lined up, we can add them numerically for the total absorption according to Eq. 6 as

$$\Delta J_{parallel} = \Delta J_0 2 (1 - \exp(-k\ell)) \quad (109)$$

The difference between these cases then becomes

$$\Delta J_{parallel} - \Delta J_{series} = \Delta J_0 (1 + \exp(-k2\ell) - 2\exp(-k\ell)) \quad (110)$$

which is a positive number and indicates that the total shadowing (acceleration) by the two layers is stronger when they are in parallel than when in series by one shielding the other.

The same can be expressed also in terms of absorption fractions:

$$f_{parallel} - f_{series} = 1 + \exp(-k2\ell) - 2\exp(-k\ell) \quad (111)$$

and in terms of acceleration:

$$\Delta g = g_{parallel} - g_{series} = g_0 (1 + \exp(-k2\ell) - 2\exp(-k\ell)) \quad (112)$$

12 On direct measurement of PG

12.1 Sphere

We can inquire about the difference of acceleration derived by Newton and PG on the surface of a sphere of known density to determine if it is practically possible to detect and measure the new PG parameters directly. If the Newton acceleration on the surface is g_{RN} and the PG acceleration g_R , their difference is given by

$$\Delta g = g_{RN} - g_R = \frac{4}{3}\pi G\rho R - g_0 A_R \quad (113)$$

for which we need k in A_R given from Eq. 60 as

$$k = \frac{\pi G\rho}{g_0} \quad (114)$$

from assumed values of g_0 and the real density of the sphere. We can plot the difference like we plotted the ratio of accelerations in Fig. 5, but we prefer to see directly some numerical outputs in Table 5 by choosing, say steel with $\rho = 7500 \text{ kg/m}^3$.

We may also further work on the equation above to produce:

$$\Delta g = g_0 \left(\frac{4}{3}kR - A_R \right) \quad (115)$$

which is a function of the product kR .

For very high kR , the difference is very high, but for very small kR the difference is very small but finite. By expanding the exponential to a Taylor series $e^x = 1 + x + \frac{x^2}{2!} + \frac{x^3}{3!} + \frac{x^4}{4!}$ and taking the limit for small kR , we obtain for the difference of accelerations

$$A_{R_{kR \rightarrow 0}} = \frac{1}{6}kR(8 - 6kR + 4k^2R^2) \quad (116)$$

$$\Delta g_{kR \rightarrow 0} = \frac{1}{3}g_0k^2R^2(3 - 2kR)_{kR \rightarrow 0} = g_0k^2R^2 \quad (117)$$

For the numerical example of the table, we see that we could have used Eq. 117 for small kR , which provides that the difference is proportional to g_0 and to the square of the radius of the sphere. The practical outcome is that, for the smallest sphere, we would need an extremely sensitive gravimeter with an accuracy up to 10 orders of magnitude smaller than the expected Newtonian value. The situation improves fast as we increase the sphere diameter, except that such spheres are out of any practical use. The situation improves with decrease of g_0 .

12.2 Cone

We have further investigated whether the same reference spherical masses used above, if reshaped properly, they could yield any improved (i.e. greater) difference between Newton and PG for a possible measurement from a known density mass. This has been investigated for truncated and spherical cones with negative results (i.e. no improvement). However, interestingly enough it was found that there is an optimum cone angle yielding maximum acceleration difference at their apex, but still very close to, (but less than) the spherical shape. There is no need to present these results at present in order to give priority to more mundane issues below.

12.3 Cube

Perhaps, a large steel (or other heavy material) cube shape might be more feasible to construct by bricks, which would reduce cost by later disassembling and re-use of the steel material. The Newtonian gravitational fields has already been provided analytically by Chappel *et al.* (2012). Measurements of some gravity contour (or point) around the cube may be done with the most sensitive gravimeter to investigate possible "anomaly". With a positive outcome, we can then calculate the corresponding PG gravity contour (or point) by integrating the shading of gravions per established theory. From the known density, we will then be able to directly derive all other PG parameters.

$R=$	10	100	1000	10000	100000
$g_N=$	2.097E-05	2.097E-04	2.097E-03	2.097E-02	2.097E-01
g_0	Δg	Δg	Δg	Δg	Δg
300	8.243E-13	8.243E-11	8.243E-09	8.243E-07	8.243E-05
500	4.946E-13	4.946E-11	4.946E-09	4.946E-07	4.946E-05
1000	2.473E-13	2.473E-11	2.473E-09	2.473E-07	2.473E-05
2000	1.236E-13	1.236E-11	1.236E-09	1.236E-07	1.236E-05
5000	4.946E-14	4.946E-12	4.946E-10	4.946E-08	4.946E-06
10000	2.473E-14	2.473E-12	2.473E-10	2.473E-08	2.473E-06
20000	1.236E-14	1.236E-12	1.236E-10	1.236E-08	1.236E-06
30000	8.243E-15	8.243E-13	8.243E-11	8.243E-09	8.243E-07
50000	4.946E-15	4.946E-13	4.946E-11	4.946E-09	4.946E-07

Table 5: *Difference of acceleration between Newton and PG on the surface of an iron sphere with density 7500 kg/m³.*

12.4 The Allais effect

The previous finding on gravity superposition in PG can be used for explaining the known ‘‘Allais effect’’ recorded during total eclipses of the Sun. According to this, the gravity on Earth is increased during the eclipse, namely, the Moon+Sun have less attraction on Earth during an eclipse than just before or after the eclipse.

Qualitatively, we can say that when the Moon stands between the Sun and the Earth, it shields the shadowing of the Sun reducing the sum total of the shadows of the Moon and Sun separately prior to them being aligned. The principle of this effect, now for spherical bodies, is derived quantitatively below by PG theory.

The derivation is facilitated, since by coincidence the Sun and the Moon subtend practically about the same average solid angle of 0.53 and 0.52 degrees, respectively. Based on Fig. 14, we use R_s for the Sun radius and R_m for the Moon radius, located at distances $PQ = r_s$ and $PQ' = r_m$ from point Q.

When the two spheres are lined up, then the integral of their PG gravity acceleration is given by

$$f_g = \int_0^{\varphi_0} 2\pi \sin \varphi \cos \varphi d\varphi \cdot [1 - \exp(-k_s \ell_s(\varphi) - k_m \ell_m(\varphi))] \quad (118)$$

where we have simply added the lined-up chord lengths $AB = \ell_s$ and $A'B' = \ell_m$ of the Sun and the Moon. Using the established lengths for these chords, we substitute as follows:

$$f_g = \int_0^{\varphi_0} 2\pi \sin \varphi \cos \varphi d\varphi \cdot \left[1 - \exp\left(-2k_s r_s \sqrt{a_s^2 - \sin^2 \varphi} - 2k_m r_m \sqrt{a_m^2 - \sin^2 \varphi}\right) \right] \quad (119)$$

However, because both spheres are taken to subtend equal angles, i.e. φ_0 , we have

$$a_m = \frac{R_m}{r_m} = \frac{R_s}{r_s} = a_m = \sin \varphi_0 = a \quad (120)$$

and the integrand is simplified below:

$$f_g = 2\pi \int_0^{\varphi_0} \sin \varphi \cos \varphi d\varphi \cdot \left[1 - \exp\left(-2(k_s r_s + k_m r_m) \sqrt{a^2 - \sin^2 \varphi}\right) \right] \quad (121)$$

which is of the same form as Eq. 36 by setting $kr = k_s r_s + k_m r_m$. Thus, we obtain from

$$f_g = 2\pi \left[\frac{\sin^2 \varphi}{2} - \frac{\exp\left(-2kr \sqrt{a^2 - \sin^2 \varphi}\right) \left(2kr \sqrt{a^2 - \sin^2 \varphi} + 1\right)}{4k^2 r^2} \right]_0^{\varphi_0} \quad (122)$$

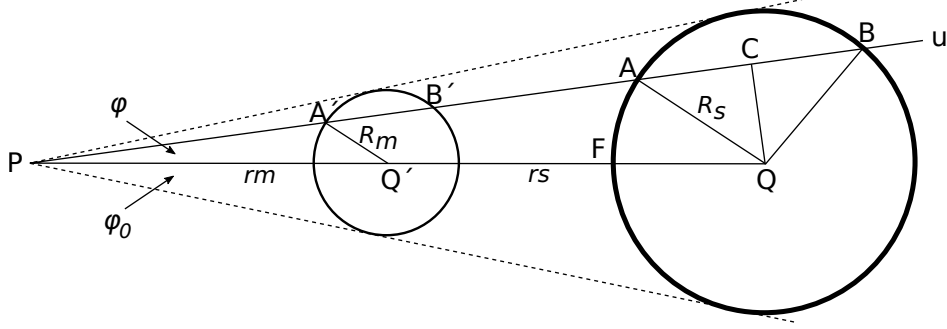


Figure 14: *PG diagram during Sun-Moon eclipse.*

g_0 , m/s ²	k , 1/m, Sun	ρ , kg/m ³	ρ/ρ_e
300	5.865327998802280E-09	8392.131445	5.459718
500	1.027835151863200E-09	2451.050109	1.594594
1000	3.894839466528660E-10	1857.583228	1.208499
2000	1.758800091947190E-10	1677.664808	1.091448
5000	6.665703761053060E-11	1589.551972	1.034124
10000	3.276671652759630E-11	1562.757685	1.016692
20000	1.624742838322570E-11	1549.791755	1.008257
30000	1.080184118890250E-11	1545.531147	1.005485
50000	6.466902304965150E-12	1542.144338	1.003282

Table 6: *Variation of Sun parameters against increasing values of g_0 with adjusted radius $R = 6.76002E08$ m corresponding to effective density $\rho_e = 1537.0998312$ kg/m³ and $g_R = 290.489290112956$, but the same mass $M_e = 1.989E30$*

the accelerating absorption fraction

$$f_g = 2\pi \left[\frac{\sin^2 \varphi}{2} - \frac{\exp\left(-2(k_s r_s + k_m r_m) \sqrt{a^2 - \sin^2 \varphi}\right) \left(2(k_s r_s + k_m r_m) \sqrt{a^2 - \sin^2 \varphi} + 1\right)}{4(k_s r_s + k_m r_m)^2} \right]_0^{\varphi_0} \quad (123)$$

By substituting the limits of integration and in view of Eq. 120, we get

$$f_g = \pi \left[\frac{R_s^2}{r_s^2} - \frac{1}{2(k_s r_s + k_m r_m)^2} + \frac{\exp(-2(k_s R_s + k_m R_m)) \cdot (2(k_s R_s + k_m R_m) + 1)}{2(k_s r_s + k_m r_m)^2} \right] \quad (124)$$

The above result applies during the eclipse, i.e. when the spheres are in “series”.

When the spheres are in “parallel” to each other, i.e. just before or just after the eclipse, we use the form of Eq. 38 to sum the separate contributions of each as

$$f_g = \pi \left[R_s^2 - \frac{1}{2k_s^2} + \frac{\exp(-2k_s R_s) \cdot (2k_s R_s + 1)}{2k_s^2} \right] \frac{1}{r_s^2} + \pi \left[R_m^2 - \frac{1}{2k_m^2} + \frac{\exp(-2k_m R_m) \cdot (2k_m R_m + 1)}{2k_m^2} \right] \frac{1}{r_m^2} \quad (125)$$

The Allais effect then should appear as the difference of acceleration in the above positions (equations)

$$g_{Allais} = g_{parallel} - g_{series} \quad (126)$$

where we have multiplied Eqs. 124 and 125 by G/Λ to obtain the factor g_0 and hence the corresponding accelerations.

We can plot calculated values of g_{Allais} against g_0 to establish for which values of g_0 we find the measured g_{Allais} . However, because we are dealing with very small numbers in these calculations, it is necessary not

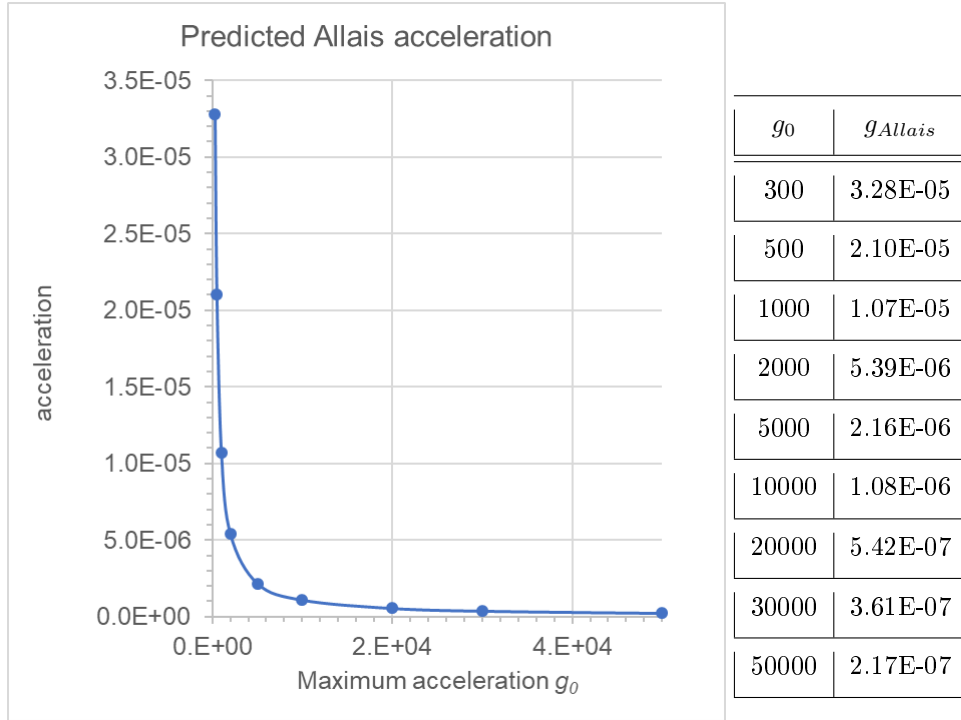


Figure 15: Predicted variation of the Allais effect acceleration vs. assumed values of g_0 .

only to use increased accuracy in the mathematical tools employed and also to eliminate the small but significant difference arising from the fact that the Moon and Sun do not subtend exactly equal angles. In other words, it was found that the small difference of the actual subtended angles overwhelms the Allais effect altogether by resulting in significant inconsistencies in the calculations. In order to test the validity of the principle, at least, we need to take the real values for one sphere and project (adjust) slightly the other so as to satisfy the condition of Eqs. 120. This is done only to be able to use the derived Allais equations above, in order to demonstrate the effect; otherwise we would be faced with considerable complexity to use PG with the actual angles, which is not needed for the present purposes. A high accuracy theoretical derivation would also require the availability of experimental measurement of the Allais effect with commensurate accuracy. Unfortunately, such measurements do not exist, because the Allais effect has been reported with significant inconsistencies. We believe that these inconsistencies are caused by the interference of various other effects on Earth, such as tidal effects and others (may be atmospheric, etc.) as well as variability of the time and position during this event. In view of these practical difficulties, it would be in vain to apply derived formulas for a direct practical outcome, except that we can use them to establish the principle and an order of magnitude. Refinement of the theory and practice of the Allais phenomenon is left for future work. Therefore, we opted to adjust the radius of the Sun to match the subtended angle of the Moon, while keeping its mass constant. We have done this and present the numerical values in Table 6, as opposed to the values presented in Table 2. We can then use these values of k for the Sun and the corresponding values from Table 3 for the Moon in Eq. 126, which we plot in Fig. 15 with tabulated numerical values of the same graph in the inserted table.

From a paper by Lorenzen (2017), we obtain an average value $g_{Allais} = 3.5E-7 \text{ m/s}^2$, which corresponds to $g_0 = 30800 \text{ m/s}$. If that were to be correct, then we would have derived the fundamental constant g_0 for our neighborhood universe. However, this is only a tentative value, most likely to be revised later. It may be that similar measurements taken from the Moon during a solar eclipse by the Earth could provide more reliable values; clearly, in that case, we should derive another equation taking into account the actual solid angles subtended by Earth and the Sun at the Moon.

With the proposed tests, PG could be verified but not disproved in the event of a very high level of g_0 reducing the effect beyond the measuring ability of our instruments at present. It is hoped that "anomalies" of Newtonian mechanics will be firmly measured and established to provide an affirmation of PG once and for all in the near future.

12.5 Other verification means for PG

We have already proposed measurements of the internal field of Earth's crust, variation of gravity in the heliosphere and other methods above. Another test may be by using very sensitive gravimeters to measure the variation of gravity on Earth during a 24 hour rotation preferably during a new Moon (or better before, during and after a solar (better total) eclipse), whereby the Earth is shadowing the Sun+Moon system overnight. The deviation from predicted values using Newtonian mechanics should provide an indication and perhaps an evaluation of the PG parameters.

Alternatively, a similar to the previous observation could be made by the variation of the orbit of an Earth satellite during a new Moon (or better before, during and after a solar (better total) eclipse, whereby the Earth is shadowing the Sun and Moon systems during the night passage of the satellite, presuming that the effect on the orbit could be measurable. Could then such a variation explain the variations (wobble) observed by Juno during orbiting Jupiter?

12.5.1 Terrestrial measurements

Perhaps, minimal experimental and logistical requirements are involved if well planned experiments are conducted on Earth. The simplest of them might be to select an appropriate location on the equator and measure the variation of gravity over a 24-hour period with the most sensitive gravimeter available. Actually, this would require minimal field work preceded by a significant amount of office work for a thorough theoretical preparation. The latter would involve the calculation of all possible effects that can be had like on a straightforward calculation of Newtonian acceleration, tidal and local density variation. Actually, theoretical work for a similar purpose has been presented in order to measure the screen effect of the Earth in the electro-thermo-dynamical theory of gravitation by Adâmuți (1982). If a difference can be established between the expected acceleration by all known factors and the measured one, then we can attribute it to an external source of radiation, such as we propose for gravions. For that purpose, we should couple corresponding computations with an expected PG value taking into account all known factors again (like eccentricity, etc.). The big unknown would be the radial density distribution of Earth, which does not enter (not needed) in the Newtonian calculation. This is a critical difference between the two derivations. Recent studies have revealed a much denser core, which could have an even greater effect on PG calculations. It might indicate the presence of PG effects even in a more pronounced manner, if we record the variation of acceleration in the entire 24-hour rotation period. The latter might reveal an anomalous variation around the midnight hour if the core presents a pronounced density difference from the mantle.

An alternative experiment would be to conduct the measurements at the poles of the Earth for a period of six months, which presumably averages out several anomalies (effects). The accuracy and precision would be increased if the measurements could be conducted concurrently at both poles over an entire year, presumably to even out most (if not all) extraneous effects.

Overall, such tests should amount for a relatively minuscule budget and effort in comparison to other ongoing experiments on deciphering gravity.

13 Discussion on gravitational law

The finding that the gravitational force is inversely proportional to distance constitutes a universal relationship now derived from the principles of static PG theory. It is unlikely that this is a fortuitous derivation, although we must wait to find the same consistency with dynamic PG. It is likely that PG can provide a genuine platform to re-work many other relationships with new physics.

We have derived some fundamental but novel relationships yielding the classical acceleration and force but revealing a different relationship with the actual of mass. The classical (Newtonian) mass is now understood to be only an apparent or effective manifestation of the real mass. The inverse square of distance law is preserved, whilst the classical gravitational constant G is itself a function of another constant like A , J_0 or g_0 , all of which are characteristic of any given region of space. It is important that these relationships are not merely empirical, but are based on a simple principle or premise of particles uniformly traveling in all directions, while they are absorbed by matter at a rate in proportion to the density of the matter. This provides a more "tangible" explanation of gravity, which, however, shifts the problem to the understanding of the nature of these particles, not less mysterious than the elusive gravity to date. Nevertheless, it looks like we can narrow down the fundamental problem of gravity to a "lesser" entity bringing us closer to the goal of a unification theory. After all, forces are already attributed to the exchange of different kind of particles: Gluons for the strong nuclear force, photons for the electromagnetic force, the bosons for the weak nuclear force and speculated gravitons for gravity. Quantum chromodynamics aims to find the smallest building block of nature and the forces that hold them together. PG may not be seen in conflict but rather it may offer a

general platform to remold and hopefully unify current quantum gravity and graviton, superstring theory, loop quantum gravity and blending quantum gravity with quantum mechanics for a theory of everything.

The validity of the gravitational law derived is further subject to ensuring that the involved gravitating bodies exist in “free space”, otherwise the space itself is filled with matter albeit of extremely low density. For in the latter case, we deal effectively with an internal field as found in Section 8 and further elaborated later in Section 24.1. Then, g_0 is *internally* variable and a function of distance r from some center of mass, while the overall gravitational law ~~ceases to be strictly~~ is inversely proportional to the square of distance. Later work has found that internal $G(r)$ is invariable and equal to the external big G . That means that the gravitational constant $G(r)$ can be a weak function of distance from the said center of mass. In the latter case, the force will be slightly weaker than Newton’s law resulting in precession for an orbiting planet. No attempt is made here to evaluate the magnitude (significant or negligible for an elliptical orbit) of possible variation of $G(r)$, before we can establish the theory PG itself. Eventually, relativistic effects may also have to be included in addition to the classical derivation of precession under PG, but this is subject to further PG analysis and development.

In one aspect, the form of Newton’s gravitational law could be considered correct with regard to $1/r^2$ (being universal), but if the mass becomes effective mass as revealed by PG, then such a law is incorrect. This is further analyzed under Section 16 establishing the variation of effective mass m_{er} with distance (in vacuum). Over and above this variation, there is also another variation due to internal effects as revealed in Section 24.1. Hence, it is this extra mass variation (not $G(r)$ variation) that may provide an alternative explanation for the missing planet "Vulcan" hypothesized in 19th century in order to account for the peculiarities in Mercury’s orbit. It remains to derive its precession based on PG theory and see if a satisfactory explanation can be found. In fact, we may not need to travel very far to realize that its value varies significantly within the heliosphere and more so as we approach the neighborhood of the Sun. Close enough to the Sun, there may be a lot of mass emitted to a significant level, which makes the closest planets effectively experiencing an “internal” gravitational field per Section 8. Mercury may be significantly affected by the variation of $G(r)$ during its orbit. Conversely, we could introduce a “fudge” factor for the variation of $g_0(r)$ or $G(r)$ to match Mercury’s precession and thus indirectly work out the unknown g_0 , but such an approach would be counter-productive for the acceptance of PG theory.

This discussion applies to gravity around stars and planets, but can we still call *gravity* the field around dwarfs, neutron stars and black holes, if it is caused by the different proposed types of push particles, according to a subsequent proposal? Each of these fields would have its own mass attenuation coefficient Λ with a different value from that corresponding to gravions. Beyond white dwarfs, a neutron star would have a variable Λ by superposition of two types of push particles, whilst black holes by superposition of more types of push particles. We may then have to introduce other terms (semantics) to differentiate the fields around these massive bodies from our familiar gravity field. In fact, we should expect to have a mixed or variable effective Λ parameter, which we might wish to denote or index with a different subscript. In those fields then the inverse square of distance law may break down again, but the math remains to be worked out. Correct terminology is important, because, when we say that the gravitational law is preserved in the cosmos, we mean that it applies to gravity due to gravions under the postulates at the outset, which is correct only regionally in the cosmos.

Last but not least is to discuss the mean free path (m.f.p.) of gravions postulated at the outset of PG. Whereas the m.f.p. is assumed to be much greater than the size of the gravitating bodies, no further qualifications were made. How much greater is it in reality? We have no knowledge of this yet, so we can only discuss the various main possibilities: (a) the m.f.p. is infinite, i.e. gravions never interact between themselves, (b) the m.f.p. is of intergalactic order and (c) the m.f.p. is of intra-galactic order. These orders of magnitude are not the only possibilities, but are sufficient for a general discussion in Part 2 of this report. These ranges of m.f.p. define corresponding regions of space, where the gravitational law varies. As soon as the postulated m.f.p. ceases to apply, push gravity behaves differently and is governed by different relationships and laws. It is of great importance to know also the forces (fields) at the transition from one region to the next and beyond. Part 1 has not dealt with such regions yet. Pending such work, we can only speculate at this stage what happens. The inadequacy of PG theory of Part 1 for those regions may correspond to the inadequacy of GR (general relativity) also at long distances, except that PG can be readily expanded and advanced in ways discussed further in the next part of this report.

Part Two (2)

The following presentation is an integral part of the whole report, but it is separated out because it contains a significant amount of speculative theory, which may have to be revised or rejected without affecting the preceding Part One (1). Part 1 should remain valid at least as a mathematical development of PG based on a set of postulates, barring inadvertent but rectifiable errors. In Part Two (2) specifically, it is proposed that the theory can be extended to a general push gravity (GPG) by borrowing some mathematical tools of general relativity (if and to the extent needed), astrophysics and other cosmological theories, or that all theories may complement one another. However, no analytical steps have been undertaken in all cases presented yet, whilst it is hoped that this would be achieved better by experts in the corresponding science fields. It is only initially attempted to introduce PG in astrophysics in the case of white dwarfs, neutron stars and black holes, but again it is hoped that this task would be best undertaken by others. The application of PG in particle physics and cosmology is barely but humbly mentioned, or discussed, in the hope that it might also spark further discussion and research for a unified field theory and a theory of everything: It makes sense to assume that all fields are created by particles, now by push particles, i.e. all with a common denominator as the only way to achieve unity.

As more material is added, re-organization of this report and its parts may become due. As a consequence, there may be some conflicting statements left unchanged, that can be better understood via a historical reading of ascending versions. It seems that some of the material of the second part can be safely included in the first part. Until this is done, it is hoped that no misunderstanding arises from the way it is currently presented. In any case, the overall spirit of the entire report remains a “what if” approach. What if the push principles do create gravity? The conventional approach has been not to proceed in considering PG, because e.g. of an alleged violation of the second law of thermodynamics. As a result, the exploration and development of PG presented in this report has been previously unknown, which has prevented science to consider new possibilities. The latter only now lay bare to see and think if they can help physics to cross through existing barriers. The only prerequisite for this to happen is to be free of preconceptions about sacred notions, like “inertia”, “mass”, “force”, “energy” and “equivalence principle”.

14 Towards a dynamic push gravity

The introduction of time in PG for moving bodies should constitute another chapter of PG dynamics still to be developed. However, an attempt to introduce some elements and ideas of it here is thought to help prepare towards a proper dynamics theory, but also address possible questions arising from the static PG of Part 1.

Since we already established that Newton’s gravitational law can actually be derived from first principles of PG, we may wonder, if we should accept the other laws of Newton by way of principle (granted), or they may also be derived wholly or in part. For clarity, we understand that Newton’s first law states that “*an object either remains at rest or continues to move at a constant velocity, unless acted upon by a force*”, in other words, material bodies have “*inertia*”. The second law states that “*the force F on an object is equal to the mass ‘ m ’ of that object multiplied by the acceleration ‘ a ’ of the object, i.e. $F=ma$* ”. The third law states that “*action = reaction, i.e. when a body exerts a force on a second body, the second body simultaneously exerts a force equal and opposite in direction on the first body*”.

Regarding a fourth law stating that “*forces exerted by different bodies add up (superimpose) like vectors, i.e. the forces obey the principle of superposition.*”, we already found that it does not apply in PG per Section 11.

Now, it is not clear, if we can mix and match the above first three laws with PG, or we should strive to derive them also from the first principles already adopted at the outset in Part 1. For example, is it legitimate to inquire as to the intrinsic meaning of inertia? Is it an a priori physical attribute for all material bodies or just a convenient empirical entity to express an experience mathematically per second law of gravity? Connected to this question is also, why “action-reaction” takes place.

Furthermore, it would be unwise to rely entirely on Newton’s laws alone without regard to subsequent revolutionary developments in many fields of physics, and in particular relativity. We already assume, at least provisionally, the existence of moving particles, the gravions, at the speed of light as an added principle of PG, hence we have to take into account at least the special theory of relativity (SR). By no means do we imply exclusion of the general theory of relativity (GR), but we can try to determine how far we can reach initially without it. We may also mix and match various attempts with all theories of gravity, by trial and error, iteratively, in order to arrive at some understanding as to how things pan out under the framework of PG. In this course, we may need to use much of the existing tools (math) and insights of other theories

without prejudice or fear. The subsequent part of this section serves only as a beginning along these lines.

14.1 Relative and absolute reference frames

Throughout Part 1, we considered only stationary material bodies relative to each other but implicitly also relative to the gravions as a whole. We already discussed the possibility of gravions with different mean free paths defining different regions of the universe. Gravions then may be treated like a gas or an aether. Such an aether, though, is not a passive medium for the propagation of light like the classical (conventional) aether in prior physics. It is an absolutely energetic medium interacting with material bodies. This medium “fills”, or better forms the space, which acts on material bodies, while at the same time this space is acted upon by the material bodies. Based on this primary interaction between space and matter, in turn, there arises interaction between matter and matter giving rise to displacement of matter (bodies) relative to it (i.e. relative to each other body) and relative to space (aether). In this way, the gravions, or space (aether) is now endowed with a privileged rest frame of reference, against which all other movements can be measured. While each body is stationary in its own reference frame and moves relative to the reference frame of other moving bodies, they all interconnect via the primary or privileged reference frame of the aether. Distance and time are now interconnected via the reference frame of the aether. If aether inflates or streams in the universe, so is its frame of reference. The analogy is the same as with the motion of an expanding (better, inflating) universe carrying with it its clocks and length-measuring-sticks, and operating under the presumably tested laws of relativity. If we can continue using some tools and concepts of relativity, we can now also flesh it out with a material (energy) content, namely, that of the gravions incessantly moving in all directions while defining an absolute frame of reference for time and distance. The aether of gravions is a source of energy, from which all other forms of energy emanate and to which they return in a perpetual cycle of cosmos.

In such an absolute reference system of a cosmic aether, we may have a better understanding of the effects on a rotating material body. PG provides an opportunity to have a fresh examination and re-think about the “Mach’s principle”.

It is important to note that the “aether of gravions” can co-exist with a host of other types of particles as proposed in Section 18.

“Statics” in physics is the branch of mechanics concerned with bodies at rest and forces in equilibrium. We may provisionally use this term in PG too, but with the qualification that there is continuous action by the relativistic moving gravions underlying the emerging forces. Until we may coin another term (if needed), we use “static PG” to describe the theory as in Part 1. Furthermore, to avoid possible confusion between the terms of “kinematics” and “kinetics”, let’s use the existing term of “dynamics” to describe the motion of bodies including its causes or not. So “dynamic PG” refers to the theory including both kinetics and kinematics. If there are disagreements with such a terminology, we may defer a possible resolution for later. After all, there may not be any need to distinguish “statics” from “dynamics” in PG.

14.2 The Equivalence Principle

We can easily reproduce Newton’s attraction force by push gravity and hopefully all other observed relationships (a task by later work). Furthermore, under the understanding of PG, we can now say that the well known equivalence principle (EP) is not violated. In fact, it is better explained as an identical process in the two systems being referred to, namely, one in a gravitational field and another accelerated by an equal force in space outside the gravitational field. That is, whether a mass is pushed “by hand” (or pulled via a rope in an elevator in free space), or the same mass is pushed by gravions by an equal force, then the outcome should be the same, namely, the mass will travel distances proportional to the square of time (t^2). Push gravity creates a force by streaming gravions through the entire mass dragging every mass element concurrently, the sum total being a force no different from a push (pull) force acting by a spring with measurable deformation on a solid mass (or an imaginary accelerating force experienced inside an elevator in space). The gravitational push force is distributed throughout the mass, whilst the spring force acts on the external surface of a **rigid** (for argument’s sake) mass and indirectly transmitted and distributed to all body elements producing an identical outcome. Then the same mass being acted by an equal force would accelerate by the same amount, i.e. we would measure distances proportional to the square of time, from the moment the mass is set free to travel (in free space or in the neighborhood of the gravitating body). If the mass is held stationary by some stationary “wall”, then the mass experiences the force (by the gravions or the spring) without moving (like pushing on or pushed by a stationary wall). The gravion force appears as a mysterious attraction force by Newton, which necessitated the adoption an “equivalence principle” to explain the observable equal outcomes by the same mass acted upon by the Earth’s gravity, or by “the rope on an enclosed elevator encompassing the same total mass”. With the insight readily provided by PG (streaming

gravions), the "equivalence principle" need not be a "principle" at all any more; it is just an identity as seen by PG, **it is** the same thing.

The Equivalence Principle (EP) is a mere and easily understood consequence of the hidden reality of the PG gravity principle, hence there is no need to postulate the EP any longer. The self-shadowing (shielding) causing an underestimation of the real mass does not refute the above understanding: To the extent that part of the mass is shielded from the action of gravions, if we push it "by hand" by the same force, as Newton would have us to use, then we would correspondingly measure the same distances. The actual mass (bigger than the apparent one) would be acted upon with an equal force, in both cases, of a falling body due to gravity or moving in space outside gravity. In both systems (cases) the same force acts on the same mass being real or effective, producing the same outcome.

Summary: PG does not require an equivalence principle, since everything exists in a real "elevator" being pushed by streaming gravions, not requiring a fictitious (gedanken) second elevator as theorized to date.

The above arguments are upgraded with an updated Section 16.

14.3 Falling bodies and Flyby anomaly

From the above description and understanding of the EP and if there is no distinction between effective and real mass (as per PG), then it follows that the gravitational and inertial mass are equivalent, actually equal. The latter equality then forms an alternative form of the Principle. In other words, the ratio of gravitational to inertial mass of any object is equal to some constant C, if and only if all objects fall at the same rate in a given gravitational field, so that C=1. The latter form of the Principle must be distinguished from its original "gedanken" description stating that "*the gravitational force we experience on Earth is identical to the force we would experience were we sitting in a spaceship accelerating at 1g*".

However such an equality of masses is clearly at variance with PG: As understood and described above, the effective mass corresponds to the gravitational mass, the force from which is transmitted to the real (entire) mass of the body, i.e. to the inertial mass of the body.

Thus, applying the PG parameters as developed so far, let us designate by M_e the mass of a large gravitating body (sphere), so that it is considered stationary, when other much smaller bodies with effective mass m_e fall to it. We consider only the case, where the falling trajectory is radial, so that the assumed steady state of PG is thought to be practically retained. A uniform (parallel) gravitational field allows the use of the static force during fall without time effects. We can use the effective mass as in Newtonian mechanics for the potential energy $GM_e m_e / r$ of the system of both masses each with an equal share of energy. We obtain the potential energy by integrating the corresponding acting force times the elementary path lengths of the falling body. Likewise, we integrate for the work done by the **same** force on the total (real/inertial) mass m to obtain the additional kinetic energy as the body falls from point (radius) r_1 to r_2 and apply the conservation of energy equation:

$$\frac{1}{2} m u_{PG}^2 = \frac{1}{2} \frac{GM_e}{r_1} m_e - \frac{1}{2} \frac{GM_e}{r_2} m_e \quad (127)$$

from which the final velocity u_{PG} is given by

$$u_{PG} = \sqrt{GM_e \left(\frac{1}{r_1} - \frac{1}{r_2} \right) \frac{m_e}{m}} \quad (128)$$

It there is no distinction between the two masses above, then, by Newtonian mechanics, the corresponding final velocity u_N would be

$$u_N = \sqrt{GM_e \left(\frac{1}{r_1} - \frac{1}{r_2} \right)} \quad (129)$$

The ratio between the above two velocities is then immediately obtained as

$$\frac{u_{PG}}{u_N} = \sqrt{\frac{m_e}{m}} \quad (130)$$

From Section 6.5, we substitute the ratio of masses to obtain:

g_0	PG over Newton velocity ratios
300	0.999999980343
500	0.999999988206
1000	0.999999994103
2000	0.999999997051
5000	0.999999998821
10000	0.999999999410
20000	0.999999999705
30000	0.999999999803
50000	0.999999999882

Table 7: *Ratio of falling velocities by PG over Newton.*

$$\frac{u_{PG}}{u_N} = \sqrt{\frac{3A_R g_0}{4\pi G \rho R}} = \sqrt{q} \quad (131)$$

as a function of the unknown parameter g_0 . The ratio of masses in Eq. 130 is independent of the gravitating center (body) and it is equal to the accelerations ratio given by Eq. 83 on the moving (gravitated) sphere (the contraction factor q). We already listed the difference of the two velocities in Table 5 for steel spheres. We repeat the same, but for the above ratios of a steel sphere with radius $R = 10$ m and density $\rho = 7500$ kg/m³ in the typical range of g_0 in Table 7.

We can apply the above figures for reported flyby velocities (at perigee) and find that the difference between velocities is of the order of mm/s. This is consistent with observed flyby anomalies and it might help further explain them, i.e. in addition to or in lieu of various other proposed explanations. The Oumuamua anomaly (Bialy & Loeb, 2018) might be another candidate to re-examine as a flyby effect.

Theoretically, a spacecraft on an elliptical orbit could experience a greater force on its inbound direction than on its outbound one by changing direction of its disk-like (for example) shape thus exhibiting a greater effective mass in one part of the orbit than in the other. This would result in incremental accretion of energy until it can reach escape velocity and then repeat the same process around a bigger planet (e.g. Jupiter), or the Sun. This explained in more detail in a later Section 23.2.4. Similarly, mass distribution in a fan-like configuration might optimize the flyby effect by opening and closing the fan accordingly. In Section 12.2, we report that there is an optimum angle for spherical and truncated cone shape, whilst other shapes may be further investigated later. This might have little practical application, but it remains to be seen, if there is some benefit in furthering such an investigation. For an elliptical orbit, time effects on the shadow (push force) of relativistic gravions become important in PG, a problem not yet formulated.

In general, this effect says that a steel ball and a feather do not fall at the same speed inside a vacuum chamber: Let us consider a flat feather falling with its plane parallel or vertical to the direction of the gravitational field. In both cases it has the same real mass but different effective mass. When it falls with its plane vector parallel to the field, the effective mass is greater than when it falls with its plane vector normal to the field. In both cases, we have the same object (mass) and the same inertial mass. However, it will fall faster in the first case than in the second. The maximum speed (and acceleration) will be when the effective mass is practically equal to the real mass, i.e. when the feather can be spread out as much as possible (e.g. by further thinning it down). Let us then consider a steel sphere and a very thin steel disk of the same mass; we can achieve this by first using the sphere and then the same object is flattened out to a very thin disk. Like with the feather, the steel sphere will achieve a slower final velocity than the same mass in the shape of disk. Now, the fine steel disk and the fine feather will fall at the same speed if they are both thin enough to expose their real mass to the field, and will fall in accordance with Newtonian mechanics, because they both use the real (total) mass. However, the steel sphere will be slower than the feather, because the sphere displays an effective mass further away from its real mass than the feather does. The effect of orientation of a falling body is thus a new finding by PG, an extremely small effect to measure in the laboratory, but it may become cumulative and observable during a fall towards a planet or star from a significant distance.

Corollary: All bodies fall at equal rates inside a uniform gravitational field, if and only if they all expose their real mass to gravions, or if they expose the same ratio of effective-to-real-mass, i.e. if and only if they have the same contraction factor q . (This is further confirmed in a later Section 23.2.4).

The flyby difference (referred to as an anomaly to date) might be used purposefully for the measurement of the unknown value g_0 in our solar system. Furthermore, the presented perceptions on EP itself from the perspective of PG theory might help us better understand the Principle itself and its implications in past and future physics.

g_0	velocity ratios of PG over Newton	velocity difference, m/s
300	0.990700461	-276.9402851
500	0.994442855	-165.4917729
1000	0.997229786	-82.49698282
2000	0.998616965	-41.18677725
5000	0.999447281	-16.45996439
10000	0.999723723	-8.227530833
20000	0.999861882	-4.113155718
30000	0.999907926	-2.741968791
50000	0.999944759	-1.645082695

Table 8: *Earth velocity ratios and differences by PG and Newton.*

It must be stressed that the above derivations of velocities were used for “falling bodies” acted upon by forces generated in the steady state of gravion flow, so that the time effect is presumably small and the validity of equations is tacitly assumed.

As a further approximation in this section, we have been tempted to include the flyby anomaly, but for which the time effects must be ultimately included, as it is also discussed in following sections.

IMPORTANT: The above derivations are based on conventional equations of a body in motion in combination with some PG equations based only on the stationary body situation. However, in subsequent sections, we gradually establish the meaning of mass in various forms. Furthermore, we need to consider also the concurrent role of the electric field inside a falling body, and the total balance among all forms of mass and energy. We will need to derive the equations of mass, energy and contraction factors both for a stationary and a falling (moving) body based entirely on PG principles and computations similar to work presented in the Appendix. Pure PG quantitative considerations would provide consistent outcomes. We further examine the falling body situation later in Section 23.2 and it seems that there are some exciting prospects ahead.

14.4 Advance theoretical solution

If we use the above reasoning in a similar fashion for an orbiting body in circular motion (for simplicity), we equate the inertial and gravitational force (initially) in PG:

$$m \frac{u_{PG}^2}{r} = G \frac{m_e M_e}{r^2} \quad (132)$$

where again m_e and m are the effective and real masses moving around a large (hence stationary) effective mass M_e , yielding

$$u_{PG} = \sqrt{G \frac{M_e m_e}{r m}} \quad (133)$$

In Newton we have:

$$u_N = \sqrt{G \frac{M_e}{r}} \quad (134)$$

so that we again get for the ratio of velocities:

$$\frac{u_{PG}}{u_N} = \sqrt{\frac{3A_R g_0}{4\pi G \rho R}} = \sqrt{q} \quad (135)$$

Now, if we apply this to the Sun-Earth system for simplicity assuming circular orbit, there is a significant slower than experience velocity component. We find this from the density ratio values in previous Table 2 and list them again together with the ratios and differences between PG and Newton in Table 8.

We have used the Earth’s average speed of 29.78 km/s. The tabulated outcome is clearly incompatible with experience: With $g_0 = 50000$ m/s,² the orbit length would be by 51.876 km shorter in one year. We have the option of increasing g_0 until we bring the difference to an acceptable level, but first we have to modify the above equations to include time effects. The equations used above assume instantaneous transmission of the push force, which is incorrect. After we derive the correct equations for orbital motion, we can find

the required value of g_0 to bring the velocity u_{PG} to an acceptable level and consistent with experience. This would constitute an advance theoretical solution to the problem of finding the prevailing maximum acceleration g_0 in our solar system, over and above the proposed experiments throughout this report. This work has not been done yet, whilst it is not clear how it will pan out. At present, this objective falls outside the scope of the present report and beyond the resources available to this author.

We have reached a critical point in the development of a general PG theory for moving bodies. In the following Section 15.3, we discuss the possibility of using the tools of general relativity (GR) to develop a *dynamic* PG, or further develop GR in the framework of PG. Now, this might appear to be inconsistent with GR from the outset, because PG breaches the equivalence principle, if stated as equality between inertial and gravitational mass, which is a cornerstone of GR. To reconcile this contradiction, we may inquire that the postulated equation:

$$m_{gravitational} = m_{inertial} \quad (136)$$

be replaced with the equation:

$$m_{gravitational} = qm_{inertial} \quad (137)$$

which is prompted from the corresponding relationship between effective (gravitational) and real mass (inertial) in PG:

$$m_e = qm \quad (138)$$

In other words, can we introduce the contraction factor q to redefine (or replace) the EP and carry on with a modified GR? This is where the subtle differences in the understanding of EP become important. This leaves the inquiry open on how to integrate relativity with PG. Gravions are assumed relativistic and we need to develop a relativistic theory of PG. Then, we could also address the objection listed in the following Section 15.6. Time effects must also include the almost helical Earth trajectory, as the Sun moves around the center of galaxy, which makes the overall formulation more complex.

The breakdown of the EP expressed in terms of differing inertial and gravitational mass seems to be necessitated also in new quantum theory (Kajari *et al.*, 2010), so that our finding here is not alone or alarming. In fact, coming to the same conclusion from an entirely different perspective, namely, from quantum mechanics, provides a strong reason to correlate the corresponding theories in an effort to unify quantum mechanics and gravitational field.

Should any further difficulties appear or remain in the development of a general PG theory, then we may have to look for some other counteracting (compensating) mechanism for the shortfall in orbital motion, before we can confidently abandon PG. For example, in Sections 15.7 and 15.8, an attempt is made to account for the postulated exiting forms of the absorbed gravions, not yet knowing if they have some second order perturbation on the gravitational field. Other compensating mechanisms may also be present.

At any rate, we can always resort to high enough g_0 in order to establish compatibility between theory and measurements, i.e. by bringing the fraction q much closer to unity. This alternative solution always remains on the table for consideration, except that it would make the prospect of measurements more difficult. In this case then, all the referenced gravitational anomalies (Allais effect, Greenland gravity anomaly, Pioneer anomaly, flyby anomaly, etc.) must be re-visited and conclusively discounted as been anomalies of gravity, namely, deviations from Newton and/or GR. This strengthens our proposal of the need to undertake some decisive experimental tests in the event that static PG theory (for stationary bodies) can be confirmed and measured.

The case of very high g_0 values, if needed, must also be considered in the spirit of discussion in Section 18 dealing with white dwarfs, neutron stars and black holes. Increasing g_0 only resolves the problem for our nearby solar system, but it shifts the importance of distinction between effective and real mass for much larger, or denser bodies and systems, like binary systems, black holes, etc, whereby compatibility of PG with such systems must be established. The difference between real and effective masses must be very high for such bodies, which also means that the EP would be grossly violated in terms of great inequality between gravitational and inertial mass. The proposal of establishing momentum or push gravity as the universal and unifying cause of all types of acceleration in Section 17 provides a reasonable platform to relate to the new quantum theory mentioned above (Kajari *et al.*, 2010).

14.5 Matter, inertia and mass

In continuation to the previous analysis, we can bring it to its logical conclusion below.

We intuitively identified the real mass $m \equiv m_{real}$ with the inertial mass $m_{inertial}$ and the gravitational mass $m_{gravitational}$ with the effective mass $m_{effective}$. However, this need not be necessarily so. It may be that, after all, the inertial mass is equal with the gravitational mass making the equivalence principle absolutely inviolable in all its expressions. Such a finding could lead to either of two outcomes:

(a) The PG becomes unsustainable, unless:

(b) Both PG as advanced in this report and the EP are true, even if EP includes equality of masses.

Then we have to accept some inexorable conclusions, even if they are counter-intuitive at first.

To avoid possible confusion, we write the subscripts of various masses explicitly by a full word. In case (b), it is not the entire m_{real} responsible for the phenomenon of inertia, i.e. a resistance to change in kinetic state (to move faster or slower). In reality then, it should be only the $m_{effective}$ that manifests inertia. At the same time, we can continue identifying $m_{effective} \equiv m_{gravitational}$. This implies that there is a fraction of the real mass, namely, the difference

$$m_{passive} = m_{real} - m_{effective} \quad (139)$$

being passive, oblivious and not resisting to the application of the gravitational force on the effective fraction of the total mass. If this were to be true, it would revolutionize our understanding and perceptions about the hitherto meanings of matter and mass. Newton defined (or identified) mass as the amount of matter:

$$mass_{Newton} \equiv matter = m_{inertial} \quad (140)$$

which would need to be re-appraised, if case (b) is true.

In fact, upon further considering this idea, we may also bring some intuition one way or another. In one way, we could think of the gravions constituting a sort of a “lattice” that activates the effective part of the mass. In doing so, it is this lattice that resists in changing the kinetic state, or inertia of the body. The passive part of the mass is ineffective and does not care (does not resist) moving along with the active part ($m_{effective}$) of the mass without actually offering any resistance. We could then safely identify the total mass of a body with its matter:

$$matter \equiv m_{real} \neq m_{inertial} \quad (141)$$

Yet, by further iterative thinking, we can make the inventive step that, instead of the gravion-lattice **activating** the effective mass to resist, it is the lattice itself that resists the movement of the body (matter) by engaging via the effective (active) part of the mass. The effective mass is passive by itself, except that it is somehow tied to the activating gravions. In consequence then, we can safely state that the entire mass is actually passive and hence it has no inertia; what appears as inertia of the mass (or part thereof), it is actually the resistance of the gravions opposing the mass to change its kinetic state.

The concept of gravion-lattice may take on various embodiments and conceptualizations: Gravions continuously penetrating and being absorbed through a mass could be likened to rolling ropes (albeit very inefficient way) constraining the mass from changing momentum. By whatever means and ways to describe the gravion-mass interaction, we can generally state that it is the gravions that are responsible for what appears as inertia of matter. When we try hard to move a sledge on slippery ice, it is the gravions, which resist invisibly to us, but we only experience the force on the tangible sledge. By such thinking, we may have ultimately deciphered the mystery of controversial inertia. We may know why bodies resist, now saying that bodies actually do not resist, but it is the energetic gravions that want to “push back” on us via the mass ($m_{effective}$). There remains to better conceptualize how they do this and why they only do it when we accelerate or decelerate a body. For the time being, we can summarize our possibly new understanding as follows:

$$m_{inertial} = m_{gravitational} = m_{effective} = qm_{real} \equiv q \cdot matter \quad (142)$$

We note that the above equation is similar to Eq. 137 except for the semantics on masses, i.e. which mass is which and what they do. If the above is true, the consequences would be immense. For example, the inertial mass of a very dense body, like a neutron particle, or a white dwarf, or a neutron star, or a black hole is much-much smaller that it could be if the same body is expanded (dilated) to produce an effective mass close to its real mass. The *dynamics* of an exploding star would be far different from what we would derive by allowing for a constant mass. Mass, inertia and matter now (in PG) mean different and variable entities. As another example, the flyby gravitational anomaly still applies, so that if we are able to vary the effective mass by a large factor minimizing it during the outbound trajectory, we could hurdle a body into space at huge velocities.

In all above, we made no mention of relativity implying that we considered only low speeds. When we go to relativistic speeds, then we have to expand on additional notions of masses, namely, that of rest mass m_{rest} and that of relativistic mass $m_{relativistic}$. In doing so, we may not be in conflict with GR and we may just carry on with established relativistic theory. Actually, it seems that we may even have a better understanding of the meaning of relativistic mass, which has been often misconstrued by many GR proponents for over a century. Relativistic mass has been so confusing even among notables in relativity, that it has been called “the pedagogical virus” (Okun, 2006). For consistency with our introduced terminology and semantics, we should set for the rest mass:

$$m_{rest} \equiv m_{effective} \quad (143)$$

so that the relativistic mass can be given by:

$$m_{relativistic} = \gamma m_{effective} \quad (144)$$

with the usual relativistic factor

$$\gamma = \frac{1}{\sqrt{1 - v^2/c^2}} \quad (145)$$

There remains now only to conceptualize and formulate how exactly the relativistic mass comes into being. Nevertheless, the important conclusion must be that the gravions remain responsible for this mass too, which is not a “mass” per se, i.e. it is not matter (stuff), but only an inertial mass. Such a conceptualization is then closely consistent with the “orthodox” and rigorous teachings of the theory of relativity, namely, that the relativistic mass is not a “mass”. However, this is a close agreement with GR but not a total agreement, because GR teaches that the “*only true mass is the rest mass*”. We may now have found that even the rest mass is not true mass, because it is only an effective mass, which can vary with density and orientation for any given body. The only true mass is actually the real mass as has been established by the present PG theory, which is non other than the matter of the body. In any case, non of all these masses has an inertia (a will to resist), but the energetic gravions are responsible for the quantity (parameter) of mass that enters our equations in physics. Therefore, gravions create both gravitational fields and apparent masses. This should be in happy agreement with GR originating from an “opposite” direction.

From the preceding analysis, it seems that PG reaches a critical point as soon as we apply the concept of effective and real mass to moving bodies. This could be either the end of PG, or a long awaited breakthrough in physics. The latter might occur in one sense, if we are prepared to review and re-appraise the notion of “inertia”. It is interesting to note that the dictionary synonyms of “inert” are “dormant, immobile, impotent, inactive, listless, motionless, paralyzed, passive, powerless”. However, in physics, we associate inertia with a resistance or refusal of a body to change its kinetic status, which is not passivity or inactivity. A resistance to the change of movement implies a power, or will, or action to resist, i.e. a reaction. Where does this power for objection to an action comes from? It might have been a misnomer to use the word “inertia” to describe our experience, when we try to change the kinetic state of a body. A more appropriate word might have been “reactivity”. In chemistry, it is more appropriate to call an inert element so, because the element does nothing by way of (chemical) reaction; it is action-neutral, However, in physics, all bodies are not action-neutral, when prompted to move or stop or change velocity. They all present reactivity and not “inertia” per the outside-of-physics use of the word. “Inertia” means inaction, the same as in other languages, e.g. in Greek inertia $\iff \alpha\delta\rho\acute{\alpha}\nu\epsilon\iota\alpha \iff$ inaction. Of course, word-play does not make physics, except that we may have fortuitously come to use the word “inertia” for what it actually means for the real mass. As a result, the word “effective” mass may now assume the role of the formerly “inertial” mass.

In the preceding analysis, we reached the dilemma of either abandoning PG, or abandoning the classical inertia meaning. We also used the word “passive” for a passive mass $m_{passive}$ of a material body.

We can better appreciate why, the EP stated as per “gedanken elevator”, is a different thing than stated as equality of masses. We may provisionally use the equality of masses in PG to learn that the “effective” mass plays the role of both the “inertial” and the “gravitational” mass of prior physics. If we can established such a finding by other means, then there is no distinction between those two prior masses, and the EP becomes redundant again. A good way to this end is to start by experimentally verifying the static PG, namely, the existence of effective mass as already proposed, or by some other experimental means. Theoretical means are also welcome, but practice is the ultimate criterion of truth.

14.6 Mass, energy and black holes

As a result of the previous potential discovery of possible properties of the effective and real mass, we further investigate the consequences on mass and energy of bodies with increasing density all the way to the creation

of black holes. We have already considered the effect of increasing density, but we also need to account for the distribution of effective mass inside a given material sphere at very high density.

14.6.1 Material sphere

We need first to clarify and summarize some previous findings to help us make an important step without laborious cross referencing: If the real density ρ is known in advance, we can find the absorption factor k directly from $k = \pi\rho G/g_0$, which substituted in Eq. 44 yields the contraction factor

$$q = \frac{3A_R}{4kR} = \frac{3}{4kR} \left(1 - \frac{1}{2k^2R^2} + \frac{\exp(-2kR) \cdot (2kR + 1)}{2k^2R^2} \right) = \frac{\rho_e}{\rho} = \frac{m_e}{m} \quad (146)$$

From the above, we obtain the effective mass and effective density:

$$m_e = \frac{3A_R}{4kR} m = \frac{\pi R^2 A_R}{k} \rho = \frac{\pi R^2}{\Lambda} A_R = \frac{g_0}{G} R^2 A_R \quad (147)$$

$$\rho_e = \frac{3A_R}{4kR} \rho = \frac{3A_R}{4\Lambda R} = \frac{3g_0 A_R}{4\pi G R} \quad (148)$$

The above equations state that, we as increase the real mass arbitrarily inside any fixed radius sphere, the corresponding effective mass increases monotonically to an asymptotic value as the absorptivity A_R approaches unity. At the same time, the contraction factor vanishes to a zero value but never reached.

We can also arrive at the same equations by starting with a given (known from Newtonian mechanics) effective mass, or effective density. Then, we find the coefficient k directly by solving Eq. 63 written as:

$$g_0 A_R - g_R = g_0 \left[1 - \frac{1}{2k^2 R^2} + \frac{\exp(-2kR)(2kR + 1)}{2k^2 R^2} \right] - G \frac{m_e}{R^2} = 0 \quad (149)$$

from which we immediately obtain again (as from Eq. 80):

$$m_e = \frac{g_0}{G} R^2 A_R = \frac{\pi R^2}{\Lambda} A_R \quad (150)$$

The above findings state that we cannot pack any arbitrary Newtonian mass (i.e. effective mass) inside a given radius sphere for a given universal constant Λ , or a combination of constants G with g_0 ; there is a limit approached asymptotically as A_R approaches unity. That limit is given by

$$m_{emax} = \frac{g_0}{G} R^2 = \frac{\pi R^2}{\Lambda} \quad (151)$$

and

$$\rho_{emax} = \frac{3g_0}{4\pi G R} = \frac{3}{4\Lambda R} \quad (152)$$

By way of example and comparison, we use a sphere with the radius of Earth ($R = 6.37 \times 10^6$ m) and $g_0 = 1000$ m/s², and find the maximum possible effective M_{emax}

$$M_{emax} = \frac{g_0}{G} R^2 = \frac{1000}{G} \cdot (6.37E + 06)^2 = 6.08 \times 10^{26} \text{ kg} \quad (153)$$

That limit would be achieved, if a near infinite amount of real mass could be accreted. For the particular example here, the ratio of that limiting value over the Earth's effective (Newtonian) mass is $M_{emax}/M_e = 101.8303172467580$.

Even risking of becoming pedantic, we need some further clarifications, because there is a bigger risk from misusing the two densities in the new situation of PG. The contraction factor q was defined for a condition outside a sphere. Thus, initially we assumed that the density is known and real, so that, if we use it in both PG and Newton, we arrive at different outcomes correspondingly, the ratio of which is provided by $q(\rho)$ being a function of real density. Subsequently, we introduced the effective density to match Newton with PG. If we use the two densities at the same time in the contraction factor, we obtain unity:

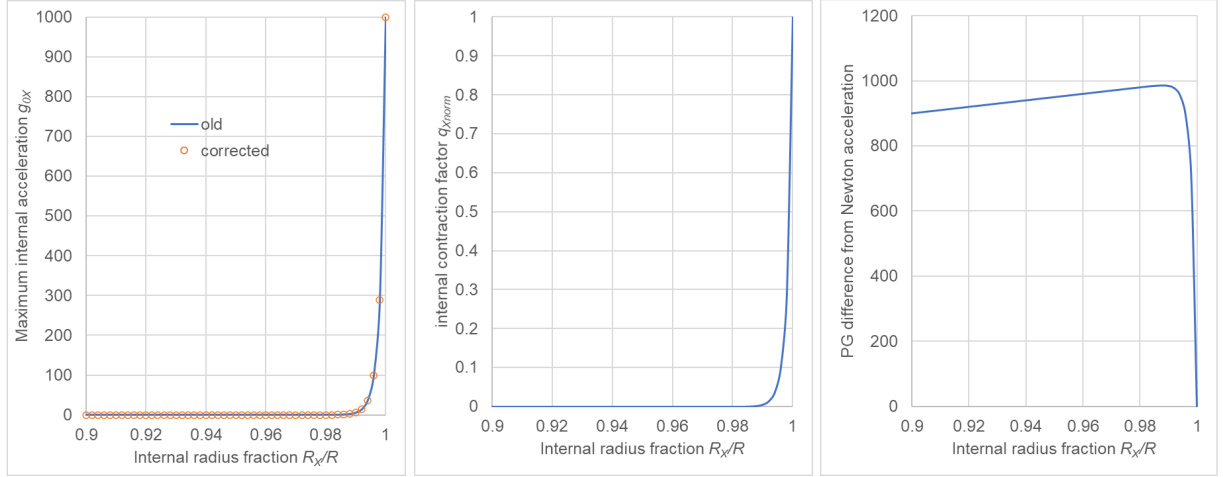


Figure 16: *Internal maximum acceleration g_{0X} , normalized contraction factor q_{Xnorm} and difference $g_{NX} - g_{0X}$ near maximum effective mass limit $M_{e-test} = 101.83M_e$ using Earth's diameter and $g_0 = 1000 \text{ m/s}^2$.*

$$q(\rho, \rho_e) = \frac{g_{PG}(\rho)}{g_N(\rho_e)} = \frac{g_0 A_R}{\frac{4}{3}\pi G R \rho_e} = 1 \quad (154)$$

after substituting ρ_e from Eq. 148. This is useful background to correctly understand the internal accelerations ratio used in Section 8 for a low (typical) density-of-the-Earth example. There, we found the internal parameters of g_{0X} , $q_X = g_X/g_{XN}$ and the difference $\Delta g_X = g_{XN} - g_X$ at any point X inside a sphere per Fig. 7 defining the internal radius R_X and the fractional radius R_X/R of the sphere with radius R . Explicitly, we have:

$$q_X(\rho, \rho_e) = \frac{g_X}{g_{XN}} = \frac{3g_{0X} A_{R_X}}{4\pi G \rho_e R_X} \quad (155)$$

where we use both the real and effective densities already established for the material sphere from the outside, whilst they do not change once found.

With q_X known per process in Section 8, we can find the corresponding density ρ_{eX} at point X required to balance the PG acceleration at that internal point for the internal sphere, for which we have:

$$q_X = \frac{\rho_{eX}}{\rho_e} \quad (156)$$

This finds the effective density for any internal sphere with radius R_X , which, in effect, provides also the desired overall distribution of the total effective mass for the entire sphere as a function of R_X . Thus, we can verify that for $R_X = R$, we get $q_X = q = \rho_e/\rho_e = 1$ as expected. Therefore, q_X provides solution to our inquiry.

Now, we are ready to plot the same internal parameters as per Fig. 8, but close to (i.e. a little under) the limiting value of M_{emax} found above. This is done in Fig. 16 using $M_{e-test} = 101.83M_e$, for which the corresponding densities are $\rho_{e-test} = 561449.92 \text{ kg/m}^3$ and $\rho_{ttest} = 299899725.44 \text{ kg/m}^3$ with a contraction factor $q_{ttest} = 0.01829587874417$. The latter factor indicates that the total effective mass is only $\approx 1.83\%$ of the total mass, i.e. relatively low but over $100\times$ the Earth's mass. The graph of the same factor internally decreases extremely fast from the surface to the center of the sphere. The effective mass is practically concentrated in the top 1% of the radius forming a very thin active layer very close to the surface. It should be noted that to reproduce the graphed numerical example, one needs to apply high precision computations. The distribution of the same and other internal parameters is further explored for the general case in Section 24, whereby the g_{0X} has been theoretically corrected and now redrawn with red circles in Fig. 16; the correction is hardly distinguishable on the graph in this range of fractional radius (approaching unity). The contraction factor is renamed as “*normalized contraction factor*” q_{Xnorm} in the figure. We used corresponding $k = 0.0000628806972857207 \text{ m}^{-1}$.

If the hypothesis that the real mass is inactive and passive (i.e. without classical inertia), whilst the only bearer of active (reactive) mass is the effective mass, it might provide us with what looks like a black hole.

There are generally different ideas about what happens inside a black hole. Especially from our reference frame, it is generally unknown what happens, other than a singularity to in-falling material. Some say nothing happens at all, not even a vacuum, it has no properties and it is not even a hole; whilst matter approaches the black hole, it slows down and finally stops at the event horizon. They also say that all mass becomes concentrated at the two-dimensional surface of the event horizon. The latter is very close to what we also find in Fig. 16. They also say that it seems that a black hole destroys energy, which is again similar to what we say, i.e. that the real mass has no energy, but also no inertia (new finding). Actually, with our approach, there is no paradox, except that we might have been misguided about the meaning of our experienced inertia. The Schwarzschild envelope or boundary and the Schwarzschild radius may be exactly, what we find for the limiting case by Eq. 151.

Actually, a close examination of Eqs. 150 and 151 may be full of meaning: The effective mass is proportional to the surface area of the sphere (πR^2) over the universal constant Λ and how close the absorptivity A_R is to unity. It is a simple equation and, hopefully, it is also true.

We further understand that: By increasing g_0 , say by a factor of $10\times$ or $100\times$ with all other parameters constant, the distribution of the effective mass is pushed inward toward the center of the sphere. However, if we also increase the effective mass by the same factor, then we recover the same distribution, i.e. resembling the event horizon. So far, it is arbitrary to keep the sphere radius constant while mass is accreted, unless we can find or propose a mechanism to achieve exactly that. For this, we need to consider what happens in the formation of high surface acceleration on white dwarfs, neutron stars and black holes together with an interim presentation of some other issues below. We continue with more on mass, energy and black holes in Section 18.1

14.6.2 Material line segment

Based on what appears to be an important development for a high density material sphere, we need to repeat a similar formulation for a material line segment; all this will help us derive a possible relationship between the contraction factors in PG with the Lorentz contraction factor in GR. We could take a similar approach for a material thin rod, but we greatly simplify the mathematical formulation required by using the shape of Fig. 1, within a very small (differential) solid angle $d\Omega$, length $\ell = BC$, absorption coefficient k and real density ρ . All corresponding referenced parameters for this case will have the subscript ℓ font. The contraction factor q_ℓ for a material line segment was given by Eq. 46 actually written for chord lengths of a sphere. However, it is better to repeat and review all needed PG parameters with a fast-track derivation below.

We should point out that the material body in Fig. 1 is traversed by gravions in all possible directions interacting with it, but all such interactions are not transmitted to an observer at point O. Point O is affected by all gravions arriving from all possible directions in a full 4π solid angle at that point; they all have a null effect except for those inside the bi-directional elementary solid angle subtended by the material object in the drawing.

Axial external points of line segment: We aim to find the (external) contraction factor along the axis at any distance up to and including the end points of the line length together with other parameters needed for further work and analysis.

The elementary absorption factor df_a (no need for f_g here) is given by Eq. 7 in PG:

$$df_{aPG} = [1 - \exp(-k\ell)] d\Omega \equiv f_{\ell PG} \quad (157)$$

where, for convenience, we abbreviate the differential absorption factor within the differential solid angle $d\Omega$ by $f_{\ell PG}$; the above equation also defines the corresponding absorptivity A_ℓ of the line body with

$$A_\ell = 1 - \exp(-k\ell) \quad (158)$$

It is worth noticing that the ratio A_ℓ/k now is an effective length ℓ_e as opposed to the spherical parameter ratio A/k producing an effective volume V_e per Eq. 52.

The corresponding absorption factor for Newton (i.e. with extremely small k) is:

$$df_{\ell N} = k\ell d\Omega \equiv f_{\ell N} \quad (159)$$

The length contraction factor is the ratio of the two accelerations:

$$q_\ell(\rho) = \frac{f_{\ell PG}}{f_{\ell N}} = \frac{1 - \exp(-k\ell)}{k\ell} = \frac{\ell_e}{\ell} \quad (160)$$

which is the same as for the length contraction found for the chords of the sphere in Eq. 46.

Next, we need to introduce the relationship of effective to real density ratio. For this, we follow the same steps as for a sphere by introducing a small test mass to find the accelerations, and easily obtain the corresponding equations:

$$g_{\ell PG}(\rho) = \frac{J_0}{c} \Lambda A_\ell = \frac{G}{\Lambda} A_\ell = G\rho \frac{A_\ell}{k} = G\rho \ell_e \quad (161)$$

$$g_{\ell N}(\rho) = G\rho \ell \quad (162)$$

Thus

$$q_\ell = \frac{g_{\ell PG}(\rho)}{g_{\ell N}(\rho)} = \frac{\ell_e}{\ell} \quad (163)$$

By introducing an effective density for Newton equation to produce the same acceleration as with PG:

$$g_{\ell N}(\rho_e) = \frac{J_0}{c} \Lambda^2 \rho_e \ell = G\rho_e \ell \quad (164)$$

we obtain the ratio of accelerations being unity:

$$\frac{g_{\ell PG}}{g_{\ell N}} = \frac{\rho \ell_e}{\rho_e \ell} = \frac{\ell_e}{\ell} \frac{\rho_e}{\rho} = 1 \quad (165)$$

and the absorptivity and ratio of densities given by

$$A_\ell = \Lambda \rho_e \ell \quad (166)$$

$$\frac{\rho_e}{\rho} = \frac{\ell_e}{\ell} = \frac{A_\ell}{k\ell} = q_\ell \quad (167)$$

This tells us that the ratio of densities for an elongated shape, like the thin truncated cone of Fig. 1, is different from a sphere. A material line body has different PG effects, whilst all other shapes should have PG effects between the extreme cases of a line segment and a sphere.

With sufficiently large $k\ell$, we get $A_\ell = 1$, so that there is a maximum acceleration $g_{\ell max}$ at the end of the length, or at any distance away from it on the axis, $g_{\ell max} \equiv g_{\ell 0} = g_0$

$$g_0 = \frac{G}{\Lambda} = \frac{G\rho}{k} \quad (168)$$

which corresponds to Eq. 60 without the factor π . From any given k , we obtain the real density for a material line segment:

$$\rho = \frac{g_0}{G} k \quad (169)$$

and for the effective density:

$$\rho_e = q_\ell \rho = \frac{A_\ell}{k\ell} \rho = \frac{1 - \exp(-k\ell)}{k\ell} \rho = \frac{g_0 [1 - \exp(-k\ell)]}{G\ell} \quad (170)$$

Finally, the distribution of the effective mass along the line segment is the derivative of $f_{\ell PG}$ in Eq. 157 with respect to fractional distance $h = \chi/\ell$ from the end of the line segment in the range $0 \leq h \leq 1$

$$\frac{df_{\ell PG}}{dh} = k\ell \exp(-k\ell h) \quad (171)$$

from which the normalized over $k\ell$ distribution is

$$\frac{1}{k\ell} \frac{df_{\ell PG}}{dh} = \exp(-k\ell h) \quad (172)$$

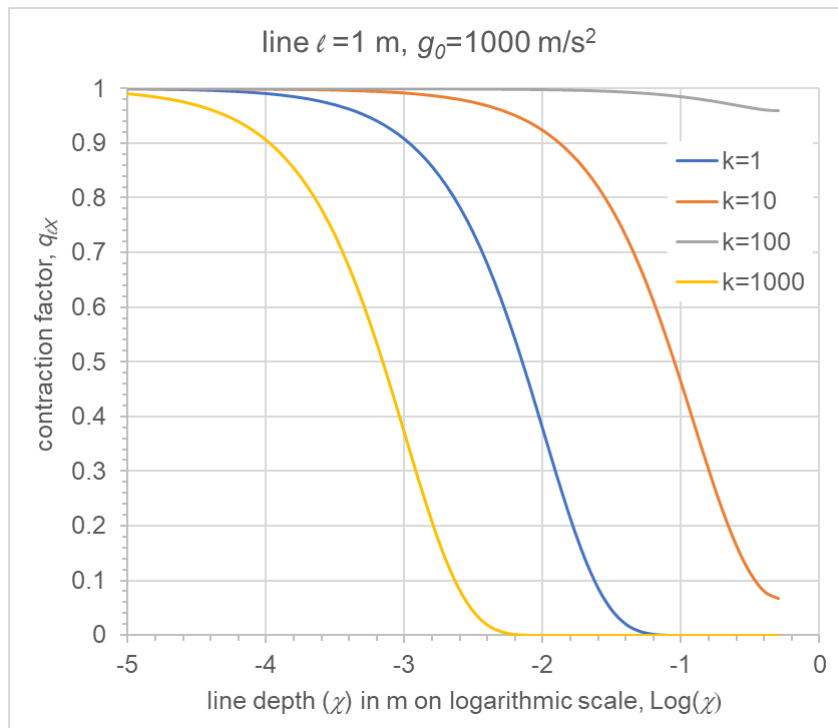
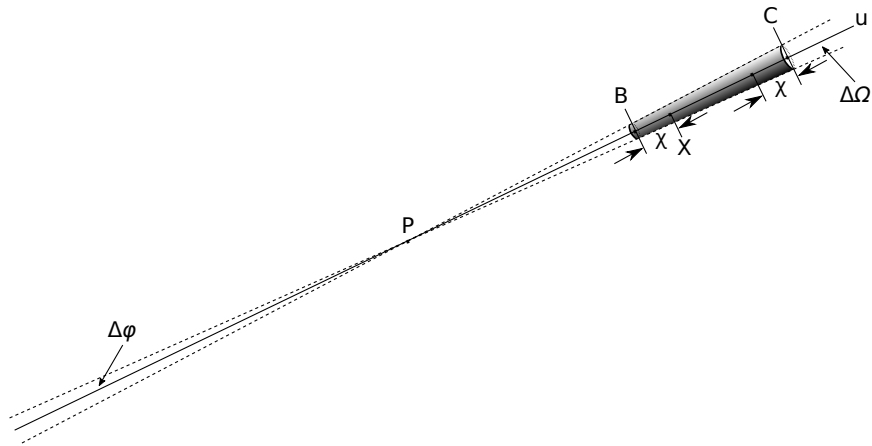


Figure 17: Line segment geometry (upper) and internal contraction factor $q_{\ell\chi}$ against depth χ (lower), for line length ℓ , maximum acceleration g_0 and fixed absorption factors k indicated

Axial internal points of line segment: We aim also to find the internal contraction factor at any point inside the line length together with other important parameters needed for further work and analysis.

The upper drawing in Fig. 17 is the same material line object: At any point X inside at a distance (depth) χ from either end point, there is a net length $\ell_X = \ell - 2\chi$ responsible for the net absorption at that point, because the absorption by the two outer layers χ cancel out. Thus, at point X, we have:

$$g_{\ell_X PG} = g_{0X} [1 - \exp(-k\ell_X)] \equiv g_{0X} A_{\ell_X} \quad (173)$$

where A_{ℓ_X} is the familiar A_ℓ factor but at the end point of the internal line length ℓ_X , and $g_{0X} < g_0$ due to the shielding of the outer layer length from X.

$$A_{\ell_X} = 1 - \exp(-k\ell_X) = 1 - \exp(-k(\ell - 2\chi)) \quad (174)$$

We can find g_{0X} by resorting to the usual absorption factor $f_{\ell_X PG}$ at point X simply by

$$f_{\ell_X PG} = [\exp(-k\chi) - \exp(-k\ell + k\chi)] d\Omega \quad (175)$$

without the need to integrate over the sphere as previously.

From this found, we can derive the acceleration g_{ℓ_X} at X by the product with the factor g_0 and equate it to its value given above by Eq. 173:

$$g_{\ell_X PG} = g_0 f_{\ell_X PG} = g_{0X} A_{\ell_X} \quad (176)$$

from which we can find the relationship between the internal g_{0X} and external g_0 .

$$g_{0X} = \frac{g_0 f_{\ell_X PG}}{A_{\ell_X}} \quad (177)$$

The expected Newtonian acceleration at X per Eq. 164 is given by:

$$g_{\ell_X N} = G\rho_e \ell_X = G\rho_e(\ell - 2\chi) \quad (178)$$

The ratio of PG over Newton accelerations at point X per above provides the corresponding internal contraction factor for the line length:

$$q_{\ell_X} = \frac{g_{\ell_X PG}}{g_{\ell_X N}} = \frac{g_0 [\exp(-k\chi) - \exp(-k\ell + k\chi)]}{G\rho_e(\ell - 2\chi)} \quad (179)$$

With q_{ℓ_X} known per above, we can find the corresponding effective density ρ_{eX} at point X required to balance the PG acceleration at that internal point for the internal line length ℓ_X , namely:

$$g_{\ell_X PG} = g_{\ell_X N}(\rho_{eX}) = G\rho_{eX}(\ell - 2\chi) \quad (180)$$

from which we have:

$$q_{\ell_X} = \frac{\rho_{eX}}{\rho_e} \quad (181)$$

This finds the effective density for any internal line length ℓ_X , which, in effect, provides also the desired overall distribution of the total effective mass for the entire length as a function of ℓ_X , or the depth χ with $0 \leq \chi \leq \ell/2$; we can verify that for $\ell_X = \ell$, we get $q_{\ell_X} = q_\ell = \rho_e/\rho_e = 1$, as expected. We plot the internal contraction factor for a line length $\ell = 1$ m and $g_0 = 1000$ m/s² as a demonstration in Fig. 17 with some fixed values of the absorption coefficient k . This is a monotonically decreasing function of χ , which decreases extremely fast at very high values of the absorption coefficient k (or the real density ρ). This means that there is a look-like “event horizon” at the two ends of the material line segment, like with the sphere found before. Of course, this is only a theoretical outcome, because any “rod”-like structure would collapse to a spherical geometry at high accretion of mass. Nevertheless, it is useful to consider this contraction too in the following presentation.

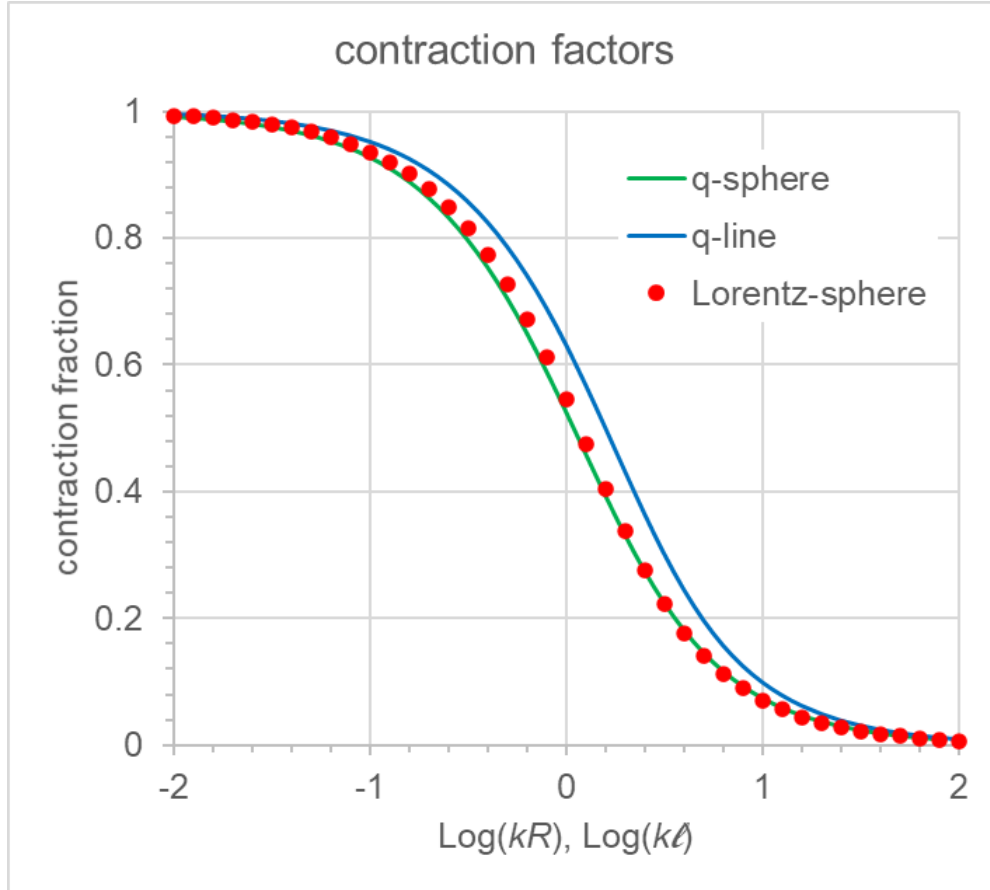


Figure 18: Comparison of PG contraction factors with Lorentz factor fitted with A_R .

14.7 PG contraction factors versus Lorentz factor

The previous suggestion that we may have already discovered an alternative explanation for the Schwarzschild event horizon in black holes prompts us to have a closer investigation of the meaning of the contraction factors given by Eqs. 45 and 46. We further attempt to establish a possible relationship with the Lorentz contraction factor. These attempts are made in a kind of round-about-way, not strictly building the dynamics of PG theory from ground up yet. Trialing such attempts involves a mix-and-match of prior principles and understandings. We already acted like that in arriving at the proposal that the effective mass could be the same as the prior “inertial” mass. This potential conclusion was based on the use of the EP despite its possible redundancy in PG. We are fully aware about this on/off relationship with the principle. Redundant does not mean invalid. Valid or invalid will be determined as we develop the theory and practice of PG. With this proviso, we should be entitled to continue trialing various novel possibilities now open with PG, which are not yet well understood or finally accepted. We aim at eventually using as fewer postulates or “principles” as possible, which entails or presupposes better knowledge of the physical processes behind the principles.

Let us rehash some of the things already learned from Part 1, as a prelude to make an important next step towards a dynamic PG theory. The presumably event horizon in PG was deduced by observing the sphere’s internal mass distribution at an ever increasing density. However, for an observer (or small test mass) on the surface or away from the sphere, the experience would be described differently. As we increase the mass of the sphere, the observer would feel an increased attraction from the direction of the sphere in proportion to the factor f_g . If the observer was trained only in Newtonian mechanics, he/she would report that the sphere was increasing its mass to an amount equal to what we **now** call effective mass. However, if the observer could view and count all the gravions arriving at the test particle, then he/she would report no change in all directions but from those in the solid angle subtended by the sphere. In more detail, it would be reported that a maximum variation (depletion) comes from the center of the sphere. In the case of observation from a point at 100 radii from the gravitating sphere, the directional depletion of gravions would correspond to the gravitoid shapes calculated by PG theory in Fig. 71. A PG observer would report that

a net push is experienced from the opposite direction of depletion. The Newtonian observer would report only an attraction by the visible spherical geometry (real one) with an apparent mass coming from the entire sphere, although it could be pointed out (with PG hindsight) that an equal effect could result from the real mass contained in the said gravitoid (unbeknown to the Newtonian observer).

Since we introduced the possibility of the effective mass playing the role of “inertial” mass in Section 14.5, which was not anticipated when the concept was first introduced in Part 1, it is helpful to review and clarify the following (even with some repetition): The effective mass and density are initially distributed uniformly over the real volume of a sphere and produce the measured (Newtonian) acceleration (or force F) at any external point. However, there exist a greater real mass and density also distributed uniformly but with a part of it being shielded from gravion action and without inertia; this part is probably the “stuff” of black holes, but possibly also ever present along with “ordinary” effective mass. We have also devised an effective spherical volume (smaller than the real volume), which, filled with real mass, produces the same Newtonian force F . Furthermore, we have devised gravitoids, which, filled also with real mass, produce the same force F . Since we attached a special interest to the effective mass, we have also become interested in finding its actual distribution inside a sphere (or line segment). Effective mass is created, where a gravion is absorbed. The outer layers are the most active with diminishing effect towards the center of the sphere. We have found the internal distribution for a stationary sphere relative to an observer (or small test mass) inside the sphere. However, for an external observer, the distribution of effective mass starts with highest concentration at the opposite end of the chord relative to the observer. Eq. 172 was derived for this purpose. Plotting the latter distribution (no need to be shown here) yields corresponding curves as in Fig. 17 but for the full line (chord) length. It is this distribution, which directly describes an important physical process, whilst other parameters are only mathematical tools and notions helping in the development of PG. We also note that we introduce a kind of relativity with respect to the observer’s location: At a point outside the sphere, only the interactions of gravions inside the subtended solid angle by the gravitating body enter in making the force F , whereas at a point inside the sphere all gravions from all directions are involved in finding the internal force F . With all these clarifications, we realize that increasing the density of a material sphere produces a Moon-like meniscus of effective mass towards the outer surface away from the observer, or correspondingly, a gravitoid (imaginary) meniscus of real mass towards the near side of the sphere to the observer. For an observer inside the sphere, we report a maximum concentration of effective mass towards an envelop close to the surface of the sphere (probably the “event horizon”). In all cases, the geometrical integrity of the sphere remains invariant, whilst it is only the amount and distribution of effective mass that varies by Eq. 147 towards some extreme state (and effective shape), which might correspond to certain mathematical outcomes by GR.

The above is according to PG theory about the effects of increasing the mass (and acceleration) to very high levels, which is an analog to the paradigm of relativity, but without establishing any relationship between the two theories yet. We only establish a concept of contraction in PG, more precisely a concentration of effective mass, possibly corresponding to a contraction of length in relativity. Clearly, these two kinds of contraction are two different things, but they may share a common underlying process, which GR is not telling us about, but which PG is being built on. It is said(?) that in GR time dilation and length contraction near a massive body are not the same as time dilation and length contraction at relativistic speeds. Correspondingly in PG, we may not say from the outset that the contraction factors derived for a stationary body are the same for a moving body at relativistic speeds. However, it is reasonable to envisage that as we increase the speed of a moving sphere, the amount of gravion intensity traversing and interacting with the sphere increases with concomitant increase of the effective mass and variation of its distribution (see Eq. 147). That means that there is a correlation and possibly a relationship between speed v and kR . It is the task of PG to establish such a relationship, if it exists. Pending such rigorous development though, it can be helpful to attempt and try some intuitive steps as a kind of advance scouting exercise.

For a possible connection between PG and relativity, we can initially try to express the PG contraction factor as a function of velocity, or the velocity as a function of kR , since we already have the function of $q(kR)$ (per Eq. 45). We try the latter by proposing some impromptu functions for the ratio of velocities v^2/c^2 in the Lorentz contraction factor $L(v^2/c^2)$

$$L = \gamma^{-1} = \sqrt{1 - \frac{v^2}{c^2}} \quad (182)$$

We note that both types of contraction (in PG and relativity) are functions of the same form (sigmoids) varying between 1 and 0. We inquire, if v^2/c^2 can be expressed as a function of kR preferably without a “fudge” coefficient to bring both $q(kR)$ and $L(kR)$ to agreement. Fudge coefficients are often detested and preferably avoided. We further note that the absorptivity factor A_R has a sigmoid form without any arbitrary constant to “fudge” with, which conveniently prompts us to try first by simply setting:

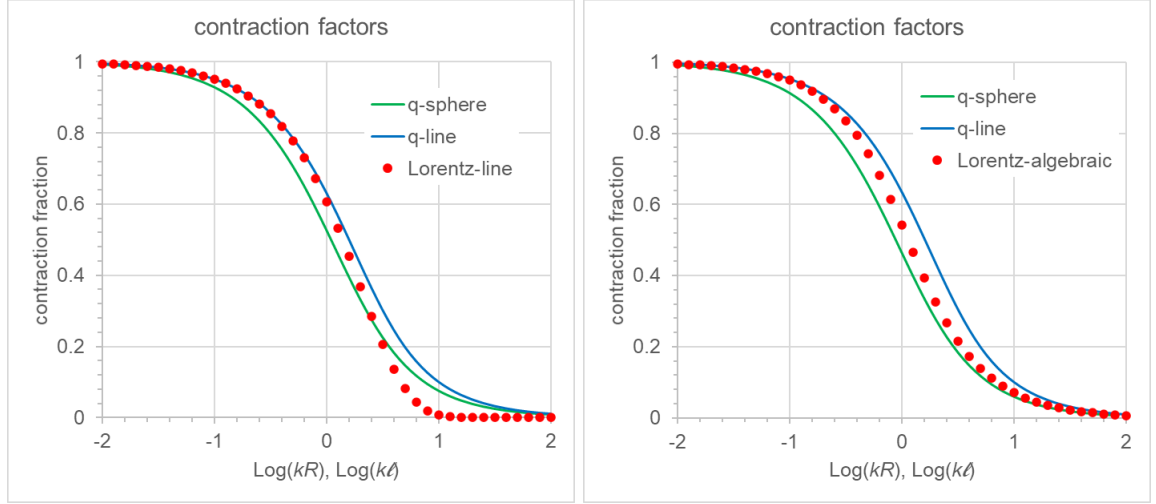


Figure 19: Comparison of PG contraction factors q -sphere (q) and q -line (q_ℓ) with Lorentz factor fitted with A_ℓ from line segment (left) and algebraic sigmoid (right)

$$\frac{v^2}{c^2} = A_R = 1 - \frac{1}{2(kR)^2} + \frac{\exp(-2kR) \cdot (2kR + 1)}{2(kR)^2} \quad (183)$$

The result is plotted in Fig. 18 with curve points (in red) labeled “*Lorentz-sphere*” along with the two PG contraction factors for sphere $q(kR)$ and line segment $q_\ell(k\ell)$. There is an immediate very good-to-excellent agreement between “*Lorentz-sphere*” and “*q-sphere*”. This is very encouraging and may be used as guidance to proceed further with PG.

We can also try to replace the Lorentz velocities ratio with the absorptivity factor of line length per Eq. 158:

$$\frac{v^2}{c^2} = A_\ell = 1 - \exp(-k\ell) \quad (184)$$

and plot the outcome (*Lorentz-line*) together with q -line and q -sphere as before in Fig. 19 (left). We now see a significant deviation from both q -sphere and q -line. Actually, there is good agreement with about the first half of the q -line curve. The deviation is surprising at first, but considering that distribution of mass and shape in a body are important in PG, the outcome may be justified. It could be that both q -line and q -sphere are correct, whilst all other body shapes may be characterized by curves lying in-between those two. In that case, if PG can express the correct contraction for any shape, then the Lorentz contraction may be a good approximation of reality, either for sphere or line segment, but not an exact one. The shape of the accelerating body does not appear in relativity(?).

For good measure, we have also tried several other sigmoid fitting forms, like the so called “generalized logistic”, “hyperbolic” and “algebraic” sigmoid functions. All failed to produce any reasonable or better fit, except for the algebraic function:

$$\frac{v^2}{c^2} = f(z) = \frac{z}{\sqrt{1+z^2}} \quad (185)$$

where z is the product of some characteristic *length* times the absorption coefficient: $z = k \cdot \text{length}$. The outcome is provided in Fig. 19 (right). Interestingly, the Lorentz factor fits well with q -line at low values of z and well with q -sphere at high values of z , with transition values in-between.

If the “*Lorentz-sphere*” fitting curve in Fig. 18 is the correct one, then we could write that:

$$q = \frac{3A_R}{4kR} \approx \sqrt{\left(1 - \frac{v^2}{c^2}\right)} \quad (186)$$

which could herald an initial (tentative) expression of the PG contraction factor as a function of velocity. If in any way it can be shown that the PG contraction is equivalent or near equivalent to the relativistic contraction, then it could have enormous consequences in physics. It is impractical to exhaustively mention

and discuss all those consequences here. A lot of work should follow. In the meantime, we may provide some tentative thoughts about the significance of the above findings.

First, some serious questions arise, which can have critical repercussions not only for PG but probably also for GR. The discussion of these questions will determine if PG and GR can coexist and complement each other, or one of them has to give way to the other.

In one aspect and by way of Eq. 186, it follows that an increased speed is accompanied by an increase of the absorption coefficient k for a fixed body radius, or length. This means an increase in mass or density. This means that the relativistic mass is not simply a mathematical intervention to enforce the light speed limit. The relativistic mass can be an effective mass increasing with the speed of the body.

It may be argued that no such new mass is consistent with experiment. For example, in the Large Hadron Collider at CERN, both Xe and Pb ions are accelerated to energies of about 2–4 TeV and nothing seems to happen to the ions. However, we may wonder, if all is taken correctly into account in arriving at such a conclusion. By no means do we challenge that conclusion here, except to draw attention to the possibility of other parameters playing a role too. For example, it is said that two “up/down quarks” are found in “ordinary” matter, but another four “other types of quarks” are found only in accelerator collisions. It is not clear why this happens (at least to the present author). Could then accretion of mass take place in nuclear and sub-nuclear structures that do not alter the macroscopic appearance of matter? If the PG “real mass” contains one active fraction (effective mass) and one inactive fraction without classical inertia, could we then allow and account for mass accretion in an accelerated ion beam in the LHC experiments?

Therefore, it seems that accelerating a body to relativistic speeds is equivalent to increasing its mass to an asymptotic upper limit, but not to infinity. We may initially surmise that the effective mass is gradually created and redistributed preferentially in the direction of motion. The increase of effective mass could only come about by a concomitant increase of the total real mass at fixed g_0 . The length itself in the direction of motion does not actually contract, but the amount of effective mass is compressed close to the head of the moving body and away from its tail. This is a point of fundamental departure from GR preaching that the actual mass does not increase, since there is only one mass, namely, the rest mass, whilst the physical length contracts. Theorists insist that relativistic mass per se has been thoroughly deprecated from the outset of GR, whilst it was introduced mathematically only to make the limit of speed of light look natural. However, PG can accommodate, literally, an actual increase of mass, namely, real mass, part of which constitutes an increasing amount of effective in lieu of relativistic mass. There is a balance between the rate of accreted and the rate of re-emitted mass according to a forthcoming Eq. 201. This novel finding of PG could resolve a persisting debate (or misunderstanding) and revolutionize the understanding of relativity.

There is no doubt that the problem of mass is one of the key problems of modern physics, whilst one wonders why the "debate" or corrective steps on the meaning of relativistic mass has continued since the inception of GR. Even notables like Penrose and Hawking did not come clear on this issue for whatever reasons (Okun, 2006). The relativistic mass may not be a “pedagogical virus”, after all, it might be a common sense reality. More about the concepts of mass and force have been worked out in Section 16 with a possible explanation on how new matter could be generated in particle accelerators. That is, the particle mass can acquire an effective mass over and above the maximum permitted outside the accelerator. The latter creates an artificially increased value of g_0 , so that when the particle decelerates at the end of its journey, it has to shed the extra mass in the form of new particles inside the accelerator. This re-adjustment of particle mass continues as long as it violates the PG law of maximum effective mass. ~~The artificially increased value of g_0 is understood to originate during acceleration via a mechanism not yet described at this point.~~ The extra effective mass accrues during acceleration but more details are now presented in Section 23 after we also consider the electric field under “push electricity” (PE) in Section 21 and other developments.

In another aspect and by way of Eq. 186, we may have another more serious conflict between PG and GR: The Lorentz factor necessitates an arbitrary increase of the relativistic mass, as we approach the speed of light. That would require PG to be able to also increase the effective mass to infinity, correspondingly. However, PG anticipates an upper acceleration limit g_0 for a stationary body. If accelerating a body by motion is equivalent to accelerating it by a nearby massive body, then either PG, or GR, or both should be adapted to produce equivalent outcomes. It is unclear if this is possible at this stage of development, especially if GR rules out(?) relativistic-speed and nearby-massive-body equivalence. May be this equivalence breaks down at relativistic speed extremely close to the speed of light. May be GR cannot be verified too close to the speed of light. May be GR needs to modify its prediction from an infinite relativistic mass to some maximum (limiting) value relativistic mass corresponding to a PG upper limit of acceleration and effective mass. The alternative for PG is to think of a way (formulation or whatever) that increases the amount of absorbed gravions to infinity as we get too close to the speed of light, something waiting to be worked out. As a last resort for PG would be to apply superluminal speeds of the body absorbing an arbitrarily increasing amount of gravions, but not likely. After all these combinations of possibilities, it is also quite possible that

all three curves in Fig. 18 are valid considering that contraction factors may not be the same for a moving body at relativistic speeds and for a nearby massive body! This means that the Lorentz contraction factor for a moving body remains to be found in PG.

In summary of above ideas, PG may anticipate that all gravions swept at the head of the moving body are (near) totally absorbed, whilst (nearly) no gravions are absorbed at the tail, when motion is very close to the speed of light. Total absorption occurs at the limit of maximum acceleration g_0 , at some maximum effective mass $m_{emax-moving}$, or density $\rho_{emax-moving}$ and provided that the real geometric integrity of the body is preserved, i.e. the radius for a sphere remains constant; otherwise, the situation becomes more complex. The details for such outcomes remain to be worked out.

Whilst GR has been verified on many occasions, it is not known (at least to the present author), if it has been verified at speeds somewhere sufficiently close to the speed of light. Could it be that the Lorentz factor is an approximate manifestation of another “contraction” process as now described by PG? It may be that one of the two theories is the true one, whilst the other is an approximation. They both appear to converge (agree) at low enough speeds (whilst disagreeing on the meaning of relativistic mass), but they are in conflict too close to the speed of light. For a proper answer, we have to wait until PG is put to the test for verification or not, while we also continue to develop it theoretically.

We are aware that we did not derive the Lorentz contraction factor above from PG principles, except to demonstrate the possibility that the PG contraction factors may already describe what the Lorentz factor exists for and much more. We have derived, hopefully, equivalent contraction factors and the Schwarzschild envelope without even resorting to relativity yet. At the outset, we have added the postulates (or principles) #5 and #6 provisionally on the assumption that PG may be built as an expansion of relativity taken for granted. Furthermore, a significant discussion on postulate #3 is presented and proposed in the following sections of Part 2, which could make this principle redundant too. Part 2 of this report is an open-ended discussion towards elaboration of a fully fledged, self contained PG theory and practice.

We are pioneering a totally new ground with PG necessitating a re-examination of a large number of problems in physics. For another example, the new concept of PG contraction factors could provide another understanding of the Michelson-Morley experiment. There is a need to re-trace the founding steps of relativity in order to juxtapose them with those of PG and explain why the two theories result in similar but also mutually exclusive outcomes in an increasing number of cases. There is both commonality and departure between the two, like between PG and Newton, and like GR and Newton. Which one is the bigger one? There is a lot of work (rework) to be done by re-visiting a lot of outstanding or seemingly established topics in physics. For one thing, though, so far PG demonstrates a lot of promise with fresh ideas and outcomes.

In the preceding analysis, we advanced some bold assumptions and assertions not necessarily exhausting the gamut of possibilities under PG. That means that we may continue to try and reconcile the aspects of PG with prior prevailing theories on the nature of matter, mass, energy and inertia. For example, see some additional aspects possible in Section 19. All options remain on the table. For this reason, it should be appreciated that the current single-author advancement of PG ideas has its limits, which can be overcome by the participation of the broader scientific community.

15 Response to criticisms

As mentioned at the outset of this report, there have been numerous objections to the idea of push gravity since the original proposal by Fatio. This has applied to all hitherto variants of PG, but it is hoped that all these objections may be overcome in part by the preceding findings and in part by some new arguments and models presented in this Part 2. Most of the objections may be overcome without further ado, but the main problem of energy absorption and mass accretion can only be tackled speculatively at this point, if we have to face the dilemma of abandoning the preceding findings, or advancing forward on those findings. The best known objections, as outlined in this referenced version of Wikipedia contributors (2018a), are discussed next.

15.1 Weak absorption, range and gravitational shielding

Whilst early conceptions of push gravity maintained that it was mandatory to assume very minimal absorption of gravions in order to avoid the objectionable gravitational shielding, it is exactly the opposite consideration that frees push gravity and explains some of its intrinsic workings. Gravitational shielding or self-shadowing by mass is now at the core of the workings and understanding of PG. This is not something to object to, because via and by its presence we can actually derive the gravitational law, in fact, in a new form that can account for a lot of missing information in Newtonian mechanics including singularities.

By the same token, gravitational shielding leads to a distinction between real and effective mass, which, in turn, may lead to a re-appraisal or re-think of the notion of inertia and mass per Section 14. When we can faithfully describe the observed motion of bodies with a theory of the dynamics of PG, we will finally put this objection to rest, unless we better achieve verification of PG by experimental means first.

15.2 Equivalence Principle

The allegation that PG would violate the Equivalence Principle must have been a misconception in view of our previous explanation. PG actually frees us from having to resort to the Equivalence Principle, which arose out of the need to understand the nature of force initially perceived as arising either from a gravitational field or from a moving mass under acceleration by an applied external force. PG finds no distinction between these two kinds of force, as the flow of gravions produces the same force in both situations (systems). For the first time, we have a tangible explanation of the **phenomenon** of equivalence of force. The gravitational force experienced by a body as attraction (pull) is actually a push force, namely, the sum total of all elementary push forces distributed in the bulk of the mass and arising from absorbed gravions. The latter force is of the same nature as the push force applied to a hypothetical elevator in free space, inside which we would experience an equivalent force. This equivalent force need not be such (equivalent) axiomatically, because it is “prima-facie” push in nature. Hence the Equivalence Principle per se vanishes without ever being in conflict with PG.

Nevertheless, if the Principle emanates from (or is based upon) the equality of the gravitating mass to the inertial mass, then PG is clearly at variance. However, PG quantifies the variance as being extremely small to easily detect in the human laboratory, but, hopefully, big enough to measure in flyby experiments and planetary orbits. If the EP is described as equality of masses (gravitational and inertial) then PG clearly violates it. Conversely, if PG provides the true relationship between the two masses via $m_e = qm$, then EP violates nature and becomes redundant under PG. Expressed differently, if “equivalence” means true proportionality but not equality, then PG provides exactly this proportionality in a tangible, physical and explanatory form.

The above ideas summarize the analysis of Section 14.2, but we should also stress that the EP seems to be only an arbitrary approximation for scales of our immediate experience. This approximation breaks down at very large masses, or densities. Large densities occur in white dwarfs, neutron stars and black holes (large scales), but they also occur at nuclear and sub-nuclear particles (small scales). Thus, the finding that EP clearly breaks down at quantum levels (Kajari *et al.*, 2010) may not be a mere coincidence, but a great consistency with our independent findings on EP. The inertial and gravitational masses are not equal, whilst the original “gedanken” conception of the EP is now redundant needlessly locking down further development of physics for over a century.

Finally, in view of the possibility to decipher the meanings of matter, inertia and mass per Sections 14.5 and 16, PG appears to be on strong ground but not necessarily consistent with the EP, or with the theory of relativity in every respect.

15.3 Theory of relativity

It has been argued that PG is incompatible with the established theories of relativity. It is often argued that since the general theory of relativity (GR) is continually verified by contemporary measurements with great accuracy, PG not emanating from within GR must be wrong. However, the counter-argument may be that PG is a re-appraisal of classical Newtonian mechanics, upon which to build and extend the current relational developments of relativity. PG explains the generation of a gravitational field around a mass that presumably can be observed and measured identically with existing data. We would suggest that it is prejudicial to think that PG has to arise out of (or fit in) GR, whilst the opposite might be true. Therefore, the two theories may not have to be in conflict upon closer examination.

If gravions travel with the speed of light, then in the steady state, they establish a pushing field that fictitiously appears as an attractive field around the shadowing (gravitating) mass. This field is being established at the speed of light without emanating from the mass, but rather emanating from the surrounding universe. If the mass starts moving at speeds comparable to the speed of gravions (and light), then there will be a disturbance of the surrounding shadowing or warped space (field) due to a time lag that propagates at the gravion speed. This disturbance would be consistent with the gravitational waves scientists are trying to detect.

An analogy may be found in solid state physics near a PN-junction, where “holes” are formed from the absence of electrons on one side of the junction with an equal amount of excess electrons on the other side. These holes are treated, or behave, like a positive current of charge moving in the opposite direction to electrons with negative current. GR then is like it is treating gravity as gravion-holes apparently emanating

from (or associated with) the mass, whilst in reality it is the real gravions (particles) moving in the opposite direction towards the gravitating mass that should be considered, or equivalently considered. The end result (force and acceleration) appears to be the same by both approaches. Both ways of creating a field around a mass presumably create identical apparent outcomes.

We propose then that the gravitational field described by PG and the field described by GR are quantitatively identical at every point around a stationary material body. The difference is that PG tells us how/why this is formed (i.e. its origins), whilst GR remains mute about the origin of the same field, but it yields verifiable measurements, anyway. The latter is sometimes described like “GR generates correct results for the wrong reasons”. However, knowing the origins of gravity is a fundamental difference between GR and PG that could get us over the existing barriers in physics.

When we start applying PG to moving bodies with significant speed relative to the speed of gravions, then we may be able to borrow the mathematical tools already developed for relativity, special and general, to describe the same resulting effects and measurements. There is probably no restriction to the importation of Special Relativity as is. The mathematical derivations and achievements of GR may also be transferred and used in PG, in particular as they relate space and time. This transfer might be particularly useful where GR actually succeeds and discarded where GR fails (e.g. at very long distances, etc). The present work has only dealt with PG in the steady state without ever involving time effects yet. Therefore, it might be premature to argue that the two theories are in conflict.

Arguments of the type, for example, that because the Mercurial precession can be explained by GR is proof and manifestation of the success of GR should by no means be used to oppose PG. The same fields being established also by PG should arrive at the same outcomes. In fact, PG provides a new framework to re-appraise the contributions of other planets on Mercury’s precession by expanding classical mechanics with PG, which may produce a further refinement of the same calculations taking into account the real density and mass distributions of all the planets contributing to this precession. The other argument that the Sun bends the star light is not the privilege of GR only, because PG can do the same thing on photons by the pushing gravions presumably at the same (correct) deflection angle.

If at first sight the above assertions might seem simplistic, it is because there is a large volume of phenomena to be understood under PG, before we make further assertions. For example, could the temporal part of the metric in relativity, which determines the rate at which clocks tick and is responsible for Newtonian gravity, relate to the rate of gravion flux intensity? Could the increase of mass (relativistic mass) of a moving body as it approaches the speed of light be tied and explained in the new terms of real and effective mass? Should we, perhaps, re-appraise the meaning of inertial mass in conjunction with the meaning of matter and “stuff”? In general, could the theoretical concepts of relativity achieve an embodiment in PG theory?

The above important questions together with issues raised in Section 14 may now be better understood in the hope to further an inquiry into the novel PG theory. We may be faced with any of the following outcomes: (a) PG and GR may complement each other, (b) GR may be expanded to incorporate PG ideas, (c) PG may replace GR as an all inclusive description of experience, or (d) PG becomes unsustainable. The examination of these possibilities is the next challenge that we face for building a dynamic PG. The preceding trials may serve to provide some indication of what may come next. Clearly, such a task is huge and falls outside the capacity and resources of a single author. Hopefully, the learned adherents of GR can make a critical contribution.

In summary to the related objections, relativity may not be presented as reason for rejection of PG. Even if it appears that PG is not consistent with certain established ideas of GR, the “jury remains out” until sufficient experimental evidence is gathered in support or not of PG. It may ultimately be that there is a substantial overlap or correspondence of ideas and conclusions between PG and GR, but also with a fundamental departure between the two theories from some point onward (see Section 16).

15.4 Drag

It has been argued that push particles (original ultramundane corpuscles) would introduce a drag force on the orbiting Earth, eventually slowing down the planet to ever closer orbits around the Sun. This would indeed be a consequence, if the particles were acting like classical mechanical balls. However, the gravions are relativistic with no difference in speed relative to the planet motion. Gravions are not expected to make a difference over any effects already experienced with photons over the broadest spectrum of wavelengths originating from outer space.

In view of the attempted explanations on the nature of matter, mass, energy and inertia in Section 14, it is implied that the gravions have no drag on the effective mass being energized (generated) by the very same gravions. This is an assumption pending further investigation on the nature of gravions and their interactions with real mass and with themselves.

Further work on PG (see later versions of it) has now advanced an even better understanding of mass and matter (hyle). Attempts have been made to find a relationship between absorptivity and speed, a relationship between mass and speed, and a relationship between mass and hyle. It seems that we may be able to derive some relativistic relationships from the premises of PG theory. We have found that while gravions (and hyle) are being absorbed, hyle is also concurrently emitted by a moving body with a steady state established at constant speed. The net variation of hyle (and mass) takes place only during acceleration (deceleration) of the moving body. It seems that PG may be self sufficient in explaining away the “drag problem” without even having to resort to the special theory of relativity. It should be appreciated that this work remains incomplete needing contributions by many other workers (and time) before uninterested parties rush to dismiss it out of hand on this or that account from the perspective of prior theories.

15.5 Superluminal speed

During the early stages of push gravity theories, the hypothetical corpuscles were required to have some superluminal speed to reduce the expected drag to a practically ineffective minimum. However, this is not required after the advent of relativity and in the light of the present arguments.

15.6 Orbital aberration

It has been further argued that PG would introduce orbital aberration due to the finite speed of gravity created by gravions. This aberration would tend to accelerate an orbiting body away from the other, unless gravity propagates much faster than the speed of light, or must not be a purely central force. It has been further argued that the same finite speed of gravity problem is almost exactly canceled by the mathematics in GR. Now, it is not clear why PG cannot overcome this problem in the same way, if GR can. It is proposed that we may continue to use and adapt aspects and derivations of GR, or postulate an equivalence between GR and PG (at least in part), until it can be finally clarified if this is at all appropriate, or under what conditions.

Nevertheless, recent measurements report that planetary orbits are widening faster than if this were solely through the Sun losing mass by radiating energy. This results in an anomalous increase of the astronomical unit, which might then be explained by the above PG criticism pending further analysis of the situation.

As discussed in Section 14.4, and until we can quantify time effects, PG theory remains incomplete. Any verdict can be postponed, until at least some tests are done to possibly verify the principle of PG.

15.7 Energy and mass considerations

15.7.1 Single sphere absorption

Basically, the most serious criticism arises from the need that the gravions must be absorbed in order to produce a force, but the amount of energy absorption would then be so high as to be unsustainable by the gravitating body. This is the main reason, for which notables like Kelvin, Maxwell and Poincaré (Wikipedia contributors, 2018a; Poincaré, 1908), after initial consideration, moved away from PG. There is no obvious or immediate solution to this major problem haunting any PG theory. For this reason, we based the entire development of PG on the assumption that the absorbed energy is somehow re-emitted. However, until some experiments provide encouragement at least, we are entitled to speculate with some improved models in continuation to previous attempts to overcome this hurdle. Let’s first formulate the energy absorption problem based on derivations in Part 1.

We find the total energy passing per unit surface area of a sphere and absorbed by the bulk in the sphere: We start with the absorbed gravions (energy) inside the solid angle subtended by the sphere at point O (see Fig. 2), which is given by the previously defined J_a (not J_g):

$$J_a = J_0 f_a = J_0 \int_0^{\varphi_0} 2\pi \sin \varphi d\varphi \cdot [1 - \exp(-k\ell(\varphi))] \quad (187)$$

$$J_a = 2\pi J_0 \int_0^{\varphi_0} \sin \varphi \left[1 - \exp \left(-2kr \sqrt{a^2 - \sin^2 \varphi} \right) \right] d\varphi \quad (188)$$

The above provides the per unit area absorption at each gravion trace direction (not the per unit area of the surface of the sphere). However, at the surface of the sphere (with $r = R$ and $a = 1$), for the absorbed flux density per unit area of the sphere, we must apply the cosine law for oblique incidence and multiply by $\cos \varphi$ yielding the parameter J_{aR} :

$$J_{aR} = 2\pi J_0 \int_0^{\varphi_0} [1 - \exp(-2kR\cos\varphi)] \sin\varphi \cos\varphi d\varphi \quad (189)$$

which can be integrated analytically as per Eq. 36 including the established absorptivity A_R :

$$J_{aR} = \pi J_0 A_R \quad (190)$$

The above provides the absorbed density flux per unit area of the sphere from all directions inside a hemispherical solid angle, i.e by integrating from 0 to $\pi/2$. Thus, we multiply by the surface area of the sphere to obtain the total absorbed density flux, i.e. the total energy per unit time, or power W as:

$$W = 4\pi^2 J_0 A_R R^2 \quad (191)$$

By replacing J_0 from Eqs. 68 and 73:

$$J_0 = \frac{cg_0}{\pi\Lambda} = \frac{cg_0 M_e}{\pi^2 R^2 A_R} \quad (192)$$

we finally obtain

$$W = 4cg_0 M_e \quad (193)$$

from which we have an energy absorption rate per unit effective mass W_{M_e}

$$W_{M_e} = \frac{W}{M_e} = 4cg_0 \quad (194)$$

If we want to use the equation $E = mc^2$, the above energy is equivalent to a mass accretion rate per unit mass:

$$mass_accretion_rate = \frac{4g_0}{c} \quad (195)$$

from which, depending on the prevailing g_0 , we find the absorbed energy. With a moderate level of $g_0 = 10^4$ m/s², we would get about 1.3×10^{-4} kg for every kg of the sphere (say, Earth) every second. This is clearly an enormous amount of energy (mass) that cannot be accounted for by our experience on the planet. An early criticism leveled against PG claimed that the absorbing mass would be doubling every second. This criticism is generally valid even with our much lower accretion rate found here, which we can formulate as follows:

If we again borrow the “ $E = mc^2$ ” equation, we use Eq. 193 to find this accretion or decay as a function of time:

$$W = \frac{dE}{dt} = c^2 \frac{dM_e}{dt} = \pm 4cg_0 M_e \quad (196)$$

$$\frac{dM_e}{M_e} = \pm \frac{4g_0}{c} dt$$

$$\ln M_e = \pm \frac{4g_0}{c} t + constant$$

$$M_e(t) = M_{e0} \exp\left(\pm \frac{4g_0}{c} t\right) \quad (197)$$

where $M_{e0} = 4\pi^2 J_0 A_R R^2 / 4cg_0$ is the initial effective mass at $t = 0$ s, when we imagine a cessation of mass emission or a cessation of the gravion field (mass accretion). This “initial” mass is the effective mass we have introduced up to now, which, for the record, can be expressed also by:

$$M_{e0} \equiv M_e = \frac{\pi^2 J_0 A_R R^2}{cg_0} = \frac{\pi R^2 A_R}{\Lambda} = \frac{S_{xsection} A_R}{\Lambda} = \frac{S_{a-xsection}}{\Lambda} \quad (198)$$

where $S_{xsection}$ is the geometric cross-section of the sphere and $S_{a-xsection}$ is the absorption cross-section.

Eq. 197 provides a time constant $t_0 = c/4g_0$, in which the mass increases by $e = 2.718$ times the initial value or decays to $1/e = 0.368$ of its initial value M_{e0} . Equivalently, the mass doubles or halves in time $t_{double} = t_0 \ln 2 = t_{half} = -t_0 \ln(1/2)$. Caution is drawn to the possibility that these rates of absorption

and decay may characterize the process only around the equilibrium point of the steady-state condition; the entire process of effective mass emergence from real mass, or the decay of effective mass back to real mass may be a multi-staged process, a topic for further study.

The characteristic time constants t_0 , or t_{half} , or t_{double} are additional fundamental constants along with g_0 , J_0 and Λ all directly relating with each other.

To continue with numerical examples, we may use the tentative value of $g_0 = 30000 \text{ ms}^{-2}$ (say, from a “claimed” Allais effect measurement) and with $c = 3 \times 10^8 \text{ ms}^{-1}$, we get $t_0 = 2.5 \times 10^3 \text{ s}$ (i.e. 41.7 min) and $t_{half} = t_{double} = 1732.87 \text{ s}$, i.e. 28.9 min. This is akin to radioactivity, the theories of which may also be better understood on the basis of PG. [Curiously, the decay time of free neutrons falls within the range of the given numerical example. The mean lifetime of a neutron is 879.6 s, which curiously is about half of the preceding halftime]. Incidentally, we have considered only the energy-rates, but not the number-rate of absorbed gravions and the number-rate of emitted particles. These two number-rates are thought to be very different from each other, presumably by many orders of magnitude. The mechanism for possible re-emission is discussed under considerations of the second law of thermodynamics in the next section. This issue will be the subject also of a quantum push gravity (QPG) theory later.

The above derivations about an absorbed energy (mass) that allegedly cannot not be re-emitted at a steady-state point are the most telling reason for the rejection of PG, as has been the case with mainstream physics to date. Therefore, this constitutes a critical point whether to continue with this theory or come to an end of this investigation once more. The present author is of the opinion to persist in finding some way(s) to push through this barrier, literally. That is because the preceding findings have produced a system of consistent outcomes with Newtonian mechanics as the limiting case, and because it promises to resolve many other cosmological problems on a new basis. At any rate, we investigate the “what if” case, the outcomes of which may be compatible with experience. We may recall an analog situation early in the 20th century, when the orbiting electrons should be emitting electromagnetic radiation, the lack of which did not deter the then visionary scientists to introduce and accept the orbital model of the atom. Thus, instead of rejecting the PG theory, we may have to accept that the dissipated energy by gravions manages somehow to escape out of the absorbing mass in a different form of radiating particles. A new motto could then be “*what goes in must come out*”, but catchphrases don’t make science on their own, unless they are confirmed without leading to another impasse: The above demand allegedly leads to another violation, namely, of the second law of thermodynamics, an objection discussed separately next.

Equivalent alternative formulations to derive the gravion absorption rate by a single (lone) material sphere are provided in Appendix D.2.1, etc.

15.7.2 Planetary absorption

The preceding analysis of energy absorption by a single sphere is further expanded for the case of two spheres in section 16, whereby we also find a relationship between force and mass. This finding goes beyond the criticism based on the alleged catastrophic energy absorption. It constitutes a novel understanding that can be used for the multi-body interaction, of which the planetary absorption is just one aspect of PG theory and should be treated in its own right.

15.8 Second law of thermodynamics

It has been argued that the gravions, if re-emitted as different particles to carry away the dissipated energy, would violate the second law of thermodynamics, which was the reason for rejecting the re-emission of particles/energy as initially (tentatively) proposed but abandoned by notables such as Kelvin, Poincaré, Lorentz and Thomson (Wikipedia contributors, 2018a). However, if we look closer at the intrinsic meaning of this law, it may not necessarily be violated overall. This arises from the fact that the law relates to the most probable state of a closed system having the maximum entropy. The entropy S relates with the number of accessible states Ω via

$$\Omega = \exp(S/k) \tag{199}$$

(k here is the Boltzmann constant) and the probability P of finding the system in that state is

$$P \sim \Omega = \exp(S/k) \tag{200}$$

Now, when the system has a relatively small number of accessible states, the fluctuations can be very frequent, wide and repeatable, i.e. recurrence of unstable states may be quite feasible within the time scale of gravion frequency absorption. The consequence of this is that the system can often be found “momentarily” in a state of decreased entropy favoring the emission of some augmented (with accreted mass) particle out

of the system. This happens when by random redistribution of mass and energy within the subsystem generates a sub-particle capable of overcoming the constraints that keep the subsystem together. When enough quantitative material and energy accumulation has occurred (accreted), the subsystem bounces emitting a new particle, all of this on an extremely short time-scale (appearing to us). The particles of the subsystem co-operate to get rid of and push out one of their own members every-now-and-then, often or not in the time scale of the subsystem. In other words, the second law of thermodynamics does not prevent us from accepting that matter/energy can be re-emitted after a number of trial fluctuations following a certain number of gravion absorption inside a proton, electron, neutron or any other nuclear, sub-nuclear, or elementary particle (subsystem). Thus, what was initially conceived by the critics as thermal dissipation inside matter in general, it will not appear as known chemical (molecular) heat that would melt and evaporate the planet. It would only appear as internal energy of a particle that is not thermally coupled with an atom or molecule via some sort of recoil action during the said re-emission. The re-coil produced by the proposed re-emission is taken up and averaged out by the subsystem behaving under the established quantum mechanical laws. In fact, it might be that the underlying mechanism of quantum mechanical randomness may be caused exactly by such re-coil of the subsystems of particles. Electrons and nuclear particles move about randomly per quantum mechanics. This model further assumes that the re-emitted particles are also penetrating the surrounding matter out of the planet with a long enough mean free path as not to heat the planet catastrophically but not long enough as to act like gravions in generating gravity (i.e. canceling out gravity). It is only the very long mean free paths of gravions that generate gravity among planets and stars, while the second generation emitted particles, as proposed here, behave like a diffusing gas out of the planet, perhaps, with some but not catastrophic heat dissipation. It may be that part of, if not all, the heat in the core of planets is generated by this mechanism in an analogous way, in addition to, or in lieu of, the heat being produced by radioactivity per prevailing theories.

We need not at this point specify the exact nature of the particles being re-emitted, other than for them to be able to carry away the absorbed gravion energy, or a critical part thereof. It is left for further investigation by particle and nuclear physics to establish if any of the known particles qualifies to play this role, as for example, neutrinos might (or might not) serve this purpose. Alternatively, we may build on a new model to describe the properties and consequences of this second generation of particles emanating from the primary gravion flow.

In support of the above general proposal, we may site a similar situation that explains radioactivity. Particles can rearrange in the nucleus, or change from one type to another statistically over time. Random quantum fluctuations can promote relaxation to a lower energy state and decay via quantum tunneling. Radioactive decay half-life varies over many orders of magnitude on a timescale down to 10^{-23} seconds (Wikipedia contributors, 2019d). In our proposed analog, we may envisage all sub-nuclear particles including protons, electrons, positrons, etc. to undergo such statistical fluctuations inside themselves at even extremely smaller time scales beyond the range of our measuring instruments, in effect, appearing like providing a continuous absorption of gravions and re-emission of secondary type-II particles diffusing in the surrounding material space without causing further gravitation or catastrophic heat. This continuous absorption then is tantamount to a continuous push without the feared catastrophic melting down.

The above proposed model should not be less plausible than the latest quantum fluctuation theories (Wikipedia contributors, 2019c). It is in accord with the fluctuation theorem and the ongoing discussion, research and experiments relating to Maxwell's demon.

Thus, the present framework in understanding gravity should not be inconsistent with modern theories. Quantum field theory is about very small stuff, small particles (the standard model). Gluons bind quarks together. Quantum gravity considers loops of gravitational force, then we get knots, loop quantum gravity and time disappears (problem of frozen time). These quantum states of space fluctuate, fluctuations in the quantum states of space create the appearance of time. These loops exist on the scale of Plank length. A proton contains 10^{65} quantum volumes, whilst gravitons is said to carry the force of gravity by exchanging them, (the photon carries the electromagnetic force, so the graviton carries the gravitational force), but gravitons are thought to be pseudo-force particles according to loop theory. The quantum nature of space does not allow singularities, whilst the universe did not come about with a bang but with a big bounce [Jim Baggott: <https://www.youtube.com/watch?v=dW7J49UTns8>]. All these latest conceptions might be further adjusted and advanced by the new understanding of PG, so that our approach should not be less plausible than all these other modern models and proposals. In fact, PG seems to be consistent with the above theories so that PG may act as a resolution by binding together of the best of elements in those theories.

Finally, if the main concern of PG theory has been the huge amount of energy or mass required to be absorbed in order to result in the measured acceleration on a planet, the likely revelation in Section 14.5 may help. In view of the idea of the creation of effective mass (Newtonian mass) by gravion absorption, the

absorption becomes a blessing rather than a curse: The large absorption is consistent with a large presence of planet mass, however, subject to a balancing rate of outflow of the same energy. We proposed a mechanism for such an outflow via the fluctuation theorem above. In the steady state, the outflow must be proportional to the steady state effective mass m_e as in the general formulation found by Eq. 196:

$$\frac{dE}{dt}(\text{inflow}) = \frac{dE}{dt}(\text{outflow}) = \text{constant} \cdot M_e \quad (201)$$

16 Two-sphere variation of mass and force

In continuation to and based on preceding analysis, we can derive some important relationships between mass or energy and force for two material spheres. The energy absorption rate given for a single sphere by Eq. 191 is derived by the universal graviton intensity J_0 times a factor S_a . For a single (lone) sphere and according to Eq. 191 the latter factor is:

$$S_a = 4\pi^2 R^2 A_R \quad (202)$$

and is involved in the known relationships:

$$S_a J_0 = 4cg_0 M_e \quad (203)$$

$$S_a \frac{cg_0^2}{\pi^2 G} = 4cg_0 M_e \quad (204)$$

$$S_a = 4\pi^2 G \frac{M_e}{g_0} \quad (205)$$

The S_a is a characteristic surface area pertaining to the omnidirectional absorption of gravitons from all directions around the sphere with radius R and can be also computed directly from the constitutional equations of graviton absorption provided in the Appendix. We will later see that this relates via a factor 4π to an effective cross-section for a classical unidirectional absorption of a beam of particles.

With S_a derived (or computed), we can then find the corresponding effective mass as:

$$M_e = \frac{g_0}{4\pi^2 G} S_a = \frac{S_a}{4\pi\Lambda} \quad (206)$$

We can readily ascertain that, S_a being an effective absorption area and the universal constant Λ being an area per unit mass, correctly yields a mass M_e . It is an important finding and understanding that the effective mass is the ratio of these two parameters. Note: $S_a = 4\pi S_{a-xsection}$ from Eq. 198.

Up this point, we have considered a single (or lone) material sphere, but this begs the question what happens in the presence of another material sphere at a distance r in the neighborhood. The answer is found by considering the constitutional equations of absorption simultaneously for the two spheres. This is done in considerable detail in the Appendix. We apply those methods here to three representative cases with a brief description of the approach. To discuss and understand what happens, we have computed in one case, by way of example, the Earth-Moon interaction as we vary the distance. In a second case, we repeat the same for two very dense spheres, one of which is very small. In the third case, we use two very dense sphere with both being also extensive (large).

We have developed and used two equivalent methods in the Appendix, namely, one integrating through the bulk of each sphere, the other around the surface of the sphere. This is possible by noting that for every internal point (in the bulk), all possible graviton traces must cross the surface. Conversely, all graviton traces through every point on the surface account for the entire bulk points twice (note that in Eq. 191, we used only one direction of flow at each point, so that we summed over the entire surface without dividing by 2).

With reference to the Appendix and related figures, we compute various fractions of graviton absorption pertaining to two kinds or classes of graviton traces or paths through each sphere. There is one class of traces crossing only one sphere, to which we refer with the term “single”, or “lone” trace. The other class of traces belongs to (i.e. they cross) both spheres, to which we refer with the term “joint” trace. Gravitons along single paths produce no net force as they travel in opposite directions in equal numbers. Nevertheless, they are absorbed by a certain amount in each direction along the chord length of a sphere, the total amount of which relates to certain effective mass. Gravitons along joint paths produce a net force along the trace due to the unequal amount of gravitons entering from the two ends of the chord. In addition, they are also absorbed by a certain amount in each direction, the total of which again relates to a certain effective mass. The task is

to find both the net force exerted on one of the spheres by the other and at the same time the total effective mass of the sphere “created” by (or related to) the absorbed gravions.

At the outset, we need to choose one of the two spheres for investigation of force and total absorption. Let this be sphere_2 and let’s apply the “surface” method of investigation to find the total gravions absorbed (we investigate the force afterwards). We consider what happens at every point O on the surface of this sphere and integrate over the entire surface for the total result of absorption relating to force or effective mass. A chord OC traversed by “single” traces yields an absorption factor $2(1 - \exp(-k_2OC))$. However, if chord OC is traversed by “joint” gravion traces, the absorption factor becomes $(1 - \exp(-k_2OC))(1 + \exp(-k_1AB))$, where A_1B_1 is the jointly traced chord of the other sphere_1, with corresponding absorption coefficients k_2 and k_1 . We integrate at point O separately all single and all joint traces with respect to the azimuth and zenith angles around the axis normal to the surface of the sphere at point O:

$$M_{ar-single} = \int_{\varphi_1}^{\varphi_2} \int_{\theta_1}^{\theta_2} (2(1 - \exp(-k_2OC))) \sin \varphi_z \cos \varphi_z d\theta_z d\varphi_z \quad (207)$$

The above outcome is the same for all points on an elementary surface annulus by rotation around the axis joining the two spheres at angle ω . This elementary surface is $2\pi \sin \omega R_2^2 d\omega$, so that by a final integration over this angle, we obtain the end result:

$$S_{ar-single} = \int_0^\pi M_{ar-single} \cdot 2\pi \sin \omega R_2^2 d\omega \quad (208)$$

We follow the same steps for the “joint” traces of sphere_2:

$$M_{ar-joint} = \int_{\varphi_1}^{\varphi_2} \int_{\theta_1}^{\theta_2} (1 - \exp(-k_2OC))(1 + \exp(-k_1AB)) \sin \varphi_z \cos \varphi_z d\theta_z d\varphi_z \quad (209)$$

$$S_{ar-joint} = \int_0^\pi M_{ar-joint} \cdot 2\pi \sin \omega R_2^2 d\omega \quad (210)$$

The total characteristic absorption surface is:

$$S_{ar-total} = S_{ar-single} + S_{ar-joint} \quad (211)$$

The notation “ ar ” in the subscripts above stands for “absorption” at distance “ r ”. Now, there is an important new quantity to consider. That is the difference between the total absorption of sphere_2 being at distance r from sphere_1 and the absorption that sphere_2 has when it is at infinite distance from the other, in other words, when it is away from the influence of any other bodies. We have already found the latter by Eq. 202. It is instructive to write the corresponding equations for this quantity starting with the corresponding factor for a chord OC. The “single” contributions cancel out leaving only the difference of the “joint” terms between the two situations. This is easily found to be $(1 - \exp(-k_2OC))(1 - \exp(-k_1AB))$, with which we can write the corresponding integrations:

$$M_{ar-netloss} = \int_{\varphi_1}^{\varphi_2} \int_{\theta_1}^{\theta_2} (1 - \exp(-k_2OC))(1 - \exp(-k_1AB)) \sin \varphi_z \cos \varphi_z d\theta_z d\varphi_z \quad (212)$$

$$S_{ar-netloss} = \int_0^\pi M_{ar-netloss} \cdot 2\pi \sin \omega R_2^2 d\omega \quad (213)$$

We use the term “net loss” to refer to this absorption in an effort to distinguish it from present (current) absorption taking place at distance r , because it does not exist, i.e. it is not current, but was present when the sphere was “lone” but now this amount of gravion absorption has gone missing. This is caused by the perturbation of the universal gravion flux by the other sphere. We can then write the more general equation with these parameters as:

$$S_a \equiv S_{a-sum} = S_{ar-total} + S_{ar-netloss} = S_{ar-single} + S_{ar-joint} + S_{ar-netloss} \quad (214)$$

All this will be better understood and discussed looking at the results of the following three cases.

r , m	$M_{er-single}$, kg	$M_{er-joint}$, kg	$M_{er-loss}$, kg	M_{e-sum} , kg	<i>Asymptotic loss</i>
12742000	5.9134E+24	5.8939E+22	<i>4.7876E+19</i>	5.9724E+24	<i>4.5098E+19</i>
25484000	5.9583E+24	1.4058E+22	<i>1.1431E+19</i>	5.9724E+24	<i>1.1274E+19</i>
50968000	5.9689E+24	3.4775E+21	<i>2.8281E+18</i>	5.9724E+24	<i>2.8186E+18</i>
101936000	5.9715E+24	8.6712E+20	<i>7.0524E+17</i>	5.9724E+24	<i>7.0465E+17</i>
203872000	5.9722E+24	2.1664E+20	<i>1.7620E+17</i>	5.9724E+24	<i>1.7616E+17</i>
407744000	5.9723E+24	5.4152E+19	<i>4.4043E+16</i>	5.9724E+24	<i>4.4041E+16</i>
815488000	5.9724E+24	1.3537E+19	<i>1.1010E+16</i>	5.9724E+24	<i>1.1010E+16</i>

Table 9: Variation of various fractions of the Earth effective mass versus distance using $R = 6371000$ m, $k = 1.16248157479707E - 09$ m⁻¹ and $g_0 = 1000$ ms⁻² (CASE_1)

r , m	$M_{er-single}$, kg	$M_{er-joint}$, kg	$M_{er-loss}$, kg	M_{e-sum} , kg	<i>Asymptotic loss</i>
12742000	6.3579E+22	9.8495E+21	<i>4.7876E+19</i>	7.3477E+22	<i>4.5098E+19</i>
25484000	7.1141E+22	2.3241E+21	<i>1.1431E+19</i>	7.3477E+22	<i>1.1274E+19</i>
50968000	7.2900E+22	5.7361E+20	<i>2.8281E+18</i>	7.3477E+22	<i>2.8186E+18</i>
101936000	7.3333E+22	1.4295E+20	<i>7.0524E+17</i>	7.3477E+22	<i>7.0465E+17</i>
203872000	7.3441E+22	3.5710E+19	<i>1.7620E+17</i>	7.3477E+22	<i>1.7616E+17</i>
407744000	7.3468E+22	8.9259E+18	<i>4.4043E+16</i>	7.3477E+22	<i>4.4041E+16</i>
815488000	7.3474E+22	2.2314E+18	<i>1.1010E+16</i>	7.3477E+22	<i>1.1010E+16</i>

Table 10: Variation of various fractions of the Moon effective mass versus distance using $R = 1737000$ m, $k = 7.02425385602087E - 10$ m⁻¹ and $g_0 = 1000$ ms⁻² (CASE_1)

CASE_1 (Earth-Moon). The masses and radii used are taken from Table 3 together with their absorption coefficients from Table 2. We performed the above integrations separately for the Earth and Moon, each one being the sphere of investigation with regards to its own graviton absorption. The numerical results of the above integrals are better shown first in table form for all three factors for Earth and Moon in Tables 9 and 10. The distance is varied in multiples of Earth radius from 2 to 128 radii doubling each distance. Actually, we have converted the S_- parameters to an effective mass via the conversion Eq. 206, in order to make it more tangible with our familiar (perhaps) “mass” concept. These masses $M_{er-single}$, $M_{er-joint}$, $M_{er-loss}$ and $M_e = M_{e-sum}$ correspond to the terms of above Eq. 214.

We note that the variation of mass is small but significant within a few radii distance, but it approaches fast and asymptotically the “lone” mass, as we increase the distance; the sum of the three fractions of mass is constant with distance and equal to the lone mass, as it should. The “single” component increases, whilst the “joint” component decreases as we increase the distance, so that their sum is always much closer to the “lone” mass. We can see this by the variation of mass loss being 5 orders of magnitude for the Earth and 3 orders for the Moon at the shortest distance below the “lone” mass, whilst it becomes 8 and 6 orders of magnitude at 128 Earth radii. We further note that the net loss is the same for the Moon and Earth, as should be expected on account of the symmetry in the chords of the net loss factor. We investigate the mass loss also in graph form in Fig. 20 but by plotting the net loss of absorption factor $S_{a-netloss}$ on logarithmic scales for both axes. We have also added an extra four point up to 2048 radii distance to assist the look of a trendline. The fitted straight line ($y = -2.0048x + 22.33$) is indistinguishable from the computed curve indicating a strong inverse square distance relationship. We suspected that this overlap may be only due to a Newtonian approximation for this case; the absorptivity for Earth being $A_{R-earth} = 0.00982$ and for Moon $A_{R-moon} = 0.00162$ with $g_0 = 1000$ ms⁻² clearly place the case very early on the A_R graph in Fig. 3. This prompted us to repeat the same investigation for other denser and/or more extensive spheres below.

CASE_2 (Small-and-large-dense-spheres). An extreme case at the other end of Newtonian regime is to use $A_R = 0.99$ (near saturation absorption). We can do this using the Earth radius R_2 and corresponding $k_2 = 1.10987744324188E - 06$ m⁻¹. We can pack a large amount of effective mass inside the given radius depending on the g_0 that we can choose according to Eq. 206. Let’s choose $g_0 = 10^5$ ms⁻². For the second interacting sphere, we chose a very small one with radius $R_1 = 1$ m but with the same $A_R = 0.99$ corresponding to $k_1 = 7.07102919089469E + 00$ m⁻¹. The results for each sphere are given in Tables 11 and 12. Then likewise, we plot the net loss factor $S_{a-netloss}$ in Fig. 21.

Now, we can make the following observations: The mass losses for the large gravitating sphere are practically (relatively) negligible being 14 orders of magnitude below that of the lone mass, as is also the “joint” fraction of mass, whilst the “single” fraction is practically equal to the lone (not enough decimal places are provided in the limited width of the table). However, the joint and net loss masses of the small sphere

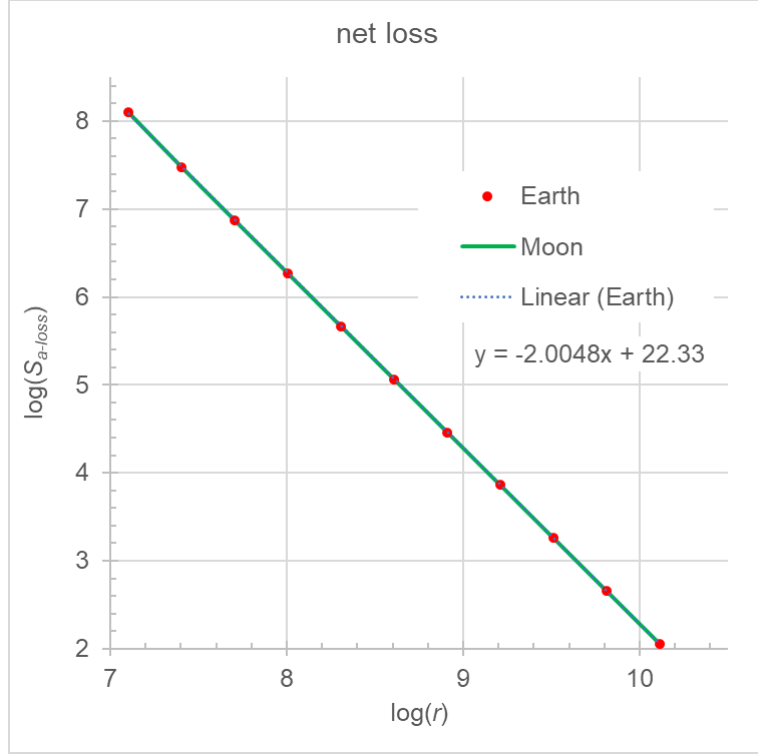


Figure 20: Absorption loss of Earth and Moon versus distance (CASE_1)

r , m	$M_{er-single}$, kg	$M_{er-joint}$, kg	$M_{er-loss}$, kg	M_{e-sum} , kg	Asymptotic loss
6371002.0	6.0209E+28	7.0314E+14	6.8921E+14	6.0209E+28	3.6713E+14
6.3711E+06	6.0209E+28	7.0065E+14	6.8887E+14	6.0209E+28	3.6712E+14
6.3716E+06	6.0209E+28	6.8829E+14	6.8678E+14	6.0209E+28	3.6706E+14
6377371.0	6.0209E+28	6.3098E+14	6.7466E+14	6.0209E+28	3.6640E+14
7008100.0	6.0209E+28	4.3435E+14	4.2575E+14	6.0209E+28	3.0341E+14
7645200.0	6.0209E+28	3.3379E+14	3.2718E+14	6.0209E+28	2.5495E+14
8919400.0	6.0209E+28	2.2439E+14	2.1995E+14	6.0209E+28	1.8731E+14
12742000.0	6.0209E+28	1.0029E+14	9.8300E+13	6.0209E+28	9.1782E+13
25484000.0	6.0209E+28	2.3783E+13	2.3312E+13	6.0209E+28	2.2946E+13
50968000.0	6.0209E+28	5.8751E+12	5.7588E+12	6.0209E+28	5.7364E+12
101936000.0	6.0209E+28	1.4645E+12	1.4355E+12	6.0209E+28	1.4341E+12
203872000.0	6.0209E+28	3.6586E+11	3.5861E+11	6.0209E+28	3.5852E+11
407744000.0	6.0209E+28	9.1447E+10	8.9637E+10	6.0209E+28	8.9631E+10
815488000.0	6.0209E+28	2.2861E+10	2.2408E+10	6.0209E+28	2.2408E+10

Table 11: Variation of various fractions of the effective mass of the large dense sphere versus distance, i.e with $R_2 = 6371000$ m and $k_2 = 1.10987744324188E - 06$ m⁻¹(CASE_2)

r , m	$M_{er-single}$, kg	$M_{er-joint}$, kg	$M_{er-loss}$, kg	M_{e-sum} , kg	$Asymptotic\ loss$
6371002.0	1.1659E+12	7.9297E+14	<i>6.8921E+14</i>	1.4834E+15	<i>3.6713E+14</i>
6371063.7	6.6336E+12	7.8784E+14	<i>6.8887E+14</i>	1.4834E+15	<i>3.6712E+14</i>
6371637.1	2.0976E+13	7.7560E+14	<i>6.8678E+14</i>	1.4834E+15	<i>3.6706E+14</i>
6377371.0	6.6288E+13	7.4240E+14	<i>6.7466E+14</i>	1.4834E+15	<i>3.6640E+14</i>
6434710.0	2.0822E+14	6.5665E+14	<i>6.1848E+14</i>	1.4834E+15	<i>3.5990E+14</i>
7008100.0	6.1796E+14	4.3964E+14	<i>4.2575E+14</i>	1.4834E+15	<i>3.0341E+14</i>
7645200.0	8.1995E+14	3.3622E+14	<i>3.2718E+14</i>	1.4834E+15	<i>2.5495E+14</i>
8919400.0	1.0381E+15	2.2527E+14	<i>2.1995E+14</i>	1.4834E+15	<i>1.8731E+14</i>
9556500.0	1.1056E+15	1.9105E+14	<i>1.8668E+14</i>	1.4834E+15	<i>1.6317E+14</i>
12742000.0	1.2846E+15	1.0043E+14	<i>9.8300E+13</i>	1.4834E+15	<i>9.1782E+13</i>
25484000.0	1.4362E+15	2.3790E+13	<i>2.3312E+13</i>	1.4834E+15	<i>2.2946E+13</i>
50968000.0	1.4717E+15	5.8755E+12	<i>5.7588E+12</i>	1.4834E+15	<i>5.7364E+12</i>
101936000.0	1.4805E+15	1.4645E+12	<i>1.4355E+12</i>	1.4834E+15	<i>1.4341E+12</i>
203872000.0	1.4826E+15	3.6586E+11	<i>3.5861E+11</i>	1.4834E+15	<i>3.5852E+11</i>
407744000.0	1.4832E+15	9.1448E+10	<i>8.9637E+10</i>	1.4834E+15	<i>8.9631E+10</i>
815488000.0	1.4833E+15	2.2861E+10	<i>2.2408E+10</i>	1.4834E+15	<i>2.2408E+10</i>

Table 12: Variation of various fractions of the effective mass of the small dense sphere versus distance, i.e with $R_1 = 1$ m and $k_1 = 7.07102919089469E+00$ m⁻¹ (CASE_2)

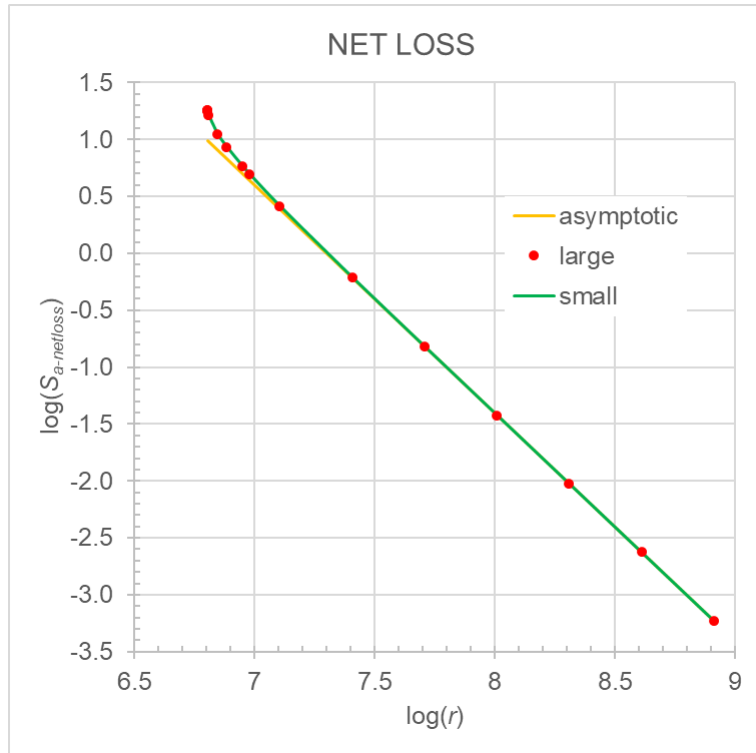


Figure 21: Net loss of small and large dense spheres with asymptotic loss versus distance (CASE_2)

r , m	$M_{er-single}$, kg	$M_{er-joint}$, kg	$M_{er-loss}$, kg	M_{e-sum} , kg	<i>Asymptotic loss</i>
12742000	6.0010E+28	1.0051E+26	<i>9.8516E+25</i>	6.0209E+28	<i>9.1782E+25</i>
25484000	6.0162E+28	2.3793E+25	<i>2.3322E+25</i>	6.0209E+28	<i>2.2946E+25</i>
50968000	6.0197E+28	5.8757E+24	<i>5.7593E+24</i>	6.0209E+28	<i>5.7364E+24</i>
101936000	6.0206E+28	1.4645E+24	<i>1.4355E+24</i>	6.0209E+28	<i>1.4341E+24</i>
203872000	6.0208E+28	3.6586E+23	<i>3.5861E+23</i>	6.0209E+28	<i>3.5852E+23</i>
407744000	6.0208E+28	9.1448E+22	<i>8.9637E+22</i>	6.0209E+28	<i>8.9631E+22</i>
815488000	6.0209E+28	2.2861E+22	<i>2.2408E+22</i>	6.0209E+28	<i>2.2408E+22</i>

Table 13: Variation of various fractions of the effective mass of the bigger dense sphere versus distance with $R_2 = 6371000$ m and $k_2 = 1.10987744324188E - 06$ m⁻¹ (CASE_3)

r , m	$M_{er-single}$, kg	$M_{er-joint}$, kg	$M_{er-loss}$, kg	M_{e-sum} , kg	<i>Asymptotic loss</i>
1.2742E+07	1.2842E+27	1.0065E+26	<i>9.8516E+25</i>	1.4834E+27	<i>9.1782E+25</i>
2.5484E+07	1.4362E+27	2.3800E+25	<i>2.3322E+25</i>	1.4834E+27	<i>2.2946E+25</i>
5.0968E+07	1.4717E+27	5.8761E+24	<i>5.7593E+24</i>	1.4834E+27	<i>5.7364E+24</i>
1.0194E+08	1.4805E+27	1.4646E+24	<i>1.4355E+24</i>	1.4834E+27	<i>1.4341E+24</i>
2.0387E+08	1.4826E+27	3.6586E+23	<i>3.5861E+23</i>	1.4834E+27	<i>3.5852E+23</i>
4.0774E+08	1.4832E+27	9.1448E+22	<i>8.9637E+22</i>	1.4834E+27	<i>8.9631E+22</i>
8.1549E+08	1.4833E+27	2.2861E+22	<i>2.2408E+22</i>	1.4834E+27	<i>2.2408E+22</i>

Table 14: Variation of various fractions of the effective mass of the smaller dense sphere versus distance with $R_1 = 1000000$ m and $k_1 = 7.07102919089467E - 06$ m⁻¹ (CASE_3)

are of the same order of magnitude as the lone, whilst the single mass is a few orders of magnitude less. This was to be expected, since the small sphere, when brought only 2 m above the surface of the large sphere, is practically shielded from about half the gravions from the direction of the large sphere. The unforeseen behavior is that of the net loss, which is better shown in graph form in the provided figure. The curve looks for the most part close to a straight line especially at long distance, but it significantly deviates from the straight line at close range. Further and most importantly, we have now found that the curve becomes asymptotic with a special straight line (on log-log scales) given by:

$$S_{F0} \equiv \frac{\pi A_1 \pi A_2}{r^2} = \frac{\pi^2 A_{R_1} A_{R_2} R_1^2 R_2^2}{r^2} \quad (215)$$

which is identical with the factor in deriving the force between the two spheres in Eq. 85. This is an extraordinary novel finding in PG, which we discuss and analyze after we tabulate the corresponding results of an additional extreme case below.

CASE_3 (Two-large-and-dense-spheres). We again choose a near saturation regime with $A_R = 0.99$, but with both spheres being extensive, i.e. with $R_1 = 1000000$ m, $R_2 = 6371000$ m and corresponding $k_1 = 7.07102919089467E - 06$ m⁻¹, $k_2 = 1.10987744324188E - 06$ m⁻¹. The results are given in Tables 13 and 14. Also, the net loss is plotted in Fig. 22.

Due to the chosen radii, we can't have the situation of a very close range equivalent to that of case_2, so that the asymptotic in case_3 is hardly distinguishable on the plot. However, we can compare at the same short distance of $r = 2R_2$. We note that the deviation of the mass loss from the asymptotic line at $r = 2R_2$ distance is about the same in all three cases, namely, the ratio of $M_{e-loss}/M_{e-asymptotic}$ is 1.062, 1.070 and 1.073 as can be found from the corresponding tables. That is, the variation of mass loss is nearly inversely proportional to the square of distance almost regardless of density, whilst it is the distance, or better the geometry that is the main controlling parameter.

We recall that the gravitational force in Eq. 85 was derived by a simple “reverse engineering approach” from the associated single (or lone) effective masses of each sphere, to which we attached their characteristic absorptivity. We then confirmed the same outcome from the integration of equations constituted from first PG principles (see “bulk method” in the Appendix). We have now further confirmed the same outcome with an alternative approach involving three integrations (the “surface” method), which allowed much improved precision with much shorter computation times including the cases of high absorption with A_R values close to unity. Thus, if we normalize the computed force factor S_F over the theoretical (reverse engineering) force factor denoted by S_{F0} , we invariably find unity as a function of distance, as can be seen by some representative results now shown in Table 15. The deviation from unity beyond 9 decimal places is caused by the set relative integration tolerance of errors, namely, of $epsrel = E - 06$, $E - 05$ and $E - 04$ for the

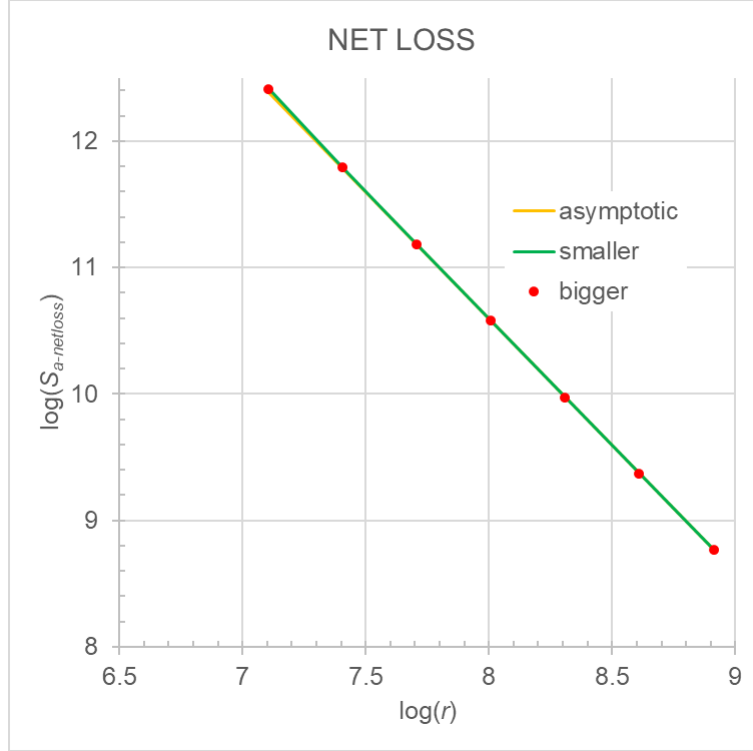


Figure 22: Net loss of two large (smaller, bigger) and dense spheres with asymptotic loss versus distance (CASE_3).

first, second and third integral. By decreasing the tolerance by four orders of magnitude in each integral, we obtain $S_F/S_{F0} = 0.9999999999999999$ (at $r = 12742000.0$, see table).

Now, the variation of effective mass with distance, i.e. a decrease of mass with decrease of distance, means that Newton's gravitational law, if applied using the effective masses, yields a smaller value of force than if the masses were independent of distance as is assumed by Newton. PG finds exactly the latter, i.e. the force behaves as if the masses were invariant without actually being so! This is a novel understanding, unexpected by Newton. It is a consequence of the underlying mathematical (better physical) relationship among the PG parameters involved via the graviton absorption.

The above difference between PG and Newton gravitational laws is fundamental, although they can be both written by a similar equation. They differ in the concept of mass, which is not trivial. Newton does not distinguish the "lone" mass from the mass acted upon by another mass. Thus, we can now distinguish between the two laws as follows:

If we use the actual masses (i.e. acting or effective) then Newton's force should be:

$$F_{Newton} = G \frac{M_{e1r} M_{e2r}}{r^2} = G \frac{(M_{e1r-single} + M_{e1r-joint})(M_{e2r-single} + M_{e2r-joint})}{r^2} \quad (216)$$

whereas PG law using the far away lone masses (see also 85) is:

$$F_{PG} = G \frac{M_{e1} M_{e2}}{r^2} \quad (217)$$

The ratio of the above forces can be written also as a ratio involving the S_- parameters via the proportionality Eq. 205:

$$\frac{F_{Newton}}{F_{PG}} = \frac{S_{a1r} S_{a2r}}{S_{a1} S_{a2}} = \frac{(S_{a1r-single} + S_{a1r-joint})(S_{a2r-single} + S_{a2r-joint})}{S_{a1} S_{a2}} \quad (218)$$

We illustrate the difference between Newton and PG in Fig. 23 by plotting the above ratio (normalizing) as a function of distance for the same three cases. The importance of this difference can now be better appreciated by considering the involvement of the mathematical derivations dictated by PG and presented in the Appendix. The coincidence in mathematical form is uncanny, except that Newton's gravitational law is both empirical and approximate, whereas PG gravitational law is derivable and precise.

	CASE_2	CASE_3
r	S_F/S_{F0}	S_F/S_{F0}
6371002.0	0.9999999942	
6377373.0	1.0000000084	
6434712.0	1.0000000068	
7008102.2	1.0000000035	
8919402.8	1.0000000030	
9556500.0	1.0000000029	
12742000.0	0.9999999747	0.9999999726 0.999999999990
31855000.0	1.0000000023	
63710000.0	1.0000000021	1.0000000021
318550000.0	1.0000000020	1.0000000020
637100000.0	1.0000000020	1.0000000020

Table 15: Computed S_F over theoretical S_{F0} force factor ratio versus distance for CASE_2 and CASE_3; second value with decreased tolerance at $r = 12742000.0$ m

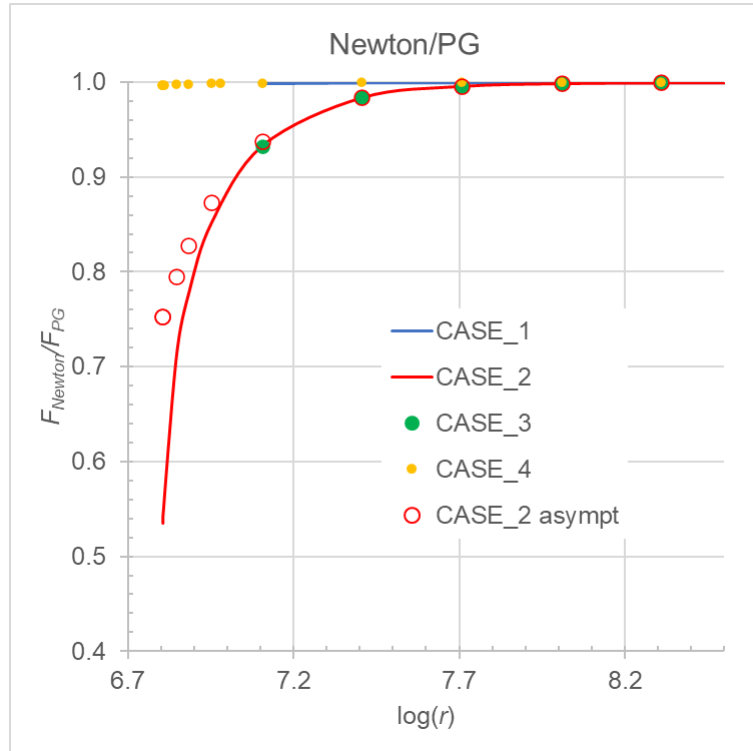


Figure 23: Ratio of Newton/PG forces against distance for four cases of density and size of spherical masses

We see that case_1 (Earth-Moon) is very close to Newtonian behavior, but not so when the absorptivity A_R increases. Has conventional physics found how very dense bodies interact at close range, or only now PG reveals exactly that behavior? The present findings can afford us a deeper understanding of the notions of mass and force. We note that the initial integrand during the derivation of force and net loss have an identical factor apart from the trigonometric factors used to calculate the directional (projection of) flow of gravions. This applies with both methods, bulk or surface (see Appendix). There is clearly a common denominator under the idea of force and mass. The common denominator is the push gravions. Whereas the effective mass is made from gravions being absorbed from all possible directions, force is made from the net directional absorption of gravions between the centers of spheres, or presumably between the “centers of gravity” of any two bodies in a general case (to be shown in later PG development). In other words, effective mass and force have a common cause, namely, the rate of gravion absorption. Mass is the omnidirectional gravion absorption resulting in a scalar quantity, whilst force is the component of gravion absorption in a particular direction defined by two bodies at a distance apart, resulting to a vector quantity.

16.1 Discussion

If PG can be experimentally confirmed and if Fig. 23 correctly reveals the deviation of Newtonian mechanics from actual physical processes, then EP, the equivalence principle emanating from Newtonian experience and carried over to GR, ceases to apply. That means that EP is not only redundant as previously suggested, but it may be an invalid one. We may have to reassess our own stance vis-a-vis EP (see Section 15.2), i.e. we may have to go from a defensive argument to a critical one against it. Here, it is important to clarify that the critics of PG citing the equivalence principle as reason for rejection of PG have presumably done so for different reasons, because they did not have our development of PG in front of them. In the light of the present findings, we have to say that PG seems to contradict the EP, but this is no reason to oppose PG. Conversely, it may be a reason to reassess the theories based on EP. It may be the reason why current theories have unsolved fundamental problems. Then, use of EP as basis for rejection of PG would be arbitrary. It may eventually be that EP is the pivot point between GR and PG, i.e. which direction to take. This can only be arbitrated by a proper experimental assessment of PG, whilst all hitherto tests of EP may have been simply inadequate.

Should we then realign the conventional meaning of “intrinsic” mass? Should this be the effective mass of a body away from other material bodies, because the effective mass varies with the distance from other bodies, albeit imperceptibly in Newtonian mechanics? This is clearly explained under the platform of PG. We distinguish the three components of effective mass, namely, “joint”, “single” and “loss” mass. The sum of these three components is a constant (at the prevailing J_0 , or g_0 or Λ) equal to the isolated lone body’s mass, which we may now call “intrinsic” mass, or use another term to describe the new understanding (sooner or later, we will have to deal with the question of terminology in a more consistent and comprehensive way, but we can await for more results, especially a confirmation of PG). The finding that the force is derived from the product of such intrinsic masses, whilst they are actually smaller at a given distance, could be the key for explaining why the equivalence principle has imposed itself for such a long time. It provides a fortuitous condition that yields correct answers for things that don’t really exist. It assumes masses that don’t exist, but their assumed value yields correct outputs such as the gravitational law. It may be that PG for the first time deciphers a trick that nature has played on science.

It should be appreciated that throughout this report we have loosely used the notions of mass, force and energy, which is an unavoidable situation, if we have to evolve from our standard education in physics; not only pedagogical but fundamental errors may creep in science for these and other concepts. Like GR redefines these concepts in terms of space-time, etc., PG now also seems to afford us an alternative understanding of the same concepts, as they evolve from an assumed universal gravion absorption. Only by persistence in developing and evolving PG theory backed by purposeful experiments, may we ultimately understand and re-define the concepts of energy, mass and force. We have started with a set of principles, which themselves will evolve dialectically (back-and-forth) as we move forward and the pig picture of cosmos unravels more clearly.

The new understanding of mass and force can further lead to an ultimate understanding of energy in the form of work ($force \times distance$), potential and kinetic energy and the $E = mc^2$ relationship. An initial check does not equate the potential energy with the mass-energy equivalence conversion, but this should be of no concern. We should bear in mind that a system of bodies acted upon by their associated gravitational fields does not constitute a closed system. The bodies are inside an “aether” of gravions coupled with them. They constitute an open thermodynamic system that exchanges gravions with the surrounding universal reservoir of gravions. The bodies must always be seen together with the surrounding universe acting from both short and long range. This universe is intimately connected with any system of bodies, small or big, at any moment of time and space, “here and now” (whatever this may mean!). The interconnection is such

that the body resists any change of its steady-state status. This resistance is the conventional “inertia”. Therefore, when the gravitational “pulling” force is doing “work” by displacing a body between two points, the interchange between work and gravitational energy must be computed as a balance of graviton exchange with the surrounding universe. An analogous system in physics is an electronics signal (current or power) amplifier, whereby a given signal input is amplified in conjunction with an external supply circuit of electrons (energy).

Actually, the new notion of mass variation inside the gravitational field of interacting bodies is not limited to dense and massive bodies in astrophysics, but it must apply also to very small but dense particles. This seems to be consistent with particle physics phenomena. Let’s recall that within a given radius, there is an upper limit of effective mass that we can pack. This upper limit is determined by the surrounding maximum J_0 (or g_0 , see also Eqs. 202 and 205). If we can think of a particle in an accelerator that it absorbs more push particles at more speed, it is like creating an artificially increased g_0 enabling the particle to pack more effective mass over and above the maximum it might have prior to its entry in the accelerator. When the particle “stops”, it cannot retain the extra mass above the limit it acquired during its acceleration. Then, it has to shed this “unnatural” load of mass in the form of new particles inside the accelerator. Those new particles themselves usually have very short lives, if they still have to readjust and obey the PG law of an upper limit of effective mass. As it was also theorized in Section 14.7, the approach to an upper speed limit is not because the mass becomes mathematically infinite, but because the real mass becomes saturated with graviton absorption as A_R approaches the upper value of unity.

If the above understanding could prove correct, it would have enormous consequences. While more cases have been studied with the formulations of PG in the Appendix, they and many more can be the subject of continuing work by the scientific community under the new physics of PG. The case of three or more interacting spheres can be investigated by expanding the work presented in the Appendix; then, we can study the eclipses of Moon and Sun over and above the simplified study outlined in Section 12.4. All this requires more resources, but also makes it ever more imperative that PG should be verified by the relevant organizations.

To summarize and avoid possible contradiction of terms (words), let’s clarify (again) the following: The effective mass is a different quantity from the real mass, whilst they are expressed in the same units. The first is the active part (fraction) of the second and relates to an experienced force. We generally experience an object as “stuff”, which we can safely identify with the real mass. The force acts on the object via its effective mass, i.e. it does not directly act on the entire object, because part of it (no matter how small or big) is shielded from the action of gravitons. The effective mass of the object is different when the object is alone from that when it is in the neighborhood of other objects. For convenience of description, let’s call the lone effective mass “intrinsic” mass (same as rest mass) as opposed to the “current” mass being the effective mass in any case. The force between two objects can be found from the intrinsic mass of the objects even though the force is acted upon each other via their current masses. With these clarifications, we can return to the equivalence principle as it originally started and as it can be now explained under PG theory. This principle has been described in the following way(s):

An object under its weight by the Earth’s gravity travels the same distance over time as when the same object is under the same force in space outside a gravitational field. By the same token, this principle says that the object’s mass is the same in both cases, i.e. its gravitational mass is equal to its inertial mass, where the two types of mass are simply the constant of proportionality between force and acceleration and this proportionality is the same in both cases.

Now, under PG we find that the proportionality between force and mass applies only when we use the intrinsic mass of the object, but not when we use its current mass. The use of intrinsic mass necessitates that we operate away from other objects, so that when we bring the object inside the gravity of another object, then its current mass is smaller. However, our experience of the falling object inside the gravity of the second object is as if it has a mass equal to its intrinsic mass. This explains exactly the equivalence principle, but the equivalence principle does not explain the nature of mass, because it fails to distinguish the current effective mass from the lone effective mass. In other words, the expression of “gravitational mass” being the same as the “inertial mass” bypasses the physics about force and real mass (stuff), it overlooks the underlying mechanism resulting in what we experience as force and stuff, as force and object. This omission is not trivial, but it explains why we get the correct result for the wrong reason. PG is about revealing the reason operating behind our experience of an object and force, and much more. In doing so, it frees the ground to unravel some discrepancies and impasses of conventional physics. Furthermore, real mass as revealed by PG bears no compatibility with EP, which makes it even more fundamental to be able to decipher and decouple the various notions of mass from the stuff an object actually has.

Based on the above clarification, we can see again why EP is at least redundant (not needed for PG by way of a “space elevator”), or even invalid (by way of mass equivalence) under the terminology and concepts

of mass in PG. This is another or better re-affirmation of our stance in previous sections. The bottom line is that EP can by no means be used against PG, whilst EP stands on precarious grounds itself.

On the previously asked question whether conventional physics has found how very dense bodies interact at close range, the implication was if such findings correspond to reality. More specifically, the question is if general relativity (GR) correctly describes the interaction of very dense objects based on parameters of bodies that may be incorrectly measured. The latter possibility exists and is better explained according to the ideas expounded in Section 18.2.

16.2 Ramifications and importance of mass variation

Having said all of the above about effective mass variation with distance between two spheres and what it means under PG so far, we must stress that we have considered only the static steady-state situation. However, it is important to clarify what the “static” condition means in an actual situation by explaining what it is not, i.e. not yet before we investigate the following cases:

(a) It is not the situation whereby the two spheres are held at a fixed distance by some other medium, such as a rod between them. In the latter case, the rod would exert a force opposing the gravitational force begging the question about the underlying mechanism of this opposing force. We may know that this is an electric force created by compression at the atomic scale. This then necessitates that we explain the electric force too, which for consistency we have proposed that it be also a push particle force. This may influence the prevailing effective mass via another mechanism. That is the subject of a following Section 21 that expands the push particle principle to a “push electricity (PE)” theory.

Therefore, the way to imagine what we described and quantified in the present section is what happens moments just after we remove the holding rod and before the spheres acquire any significant velocity by “falling”. In other words, the spheres are both stationary and in a steady state situation with regard to absorption of gravions and re-emission of their energy into something else (let’s say electrions) and are free in space without influence by anything else like a rod.

(b) It is not the situation whereby the two spheres are held at a fixed distance while moving at an orbit with respect to each other, like in a binary system, or one very small (light) sphere orbiting around another large (heavy) sphere. Also, it is not the situation whereby the two spheres are falling to each other having acquired a significant velocity. For a falling body, we have not yet established what happens to the current effective mass (at time t) and how (if) the gravion flux varies and differs from the postulated static situation. This problem could be solved under Section 14 for the development of a dynamic PG theory. The prospects are very interesting and important, if we can only speculate thus now: A sphere orbiting around or falling towards another “stationary” sphere may have yet another current effective mass, quantitatively different from the stationary one.

(c) It is not the situation whereby one sphere (with or without the presence of the other sphere) is pushed by some medium like a rocket. We can imagine this happening in different ways. While the two spheres are held apart with a fixing rod, one sphere disappears or is let loose while the rod-rocket continues to act on the other sphere. We have not examined these two cases yet. In other words, moment(s) after the disappearance or letting loose of one sphere, the other sphere exists at practically the same (prior fixed) distance before it acquires a significant velocity being propelled by the rod-rocket. It would be a mistake to apply our derived equations in this section for the prevailing effective mass of the sphere. This is because we have to consider the mechanism of the rocket force, which we again expect it to be an electrical force. Therefore, we should examine these cases also after we first develop and understand push electricity. Later work has now been done in Section 23.

From the above clarifications, we can see the reasons why the effective mass may be different depending on the prevailing conditions. If we postulate that the “mass” is the same (equivalent) in all situations, which is exactly what the Equivalence Principle has demanded from the mainstream physics, then we have not seen the above described fundamental differences. Current theories have overlooked the above analysis, exactly because they have adopted a problematic EP. In other words, EP has imposed a severe constraint limiting further developments in physics, in fact leading to impasses. For if we let the mass vary and/or transfer under static and dynamic situations, we can free ourselves for much better explanations of experiments, phenomena and the cosmos. Now, we understand that “mass” is an objective entity in various forms like “stuff” = matter = real mass, with subsets of effective mass and black mass. Mass is not a mere mathematical multiplier factor to an invariable conventional rest mass.

16.3 Supplementary study of two sphere interaction cases

Due to the need for better understanding of the positional variation of two spherical masses, we undertook the study of many more cases. The relationship of geometry (radii and distance) with nature of material

(absorptivity) is the main purpose of the study. This work has revealed some important patterns of behavior that is necessary to know in further studies, development and applications of the theory of PG. The salient aspects of this behavior are described by some representative cases presented below.

CASE_4 involves the Earth and a small sphere with $R_1 = 1$ m having Earth-like density, for which we used $k_1 = 1.15604978409807E - 09$ m⁻¹, at $g_0 = 1000$ ms⁻². [Note: Throughout this report, we often provide numerals with the same many decimal places used to allow other workers to reproduce the same numerical results]. This is a Newtonian (or close to it) case where the small diameter of one sphere allows to bring it down to 2 m above the Earth surface (i.e. at $r = 6371002$ m). We plot the net loss of mass against distance in Fig. 24a along with the corresponding asymptotic line given by Eq. 215. The difference

$$\Delta S_{loss}(r) = S_{a-netloss}(r) - S_{F0}(r) \quad (219)$$

and ratio

$$\mathfrak{R}(r) = \frac{S_{a-netloss}(r)}{S_{F0}(r)} \quad (220)$$

between actual and asymptotic values are also plotted against distance in Fig. 24b&c. We note that the deviation from the asymptotic is as significant as in Fig. 21 done for the very dense (non-Newtonian) spheres with identical geometry. This knowledge is needed for studies involving the $S_{a-netloss}(r)$ function in other parameters describing the behavior of bodies with different density (absorptivity). One such parameter is the ratio of Newton/PG forces given by Fig. 23, to which we now add CASE_4 and note that the points remain close to unity even at close range.

The approach (or deviation) of the net loss function to (from) the asymptotic straight line is an important consideration. If we use the asymptotic function of CASE_4 instead of the actual values of the net loss function in the same Fig. 23, the difference is not visible on the graph. However, if we apply the asymptotic function for CASE_2, the deviation from the actual function becomes quite obvious (red circle points now added in the same figure). From this, we may conclude that use of the asymptotic function is a good approximation in the Newtonian regime, which may be allowed for some parameters, like the one plotted in Fig. 23. However, this may also provide erroneous outcomes for other parameters, like the falling speed between bodies. The speed that results from the action of force at various points is a cumulative parameter that can result in significant deviation between using the asymptotic or the actual function of net loss of mass. We have already suggested (per Section 14.3) that the falling speed is a function of the contraction factor, so that later studies should take into account even the smallest deviation, even in the Newtonian regime. (Note that we do not need to use a subscript (₁ or ₂) to designate the net loss of mass for either sphere 1 or 2, because they share the same mass loss).

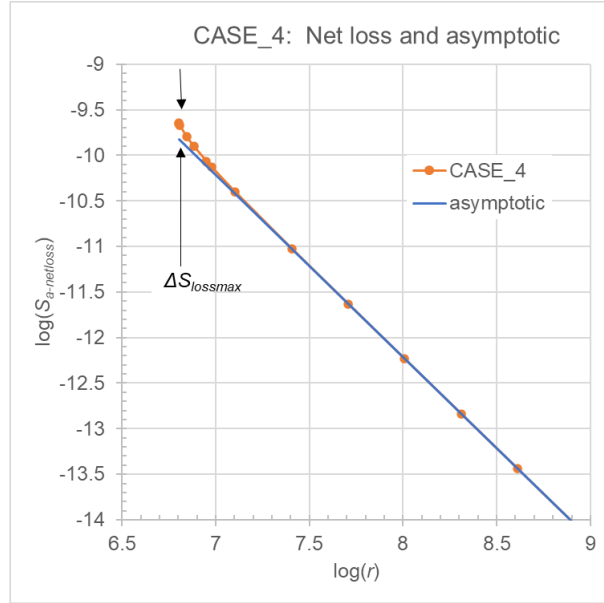
The above findings prompted us to study further cases in an effort to establish some patterns or “rules” about the behavior of the $S_{a-netloss}(r)$ function. This behavior is not obvious directly from the integrals involved for computing the net loss for a set of two spherical masses with different absorptivities by use of the method in Appendix E. Closer to practical application for our study, we fix the gravitating “large” sphere_2 to the Earth radius and the “small” sphere to the radius of $R_1 = 1$ m. We vary the absorptivity (or k_2 factor) of the large sphere over a wide range of values in conjunction with some fixed absorptivities (or k_1 factors) for the small sphere between extreme densities; we found that three fixed values, namely, $k_{1a} = 2.09672407007571E - 10$ m⁻¹ (case_ka), $k_{1b} = 2.09672407007571E - 06$ m⁻¹ (case_kb) and $k_{1c} = 2.09672407007571E - 01$ m⁻¹ (case_kc), chosen arbitrarily, are sufficient for the current purposes. We generalize the presentation by plotting the results against the usual product of $k_2 R_2$. To minimize the work and reporting, we computed only the maximum value $S_{lossmax} \equiv S_{a-netloss}(r_{min})$ at the closest distance $r_{min} = 6371002$ m, where the deviation from the asymptotic function $S_{F0}(r_{min})$ is maximum. Then the ratio \mathfrak{R}_{max} of these quantities at the minimum distance:

$$\mathfrak{R}_{max} = \frac{S_{a-netloss}(r_{min})}{S_{F0}(r_{min})} \quad (221)$$

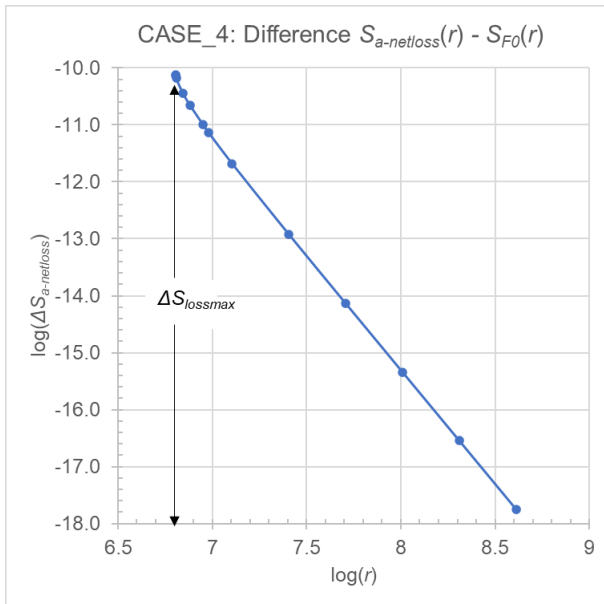
has been found to be a good indicator of the regime behavior for the given k factors (absorptivities) of any set of sphere densities. The corresponding difference $\Delta S_{lossmax}$ of the same values:

$$\Delta S_{lossmax} = S_{a-netloss}(r_{min}) - S_{F0}(r_{min}) \quad (222)$$

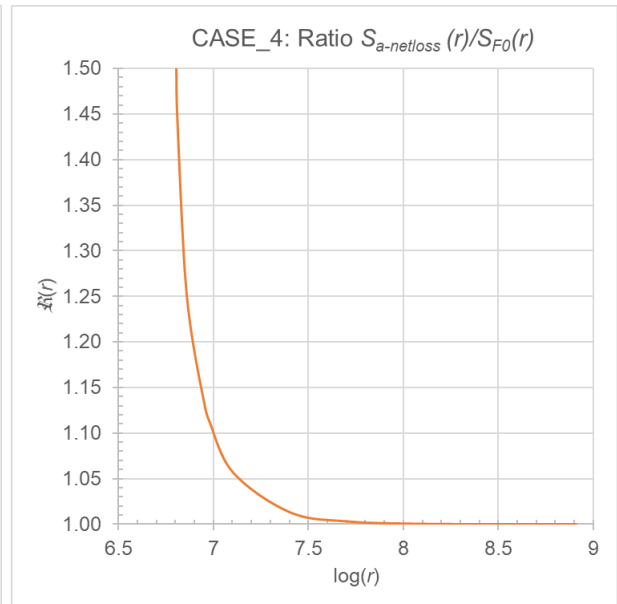
is more cumbersome to use because it provides absolute values varying over many orders of magnitude, which cancel out in the ratio \mathfrak{R}_{max} . We can see the variation of net loss $S_{a-netloss}(r_{min})$ in absolute values plotted in Fig. 25a. However, plotting the ratio by Eq. 221 results in grouping all three cases very close together, but not exactly overlapping, as can be seen in Fig. 25b. The latter closeness may simplify some



a



b



c

Figure 24: CASE_4 using a small sphere with $R_1 = 1$ m, $k_1 = 1.15604978409807E - 09$ m $^{-1}$ and Earth with $R_2 = 6371000$ m, $k_2 = 1.16248157479707E - 09$ m $^{-1}$, and $g_0 = 1000$ ms $^{-2}$; (a) net_loss_function and asymptotic, (b) difference between net loss and asymptotic and (c) ratio of net_loss_function over asymptotic, all plotted against distance between spheres

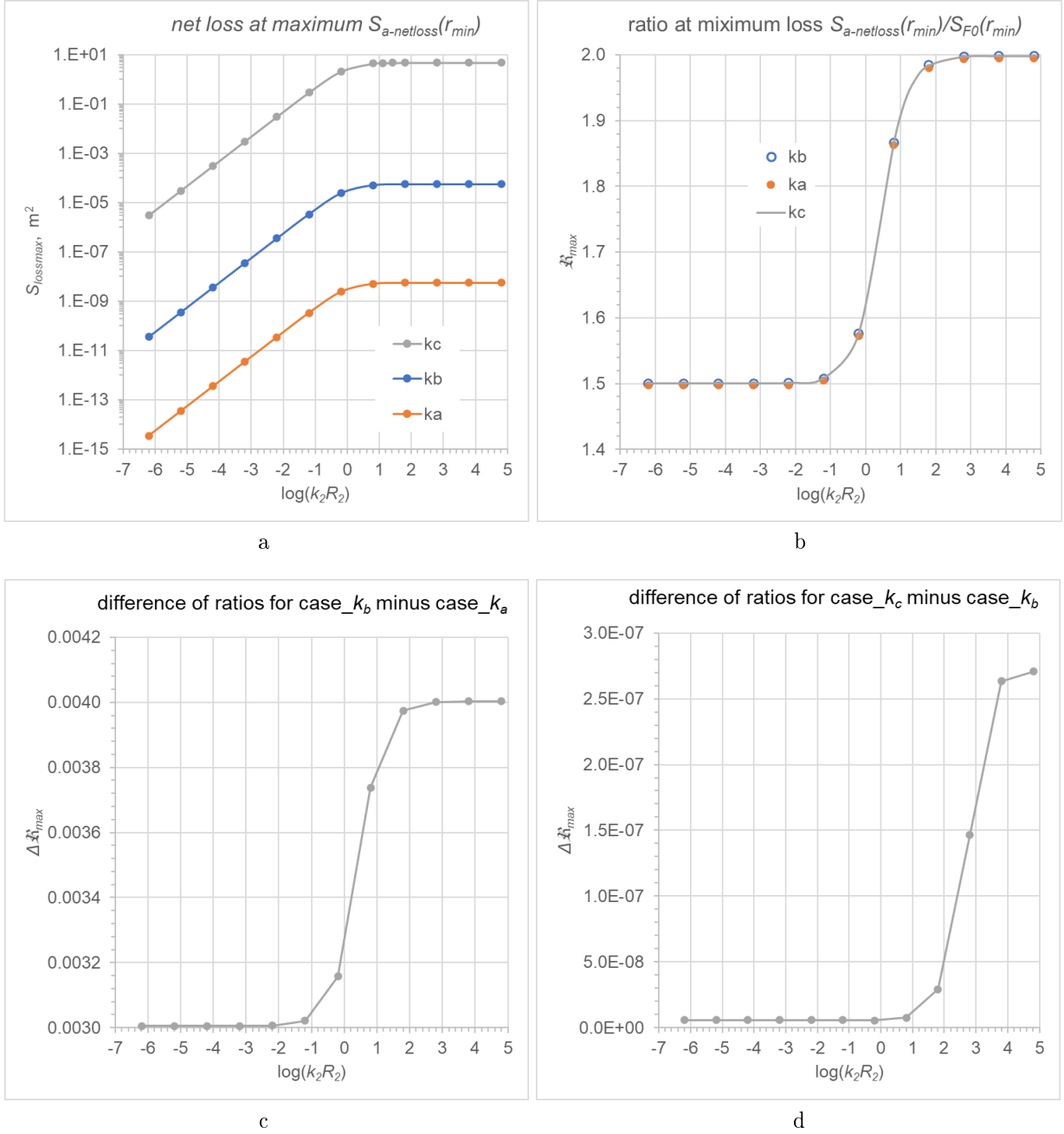


Figure 25: Variation of the small sphere parameters against $k_2 R_2$ of the large sphere for three fixed values k_1 of the small sphere: (a) Absolute values of the net loss function, (b) ratio of max net_loss over max asymptotic_loss, (c) difference of ratios corresponding to case_ka minus case_kb and (d) difference of ratios corresponding to case_kc minus case_kb.

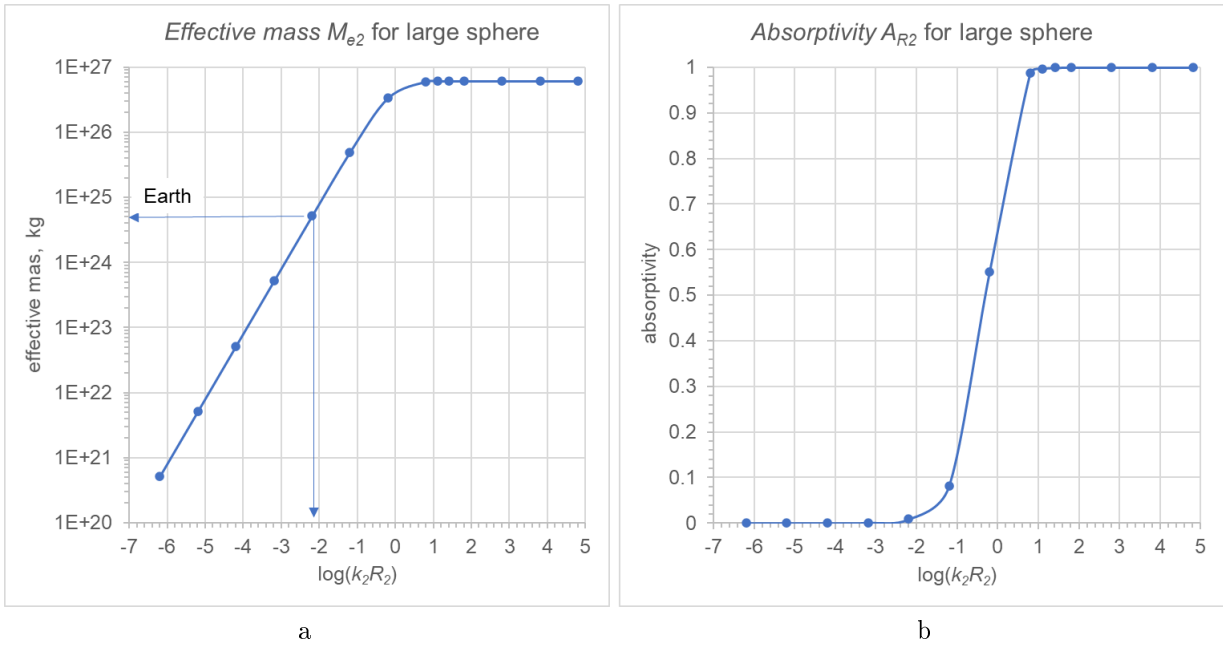


Figure 26: (a) Effective mass and (b) absorptivity for the large (Earth size) sphere against $k_2 R_2$

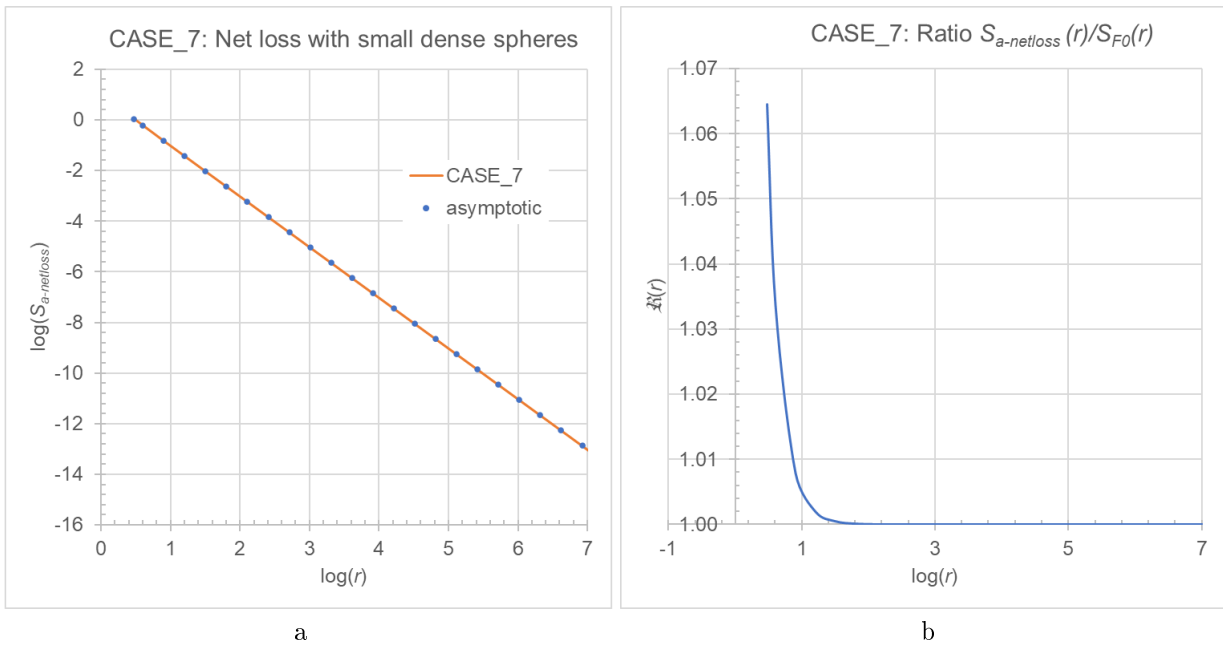


Figure 27: CASE_7: Two identical small and dense spheres with $R = 1$ m and $k = 7.07102919089469$ m^{-1}

engineering problems, but the subtle difference may be important in further development and understanding of PG application. For good measure, the difference between the closely presenting graphs are given in the same Fig. 25c&d. Therefore, the multiplier factor $\mathfrak{R}(r)$ is itself also a function of the absorptivity of both spheres, so that we can write an overall general function for $S_{a-netloss}$ as:

$$S_{a-netloss}(A_{R_1}, A_{R_2}, r) = \frac{\pi^2 A_{R_1} A_{R_2} R_1^2 R_2^2}{r^2} \mathfrak{R}(A_{R_1}, A_{R_2}, r) \quad (223)$$

Recalling that the absorptivity itself is a function of the radius R (geometry) and absorption factor k (nature of material), namely, of the product kR at a given universal acceleration g_0 , the net_loss of mass is function of the geometry, determined by the radii of spheres and distance between them, as well as the nature of the materials for each sphere. Therefore, the system of two spherical masses is always described by a peculiar function above including the Newtonian regime, whereby we may or may not reduce it to the asymptotic function depending on the associated parameter under examination.

As for a rule, we may say that cases involving the interaction of two bodies differing greatly by size and/or density, it is the larger body that imposes its dominance and a characteristic pattern like the one we see in Fig. 25. The smaller sphere appears to be overwhelmed by the large one throughout the entire range of $k_2 R_2$ variation of the large sphere; that is, when the small sphere is “immersed” in, or “engulfed” by the gravitational field of the large sphere. The small sphere appears to play a secondary role with second order significance from a “practical” point of view, but nonetheless its role is ever present and non-trivial for an overall theoretical examination and in problems involving a cumulative effect of what appears as a secondary role at first. It is striking that the factor \mathfrak{R}_{max} varies very closely only between 1.5 and 2.0 for a large number of cases. Planet Earth seems to be around the onset of an abrupt transition from $\log(k_2 R_2) > 2$ according to Fig. 26a providing the variation of effective mass; the corresponding variation of absorptivity is given in (b).

A deviation from the above rule and the effect of geometry alone can be readily seen if use a case with comparable size spheres, as we present CASE_7 in Fig. 27 involving two identical small-and-dense spheres with 1 m radius (identical with the small sphere of CASE_2). Neither sphere exerts a dominance, and one is not “engulfed” by the field of the other; they interact on an “equal footing” at all distances possible. This geometry brings closer together the net_loss function with its asymptotic as seen in (a) but there is a difference, albeit much smaller, as can be seen by plotting the $\mathfrak{R}(r)$ factor in (b) of the same figure.

Important: This entire Section 16 is fundamental for the development of PG and should be moved to Part 1 in continuation of Section 7 during a later revision of the report.

17 Momentum or push gravity as the universal and unifying cause of all types of acceleration (force)

If gravity is finally proven to be caused by gravions under the working of PG, then it could be a logical conclusion that all forces may be attributable to a similar cause, albeit by different kind of push particles. What would then be needed is that each kind of particles have a mean free path much longer than the dimensions of the masses (particles) acted upon. This requirement is already fulfilled for planets and stars by gravions, to which we may also refer as the first type-I push particles. The force is then generated by the law of conservation of momentum and energy. This momentum force is well established in physics as it is also a tangible phenomenon, i.e. understood by common experience. We may then extend the proposal to apply to all kinds of force fields regardless of the size of the field generating body. This may be a sensible proposition, because size should not be an obstacle at least for all experimentally known particles. Given that the size of an atom is of the order of $\approx 10^{-9}$ m, we still have 16 orders of magnitude to reach the Planck particle, the length ℓ_P of which is defined as:

$$\ell_P = \sqrt{\frac{\hbar G}{c^3}} \quad (224)$$

where \hbar is the reduced Planck constant. The Planck length is about 10^{-20} times the diameter of a proton.

Thus, nucleons may be maintained by their own surrounding push (momentum) particles, the nucleus may be maintained by yet another kind of push particles, and so on for atoms, each group maintained by their own associated type of momentum particles. The universal situation may be that the space is filled by particles with a wide range of sizes (energies/wavelengths) corresponding to an equally wide range of mean free paths, acting as push particles to their matching (corresponding) relatively much bigger particles (bodies). The entire universe may then be thought as an agglomeration of varying concentrations of matter automatically sorting out themselves by the surrounding push particles. This proposition may then constitute

a likely basis for a unification of all force fields in the cosmos from the smallest to the largest phenomena. Le Sage made a similar attempt to account for forces of different chemical strengths, by the existence of different species of “ultramundane” corpuscles of different sizes, whilst all this should be reconsidered and re-appraised in the light of modern particle physics, quantum mechanics, relativity and astrophysics.

Ultimately and inexorably, however, the above model only shifts the problem to what keeps the “ultimate” mysterious particle as a unity (re gravion), if not for an attractive force, according to Kant’s philosophical reasoning. However, the lack of understanding of the nature of an ultimate particle is not yet reason good enough to reject a possible unifying model that allows us to concentrate our attention more to a smaller “area” of the cosmos that underlies as a common denominator to all other processes.

From the above broad model, we may narrow down the cosmological questions to assuming the existence of types of particles corresponding at least to the known force fields. Thus, gravions are type-I push particles that mediate the gravitational force, type-II push particles are those mediating the electrical field forces, type-III those mediating the nuclear forces, etc. Already, in quantum theory the electric field is thought to be due to a continuous stream of exchange of photons (say, here type-II particles). Dibrov (2011) believes that the core of electrons and positrons remains stable by pressure of the bombardment of “fations”. The electron, in his proposed model, “*as against the static Abraham–Lorentz electron, is the dynamic object transforming the gravitational field energy into the energy of the electric field, and periodically exploding up.*” However, he probably means something very different to our proposed model in this report, because he talks about charge already being present in the electron, and he only tries to justify the re-emission of the “fation” energy in the form of electric field sub-particles. Considering various parameters quantitatively and his main conclusions, it is clear that his theory is not consistent with our findings. For example, “the active mass is not equal to the passive mass”, he discovers a “violation of equivalence principle for the electron” and that the “gravitation constant G is not equal to the actual one”, to mention a few aspects of his push gravity theory that are in clear variance to the ideas proposed herewith. Nevertheless, an “exploding electron” seems consistent with re-emission of absorbed gravion energy.

We may go on to elaborate on our general proposal (model). For example, the type-II particles, in particular, may be subdivided either in two sub-classes responsible for the positive and negative electrical force (such as opposite spin or an as yet unknown attribute), or may emanate from two complementary types of matter organization at the electron and positron level. The emanated energy (type-II) carriers exit as a result of the absorbed type-I push particles by protons and electrons, and so on and so forth.

In summary, for a field unification theory, it is logical and consistent to envisage and assume that all force fields are created by particles including gravity. This general idea of the underlying particles for all fields is then greatly facilitated by a push/momentum mechanism in a PG framework advanced in this report. A general push particle field principle may then be seen as one kind of self-similarity as used in fractal theory. Could self-similarity be used to recreate a new standard model in physics?

18 White dwarfs, neutron stars and black holes

It is reported that the gravitational field on a white dwarf is of the order of 10^6 m/s², whilst that on a neutron star is of the order of 10^{12} m/s², and much greater on black holes. If these extreme accelerations are caused by gravions (in that case being the universal cause of all gravitational fields), then it might be unlikely that we can practically detect them directly by the methods proposed here, because of the need for extremely sensitive gravimeters. However, if it were found that the maximum g_0 is, say, around 30000 m/s² by some careful measurement, then we would be faced to explain the super high values of acceleration on white dwarfs, neutron stars and black holes. Then, one possible explanation would be to assume that those extreme accelerations may be caused by different, more energetic types of push particles. Before we further speculate on these other hypothetical types of push particle, let us apply a little further the already found PG relationships below.

We continue our investigation from where we left off in Section 9.1. By increasing the maximum prevailing acceleration g_0 in the neighboring universe, we inversely decrease the corresponding k (see Eq. 60) by

$$k = \frac{\pi G \rho}{g_0} = \frac{3GM}{4g_0 R^3} \quad (225)$$

so that by keeping the mass and radius of a star constant, the PG equation is reduced to the value provided by Newton, namely, to $\frac{4}{3}\pi G \rho R = GM/R^2$, which is the saturation (asymptotic) value(s) observed in Fig. 10, when k becomes sufficiently small.

Let us now see the values of surface acceleration g_R against the prevailing maximum acceleration g_0 possible in a particular space of the universe for stars having various combinations of masses M with radii

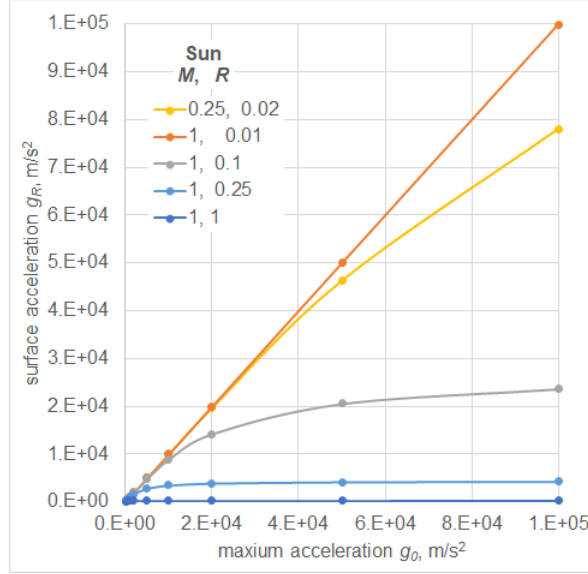


Figure 28: *Surface g_R against maximum g_0 for stars with mass and radius (M, R) in units of Sun mass and Sun radius.*

R . This is shown in Fig. 28, where both mass and radius are expressed in units of Sun (\odot) mass and radius. The masses used are those of the apparent Sun mass but taken to be the real mass of a hypothetical star as a first approximation to get a feel of the situation. Then as expected, the pair $(M, R)=(1, 1)$ reproduces the curve in Fig. 10 very close to the abscissa (visibly touching it) with an asymptotic value approaching the Newtonian value of surface acceleration of our Sun. The additional curves now show the outcomes of different values of the pair (M, R) , which can be understood by the above Eq. 225: For any fixed, g_0 and M , the value of k increases very fast with a decrease of radius, which forces the surface acceleration to be well below the saturation values is reached, as noted by the curves on the figure. When R reduces below a sufficiently low value, k becomes so large that the factor A_R in PG becomes unity and $g = g_0$, which is the straight line at unity slope in the figure.

In the event that we can safely measure g_0 and find that this is not as high as on the surface of a dwarf, however, it may be sufficient to trigger gravitational collapse in the presence of a critical mass. After the collapse, a white dwarf is formed that may be sustained also by push particles of a different kind (type-II). Likewise, upon formation of a neutron star, the forces holding it together may further be provided by push particles of a third kind (type-III) as they evolve upon the onset of a further collapse. This proposal forms initially a qualitative model, which is depicted with some hypothetical quantitative dimensions in logarithmic scales (powers of 10) in Fig. 29. The validity of such a hypothesis should by all means be cross-examined against existing data and theories in astrophysics to be further refined or even rejected, if not appropriate.

For the general reader and to better describe the proposed model here, it is helpful to summarize the current understanding of these dense bodies by conveniently referring to a brief description provided in relevant articles by Wikipedia contributors (2019f). The summary descriptions below are needed to precede a new idea here attempting to connect the neutron star field with the atomic nuclear field, both unified under the proposed PG field model.

A white dwarf is a very dense stellar core remnant composed mainly of electron-degenerate matter. It has a mass like the Sun with a volume like the Earth. Because it no longer undergoes fusion reactions, it has no source of energy, so that it cannot support itself by fusion heat against gravitational collapse. It is supported by electron degeneracy pressure and is extremely dense. Accretion takes place by accumulating particles into a massive object, typically gaseous matter. Galaxies, stars, and planets, are formed by accretion processes. Neutrinos are radiated by white dwarfs through the Urca process (Wikipedia contributors, 2019e), which is a neutrino-emitting process playing a central role in the cooling of neutron stars.... White dwarfs have masses from about 0.07 to 10 M_\odot .

An astronomical body can collapse by its own gravity drawing matter inward toward its center. Gravitational collapse is a fundamental mechanism for structure formation in the universe. It can all start from relatively smooth distribution of matter gradually collapsing to form pockets of higher density, stars and planets, stellar groups and clusters of galaxies.

A giant star with a total of between 10 and 29 solar masses collapses to a neutron star (Wikipedia contributors, 2019b). Other than black holes, neutron stars are the smallest and densest stars with a radius

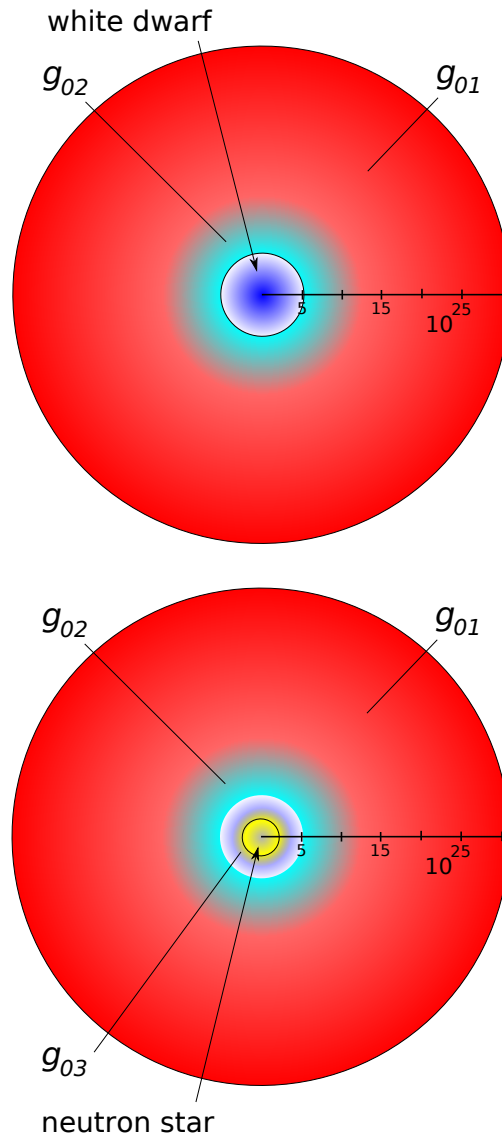


Figure 29: Diagrammatic perception of a white dwarf (above) with its surrounding PG type-II (g_{02}) field inside the universal type-I (g_{01}) field, and a neutron star (below) with its surrounding PG type-III field (g_{03}) inside a dwarf type-II (g_{02}) field inside the universal type-I (g_{01}) field; the scales in m are logarithmic and approximate.

on the order of 10 km and a mass less than 2.16 solar masses. They are produced from the supernova explosion of a massive star, and together with gravitational collapse achieve the density of atomic nuclei.

Binary systems of neutron stars can undergo accretion making the system bright in X-rays and a source of short-duration gamma-ray bursts, as well as produce gravitational disturbance. At soaring temperatures, electrons and protons combine to form neutrons via electron capture, releasing a flood of neutrinos. It is important for our model proposed here to quote verbatim from Wikipedia the following: *“When densities reach nuclear density of 4×10^{17} kg/m³, neutron degeneracy pressure halts the contraction. The in-falling outer envelope of the star is halted and flung outwards by a flux of neutrinos produced in the creation of the neutrons, becoming a supernova. The remnant left is a neutron star. If the remnant has a mass greater than about $3 M_{\odot}$, it collapses further to become a black hole”*.

The temperature inside a newly formed neutron star is from around 10^{11} to 10^{12} Kelvin. However, the huge number of neutrinos it emits carry away so much energy that the temperature of an isolated neutron star falls within a few years to around 10^6 kelvin. At this lower temperature, most of the light generated by a neutron star is in X-rays.

A neutron star has some of the properties of an atomic nucleus, including density (within an order of magnitude) and being composed of nucleons. In popular scientific writing, neutron stars are therefore sometimes described as ‘giant nuclei’. However, in other respects, neutron stars and atomic nuclei are quite different. A nucleus is held together by the strong interaction, whereas a neutron star is held together by gravity. The density of a nucleus is uniform, while neutron stars are predicted to consist of multiple layers with varying compositions and densities.”

It is the above last statement that we can seize upon to support the PG model here, namely, we say here **that a nucleus and a neutron star are both held by the same force: That force is the pressure exerted by the presumed type-III push particles.** We propose that the strong nuclear interaction is no different from the neutron star gravity, namely, both being created by push particles of the same type. In consequence of this model, the space around any atomic nucleus inside the electron orbitals is occupied by push particles holding the nucleus together. The current understanding is that this space seems relatively more “empty” than the interplanetary space, so there is nothing weird about our hypothesis that push particles small enough occupy this space fulfilling the requirements of PG with regard to mean free path and absorption coefficient of the nucleus. There is plenty of “room” for such superfine particles on the scale all way down to the Plank length. It may turn out that these push particles are x-rays and gamma-rays of sufficiently short wavelength, which would be consistent with the strong x-ray emission by neutron stars. That may also provide the existence/mechanism of x-ray emission by the orbital electrons in atoms adjusting to different energy levels, as well as somehow explain the original mystery of stable electron orbitals of accelerating orbital charges. Thus, the atom is a micro-neutron star created from (after) breaking down a neutron star. We might want to call the corresponding type-III push particles *neutrions* (neutron + $\iota\nu$) in analogy to gravions. However, in proposing this model, it may not be clear how to differentiate between a nucleus and a neutron particle, so that we may have to refine the various distinctions of push particles mediating strong and weak interactions and all other sub-nuclear forces. The proposed model is only a general approach towards a unification of fields, which requires the cooperation of particle physics and astrophysics.

The above proposed scheme for neutron stars and atoms may not be acting alone, as it requires the simultaneous cooperation of a type-II push particles holding electrons and nuclei together in the atom. In a similar fashion, white dwarfs are the plasma state by free electrons and nuclei having released their mediating binding (type-II) particles around the white dwarf. These mediating particles responsible for the appearance of electric field might be called *electrions* (from electricity + $\iota\nu$). “Neutrions” and “electrions” are finally redistributed after explosion to form atoms.

At any rate, the above general model could be described in more specific terms of particle physics such as: Gluons participate in the strong interaction in addition to mediating it. This is unlike the photons, which mediate the electromagnetic interaction but lacks an electric charge. Gluons also share this property of being confined within hadrons. One consequence is that gluons are not directly involved in the nuclear forces between hadrons. The force mediators for these are other hadrons called mesons. Although in the normal phase of QCD single gluons may not travel freely, it is predicted that there exist hadrons that are formed entirely of gluons — called glueballs. There are also conjectures about other exotic hadrons, in which real gluons (as opposed to virtual ones found in ordinary hadrons) would be primary constituents.

The above intermittent extracts from established theories and observations from astrophysics and particle physics serve only to stimulate further discussion, one way or another, that could involve the push theory principle consistent with the findings of this report.

In continuation to the proposed “aether of gravions” in Section 14.1 and generalized push particles in Section 17, it is envisaged that other types of push particles finally “leak out” into space together with

gravions achieving some steady state concentration in various regions of space. Whilst their concentration is highest around their associated specific fields, which they mediate, like around white dwarfs, neutron stars and black holes, and various atomic and nuclear fields, the “aether” is a “soup” of various types of extremely fine particles. The “electrions” after mediating the electric field in matter, they leak out of bodies and fill the space. Thus, they might mediate also the propagation of photons in space, which is not an absolute vacuum, whilst they are also entrained by bodies. Electrions are also “energetic” particles, like gravions activating (or mediating) corresponding physical processes in electricity; they permeate not only space but also matter. Electrions seem to be responsible for charge and electricity, in a similar fashion to gravions being responsible for creating effective (active) mass, i.e. the conventional mass we are familiar with. Nikola Tesla, forgotten genius of electricity and the man who invented the twentieth century (Lomas, 1999), may have already envisaged the medium for the electric field and the propagation of lightning, when he was suggesting that we swim inside an inexhaustible source of energy.

18.1 More on mass, energy and black holes

We now continue from where we left off in Section 14.6 canvassing the possibility that black holes consist mainly of passive mass per Eq. 139.

From the preceding discussion on massive bodies in general, we have proposed the possibility that these bodies are surrounded by different layers of different fields generated by the corresponding different types of push particles. For the dynamics of such bodies (kinematics and kinetics) in push gravity, it is important to consider the distance between any two given bodies. For long enough distance, they will be governed by our familiar long range gravity field due to gravions, but at closer range other types of field will take over or prevail, like the fields around white dwarfs, neutron stars and black holes. It is not yet known to the present author whether the proposed hypothesis agrees with data from astronomy and astrophysics. It is not known how the “gravitational” fields and masses have been calculated, whether these data are amenable to review, and overall if PG and the data can be inter-interpreted, re-interpreted, and/or mutually adapted, or the PG theory must be modified or be aborted. These questions need to be addressed by many more workers with appropriate expertise. Nevertheless, some tentative ideas are put forward next by way of trialing conjectures.

In a recent report, an active galactic nucleus (AGN) believed to be the explosion from a supermassive black hole has been announced (Giacintucci *et al.*, 2020). It looks like an outburst in slow motion that *“would take at least 240 Myr to rise to the current radius moving with the sound speed, which is an upper limit on the velocity, so the actual age would be greater than that”*. In our proposed model of a black hole, a small disturbance could create an instability to the spherical geometry exposing some internal mass near the surface to the action of push particles, in turn, setting off a chain reaction to a full blown explosion. The explosion would be necessary because, otherwise, the stable sphere can only hold a maximum limit of effective mass. As more passive mass is accessed by push particles, more effective mass is created by a process continuing for a long time. The internal passive mass of a black hole may resemble black powder waiting to explode. The end result is the creation of active mass (effective mass) in a huge cloud that will later start yet another cycle of galaxy and star formation according to prevailing theories.

The internal stuff, from which black holes are made of, is completely shielded from the action of push particles of various types, like gravions, electrions, neutrinos and black-hole-field push particles. All these types of particles can actually exist in all of our everyday materials according to the preceding model. Even black hole stuff may be present in the smallest possible quantities corresponding to what we initially have called “real mass”. By way of self-similarity, the universe is deconstructed and reconstructed recursively.

We may have a tangible illustration of particle-matter transformation to energy in the $E = mc^2$ equation and conversely.

The above may not be implausible, as there is some similarity with current theories about the Higgs boson (field) giving mass to subatomic particles. Without the Higgs field, we wouldn’t exist, i.e. mass would “evaporate”. Similarly, we may say that push particles maintain the integrity of material bodies at all levels of organization, whilst in the absence of said push particles (fields), the effective mass would cease to exist too. We may now have a reason, why the Higgs field exists. Matter cannot exist in absolute vacuum, and so PG theory is on the same page with some prevailing theories. There remains to work out an understanding on the relationship between gravions and black hole passive matter, as well as the interaction between gravions and all matter manifested in the universal constant Λ , i.e. the number of scattering events per unit mass thickness (area density).

Mathematics provide relationships about things, but not what the things are, whilst theorists often are not concerned as to what it means. Thus, we hope that PG can fulfill such a gap haunting several areas in physics. The physics/maths ratio needs a substantial overhaul, where physics lags behind mathematical formulations; mathematics is supposed to serve physics, whereas physics has become subservient to mathematics. For

example, the mathematicians(?) invented the Higgs field, but they don't tell us what it is, not to mention a long standing difficulty in conceptualizing relativity outside a narrow circle of high expertise scientists.

18.2 Total absorption layers and black holes

In continuation to the conceptualization of possible gravitational fields around massive bodies per Fig. 29, below we attempt to provide also a conceptualization of the interior of massive (very dense) bodies by some simple qualitative considerations.

In Sections 14.6 and 14.7, we found that the effective mass becomes concentrated towards the outer layers of a material body, be it a sphere, or a line segment, or any other shape, when we sufficiently increase the product $k \cdot \text{length}$. At a very high value of the latter product with a characteristic low value of contraction factor per Fig. 5, the effective mass is concentrated in a relatively thin outer layer resembling the event horizon (Schwarzschild surface). Associated with this is the limiting graviton parameter of maximum acceleration g_0 together with the governing Eqs. 151 and 152. From the preceding proposals about white dwarfs, neutron stars and black holes, they may also be characterized by their own corresponding limiting (maximum) acceleration parameters, so that we can suggest similar outer layer concentrations of effective masses due to absorption of the corresponding type of push particles. To clarify and avoid confusion about this emerging novel situation, we need to introduce an appropriate terminology of the more general case of the look-alike “event horizon” or “Schwarzschild” parameters with reference to gravions and other push particles, i.e. over and above the existing terminology. The established terms for event horizon and Schwarzschild radius are expressed differently from the corresponding ones arising from gravions. The well known Schwarzschild radius R_S is given by

$$R_S = \frac{2GM}{c^2} \quad (226)$$

whereas our PG limiting radius R_0 (at $A_R = 1$) due to gravions is given by

$$R_0 = \sqrt{\frac{GM_e}{g_0}} \quad (227)$$

A possible correlation (and numerical comparison) between the two quantities and the correspondence between the said event horizons should be done in conjunction with possible values of g_0 with different types of push particles. We can return to this issue after we outline the various regimes below. In fact, a possible agreement of the above two equations seems to be born out during the development of push electricity reported in Section 21.

From the Beer-Lambert law, we generally define an attenuation or absorption length as the distance inside a material, whereby the incident intensity drops to $1/e$ of the initial value; that is, the transmitted intensity decreases to about 37% with 63% being absorbed. We generally define the transmission fraction or transmittance T , and transmission depth τ by:

$$T = \frac{J}{J_0} = \exp(-\tau) = \exp(-k\chi) \quad (228)$$

where we use our parameters of k and χ with $\tau = k\chi$. We can also define a particular transmission depth resulting in an arbitrary amount of absorption of practically “all” gravions, say, 99% absorption allowing only 1% transmission. We designate such a depth with $\chi_{0.01}$, when $\tau_{0.01} = -\ln 0.01 = 4.60517 = k\chi_{0.01}$, so that $\chi_{0.01} = 4.60517/k$. For a line segment ℓ or radius R and, depending on the value of k , we can have $\chi_{0.01} \stackrel{\geq}{\leq} \ell$ or R . By convention and for practical purposes, we may define the 99% absorption layer, or any other convenient absorption fraction, as the “*total absorption layer (TAL)*”. Theoretically, there is no “total” absorption layer on account of the exponential form of the absorption, but in reality, we can assume there must be one by introducing a quantum mechanism of absorption in a quantum push gravity theory (QPG) later.

With reference to Fig. 29, we can continue with the terms of push particles being “type-I”, “type-II”, type-III, “type-IV” and so on. Now, each of these bodies should have their own TAL for the corresponding type of push particle. We have also reserved more explicit terms for each of those types, like gravions, electrions, neutrions and possibly others to be used later as the need arises. We may use the Roman or Arabic numerals in ascending order of field strength or ascending order of generating process, something to be finally determined again later. The use/attachment of expressive (explicit) words have been used provisionally in this report, whilst their order may evolve and change as we more firmly establish the associated processes that generate those fields in PG. Thus, we can envisage a (nearly) total absorption layer relative to gravions and abbreviate it with a subscripted acronym TAL_1 or TAL_I (“*type-I total absorption*”).

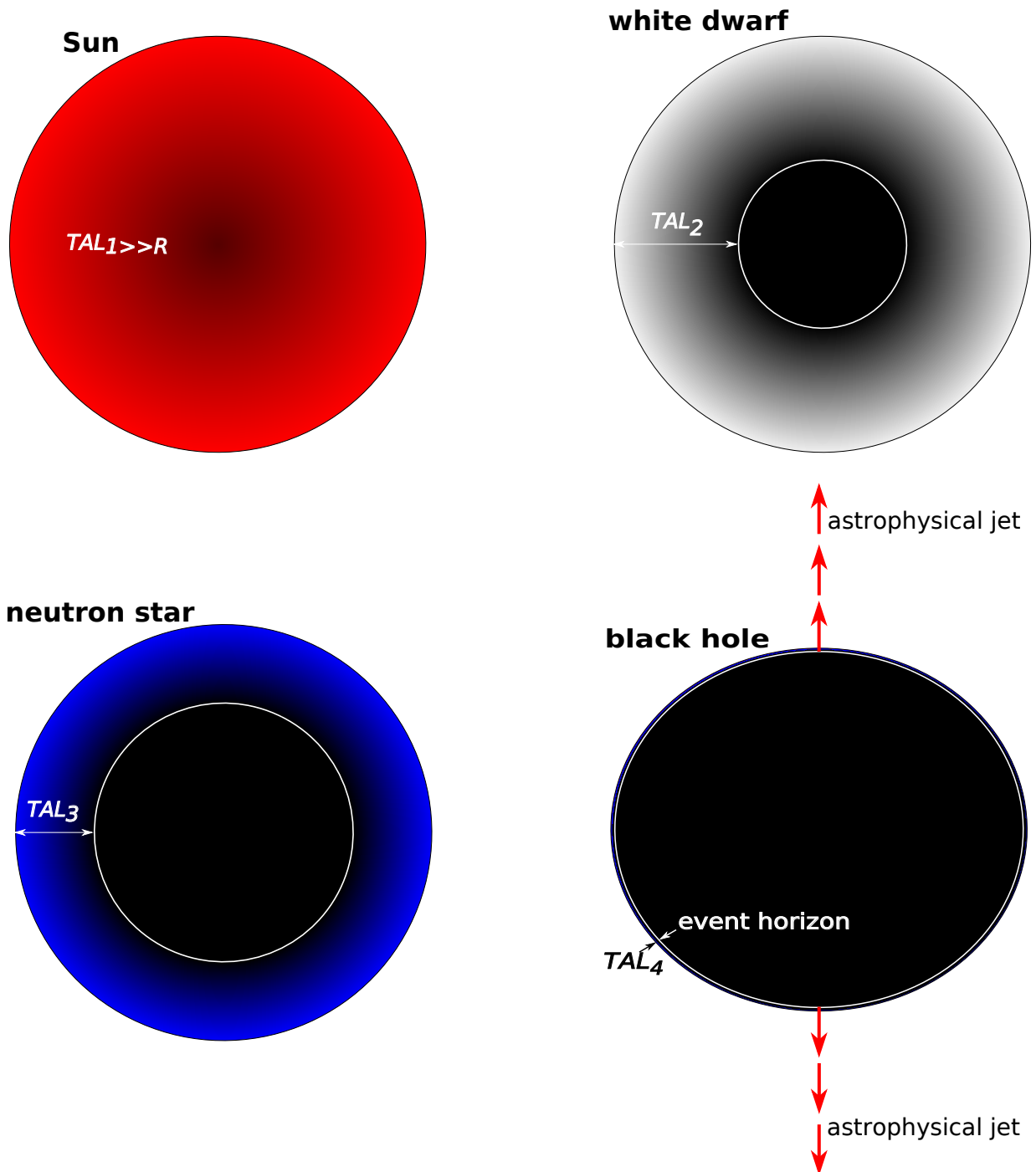


Figure 30: Diagrammatic perception of the Sun (upper-left), white dwarf (upper-right), neutron star (lower-left) and black hole (lower-right) with their corresponding total absorption layer

layer”). Similarly, we may apply the same scheme for subsequent denser bodies: We can envisage a “*type-II total absorption layer*” TAL_{II} or TAL_2 for white dwarfs, a “*type-III total absorption layer*” TAL_{III} or TAL_3 for neutron stars, also a “*type-IV total absorption layer*” TAL_{IV} or TAL_4 for black holes, and so on for other possible intermediate fields/bodies/particles. We initially (tentatively) think that these thicknesses may rank as $TAL_1 > TAL_2 > TAL_3 > TAL_4$.

By applying the workings of internal spherical field for the Sun, the internal contraction factor is only a little less than for Earth and both a little less than unity. By way of visual illustration (not to scale), we show the Sun’s distribution of effective mass in Fig. 30 (upper-left). Thus, we deem that $TAL_1 \gg R_{Sun}$. For a white dwarf, we may initially assume that $TAL_1 < R_{dwarf}$, for which a visual representation is provided in Fig. 30 (upper-right). Likewise, we have conceptualized a neutron star (lower-left) and a black hole (lower-right) in the same figure. We don’t know at this stage how the various types of push particles and total absorption layers may superpose or interact with each other and how we may rank them. We have not considered the possibilities of other, or intermediate situations, like the existence of quark stars.

At a later stage, we should compute the effective mass envelop of a black hole also in the shape of a rotating spheroid. We then find the dependence of the thickness of this envelop on the curvature of the spheroid. If the thickness is significantly less at the poles than at the equator, then an astrophysical jet could be formed at the poles on account of internal hydraulic pressure exerted by the envelop membrane everywhere inside the body. This weakening at the poles may be further enhanced by forces due to rotation. Also, the size of the black hole can be significant for such a process, but all this remains to be answered by formulating the entire dynamics of such a system. As soon as the black matter is squeezed out and exposed to push particles of all kinds, it becomes effective (active) mass and literally “lights up”. This is consistent with observed jets of plasma material coming out from the center of galaxies presumably occupied by black holes. It is plausible that black hole matter is jettisoned by squeezing out initially non-inertial (passive and inert) mass to form astrophysical jets.

A rough analog, in some respects, to conceptualize black holes may be the formation of liquid droplets or soap bubbles in the atmosphere in the absence of gravity (e.g. inside the international space station). The surface tension plays a decisive role for the spherical shape of the smallest of droplets, whilst its role changes as more mass is accreted. When the droplets becomes very large, any small perturbation causes the droplet to wobble and deviate from the spherical shape. The eccentricity of a rotating bubble can be also a contributing condition. Some resemblance may take place with black holes but with properties unparalleled by our familiar bubbles: There is no surface “tension” per se, whilst the interior is an incompressible and non-inertial (conventionally) mass being literally inert and inactive. The interior does not generate any force but can be acted upon by the membrane forces. Black holes can in principle grow to arbitrary large sizes, but as they do so, they become more unstable by nearby disturbances and/or by rotation. A breach at the poles will squirt out inert mass at extreme acceleration and velocity while the exterior surface of the forming jet becomes activated. This situation is governed by new mechanics to be worked out.

Earlier, we referred to the difference between real and effective mass as “passive” mass $m_{passive}$ (per Eq. 139). We could also call it “black matter” or “black mass” and designate it with $m_b \equiv m_{black}$, which should not be confused with the term “dark” matter already in use by existing physics terminology but with a different meaning. Thus, we can write for the real mass (and matter) in PG:

$$m = m_e + m_b \tag{229}$$

Based on the above equation, we can say that there is some fraction of black matter even in ordinary objects. That fraction can be exceedingly small, moderate or excessive depending on the size and density of the object. There must be more of this stuff in the Sun than in the Earth. The amount of gray color-level showing in the diagrams in Fig. 30 gives some idea about it (not to scale). We may visualize more black matter towards the center of celestial bodies. In doing all this, it is important that we have only considered some average density throughout each of the above bodies, whereas in reality the density is variable. We have seen in Section 10 that actual density distribution can alter all other parameters involved. The same applies for the planets and stars, so that the picture conveyed by Fig. 30 for the Sun could be misleading. Those who have all the relevant data about the Sun may like to see how we can build the correct PG picture of the Sun. The same applies for all other bodies in Fig. 30 and not only. We have selected those four typical types of bodies, but all other intermediate bodies with all available data could be re-worked to fit, or to see if they can fit under PG.

The above is an initial conceptualization of what might happen around and inside stars and other massive bodies, but is subject to later modification as we develop and better understand PG theory. Even the proposed classification of various fields and various types of push particles may be entirely or partially incorrect needing proper adjustments along with corresponding fractions of effective and black mass, for example, if existing information on surface gravity of those bodies is revised.

In the above general scheme, we imply that the maximum value of a starting g_0 is sufficient to trigger the first transition of a star to a white dwarf. Depending on the literature source, the pressure at the center of the Sun may range between 3×10^{13} - 3.5×10^{16} Pa. This is expected to be well below the maximum pressure by gravions predicted by Eq. 31

$$p_{0g} = \frac{J_0}{c} = \frac{g_0^2}{\pi^2 G} \quad (230)$$

which will be known when J_0 or g_0 is finally measured. For a tentative $g_0 = 4 \times 10^4$ m/s², we have $p_{0g} = (4 \times 10^4)^2 / (\pi^2 G) = 2.43 \times 10^{18}$ Pa. Therefore, this pressure is consistent with existing requirements for a star on the main sequence to collapse to a white dwarf. The pressure at the core of Sirius B (white dwarf) is estimated to be $\times 10^6$ that of the sun, which means that we need a $g_{02} > 10^3 g_0$.

If the conceptualization of various bodies in Fig. 30 is generally correct, it would question the validity of existing methods for finding their mass, radius and distance. There shouldn't be a serious problem for the main sequence stars, if their contraction factor q is not far from unity. From the observed (intrinsic) brightness, color (temperature) and distance, the established measurements of mass and radius might involve only a small correction, but for stars outside the main sequence, in particular for white dwarfs etc, we may have significant discrepancies between existing values and reality. To address this problem, we would probably also need to develop a concurrent quantum theory of push gravity. We need to re-appraise conceptions and requirements of established theories of nuclear particles and force fields. We now see that PG opens new possibilities for modeling our physical observations. For example, the Chandrasekhar curve may need re-adjustment, if we note some discrepancy with PG, rather than object to PG. We will return to the question of white dwarfs later after we attempt an inquiry at the small particles level. Like the flying shuttle weaves the fabric out of yarn, so may push particles weave the fabric of effective mass out of real mass (matter, or stuff). The material form of objects as we experience them is created from an amorphous substrate/matter through the action of gravions and other push particles by as yet unknown staged processes. We would need to bring together all particle physics data to date and attempt to explain them by PG.

One important corollary here is to indicate that the current scales of the cosmos may require adjustment. This should not be overlooked even if specific mechanisms above might turn out to be fallacious simplifications. Therefore, prospective criticisms against PG may themselves be based on false grounds. In turn, agreement or not by various theories (including GR) involving existing measurements of dwarfs, neutron stars and black holes may have to be revised. As a result, the findings of PG, like in Section 16 of the novel relationship between mass and force should not be dismissed (based on some other theory) until an integrated resolution of all emerging issues is obtained.

Note: The transmission depth τ defined above is based on an assumed exponential variation of J with depth. In a later development on mass-matter relationship in Section 24, we have derived the exact variation of several parameters as a function of radius in spherical geometry bodies. They are not pure exponential functions, but we can still define an equivalent or effective transmission depth to convey the same main ideas above.

19 Towards a quantum push gravity (QPG) theory

The explanation of gravity as arising from push particles (the gravions) already indicates the quantum nature of the generated field. However, so far we have described and discussed the absorption of gravions by material bodies in general without much regard about the nature of the absorbing body. We have introduced an absorption coefficient k only to denote the number of absorption events per unit length inside the body. So far, the body may be a continuum, inside which the absorption process takes place; the process obeys Lambert's law on the propagation of general radiation or beam transmission inside matter. It is the interaction of push particles with another material entity that completes the phenomenon of gravity. We attempt to complement our study by investigating the other side (member) of this process, i.e. the absorbing body including material particles like protons and electrons. In doing so, we must be reminded about the provisos of Part Two, namely, that these attempts may be revised by the author and the readers freely without harm to the outcomes of Part One.

The attempted development of a quantum push gravity (QPG) theory here follows an independent path from existing quantum gravity and quantum field theories. This happens either because the theory is self-sufficient without the need to introduce extraneous concepts, or because of limitations already outlined in the introduction of this report, which make a thorough literature survey impractical. The connection with existing theories may be effected as it becomes apparent to this author now or in later writing, but the onus is mainly on the expert reader to take over from all the loose ends created by, or left off from this report. The present sections may extend beyond the original scope of providing an early mathematical background

of a push gravity theory for the purpose of designing experimental verification of its principles. Pending such verification, we are only left with a continuation of the theoretical development and a compilation of thought experiments.

It is generally accepted that force fields are responsible for the force exerted between two particles, or the force is the result of the exchange of virtual-force-carrier-particles between the said two particles. The force field generated by each particle acts on the other particle. Furthermore, it is said that particles are interpreted as the quantum excitations of each field. Thus, photons are the excitations of the electromagnetic field, gluons are excitations of the strong gauge field, Higgs bosons are excitations of one component of the Higgs field and gravitons are presumed to be excitations of gravitational field or waves.

PG starts with a presumed existence of gravion particles, a consequence of which is the gravitational field. In that sense, gravions create (underlie) the gravitational field. If a disturbance of the steady-state gravitational field is thought of as a wave, and if the graviton (per literature) is that wave, then gravions and gravitons are two separate and different entities. The gravions precede the gravitons, and we were justified at the outset to introduce a new term for the push particle of gravity, namely, the gravion or type-I push particle. In subsequent extension of PG, we introduced the electrion (type-II) push particle underlying the electric field. As such and following a parallel reasoning as with gravity, we may say that a photon is a perturbation of electrions from their steady-state equilibrium. In other words, if the underlying quantum fields are more fundamental than particles, then we take it one step deeper by understanding that fields themselves are made up by more fundamental particles, the nature of which is yet to be comprehended. We may repeat the same reasoning for any other type of push particles responsible for other force fields. We realize that the term “particle” used here may differ from its meaning in the literature, so that we try to use the qualifier word “push” often.

In the following sections, we continue with possible forms of quantization of absorbing bodies, some absorption parameters and a description of the proton, electron and positron under the laws of PG.

19.1 Minimum absorption center (MAC)

A particle beam or any radiation, in general, traversing a material body may be scattered or absorbed by the body, partially or totally. That is, we may have partial or total reflection, partial absorption and scattering or total absorption with concomitant changes in the reacting body. For push gravity, we have considered only total absorption of gravions as a necessary condition to develop the theory, whilst we defer consideration about some other type of scattering also taking place; we should stress that our going assumption applies only to gravity, i.e. other types of force field may behave differently.

Around the absorption "point" of a gravion, there must be a minimal amount of a material entity or mechanism performing the absorption process. This process must also allow additional gravions to accumulate up to a critical limit, whereupon the accreted gravions are lumped and emitted in another form of radiation by the reasoning proposed in Section 15.8. That is, the absorption “point” constitutes a minimum thermodynamic subsystem evolving by fluctuations in time to a state that can emit the accumulated gravion mass (and energy) as permitted by the fluctuation theorem. We may refer to this quantum subsystem or minimal material entity as gravion absorption center, or quantum gravion absorption center, or simply as minimum absorption center (MAC). The distribution of MACs depends on the nature and state of any given material body, be it a gas, liquid or solid, plasma, electron, nucleon, etc. Some conceivable distribution patterns are depicted in Fig. 31 to help in the ensuing analysis, but they are not the only ones, whilst other appropriate patterns can be devised as we evolve our understanding. A given MAC is drawn in full red color to indicate that it is fully active and free of any shadowing effect by other “neighboring” matter. A MAC can only be active or inactive, so that it should be drawn either red or black correspondingly. At and near the surface of a body, there is a maximum time exposure to push particles, whilst, as the depth inside the bulk of a material increases and due to the shadowing (shielding) effect by the overlaying layers, the time exposure decreases exponentially. In any situation, a MAC can be active or inactive, ON or OFF, one of two states, i.e. a process thought to be governed by a Poisson distribution probability. The variation of gray level in its mixture with red color in the diagrams describes just the time averages of them being between the active and inactive state, i.e. between effective or black mass (or matter).

The four spacial distributions shown in Fig. 31 are entirely arbitrary at this point of our understanding: They may be distributed at the highest packing order (compacted) as in a cuboctahedron, or at the most dispersed, or a mixed type of distribution. These distributions are determined by the fixed or averaged spacial distribution of matter determined by other forces, like the chemical bonds pertaining to the electric field. That means that another type of force field (say, the electric field) is also present and takes precedence prior to the gravion force field (gravity). If the hypothesis is correct that the other fields are also due to push particles, then those other push particles must be permeating in the interstices of matter at the appropriate scales to maintain the material body in its macroscopic form. We will consider the electric field

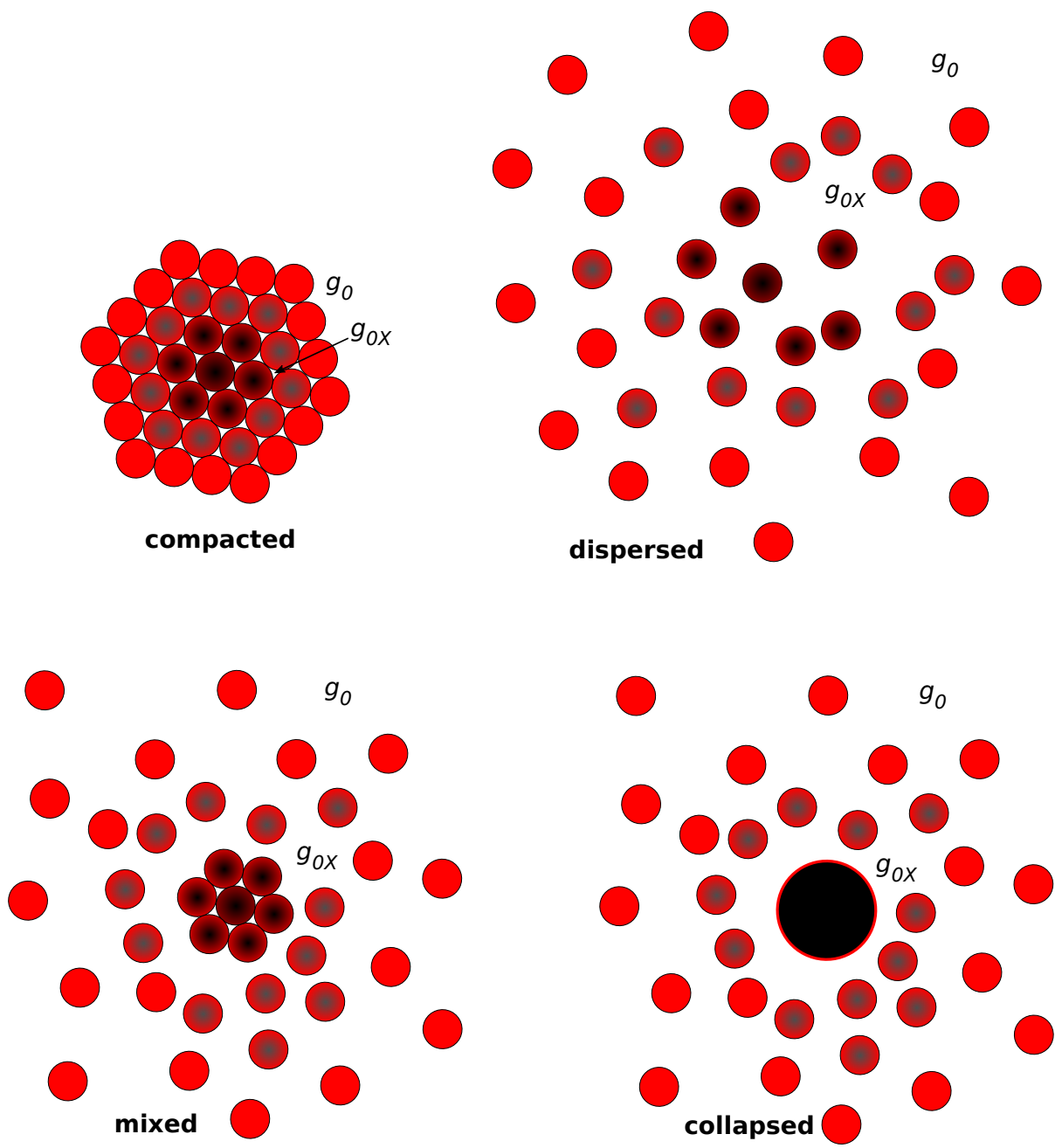


Figure 31: Conceptualization and configurations of minimum graviton absorption centers

in an upcoming version of the report, but we may remain with the gravitational (gravion) field for a while. The “collapsed” depiction of MACs in the provided diagram is an anticipated collapse of ordinary matter to the next or further finer-ingredient state, whereby the gravions can only penetrate a relatively small depth leaving the core as inactive mass with reference to gravions. However, this collapsed central region is a matter of concern whether we understand it correctly at this point, i.e. whether it is composed of plasma particles, neutrons, or quarks (not shown/resolved as finer spheres), or whether it is the ultimate black mass of a black hole. We have to return back to this section at a later stage of theory development.

It should be appreciated that the depictions in Fig. 31 are exaggerated in scale, because we already saw how little absorption takes place over the scale of planet sizes. The effects shown may become more evident above the scales of stars, etc. envisaged in the preceding Fig. 30.

19.2 Absorption coefficient vs. absorption cross-section

We can generally liaise microscopic with macroscopic processes, like those of microscopic particles with a (macroscopic) planet. We can apply the standard/general formulation of a directional particle beam scattering and absorption by a material body. Any macroscopic body may be composed of individual particles (including MACs) responsible for absorption events. Whether MACs may be thought of as particles themselves is a different question, because such “particles” may be impossible to isolate, or they may have an extremely short life to ever become observable. Nevertheless, we can say that the total number of absorbing particles, in whatever form, composing a planet would be the ratio M/m of the respective real masses of the planet and particles, of which the number density n is

$$n = \frac{M}{m} / \left(\frac{4}{3} \pi R^3 \right) = \frac{\rho}{m} \quad (231)$$

where R is the radius of the planet. A single particle has a characteristic radius R_0 , which defines a total absorption cross-section σ :

$$\sigma = \pi R_0^2 \quad (232)$$

The number of absorption events of a beam of gravions traversing our typical length ℓ is $k\ell$ with the generally known relationship for k :

$$k = n\sigma = \frac{\rho}{m} \pi R_0^2 \quad (233)$$

We also have from Eq. 114

$$k = \frac{\pi G \rho}{g_0} = \frac{\pi G \rho_e}{g_0 q} = \frac{k_e}{q} \quad (234)$$

where we similarly introduce a corresponding effective absorption coefficient k_e by:

$$k_e = \frac{\pi G \rho_e}{g_0} \quad (235)$$

and supplement yet another equation (formula) for the contraction factor:

$$q = \frac{k_e}{k} \quad (236)$$

The practical application of this effective absorption coefficient is that we can use the known effective mass of the used particle and the known effective mass of the planet, from the outset, to obtain a corresponding effective number density of the scattering particles:

$$n_e = \frac{\rho_e}{m_e} \quad (237)$$

The latter allows us to derive, or connect either of the absorption coefficients with the total absorption cross-section of the particle as:

$$k_e = n_e \sigma = \frac{\rho_e}{m_e} \pi R_0^2 = qk \quad (238)$$

The above method relates the microscopic absorption cross-sections with the macroscopic parameters of a planet, but the absorption cross-section can be taken to correspond to particles (including MACs) of any size with a given (absorption) effective mass. The particle can be an electron, proton, positron or any other

body including the entire planet itself. In the latter case, from Eq. 227, the planet's minimum radius at $A_R = 1$ is

$$R_{0-planet} = \sqrt{\frac{GM_e}{g_0}} \quad (239)$$

Then we can write the following useful relationships:

$$k_e = n_e \sigma = \frac{\rho_e}{M_e} \pi R_{0-planet}^2 = \frac{3R_{0-planet}^2}{4R^3} = \frac{3GM_e}{4g_0 R^3} = \frac{\pi G \rho_e}{g_0} = qk \quad (240)$$

From the above equations, we can obtain the minimum absorption radius of the Earth (i.e. its absorption cross-section) as a function of the prevailing g_0 . For example, we get $R_{0-Earth} = 8.928614 \times 10^4$ m, a total absorption cross-section $\sigma_{Earth} = 2.504482386487 \times 10^{10}$ m² and $k = 2.31236 \times 10^{-11}$ m⁻¹ for $g_0 = 50000$ ms⁻¹, as can also be cross-examined against Table 2 with use of data from Table 3. Again, these values are produced based on an average density distribution of Earth and should be re-evaluated by proper accounting of the actual prevailing density situation in the future.

19.3 Proton and electron parameters

Before we theorize a description of the electric field under push particle principles, we consider the graviton field (gravity) effect at the microscopic scales of proton and electron according to PG for a series of assumed cases with regard to their absorptivity and the amount of black mass possibly contained in them. We know that these particles have a gravitational mass, i.e. they have weight under gravity regardless of their very small size. We can use the available radius for proton, but no such radius is readily accepted for electron, for which it is said to be zero, or some very small value not yet found, or the so called "classical electron radius". We can return to these and other questions after we attempt to solve a series of cases in the form of exercises below. We take this approach initially, because of unknown parameters for these particles, with an intent to return for a another pass of computations later. None of the presented cases are claimed to represent actual cases, but they serve to alert us about some important issues.

19.3.1 Exercise: Proton parameters

Like for planets, we find the corresponding parameters for proton from Eqs. 147 and 149 given its (charge) radius and effective mass; the "charge" radius is used to be also the mass radius at this stage. The contraction q_p , absorption coefficient k_p and absorptivity A_{R-p} are given in Table 16 in the typical range for g_0 (we use p in the subscript for proton). We use the prevailing radius $R_p = 8.414000 \times 10^{-16}$ m and mass $m_{e-p} = 1.672622E \times 10^{-27}$ kg as its effective mass. We find that the contraction factor is very close to unity, which means that the real mass is very close to the measured effective mass.

From the above known parameters of proton, we find its total real mass m_p and its black mass component m_{b-p} from the contraction factor:

$$m_{b-p} = m_p - m_{e-p} = \frac{m_{e-p}}{q_p} - m_{e-p} = \left(\frac{1}{q_p} - 1 \right) m_{e-p} \quad (241)$$

We note that only an extremely small fraction of mass is inactive (black), whilst correspondingly the absorptivity is also very low. However, all these parameters may need revision as soon as the radius of the proton is further revised; in fact, we feel that such a revision is overdue, whilst PG will assist in doing so.

19.3.2 Exercise: Electron parameters in case of equal electron-proton real mass

The electron is considered an elementary or fundamental particle that cannot be decomposed to other particles, yet it presents some sort of a connection with proton by its constant (effective) mass ratio $\mu = m_{e-p}/m_{e-e}$, its equal but opposite charge and by both particles being stable in time (i.e. extremely long - if not infinite- lifetimes). The β^+ decay or "inverse beta decay" inside a nucleus is written by:



where e^+ is a positron, ν_e is an electron neutrino and $\bar{\nu}_e$ an electron antineutrino. Likewise, the beta decay for the neutron (β^- decay) is written by:

$$n^0 \rightarrow p^+ + e^- + \bar{\nu}_e \quad (244)$$

It is said that all particles can be made from leptons. Without specifying the kinds of particles, the idea of building particles from other particles is consistent with the general concepts of PG and its framework. They could be described under PG too in balancing the energy and total mass yielding a tiny rest mass for the electron neutrino/antineutrino. We cannot enter into a detailed correlation or explanation of particle physics data under PG yet.

There seems to be a fundamental relationship between proton and electron, which can now be revisited under various possibilities presented by PG. These possibilities arise from the existence of and distinction between real, effective and black mass, which could presumably be used to establish that relationship. The possibility of combining gravion absorption with black mass in various proportions to produce effective mass for any given particle might assist existing theories in nuclear reactions and particle physics in general, as we might be able to better understand and explain the above reactions. For this purpose, we present some results in the form of a series of “exercises”, which might point to a direction, or provide the means to address the problem in due course.

For convenience, we repeat our previous equations: The radius of a particle is given by

$$R = \sqrt{\frac{Gm_e}{g_0 A_R}} \quad (245)$$

where in the limiting case of $A_R = 1$, we obtain the characteristic minimum radius R_0

$$R_0 = \sqrt{\frac{Gm_e}{g_0}} \quad (246)$$

It is said that electrons have zero radius, being point masses, or on account of its mass ratio with proton it may be less than 10^{-18} m, but the radius is as yet unspecified. There is also the classical electron radius of $R = 2.8179403227(19) \times 10^{-15}$ m, which, being greater than the proton radius, it is said to have only a theoretical value. Now, we could initially obtain a radius from the above formula, except that we don't know A_R . The value of $A_R = 1$ means an absolutely total absorption layer forming an effective mass with “zero” thickness. This would also imply an infinite, or extremely large real mass, which would be very difficult to explain. However, this idealized situation is simply a mathematical artifact that can be dealt with in a quantum PG. We can only accept a finite value for the real mass accompanied by a finite absorption layer thickness (TAL) for the existing (established) effective mass of the electron. We have no indication what the real mass of the electron may, or should be. That could perhaps be derived during a concerted effort to fit various existing data of the “standard model” or other data under the framework of PG. The present author is in no position to achieve this goal for lack of readily available knowledge of the existing vast pool of information. However, we can demonstrate by simple algebra how to go about with some tentative considerations in a possible relationship between proton and electron (or positron).

We have generally considered the effect of shrinking a given constant spherical mass in Section 9.1. We apply this situation to the case of a proton and see what happens. Because its contraction factor is very close to unity and its absorptivity very small getting smaller at higher g_0 , it can be envisaged as being very “fluffy” or “compressible”. This is consistent with its structure of three quarks. In plain terms, the proton seems to be very “transparent” to gravions.

g_0	q_p	k_p	A_{R-p}	m_{b-p}
300	0.99999999704344	4.68513035281366E+05	5.25609157025589E-10	4.945210E-37
500	0.99999999822606	2.81107821135575E+05	3.15365494215353E-10	2.967133E-37
1000	0.99999999911303	1.40553910555320E+05	1.57682747107676E-10	1.483566E-37
2000	0.99999999955651	7.02769552745438E+04	7.88413735538384E-11	7.417906E-38
5000	0.99999999982260	2.81107821090695E+04	3.15365494215353E-11	2.967237E-38
10000	0.99999999991130	1.40553910544101E+04	1.57682747107676E-11	1.483618E-38
20000	0.99999999995565	7.02769552717388E+03	7.88413735538384E-12	7.418277E-39
30000	0.99999999997043	4.68513035144233E+03	5.25609157025589E-12	4.945890E-39
50000	0.99999999998226	2.81107821086207E+03	3.15365494215353E-12	2.967459E-39

Table 16: PG parameters for proton

Initially, we consider what would happen, if we could compress the proton to a much smaller radius keeping its real mass constant. We re-write Eq. 147 both for a proton and an electron together with their contraction factors, whereby we also use the same real mass m for both:

$$m_{e-p} = q_p m = \frac{g_0}{G} A_{R-p} R_p^2 \quad (247)$$

$$m_{e-e} = q_e m = \frac{g_0}{G} A_{R-e} R_{-e}^2 \quad (248)$$

[Note: the subscript $_e$ stands for “effective”, the subscript $_{-e}$ stands for “electron”, whilst the subscript $_p$ or $_{-p}$ stands for “proton”]. In other words, we consider that we compress the proton to such a radius that its effective mass reduces to become equal to the published (effective) mass of an electron, namely, $m_{e-e} = 9.1093837015 \times 10^{-31}$ kg. We expect that the effective mass of a sphere decreases, if we keep the real mass constant: Because A_R can never exceed unity, by arbitrarily reducing the radius in the above equations, the only compensation can be a reduction of the contraction factor and hence by a corresponding decrease of the effective mass.

The proton-to-electron mass ratio μ is well known to be:

$$\mu = \frac{m_{e-p}}{m_{e-e}} = \frac{q_p}{q_{-e}} = 1836.15267343 \quad (249)$$

where we have canceled the common m and also relate the above by:

$$\mu = \frac{A_{R-p} R_p^2}{A_{R-e} R_{-e}^2} \quad (250)$$

from which we find the electron radius as:

$$R_{-e} = \sqrt{\frac{A_{R-p}}{\mu A_{R-e}}} R_p \quad (251)$$

We can find the unknown A_{R-e} as follows: The contraction factor for the electron is given by:

$$q_{-e} = \frac{q_p}{\mu} = \frac{3A_{R-e}}{4kR_{-e}} \quad (252)$$

which yields the equation

$$\frac{3A_{R-e}}{4kR_{-e}} - \frac{q_p}{\mu} = 0 \quad (253)$$

The above can be solved first for the unknown product kR_{-e} (for electron), which appears also inside A_{R-e} (see Eq. 44), and from which we obtain A_{R-e} and then the electron radius from Eq. 251. We have done this numerically and list the final results in Table 17. Like for proton, we find the black (inactive) mass m_{b-e} for the electron (positron) under this particular condition of maintaining a constant real mass $m_p = m_{-e} = m$ by

$$m_{b-e} = m_{-e} - m_{e-e} = \frac{m_{e-e}}{q_e} - m_{e-e} = \left(\frac{1}{q_e} - 1 \right) m_{e-e} \quad (254)$$

Notable is the comparatively large black mass in the electron (positron). We also find and list the theoretical limiting radius R_{0-e} , which is the same and repeated in all tables for easy reference; the difference between the two radii $R_{-e} - R_{0-e} \equiv \Delta R_{-e}$ is discussed below.

Since the positron is the counterpart of the electron having the same effective mass, we could imagine the positron as being a compressed proton by the above means, or conversely, the proton as a “blown-up” positron. We are aware of the theory that the proton consists of quarks and muons, but the imagined contraction or expansion of real mass does not necessarily negate an internal structure of the proton as a function of that of a positron.

The above analysis presents only a methodology on how to deal with real and effective mass and with their associated parameters without claiming to have found the actual electron radius yet. The latter may have any value subject to the electron absorptivity factor A_{R-e} as it deviates from unity. The greater the deviation, the greater the electron radius. To be able to finally solve this question, we need to apply the above methodology in a way that produces outcomes consistent with other existing data and general information not only relating to electrons but also spanning the entire physical world at various scales.

g_0	q_{-e}	kR_{-e}	$A_{R_{-e}}$	$m_{b_{-e}}$
300	5.44617021326613E-04	1.37711414240144E+03	0.9999997363485721592	1.67171098512473E-27
500	5.44617021391021E-04	1.37711414223858E+03	0.9999997363485720969	1.67171098492693E-27
1000	5.44617021439326E-04	1.37711414211643E+03	0.9999997363485720501	1.67171098477857E-27
2000	5.44617021463479E-04	1.37711414205536E+03	0.9999997363485720267	1.67171098470439E-27
5000	5.44617021477971E-04	1.37711414201872E+03	0.9999997363485720127	1.67171098465989E-27
10000	5.44617021482801E-04	1.37711414200650E+03	0.9999997363485720080	1.67171098464505E-27
20000	5.44617021485217E-04	1.37711414200040E+03	0.9999997363485720057	1.67171098463763E-27
30000	5.44617021486022E-04	1.37711414199836E+03	0.9999997363485720049	1.67171098463516E-27
50000	5.44617021486666E-04	1.37711414199673E+03	0.9999997363485720043	1.67171098463318E-27
g_0	R_{-e}	$R_{0_{-e}}$	ΔR_{-e}	k_{-e}
300	4.50173194740697E-22	4.50173135396290E-22	5.93444066960637E-29	3.05907628106260E+24
500	3.48702657227941E-22	3.48702611259961E-22	4.59679797757554E-29	3.94925049664415E+24
1000	2.46570013543645E-22	2.46569981039375E-22	3.25042702226488E-29	5.58508361306745E+24
2000	1.74351328613970E-22	1.74351305629980E-22	2.29839898939935E-29	7.89850099223745E+24
5000	1.10269462299327E-22	1.10269447762975E-22	1.45363515574359E-29	1.24886266179528E+25
10000	7.79722845496485E-23	7.79722742708958E-23	1.02787527601569E-29	1.76615851383658E+25
20000	5.51347311496635E-23	5.51347238814878E-23	7.26817577891135E-30	2.49772532355734E+25
30000	4.50173194740697E-23	4.50173135396290E-23	5.93444067308037E-30	3.05907628016721E+25
50000	3.48702657227941E-23	3.48702611259961E-23	4.59679797919012E-30	3.94925049595058E+25

Table 17: Derived PG parameters for electron (positron) in the case of constant (equal) real mass between electron-proton.

The example analyzed above is just one possibility among many. There is a variety of combinations of effective mass with black mass, g_0 value and radius. We demonstrate some of those other possibilities below, which may later help us derive not only the electron radius but also the proton-to-electron mass ratio μ and other particle relationships.

[Note: Could PG theory help in the mysterious discrepancy of proton diameter measurements and other anomalies with muon technologies? From Wikipedia article on hadrons, we quote a relevant statement: *"In other phases of matter the hadrons may disappear. For example, at very high temperature and high pressure, unless there are sufficiently many flavors of quarks, the theory of quantum chromodynamics (QCD) predicts that quarks and gluons will no longer be confined within hadrons, "because the strength of the strong interaction diminishes with energy". This property, which is known as asymptotic freedom, has been experimentally confirmed in the energy range between 1 GeV and 1 TeV "*]

19.3.3 Exercises: Electron parameters in case of x:y gravion accretion

We can repeat the previous exercise by setting various other conditions between the different types of mass. We can generalize the previous derivations for the following hypothetical particle relationship like:

$$p^+ \rightarrow e^+ + \nu \quad (255)$$

where ν is a hypothetical particle (in lieu of a known neutrino) with all particles being at rest with no kinetic energy, so that we write for their masses the equation:

$$m_{e-p} = m_{e-e} + m_{e-\nu} \quad (256)$$

where the masses of the positron and electron are the same ($m_{e-positron} = m_{e-e}$) and $m_{e-\nu}$ is the effective mass of the hypothetical emitted (balancing) particle in lieu of a known neutrino. This hypothesis allows us to add mass to the electron (positron) from an external source, which can be an accretion of gravions. Now, instead of keeping the same real mass for the electron and proton, we can try to vary the real mass from m_p to m_{-e} , or from m_{-e} to m_p and re-write their equations as

$$m_{e-p} = q_p m_p = \frac{g_0}{G} A_{R-p} R_p^2 \quad (257)$$

$$m_{e-e} = q_e m_{-e} = \frac{g_0}{G} A_{R-e} R_{-e}^2 \quad (258)$$

with corresponding contraction factors q_p and q_e . The absorptivities and radii of the proton and electron are still related via Eq. 250 (by dividing the above equations), but the contraction factors relate differently. The proton's effective mass can be written as the above sum by

$$m_{e-p} = m_{e-e} + m_{e-\nu} = \frac{m_{e-p}}{\mu} + m_{e-\nu} \quad (259)$$

where we factor in their observed (effective) mass relationship μ between electron(positron)-proton. The above equation is only a starting approach to help build the required term $m_{e-\nu}$ in various ways of combining added gravion mass with existing black mass in the electron to produce effective mass in the proton; in this process, mass and energy are interchangeable in the summed terms by lumping them together. To build a proton from an electron(positron) in this way, we need an available amount of black mass $m_{b-available}$ in the electron over and above the final remnant black mass m_{b-p} in the proton, i.e. we must have for the electron total real mass:

$$m_{-e} = \frac{m_{e-p}}{\mu} + m_{b-available} + m_{b-p} \quad (260)$$

with a total electron black mass being $m_{b-e} = m_{b-available} + m_{b-p}$.

Now, we can build the term $m_{e-\nu}$ from a given amount of the "available" black mass ($m_{b-available}$) via the absorption of gravions in various ways. Let's designate the energy/mass of a single gravion by ω , which when absorbed adds a quantum of ω mass/energy to the absorbing center. We can generalize so that x accreted gravions (or mass parts) combine with y parts of black mass in the electron (positron), i.e. we make the rule $x : y$ with the meaning that an amount of $y\omega$ black mass combines with an amount of $x\omega$ gravion mass to yield an amount of $x\omega + y\omega$ effective mass towards building the proton. In this connection, we envisaged that the black mass is "granulated" with grains of ω mass each, but this is not a necessary condition, whilst it is used for convenience in our mathematical formulation. What we actually need is the fraction $x\omega/(x\omega + y\omega) = x/(x + y)$, from which we find the available (needed) black mass in the electron to be present,

$$m_{b-available} = \frac{y}{x + y} m_{e-\nu} = \frac{y}{x + y} \left(m_{e-p} - \frac{m_{e-p}}{\mu} \right) \quad (261)$$

so that the total real mass of the electron (positron) should be:

$$m_{-e} = \frac{m_{e-p}}{\mu} + \frac{y}{x + y} \left(m_{e-p} - \frac{m_{e-p}}{\mu} \right) + m_{b-p} = m_{e-p} \left[\frac{x}{(x + y)\mu} + \frac{1}{q_p} - \left(\frac{x}{x + y} \right) \right] \quad (262)$$

where we used Eq. 241 for the proton black mass. From this, we derive the overall general equation for the electron contraction:

$$q_{-e} = \frac{m_{e-e}}{m_{-e}} = \left(\frac{x}{x + y} (1 - \mu) + \frac{\mu}{q_p} \right)^{-1} \quad (263)$$

that is used in the below equation (like in 253) to find all the electron parameters in the usual way:

$$\frac{3A_{R-e}}{4kR_{-e}} - \left(\frac{x}{x + y} (1 - \mu) + \frac{\mu}{q_p} \right)^{-1} = 0 \quad (264)$$

We can vary the fraction x/y in the range $0 \rightarrow \infty$. When $x = 0$, we recover Eqs. 252 and 253, i.e. the case for constant real mass without external contribution. When $x = \infty$, i.e. there is no need to have any available $m_{b-available}$ mass, so that the above equations reduce to:

$$q_{-e} = \left(1 - \mu + \frac{\mu}{q_p} \right)^{-1} \quad (265)$$

$$\frac{3A_{R-e}}{4kR_{-e}} - \left(1 - \mu + \frac{\mu}{q_p} \right)^{-1} = 0 \quad (266)$$

from which we found the results of Table 21; in this case, the added effective mass originates exclusively from external contribution. We present some examples for the electron parameters as before in Tables 18 through to 21 for a selection of ratios $x : y$. Furthermore, we have extended the computations to include more results (points) for this ratio in the range $0 \rightarrow \infty$ in Table 22 for two values of g_0 . The results are also presented for many more points in graph form with logarithmic scales in Fig. 32. These outcomes are discussed in more detail next.

g_0	q_{-e}	kR_{-e}	$A_{R_{-e}}$	$m_{b_{-e}}$
300	1.08864114983105E-03	6.88931527181105E+02	0.9999989465403999087	8.35855492809629E-28
500	1.08864115008840E-03	6.88931527018244E+02	0.9999989465403994106	8.35855492611821E-28
1000	1.08864115028141E-03	6.88931526896099E+02	0.9999989465403990371	8.35855492463466E-28
2000	1.08864115037791E-03	6.88931526835026E+02	0.9999989465403988503	8.35855492389288E-28
5000	1.08864115043582E-03	6.88931526798382E+02	0.9999989465403987382	8.35855492344781E-28
10000	1.08864115045512E-03	6.88931526786168E+02	0.9999989465403987009	8.35855492329945E-28
20000	1.08864115046477E-03	6.88931526780061E+02	0.9999989465403986822	8.35855492322528E-28
30000	1.08864115046799E-03	6.88931526778025E+02	0.9999989465403986760	8.35855492320055E-28
50000	1.08864115047056E-03	6.88931526776396E+02	0.9999989465403986710	8.35855492318077E-28
g_0	R_{-e}	$R_{0_{-e}}$	ΔR_{-e}	k_{-e}
300	4.50173372516083E-22	4.50173135396290E-22	2.37119792940316E-28	1.53036934044004E+24
500	3.48702794932163E-22	3.48702611259961E-22	1.83672201909637E-28	1.97569832255652E+24
1000	2.46570110915235E-22	2.46569981039375E-22	1.29875859531822E-28	2.79405936242182E+24
2000	1.74351397466081E-22	1.74351305629980E-22	9.18361010036657E-29	3.95139664406219E+24
5000	1.10269505845225E-22	1.10269447762975E-22	5.80822501263505E-29	6.24770666665878E+24
10000	7.79723153412487E-23	7.79722742708958E-23	4.10703529323719E-29	8.83559150156096E+24
20000	5.51347529226128E-23	5.51347238814878E-23	2.90411250647199E-29	1.24954133329852E+25
30000	4.50173372516083E-23	4.50173135396290E-23	2.37119793217784E-29	1.53036933954465E+25
50000	3.48702794932163E-23	3.48702611259961E-23	1.83672202038593E-29	1.97569832186295E+25

Table 18: Derived PG parameters for electron (positron) in the case of variable mass rule 1:1

g_0	q_{-e}	kR_{-e}	$A_{R_{-e}}$	$m_{b_{-e}}$
300	7.03405088619216E-03	1.06619503325234E+02	9.99956015800314E-01	1.28593153158382E-28
500	7.03405089693614E-03	1.06619503162367E+02	9.99956015800180E-01	1.28593152960574E-28
1000	7.03405090499413E-03	1.06619503040216E+02	9.99956015800079E-01	1.28593152812218E-28
2000	7.03405090902312E-03	1.06619502979141E+02	9.99956015800029E-01	1.28593152738040E-28
5000	7.03405091144052E-03	1.06619502942495E+02	9.99956015799998E-01	1.28593152693534E-28
10000	7.03405091224632E-03	1.06619502930280E+02	9.99956015799988E-01	1.28593152678698E-28
20000	7.03405091264922E-03	1.06619502924173E+02	9.99956015799983E-01	1.28593152671280E-28
30000	7.03405091278352E-03	1.06619502922137E+02	9.99956015799982E-01	1.28593152668808E-28
50000	7.03405091289096E-03	1.06619502920508E+02	9.99956015799980E-01	1.28593152666830E-28
g_0	R_{-e}	$R_{0_{-e}}$	ΔR_{-e}	k_{-e}
300	4.50183035975433E-22	4.50173135396290E-22	9.90057914308844E-27	2.36835897412741E+23
500	3.48710280215613E-22	3.48702611259961E-22	7.66895565122834E-27	3.05753828354135E+23
1000	2.46575403809933E-22	2.46569981039375E-22	5.42277055802827E-27	4.32401210310503E+23
2000	1.74355140107819E-22	1.74351305629980E-22	3.83447783879373E-27	6.11507655657349E+23
5000	1.10271872899698E-22	1.10269447762975E-22	2.42513672327273E-27	9.66878498921251E+23
10000	7.79739891015185E-23	7.79722742708958E-23	1.71483062272360E-27	1.36737268618470E+24
20000	5.51359364498498E-23	5.51347238814878E-23	1.21256836205313E-27	1.93375699751017E+24
30000	4.50183035975508E-23	4.50173135396290E-23	9.90057921795331E-28	2.36835896517295E+24
50000	3.48710280215647E-23	3.48702611259961E-23	7.66895568602239E-28	3.05753827660524E+24

Table 19: Derived PG parameters for electron (positron) in the case of variable mass rule 12:1

g_0	q_{-e}	kR_{-e}	$A_{R_{-e}}$	$m_{b_{-e}}$
300	9.63934186896923E-01	4.93609383070407E-02	6.34409279086220E-02	3.40829627576949E-32
500	9.63934388663436E-01	4.93606548086926E-02	6.34405768227254E-02	3.40827649499800E-32
1000	9.63934539988376E-01	4.93604421849095E-02	6.34403135081781E-02	3.40826165941939E-32
2000	9.63934615650864E-01	4.93603358730108E-02	6.34401818508643E-02	3.40825424163008E-32
5000	9.63934661048362E-01	4.93602720858693E-02	6.34401028564632E-02	3.40824979095650E-32
10000	9.63934676180862E-01	4.93602508234885E-02	6.34400765249941E-02	3.40824830739864E-32
20000	9.63934683747113E-01	4.93602401922980E-02	6.34400633592591E-02	3.40824756561971E-32
30000	9.63934686269196E-01	4.93602366485678E-02	6.34400589706807E-02	3.40824731836007E-32
40000	9.63934687530238E-01	4.93602348767027E-02	6.34400567763915E-02	3.40824719473024E-32
50000	9.63934688286863E-01	4.93602338135836E-02	6.34400554598180E-02	3.40824712055235E-32
g_0	R_{-e}	$R_{0_{-e}}$	ΔR_{-e}	k_{-e}
300	1.78728911805991E-21	4.50173135396290E-22	1.33711598266362E-21	2.76177691724670E+19
500	1.38443202859096E-21	3.48702611259961E-22	1.03572941733100E-21	3.56540832553048E+19
1000	9.78943307096927E-22	2.46569981039375E-22	7.32373326057552E-22	5.04221662552541E+19
2000	6.92218169123965E-22	1.74351305629980E-22	5.17866863493985E-22	7.13074837886423E+19
5000	4.37797483004940E-22	1.10269447762975E-22	3.27528035241965E-22	1.12746815598555E+20
10000	3.09569633264237E-22	7.79722742708958E-23	2.31597358993341E-22	1.59447973959889E+20
20000	2.18898809644638E-22	5.51347238814878E-23	1.63764085763150E-22	2.25493415301937E+20
30000	1.78730135825983E-22	4.50173135396290E-23	1.33712822286354E-22	2.76171874544013E+20
40000	1.54784840724023E-22	3.89861371354479E-23	1.15798703588575E-22	3.18895795258856E+20
50000	1.38443771734721E-22	3.48702611259961E-23	1.03573510608725E-22	3.56536326590157E+20

Table 20: Derived PG parameters for electron (positron) in the case of variable mass rule 49048:1.

g_0	q_{-e}	kR_{-e}	$A_{R_{-e}}$	$m_{b_{-e}}$
300	9.99999457132400E-01	7.23823744995925E-07	9.65097802740621E-07	4.94519194260210E-37
500	9.99999674279410E-01	4.34294219814202E-07	5.79058771140844E-07	2.96711479371232E-37
1000	9.99999837139729E-01	2.17147052147437E-07	2.89529355710413E-07	1.48355693244071E-37
2000	9.99999918569909E-01	1.08573460670328E-07	1.44764602438909E-07	7.41778001932116E-38
5000	9.99999967428023E-01	4.34293033380708E-08	5.79057358979900E-08	2.96710643667659E-38
10000	9.99999983714062E-01	2.17145838196526E-08	2.89527779546803E-08	1.48354857586291E-38
20000	9.99999991857082E-01	1.08572239840062E-08	1.44762985274623E-08	7.41769645468789E-39
30000	9.99999994571422E-01	7.23810402746675E-09	9.65080531756552E-09	4.94510002005967E-39
50000	9.99999996742893E-01	4.34280805815849E-09	5.79041072535134E-09	2.96702287236387E-39
g_0	R_{-e}	$R_{0_{-e}}$	ΔR_{-e}	k_{-e}
300	4.58240965125915E-19	4.50173135396290E-22	4.57790791990518E-19	1.57957013903598E+12
500	4.58240929714180E-19	3.48702611259961E-22	4.57892227102920E-19	9.47742097339680E+11
1000	4.58240953344043E-19	2.46569981039375E-22	4.57994383363003E-19	4.73870898187498E+11
2000	4.58241072706203E-19	1.74351305629980E-22	4.58066721400573E-19	2.36935244650012E+11
5000	4.58241488475362E-19	1.10269447762975E-22	4.58131219027599E-19	9.47738352600211E+10
10000	4.58242200653944E-19	7.79722742708958E-23	4.58164228379673E-19	4.73866959190235E+10
20000	4.58243632231437E-19	5.51347238814878E-23	4.58188497507556E-19	2.36931257094321E+10
30000	4.58245065424667E-19	4.50173135396290E-23	4.58200048111127E-19	1.57952688934228E+10
50000	4.58247932812879E-19	3.48702611259961E-23	4.58213062551753E-19	9.47698341267113E+09

Table 21: Derived PG parameters for electron (positron) in the case of variable mass rule $\infty : 0$

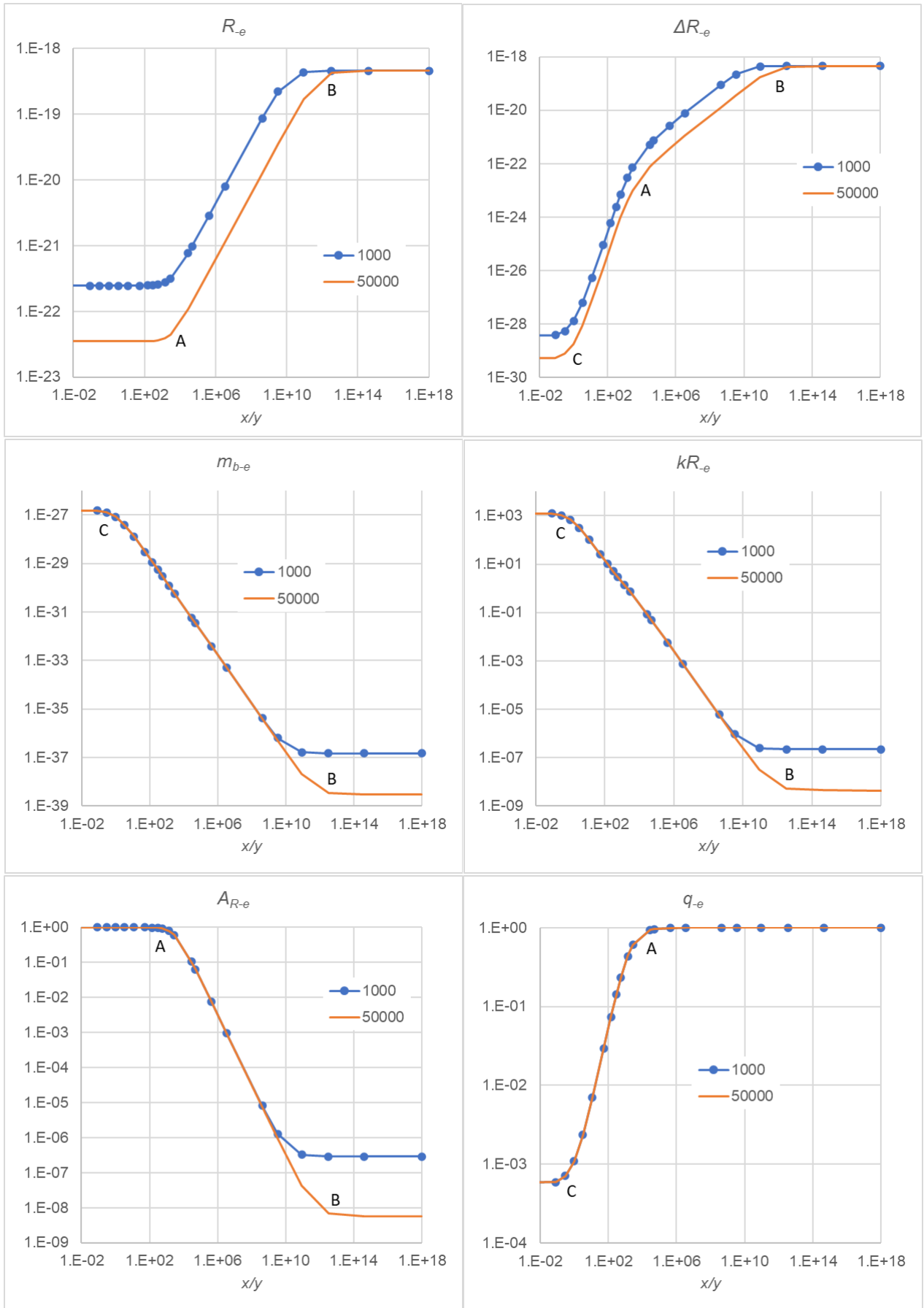


Figure 32: Plotting the electron parameters per Table 22 versus the ratio x/y for two fixed values 1000 and 50000 of g_0

x/y	g_0	q_{-e}	kR_{-e}	$A_{R_{-e}}$	m_{b-e}	R_{-e}	ΔR_{-e}
0/1	1000	0.0005446170	1377.11414212	0.99999974	1.67171098E-27	2.46570014E-22	3.25E-29
	50000	0.0005446170	1377.11414200	0.99999974	1.67171098E-27	3.48702657E-23	4.60E-30
1/12	1000	0.0005899750	1271.23991918	0.99999969	1.54311783E-27	2.46570019E-22	3.81E-29
	50000	0.0005899750	1271.23991906	0.99999969	1.54311783E-27	3.48702665E-23	5.39E-30
3/10	1000	0.0007078865	1059.49145518	0.99999955	1.28593153E-27	2.46570036E-22	5.49E-29
	50000	0.0007078865	1059.49145506	0.99999955	1.28593153E-27	3.48702689E-23	7.77E-30
1/1	1000	0.0010886412	688.93152690	0.99999895	8.35855492E-28	2.46570111E-22	1.30E-28
	50000	0.0010886412	688.93152678	0.99999895	8.35855492E-28	3.48702795E-23	1.84E-29
10/3	1000	0.0023557305	318.37100771	0.99999507	3.85779458E-28	2.46570589E-22	6.08E-28
	50000	0.0023557305	318.37100759	0.99999507	3.85779458E-28	3.48703471E-23	8.60E-29
12/1	1000	0.0070340509	106.61950304	0.99995602	1.28593153E-28	2.46575404E-22	5.42E-27
	50000	0.0070340509	106.61950292	0.99995602	1.28593153E-28	3.48710280E-23	7.67E-28
54/1	1000	0.0290981784	25.75538124	0.99924624	3.03947453E-29	2.46662961E-22	9.30E-26
	50000	0.0290981786	25.75538112	0.99924624	3.03947452E-29	3.48834105E-23	1.31E-26
146/1	1000	0.0741617940	10.06309090	0.99506250	1.13721837E-29	2.47180964E-22	6.11E-25
	50000	0.0741617949	10.06309078	0.99506250	1.13721836E-29	3.49566672E-23	8.64E-26
49048/1	1000	0.9639345400	0.04936044	0.06344031	3.40826166E-32	9.78943307E-22	7.32E-22
	50000	0.9639346883	0.04936023	0.06344006	3.40824712E-32	1.38443772E-22	1.04E-22
$\infty/0$	1000	0.9999998371	2.1714705E-07	2.8952E-07	1.48355693E-37	4.58240953E-19	4.58E-19
	50000	9.999999E-01	4.3428080E-09	5.7904E-09	2.96702287E-39	4.58247932E-19	4.58E-19

Table 22: Electron (positron) parameter variation with admixture effective/black_mass m_e/m_b at two values of g_0

19.3.4 Discussion

From the provided tables and graphs, we note some salient outcomes:

- The electron radius R_{-e} lies in the range $3.4870266 \times 10^{-23} \rightarrow 4.58 \times 10^{-19}$ m for the highest value of g_0 used and in a sub-range of the same for lower values of g_0 . The lowest value of radius is only slightly above the characteristic limiting electron radius $R_{0-e} = 3.4870261 \times 10^{-23}$ for the high g_0 (see Table 17).
- The slope (on log-log scales) of the radius variation is initially close to zero followed with a nearly fixed slope up to the maximum radius. The middle range of variation is re-plotted in Fig. 33, where the straight line is fitted with a power function for the two values of g_0 . There are two characteristic inflection points A and B at specific values of the ratio x/y .
- The radii difference ΔR_{-e} simply follows the variation of R_{-e} where R_{-e} is much greater than R_{0-e} , otherwise it shows some additional information: There is a new inflection point C very early before point A is shifted upwards. Point C occurs around $x/y=3/10$, point A around $x/y=560/1$ and point B around $x/y=3338337000/1$.
- Either only two combinations or all three of points A, B and C appear with each of the electron parameters at the same x/y .
- From the previous parameters, we have further extracted the absorption coefficient k_{-e} , the effective ρ_e and real ρ densities as well as the universal constant Λ as shown in Fig. 33. The latter constant depends only on the chosen g_0 and the values shown confirm those already provided in Table 2 for large bodies, as it should.
- All electron parameters present the usual ‘‘sigmoid’’ shape like in Fig. 3, except we have now used logarithmic scales for both axes, which allows us to distinguish differences at the very small scale of the ordinate axis: Thus all parameters are affected by a change in g_0 , except the contraction coefficient (albeit to a very small extent). It is interesting to observe how the effect of g_0 takes place in the ranges between points A, B and C. Furthermore, it should be noted that even where the curves appear indistinguishable, there is still some very small difference for all parameters per numerical values in tables (less than the fifth decimal place).

The above summary of results may be important in attempting to explain the properties of the electron and positron in this report but also by other workers in particle physics and cosmology in general. The electron radius seems to assume a finite value in a definite range as noted above.

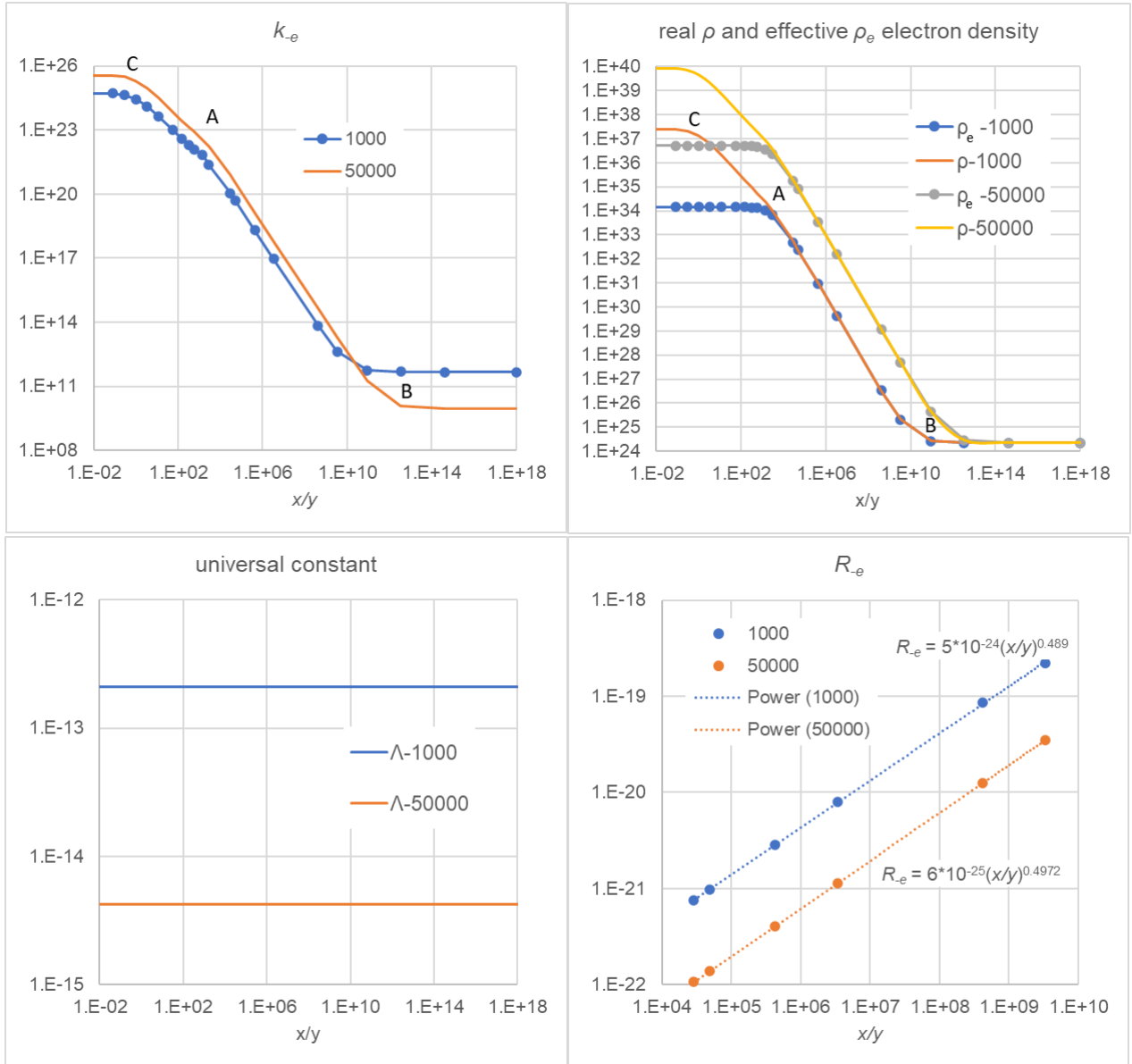


Figure 33: Absorption coefficient k_e , real ρ and effective ρ_e densities, universal constant Λ and repeat of the electron radius in the transition range versus ratio x/y for two values of $g_0 = 1000$ and 50000 ms^{-2} [Note: densities graphs corrected from previous version inadvertently inputting the wrong data columns]

The parameter ΔR_{-e} is many orders of magnitude smaller than the electron radius up to point A, whereupon it reaches about the value of the electron radius. This indicates that the absorption layer initially distributes itself around the characteristic (minimum) electron radius with $TAL_{-e} < R_{-e}$, until it becomes $TAL_{-e} \approx R_{-e}$ around point A. Afterwards, the radius “swells” up to point B and then it appears to have reached a saturation (maximum) value.

In this connection, it is important to quote from Dehmelt’s (Nobel prize) lecture on “experiments with an isolated subatomic particle at rest” (Dehmelt, 1989), where he suggests that “*the electron may have size and structure!*”. He calculates a radius $R \approx 10^{-22}$ m with an upper limit $R \approx 10^{-19}$ m. This is entirely consistent with our preceding values. Another “unofficial” report is found giving a more precise electron radius $R = 1.61 \times 10^{-22}$ m, but this and other formulae were “*published without detailed explanations of how they were derived*” (Sukhorukov, 2017-2020). This value can be found also in some of our tables in the preceding exercises, whilst Table 20 was specifically compiled to contain a case close to this value in the suspected range between 30000-40000 m/s² for g_0 ; this range is “suspected” from the Allais effect calculations in Section 12.4.

If we have not provided a definitive answer yet, we have at least demonstrated the plausibility of PG schemes. The Standard Model does not allow a finite radius for the electron. However, if this is to be remodeled, then PG offers a candidate platform: The electron and positron having a finite mass can also have a finite radius, which depends on the relative amounts of the two types of real mass present. Since gravitation is not described by the Standard Model and a quantum theory of gravity is not yet established, the final observation of the top quark with a mass much larger than had previously expected, almost as large as a gold atom, it might make us think again with an understanding of the meaning of mass under PG.

Neutrinos with great range of energy and mass, from supernova neutrinos and solar neutrinos to cosmic neutrino background radiation with minimal energy may provide some hint on their possible role in PG. It is said that the three known neutrino flavors are the only established elementary particle candidates for dark matter, but they may also relate to black matter. To accommodate the large amount of all neutrinos in the universe, the summed masses of the three neutrinos must be less than 0.26 eV ($1 \text{ eV} = 1.782662 \times 10^{-36}$ kg). We may be able to do away with the Standard Model’s neutrinos as fundamental point-like particles (no volume), whilst they involve mass differences between neutrino mass eigenstates. Loureiro *et al.* (2019) report a species of neutrino with a mass no greater than 0.086 eV, i.e. about $\times 10^7$ (times) smaller mass than an single electron. This implies the existence of physics beyond the Standard Model.

Neutrinos have been detected with a large variety of mass/energy in nuclear reactors and in South Pole IceCube Neutrino Observatory (Stein *et al.*, 2021), all of which may be attributed to fragments of black mass from black holes and other massive bodies all the way down to atomic nuclei. For discussion purposes, we may consider the following two contradicting scenarios: (1) The black mass fragments become activated, as they are hurled away from the source, whilst they have subsequently high penetration range through material bodies. (2) The black mass fragments are difficult to detect, if they remain inactivated (inert) during their transit from the source to a detector event. These ghost particles then may have even superluminal speed of immense magnitude, if they are actually inert and without classical inertia meaning that they can be hurled from their source across the universe at unimaginable speed. However, the second scenario cannot justify the principle of imparting a push (momentum) required by PG. So, gravions themselves may be the smallest possible neutrinos (or neutrino like) from initially black mass traversing the universe and manifesting themselves as gravitation after they are absorbed by particles, planets, stars, etc. The universal constant $\Lambda = k/\rho$ is exactly the characteristic measure of this absorption. The nature of gravions is as yet unknown, so that confirmation of their existence and measurement of g_0 is an imperative step forward. This will greatly facilitate the further development of the theory.

The big range of neutrino energy chasing the tiniest particles is consistent with taking into consideration the novel possibilities now opened with PG on the finest structure of matter. We can now return to our hypothetical proton decay expression 255 and appreciate its purpose: Whilst no nuclear reaction like that has been observed, the end products of proton, electron (positron) and neutrinos are obtained via reactions 242, 243 and 244 with mediation of neutron and energy balancing terms in the equation. It seems that our black mass m_{b-e} calculated and plotted in Fig. 32 provides the ranges required for balancing the said reactions with observed neutrinos and energy. We note that the black mass may lie anywhere between $2.96 \times 10^{-39} \rightarrow 1.67 \times 10^{-27}$ kg. If the smallest species of neutrino is about $\times 10^7$ times smaller than the electron, i.e. about $m_{e-e} = 9.1093837015 \times 10^{-38}$ kg, then PG predictions (expected range of m_{b-e}) are consistent with experiment. The task is to determine the ultimate values of the electron parameters. This can only be done with further correlation of existing or new data, a task to be undertaken by relevant physics departments.

In all above connections, we would like to further quote from Dehmelt’s lecture: “*The electron is a much more complex particle than the cosmon. It is composed of \mathcal{Z}^{C-3} cosmon-like d_c ’s, but only two particles of*

this type formed the cosmonium world-atom from which sprang the universe. In closing, I should like to cite a line from William Blake. 'to see a world in a grain of sand...' and allude to a possible parallel - to see worlds in an electron -". Our elementary investigation of the electrons and positrons in this section already reveals some exciting possibilities and prospects: If the electron has the smallest predicted radius, it would also have the highest density and the highest absorptivity close to $A_{R-e} \approx 1$. That means it has the characteristics of a black hole! Should this be shown to be the case, it would be a really extraordinary finding. Then it would be easier to think about electric charge and other properties of these fundamental particles. At the other end, should the electron have the highest possible radius predicted here, then there would be very little black mass with the lowest $A_{R-e} \approx 0$, i.e. it would be a “fluffy” object, with an effective mass equal to its real mass. Between the two extremes, it is also possible that the radius corresponds to the situation of point A on the presented graphs. It may be governed by statistics favoring an optimum state around this point. The governing statistics may be different from conventional quantum mechanics. Furthermore, we may have not exhausted all possible interpretations of the Heisenberg Principle to date. Also, as already said, the second law of thermodynamics should be considered in conjunction with the fluctuation theorem. All-in-all, we feel that there are some exciting possibilities under PG making its verification all the more urgent.

We can summarize our findings that may be used in particle physics thus: The preceding exercises demonstrate the new possibilities presented by various relationships between active (effective) and passive (black) types of mass in PG. The relative amounts of effective and black mass in a particle could accommodate the needs of particle physics. In the transformations between and among various particles, we should also consider the possible role of black mass that accompanies those transformations. Various neutrinos appear for balancing the equations of mass and energy involved. The instability and extremely short lifetimes of various particles may be attributed to their inability of containing less-or-equal to the critical mass that allows a push particle field to stabilize them as an independent entity. The large types of particles produced in nuclear reactors and elsewhere are generally fragments out of stable and unstable entities. Those fragments may not necessarily exist as independent entities inside the original particle, they may even not appear to exist at all in there. Theories contrived to reconcile their co-existence inside, for example, the nucleus or nucleons, may need reappraisal.

In the meantime, we may attempt to theorize about various possibilities in understanding the electron and positron. Neutronium and Neutron stars are said to have extremely high pressures and temperatures, nucleons and electrons are believed to collapse into bulk neutronic matter, called neutronium. This is presumed to happen in neutron stars. The extreme pressure inside a neutron star may deform the neutrons into some high packing order of neutrons like a cubic symmetry (Llanes-Estrada & Navardo, 2012). We may then think that the interior of black holes could have still the highest packing order possible, like a cuboctahedron (see also “compacted” shape in Fig. 31). With the small electron radii possible, the densities become extremely high per Fig. 33. It is for this reason that we selected most of the mass ratios x/y in the exercises herewith. We would like to examine if there is some characteristic correlation of the behavior of the electron parameters with the chosen ratios. For cuboctahedron, the count of successive layers of closely packed spheres is called frequency F , from which we find the number of the outermost layer spheres in a densely packed “ball” by:

$$\#outer - spheres = 10F^2 + 2 \quad (267)$$

and the total number of spheres by:

$$\#total - spheres = \frac{10}{3}F^3 + 5F^2 + \frac{11}{3}F + 1 \quad (268)$$

We note that point A occurs around $x/y = 308/1$, or $x/y = 560/1$, which correspond to $F = 4$ and $F = 5$. A visual observation may indicate that the outer three, or four layers could be sufficient to shield the central one sphere at the core of the “ball”; this would agree with such ratio of added effective mass to one unit of black mass. The ultimate aim is to hopefully find an explanation of the “mysterious” but firm number of $\mu = 1836.15$. We can return to this question later, while some other workers may like to take up this task.

The specific presentation of electron parameter variation with respect to the ratio x/y is aimed at the possibility of revealing some structural relationship, but the same data relate all parameters between themselves taken in arbitrary pairs. In preparation for the formulation of a push electricity (PE) theory in a following section, it is helpful to familiarize with all push gravity parameters, because the same appear also in other force fields. The equations we used to derive and describe these properties for electrons are relatively simple and straightforward, but the peculiar form of Eq. 146 and its dependence on the product kR may often lead us to some non-intuitive outcomes, or to an understanding that is not immediately obvious. Since graphic presentation is a good way to acquaint ourselves with these new parameters of PG, we have re-plotted the

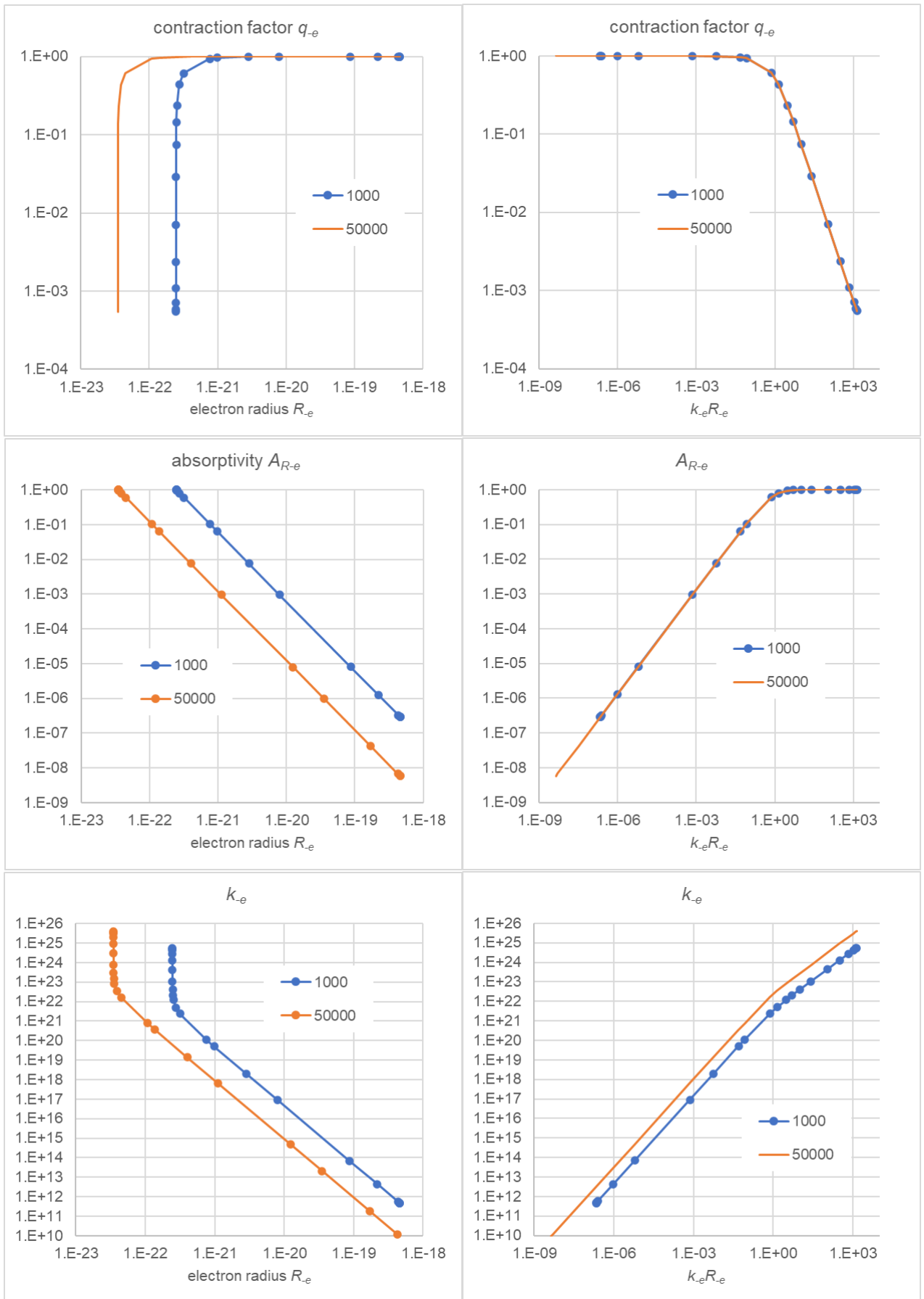


Figure 34: Plotting and comparing the electron parameters versus electron radius (left) and versus product $k_e R_e$ (right) deduced from previous plots for two fixed values 1000 and 50000 of g_0

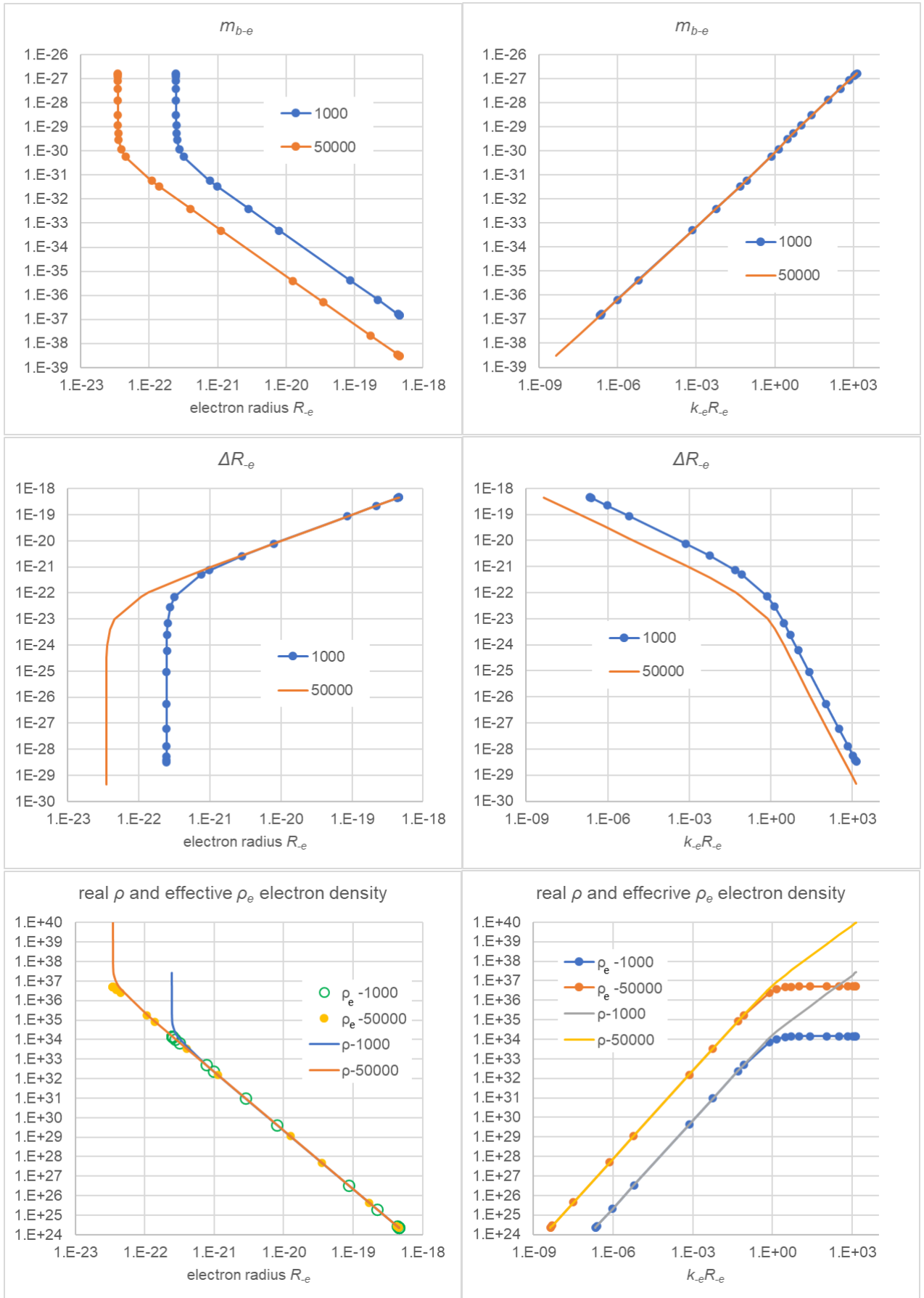


Figure 35: Plotting and comparing of more electron parameters versus electron radius (left) and versus product $k_e R_e$ (right) deduced from previous plots for two fixed values 1000 and 50000 of g_0

same numerical data in different pair combinations in Figs. 34 and 35. We juxtapose any given parameter against radius (left), and the same parameter against the characteristic product kR . There are many other combinations the reader may wish to display, but we prefer to standardize the plotting against the common dimensionless variable kR , which will also make the comparison during development of the electric field easier to comprehend.

20 Uncertainty Principle

We are well overdue for making a statement about the Uncertainty Principle (UP) in attempting to apply push particle theory at very small scales and entities. In fact, we are already working with entities assumed to be well below quantum mechanics levels. In attempting to find the radius of the electron at such small scales, the conjugate variable of momentum would be greatly uncertain. This is a concern compounded also by the as yet unspecified description of what this momentum (conjugate to radius) involves. Does it involve an oscillating mass of the electron? Which mass of the electron, the effective, the black or both masses? The radius itself would also be accompanied with an uncertainty, but how would that relate to the well defined characteristic minimum radius, or is the latter already ill-conceived? We have plotted a black mass of the order $\times 10^{-38}$ and a density of the order $\times 10^{40}$, which raise the question of how these variables and their conjugate variables enter in the uncertainty principle, or what the physical implication of the UP on these variables might be? In the next section, we will find even greater ranges of these and other variables, so can we proceed without prior application or some consideration of the UP?

The above questions and concerns are at the core of PG, especially when the latter is based on the transfer of momentum (impulse) by push particles, the nature of which is not yet specified or satisfactorily understood. A great uncertainty in momentum may be in direct conflict with the requirement of PG that gravitons impart a definite impulse at the smallest of MAC targets.

UP could make the continuation of development of PG futile unless we can integrate UP and PG together. We readily acknowledge all of the above considerations. However, how do we know that UP is or must be a universal principle applicable even to push particles and their interactions? Furthermore, there are different interpretations or “schools” for UP with significant deviations and with no need to go through them all now. After all, UP is a “principle” creating again another dilemma if we should continue with the development of PG or think more about the UP itself. We faced the same dilemma with the equivalence principle, which it seems that we can or we have overcome. Now, we have the option to continue without the uncertainty principle, at least tentatively, in order to see what outcomes we can obtain and then return to it with a judgment. After all, it may be more plausible to assume a deterministic sub-quantum-mechanics level than proclaim a universal applicability of UP everywhere. We opt to continue without a full investigation of the consequences of UP on PG, only as a way that would allow us to get at least an idea what the outcomes are if we follow this path. We might even have a better understanding of quantum mechanics, if we were willing to investigate first, as we have already been doing from the outset in this work. If we are in search of a “game changer”, we must be prepared to work outside principles that may be responsible for the constraints and impasses of the theories based on them. This is the purpose of science. After all, EP and UP are just “principles” that science has adopted to build all hitherto mainstream current theories. We reserve the right to pursue an investigation tentatively without these constraints, i.e. on the “what if” approach for anyone willing to see the outcomes first and then decide.

In other words, a statement of awareness on the above issues is a provisional license that may allow us to proceed even if we appear to trespass the uncertainty principle. We intend and hope to remedy this shortcoming after we gather sufficient information by means of an expanded PG theory.

By no means do we dispute the validity of the uncertainty principle and quantum mechanics (QM). We only want to move beyond this if and where possible. We only make brief statements in this section to let us move forward elsewhere. The presented report is only an optional investigation not a claim, but may become one if and when it is verified.

Actually, we have suggested that QM might be explained on the basis of PG. The big picture of modern physics should include a deeper and possibly hidden layer of subatomic world, which may lie beyond the uncertainty principle. The introduction of “virtual particles” and the mysterious electric field accompanying the electric charge may be replaced by real processes of real “particles”. If a conventional particle generates(?) an output field (e.g. electron \rightarrow electric field), it must also have an input of something. We cannot exclude that the processes at sub-QM levels are perfectly deterministic. A “particle” is an excitation according to QFT, but our introduced “push-particle” is not a particle in the sense of QFT. Perhaps, we should coin another name, but “push particles” lie well below the scale of QFT “particles”. Whereas QM describes and is valid at the scale of QFT particles, it would be arbitrary to want to forcefully apply it also at the scale of push particles. Therefore, without abandoning the achievements of QM, we might be able to explain it in a

tangible way instead of attributing mythical properties beyond human comprehension. That is, UP may be reformulated to include an underlying determinism, which will also put an end to the persistence of different interpretations and schools vying for the truth. We are optimistic that the following work will put to rest any concerns.

21 Push Electricity (PE)

We have proposed that the push particle principle be extended to explain all other known force fields. We attempt to do this for the electric field next. The outcomes seem to have far reaching effects in physics.

Because mass is a key “ingredient” across all force fields, we summarize the greater notion of matter already developed throughout previous sections even if we appear to be repetitive:

(a) The conventional mass appears either as inertial or gravitational mass in different situations, but they are axiomatically assumed to be the same according to the equivalence principle (EP). Both forms start with a common rest mass thought to be also an intrinsic property.

(b) In PG, we have come up with the notion of real mass, which is the same as matter, i.e. all the material (stuff) from which any object is composed of. The real mass is then subdivided into effective mass and black mass. The effective mass is understood to be the active or activated component liaised with a force. The black mass is a purely inert, passive, or inactive component without the conventional “inertia”. The effective mass is created by the absorptive action of push particles, e.g. of gravions in gravity and electrions in electricity as we will say. Effective mass is a relative and measurable quantity, whilst real mass is an absolute quantity. They are both measured in the same units of mass and their difference is the amount of black mass. The amount of effective mass is relative to whether a body (real mass) is close or very far away from other bodies (real masses). For a lone body, its effective mass is determined by the intensity of flux of particular type of push particles in the surrounding space. It is the rate of push particle and energy absorption that determines the effective mass, which is different for a lone body or for a body with other neighboring bodies. We have found a relationship between force and effective mass between two spherical bodies in Section 16. The effective mass of a lone body can be said to coincide with the conventional intrinsic mass. From this common point of agreement, we have a departure of the meaning and measure of the effective mass from the conventional inertial and gravitational mass. This departure is imperceptible for “ordinary” bodies of Newtonian mechanics, but becomes increasingly significant for neighboring dense bodies. In particular, the effective mass generally decreases by proximity with another body in contrast with conventional gravitational mass. We have briefly cautioned what may happen to the effective mass of a body orbiting around another body or accelerated in space by a rocket. In the latter case, we think that it increases in similar but not necessarily exactly the same mathematical fashion as the conventional inertial mass, and not only mathematically but also in a material sense. While we await a proper assessment of the latter case, we can still proceed to investigate the static electric field next.

We should note that the term “matter” in this report includes also “antimatter” that is well known and used in physics. This is only because we lack a commonly agreed word to include both “matter-antimatter” in elsewhere terminology. For this reason we have often used the less elegant word “stuff” to denote everything that material bodies or objects are made of including the force fields themselves. Then we can state that “stuff is conserved”, which leads us to unite the fields. We do not subscribe to a mere mathematical conception/description of force fields in the belief that only some common underlying stuff can unite them. Otherwise, physics could be reduced to a mathematical idealism, and cosmos could be the product of human existence, not the reverse. By all this, of course, we enter the realm of philosophy.

For the time being, we juxtapose only gravions and electrions and, if our findings prove successful or promising, we may continue on with other fields of force. The examination of these two fields may present us with an opportunity of their unification prior to a general push field theory (PFT).

21.1 General relationships

Little is known about the mysterious and intriguing electron: We don’t know what holds it together, what fixes its mass and its possible radius, or the nature of its electric charge. By the same token, we can say the same about the positron. We know, or consider, that the electron is a persistent and reliable “atomon” (=uncuttable), i.e. indivisible particle so far, whilst the positron has a very short life. We want to describe and quantify the electric field in a similar fashion as the gravitational field. Initially we ignore the repelling effect of same sign charges and bypass the concept of charge. The electric field between an electron and a positron (in lieu of a proton) is the simplest way resembling an “attracting” gravitational field, for which we may afford to use similar derivations. We don’t use the similar proton-electron system to avoid possible complications on account of the different proton mass and structure. The apparent similarity between Coulomb’s law and

gravitational law prompts us for this approach. Upfront we can expect that the only difference should be a difference in magnitudes, since we know that the electric field is by far much stronger than the gravitational field.

Under the provisos set in the preceding sections, our intention is to consider the options below as a first pass of the theory and then return and weed out any discrepancies that may appear. So far, we rely on the type (nature) of push particles and regard their mean-free-path as a critical parameter in delineating various fields. We delay the use of the wavelength concept until we see the need for it.

Since the real mass is the stuff that is conserved, it should be invariant under the simultaneous presence of both gravitational and electric fields. Then we think that the radius corresponding to the real mass is also invariant between the fields. The latter radius might be disputed presumably by a theoretical arrangement of a collision experiment in electromagnetic field that would produce only a “charge” radius. Instead, we have produced a theoretical electron radius from a gravitational field by PG considerations in preceding Section 19.3. Sharing Dehmelt’s vision, we also assume that the electron has an absolute finite (real) radius determined by its real mass, i.e. independently and prior of any applied measuring methods or an assumed nature’s indeterminism. At any rate, should any objections be raised, we can always return after we proceed as repeatedly suggested.

For the electric field and its associated electrion, i.e. push particle type-II, we can apply the same equations as for the gravitational field simply by introducing the subscript 2 (2) following the same terminology used in previous sections. Thus, we write G_2 for universal “electrical” (big G_2) constant, m_{2e-e} for effective mass, A_{2R-e} for absorptivity, q_{2-e} for contraction factor, k_{2-e} for absorption coefficient, g_{02} for maximum acceleration, J_{02} for flux 2 density (intensity), Λ_2 for new universal 2 constant, m_{2b-e} for black mass, ρ_{2-e} for real density, R_{02} for characteristic minimum radius, $\Delta_2 R_{-e}$ for radius difference, and product $k_{2-e} R_{-e}$ for the characteristic dimensionless variable. We may use no subscript or occasionally the subscript 1 (1) for the gravitational field, like $g_{01} \equiv g_0$.

Since the real mass m_{-e} of the electron (positron) is the same under both fields (i.e. $m_{2-e} = m_{1-e} \equiv m_{-e}$), we immediately have that:

$$m_{-e} = \frac{m_{e-e}}{q_{-e}} = \frac{m_{2e-e}}{q_{2-e}} \quad (269)$$

or

$$m_{2e-e} = \frac{q_{2-e}}{q_{-e}} m_{e-e} \quad (270)$$

If the radius R_{-e} for the electron (positron) is the same (i.e. $R_{2-e} = R_{1-e} \equiv R_{-e}$), then:

$$R_{-e}^2 = \frac{G m_{e-e}}{A_{R-e} g_0} = \frac{G_2 m_{2e-e}}{A_{2R-e} g_{02}} \quad (271)$$

or

$$g_{02} = \frac{m_{2e-e} G_2 A_{R-e}}{m_{e-e} G A_{2R-e}} g_0 = \frac{q_{2-e} G_2 A_{R-e}}{q_{-e} G A_{2R-e}} g_0 = \frac{G_2}{G} \frac{k_{-e}}{k_{2-e}} g_0 \quad (272)$$

where we used also the general equation $q = 3A_R/(4kR)$. [Note: Throughout this report we often expand an equation to include various forms and parameters, because they can be easily referenced, verified and better understood as we experience new variables over conventional physics].

We also have a corresponding characteristic limiting radius R_{20-e} for each value of g_{02} :

$$R_{20-e} = \sqrt{\frac{G_2 m_{2e-e}}{g_{02}}} = R_{-e} \sqrt{A_{2R-e}} \quad (273)$$

so that we can again define the two radii difference ΔR_{-e} by:

$$\Delta R_{2-e} = R_{-e} - R_{20-e} = R_{-e} \left(1 - \sqrt{A_{2R-e}}\right) \quad (274)$$

Further, from the known (given) m_{e-e} , m_{2e-e} and q_{2-e} and the equation of contraction factor below:

$$q_{2-e} = \frac{3A_{2R-e}}{4k_{2-e} R_{-e}} = \frac{m_{2e-e}}{m_{e-e}} q_{-e} \quad (275)$$

we solve first for the unknown product $k_{2-e} R_{-e}$ (also contained in A_{2R-e}) and then we deduce k_{2-e} and A_{2R-e} from the given electron radius.

The new universal constant Λ_2 and other parameters of the electric field are given below from the corresponding parameters of the gravitational field without further comment:

$$\Lambda_2 = \frac{k_{2-e}}{\rho} \quad (276)$$

$$\Lambda_2 = \frac{\pi R_{-e}^2 A_{2R-e}}{m_{2e-e}} = \frac{\pi R_{-e}^2 A_{R-e}}{m_{e-e}} \frac{k_{2-e}}{k_{-e}} = \Lambda_1 \frac{k_{2-e}}{k_{-e}} \quad (277)$$

$$J_{02} = \frac{cg_{02}}{\pi\Lambda_2} = \frac{k_{-e}^2 G_2}{k_{2-e}^2 G} \frac{c}{\pi\Lambda_1} g_0 = \frac{k_{-e}^2 G_2}{k_{2-e}^2 G} J_0 = \frac{k_{-e}^2 G_2}{k_{2-e}^2 G^2} \frac{c}{\pi^2} g_0^2 = \frac{cG_2}{\pi^2} \frac{k_{-e}^2}{k_{2-e}^2} \left(\frac{m_{e-e}}{A_{R-e} R_{-e}^2} \right)^2 \quad (278)$$

$$J_{02} = \frac{c}{\pi^2 G_2} g_{02}^2 = \frac{c}{\pi^2 G^2} \left(\frac{k_{-e}}{k_{2-e}} g_0 \right)^2 \quad (279)$$

$$\frac{k_{-e}}{k_{2-e}} \frac{g_0}{g_{02}} \frac{G_2}{G} = 1 \quad (280)$$

$$\frac{J_{02}}{J_0} = \frac{g_{02}^2}{g_0^2} \frac{G}{G_2} = \frac{k_{-e}^2 G_2}{k_{2-e}^2 G} = \frac{g_{02}}{g_0} \frac{k_{-e}}{k_{2-e}} \quad (281)$$

The above considerations require generally two alternative effective masses, which may be in question because the electron “mass” is generally considered to be well established. If the effective mass created by (or corresponding to) electrons were generally different from that created by gravions, it would presumably be contrary to our experience with mass measurements of the electron and established theories. Masses with an electric charge are generally measured inside electric (and/or magnetic) fields, but they are also measured in macroscopic charge-neutral-form inside the gravitational field and found to be the same in the sum-total of all particles comprising a given material body. No distinction is generally made for the masses inside electric and gravitational fields in compliance with the Equivalence Principle. Nevertheless, we wish to go through the exercise of the available options below.

The above general relationship by Eq. 270, states that the ratio of the two effective masses is equal to the ratio of the two corresponding contraction factors for the two fields. We have now two options to consider, namely, that the two masses are equal $m_{2e-e} = m_{e-e}$ for the sake of preserving the equivalence principle, or distinctly different $m_{2e-e} \neq m_{e-e}$. The unequal masses case clearly violates the EP, but we have already concluded in Section 16 that EP should not be a constraint that we always have to adhere to.

Addendum:

As a separate supplementary relationship often encountered in conventional physics is the product Gm_e called “standard gravitational parameter” μ_{sp} , which we can also express in our parameters as:

$$\mu_{sp} = Gm_e = A_{R-e} R_{-e}^2 g_0 \quad (282)$$

This is often quoted to be the “best known or measured quantity”. We can also introduce a corresponding “standard electric parameter” μ_{2sp} for the electric field by

$$\mu_{2sp} \equiv A_2 g_{02} = A_{2R-e} R_{-e}^2 g_{02} = G_2 m_{2e-e} \quad (283)$$

Noted that the sub-scripted symbol $\mu_{subscript}$ here denotes a different parameter from the plain μ previously used for the proton-to-electron mass ratio.

We can also transfer other corresponding equations from the summary Section 6.5 and elsewhere in Part One of this report for use in the electric field.

21.1.1 Case with equal masses $m_{2e-e} = m_{e-e}$

Let’s assume that the gravitational mass of the electron m_{e-e} is equal to its electrical mass m_{2e-e} . Then $q_{2-e} = q_{-e}$ and $k_{2-e} R_{-e} = k_{-e} R_{-e}$ from Eq. 45 of contraction; then $k_{2-e} = k_{-e}$ and $A_{2R-e} = A_{R-e}$. As a result, the above Eq. 272 between fields reduces to a simple formula of proportionality:

$$g_{02} = \frac{G_2}{G} g_0 \quad (284)$$

In electricity, the Coulomb force F_2 at distance r between an electron and a positron charge e is

$$F_2 = \frac{1}{4\pi\epsilon_0} \frac{e^2}{r^2} \equiv b \frac{e^2}{r^2} \quad (285)$$

where for simplicity in expressions we use Coulomb's factor $b = 8.987552 \times 10^9 \text{ m} \cdot \text{N}^2/\text{C}^2$ instead of the electric permittivity constant ϵ_0 . We may now theorize that the same force is generated by a corresponding effective electron mass m_{2e-e} at the same distance:

$$F_2 = G_2 \frac{m_{2e-e}^2}{r^2} \quad (286)$$

where G_2 is the (electrical) universal constant for this field. By equating the two expressions of the same (equal) force, we derive

$$G_2 = b \frac{e^2}{m_{2e-e}^2} = 2.7803909099 \times 10^{32} \text{ m}^3 \text{ kg}^{-1} \text{ s}^{-2} \quad (287)$$

where we used for the charge $e = 1.6021766340 \times 10^{-19} \text{ Cb}$ and the established effective electron mass $m_{2e-e} = 9.1093837015 \times 10^{-31} \text{ kg}$. From this, we derive the remaining corresponding PG parameters for the electric field as summarized without further comment below:

$$\Lambda_2 = \frac{\pi R_{-e}^2 A_{2R-e}}{m_{2e-e}} = \Lambda_1 \quad (288)$$

$$J_{02} = \frac{c g_{02}}{\pi \Lambda_2} = \frac{c g_0}{\pi \Lambda_1} \frac{G_2}{G} = \frac{G_2}{G} J_0 = \frac{c G_2}{\pi^2 G^2} g_0^2 = \frac{c G_2}{\pi^2} \left(\frac{m_{e-e}}{A_{R-e} R_{-e}^2} \right)^2 \quad (289)$$

$$J_{02} = \frac{c}{\pi^2 G_2} g_{02}^2 = \frac{c G_2}{\pi^2 G^2} g_0^2 \quad (290)$$

$$g_{02} = \frac{G_2 m_{2e-e}}{A_{2R-e} R_{-e}^2} = \frac{G_2 m_{e-e}}{A_{R-e} R_{-e}^2} \quad (291)$$

$$F_2 = G_2 \frac{m_{2e-e}^2}{r^2} = \frac{g_{02}}{g_0} G \frac{m_{e-e}^2}{r^2} = \frac{g_{02}}{g_0} F_1 \quad (292)$$

where F_1 is the gravitational force and how it relates to the electric force F_2 .

Now, we try to understand the physical meanings for this case of equal masses in the two fields. We need to introduce the number density n_ω for gravions with a quantum energy ω and the number n_ϵ density for electrions with a quantum energy ϵ and relate them via the corresponding energy flux densities with J_0 and J_{02} by:

$$J_0 = n_\omega \omega c \quad (293)$$

$$J_{02} = n_\epsilon \epsilon c \quad (294)$$

$$\frac{J_{02}}{J_0} = \frac{n_\epsilon \epsilon}{n_\omega \omega} = \frac{G_2}{G} = 4.1659538241 \times 10^{42} \quad (295)$$

The equation $k_{-e} = k_{2-e}$ found says that the number of absorption events per unit length is the same for the gravion and the electron. Then we must have $n_\omega = n_\epsilon$, otherwise the accrued absorption events would be different for gravions and electrions resulting in different effective masses that would contradict the case of equal masses here. Thus the above equation is simplified to:

$$\frac{J_{02}}{J_0} = \frac{\epsilon}{\omega} = \frac{G_2}{G} = 4.1659538241 \times 10^{42} \quad (296)$$

Then we face a dilemma to reconsider the interpretation of the meaning of effective mass: The impulse transmitted to the common effective mass by each electron is G_2/G times the impulse transmitted by each gravion. This means that the effective mass is proportional to the number rate of push particles not to the energy rate (power) and each electron is not reduced to an equivalent number of gravions after absorption, otherwise the effective mass should be by many orders of magnitude greater. The reasoning of the electron "dissolving" to equivalent gravions after absorption forces a contradiction of terms, unless the electron is a type of matter that retains its identity after absorption. In other words, the electron must have some

unique attribute like, say, the conventional charge which is conserved. In other words, the electron is not lumped together with the absorbing matter, it is not integrated with stuff of the electron but its entity is preserved inside the electron. Then, we may as well identify it with our well known charge. By this then, we conclude that the charge of an electron originates by absorption of peculiar electrons being small push particles with a density flux J_{02} in the surrounding space. Then, gravions and electrons perform different functions upon absorption in their own right and their own separate identity. We are forced to conclude that whilst the electron imparts much greater impulse and energy into the absorbed center, the effective mass is not increased in proportion but remains the same. Such a conclusion and re-interpretation of “effective” mass may be difficult to incorporate into a unifying theory of fields and matter, if not met with an outright rejection. Nevertheless, we must keep note of this case, if keeping true to our scientific endeavor.

21.1.2 Case with unequal masses $m_{2e-e} \neq m_{e-e}$

Let us now investigate the challenging case of unequal effective masses between the two fields. Given the identical form of Coulomb’s law with the gravitational law, we are tempted to replace Coulomb’s charge with effective mass, as if the electric field were to be considered like a gravitational field. In other words, we set the numerical value of the electrical effective mass equal to the numerical value of the electron charge as a likely case of unequal gravitational and electrical masses. We cannot immediately envisage any reason for another choice of a numerical value of electrical mass without upsetting the well established physics of electricity. Thus, we set:

$$m_{2e-e} \equiv 1.6021766340 \times 10^{-19} \text{ kg} \quad (297)$$

and so the universal electrical constant should be numerically equal to b :

$$G_2 \equiv b = 8.987552 \times 10^9 m^3 kg^{-1} s^{-2} \quad (298)$$

i.e. a greatly different value from Eq. 287 for this parameter. Coulomb’s law is then replaced with a gravitational-like law, as previously by:

$$F_2 = G_2 \frac{m_{2e-e}^2}{r^2} \quad (299)$$

Substituting the electrical mass in terms of PG parameters as we did for the gravitational mass via Eq. 270, we obtain:

$$F_2 = G_2 \left(\frac{q_{2-e} m_{e-e}}{q_{-e}} \right)^2 \frac{1}{r^2} = \frac{k_{2-e} g_{02} q_{2-e}^2}{k_{-e} g_0 q_{-e}^2} G \frac{m_{e-e}^2}{r^2} = \frac{k_{2-e} q_{2-e}^2 g_{02}}{k_{-e} q_{-e}^2 g_0} F_1 \quad (300)$$

where F_1 is the gravitational force and how it relates to the electric force F_2 .

We find some numerical values and see the consequences of the above derivations. For the known (given) ratio of the two effective masses, we find the magnitude of contraction ratio:

$$\frac{q_{2-e}}{q_{-e}} = \frac{m_{2e-e}}{m_{e-e}} = 1.758820010772160 \times 10^{11} \quad (301)$$

i.e. the electrical effective mass is 11 orders of magnitude greater than the gravitational mass and so are the contraction factors. This is the known electron charge-to-mass quotient, which is not a tautology or a mere change of the word charge with the word mass, as we will shortly realize by introducing and understanding the physical meaning and consequences below.

The above “quotient” expresses an enormous difference between the two masses that cannot be reconciled if we start with (accept) the gravitational parameters already calculated for the electron in Section 19.3, because the contraction factor and the absorptivity cannot be greater than unity in either the gravitational or electric field. The only way to apply the above relationships between the two fields is to start with a range of values for the electrical field and work backwards (in reverse) to find the corresponding parameters for the gravitational field. Since we have no idea about choosing a range for g_{02} (as we did for g_0), we can choose a range for the contraction or the absorptivity both known to vary in the range between zero and one. We opted to do so by choosing the absorptivity as the independent (starting) variable with a selection of representative values in the range $0 < A_{2R-e} < 1$. Then we find all other electrical parameters corresponding to these values of A_{2R-e} and all corresponding gravitational parameters from the above relationships between the two fields. The only proviso in doing all these computations is that we have to specify (choose) an arbitrary electron radius at least among the range of radii already found from the gravitational field. For every choice of radius value, we obtain a different family of relationships between all other parameters. We present results for three electron radii at the extreme cases previously found

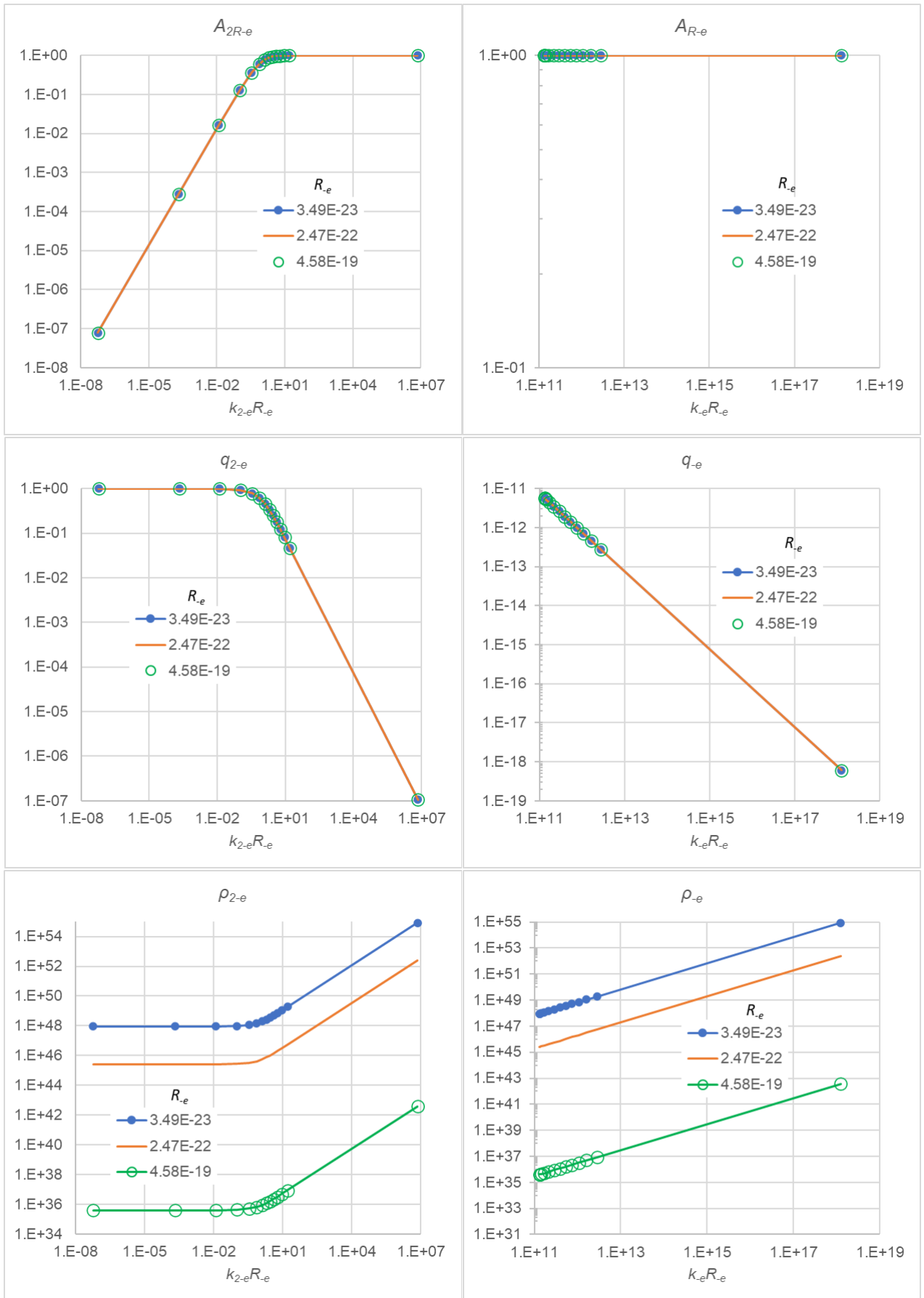


Figure 36: Electron parameters against the electrical product $k_{2-e}R_e$ (left) and same juxtaposed against the gravitational product $k_e R_e$ (right) for three extreme cases of fixed electron radii.

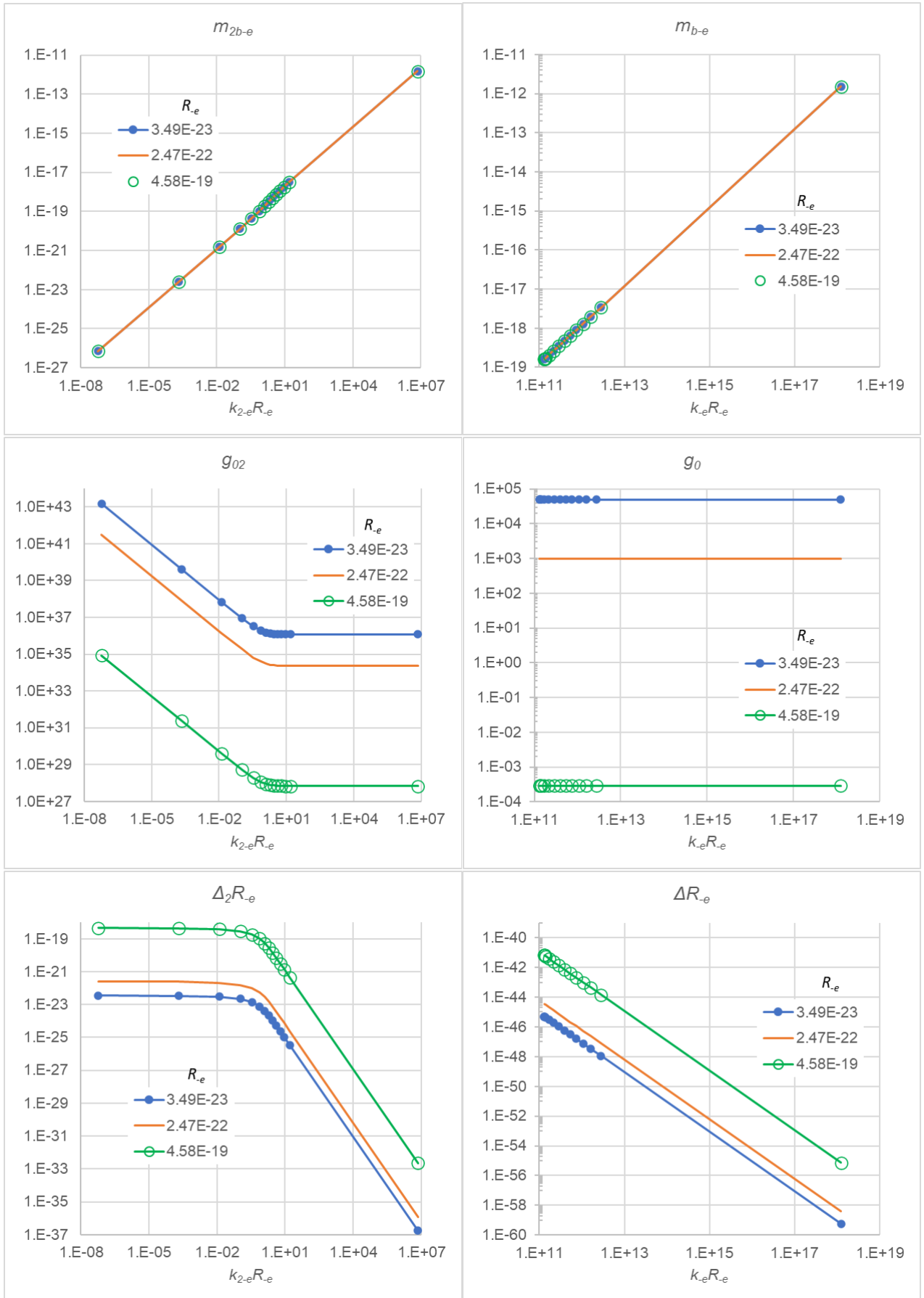


Figure 37: Electron parameters against the electrical product $k_{2-e}R_e$ (left) and same juxtaposed against the gravitational product $k_e R_e$ (right) for three extreme cases of fixed electron radii.

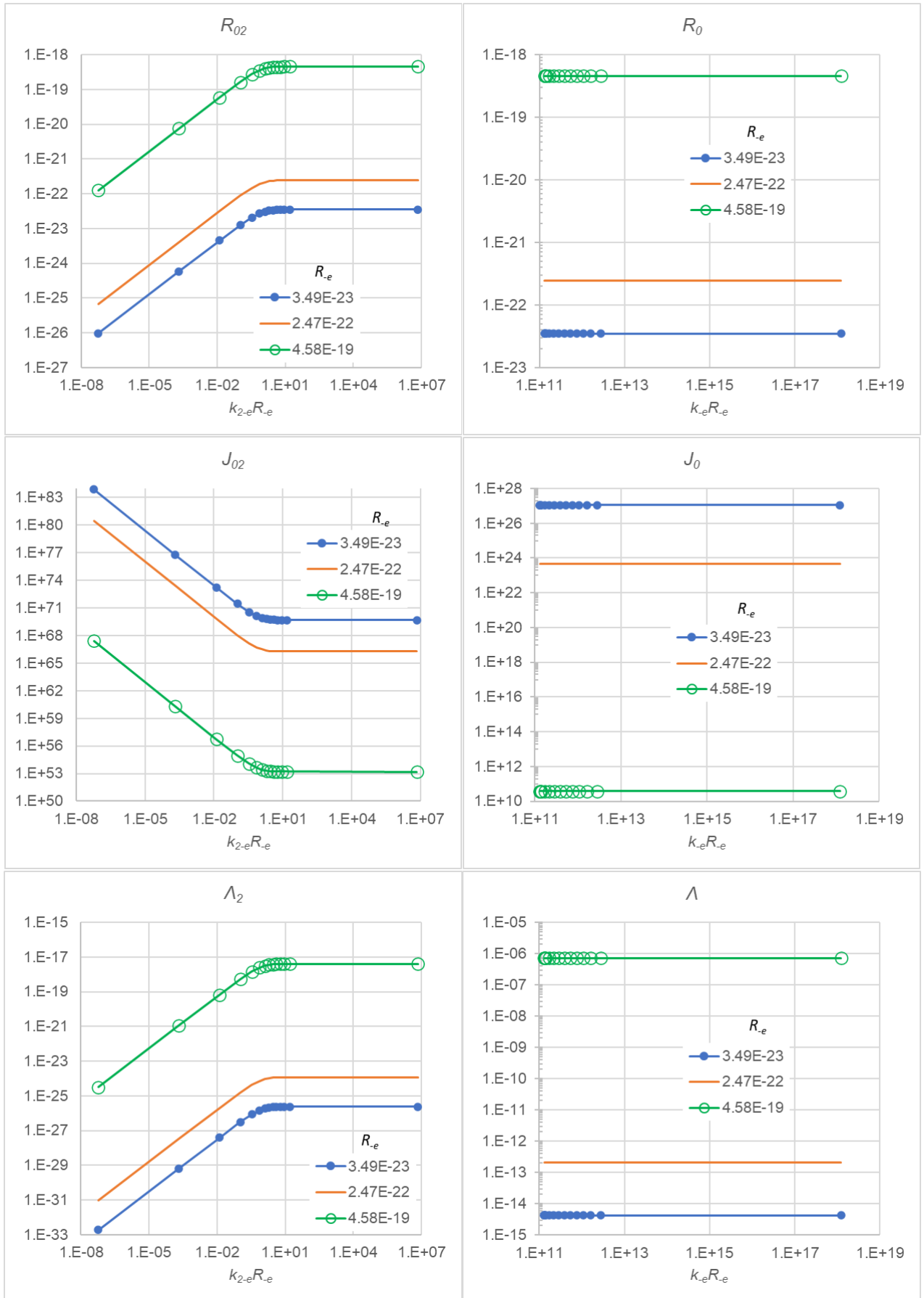


Figure 38: Electron parameters against the electrical product $k_{2-e}R_{-e}$ (left) and same juxtaposed against the gravitational product k_eR_{-e} (right) for three extreme cases of fixed electron radii.

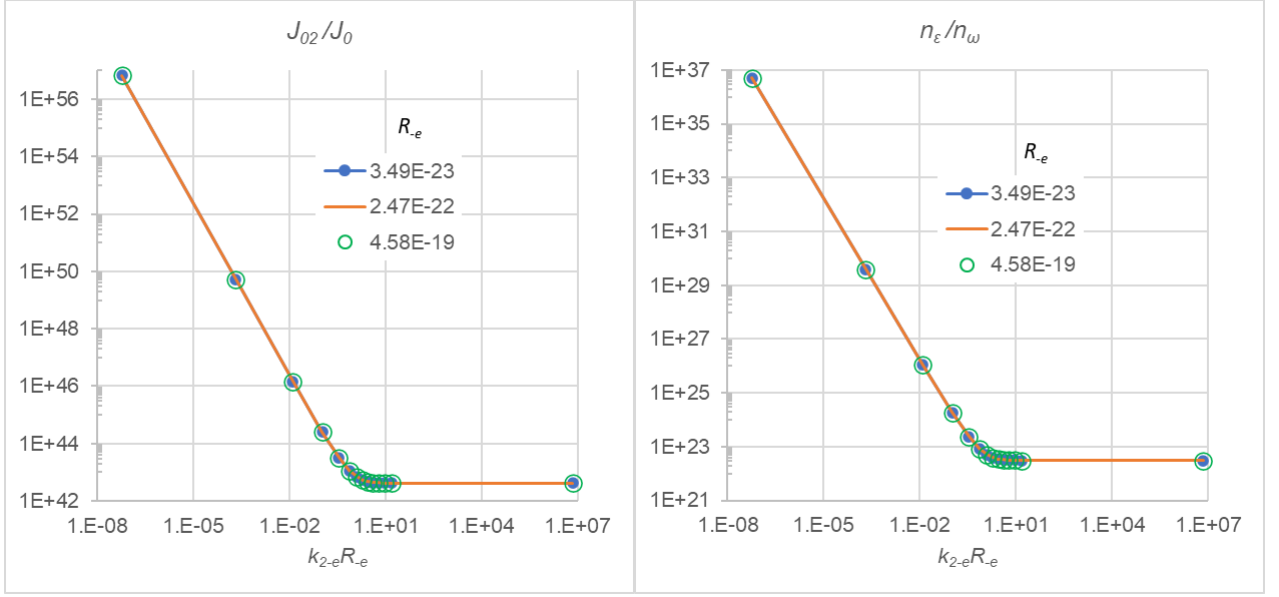


Figure 39: Ratios of density flux (left) and number density (right) of corresponding push particles of electrical over gravitational fields against electrical product $k_{2-e}R_{-e}$ for three extreme cases of fixed electron radii.

in Section 19.3. Two radii are taken from the lowest values at $g_0 = 1000 \text{ ms}^{-2}$ and $g_0 = 50000 \text{ ms}^{-2}$, namely, $R_{-e} = 2.46570013543645 \times 10^{-22} \text{ m}$ and $R_{-e} = 3.48702657227941 \times 10^{-23} \text{ m}$ from Table 17, and one maximum radius $R_{-e} = 4.58247932812879 \times 10^{-19} \text{ m}$ from Table 21 with $g_0 = 50000 \text{ ms}^{-2}$. Having calculated the corresponding values of all parameters, we can plot any arbitrary pair of them and observe their variation. We have done this by plotting parameters against the generalized products $k_{2-e}R_{-e}$ and $k_{-e}R_{-e}$ for the electric and gravitational field juxtaposed in the left and right columns in Figs. 36, 37 and 38.

There are many conclusions to draw from those graphs, some of which are given below.

We note that for the electric field there is generally a straight line portion of the graphs corresponding to a Newtonian mass, another straight line portion corresponding to a prevailing black mass and an inflection region corresponding to a transition between the two masses. This is because we have purposefully chosen a wide range of values of the variable $k_{2-e}R_{-e}$ to cover all regimes of electron absorption. In contrast, the juxtaposed parameters for the gravitational field are all straight lines well beyond the Newtonian masses and into the total absorption of black masses as judged by the very near unity value of the absorptivity, or the very near zero values of the contraction factors, all with extremely low values of variation invisible by the drawn lines. The graphs were produced with an excel worksheet not permitting precision with more than 15 decimal places, so the absorptivity appears a parallel line very close to unity, but there is no need to zoom in such small details here.

Another salient feature is that the black mass of the electron should be many orders of magnitude greater than that worked out by the exercises on possible electron-proton relationship in previous Section 19.3. The large amount of possible black mass in the electron (positron) may allow even more flexibility to find not only the ultimate relationship between proton and electron but also to explain many other relationships in nuclear and particle reactions, where these three particles are present. Importantly, we have not found a unique single value of possible black mass yet, as we only have a large range of possible electron densities J_{02} . However, we learn that black mass can be used as a “wild” card for fitting and understanding many or all particles already found for the Standard Model and beyond. This is a next task that can only be undertaken by the relevant experts. We only reveal the new possibilities now opened by PG.

Another salient feature found by examining the graphs for g_0 is that it requires an extremely low value of $g_0 = 0.0002895 \text{ ms}^{-2}$ with the maximum radius used, which is unacceptable. It must be understood that for any fixed radius R_{-e} the variation of g_0 appears constant on the graphs, but there is an invisible but extremely small variation. For example, in the case with $R_{-e} = 4.58 \times 10^{-19} \text{ m}$ the variation is beyond the 25th decimal place, with $R_{-e} = 2.47 \times 10^{-22} \text{ m}$ beyond the 19th decimal place and with $R_{-e} = 3.49 \times 10^{-23} \text{ m}$ beyond the 16th decimal place. In practice, this means that if we could measure experimentally the gravitational g_0 , then we can determine the electron beam radius. To these fixed values of g_0 and R_{-e} there corresponds a range of values for the electron g_{02} . The actual value for g_{02} will then have to be determined by other means such as from existing data in particle physics and possibly from similar relationships between

subsequent field strengths, until we close the “loop” of necessary relationships.

In Table 23, we present possible magnitudes of the maximum (limiting) electrical acceleration g_{02} and density flux J_{02} against the gravitational g_0 for the cases of equal and unequal masses using Eqs. 284 and 272 correspondingly. We see (as expected) that there is a one-to-one correspondence between electrical and gravitational fields for the case of equal masses. However, for every given value of g_0 at a fixed radius, we have a corresponding range of values for g_{02} and J_{02} in the case of unequal masses, where we equated the electrical mass to the charge of the electron. [Note: The above range of values are by far much greater than the minimum requirement of $g_{02} > 10^3 g_0$ to achieve expected core pressures in white dwarfs.]

Now, we can describe further the meaning of the case with unequal masses in the two fields with energy flux densities J_0 and J_{02} . We use Eqs. 293 and 294 again, but with $n_\omega \neq n_\varepsilon$ we obtain the corresponding ratio of flux densities from Eq. 278 as:

$$\frac{J_{02}}{J_0} = \frac{n_\varepsilon \varepsilon}{n_\omega \omega} = \frac{G_2 k_{2-e}^2}{G k_{2-e}^2} = \frac{G g_{02}^2}{G_2 g_0^2} = \frac{g_{02}}{g_0} \frac{k}{k_{2-e}} \quad (302)$$

Then we can relate the ratios $\frac{\varepsilon}{\omega}$ and $\frac{n_\omega}{n_\varepsilon}$ as:

$$\frac{n_\varepsilon}{n_\omega} = \frac{\omega J_{02}}{\varepsilon J_0} = \frac{\omega G_2 k_{2-e}^2}{\varepsilon G k_{2-e}^2} = 1.347 \times 10^{20} \frac{k_{2-e}^2 \omega}{k_{2-e}^2 \varepsilon} \quad (303)$$

or the same by

$$\frac{n_\varepsilon}{n_\omega} = \frac{\omega J_{02}}{\varepsilon J_0} = \frac{\omega G g_{02}^2}{\varepsilon G_2 g_0^2} = 7.426 \times 10^{-21} \frac{g_{02}^2 \omega}{g_0^2 \varepsilon} \quad (304)$$

If we set

$$\frac{\omega}{\varepsilon} = \frac{G}{G_2} \quad (305)$$

then

$$\frac{n_\varepsilon}{n_\omega} = \frac{k_{2-e}^2}{k_{2-e}^2} = \frac{G^2 g_{02}^2}{G_2^2 g_0^2} \quad (306)$$

In other words, the impulse transmitted to the different effective masses by each electrion is a lot greater than the impulse transmitted by each gravion but a lot smaller than the impulse of the electrion in the case of equal masses. The ratio of these impulses will be determined if and when we know the number density ratio n_ω/n_ε . These numbers may be easier to physically justify in a subsequent modeling for the two fields using the unequal masses case. The ratios of flux densities and number densities for the two fields are plotted in Fig. 39.

We will use the above findings further in building an electricity model and draw more conclusions and insights in the course of more detailed development of the theory.

21.2 Minimum emission centers (MEC)

According to the third postulate of PG theory, “gravions (or energy) absorbed are also re-emitted in a different form of particles (energy) with much shorter mean free path so as not to pertain (mediate) further to gravitational force, but likely to pertain to other types of forces or reactions”. That is, the rates of absorption and emission (decay) are equal in the steady state with a characteristic time constant, as we have also discussed in Section 15.7.1. The number-rate of absorbed gravions and the number-rate of emitted particles differ in inverse proportion to the energy of each type of push particle. They differ by many orders of magnitude as we have found for both cases of equal or unequal electron masses in the two fields. Having previously introduced the minimum absorption center (MAC), we can now introduce equivalently a minimum emission center (MEC) for and around points distributed inside any material body. That is, we can say that every “point” of a body appears “dark” with respect to gravions and “bright” with respect to emitted push particles, which we have tentatively called electrions, but may be called with any other name according to their function. At this point of development we don’t know if the nature of a MAC or the type of push particle absorbed or both determine the nature of emitted push particles. For an electron and positron, in particular, we may guess that they are type-II push particles (electrions) subject to possible revision later.

Let us concentrate on the electron and positron here. The acceleration (force) around them may be generated as follows: The sphere of Fig. 1 used for founding gravity is now considered an electron. Now, there is an excess amount of emitted electrions inside the differential solid angle subtended by O, not a

	$m_{2e-e} = m_{e-e}$		$m_{2e-e} = 1.6E - 19$	
g_0	g_{02}	$\frac{J_{02}}{J_0}$	g_{02}	$\frac{J_{02}}{J_0}$
300	1.24979E45	4.16595E42		
500	2.08298E45	4.16595E42		
1000	4.16595E45	4.16595E42	2.4E34 → 3.0E41 ($R_{-e}=2.47E-22$)	4.16575E42 → 6.83450E56
2000	8.33191E45	4.16595E42		
5000	2.08298E46	4.16595E42		
10000	4.16595E46	4.16595E42		
20000	8.33191E46	4.16595E42		
30000	1.24979E47	4.16595E42		
50000	2.08298E47	4.16595E42	1.2E36 → 1.5E43 ($R_{-e}=3.49E-23$)	4.16575E42 → 6.83450E56

Table 23: Relationship between g_{02} of electric field and g_0 of gravitational field for equal masses case (left columns) and $m_{2e-e} = 1.6E - 19$ kg case (right columns) with two electron radii at $g_0 = 1000$ and 50000 ms^{-2} .

depletion as applied for gravions. This will produce a repulsive force in the opposite direction. The emitted electrions ε^- will be produced along lines of sight from O with an emission coefficient k_{2-e} inside the sphere, corresponding to the gravion absorption coefficient $k \equiv k_1$. Therefore, we expect a net emission factor, or acceleration and force expressed by the same formulas as in the gravitation field. Thus the repulsive force should have the same form as the corresponding attractive force expressed by Eqs. 292 or 300 for equal or unequal electrical masses between the fields.

With the above understanding, we can adopt a similar reasoning for the positron as being the source of MECs radiating electrions ε^+ with a positive attribute. We can combine these ideas to build an electrical push model next.

By virtue of the above description, there are various possibilities about the proposed MACs and MECs. They may be equal in number and distribution, or vary to explain differences between gravity and electricity. They perform certain functions, two of which are the absorption of gravions ω and the emission of electrions ε^- or ε^+ . In building a model, we are entitled to allocate attributes in similar fashion as practiced by other theories like “flavors”, “colors”, “exclusive” principle, etc. We hope to be able to explain any introduced attributes as PG theory evolves, otherwise we simply augment the list of incomprehensible properties. The task of physics should be to make the cosmos understood by humans and not appeal to human weakness to evade the task.

21.3 Unifying gravitational and electric fields

From the numerical examples worked out for the force and other parameters for the electron, it is immediately clear that the gravion density is too weak to produce enough electrions to generate the electric force, i.e. if gravions are re-emitted as electrions. Therefore, there must be another source of push particles type-III that we call “*somions*” (ς) [see below note (*) for terminology], which after being absorbed by an electron generate the required flux density J_{02} of emitted electrions ε^- . We require that this other source has a density flux $J_{03} \geq J_{02}$ producing a maximum secondary acceleration g_{02} at the exit surface of electrons and positrons and all the other parameters that we worked with for the electric field. This rightly evokes the question about the origin and extent of the source of somions ς , i.e. if they are “locally” stagnating in the “vacuum” inside material bodies or they pervade the outer universe (“vacuum”) as well. Are they recycled locally or are they supplied continuously from outside?

Since electrons and positrons contain MECs, they are emitters of electrions and appear as “bright-gray” bodies generally, not as “dark-gray” bodies like in the case of gravity. The depth distribution of bright MECs is an open end question to determine together with nuclear force fields later as needed.

We now need to disengage the functions of the primary supply density J_{03} of somions from the secondary supply density J_{02} of electrions. To assist in this, we describe an outline of a model as follows:

Fig. 40 shows an electron and a positron surrounded by a dense medium of somion particles ς . These particles have a uniform density and move homogeneously in all directions presumably at the constant speed of light. They are characterized by a uniform flux density J_{03} . We posit that the mean free path of these particles is much smaller than atomic sizes, so that no attractive force is generated by them between

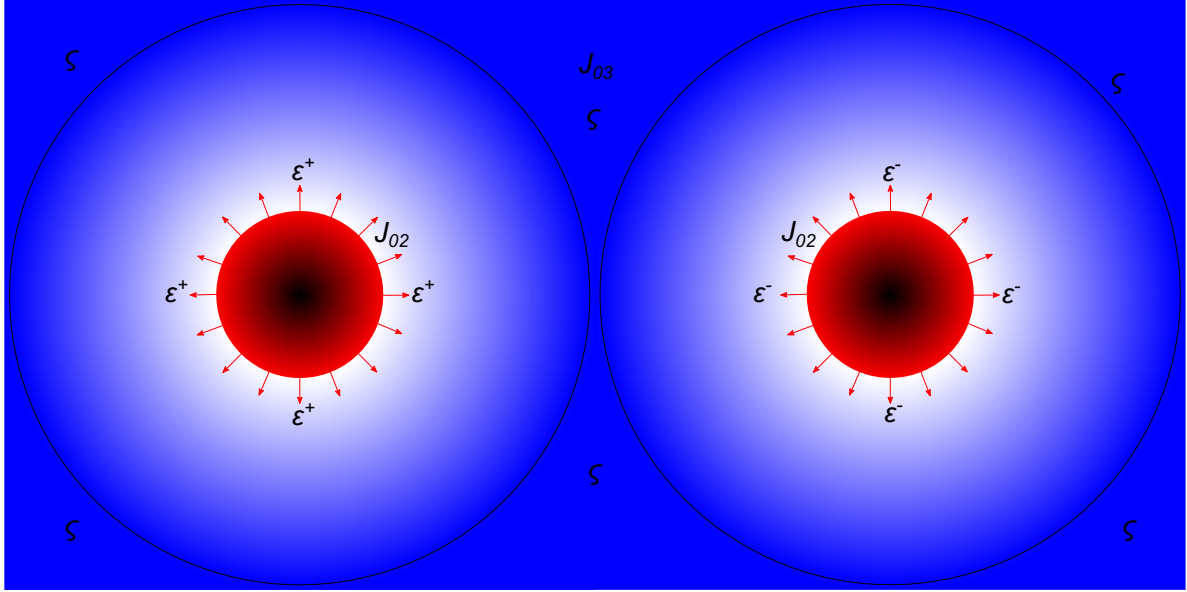


Figure 40: Primary somion field ζ (blue background) with flux density J_{03} generating secondary emitted electron field ε^+ or ε^- with flux density J_{02} at the electron and positron surface correspondingly.

electron-proton in an atom (or electron-positron in the figure) by way of absorption from J_{03} , as it happens with gravity (note that the diameters and distance in the figure are disproportionate). We further posit that push particles ε^- and ε^+ emitted from the electron and positron correspondingly have a mean free path much longer than the atomic dimensions (also the dimensions in the figure). We show this emission by red arrows emanating from the surface of the particles, where the maximum intensity J_{02} takes place. This maximum decreases with the inverse square distance law as expected by Coulomb's law for the electric field. The latter field is not fully shown by the diagram, but we can extrapolate the red arrows emanating from the surface of each particle. The signs $+$ and $-$ designate two attributes of the emitted electrons the nature of which remains to be explained. These attributes are introduced to explain the repulsive force between two electrons or between two positrons, and an attractive force between an electron and a positron (as in proton). For convenience, we may refer to them as "positive" and "negative" electrons but without the meaning of "charge" conventionally known for the electron and positron (or proton). In consequence of the relatively much longer mean free paths, these secondary electrons ε^+ and ε^- are thought to be much lighter (less mass/energy per particle) than the primary neutral somions ζ . A positive electron striking a positron is probably reflected, and so a negative electron is probably reflected from an electron. Instead of reflection, there may be absorption and re-emission via a processing mechanism if a final model requires it. In either case, the electrons create repulsive forces between electrons or between positrons.

We proceed step-by-step in building a model. For now, we further posit that a negative electron is readily absorbed by a positron, like a positive electron is absorbed by an electron. At the point of this absorption (MAC), the previous mechanism of electron generation and emission (MEC) is neutralized and momentum is transferred from the impinging ε^+ or ε^- to the receiving electron or positron. In this way, we may also say that MECs are "annihilated" or lost, i.e. the mechanism is lost but not the incoming electrons that may re-emerge as something else in another "grouping" that is not pertaining to the process of generating the electrical force. We need to stress that the "annihilation" here is about the mechanism (or MEC) without annihilation of matter from the absorbing body or the absorbed electron. As a result of this annihilation, there will be a shortage of electrons between and across an electron and a positron.

What eventually happens to the emitted electrons, if they do not meet with an electron or positron, does not concern us here yet; it is another open end to be dealt with as needed later, but we must assume that they dissipate or drain out to a steady-state density orders of magnitude below the density of emitted electrons at close range to the nucleus. Orbital electrons are already relatively far from the nucleus and may experience a density somewhere between the maximum J_{02} and the background electron aether. We do not attempt to address several questions until we have a more complete theory about other known force fields and until we can fit the general approach of PG with specific experimental information from particle physics and other related data. Then we should be able to learn how the background density dissipates or drains out and what happens to the absorbed electrons with annihilated MECs. This is only an initial qualitative attempt towards connecting electricity with gravity pending a quantitative analysis of the model.

By conjecture, we anticipate similar outcomes as from the gravitational computations in the Appendices with a difference arising from the background electrion flux superimposed on the emitted electrion flux. We are compelled to have or produce an explanation for the outcomes and choices of electrical parameters used in this section.

If electrions are practically reflected without prior deep absorption, then electrons and positrons should appear like white-holes in an opposite sense to black-holes. In that case, the values for J_{02} and g_{02} should be in a range corresponding to $k_{2-e}R_e > \sim \times 10$ according to Figs. 37 and 38. That is $J_{02} \sim \times 10^{68}$ and $g_{02} \sim \times 10^{35}$, for which there is practically no variation. Thus, electrons and positrons may be like black holes with respect to gravions and bright holes with respect to electrions. In that case, we may be much closer to understanding what happens physically when an electron comes sufficiently close to a positron: The adjacent surfaces coalesce, the masses merge and re-emerge as two gamma rays, and other particles. That is because a particle with an effective mass twice that of the electron (positron) cannot be sustained under PG rules. An explanation of the coalescence of electron-positron like this may help dissolve the long standing mysteries of “matter-antimatter”.

In consequence of the above description of the model, we can account of the repulsive and attractive forces as mediated by the exchange of electrions with same or opposite sign attribute. This may be a counterpart of the concept of “virtual” particles exchanged and transmitting force found in existing literature. Our model then explains known behavior of charges. However, the next key here is to explain the nature of positive and negative attribute of the emitted electrions by the electrons and positrons towards completing a unification theory. This outstanding attribute might relate to spin or revolution or another physical property, and we might be able to draw from the experimental data that have led to the Standard Model, if now the same data can be re-appraised under PG.

In drawing a parallel between Fig. 1 for establishing other force fields, we do not know at present about the depth distribution of MACs and MECs in relation to somions and electrions. They might penetrate deep enough or they may be restricted to an event-horizon-like layer. We bear this in mind when we attempt to reconcile experimental data and adapt this model accordingly.

In a macroscopic material body we expect a huge number of electrions around emitted from local sources like in Fig. 40 effectively producing a background of equal number density of ε^+ and ε^- in the “vacuum” away from the sources. As a result, we must superimpose the effect of this homogeneous background to the local picture of 40. Pending a detailed computation, we anticipate that the effect of this background on the total local force to be practically negligible. Also, whilst the ε^+ neutralize a number of MECs on an electron, an equal number is recreated continuously by somions. The same applies for a positron. An electron must be so organized internally as to always have a net amount of MECs specializing in ε^- emission and the positron in ε^+ emission. It is generally the short range interactions emanating from the immediate and near neighbors which determine the electrical force in atoms and between atoms. Now, the mean free path and range of ε^+ and ε^- depends on the surrounding medium (nature and state of material, like permittivity), but it must be consistent with observed macroscopic electric properties. A macroscopic electric field arises from an excess of ε^+ and ε^- on/from the corresponding “charged” bodies. We cannot complete the model until we can take into account an integrated flow and inter-conversions of push particles from all available sources of various force fields around.

We need to calculate the details of distribution of ε^+ and ε^- at both the microscopic and macroscopic level to gain a new insight of the ultimate mechanisms of electricity. For example, push electricity may provide a direct explanation also of the Casimir effect on account of the inhomogeneous distribution of ε^+ and ε^- around surfaces at close range. Also push electricity should explain long range observations like discharging and atmospheric lightning.

Most importantly, we have not accounted yet why the electrical mass should be constant by equating it numerically with the charge. Like with gravitation, we should be having a variable electrical mass with distance, say, from the nucleus of the atom. We can offer the following initial explanation: The electron has an intrinsic electrical mass m_{2e-e} acquired in a region where it is free from surrounding spherical nuclei. That region is characterized by a fixed density flux of electrions, from which the intrinsic electrical mass emerges. Whilst this mass is variable with distance from another spherical mass, it is not variable with distance from a “charged” flat plane. It is known that the electric force on a charge is independent of distance from an infinite plane conductor at fixed potential. Even simpler, we know that the force in a homogeneous electric field between two parallel plane conductors is independent of location. By increasing the potential of the conductors, we increase the electrical mass of the electron, generally speaking. For determining the charge of the electron, the experimental fields applied by Millikan and Fletcher create a net excess of effective mass due to extra electrion flux created by the external field only and not by changing position in the field. That is, we only vary the total flux of J_{02} . However, the magnitude of the extra applied flux is much-much smaller than the naturally prevailing electrion flux by many orders of magnitude. The naturally prevailing electrion flux

is that around a bound or “free” electron, the magnitude of which remains to be found. Thus the variation of electrical mass is practically vanishing and undetectable during experiment. This is the reason why we have invariably found the electron charge to be constant, whereas in reality it is not, if our push electricity theory can be verified. In other words, we do expect theoretically a significant net excess of effective mass to accrue on an electron with decreasing distance from another electron with spherical geometry, but we do not expect any net excess mass to accrue on an electron with variable location in a uniform electric field. In practice (experiment), if the position of an orbital electron from the nucleus in an atom changes slightly, the surrounding electrion flux variation may not be measurable either, whereby motion must be considered too. The added effect of the external field itself is practically insignificant and presumably undetectable to date. The naturally prevailing density of electrions trumps the applied fields during our charge measurements. The variation of electrical mass due to proximity with another electrical mass like the in-situ electrical mass of the electron in the atom remains an issue to investigate. This is another loose end to pick up on the way towards completing a push particle theory for all known forces.

We note reported values of the electron charge up to the 9th decimal place, which seems to be out of the expected range of charge variation vs. experimental applied electric field. Theoretically, if we could conduct measurements better than that to detect variation of the electron charge as a function of the applied field, then that would be a direct way to verify push electricity.

We should be able to independently confirm a similar theorem for the constancy of gravitational or electrical effective mass of a spherical body from an infinite plane sheet of matter (neutral or charged) using the fluxes of gravions and electrions as we did in Appendix C and E.

21.3.1 Precursor of nuclear field

The short mean free path relative to atomic sizes described above for neutral somions ς may be very long relative to nuclear sizes. In the latter case, nuclear particles would be pushed against each other, i.e. they would appear attracted to each other like with a strong force holding the nucleus together. In other words, we have a situation like with gravions but with an immensely greater flux density. Also, the weak nuclear force might not need a separate reservoir of push particles. The nature of the absorbing particles may determine the interaction with various types of push particles. Furthermore, the nuclear force arising from somions can be strong enough to overcome the repelling forces between the positive charges “residing” somewhere inside the protons. This is all a matter of the reservoir of somions having enough density to accommodate both electrical and nuclear forces by way of properly apportioning the absorptivity and emissivity of each constituent of an atom. This apportioning must be properly balanced out to preserve the real mass and energy of atoms being coupled with surrounding push particles (so far gravions, somions and electrions). The system of atoms and push particles must complete a “loop” of a continuous flow of real mass. This model will be finally complete when we can relate these push particles in closing the said loop.

Alternative to the the above suggestion (but unlikely), there is also the (theoretical) possibility that J_0 (and g_0) is far (immensely) stronger than we expect to ever be able to measure, in fact so strong as to be the primary source from which all other secondary push particles draw from, like secondaries in required in J_{02} and/or other flux densities J_{0x} with x as required. However, this possibility might extinguish our desire for a direct verification of PG, which makes it (again) imperative to organize some independent testing measurements for the gravion flux J_0 (or g_0).

Yet a simpler explanation for the presence of somions may be non other than they are gravions with the same mean free path and intensity (density) as the hypothesized somions. This idea is in accord with gravions being characterized by an appropriate distribution of density over mean free paths. In other words, the gravion density varies by orders of magnitude that corresponds to the magnitudes of force of various fields, like nuclear and electric fields. Correspondingly, the mean free paths also vary by many orders of magnitude commensurate with the range of forces of the said fields. This is further discussed in Section 28.4

[Note (*). We have determined the term “somion” like this: Since we think that the pool of push particles may be a common source for the electric and nuclear forces and since these forces create or hold the atom together and since atoms make up the everyday bodies that we experience, we want the new term to relate to embodiment. We mean something pertaining to the creation of bodies, or to the fleshing out of objects. Thus “bodings” might have been one, which could probably raise some eyebrows. Another term might be “union” since it unifies and unites particles, but it seems a too common and likely confusing word. So we decided for a more exotic name from Greek word “σώμα” for “body” and adding our suffix “-ίον” (ion), as we did for gravion and electrion. That is, “soma” + “ion” = “somion”. The symbol for somion could be sigma σ , but this has had many other uses and so we coined the variant-sigma ς . “Somation” (from known somatic) is a bit longer for economy, also “formion” in body-forming might be a bit less descriptive. Thus, somion is not more unsuitable than gluon, which would be a good choice too, if it were not already in use (unless we made it “gluion:” for consistency with “ion”). Somion implies the function of gluon

but for a larger group of composite particles and atoms. If the nucleus is found to be held together by its own special push particles, we have used the term “nuclions”, but all these are in a state of revision subject to how exactly the theory evolves. A review could be due any time.]

21.4 Discussion

The oil drop experiment by Millikan and Fletcher for measuring the elementary electric charge is now perfectly understood in physical terms without the use of an exotic “charge”. The oil drop becomes stationary by the equally opposing flows of gravions and electrions imparting a total of equal impulses. The same particle, namely, the electron has two distinct masses each acted upon by different types of push particles with different strength. In a stationary steady-state situation, both gravitational and electrical masses appear to be constant, whilst possible variations have been beyond detection to date. The “constant” electron charge may not be absolutely constant after all, as now revealed by PE, but we can have a simple explanation for its constancy too. If our theory is correct, the consequences are enormous even for the structure of the atom in view of the possibility that the in-situ electrical mass is different from the constant “charge” used to date. This could influence novel theoretical modeling of the atom and quantum mechanics. However, the picture is incomplete until we formulate the magnitudes of both electrical and gravitational effective masses in motion that actually (finally) yields the known constant effective mass or “charge”. Here, we repeat the thought process on the variation of gravitational mass in a stationary or moving state per Section 16.2, as it is also further developed in following sections.

Another issue may appear to be during finding the mass-to-charge ratio (m/Q) in electrodynamics experiments, which can be performed away from a planet, i.e. believed to be independent of the influence of gravity. There, it appears that we need the use of an inertial mass of the electron resisting the action of the electric force. However, even far enough from a planet, we have the ever present gravion flux creating an effective mass, which appears to resist (presenting classical inertia) an applied force. We have said that this apparent resistance is due the gravions acting via the activated part of the real matter. Thus, we have again the action by gravitational and electric fields on the same particle with different masses emerging from the energy rate of absorption from the respective fields. Again, there would no mystery of a separate and needless entity of “charge”, had we properly understood the meaning of mass used conventionally. In other words, we could have understood the above experiments in a straightforward and natural manner without the intervention of an “equivalence principle”. If our understanding could be verified, then we would be justified by proclaiming at the outset in version 1 of our reports that this principle is redundant. In fact, it would be worse than redundant, because it may have created a lot of needless mathematical physics around it. In fact, we still need a lot of basic mathematics to further develop PG and PE in the manner we have used in Section 16. With a similar approach, we should quantify the creation and variation of electrical mass. We listed the cases that we have not addressed yet in Section 16.2 and mentioned the need to incorporate a PE theory, an outline of which we have only started to describe qualitatively. The case of accelerating a body inside a gravitational and/or an electrical field remains incomplete. Even so, we have achieved a good understanding of the nature of both fields as we also understand that Newton’s gravitational law and Coulomb’s law are the same differing only in the type of effective mass used without the need of a distinct and cloudy entity like charge. The case of a falling “mass” in gravity corresponds to a falling “charge” in an electric field. When one of the two is driving the movement, the other is receiving the effects appearing as inter-conversion between mechanical and electrical energy. We have dealt only with a stationary steady-state situation for both fields, whilst Section 14 remains only a “stub” open for further work. In this respect, one worker alone cannot accomplish the entire task, should some readers feel that we leave many loose ends or obfuscate the problems. The groundwork of the theory should by now be sufficient to warrant participation of readers keen to solve all the ensuing issues.

Corollary: It is said that the mass-to-charge ratio (m/Q) in high energy particle accelerators remains constant and, because the charge is invariant, the mass must also be invariant and equal to the rest mass; it is then concluded that the relativistic mass increase is not an actual mass increase but only a theoretical consideration. However, we now lay bare the possibility that charge actually being also a mass may be subject to a simultaneous increase by the same factor that cancels out in the quotient. There is plenty of black mass converting to effective mass at the elementary particle level without creating new atoms. This possibility should raise an alarm about what really happens.

The reduction of all fields to push particles together with real mass in bodies provides a more tangible basis to understand and analyze in lieu of a mathematical abstraction by merely allotting a “force” to every point of a field by quantum field theory. For example, the electromagnetic potential field may have a real physical substrate rather than being mathematical concept(s) not readily comprehensible by humans. All push particles may be thought of as being a form of matter, so that we are left with finding how they relate or transform to each other through the mediation of other material bodies (e.g. electrons, positrons, neutrons

protons, etc) containing also black matter in the right amount to fit experiments. The substrate of fields in PG and PE is a form of real mass (stuff) that is conserved during transformations. One such transformation is to the effective mass. Black mass is another form of real mass with probably a true “zero-ground-state” that can be excited to effective mass at different states.

Another corollary of the above description is that we may be able to explain the underlying mechanism of the classical conservation of energy (potential and kinetic) as being one of conservation of gravions together with their momentum, if for example electrions upon absorption are equivalent to the absorption of a lump of gravions.

If the advent of electrical mass in lieu of “charge” creates a sensible basis for the unification of gravity with electricity, but at the cost of the equivalence principle, then why not do it? After all, Kajari *et al.* (2010) have already forecast such a possibility by their study on “inertial and gravitational mass in quantum mechanics”.

In view of the quantitative analysis and results, we can also return to the proton and review its black mass to fit with our upgraded finding for the electron on account of the electrion field. We can envisage that the “charge” in the proton is still connected to a fractional mass corresponding to that of a positron because of the composite nature of proton. The quark model of the proton may provide one form of connection with the evolving theory here by modeling the quarks with appropriate combinations of effective and black mass. However, we must also consider alternative possibilities about the structure of the proton. In this regard, we note some recent reports by Vayenas *et al.* (2020); Vayenas & Grigoriou (2020) claiming a fundamental departure from the Standard Model. They propose a “rotating lepton model” with a three-neutrino ring around a positron. Whilst this may be at odds with other theories, it may be consistent with our findings about mass so that the idea of revolving sub-particles may be validated with appropriate modifications. For example, their model for the neutron involving three revolving neutrinos around a stationary neutrino at the center may not explain the observed neutron magnetic moment, but we might use a different combination of revolving, rotating and spinning particles to explain the neutron properties: It might involve a central binary system of a positron (or electron) with a heavy neutrino both acted upon by gravitational force at very close range, around which revolve correspondingly an electron (or positron) together with one or more light neutrinos all acted upon by gravions while the electron and positron are acted upon also by electrions. Such a system would display a neutral charge but have a magnetic moment by the orbiting charge. There may be better combinations of particles among the plethora of experimentally existing particles to improve or replace the alternative proposed combinations of particles just mentioned. Revolving and rotating/spinning systems of smaller particles at the ultra-small scales inside all known/unknown particles seems a plausible way to proceed, if we wish to move beyond the Standard Model. If it can be shown that gravions, somions and electrions are sufficient to explain all known forces, the model can be simplified greatly. Then it may be that all composite particles are made of much fewer elementary particles in one way or another, such as Vayenas *et al.* propose or variant(s) of it; their model might warrant a closer examination and attention by authoritative experts. Of course, even if all this could explain the known forces, we would still be left with Kant’s query of how the elementary particles themselves are held together, but we do not aspire to reach the “ultimate” end by the present theory other than having made a bold stride forward.

By the same token, another “unofficial” theory on “*a sensible model for the confinement and asymptotic freedom of quarks*” (Watkins, 2020b) and on “*estimates of the mass densities of up and down quarks and estimates of the outer radii of the small, medium and large up and down quarks*” (Watkins, 2020a) may also be considered in relation to another possible “charge” distribution inside a proton under our interpretation of charge by PG. Again, the present author is in no position to support or reject any of those claims, other than to state the need for some new understanding of hadrons. We should not reject an alternative theory only on grounds of disagreement with existing theories and principles, or by the prejudicial demand that any new theory must only constitute an extension (continuation) of and subject to existing theories. We more probably need a radical breakout before we can determine some common grounds and return with an all encompassing theory. At the moment, we can speculate various possibilities, or at best we can sideline the problem until we can think of compatible models for hadrons and other particles. We hope that a better particle model will be found under the platform of a general PG, but that work is left for the relevant scientific community to accomplish.

Furthermore, the structure of the electron and positron could be entirely remodeled based on evolving theories of toroidal vortex structures (Rankine, 1855; Kelvin, 1867; Parson, 1915; Bulgac *et al.*, 2014; Falconer, 2019) as are proposed in following sections.

It is said that hadrons feel the strong nuclear force, but leptons do not, whilst all particles feel the weak nuclear force. Now, we may think that both forces may arise from the pool of somions, if their flux density is sufficient to satisfy the production of both electric force and nuclear forces. To this end, the presence of black matter in various particles may be such as to satisfy all experimental nuclear reactions.

Our above model per Fig. 40 may be enriched or modified by incorporating any compatible aspects of other existing field theories. For example, the zero-point energy (ZPE), or zero-point radiation and ground state energy may correspond to the somion concentration, a kind of an aether. The term ZPF is in reference to quantum electrodynamics (QED) vacuum dealing with electromagnetic interactions between photons, electrons and the “vacuum”, or to the quantum chromodynamics (QCD) vacuum dealing with color charge interactions between quarks, etc. A “vacuum” is viewed as the summation of all zero-point fields, the “vacuum state” in quantum field theory (QFT) with an energy density known as the cosmological constant. In this connection, we have correspondingly introduced and used the gravion flux density J_{01} and now the electrion flux density J_{02} and/or somion J_{03} . From the flux densities, we obtain the pressures J_{01}/c and J_{02}/c , which are also energy densities. For a cosmological ground state constant C , we may write:

$$C = \frac{J_{01}}{c} + \frac{J_{02}}{c} + \dots + \frac{J_{0x}}{c} = \frac{J_{0-total}}{c} \quad (307)$$

where x is the x^{th} known type of push particles. We note that our previous symbol Λ is also used in the literature to denote the cosmological constant, so care should be taken to avoid any confusion arising from the use of symbols. Our Λ denotes a new “cosmic” constant (in lieu of G) being different from the above cosmological constant C , but both bearing a direct relationship with each other. The above ideas might assist in removing the “infinite zero-point energy and the need for re-normalization”. In the event that the somion flux density provides a common source for all fields other than gravity, then the above equation would be simplified to:

$$C = \frac{J_{01}}{c} + \frac{J_{03}}{c} \quad (308)$$

Initially, we have no guide about the range of the somion or electrion flux density. Perhaps, we may have such a guide by previous Eqs. 226 and 227 on Schwarzschild radius and PG limiting radius. We had hoped to find an agreement once we find the maximum acceleration of other force fields. We can now try our preceding findings for the electric field. By equating the radii obtained for the Schwarzschild and PG derivation, we obtain for the required maximum acceleration g_{0max} :

$$g_{0max} = \frac{c^4}{4G_{max}M_{maxe}} \quad (309)$$

where the subscript *max* denotes the strongest force field producing an effective mass M_{maxe} and constant G_{max} , if all other fields are orders of magnitude weaker than this. Using the values for the electrion field in the case of unequal masses in the above equation, we find $g_{0max} = 1.4 \times 10^{42} \text{ ms}^{-2}$. This is the value of J_{02} around and between the graphs for the two smaller electron radii of $\sim 10^{-22}$ and $\sim 10^{-23}$ m at around $k_2R_{-e} \approx 10^{-7} \rightarrow 10^{-8}$ in Fig. 37. We do not expect an exact agreement between PG and GR, especially if one theory is better than the other. However, an astonishing compatibility is obtained by these values bearing in mind that we converge from totally independent derivations. In addition, we see convergence with Dehmelt (1989) and Sukhorukov (2017-2020) for the radius of the electron.

In contrast, using the case of equal masses, we get $g_{0max} = 7.97 \times 10^{30} \text{ ms}^{-2}$, which conflicts the corresponding range in Table 23. That is, we would need an unacceptably (unnatural) low value for g_0 for this value of g_{02} leading to an impossible situation. This seems to be a strong argument against the case of the gravitational mass being equal to the electrical mass.

We can obtain an interim cosmological constant by using the above value of $g_{02} = 1.4 \times 10^{42} \text{ ms}^{-2}$: The corresponding flux density is $J_{02} \approx \times 10^{82} \text{ Jm}^{-2}\text{s}^{-1}$, so that the cosmological constant may be around $C = J_{02}/c \approx \times 10^{74} \text{ Jm}^{-3}$ ignoring the relatively much smaller contribution from the gravitational flux density of $J_0 \approx \times 10^{26} \text{ Jm}^{-2}\text{s}^{-1}$. The actual J_{02} may be finally found to be several orders of magnitude less, which means that the difference from the cosmological constant is used for nuclear forces, like we proposed for the somion density, i.e. $J_{03} = J_{0max}$. However, we may ask if the energy density of vacuum is the same inside and outside a material body, which may be one reason for the big discrepancies found in the literature. It may be that there is a stagnation density of energy accompanying celestial bodies that is different from the rest of the universe, or different in various regions. We have already assumed the latter variability to be the case throughout this report.

The above cross-correlation example, if proven correct, indicates that there are probably many other examples of cross-examination between PG and existing data. Then this should serve as an invitation for the broad scientific community to start transferring their information on the PG platform in the hope that they will help PG to develop but, conversely, also their information to be better explained.

22 Action and reaction

We can now illustrate a conceptualization of the effects of gravitational and electrical fields between two macroscopic material spheres as shown in Fig. 41. The gravitational (effective) mass of the spheres is depicted with red color (top pair) and the electrical (effective) mass in blue color (middle pair). To avoid possible confusion, it should be noted that the color coding for each field here is different from that used in previous or other figures; also the density variation is not computed but it is only an indicative schematic (graphic) illustration. We have learned in Section 16 that the force arises from the loss of effective mass during the interaction of two spheres, which (loss) is depicted by yellow color (top pair). Correspondingly, we expect that an electrical force arises from the excess of effective electrical mass during interaction via same attribute electrions. While corresponding forces arise from the loss and excess of corresponding effective masses, these forces are distributed and exerted throughout the entire effective masses. We have not yet described the detailed distribution of electrical mass at the atomic level, but we may skip ahead and say that a shortening (albeit extremely small) of the distance between electrons prevails where there is compression, which means that a net excess amount of electrions is stored between atomic charges (masses) within each atom at a steady-state. This excess amount gives rise to an excess amount of electrical mass which becomes equal to the loss of gravitational mass, at equilibrium, as it is shown also in yellow color in the middle pair of spheres. The depth distribution of the electrical loss must be the same for both fields. The end result is a null force schematically depicted by the spherical distribution of red color for a restored effective mass in the bottom pair of spheres. The red color depiction is again approximate and without computation, to indicate the distribution of effective mass towards the outer surface with mass loss towards the center of the spheres shown again in yellow; the net effect is to restore the “lone” sphere distribution of effective mass.

It must be clear again that the schematic depiction above is about macroscopic bodies and not the interaction between elementary electrons. Until we find the correct quantitative relationships, the latter particles behave like a black-hole with respect to gravions and either (a) like a white hole or (b) like a bright hole with respect to electrions. The distribution of those masses would look like a very thin or thick meniscus accordingly (see gravitoids in Fig. 71) as each particle is facing the other. The magnitude of the absolute values will differ by many orders of magnitude between the two types of masses, which is not possible to depict graphically and simultaneously in the figures provided. The distribution of effective masses and their loss or excess for elementary particles can be computed accordingly but left for future work as needed.

In effect, we have explained the underlying processes during action and reaction between stationary macroscopic bodies. This involves a redistribution of the rate of absorbed push particles that is also an exchange and variation of effective mass. At first, it may look like electrions are squeezed out from the rod and transferred to the sphere, but actually they are squeezed out of the sphere itself locally (at the atomic/molecular level) originating from the local pool of electrions and transferred back into the sphere to replenish the loss of gravitational effective mass due to the shadowing by the other sphere. This is reminiscing of the piezoelectric effect converting mechanical compression to electric voltage and vice-versa. In combination, the ultimate balance of masses is supplied from the pool of gravions and electrions pervading the “vacuum” within and outside material objects. This may complete, for now qualitatively, the incomplete picture anticipated in Section 16.

The above description may also serve first for a qualitative description and introduction to a proper development of a dynamic push particle theory for Section 14. This can be done by upsetting the static equilibrium of the picture in Fig. 41 in any of the following two ways:

(i) Remove one sphere leaving the rod acting on the other sphere like a rocket per Fig. 42(bottom). Then the sphere has no mass loss on account of the presence (shadowing) of the other sphere, but retains the net excess electrion rate as long as the rod acts on the sphere imparting acceleration. While the acceleration persists, the net excess of electrions accrues real mass in the form of effective and black mass. It is important that this accrual takes place inside elementary particles of the atoms not by creating new atoms; in other words, the chemistry is preserved. This continues for the duration of acceleration. When the rod (rocket) ceases to act, which is the practical situation, acceleration ceases, the body moves at constant velocity but retains an excess mass establishing a new steady-state energy exchange rate with the surrounding gravion flux. It remains to work out how exactly the new equilibrium flux is distributed around the moving sphere. There must be an equal rate of absorption of gravions at least from the back and front in the direction of velocity to avoid drag. The rate of absorption and emission around the perpendicular direction may differ, but this plane of symmetry does not affect the constant velocity. During acceleration, it is the electric field (electrions) driving the body whilst the gravion field acts as buffer in a passive manner for the balancing of energy flow consisting of push particles. Energy flows from the electrion medium to the gravion medium. We attempt to write equations for the mass accrued at constant speed below.

(ii) Remove the supporting rod between the two spheres per Fig. 42(top). Then the internal compression in each sphere will be undone and the emanating excess electrions will vanish over a very short transition

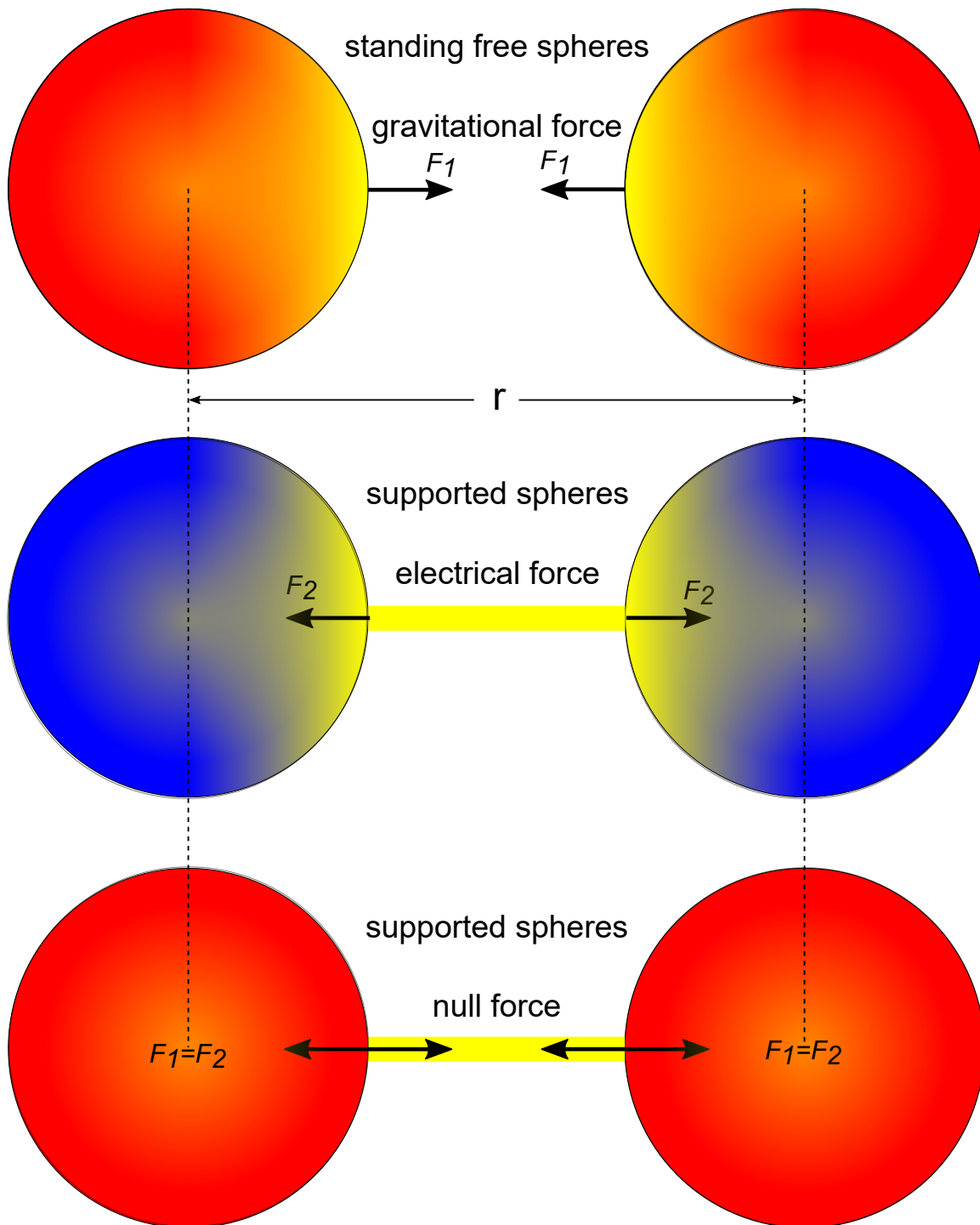


Figure 41: Unification of gravitational and electric fields: Red represents gravitational effective mass, blue electrical effective mass and yellow the loss of effective mass being the same in both fields. The resulting gravitational F_1 and electric F_2 forces arising from the equal mass loss are also equal

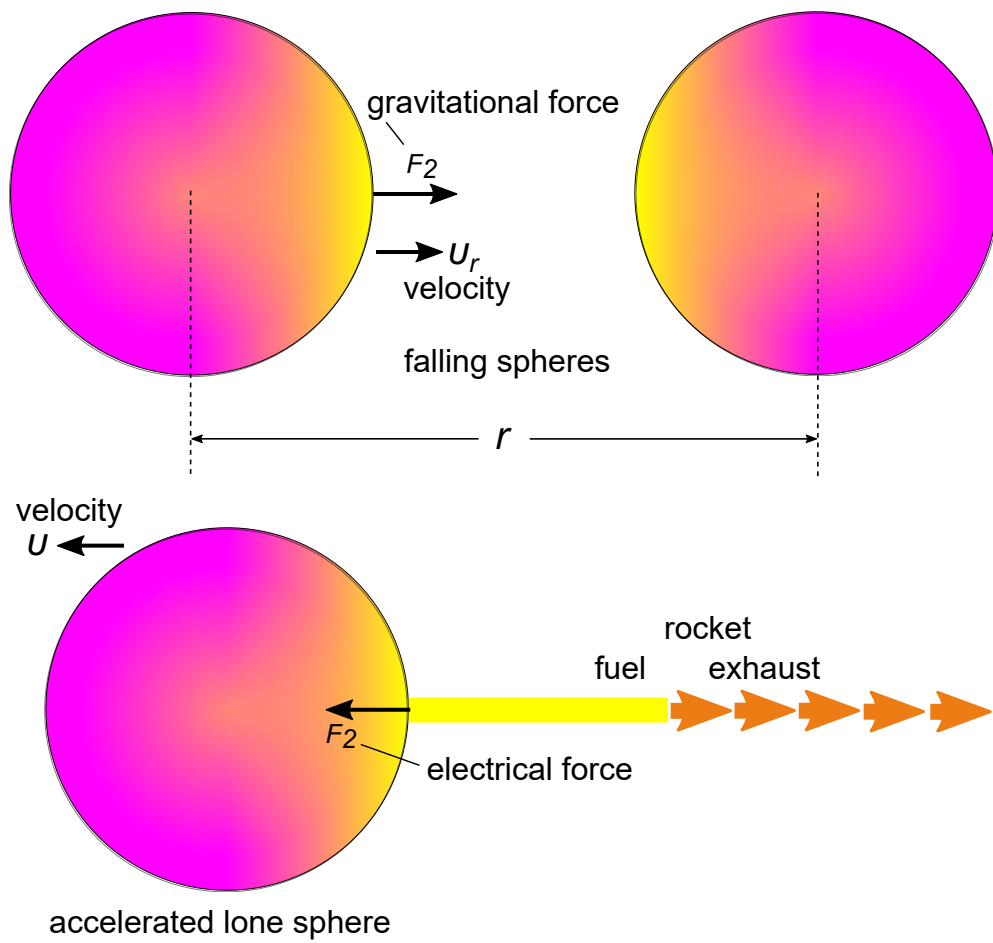


Figure 42: Falling spheres (top) and rocket acting on sphere (bottom)

time, during which masses of different types vary and redistribute themselves. The force present from the net rate of loss of gravions (= effective mass loss) will accelerate the spheres closer to each other increasing the said loss on account of proximity. We attempt to quantify the situation of falling spheres also below.

23 Mass versus speed

This is in continuation of Sections 14.7 and 16 dealing with variation of mass against distance or speed, under the understanding on developments on electricity and electron structure in preceding sections. We test and investigate a conjectural relationship between velocity and parameter kR of a moving material sphere for two distinct situations: (a) acceleration by a rocket away from (outside) other gravitational fields and (b) acceleration of a falling sphere on another under their gravitational field.

It is still undecided how to correctly handle special relativity under PG in order to start working out the dynamics of push gravity. In the interim, we have attempted a trial connection between the Lorentz contraction factor and the PG contraction factors in Section 14.7. With some further analysis and in view of the findings on mass composition of the electron (positron), we can obtain a new insight of this attempt. We use again the conjectures for connecting speed v to absorptivity A_R . A close agreement was obtained with one hypothesis by setting:

$$\frac{v^2}{c^2} = A_R = 1 - \frac{1}{2k^2R^2} + \frac{\exp(-2kR) \cdot (2kR + 1)}{2k^2R^2} \quad (310)$$

The above conjecture is arbitrary and can be replaced by another form as suggested previously. The simplest variation is to apply a power form of the above equation, like:

$$\left(\frac{v}{c}\right)^n = A_R \quad (311)$$

where n may be chosen in a way to yield outcomes consistent with experiment. We will discuss this possibility afterwards.

In the following, we first use the above Eq. 310 to help us draw some important conclusions, which may not differ if we use or find other relationships later, including some not yet proposed; it is worthwhile to ponder on the outcomes of the following investigation. The work of these sections here is undertaken under the provisos set at the outset of Part 2, that is, they have an exploratory purpose and by no means bound the groundwork of Part 1.

23.1 Rocket acceleration

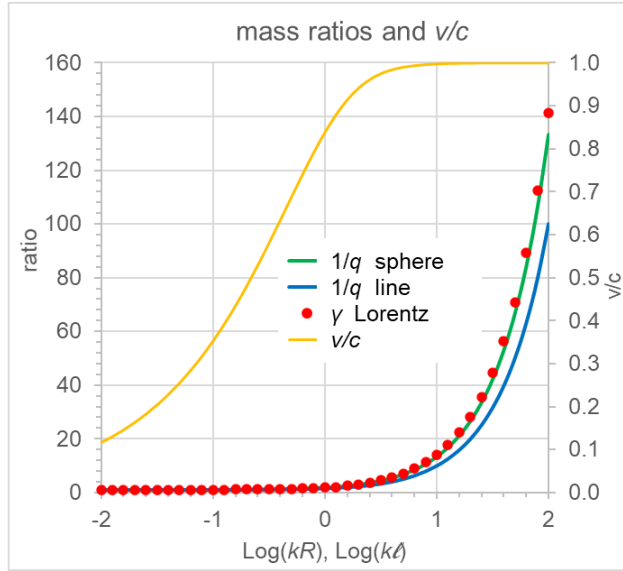
First, we compare the ratio of *relativistic mass* m_{rel} over the *rest mass* m_0 used by $\gamma = m_{rel}/m_0$ simultaneously with the PG ratio of *real mass* over *effective mass* given by $1/q = m/m_e$. We actually repeat the findings of Fig. 18 by now explicitly plotting the ratio of masses from the two theories, because we will continue to use various types of masses in continuation to these plots. The results are given in Fig. 43(a) in the same range of kR as before for the three cases, namely, of a “sphere”, “line” and “Lorentz” (left ordinate axis), where we also plot the corresponding speed fraction v/c on the secondary axis (right ordinate axis). The same three cases are re-plotted against the more familiar variable of speed fraction v/c in (b). As expected, we repeat the close agreement between $1/q$ and γ factor for the “sphere”. If our relational conjecture is correct, then this is an important outcome beyond just a good or fortuitous agreement, as found below.

We note in Fig. 43(b) that the speed ratio v/c starts from a non-zero value, because we arbitrarily started with a non-zero value of kR . This is a consequence of the applied Eq. 310 stating that only at the limit of zero kR would we have a non-moving body. This means that the absorption coefficient k (or absorptivity A_R) is practically zero at zero velocity. The latter condition may have only theoretical meaning or importance, because we must actually start with some finite value of absorptivity, i.e. A_R is non-zero before the sphere starts moving. In this case, Eq. 310 yields a speed-like quantity for a stationary body, which we may call *intrinsic speed* v_0

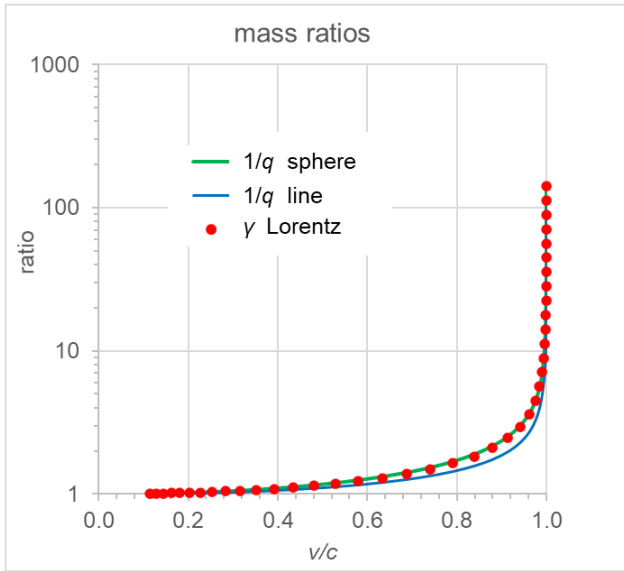
$$v_0 = c\sqrt{A_R} \quad (312)$$

This appears to be a misnomer for a non-moving body in the absolute reference frame of the gravion medium, but we introduce it for uniformity of terms in the ensuing formulation. At any rate, this speed corresponds to an initial (starting) value $(kR)_0$, or k_0R for a fixed sphere radius R , as given by:

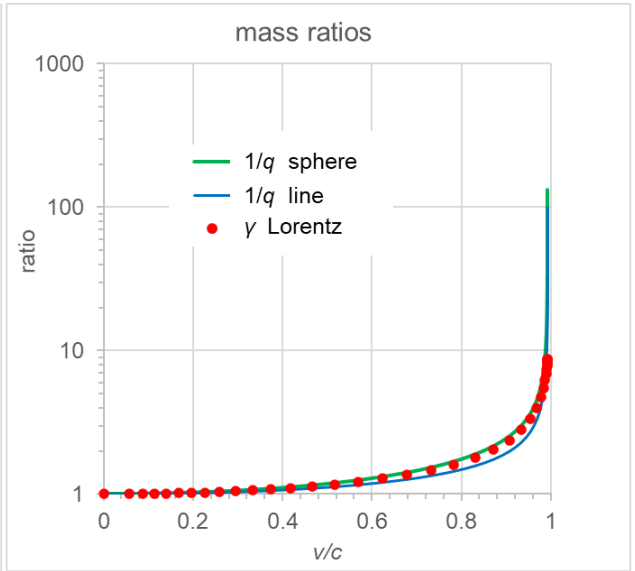
$$\frac{v_0^2}{c^2} = A_R = 1 - \frac{1}{2k_0^2R^2} + \frac{\exp(-2k_0R) \cdot (2k_0R + 1)}{2k_0^2R^2} \quad (313)$$



a



b



c

Figure 43: (a) Mass ratios and speed against kR , (b and c) mass ratios against speed.

Noted that we want to retain the notation A_R instead of a would be more appropriate A_{R0} for what should now be called the *intrinsic absorptivity*, because we prefer to avoid changing the notation in all of the preceding work; it is exactly what we have used and meant under the static regime of our theory. As we move in a range $kR > k_0R$, absorptivity increases monotonically to values which we designate by $A_{Rc} > A_R$, where the subscript c (c) refers to “*composite*”, as in composite absorptivity pertaining to combined (integrated) intrinsic and kinetic (moving) components of absorptivity. The term “composite” means the same as the term “current” (like *current effective mass*) in previous discussion of Section 16.1, but “composite” now ensures the presence of actual speed. From the absorptivity, we aim to derive the corresponding types of mass like real, effective, black and now kinetic and composite masses being simply proportional to types of absorptivity by the ubiquitous equation:

$$M_e = \frac{g_0 R^2}{G} A_R \quad (314)$$

Because the masses are additive quantities, so are the absorptivities. Therefore, the *composite absorptivity* A_{Rc} in the range $k_c R > k_0 R$ is the sum of the intrinsic absorptivity plus a component of absorptivity arising from the actual speed v of the moving body. Let us call the latter component as the *kinetic absorptivity* $A_{R\kappa}$, so that we have :

$$A_{Rc} = A_R + A_{R\kappa} \quad (315)$$

Then we obtain the *composite speed* v_c from the relationship:

$$\frac{v_c^2}{c^2} = \frac{v_0^2}{c^2} + \frac{v^2}{c^2} \quad \text{or} \quad v_c^2 = v_0^2 + v^2 \quad (316)$$

where we reserve the notation v without subscript for the actual speed to be consistent with convention. The corresponding absorptivities then are given explicitly by:

$$\frac{v_c^2}{c^2} = A_{Rc} = 1 - \frac{1}{2k_c^2 R^2} + \frac{\exp(-2k_c R) \cdot (2k_c R + 1)}{2k_c^2 R^2} \quad (317)$$

$$\frac{v^2}{c^2} = A_{R\kappa} = 1 - \frac{1}{2k_\kappa^2 R^2} + \frac{\exp(-2k_\kappa R) \cdot (2k_\kappa R + 1)}{2k_\kappa^2 R^2} \quad (318)$$

Among the three types of speed introduced above, only v is the real one, while the other two (v_0 and v_c) have theoretical significance (initially) in the formulation derived. However, the composite absorptivity A_{Rc} may be viewed as the absorptivity in the reference frame of the moving body, like the intrinsic absorptivity is with reference to the stationary frame of the gravion medium.

As a result, we adjust the graphs on contraction factors against actual speed using:

$$A_{R\kappa} = A_{Rc} - A_R \quad (319)$$

We substitute velocities for absorptivities per above to obtain:

$$\frac{v^2}{c^2} = 1 - \frac{1}{2k_\kappa^2 R^2} + \frac{\exp(-2k_\kappa R) \cdot (2k_\kappa R + 1)}{2k_\kappa^2 R^2} - A_R \quad (320)$$

As demonstration, we use again the starting (arbitrary) value $k_0 R = 0.01$ to establish an intrinsic A_R at $v/c = 0$ and plot the same mass ratios against speed (v/c) for $kR \equiv k_c R > k_0 R$ in Fig. 43(c). It should be noted that the deviation between GR and PG, (γ and $1/q$) now becomes greater towards high speeds. This deviation decreases if we start at smaller starting values of $k_0 R$ instead of the arbitrarily chosen 0.01. Smaller $k_0 R$ implies operation closer to Newtonian regime. Higher $k_0 R$ means starting to move a denser body, which has a higher intrinsic velocity v_0 . As a result, GR using the lesser actual speed v yields a lesser value for γ than PG using a corresponding higher composite speed v_c yields a higher value for $1/q$. Now, if one of the two theories is correct, the other should be wrong. We think that GR has not been verified at very high speed with v/c very close to unity for macroscopic bodies, while with small particles the existence of real and black mass has not been taken into account. Therefore, we may not dismiss PG being the correct one. In the latter case, we anticipate much higher real mass than a corresponding relativistic mass (theoretical or real), the significance of which can be thrown into question.

We can readily find the corresponding contraction factors, effective masses and real masses from previous known equations. We only need to qualify these new quantities as being *intrinsic*, *kinetic* or *composite* accordingly. Thus we use the notations m , m_κ and m_c for the real masses, m_e , $m_{e\kappa}$ and m_{ec} for the effective

masses, m_b , $m_{b\kappa}$ and m_{bc} for the black masses and q , q_κ , q_c for the contraction factors and so on for other variables.

To avoid possible ambiguity, we summarize the old and new notations and symbols of the variation of mass of a moving sphere in Fig. 44: This is for a sphere with radius $R = 1$ m, for which we set (arbitrarily) $k_0R = 0.01$ and $g_0 = 1000 \text{ ms}^{-2}$. The latter values determine the intrinsic (lone and stationary) effective mass m_e at the start of the abscissa. We note that it is already a very massive body at this value of kR (left point). From Eq. 314, we find and plot the new effective mass in motion m_{ec} that we termed “composite effective mass” and is the sum of masses corresponding to Eq. 315:

$$m_{ec} = m_e + m_{e\kappa} \quad (321)$$

where $m_{e\kappa}$ is the kinetic mass. The real mass in motion m_c (composite real mass) is found from the effective mass divided by the contraction factor to be:

$$m_c = \frac{4g_0R^2}{3G}k_cR \quad (322)$$

which is the straight line graph in 44(a). It must be noted that $m > m_e$ at the starting point of k_0R , but the difference is not visible on the graphs. The difference $m_{bc} = m_c - m_{ec}$ is the *composite black mass*. For good measure, we plot the same masses against the corresponding real velocity in the same figure on the right (b), where we also add the relativistic mass. We note the significant disagreement of the latter with the real and effective masses, where the m_{rel} lies consistently below the the PG masses. The disagreement is due to the choice of this unusually dense sphere, which has a large intrinsic “velocity”. If we chose an ordinary density sphere, the disagreement would be exceedingly small as the reader can easily verify (e.g. use a steel sphere with $\rho_e = 7500 \text{ kgm}^{-3}$ and $R = 1$ m characterized by $k_0 = 1.57 \times 10^{-9} \text{ m}^{-1}$ at $g_0 = 1000 \text{ ms}^{-2}$, or $k_0R = 3.15 \times 10^{-11}$ with a more likely $g_0 = 50000 \text{ ms}^{-2}$). It is this difference (small or big), which we find that GR may have missed. Hopefully, we have correctly accounted for this miss now. [Note: The apparent much better agreement in Fig. 43 is because we use the mass ratios, not the absolute values of masses].

We have examined the situation of a continuous application of force (acceleration), but we need also to consider what happens at cessation of acceleration. There must be initially an “instantaneous”, actually extremely short duration, transition of some internal re-adjustment of masses followed by a new steady state situation of the body moving at constant speed. This transition is needed to restore the effects of “deformation” of the internal electric field that took place at the outset of application of force, but the cumulative effects accruing in the entire acceleration period must remain intact after this transition under a new steady-state rate of gravion absorption and emission. These matters are pending examination in conjunction with and after investigation of a falling body and then of possible internal structure of matter at the fundamental level in following work.

Note: Compare Eq. 316 with relativity equation $E^2 = (m_0^2c^2 + p^2) c^2$ or

$$\left(\frac{E}{c^2}\right)^2 = m_0 + \frac{p^2}{c^2} \quad (323)$$

which corresponds to Eq. 321 relating composite_effective, effective and kinetic masses. The difference between the two theories lies in the understanding that the effective mass per PG corresponds to the “rest” mass per SR, but they are not the same. Our effective mass varies with speed, which added to the kinetic mass yields the total (composite) effective mass. It is said that “relativistic mass corresponds to the total energy” which we could relate to the composite mass here.

Further, we can briefly see what the effect is on the mass-speed relationship, if we use Eq. 311 in the case of $n = 1$, or $n = 4$ (we already investigated the case with $n = 2$) below. That is, we if we use the alternative conjecture of:

$$\frac{v}{c} = A_R \quad (324)$$

or

$$\left(\frac{v}{c}\right)^4 = A_R \quad (325)$$

We plot the alternative mass-speed relationships in Fig. 45a for $n = 1$. We can see by comparison with the previous Fig. 44b that the accrued kinetic mass is now greater for any given speed. The opposite effect is if we use $n = 4$, the quantitative relationship for which is plotted in Fig. 45b. Hence, it is possible to adjust the accrued mass as needed in later theoretical formulations. In the latter case, it looks like the effective mass

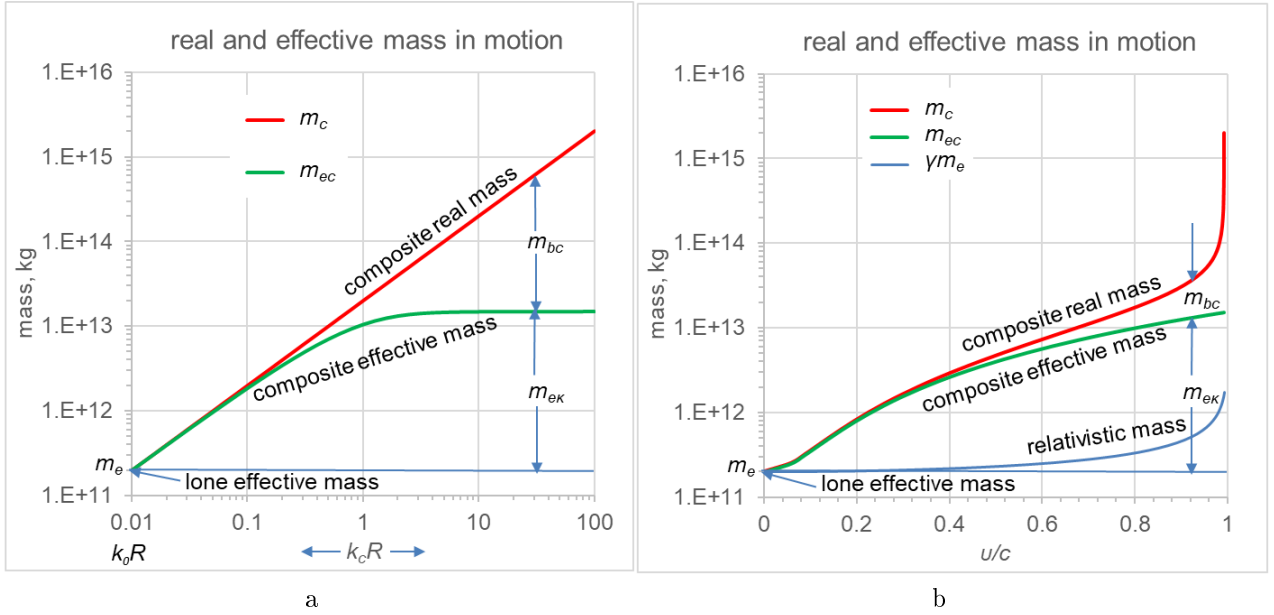


Figure 44: Composite real mass m_c and composite effective mass m_{ec} of a moving material sphere starting with an intrinsic effective mass m_e at $v/c=0$ are plotted against kR in (a) and against v/c in (b), based on Eq. 310; the relativistic mass is added for comparison.

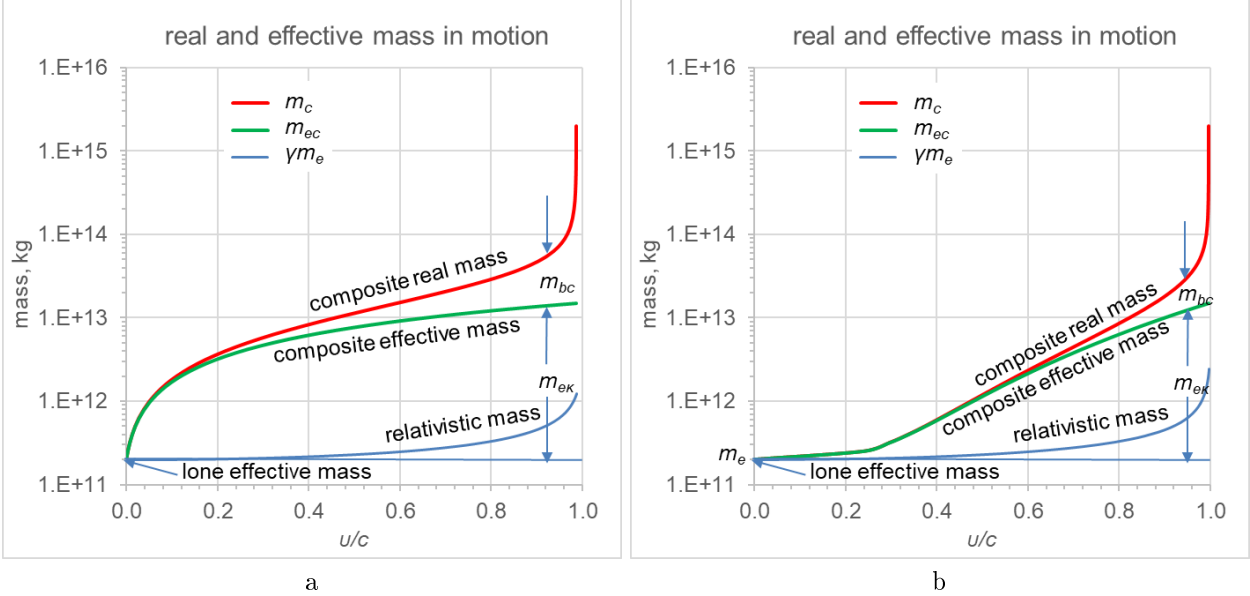


Figure 45: Composite real mass m_c and composite effective mass m_{ec} of a moving material sphere starting with an intrinsic effective mass m_e at $v/c=0$ are plotted against v/c , for alternative conjectures (a) with power of $n = 1$ and (b) with power of $n = 4$; the relativistic mass is added for comparison.

is much closer to the relativistic mass up to considerable speed of $v/c \approx 0.2$; could that mean that this is sufficient agreement, if relativistic mass has not been experimentally verified with sufficient accuracy above this speed? Otherwise, could we adjust the conjecture to achieve the experimentally required accuracy? Interestingly, both effective and real mass move closer together up to around $v/c \approx 0.8$, meaning that the black mass accrued is not great, but becomes so as we approach very close to the speed of gravions.

Introducing again a distinction between intrinsic, kinetic and composite absorptivities, we sum them by Eq. 315 in the form of speeds by the above alternative conjectures to obtain correspondingly:

$$\frac{v_c}{c} = \frac{v_0}{c} + \frac{v}{c} \quad (326)$$

or

$$\left(\frac{v_c}{c}\right)^4 = \left(\frac{v_0}{c}\right)^4 + \left(\frac{v}{c}\right)^4 \quad (327)$$

The issue of speed-mass relationship is taken up again in Section 23.2.2.

Alternatively, we might want to force an equation between our contraction factor q and Lorentz factor L $q = L$ as proposed by Eq. 186, to but not carried through yet. From that equation, we derive the relationship between speed and absorptivity (connected to mass) for sphere and line, as we did in Section 14.7:

$$\frac{v^2}{c^2} = 1 - q^2 \quad (328)$$

Sphere

$$\frac{v^2}{c^2} = 1 - \left(\frac{3A_{R\kappa}}{4k_\kappa R}\right)^2 \quad (329)$$

$$\frac{v_0^2}{c^2} = 1 - \left(\frac{3A_R}{4kR}\right)^2 \quad (330)$$

$$\frac{v_c^2}{c^2} = 1 - \left(\frac{3A_{Rc}}{4k_c R}\right)^2 \quad (331)$$

We have done the calculations and plotted the results for this case too. However, the graphs are very close to those presented in Fig. 44; we can only a small numerical shift on the corresponding speed axis for the relativistic mass. This outcome is expected on account of the very close graphs for the two factors seen in Fig. 18. The reader may like to repeat our computation steps as follows:

We set an initial value of $k_0 R = 0.009999999999999 \approx 0.01$ and find A_R . Then for any subsequent $k_c R$ we have the A_{Rc} yielding the kinetic absorptivity from:

$$A_{R\kappa} = A_{Rc} - A_R \quad (332)$$

which we solve for $k_\kappa R$, namely, the equation:

$$1 - \frac{1}{2k_\kappa^2 R^2} + \frac{\exp(-2k_\kappa R) \cdot (2k_\kappa R + 1)}{2k_\kappa^2 R^2} - (A_{Rc} - A_R) = 0$$

Finally, the speed ratio is given by:

$$\frac{v}{c} = \sqrt{1 - \left[\frac{3(A_{Rc} - A_R)}{4(k_\kappa R)}\right]^2}$$

The initial value of $k_0 R$ was chosen very close (not equal) to 0.01 to avoid a singularity in solving the above equation at this point $k_0 R$ and then increased to step by the factor of $10^{0.1}$ up to $k_\kappa R = 100$ spanning the typical 4 orders of magnitude variation.

If we wish to apply the “line” contraction factor, we may proceed like:

Line

$$\frac{v^2}{c^2} = 1 - \left(\frac{A_\ell}{k\ell}\right)^2 = 1 - \left(\frac{1 - \exp(-k\ell)}{k\ell}\right)^2 \quad (333)$$

where the contraction of material line q_ℓ is given by Eq. 46 and the line-absorptivity $A_\ell = 1 - \exp(-k\ell)$ was defined in Eq. 184.

We can retrace our steps in the entire Section 23 for both rocket acceleration and falling acceleration using the above speed-absorptivity equations.

23.2 Falling body acceleration

We further apply the above formulations in the special case of two spheres falling to each other. However, we already found that this is a different situation, so that we must adapt the previous derivations properly. One difference is that with a rocket acceleration we have the action of an electric field from the “outside”, whereas in the case of a falling body we have action of the gravitational field within itself. There is no outside accretion of mass (by an “external” agent like a rocket), only a variation of the existing falling mass(es) by gravity. We have seen this in Section 16, where the distance between gravitating spheres is an additional parameter to be incorporated in our derivations of motion. Those simple findings are enough to see that “falling body acceleration” is different from the “rocket acceleration”. We simply cannot assume any equivalence, as will also become more evident below. Now, we need to introduce the additional parameter of distance r and incorporate it as an additional subscript (r) accordingly.

It is instructive to continue on from the three cases worked out in Section 16 for static pairs of material spheres. We start with CASE_1 involving the Earth and Moon. We calculate the components of effective mass for the Moon falling to Earth. We previously found the effective mass of a stationary and unsupported Moon at various distances. However, the effective mass of a falling Moon is increased by the kinetic mass component over and above the static one. Therefore, we must distinguish the effective masses in previous Tables 9 and 10 by denoting them as m_{er} for *static effective mass at distance r* . As explained previously, “static” means that the sphere is stationary at distance r but without any supporting means. If the sphere is moving at r in consequence of prior falling, then we use m_{erc} for the *composite (current) effective mass at distance r* . For the lone (very far away) effective masses of the Moon and Earth we maintain the same subscripts in m_e and M_e correspondingly for the masses but now with lower and upper case letters in lieu of numerals (1 and 2); we use one plain upper case R for the radius of the “smaller” sphere falling towards the “larger” sphere in the three cases (we do not examine the falling of the “larger” sphere to the “smaller” one at present). Now, the static effective mass plays the role of an intrinsic mass at each distance, if we apply the same preceding formulation for the composite effective mass used in rocket acceleration; the rocket force is replaced by the force of the impulse of the gravion difference rate of absorption along the line of fall.

We found that Newton’s gravitational law is applicable provided we use the intrinsic (lone) masses in calculating the force vs. distance. Then, regarding the potential energy, we can use:

$$E_{potential} = \int_{\infty}^r F dr = \int_{\infty}^r G \frac{M_e m_e}{r^2} dr = G \frac{M_e m_e}{r} \quad (334)$$

which is equally shared by the two bodies. However, the speed obtained from the corresponding equivalent kinetic energy (by the action of the same force) depends on the behavior of mass during fall. If we arbitrarily use a constant mass m_e as in the classical derivation of the kinetic energy of the system:

$$E_{kinetic} = \int_{\infty}^r F dr = 2 \int_{\infty}^r \frac{dp}{dt} dr = 2 \int_{\infty}^r \frac{d(m_e v_r)}{dt} dr = 2m_e \int_{\infty}^r \frac{dv_r}{dt} v_r dt = m_e v_r^2 \quad (335)$$

the resulting speed refers only to this constant mass. which is not consistent with a variable mass m_{er} vs. distance found previously in PG. Use of the above Newtonian speed to generate the kinetic mass ($m_{e\kappa}$) by a presumed conjecture in Eq. 310 would be incorrect at least in principle. Nevertheless, we can establish procedures and relationships below, which do not affect the analysis, discussion and conclusions, other than some second order of magnitude numerical differences. After all, if PG speed is different from Newton, the difference has not been possible to measure to date. Contingent upon this clarification, we may use Newtonian mechanics to derive the corresponding speed at distance r for the Moon (to start with) by:

$$v_r^2 = G \frac{M_e}{r} \quad (336)$$

From the above, we obtain the absorptivity $A_{Rr\kappa}$ at this distance by

r , m	m_{er} , kg	m_{erloss} , kg	m_{rc} , kg	$m_{er\kappa}$, kg	m_{br} , kg	m_r , kg
12742000	7.342882E+22	4.7876E+19	7.34960070E+22	1.57E+16	6.7167536E+19	7.34959912E+22
25484000	7.346527E+22	1.1431E+19	7.35325113E+22	7.87E+15	6.7234253E+19	7.35325034E+22
50968000	7.347387E+22	2.8281E+18	7.35411257E+22	3.93E+15	6.7250002E+19	7.35411217E+22
101936000	7.347599E+22	7.0524E+17	7.35432505E+22	1.97E+15	6.7253887E+19	7.35432486E+22
203872000	7.347652E+22	1.7620E+17	7.35437796E+22	9.83E+14	6.7254854E+19	7.35437786E+22
407744000	7.347666E+22	4.4043E+16	7.35439115E+22	4.92E+14	6.7255095E+19	7.35439110E+22
815488000	7.347669E+22	1.1010E+16	7.35439444E+22	2.46E+14	6.7255155E+19	7.35439441E+22
∞	7.347670E+22	0	7.35439552E+22	0	6.7255175E+19	7.35439552E+22

Table 24: Dependence of various types of mass on distance of the Moon from Earth per prior CASE_1.

r , m	m_{er} , kg	m_{erloss} , kg	m_{rc} , kg	$m_{er\kappa}$, kg	m_{br} , kg	m_r , kg
6371002.0	7.9414E+14	6.8921E+14	1.193639E+15	1.05E+10	3.99492E+14	1.193614E+15
6371063.7	7.9448E+14	6.8887E+14	1.194452E+15	1.05E+10	3.99964E+14	1.194427E+15
6371637.1	7.9657E+14	6.8678E+14	1.199452E+15	1.05E+10	4.02869E+14	1.199427E+15
6377371.0	8.0869E+14	6.7466E+14	1.228731E+15	1.05E+10	4.20028E+14	1.228705E+15
6434710.0	8.6487E+14	6.1848E+14	1.372847E+15	1.04E+10	5.07967E+14	1.372819E+15
7008100.0	1.0576E+15	4.2575E+14	2.015524E+15	9.56E+09	9.57913E+14	2.015484E+15
7645200.0	1.1562E+15	3.2718E+14	2.494737E+15	8.76E+09	1.33856E+15	2.494687E+15
8919400.0	1.2634E+15	2.1995E+14	3.264946E+15	7.51E+09	2.00153E+15	3.264877E+15
9556500.0	1.2967E+15	1.8668E+14	3.601683E+15	7.01E+09	2.30500E+15	3.601604E+15
12742000.0	1.3851E+15	9.8300E+13	5.036353E+15	5.26E+09	3.65130E+15	5.036225E+15
25484000.0	1.4600E+15	2.3312E+13	8.830150E+15	2.63E+09	7.37011E+15	8.829845E+15
50968000.0	1.4776E+15	5.7588E+12	1.200624E+16	1.31E+09	1.05286E+16	1.200586E+16
101936000.0	1.4819E+15	1.4355E+12	1.349491E+16	6.57E+08	1.20130E+16	1.349464E+16
203872000.0	1.4830E+15	3.5861E+11	1.396041E+16	3.29E+08	1.24774E+16	1.396026E+16
407744000.0	1.4833E+15	8.9637E+10	1.408436E+16	1.64E+08	1.26011E+16	1.408428E+16
815488000.0	1.4833E+15	2.2408E+10	1.411584E+16	8.21E+07	1.26325E+16	1.411580E+16
∞	1.4834E+15	0	1.412635E+16	0	1.26430E+16	1.412635E+16

Table 25: Dependence of various types of mass on distance of the small dense sphere from the large dense sphere per prior CASE_2.

$$A_{Rr\kappa} = \frac{v_r^2}{c^2} = G \frac{M_e}{c^2 r} \quad (337)$$

Then the kinetic mass component of the composite effective mass at the same distance is

$$m_{er\kappa} = \frac{g_0 R^2}{G} A_{Rr\kappa} = \frac{g_0 R^2}{G} \frac{v_r^2}{c^2} = \frac{g_0 R^2}{c^2 r} M_e \quad (338)$$

The total or composite effective mass at distance r is

$$m_{erc} = m_{er} + m_{er\kappa} \quad (339)$$

The corresponding absorptivities are

$$A_{Rrc} = A_{Rr} + A_{Rr\kappa} \quad (340)$$

By substitution, the above equation becomes:

$$1 - \frac{1}{2k_{rc}^2 R^2} + \frac{\exp(-2k_{rc}R) \cdot (2k_{rc}R + 1)}{2k_{rc}^2 R^2} = G \frac{m_{er}}{g_0 R^2} + G \frac{M_e}{c^2 r} \quad (341)$$

which we solve for $k_{rc}R$ and then obtain the composite contraction factor q_{rc} at this distance. From the composite effective mass we also obtain the real mass m_r at each distance. The results are provided in Table 24, where we have transferred the masses m_{er} and m_{erloss} along with the same distances from Table 10. Subject to the above clarification on mass variation, we repeat the same procedure for CASE_2 and CASE_3 in compiling Tables 25 and 26. We include these tables to show any small numerical differences and variations where they occur, which are not visible in subsequent graphical form.

It is necessary to point out that the “kinetic” type of PG mass introduced above is not the same with another “kinetic mass” that we could theoretically derive from the Newtonian kinetic or potential energy of two mutually falling spherical bodies given by

$$E_{potential} = G \frac{m_e M_e}{r} = m_e v_r^2 = E_{kinetic} \quad (342)$$

We understand that orthodox (conventional) physics may not accept us to think that the above energy is convertible to mass, i.e. something outside the conventional or Newtonian intrinsic (rest) mass. However, since we have already moved away from this restriction, it would be arbitrary to avoid juxtaposing and cross-examining this quantity (actual or not) vis-à-vis with all other types of mass already introduced in our theory. This quantity can be tested together with the ubiquitous equation $E = mc^2$ used for our conversion, i.e. by dividing the above potential (or kinetic) energy by c^2 as:

$$m_{potential-at-r} \equiv m_{pr} = \frac{m_e v_r^2}{c^2} = G \frac{m_e M_e}{r c^2} \quad (343)$$

where we prefer the subscript “p” ($_p$) to avoid confusion with the subscript “ κ ” ($_{\kappa}$) already allotted to the PG kinetic mass. Then the ratio of these two masses is:

$$\frac{m_{er\kappa}}{m_{pr}} = \frac{g_0 R^2}{G m_e} \quad (344)$$

From the above, we could obtain the highly sought limiting acceleration:

$$g_0 = \frac{m_{erk}}{m_{pr}} \frac{G m_e}{R^2} \quad (345)$$

if we actually knew the value of $m_{er\kappa}$, but we do not, because the tabled values for it are based on the assumed values of g_0 arbitrarily chosen to be $g_0 = 10^3 \text{ ms}^{-2}$ for CASE_1 and $g_0 = 10^5 \text{ ms}^{-2}$ for CASE_2 and CASE_3. Then, if the conversion of potential energy to mass by division with c^2 were to be correct, i.e. if we wanted to have $m_{erk} = m_{pr}$, we would obtain:

$$g_0 = \frac{G m_e}{R^2} \quad (346)$$

The above finding is important, because we also have the universal Eq. 314 for g_0 , so that the only way to have them equated by:

$$\frac{G m_e}{R^2} = \frac{G m_e}{A_R R^2} \quad (347)$$

is on the condition that $A_R = 1$, or, in practice, close enough to unity! This indicates that if we knew the diameter and the mass of a particle opaque to gravions, then we could deduce the g_0 sought. We could have come to this understanding earlier by the known

$$g_0 A_R = \frac{G m_e}{R^2} \quad (348)$$

but we have now found this result by connecting kinetic mass to potential mass via $E = mc^2$. Conversely, the latter equation is experimentally applicable with very dense bodies. It would be nice if could measure the electron radius. However regarding measurement of g_0 , it may still be more practical to resort to some of the direct methods proposed in Part 1.

Next, we can see how the above theoretical considerations fare in comparison with the tabled results for the three computed cases. To facilitate reading of the various combinations and types of mass, for convenience and clarity in the ensuing reporting, we include a summary Table 27 with explanations of the various mass symbols used. The numerous types and combinations of mass is not a trivial or pedantic exercise, because their theoretical existence may indicate corresponding existence of material structures at the fundamental level of particles.

With regard to density of mass in the three cases examined, mention of a “dense” or “very dense” sphere simply implies operating away from Newtonian mass on the sigmoid curve of A_R against kR . Unfortunately, we do not have the actual value of g_0 yet, which has compelled us to use a hypothetical range for it, or some arbitrary values as in the example cases here. This creates some unavoidable complexity in reporting and understanding the real world situation. Thus, the choice of g_0 for the Moon corresponds to $k_0 R = 0.00122$ placing it closer to Newtonian situation, while for CASE_2&3 we have $k_0 R = 7.071$ placing them close to saturation on the absorption curve. We expect a much higher than $g_0 = 1000 \text{ ms}^{-2}$, which would correspond

r , m	m_{er} , kg	m_{erloss} , kg	m_{rc} , kg	$m_{er\kappa}$, kg	m_{br} , kg	m_r , kg
12742000	1.384834E+27	9.8516E+25	5.03111536E+27	5.26E+21	3.64628E+27	5.03098791E+27
25484000	1.460029E+27	2.3322E+25	8.82903258E+27	2.63E+21	7.36900E+27	8.82872789E+27
50968000	1.477591E+27	5.7593E+24	1.20060756E+28	1.31E+21	1.05285E+28	1.20056950E+28
101936000	1.481915E+27	1.4355E+24	1.34948947E+28	6.57E+20	1.20130E+28	1.34946246E+28
203872000	1.482992E+27	3.5861E+23	1.39604103E+28	3.29E+20	1.24774E+28	1.39602608E+28
407744000	1.483261E+27	8.9637E+22	1.40843570E+28	1.64E+20	1.26011E+28	1.40842803E+28
815488000	1.483328E+27	2.2408E+22	1.41158362E+28	8.21E+19	1.26325E+28	1.41157976E+28
∞	1.483351E+27	0	1.41263499E+28	0	1.26430E+28	1.41263499E+28

Table 26: Dependence of various types of mass on distance of the smaller dense from larger dense sphere per prior CASE_3.

Symbol	Definition
m	real mass of static lone body
m_e	effective or intrinsic mass of static lone body
m_b	black mass of static lone body
m_c	composite real mass of lone body at speed v
$m_\kappa = m_c - m$	kinetic real mass of lone body at speed v
m_{ec}	composite effective mass of lone body at speed v
$m_{e\kappa} = m_{ec} - m_e$	kinetic effective mass of lone body at speed v
m_{bc}	composite black mass of lone body at speed v
$m_{b\kappa} = m_{bc} - m_b$	kinetic black mass of lone body at speed v
m_r	real mass static at distance r
m_{rc}	composite real mass moving at distance r
m_{er}	effective or intrinsic mass static at distance r
m_{erc}	composite effective mass moving at distance r
m_{br}	black mass static at distance r
m_{brc}	composite black mass moving at distance r
$m_{r\kappa} = m_{rc} - m_r$	kinetic real mass moving at distance r
$m_{er\kappa} = m_{erc} - m_{er}$	kinetic effective mass moving at distance r
$m_{br\kappa} = m_{brc} - m_{br}$	kinetic black mass moving at distance r
$m_{rloss} = m - m_r$	loss of real mass static at distance r
$m_{erloss} = m_e - m_{er}$	loss of effective mass static at distance r
$m_{brloss} = m_b - m_{br}$	loss of black mass static at distance r
$m_{rcloss} = m - m_{rc}$	loss of real mass moving at distance r
$m_{ercloss} = m_e - m_{erc}$	loss of effective mass moving at distance r
$m_{brclloss} = m_b - m_{brc}$	loss of black mass moving at distance r
m_{pr}	potential mass static at distance r
v	real (actual) speed of lone body (moving outside gravity)
v_0	intrinsic (notional) speed of lone body by m_e
v_c	composite (notional) speed of lone body (moving outside gravity)
v_r	real (actual) speed of falling body (inside gravity)
v_{r0}	notional speed of falling body (inside gravity) by static m_{er}
v_{rN}	Newtonian falling speed from infinity to r
v_{rPGs}	real (actual) PG falling speed from infinity to r by static m_{er}
v_{rPGc}	real (actual) PG falling speed from infinity to r by composite m_{erc}
v_{r1rPGc}	real (actual) PG falling speed from r_1 to r by composite m_{erc}

Table 27: Summary of terminology on masses and speeds tabled, plotted and analyzed.

to a much lower k and kR , i.e. even closer to Newtonian situation for the Earth-Moon system, but these clarifications should help understand the results provided. It is imperative to conduct some of the proposed experiments to determine the actual g_0 and then repeat the computations to establish the actual k for real systems of bodies.

In Fig. 46(a,b,c), we plot the m_{pr} , m_{erk} , m_{erloss} and m_{rcloss} for each of the three cases. In Newtonian CASE_1, the effective mass loss is practically (not exactly) the same as the real mass loss, whereas the kinetic mass is far above the potential mass and both far below the effective mass. In contrast, the kinetic mass is practically (not exactly) the same as the potential mass in CASE_2&3, while the effective mass loss and real mass loss have separated out both lying above the potential and kinetic masses by orders of magnitude. These are important outcomes: They confirm Eq. 347 in that potential mass is (nearly) the same as kinetic mass for very dense but not for Newtonian bodies. This might seem at first that energy does not balance out in all cases. However, according to our understanding, mass is a continuous steady state rate of energy transfer between gravions (absorption) and (possibly) electrions (emission), or between different fields. The classical (conventional) potential energy represents only the agent for achieving conversion of one form of mass to another during fall (variation of distance). When we lift an object, we spend work to achieve the process of the said mass conversion to which we partner with the surrounding fields. In any energy balance we have to include not only our energy (work) but also the partnered energy. It is like the mechanism of a heat pump in an air-conditioning system, namely, we spend a small amount of energy for the pump (electrical motor) to transfer a much larger amount of energy between two different temperature reservoirs. Correspondingly, in Newtonian mechanics, we spend a small amount of potential energy (i.e. mass) to generate a much larger amount of PG kinetic mass. However, if we use extremely dense bodies, then our potential energy expended transforms almost entirely to kinetic mass. Understood that the processes described are reversible. This understanding is compatible with particle physics confirming the conversion of mass to energy, because we may assume that the particles involved are extremely dense, as we have already found for the electron and positron. Hence, the equivalence Eq. 347 blends harmoniously with $E = mc^2$ that was used to derive it. It would be profitable to trace back the original work (founding steps) in the derivation of the latter equation.

Furthermore, we also find that the total (real) mass decreases with distance between the two falling spheres in all cases. We present comparative graphs in the same Fig. 46(d). This indeed contravenes conventional theories. The conventional “rest mass” is sacrosanct. However, all types of PG mass vary with distance, including the real mass. This might at first be disturbing, but we may quickly dismiss any concerns: If the mass of a falling body decreases, it does not mean that it loses atoms or chunks of matter, but rather that it radiates push particles without changing the known structure of matter (within a certain range of conditions). This is what happens to an electron falling towards a nucleus. We are accustomed to x-rays emitted by electrons. We can claim that a similar situation exists also with a falling body in a gravitational field, except that we have not been able to detect such radiation yet, neither for a falling Moon on Earth, nor by variation of the distance of planets in elliptical orbits. Such radiation would be of extremely low frequency and extremely low intensity for us to detect. However, we do detect radiations from heavy bodies in astrophysics, so that our PG theory of mass may apply and help us understand better the astronomical/astrophysical observations available now or in the future.

In corroboration of the above, we may also note in (d) of the same figure that CASE_2 may approximately represent also an electron-proton analog system by comparing the radii used: The ratio of “large_dense” to “small_dense” radii is of the order 10^6 , while the proton/electron ratio can be in the order between 10^6 and 10^7 per Section 21.1.2. Since we found that the density of the electron is very high with a much lower proton density (making a good analog system with our spheres), then we may conclude that the variation (loss) of mass displayed in the figure is plausible. It would be very useful to repeat another test case with two “small_dense” spheres of equal diameter to simulate an analog for the fall between an electron and a positron. All this requires a lot of work which may take time to do unless readers decide to contribute to this and many other open topics.

The above findings may also provide evidence about a long standing question, or paradox, about the orbiting electron not emitting radiation. Our PG theory provides the answer: At fixed orbiting radius and numerically fixed speed there is no change of the real mass, hence there is no radiation emitted. If this might seem difficult to accept, we can suggest a physical explanation too: The centripetal force (acceleration) should accrue kinetic mass per Fig. 44 but the “fall” should also emit an amount of mass simultaneously resulting in a null effect. The rate of mass accrual (due to falling acceleration) must offset the rate of mass loss (due to distance decrease); we should be able to confirm this by carrying out analytical and/or computational work later, like in Appendix E. Readers may be encouraged to take up this work too, like many other works where we leave off unfinished tasks. However, the processes taking place during motion in PG dynamics will be better understood when we can correctly learn about the structure of fundamental

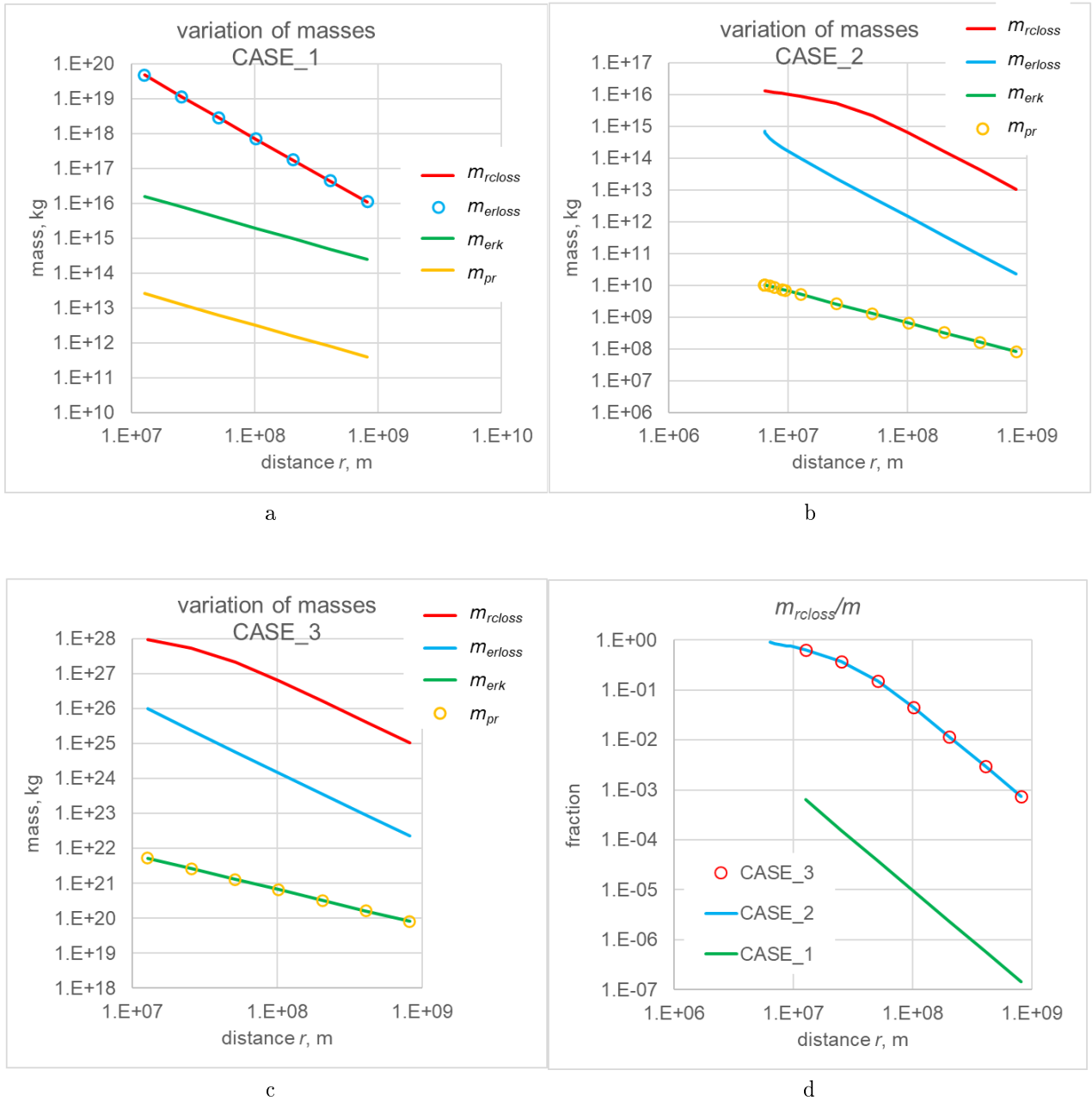
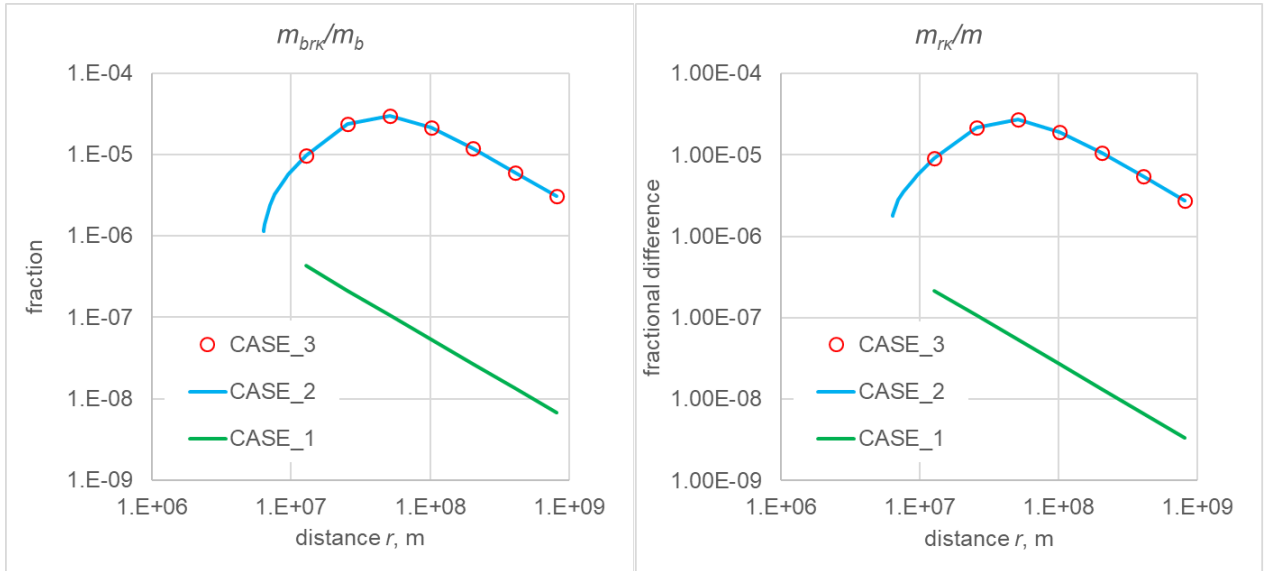
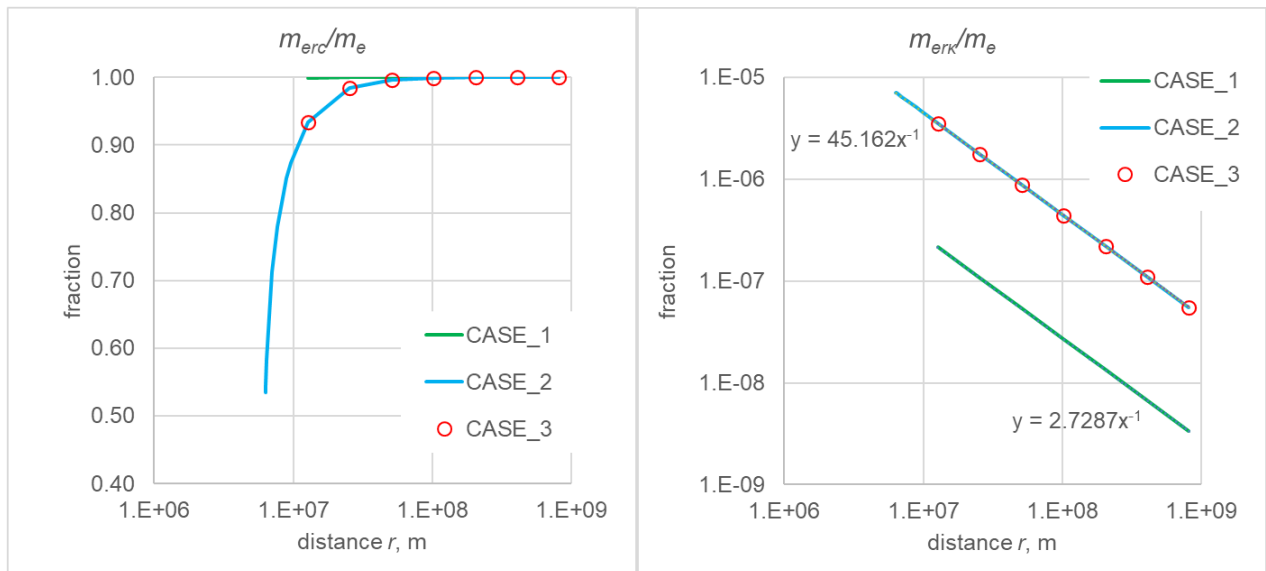


Figure 46: (a, b and c) Variation of different type of masses against distance in continuation of CASE_1, CASE_2 and CASE_3 per Section 16 in absolute values; (d) real mass loss in fractional (normalized) values.



a

b



c

d

Figure 47: Fractional (normalized) variation of various types of mass against distance.

particles once and for all.

Now, the exact distribution and other aspects of radiation emission may be speculated. The emission should be generally uniform around the falling sphere, otherwise it would affect the force along the direction of fall. However, this uniformity may be distorted at short range and/or with dense bodies resulting. Electrodynamics may be re-appraised on a PG platform.

The results presented in the tables and equations are only part of the big potential ushered. As a further example, we have also plotted the variation of other fractional masses or combinations thereof against distance in Fig. 47. While black mass may not contribute to inertia and force, it is part and parcel of the entire body structure accompanying the static and kinetic effective masses. There are corresponding fractions of black mass like *static black mass at r* m_{br} , *kinetic black mass at r* $m_{br\kappa}$ and *composite black mass at r* $m_{brc} = m_{br} + m_{br\kappa}$. We normalize and plot the fraction $m_{br\kappa}/m_b$ in order to compare the outcomes for all three cases on the same Fig. 47(a). Likewise, we plot the *kinetic real mass at r* $m_{r\kappa} = m_{rc} - m_r$ normalized by $m_{r\kappa}/m$, i.e. over the intrinsic real mass to compare the results again for all three cases in Fig. 47(b). The latter mass is the radiation (mass loss) emitted initially if we release the body fixed at r with a support rod as shown in Fig. 41; on the hypothesis that the stationary-and-supported sphere has the original intrinsic (lone) mass, upon release it must rearrange the internal mass types so that it acquires the computed static effective and black masses at this distance of an unsupported-and-not-moving sphere. Actually, this re-arrangement must be very fast determined by the magnitude of gravion and electrion exchange rate. That is what must be happening when we release a body from some altitude to start a free fall. This action-reaction process represents a transition period of time during which the body starts falling without having achieved any appreciable speed. In future studies we can examine the mathematical details of this transition. For now, we are satisfied about the general state of a stop-fall regime. That is, the dynamics of the falling sphere depends also on the point of start of the fall (the distance r). We can use the same mathematical derivations accordingly.

We are further interested in the shape of the two curves (a) and (b) of Fig. 47. For the cases of highly dense bodies, there is a maximum presumably representing some internal process in the structure of real mass. Suffice it here to note this finding until we attempt to understand better what the internal structure might be.

We add two additional sets of plots in the same Fig. 47, namely, for the *normalized composite effective mass* m_{erc}/m_e in (c) and the *normalized kinetic mass* $m_{er\kappa}$ in (d). The curves in (c) appear numerically identical with the ratio of forces in Fig. 23, but actually they are different derivations with unequal values:

$$\frac{m_{erc}}{m_e} > \frac{m_{er}M_{er}}{m_eM_e} \quad (349)$$

The seeming equality on the graphs is due to the chosen numerical values of the variables involved as can be easily verified. With variables differing by many orders of magnitude, it requires high precision computations if to avoid misleading impressions. Nevertheless, we note this similarity that might lead us to new relationships and understanding further down the track.

The curves in (d) confirm a relationship found between masses and distance if we use the previous equations by:

$$\frac{m_{er\kappa}}{m_e} = \frac{g_0 R^2 M_e}{c^2 m_e} \frac{1}{r} \quad (350)$$

The straight lines fitted on the log-log plots yield the equations $y = 2.7287x^{-1}$ for CASE_1 and $y = 45.162x^{-1}$ for CASE_2&3, i.e. an inverse to the distance relationship as predicted above or the same originally given by Eq. 338. The kinetic mass and potential energy behave the same, but they are generally unequal unless the absorptivity is close to unity.

We supplement the above presentation with the additional CASE_7 and CASE_4 now provided in Section 16.3 with corresponding results here in Figs. 48 and 49.

We comment first on CASE_7, which follows the same trend with previous cases: The variation of kinetic $m_{er\kappa}$ and potential m_{pr} masses are practically the same but not exactly equal, like we found previously for the dense bodies; the loss of real composite m_{rcloss} and effective m_{erloss} masses increases monotonically as the spheres approach each other. That is, there is a monotonic shedding of real mass with decreasing distance, most of which takes place within a few radii of distance, considering the logarithmic scale of mass loss. The fractional kinetic black mass $m_{br\kappa}/m_b$ and the fractional kinetic real mass $m_{r\kappa}/m$ at distance r follow practically the same trend and values without being equal. The fractional composite effective mass m_{erc}/m_e and the fractional kinetic effective mass $m_{er\kappa}/m_e$ at distance r are again similar at different scales for all these cases.

CASE_4 is in clear departure from the other cases: The real mass loss defined by $m_{rcloss} = m - m_{rc}$ yields a negative value. To show this on logarithmic scale along with the other masses, we changed the sign

Type of mass	kg
m_e, r_∞	2.30953136731102E+04
m, r_∞	2.30953136931349E+04
m_b, r_∞	2.00246358872391E-05
m_{er}, r_{min}	2.30102108923897E+04
m_{erloss}, r_{min}	8.51027807205368E+01
m_{erc}, r_{min}	3.34405290986513E+04
m_{rc}, r_{min}	3.34405291406330E+04
m_{brc}, r_{min}	4.19817015868788E-05
m_{rcgain}, r_{min}	1.03452154474984E+04
m_{erk}, r_{min}	1.04303182062616E+04
m_{pr}, r_{min}	1.60772894666244E-05

Table 28: Representative masses of the small sphere of CASE_4

and renamed it by $m_{rcgain} = m_{rc} - m$, because we now have a net gain of mass. The small test sphere with earthly density and only 1 m radius is characterized by a very small absorptivity and black mass, so that the effective and real masses are very close to each other. The corresponding variation of effective mass with position (m_{er}) is also extremely small to the extent that the accrual of kinetic mass during fall overwhelms all positional variation of mass loss. The real mass gain is practically equal to the kinetic mass with both being only a little under the effective lone mass of the falling sphere. Indicatively, we list some representative values of the various types of mass for the small sphere of this case in Table 28.

The above outcomes may come as surprise and for possible rejection based on existing expectation and experience. In fact, they may be contrary to data and astronomical observations and measurements of meteors and comets. However, this is no reason to discard the attempted approach. First of all, these masses are the result of the arbitrary use of Eq. 310 while they can be drastically reduced via, say, Eq. 325 up to great speeds (see also Fig. 45).

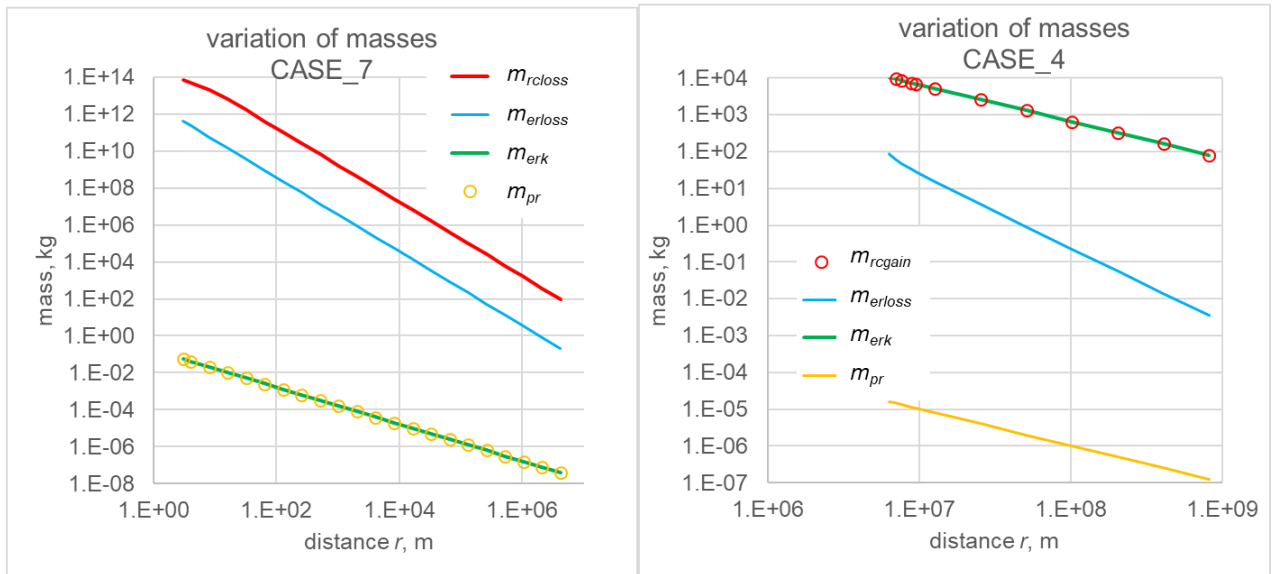
As stated previously, the use of Newtonian speed to connect with mass variation for a falling body is arbitrary but has been applied on the assumption that it would provide first order magnitudes, upon which we have already derived important lessons. We proceed to substantiate our assumption in the next two subsections, but the answers provided are themselves subject to other simplifications, which should not invalidate our hitherto conclusions. The simplifications used have other important ramifications emanating from the cumulative effects of speed computations.

We first consider the case where the falling spherical mass has a variable effective mass $m_{er}(r)$ with distance alone but not with speed yet, followed by the case of having both variations. This is a novel situation completely outside conventional physics, for which we must make our position clear: We must recognize the distinction between the two different causes of mass variation, namely, one positional variation based on the firm PG outcomes of Section 16, and another based on a proposed/speculated mass accrual (variation) determined by the given speed at any point in space and moment in time (speed-variation of mass). The first variation is fundamental to the static PG theory of Part 1 of this report, but the second variation remains to be worked out and proved, albeit also fundamental in the development of a dynamic PG theory. We skirmish with the latter development in Part 2 of this report. We attempt to explore the possibility of arriving at a dynamic theory with as little as possible reliance on conventional principles. The delay in doing so is the idea that the dynamics of motion depends also on the structure of matter at the fundamental level, i.e. motion and structure being intimately connected. We provide a sample of these ideas later, so that it should be appreciated why we have created several incomplete openings with the aim to return to, or somebody else to take over from where we leave off.

23.2.1 Speed from static mass variation

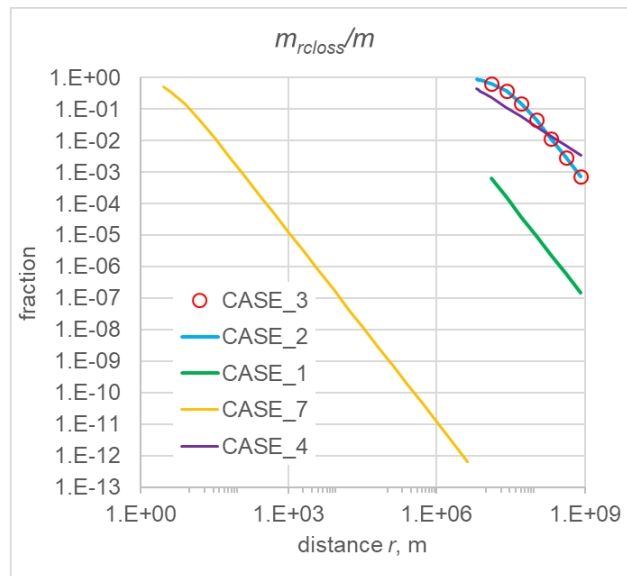
The difference between Newton and PG is that the same force acts on different masses, namely, on a constant (invariable) mass in Newton, but on a variable mass now in PG. The force is the same in both situations but the outcomes on speed and motion are different. The work done and the kinetic energy is the same in both cases, but the resulting speeds differ as they are used by different masses. The kinetic mass ($m_{e\kappa}$) created by a presumed conjecture in Eq. 310 is left out for now (to be applied in the next section), so that we can secure a novel outcome even if the said conjecture is abandoned or modified later.

We follow the mathematical steps for the work done by the same force on the variable mass below:



a

b



c

Figure 48: (a) Variation of different type of masses in absolute values against distance for CASE_7, (b) same for CASE_4 and (c) real mass loss in fractional (normalized) values for all cases together

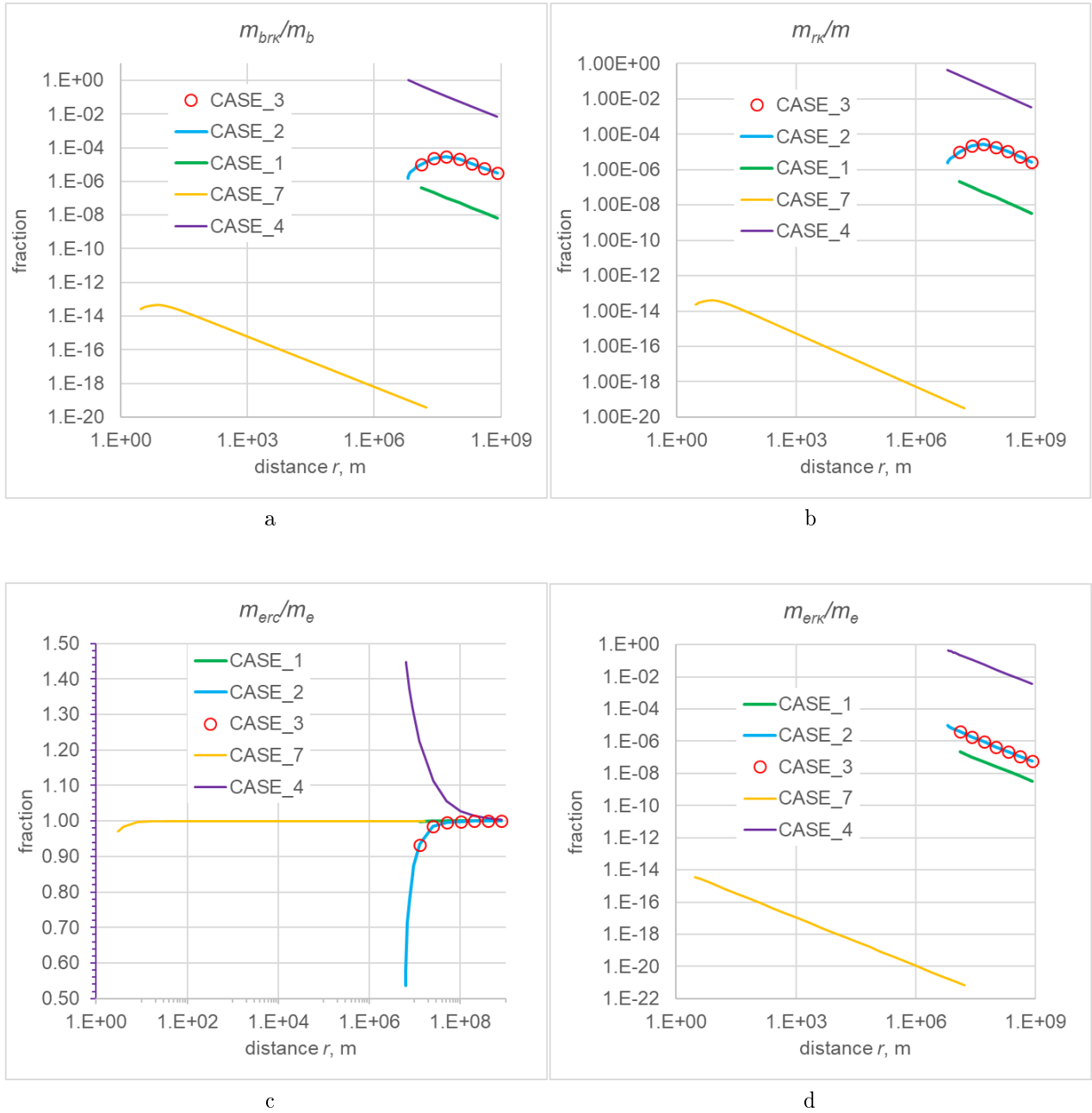


Figure 49: Fractional (normalized) variation of various types of mass against distance adding CASE_7 and CASE_4 together with all previous ones.

$$\begin{aligned}
E_{kinetic} &= \int_{\infty}^r F dr = 2 \int_{\infty}^r \frac{dp}{dt} dr = 2 \int_{\infty}^r \frac{d(m_{er} v_r)}{dt} v_r dt = 2 \int_{\infty}^r \left(v_r \frac{dm_{er}}{dt} + m_{er} \frac{dv_r}{dt} \right) v_r dt \\
&= 2 \int_{\infty}^r \left(v_r^2 \frac{dm_{er}}{dt} dt + \frac{1}{2} m_{er} \frac{dv_r^2}{dt} dt \right) = 2 \int_{\infty}^r \left(v_r^2 \frac{dm_{er}}{dr} + m_{er} \frac{dv_r^2}{dr} \right) dr
\end{aligned}$$

There remains now to furnish the effective mass $m_{er} = m_{er}(r)$ so that we can find the speed $v_r = v_r(r)$ as a function of distance by solving the differential equation:

$$2 \int_{\infty}^r \left(v_r^2 \frac{dm_{er}}{dr} + m_{er} \frac{dv_r^2}{dr} \right) dr = G \frac{M_e m_e}{r} \quad (351)$$

We use again the notation of capital M for the “gravitating” mass and lower case m for the “falling” mass. Strictly speaking, both spheres are gravitating and falling relative to each other as we use the variable distance r in the equations. For the function of $m_{er}(r)$, we can use the variation of effective mass computed in Section 16. The corresponding tables provide the variation of mass in numerical form. The graphs show the mass loss, which deducted from the “lone” mass m_e can also provide the required mass here. We draw attention again to the behavior of mass loss and the associated asymptotic line. The correct approach should be to apply the numerical outcomes on mass calculation using the computational methods in the Appendix for solving the above differential equation. We are not equipped to do that at present, but we can apply the asymptotic analytical function in an attempt to estimate at least the order of magnitude of the ensuing falling speed. Thus, from the general Eq. 206 for mass and Eq. 215 for the asymptotic line, we write again here:

$$\begin{aligned}
m_{erloss} &= \frac{g_0}{4\pi^2 G} S_{F0} \\
S_{F0} &\equiv \frac{\pi A_1 \pi A_2}{r^2} = \frac{\pi^2 A_{R_1} A_{R_2} R_1^2 R_2^2}{r^2} \\
m_{erloss} &= \frac{g_0}{4\pi^2 G} \frac{\pi^2 A_{R_1} A_{R_2} R_1^2 R_2^2}{r^2} = \frac{g_0}{4G} \frac{A_{R_1} A_{R_2} R_1^2 R_2^2}{r^2} \equiv \frac{d}{r^2}
\end{aligned} \quad (352)$$

where

$$d = \frac{g_0}{4G} A_R A_{R_2} R^2 R_2^2 = \frac{\Lambda G M_e m_e}{4\pi G} = \frac{G M_e m_e}{4g_0}$$

We reintroduce the notation R_2 for the “gravitating” sphere radius but retain the plain notation R for the “falling” sphere radius. The required effective mass of the falling sphere is the difference of the loss mass from the effective lone mass:

$$m_{er} = m_e - m_{erloss} \quad (353)$$

from which the derivative with respect to distance is

$$\frac{dm_{er}}{dr} = \frac{2d}{r^3}$$

We use the above to re-write the differential equation in a form ready for integration and find the unknown speed squared as $y \equiv v_r^2 = v_r^2(r)$. We proceed in obvious steps with comments as needed:

$$\begin{aligned}
\int_{\infty}^r \left(4v_r^2 \frac{d}{r^3} + \left(m_e - \frac{d}{r^2} \right) \frac{dv_r^2}{dr} \right) dr &= G \frac{M_e m_e}{r} \\
\int_{\infty}^r \left(4y \frac{d}{r^3} + \left(m_e - \frac{d}{r^2} \right) \frac{dy}{dr} \right) dr &= \frac{G M_e m_e}{r}
\end{aligned}$$

We divide both members of the equation by d :

$$\int_{\infty}^r \left(\left(\frac{m_e}{d} - \frac{1}{r^2} \right) \frac{dy}{dr} + 4 \frac{y}{r^3} \right) dr = \frac{4g_0}{r} \quad (354)$$

whereby it is important to note that the falling mass m_e is entirely eliminated from the equation:

$$\int_{\infty}^r \left(\left(b - \frac{1}{r^2} \right) \frac{dy}{dr} + 4 \frac{y}{r^3} \right) dr = \frac{a}{r}$$

where

$$b = \frac{4g_0}{GM_e} \quad a = 4g_0$$

By differentiating, we need to solve the equation of the form:

$$\left(b - \frac{1}{r^2} \right) y' + 4 \frac{y}{r^3} = - \frac{a}{r^2} \quad (355)$$

The solution for y is readily found to be:

$$y = \frac{\int -\frac{ae}{br^2-1} \frac{r^{\frac{4}{r(br^2-1)}} dr}{e^{\int \frac{4}{r(br^2-1)} dr}} \quad (356)$$

$$\int_{\infty}^r \frac{4}{r(br^2-1)} dr = 2 \ln \frac{br^2-1}{br^2} \quad (357)$$

$$y = \frac{\int \frac{-a \exp\left(2 \ln \frac{br^2-1}{br^2}\right)}{br^2-1}}{\exp\left(2 \ln \frac{br^2-1}{br^2}\right)} = \frac{\int -a \frac{br^2-1}{b^2 r^4}}{\left(\frac{br^2-1}{br^2}\right)^2} = \frac{a(3br^2-1)}{3b^2 r^3} = \frac{a(3br^2-1)}{3b^2 r^3} \frac{b^2 r^4}{(br^2-1)^2}$$

$$y = \frac{a(3br^2-1)r}{3(br^2-1)^2} \quad (358)$$

Reverting to the original parameters and denoting the obtained PG speed from static mass at r by v_{rPGs} with $y = v_r^2 \equiv v_{rPGs}^2$, we finally obtain:

$$v_{rPGs}^2 = \frac{4g_0 \left(\frac{12g_0}{GM_e} r^2 - 1 \right) r}{3 \left(\frac{4g_0}{GM_e} r^2 - 1 \right)^2} = \frac{4g_0 \left(\frac{12}{A_{R_2}} \frac{r^2}{R_2^2} - 1 \right) r}{3 \left(\frac{4}{A_{R_2}} \frac{r^2}{R_2^2} - 1 \right)^2} \quad (359)$$

We can immediately see that the above formula reduces to the familiar Newtonian $v_{rN}^2 \rightarrow GM_e/r$ when $r^2 \gg \frac{GM_e}{4g_0}$, or $\frac{r}{R_2} \gg \frac{\sqrt{A_{R_2}}}{2}$, or when $A_{R_2} \rightarrow 0$, in other words when we approach closely to the Newtonian regime. Beyond Newton, we arrive at a different speed, which, however, is the same for all falling bodies. The latter appears to be consistent with prevailing experience and conventional physics, namely, that all bodies fall with the same speed. However, according to the findings in Section 16.3, the falling body parameters should not be eliminated from our differential equation above, because they are ever present albeit imperceptibly in the first place. It is only because we used the linear asymptotic equation of mass loss when the falling mass was eliminated in step of Eq. 354. After all, by way of symmetry, we should have the absorptivity of both spheres involved, not only one as provided by the above equation. Then, the speed should be a function of the properties of the falling body, which presumably has escaped our experiments to date, because of its extremely small effect within the framework of our experiments. However, this can become important in long space travel between planets whereby even the smallest deviation from Newtonian mechanics would appear as an anomaly, such as those anomalies already on record.

For the present purposes, we can use the above derived equation of speed to see at least the magnitude of deviation from Newton. We do so later in tables and figures together with the outcomes of the next section including the kinetic mass.

23.2.2 Speed from composite mass variation

Here, we investigate the possibility of the falling spherical mass being dependent on both distance and speed. That is, we follow the corresponding steps as previously by using the composite mass function $m_{erc}(r, v_r)$ by including the kinetic mass component generated by the speed at each distance r , namely:

$$m_{erc} = m_{erc}(r, v_r) = m_{er}(r) + m_{er\kappa}(v_r) = m_e - m_{eloss} + \frac{g_0 R^2}{G} \frac{v_r^2}{c^2} \quad (360)$$

where we initially use Eq. 310 between speed-mass. We now arrive at a new differential equation to solve by proceeding in the same way as before. To make it more general, we can replace the starting falling point from infinity to a finite initial distance r_1 and follow the same steps without or little further comment below:

$$\begin{aligned} E_{kinetic} &= \int_{r_1}^r F dr = 2 \int_{r_1}^r \frac{dp}{dt} dr = 2 \int_{r_1}^r \frac{d(m_{erc} v_r)}{dt} v_r dt = 2 \int_{r_1}^r v_r d(m_{erc} v_r) dr \\ &= 2 \int_{r_1}^r \left(v_r \frac{dm_{erc}}{dt} + m_{erc} \frac{dv_r}{dt} \right) v_r dt = \int_{r_1}^r \left(2v_r^2 \left(\frac{\partial m_{erc}}{\partial r} + \frac{\partial m_{erc}}{\partial v_r} \right) + m_{erc} \frac{dv_r^2}{dr} \right) dr \end{aligned} \quad (361)$$

$$\begin{aligned} E_{kinetic} &= \int_{r_1}^r \left(2v^2 \left(\frac{d}{r^3} + \frac{g_0 R^2}{c^2 G} \frac{dv_r^2}{dr} \right) + \left(m_e - \frac{d}{r^2} + \frac{g_0 R^2}{G c^2} v_r^2 \right) \frac{dv_r^2}{dr} \right) dr \\ &\equiv \int_{r_1}^r \left(2y \left(\frac{d}{r^3} + \frac{g_0 R^2}{c^2 G} y' \right) + \left(m_e - \frac{d}{r^2} + \frac{g_0 R^2}{G c^2} y \right) y' \right) dr \\ &= \int_{r_1}^r \left(2y \frac{d}{r^3} + 2y \frac{g_0 R^2}{c^2 G} y' + \left(m_e - \frac{d}{r^2} + \frac{g_0 R^2}{G c^2} y \right) y' \right) dr \\ &= \int_{r_1}^r \left(\left(m_e - \frac{d}{r^2} + \frac{g_0 R^2}{G c^2} y + 2y \frac{g_0 R^2}{c^2 G} \right) y' + 2y \frac{d}{r^3} \right) dr \\ &= \int_{r_1}^r \left(\left(m_e - \frac{d}{r^2} + 3 \frac{g_0 R^2}{G c^2} y \right) y' + 2y \frac{d}{r^3} \right) dr \\ &= \int_{r_1}^r \left(\left(m_e - \frac{d}{r^2} + 3 \frac{g_0 R^2}{G c^2} y \right) y' + 2y \frac{d}{r^3} \right) dr = GM_e m_e \left(\frac{1}{r} - \frac{1}{r_1} \right) \\ &\int_{r_1}^r \left(\left(\frac{m_e}{d} - \frac{1}{r^2} + 3 \frac{g_0 R^2}{d G c^2} y \right) y' + 2y \frac{1}{r^3} \right) dr = \frac{GM_e m_e}{d} \left(\frac{1}{r} - \frac{1}{r_1} \right) = 4g_0 \left(\frac{1}{r} - \frac{1}{r_1} \right) \end{aligned} \quad (362)$$

$$\int_{r_1}^r \left(\left(\frac{4g_0}{GM_e} - \frac{1}{r^2} + 3 \frac{g_0 R^2}{d G c^2} y \right) y' + 2y \frac{1}{r^3} \right) dr = 4g_0 \left(\frac{1}{r} - \frac{1}{r_1} \right)$$

where we have use the replacements

$$a = 4g_0, \quad b = \frac{4g_0}{GM_e} = \frac{4}{A_{R_2} R_2^2}, \quad d = \frac{GM_e m_e}{4g_0} = \frac{M_e A_R R^2}{4}, \quad h = \frac{4g_0^2 R^2}{G^2 M_e m_e c^2}$$

and simplify the form of the equation as:

$$\int_{r_1}^r \left(\left(b - \frac{1}{r^2} + 3hy \right) y' + y \frac{2}{r^3} \right) dr = a \left(\frac{1}{r} - \frac{1}{r_1} \right) \quad (363)$$

By differentiating, we arrive at the differential equation:

$$\left(b - \frac{1}{r^2} + 3hy \right) y' + y \frac{2}{r^3} = -\frac{a}{r^2} \quad (364)$$

The solution of this equation is again readily available and given by:

$$y = \frac{-b + \frac{\sqrt{c_1 hr^4 + 6ahr^3 + b^2 r^4 - 2br^2 + 1} + 1}{x^2}}{3h}$$

where the integration constant c_1 is determined by the speed at r_1 . To simplify the present investigation, let us start with zero speed at r_1 getting the equation:

$$y = \frac{-b + \frac{\sqrt{c_1 hr_1^4 + 6ahr_1^3 + b^2 r_1^4 - 2br_1^2 + 1} + 1}{r_1^2}}{3h} = 0$$

from where we obtain the constant:

$$c_1 = -\frac{6a}{r_1}$$

By substituting and restoring our parameters from the interim substitutions, we finally obtain for the falling PG speed v_{rPGc} from composite mass at r over the gravion speed c squared, the formula:

$$\boxed{\frac{v_{rPGc}^2}{c^2} = -\frac{A_R}{3} + \sqrt{\frac{A_R^2}{9} + \frac{2g_0 A_R A_{R_2} R_2^2}{3c^2} \left(\frac{1}{r} - \frac{1}{r_1}\right) - \frac{A_{R_2} A_R^2 R_2^2}{18 r^2} + \left(\frac{A_{R_2} A_R R_2^2}{12 r^2}\right)^2} + \frac{A_{R_2} A_R R_2^2}{12 r^2}} \quad (365)$$

where A_{R_2} and A_R are the absorptivities for the gravitating and falling spheres accordingly given by the familiar general equation:

$$A_R = \frac{Gm_e}{g_0 R^2} \quad (366)$$

For speed notations see also a summary in Table 27. We discuss the above results next. It should also be noted that we use the words “speed” and “velocity” interchangeably in this work, while in other languages these words have only one translation (e.g. $\tau\alpha\chi\acute{\upsilon}\tau\eta\varsigma$ = tachytes or tachytis in Greek, re tachyon, etc.)

This work remains incomplete: The exact solutions to the differential equations involved require resources beyond those available to this author at present, but other workers are encouraged to make a contribution in this direction, if to move forward faster. We only attempt to introduce some dynamics in PG, i.e. new physics, which constitutes an opportunity for mathematicians to make a new contribution. We have grouped various situations by way of several “CASES” with regard only to two interacting spherical bodies, but the problem is greatly complicated in a multi-body problem like the solar system. We need devoted mathematics and software engineering to properly address a new and evolving chapter of physics, a task clearly beyond the means available to this author.

23.2.3 Speed investigation

The speed formula 359 based only on positional variation of effective mass but not on the speed itself would not be consistent with accrual of mass proposed during rocket acceleration, with an upper speed limit; that is, any kinetic mass, if present, would be inertia-less. The second speed formula 365 is consistent with a composite effective mass and would be closer to a true representation of reality, if the conjectural Eq. 313 between speed and absorptivity (or mass) were to be true; that is, the kinetic mass may be treated like effective mass acted upon by a force.

On the above basis, we can now see the effects of revised falling speeds for all CASES_1_2&_3. It is instructive to find the deviation from Newtonian mechanics, the falling speed for which we denote by v_{rN} . We do this by plotting the ratio of speeds squared v_{rPGs}^2/v_{rN}^2 and v_{rPGc}^2/v_{rN}^2 in Fig. 50. The effect is to obtain a higher PG speed than Newton, which quickly diminishes as the distance increases. The departure from Newton follows the same trend as in previous comparisons with other parameters (e.g. for the force per Fig. 23). We can better understand these results by examining also the numerical values of kinetic and composite masses for all three cases next.

Tables 29, 30 and 31 provide a comparison of kinetic masses corresponding to (or generated by) Newtonian, static and composite speeds; the Newtonian kinetic mass is copied from previous tables for convenience of comparison. We note that all kinetic masses have same order of magnitude or very close values, with the greatest deviation for CASE_2. The difference does not affect the main points of discussion based on

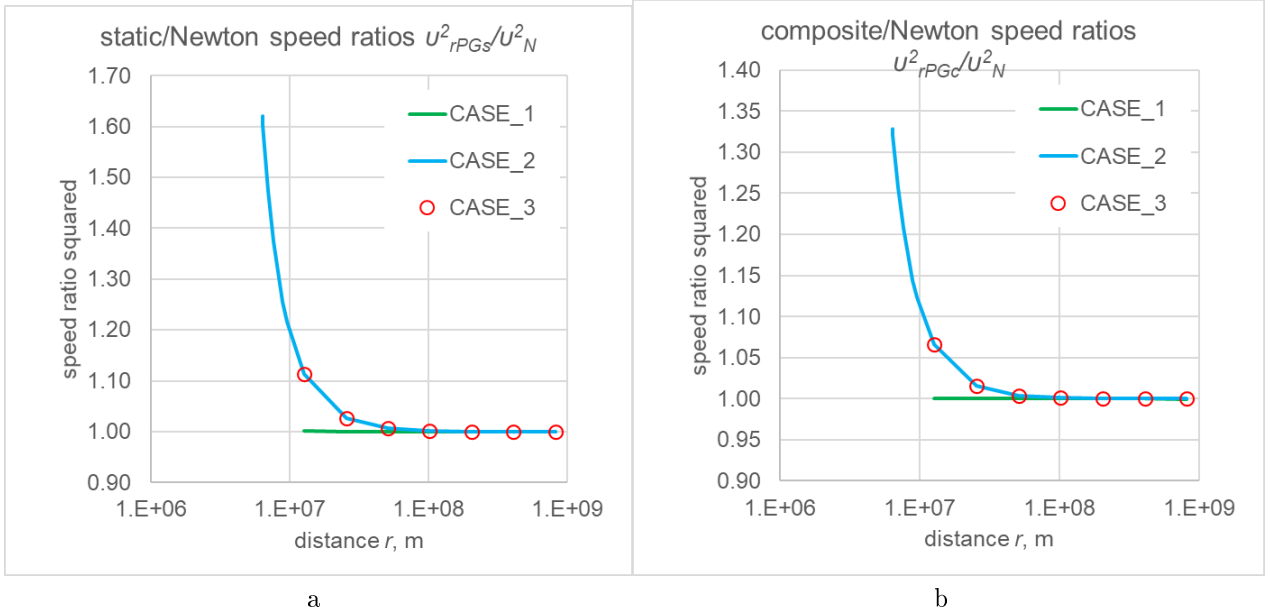


Figure 50: Ratio of speeds_squared against distance in (a) using static mass and (b) using composite mass for CASES_1, 2&3.

r, m	$m_{er\kappa}$ kg, with v_{rN}	$m_{er\kappa}$, kg with v_{rPGs}	$m_{er\kappa}$, kg with v_{rPGc}	v_{rPGs}^2/v_{rN}^2	v_{rPGc}^2/v_{rN}^2
12742000	1.5735021E+16	1.5751131E+16	1.5744680E+16	1.001024	1.000614
25484000	7.8675107E+15	7.8695231E+15	7.8687168E+15	1.000256	1.000153
50968000	3.9337553E+15	3.9340068E+15	3.9339059E+15	1.000064	1.000038
101936000	1.9668777E+15	1.9669091E+15	1.9668964E+15	1.000016	1.000010
203872000	9.8343883E+14	9.8344276E+14	9.8344117E+14	1.000004	1.000002
407744000	4.9171942E+14	4.9171991E+14	4.9171971E+14	1.000001	1.000001
815488000	2.4585971E+14	2.4585977E+14	2.4585974E+14	1.000000	1.000000
∞	0	0	0	1	1

Table 29: Dependence of kinetic mass and speed ratio_squared on distance per prior CASE_1 and comparison using Newtonian speed v_{rN} , static speed v_{rPGs} and composite speed v_{rPGc}

Newtonian speed. The corresponding speed ratios squared are also given in the last two columns noting a monotonic decrease close to unity at long enough distance; the distance in meters is given in multiples of Earth radii doubling with each point.

Similarly, the corresponding composite masses are provided in Tables 32, 33 and 34. We can verify again the similar values with the greatest effect resulting in CASE_2, all of which also do not affect the preceding discussion.

We have the same conclusion for the added CASE_7, namely, there is no visible difference for the kinetic and composite real mass loss between applying Newtonian or PG composite speed according to Fig. 51a. However, this does not apply for CASE_4 according to Fig. 51b, which is further investigated with more specific examples below.

Therefore, there is no need to redraw the graphs obtained for the cases in the previous section using Newtonian speed, or revise the ensuing findings and considerations. One remaining correction would arise from replacing the asymptotic function of Eq. 352 used above with the actual falling static effective mass m_{er} resulting by the computational means applied in Section 16 or by an analytical function, if it exists; additionally, a correction may be required by a modified relationship between absorptivity and mass (analytical, if it exists, or otherwise) in lieu of the conjectured equation. Still, we expect only second order difference on top of the previous one for the given cases. Therefore, the opening presentation of this Section 23.2 need not be altered only because it was based on Newtonian speeds. However, there would be a practical difference of the preceding analysis by way of a cumulative effect on the speed over a long trajectory between planets or between a planet and spacecraft. This is an important difference that is examined in the following Section.

Now, CASE_4 represents a family of objects from our immediate experience, as opposed to very massive, large or dense bodies lying beyond the ordinary range of perception. We have already seen the different

r , m	$m_{er\kappa}$ kg, with v_{rN}	$m_{er\kappa}$, kg with v_{rPGs}	$m_{er\kappa}$, kg with v_{rPGc}	v_{rPGs}^2/v_{rN}^2	v_{rPGc}^2/v_{rN}^2
6371002.0	1.0515014E+10	1.7037378E+10	1.3973175E+10	1.620291E+00	1.328878
6371063.7	1.0514912E+10	1.7037026E+10	1.3972951E+10	1.620273E+00	1.328870
6371637.1	1.0513966E+10	1.7033751E+10	1.3970866E+10	1.620107E+00	1.328791
6377371.0	1.0504513E+10	1.7001085E+10	1.3950061E+10	1.618455E+00	1.328006
6434710.0	1.0410908E+10	1.6681671E+10	1.3745758E+10	1.602326E+00	1.320323
7008100.0	9.5591065E+09	1.4077247E+10	1.2016979E+10	1.472653E+00	1.257124
7645200.0	8.7625143E+09	1.2045208E+10	1.0581013E+10	1.374629E+00	1.207532
8919400.0	7.5107265E+09	9.4244672E+09	8.5961329E+09	1.254801E+00	1.144514
9556500.0	7.0100114E+09	8.5254105E+09	7.8763469E+09	1.216176E+00	1.123585
12742000.0	5.2575086E+09	5.8506967E+09	5.6042391E+09	1.112827E+00	1.065950
25484000.0	2.6287543E+09	2.6980243E+09	2.6700494E+09	1.026351E+00	1.015709
50968000.0	1.3143771E+09	1.3228948E+09	1.3194781E+09	1.006480E+00	1.003881
101936000.0	6.5718857E+08	6.5824895E+08	6.5782412E+08	1.001614E+00	1.000967
203872000.0	3.2859429E+08	3.2872670E+08	3.2867362E+08	1.000403E+00	1.000241
407744000.0	1.6429714E+08	1.6431369E+08	1.6430704E+08	1.000101E+00	1.000060
815488000.0	8.2148572E+07	8.2150640E+07	8.2149806E+07	1.000025E+00	1.000015
∞	0	0	0	1	1

Table 30: Dependence of kinetic mass and speed ratio_squared on distance per prior CASE_2 and comparison using Newtonian speed v_{rN} , static speed v_{rPGs} and composite speed v_{rPGc}

r , m	$m_{er\kappa}$ kg, with v_{rN}	$m_{er\kappa}$, kg with v_{rPGs}	$m_{er\kappa}$, kg with v_{rPGc}	v_{rPGs}^2/v_{rN}^2	v_{rPGc}^2/v_{rN}^2
12742000	5.2575086E+21	5.8506967E+21	5.6042391E+21	1.112827	1.065950
25484000	2.6287543E+21	2.6980243E+21	2.6700494E+21	1.026351	1.015709
50968000	1.3143771E+21	1.3228948E+21	1.3194781E+21	1.006480	1.003881
101936000	6.5718857E+20	6.5824895E+20	6.5782412E+20	1.001614	1.000967
203872000	3.2859429E+20	3.2872670E+20	3.2867362E+20	1.000403	1.000241
407744000	1.6429714E+20	1.6431369E+20	1.6430704E+20	1.000101	1.000060
815488000	8.2148572E+19	8.2150640E+19	8.2149806E+19	1.000025	1.000015
∞	0	0	0	1	1

Table 31: Dependence of kinetic mass and speed ratio_squared on distance per prior CASE_3 and comparison using Newtonian speed v_{rN} , static speed v_{rPGs} and composite speed v_{rPGc}

r , m	m_{erc} kg, with v_{rN}	m_{erc} , kg with v_{rPGs}	m_{erc} , kg with v_{rPGc}
12742000	7.34288394267474E+22	7.34288394428572E+22	7.34288394364059E+22
25484000	7.34652770181904E+22	7.34652770202028E+22	7.34652770193965E+22
50968000	7.34738756500709E+22	7.34738756503224E+22	7.34738756502215E+22
101936000	7.34759966340501E+22	7.34759966340816E+22	7.34759966340689E+22
203872000	7.34765247337708E+22	7.34765247337747E+22	7.34765247337731E+22
407744000	7.34766564250449E+22	7.34766564250454E+22	7.34766564250452E+22
815488000	7.34766892244818E+22	7.34766892244818E+22	7.34766892244818E+22
∞	7.34767000000000E+22	7.34767000000000E+22	7.34767000000000E+22

Table 32: Dependence of composite mass on distance per prior CASE_1 and comparison using constant Newtonian speed v_{rN} , static speed v_{rPGs} and composite speed v_{rPGc}

r , m	m_{erc} kg, with v_{rN}	m_{erc} , kg with v_{rPGs}	m_{erc} , kg with v_{rPGc}
6371002.0	7.94147138242287E+14	7.94153660606427E+14	7.94150596403506E+14
6371063.7	7.94488228598695E+14	7.94494750712234E+14	7.94491686637396E+14
6371637.1	7.96583043838863E+14	7.96589563624548E+14	7.96586500739456E+14
6377371.0	8.08703233104536E+14	8.08709729676536E+14	8.08706678652915E+14
6434710.0	8.64879251436736E+14	8.64885522199615E+14	8.64882586286389E+14
7008100.0	1.05761101120192E+15	1.05761552934288E+15	1.05761346907430E+15
7645200.0	1.15618076737692E+15	1.15618405007037E+15	1.15618258587526E+15
8919400.0	1.26341138212519E+15	1.26341329586583E+15	1.26341246753153E+15
9556500.0	1.29668049750239E+15	1.29668201290149E+15	1.29668136383782E+15
12742000.0	1.38505541527468E+15	1.38505600846280E+15	1.38505576200522E+15
25484000.0	1.46004099803422E+15	1.46004106730425E+15	1.46004103932934E+15
50968000.0	1.47759306210703E+15	1.47759307062470E+15	1.47759306720794E+15
101936000.0	1.48191568110883E+15	1.48191568216921E+15	1.48191568174437E+15
203872000.0	1.48299223039647E+15	1.48299223052888E+15	1.48299223047580E+15
407744000.0	1.48326104136967E+15	1.48326104138622E+15	1.48326104137957E+15
815488000.0	1.48332818800946E+15	1.48332818801152E+15	1.48332818801069E+15
∞	1.48335051422818E+15	1.48335051422818E+15	1.48335051422818E+15

Table 33: Dependence of composite mass on distance per prior CASE_2 and comparison using constant Newtonian speed v_{rN} , static speed v_{rPGs} and composite speed v_{rPGc}

r , m	m_{erc} kg, with v_{rN}	m_{erc} , kg with v_{rPGs}	m_{erc} , kg with v_{rPGc}
12742000	1.38483965472048E+27	1.38484024790860E+27	1.38484000145102E+27
25484000	1.46003136003934E+27	1.46003142930937E+27	1.46003140133446E+27
50968000	1.47759250212494E+27	1.47759251064261E+27	1.47759250722585E+27
101936000	1.48191564673190E+27	1.48191564779228E+27	1.48191564736744E+27
203872000	1.48299222827079E+27	1.48299222840320E+27	1.48299222835012E+27
407744000	1.48326104123612E+27	1.48326104125267E+27	1.48326104124602E+27
815488000	1.48332818800111E+27	1.48332818800317E+27	1.48332818800234E+27
∞	1.48335051422818E+27	1.48335051422818E+27	1.48335051422818E+27

Table 34: Dependence of composite mass on distance per prior CASE_3 and comparison using constant Newtonian speed v_{rN} , static speed v_{rPGs} and composite speed v_{rPGc}

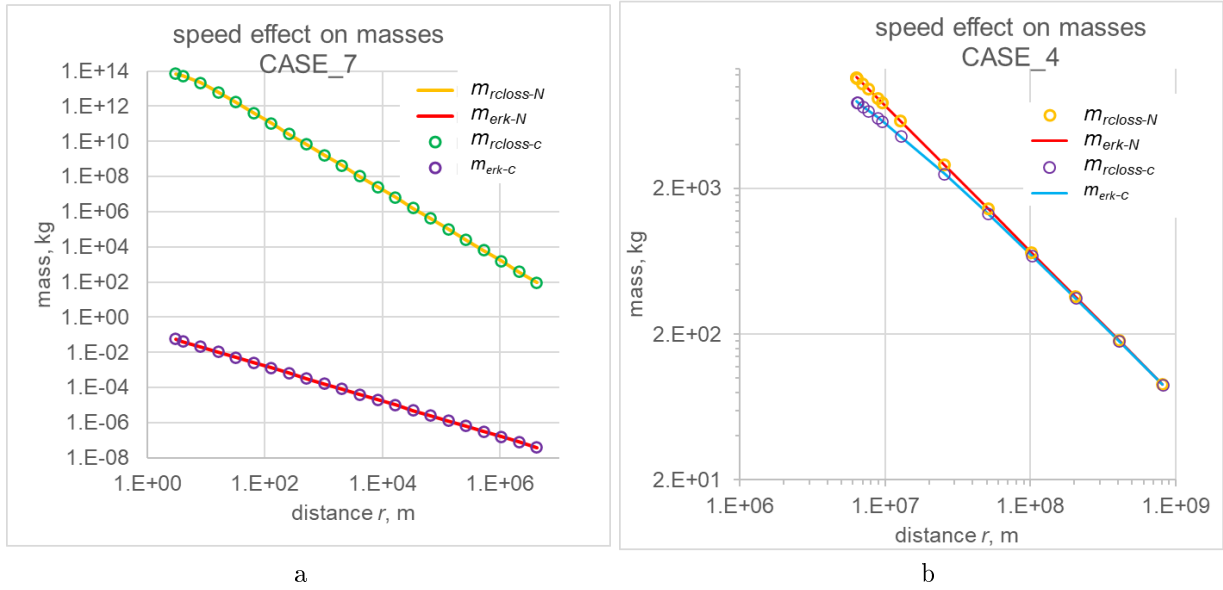


Figure 51: Speed effect on real mass loss and kinetic mass by applying Newtonian and composite speeds in (a) for CASE_7 and in (b) for CASE_4

behavior of the associated masses in Table 28 and Figs. 48 and 49 drawn according to Section 16.3. We can use cases like this to further investigate the equations of falling speed and see if they are consistent with surrounding experience. Actually, current experience dictates that our predictions should be untenable, because “*all bodies fall with equal speed*”, unless our predictions fall within the experimental errors prevailing to date.

Both equations involve the distance r and the unknown limiting acceleration g_0 . We do a preliminary examination of the behavior of the second Eq. 365, whereby we do have a variation of speed due to the absorptivity A_R of the falling body. The numerical results in Table 35 indicate that the effect of parameter g_0 seems to be minor: We note a very small variation of the ratio v_{rPGc}/v_{rN} in a wide range of absorptivity over many orders of magnitude and over a wide range of the limiting acceleration (g_0) at a fixed final distance from Earth, namely, at $r = 2R_2 = 12742000$ m. However, the absorptivity A_R of the falling body is decisive in the determination of the final speed. In a range of $A_R > 1.0E - 08$, the PG speed is very close to Newtonian speed with a ratio either a little below or a little above unity. This behavior is consistent with the outcomes from various cases: The kinetic mass adds very little in all those cases except CASE_4, where the kinetic mass overtakes the positional net loss of mass; this happens when A_R is very small.

Equivalently, we next plot the same speed ratios v_{rPGc}/v_{rN} against absorptivity for a set of final distances starting from infinity in Fig. 52(a). We note that all curves shift closer to Newton speed at long final distance. This is again important indicating that Newtonian mechanics can be applied at long enough distance from planets in interplanetary travel, but a modification becomes due as we approach a planet. The same effect is re-plotted in (b) of the same figure showing the variation of speed ratio against distance at selected absorptivities. While all graphs start from greater than unity ratios at long enough distance, they invariably undershoot unity at shorter distance. The deviation is quite large raising concern about the veracity of such outcomes.

The above are generalizations of situations similar to CASE_4. We get a better feel also by choosing for comparison two different materials of beryllium (Be) and lead (Pb) with diameters even smaller than 1 m. A similar deviation can be seen if we plot the same speed ratio against the radius of the falling sphere per Fig. 53a, since radius and absorptivity are interdependent. Corresponding to this, we further plot the absolute speed of these spheres in a smaller (more practical) range of radii in 53b.

We don't have data of falling bodies from “infinity” to compare with the numerical values between “experiment” and our findings and see if these outcomes are correct or even reasonable. However, we have applied Eq. 365 for sets of falling spheres from a height of 10 m on the surface of Earth at a guessed $g_0 = 40000$ ms^{-2} . We used the example of Be and Pb materials with sphere diameters 0.001 m, 0.01 m and 0.1 m. The time difference $\Delta t = t_{Be} - t_{Pb}$ is found to be 0.017394 s, 0.001782 s and 0.000179 s correspondingly. These values clearly fall within the detectable time range and cannot be accepted. However, while these values are no good, they are not “catastrophic” either, in the sense that their discrepancy can be manageable. The numerical values plotted are no reason to reject or abandon the preceding theory, because they can

$r = 12742000 \text{ m}$				
$g_0 =$	1000	10000	50000	100000
A_R	v_{rPGc}/v_{rN}	v_{rPGc}/v_{rN}	v_{rPGc}/v_{rN}	v_{rPGc}/v_{rN}
1.0E-13	0.117236	0.117236	0.117236	0.117236
1.0E-12	0.206925	0.206924	0.206924	0.206924
1.0E-11	0.359383	0.359376	0.359375	0.359375
1.0E-10	0.593533	0.593498	0.593495	0.593495
1.0E-09	0.851810	0.851676	0.851664	0.851662
1.0E-08	0.976295	0.976050	0.976028	0.976026
1.0E-07	0.997716	0.997443	0.997419	0.997416
1.0E-06	1.000046	0.999770	0.999745	0.999742
1.0E-05	1.000281	1.000005	0.999980	0.999977
1.0E-04	1.000304	1.000028	1.000004	1.000000
1.0E-03	1.000307	1.000030	1.000006	1.000003
1.0E-02	1.000307	1.000031	1.000006	1.000003
1.0E-01	1.000307	1.000031	1.000006	1.000003

Table 35: Speed ratios against absorptivity at selected values of g_0 using Earth as the gravitating body with a falling sphere from “infinite” distance to a perigee of $r = 12742000 \text{ m}$

be explained by the assumptions from which the equations were deduced. The equation of speed based on positional variation of mass (static speed) always yields ratio values above unity. The transition to below unity values by the equation for the composite speed is due to the accrual of mass in excess of the positional loss. We used the conventional equation between kinetic and potential energy, so that for any fixed potential energy between two points, an increase of mass would result in a reduction of the end speed. The increase of mass by use of 365 is determined by the applied conjecture of Eq. 310, but the increase of mass would be a lot less if we had used Eq. 311 with $n = 4$ as seen by Fig. 45. In the latter case, the composite speed would be considerably higher and closer but always below the static speed. There is an interplay between the two speeds, which we hope it to be such that to bring the theory in agreement with reality. The problem would still be that the effects would remain undetectable for falling bodies from a height of 10 (or similar) meters, but they might become detectable from an interplanetary “height” fall.

There are additional parameters requiring adjustment and determination, such as the true value of g_0 that is to be used in our work. We can see this by plotting the final falling velocity from 10 m height v_{10c-Pb} of the lead sphere, the same v_{10c-Be} of the beryllium sphere and their difference $\Delta v = v_{10c-Pb} - v_{10c-Be}$ against a wide range of g_0 values in Fig. 53c. This is done for the middle radius $R_1 = 0.01\text{m}$, but similar (almost inversely proportional) is the situation for the other radii too. Therefore, there is ample room for adjustment of the theoretical parameters to meet reality. This is an important conclusion confirming an early corollary of Section 14.3 that “*All bodies fall at equal rates... if and only if they have the same contraction factor q* ”, which relates to the same absorptivity. The problem is that the classical experiments of measuring velocity involve bodies all having practically equal absorptivities and thus not measurable by our equipment. If we had a body with an unusually high density for comparison, then we would have detected the difference.

It might also be said that meteors and comets provide data that do not (presumably) support any deviation of speed from that worked out by applying Newtonian mechanics. However, the question here is about their mass, not just speed and trajectory. How do we measure their mass? Is it measured by reliable independent means or is it deduced by applying/relying on the Newtonian laws of motion? How do we know if their effective mass thus deduced is not a composite type of mass as introduced herewith? The question of mass is a key question in modern physics and applies to all moving bodies in astronomy and elsewhere. We have introduced a new conception of mass that can be put to the test by numerous proposals throughout this report. The different kinds of mass in Table 27 might be explained by and correspond to different material structures. We continue with modeling of the electron and positron in a following Section 25 with some interesting possibilities. The role of kinetic mass might be connected with to propulsion of a body to motion with some degree of contribution to the ideas of inertia, action-reaction, etc; i.e., it might have a dual function. It might play a role in offsetting the gravion “drag”. So far, the theory is incomplete pending further development but mainly pending experimental research like the newly proposed next.

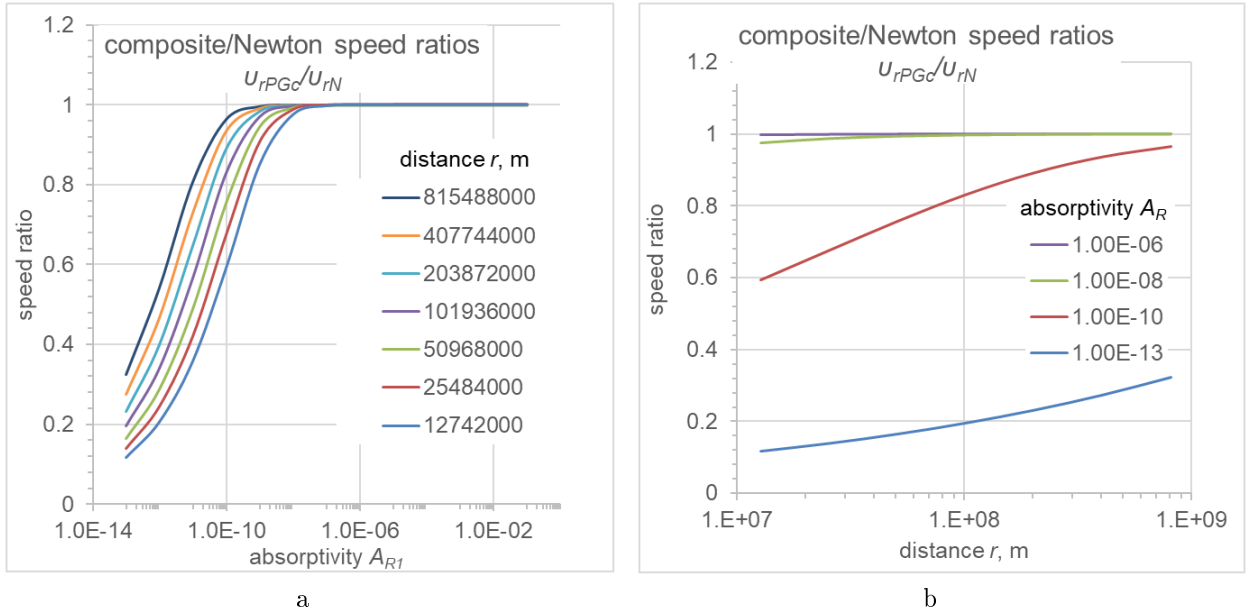


Figure 52: Ratio of speeds (a) against absorptivity at fixed final distances and (b) against distance at fixed absorptivities of the falling body

23.2.4 Interplanetary testing of falling speeds: Effect of shape, direction and contraction factor

The preceding findings lend themselves for another possible verification of PG theory involving tests during interplanetary spacecraft trajectories. A recent “space test of the equivalence principle” (STEP) with orbiting satellite measurements failed to establish any deviation from the Equivalence Principle (Touboul *et al.*, 2019). However, this negative outcome is consistent with our PG theory: We found that the real and effective mass of an orbiting object remains constant for all spherical objects and densities, whereby the associated speed and acceleration should be invariable for all objects. However, we should expect a continuous net variation of mass during fall in an interplanetary trajectory with an associated variation of speed, which can be subjected to the test by an experiment. Even the incomplete solution of Eq. 365 predicts different falling speeds. Also, even if there is no connection between speed and mass, the first Eq. 359 completed with the absorptivity of both bodies in a future correction predicts different speeds with a measurable effect over a long falling trajectory.

In fact, we have found that not only different density bodies fall with different speeds, but different size objects of the same material would also fall at different speeds, because they present different absorptivities (per Fig. 53a&b). We note that the effect of radius may be even greater than the effect of material nature, per (a).

Based on the above finding, we could perform a variety of experiments involving different combinations of body shapes, sizes and materials. Indicatively, we have illustrated some examples in Fig. 54. We show a pair of two equal radius spheres (#3 and #4) of lead and beryllium per preceding analysis, but also added two identical flattened bodies (#1 and #2) with one oriented parallel and the other perpendicular to the direction of fall. The experiment is supposed to take place between two rocket firings for correcting the trajectory, so that the fall is always free of disturbance by rocket force. We should choose this trajectory, if possible, to be the last leg of fall in an inbound trajectory with the longest possible pause of rocket engine activity.

The pair of flat bodies shown could have the shape of disk or any other convenient shape. However, this is a different case than the spherical geometry we have worked with so far. We would need to repeat the same PG computations by replacing the sphere with another desirable shape. One candidate shape is that of an oblate spheroid as depicted in Fig. 54 by #1 and #2. It is not immediately obvious if those two bodies would deviate or not during fall. We might initially think that the first (#1) with its major axis parallel to the direction of acceleration would fall faster, if it is associated with higher absorptivity. However, the subtended angle is smaller than the second body (#2), so that the combination of solid angle and absorptivity might cancel each other out. Both of these identical bodies (#1) and (#2) have equal lone absorptivities very far away from a planet, so that it is not obvious if they would retain equal absorptivities in different direction inside the gravitational field. The variation of static effective mass at different proximity locations from a

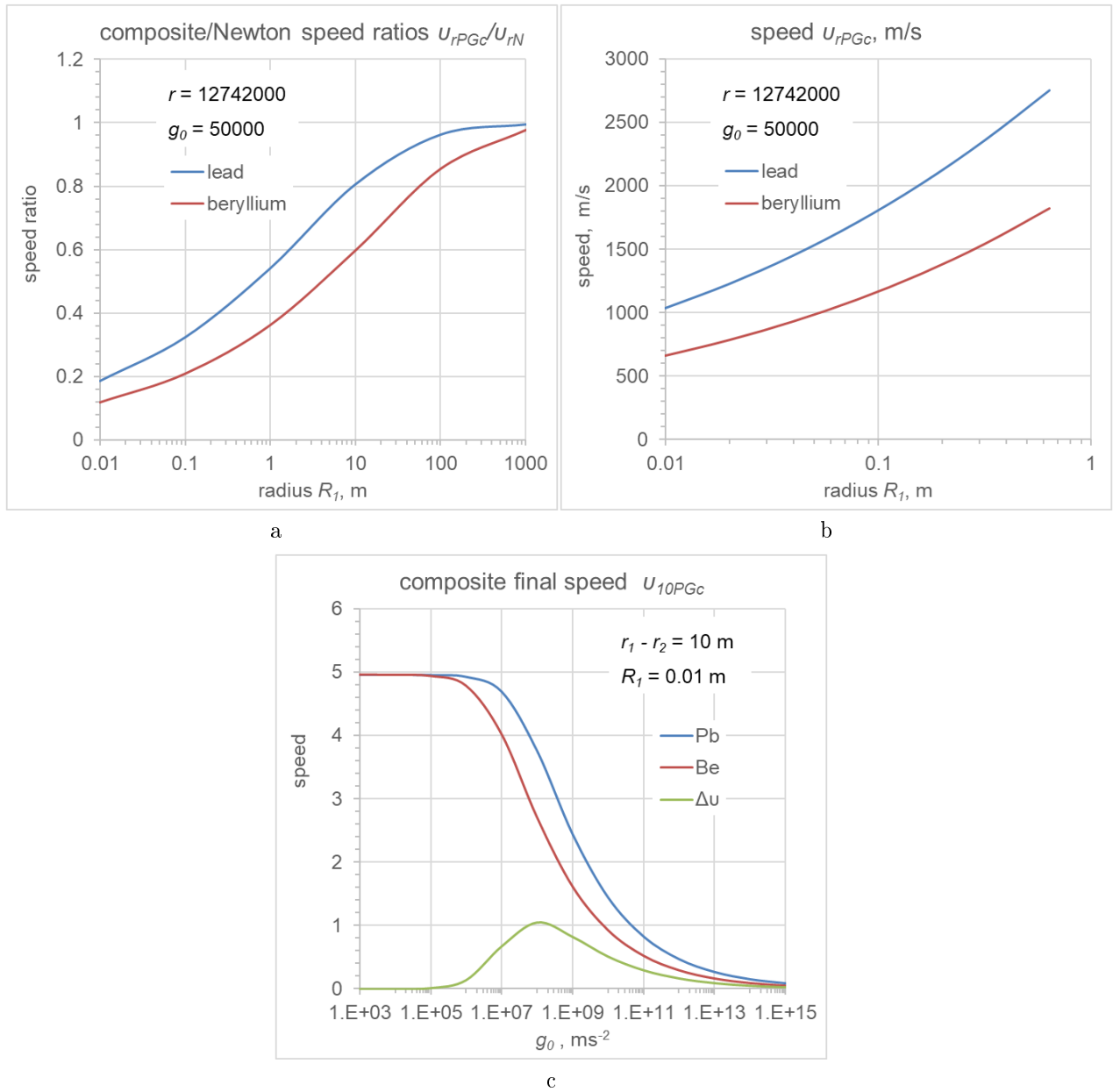


Figure 53: Comparison of final speeds for beryllium (Be) and lead (Pb) spheres falling from infinity to $r = 12742000$ m against falling sphere radius in the form of (a) Speed-ratio u_{rPGc}/u_{rN} and (b) absolute composite speed u_{rPGc} . (c) Final falling speed from 10 m height of beryllium and lead spheres with $R_1 = 0.01$ m together with their difference Δv plotted against universal acceleration g_0 .

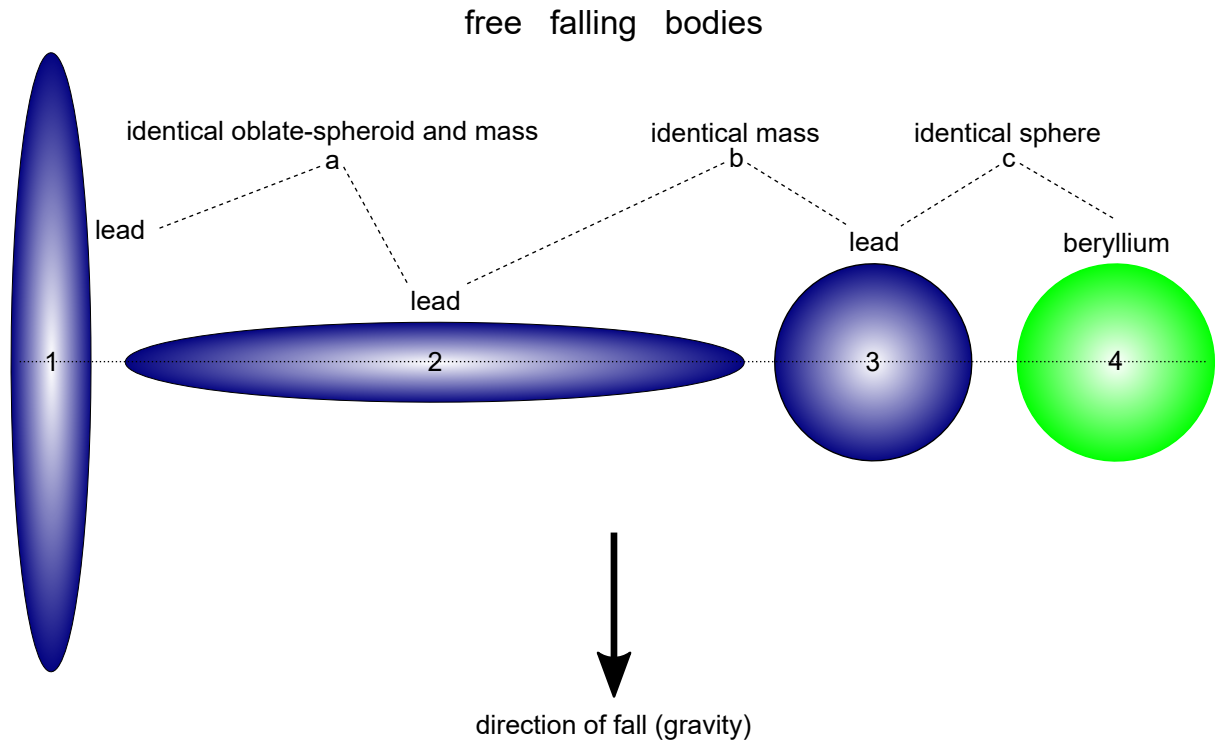


Figure 54: Inter-planetary spacecraft experiment with four (1, 2, 3, 4) free falling bodies in pairs of (a) identical oblate spheroid masses with different orientation, (b) equal masses with different shapes and (c) equal sphere size but different materials.

planet need to be worked out using the methods presented in the Appendices by replacing the spherical geometry with spheroidal one. The non-obviousness of the effect of falling orientation can be appreciated by considering the overall picture of macroscopic and microscopic structure of any given geometry body: Fig. 55 conveys an idea for the case of a “rod” in continuation of the configurations of prior Fig. 31. The shielding (depicted by shading) of the absorption centers is greatly exaggerated for demonstration only of the envisaged effects on absorptivity in the three situations involving the same amount of particles; the dark (gray) shading illustrates the amount of black matter created when the rod moves from infinite distance to a given approach inside the gravitational field of a planet. The effect is shown approximately and grossly exaggerated to demonstrate the change of black mass (and absorptivity) with a change in configuration or rod direction relative to the direction of the surrounding gravitational field. Actually, a single-stranded rod of MACs would have an infinitesimally different absorptivity at different orientation (the solid angle being infinitesimally small), but as we add stands to build a a macroscopic rod, the difference may become measurable. At any rate, the study of relative orientation could be included in the experiment to confirm or disprove in advance theoretical computations.

Judging from the “STEP” experiment, the complexity of practical details involved is appreciated. These details might be the same, simpler or even more complex in the proposed test here. For example, spinning the disks might be an option for maintaining orientation, but it might complicate an as yet unknown effect on the mass-energy relationship during fall. This and other parameters require prior, during, or a post experiment assessment.

The influence of orientation during free fall, if real, would have important theoretical ramifications but may also have important practical applications. We suggested in Section 14.3 that changing the orientation between the inbound and outbound leg of the trajectory during a flyby mission could result in a difference of speed at corresponding points of the two legs. That was based on the assumption that the spacecraft is made to exhibit a greater effective mass in one part of the orbit than in the other, but this remains both theoretically and in practice unproven. Another possibility was to vary the mass configuration by way of an opening or folding fan-like system.

Yet another conceivable mechanism for performing such a test is shown by the collapsible sphere of a toy shown in Fig. 56. The effective mass is greater in the expanded form (a) than in the collapsed form (b). The transformation between the two forms (collapsed and expanded) involves the supply (or release) of some energy commensurable with the associated gravitational field of the toy sphere itself. The amount

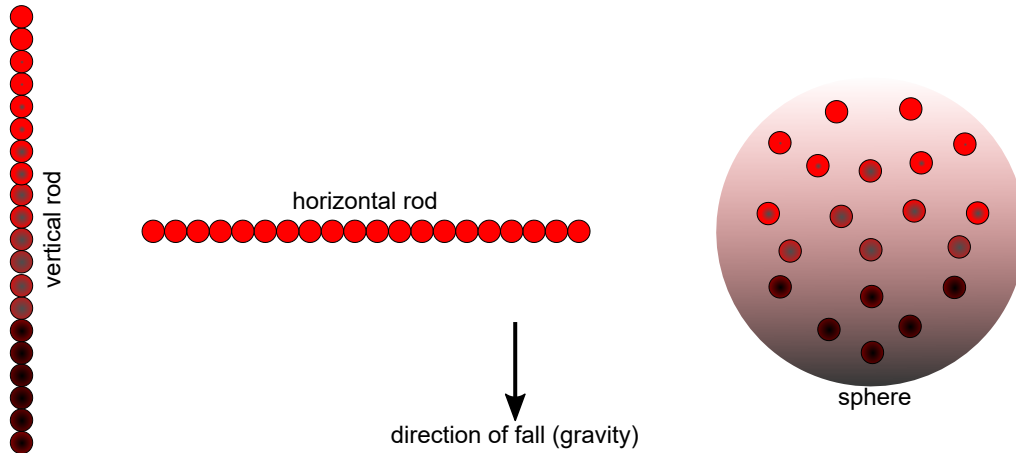


Figure 55: Absorption centers (MACs or particles) fixed in a rod configuration directed along the gravity direction (i.e. vertical), or perpendicular to it (i.e. horizontal); same particles re-distributed in a spherical configuration

of this energy must be extremely minute in comparison with the energy involved during fall of the same toy sphere towards a planet. The preceding findings that the falling speed is a function of absorptivity (or contraction factor) implies that if we can somehow vary the absorptivity during flight, then we should also vary the speed, if we are to preserve the energy of the body. That means that we can brake or accelerate the body accordingly. The effect may be very small if we can vary the absorptivity only by a very small amount, but over a long flight, the cumulative effect should be measurable. Furthermore, *“This would result in incremental accretion of energy until it can reach escape velocity and then repeat the same process around a bigger planet (e.g. Jupiter), or the Sun”*, per early statement of Section 14.3. We understand that if two spheres like that, one expanded and the other collapsed, start together at the apogee, they should both return at the apogee simultaneously, but they would pass around the perigee at different times: The contracted one would pass before the expanded one, but then the faster one would decelerate faster during the outbound leg so that the expanded one will catch up and arrive at the same time at the apogee. Now, if we consider one only sphere to start in the expanded configuration at the apogee all the way to the perigee, whereupon it contracts, it should reach and surpass the apogee where it started from. This is because it would have a lesser potential energy than it started with, so that it can continue the “ascend” to a new apogee before it starts a new descend. However, around the new apogee, it could expand again to increase its effective mass. This will be done at the cost of only a practically negligible energy. Doing so is like “inhaling” mass via graviton absorption, which results in an increased potential energy at the new apogee at negligible cost.

We can build on the preceding description as with reference to Fig. 57. We initially spend energy to establish an elliptical orbit, say around Earth, by a spacecraft equipped with a mechanism to vary its absorptivity in a manner analogous to the toy sphere. The initial (innermost) elliptical orbit (in red) is established in the expanded configuration at the cost of given rocket energy. Then we can initiate and repeat a series of the previously described sequence of maneuvers: At the perigee, it collapses and travels all the way to a new greater apogee, whereupon it expands again to travel to the perigee, whereupon it collapses, and so on. This is repeated a number of times, resulting in a cascade gain of apogee distance. We have likened the actions at the apogee and perigee to “inhaling” and “exhaling” mass, in and out. We have suggested it to be an equivalent process taking place like with a heat pump, whereby an electrical motor pumps heat (energy) “out of thin air” at a small cost. Our analog is pumping mass out of the graviton gas. There are more details around the orbit to contend with, but they all cancel out in the overall scheme. For example, we can ignore the gain or loss of kinetic energy from the tangential component of velocity at the apogee, because it is generally less from the corresponding tangential kinetic energy at the perigee. Now, the trajectories drawn in the figure are simplified to demonstrate the principle and the intended effect, but the flight engineer can later draw the correct ones. We have not accounted for possible precession and distortion from symmetrical shapes due to the variation of velocity at the corresponding points.

The presence or not of a concurrent variation of kinetic mass would not change the overall outcomes of the above proposed scheme.

To avoid disappointment for a forthcoming (anticipated) “free” space travel, we must warn that the above described effect may be so small that it might take 100 years to achieve some moderate increase of apogee with current technology for shape transformation. However, if we could find means to effectively vary the

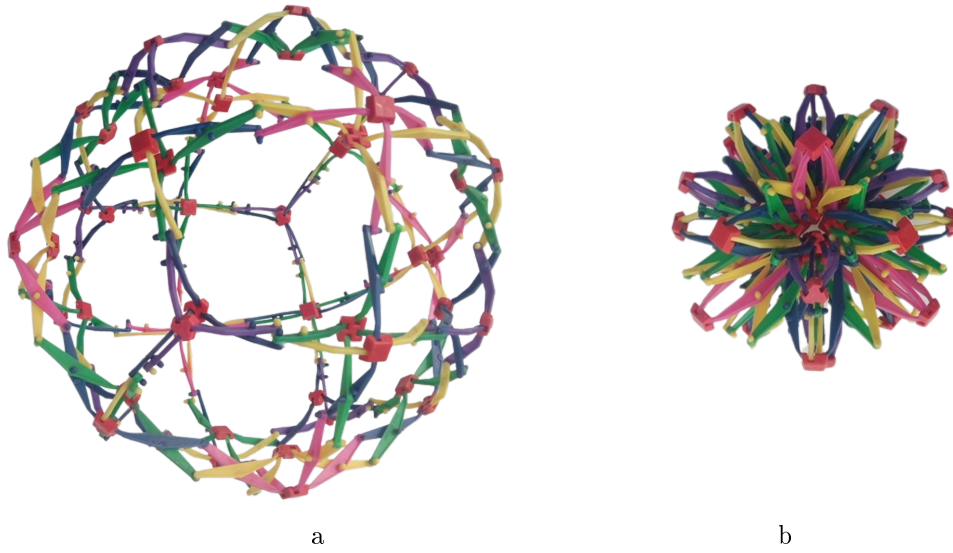


Figure 56: Toy sphere in (a) expanded form and (b) collapsed form

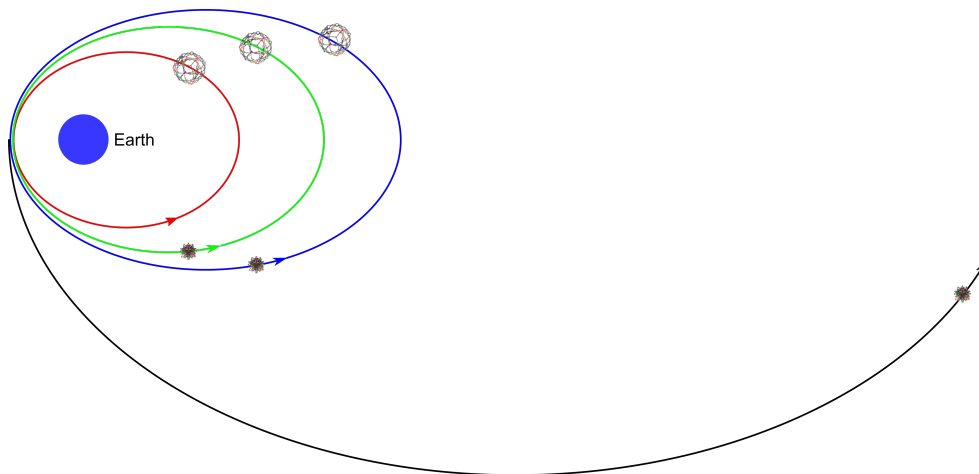


Figure 57: Schematic of principle: Cascade flyby acceleration and escape velocity obtained with the “toy sphere” falling towards the perigee in the expanded configuration while ascending towards the apogee in the contracted configuration (simplified and exaggerated trajectories)

density (to contract and expand) of an orbiting spacecraft, then the promise could become rewarding. In the meantime, the practical benefit of PG speed variation might be in controlling trajectories over a long haul accordingly by accelerating or braking a spacecraft with minimal (negligible) energy expenditure, provided the total effect is significant. The latter is to be quantified in later PG theory and engineering. Also it could furnish direct explanation for the flyby anomaly and perhaps for the Pioneer anomaly as well. We should investigate if it can also explain, at least in part, the Mercurian precession. Above all, the immediate benefit would be to validate our PG theory, which would place us in an advantageous position to progress in many other areas of scientific and technical endeavor.

23.3 Speed addition

If our theory is verified, then we have effectively arrived at a novel way to compose speeds according to Eq. 316. This supplies an alternative solution to the speed transformation in special relativity.

The actual speed of a body depends on and is limited by the composite absorptivity possible. The upper limit of absorptivity is unity, which imposes an upper limit to the effective mass and the associated speed, since the two are one-to-one connected. With given intrinsic absorptivity A_R , the kinetic absorptivity $A_{R\kappa}$ can only be in the range:

$$0 \leq A_{R\kappa} < 1 - A_R \quad (367)$$

which provides also a limited range for the real speed:

$$0 \leq \frac{v^2}{c^2} < 1 - \frac{v_0^2}{c^2} \quad \text{or} \quad 0 \leq v^2 < c^2 - v_0^2 \quad (368)$$

In other words, the intrinsic speed v_0 takes on a real meaning in the sense that it sets a handicap for the real speed of any given body: A heavy (dense) body cannot go as fast as a light body. In all this, it is implied that zero real speed is with reference to the gravion medium. A passenger in a train with real speed v_1 has already committed a composite value of speed over and above the intrinsic one before boarding the train. The passenger moving forward (or shooting a bullet) with additional speed Δv will find it more difficult to acquire that additional speed than prior to boarding the train (provided any subtle differences could be measured no matter how small they would be). The additional speed will result in a real speed $v_2 = v_1 + \Delta v$ to computed with reference to the stationary gravion system, giving:

$$\frac{v_1^2}{c^2} = A_{R\kappa 1} = A_{Rc1} - A_{R1} \quad (369)$$

$$\frac{v_2^2}{c^2} = A_{R\kappa 2} = A_{Rc2} - A_{R2} \quad (370)$$

$$\Delta v = v_2 - v_1 = c\sqrt{A_{R\kappa 2}} - c\sqrt{A_{R\kappa 1}} = c\sqrt{A_{Rc2} - A_{R2}} - c\sqrt{A_{Rc1} - A_{R1}} \quad (371)$$

which is the speed seen by the moving train reference. This gives the “transformation” (better the real speed) of v_2 relative to the stationary (absolute) system and Δv relative to the moving (train) system. The addition of speeds is straightforward with the provision that they cannot acquire arbitrary values other than those constrained by the absolute stationary medium.

When we establish another suitable equation to relate speed with absorptivity (and effective mass) in lieu of the conjectured Eq. 310, then we can adjust and expand the above equations accordingly.

23.4 Review and discussion

The present Section 23 is effectively a first attempt to usher some dynamics in PG theory initially developed only for stationary bodies. It is sort of an introductory rehearsal for the deferred Section 14 towards a dynamic push gravity theory. It is only a trial attempt based on a conjectured relationship between speed and mass, which we hope to approach from more fundamental principles in later development. In any case, the attempt remains to be completed with further work using more detailed mathematical analysis and accompanying computations. The preceding presentation contains some simplifying assumptions and relationships that we discuss below by way of alerting to remaining issues.

The absorptivity formula used in Eq. 311 was derived for a stationary lone sphere under omnidirectional gravion flux with spherical symmetry. Gravions are being absorbed with radial depth of penetration converting “neutral” (inactive) real mass to effective mass. By the introduction of speed of a sphere, we may not assume that the spherical symmetry of the distribution of effective mass is maintained. Intuitively,

we may expect a distribution of the total effective mass towards axial symmetry around the direction of velocity, but this is not clear (for now) how it takes place. It is not clear whether the intrinsic effective mass of the lone sphere is redistributed lumped together with the kinetic mass accrued at any given speed, or the kinetic mass accrued is superimposed to the lone mass. We accept that the kinetic mass must be reversible (added or subtracted) as a function of speed, which is the reason why we introduced the term “kinetic” mass to separate it out from the “intrinsic” mass. The kinetic mass must also be such that it counteracts (neutralizes or bypasses) the drag expected to appear from classical considerations. Possibilities for this to happen are canvassed in Section 25. It is difficult to envisage such mechanisms operating on amorphous matter. This prompts us to hypothesize the existence of some suitable structures around (or by) the minimal absorption-and-emission centers (MACs-MECs). One candidate structure is the vortex, which we also attempt to introduce for modeling the electron and positron in the following section. Vortices are built around axial symmetry, which we need during the introduction of kinetic mass.

In considering the free fall acceleration vis-à-vis the rocket acceleration, we have an overlap of common issues, but we also have unique issues with each of these situations. In rocket acceleration, we can understand the accrual during acceleration and radiation (release) of mass during deceleration. The addition and subtraction of mass takes place via an electrical field by the rocket. However, in free fall acceleration, the graphs show a net radiation (release) of mass, which is surprising. We can understand that the effective mass decreases with position and concurrently increases with falling speed, but any variation of total mass begs further questions and investigation. In fact, this is another opportunity to see the difference between rocket acceleration and falling acceleration, contrary to the Equivalence Principle.

To address the above concerns, it has been necessary to further study the mass-matter relationship by expanding our PG in the following Section 24. Before that, we need to spell out the details of how various parameters have been calculated and graphed for the falling body in the current section. We do so even if all the equations have been known and often applied in preceding work.

From given k and R for each sphere, we obtain the intrinsic (lone) values at infinite separation distance $r = \infty$ for A_{R_1} and A_{R_2} from the general equation:

$$A_R = 1 - \frac{1}{2k^2 R^2} + \frac{\exp(-2kR) \cdot (2kR + 1)}{2k^2 R^2}$$

The corresponding contraction factors q_1 and q_2 from the general equation:

$$q = \frac{3A_R}{4kR}$$

The corresponding effective masses $m_e \equiv m_{e1}$ and $M_e \equiv m_{e2}$ similarly from:

$$m_e = \frac{g_0 A_R R^2}{G}$$

The corresponding real masses $m = m_1$ and $M = m_2$ from:

$$m = \frac{m_e}{q}$$

After that, we need to decide what speed to use during fall, like Newtonian speed v_{rN} , PG static speed v_{rPGs} , or PG composite speed v_{rPGc} , so that we can calculate the kinetic absorptivity $A_{Rr\kappa}$ at distance r from:

$$A_{Rr\kappa} = \left(\frac{v_r}{c}\right)^2$$

where we adopt Eq. 311 with $n = 2$.

The corresponding kinetic (effective) mass $m_{er\kappa}$ from:

$$m_{er\kappa} = \frac{g_0 A_{Rr\kappa} R^2}{G} \quad (372)$$

The total (composite) effective mass from:

$$m_{erc} = m_{er} + m_{er\kappa}$$

where m_{er} is the static effective mass at r computed per Appendix E. From the latter, we find a static absorptivity A_{Rr} :

$$A_{Rr} = \frac{G m_{er}}{g_0 R^2} \quad (373)$$

and a composite A_{Rrc} at r from:

$$A_{Rrc} = A_{Rr} + A_{Rr\kappa} \quad (374)$$

Then we can find the product $k_c R$ for the composite absorptivity by solving the equation:

$$A_{Rrc} = 1 - \frac{1}{2k_c^2 R^2} + \frac{\exp(-2k_c R) \cdot (2k_c R + 1)}{2k_c^2 R^2}$$

from which we find the contraction factor for the composite mass:

$$q_{rc} = \frac{3A_{Rrc}}{4k_c R}$$

The latter is used to find the real mass at r m_{rc} from:

$$m_{rc} = \frac{m_{erc}}{q_{rc}}$$

Then the total black mass in motion at this distance r m_{brc} is:

$$m_{brc} = m_{rc} - m_{erc}$$

and the loss of real mass m_{rcloss} from:

$$m_{rcloss} = m - m_{rc}$$

For the static parameters, we correspondingly find first the static product $k_r R$ by solving the equation:

$$A_{Rr} = 1 - \frac{1}{2k_r^2 R^2} + \frac{\exp(-2k_r R) \cdot (2k_r R + 1)}{2k_r^2 R^2}$$

and then we get the static contraction factor q_r at that distance:

$$q_r = \frac{3A_{Rr}}{4k_r R}$$

The static real mass m_r :

$$m_r = \frac{m_{er}}{q_r}$$

The static black mass m_{br} :

$$m_{br} = m_r - m_{er}$$

Finally, the loss of static real mass m_{rloss} is obtained from:

$$m_{rloss} = m - m_r$$

The provision of exactly all the equations used in producing the graphs in this section may now help the reader to better stay in tune with what they mean. Our main concern above regards both Eqs. 373 and 374, whereby we insert the equation of absorptivity as it applies for lone bodies with effective masses distributed around a spherical symmetry. This is not the case for a falling sphere, where m_{er} must be axially distributed around the axis of fall, and $m_{er\kappa}$ is a new unknown type of mass with probably also a distribution around the same axis of fall. Therefore, the derivation of a composite absorptivity A_{Rrc} based on the equation for a lone body is only simplifying but arbitrary. Therefore, some of the graphs in this section (e.g. the total real mass) should be treated with caution until we can find an alternative approach for a dynamic PG. It is ascertained that m_{er} is correctly computed as a total mass following an integration, but we could also establish its distribution during the integration in future work. These concerns prompt us to undertake further work in the following section and return to them afterwards.

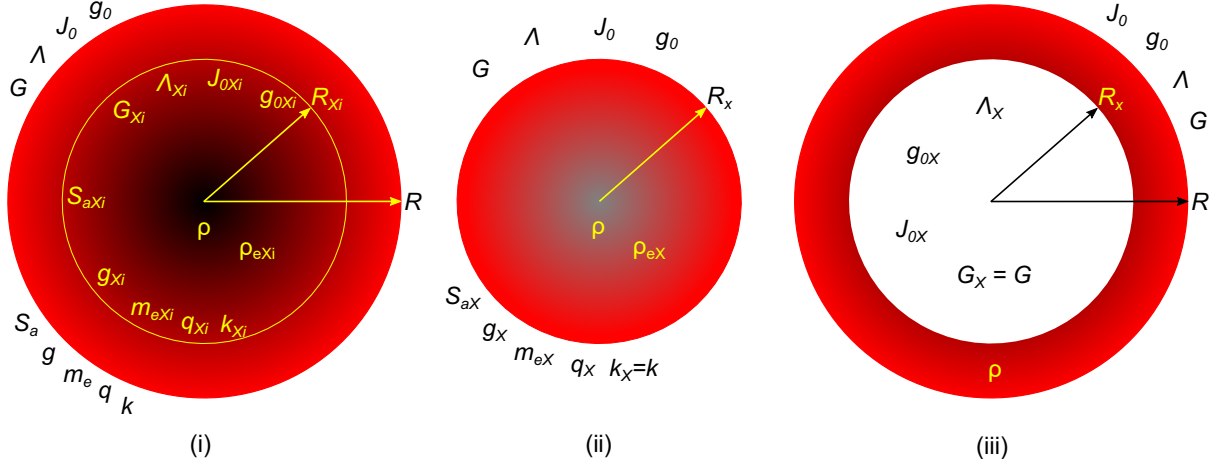


Figure 58: Internal vs. external spherical parameters and gravitational fields.

24 Mass-matter relationship

This theory has continually evolved from simple absorption relationships producing parameters with new understanding and without a priori knowledge. For example, the concept and parameter of “real mass” was necessitated as a substrate to facilitate the absorption of gravions. This led us to distinguish it from the “effective mass”, which is the activated component bearing the classical inertia as opposed to the remainder component that must be inertia-less and thus termed as “black mass”. This then has necessitated the understanding of black mass and its association with the assumed substrate; by the same token, we need to understand the association of all forms of mass with a presumed common substrate. In order to achieve this, we need to further develop the meaning and relationships of these and other parameters inside a material sphere including their connection to corresponding equations outside the sphere “in vacuum”; then we can attempt to find the desired association with the said (presumed) substrate (or matter).

We have already produced the variation of internal acceleration of a sphere in Section 8. We did the same in Section 14.6 with emphasis on the outermost layer of a very dense spherical body, after which we introduced (arrived at) the concept of black mass. It is now pertinent to review, refresh and generalize those relationships including others inside a material sphere. Since the intensity of radiant flux of gravions remains unknown, we have to theoretically continue on varying this parameter and find how all else vary with this. Equivalently, we can vary any other interdependent parameter that may be more suitable to understand or experiment with and deduce all others therefrom. In this Section, we opt to maintain a constant (fixed) real density ρ inside a fixed radius R of sphere as a more “tangible” approach in deriving the other parameters. For example, Eq. 114:

$$k = \frac{\pi G \rho}{g_0} \quad (375)$$

yields an inverse relationship between k and g_0 so that by choosing a series of values for k , we can find or imply a corresponding series of values for g_0 in a region of the universe with constant G and given ρ . Alternatively, for a given g_0 , we can choose a set of fixed values of k to which correspond a set of fixed values of ρ . We establish fundamental equations and theorems as an introduction to later analysis of more complex systems. The main purpose is to consolidate our understanding of the physical meaning of novel parameters that will reappear in future developments; it will be appreciated below that the physical meaning becomes convoluted and sometimes confusing as we move from external (vacuum) to internal condition with a given material density.

We reproduce the schematic representation of a massive star from Fig. 30 now in Fig. 58 with the aim of quantifying the schematic color shading of the internal properties. This figure illustrates three situations:

- (i) The variation of various parameters (properties) at any internal point X_i inside the sphere such as radius R_{X_i} , effective mass m_{eX_i} , Λ_{X_i} , etc. in contrast to the external ones R , m_e , Λ , etc.; we introduce the subscript (i) for the internal parameters.
- (ii) The creation of a new “external” partial sphere from the internal partial sphere with the same radius, namely, with $R_X = R_{X_i}$, in order to find the relationship of the parameters between these

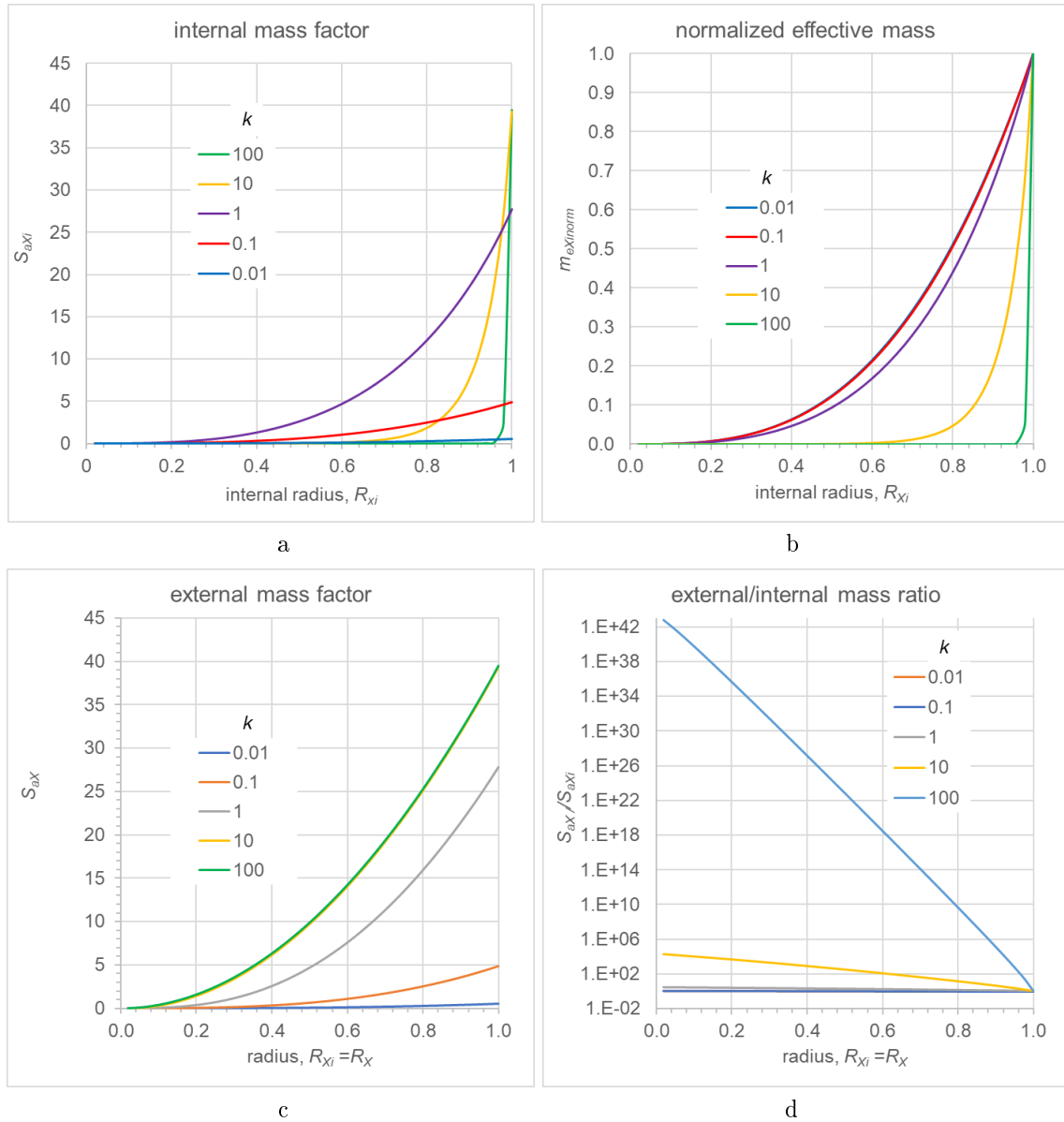


Figure 59: Internal and external mass factors, internal effective mass and ratio of external/internal mass.

two spheres; we compare various internal parameters with corresponding ones for spheres of the same radius and real density but without the outer shell, i.e. for spheres exposed to the influence of the “vacuum” g_0 as opposed to the internal spheres exposed to an internal g_{0Xi} .

- (iii) The removal of the material of the internal sphere leaving a hollow space (“vacuum”) with corresponding parameters characterizing a new internal “universe” surrounded by a material shell absorbing (shielding) in part the external graviton flux.

The subscript (i) helps avoid ambiguity and is used even if it may be redundant (obvious that something is internal), the absence of which refers to a sphere exposed to external “vacuum”. Thus, R_{Xi} replaces the R_X in Fig. 7, and the fractional radius becomes R_{Xi}/R , where we always have $R_{Xi} \leq R$; R_X is herewith reserved for a free to vacuum sphere like in (ii) but with $R_X = R_{Xi}$.

We should note that the “internal” realm regards not only solid or liquid bodies but also gaseous bodies including the heliosphere, all of which are considered non-vacuum, whilst some allow the motion of other material bodies like planets. For the present purposes, we do not include the interior of subatomic particles (electrons, protons, neutrons, etc); we consider all bodies with a given distribution of matter that is fixed either by their chemistry or by fixed statistical processes like in gases and the heliosphere.

24.1 Internal vs. external parameters (constant real density)

For the internal spherical field in (i) of the above figure, we derived the variation of a few parameters against fractional internal radius (R_X/R) per Fig. 8, which we now complement by deriving also the distribution of other parameters for a general case, starting with the effective mass and density.

Mass We examine the distribution of effective mass with radius. The computed characteristic absorption area \bar{S}_a for any sphere continues to mean S_{aR} for the external total sphere (with R) to be distinguished from S_{aR_X} for the external partial sphere (with R_X) and $S_{aR_{Xi}}$ for the internal partial sphere (with R_{Xi}). In Appendix D.2.2, point O always refers to an internal point defining an internal radius over which we integrate; that is, R_O now strictly refers to an integration variable in the range $0 \leq R_O \leq R$, or $0 \leq R_O \leq R_{Xi}$, or $0 \leq R_O \leq R_X$.

Eq. 497 used for the total (external) sphere is now re-written for the external partial sphere as :

$$S_{aX} = \int_0^{R_X} M_{aO} \cdot 4\pi k R_O^2 dR_O \quad (376)$$

and for the corresponding internal partial sphere as:

$$S_{aXi} = \int_0^{R_{Xi}} M_{aO} \cdot 4\pi k R_O^2 dR_O \quad (377)$$

which multiplied by $\frac{1}{4\pi A}$ yields the internal effective mass m_{eXi} at radius R_{Xi} .

It must be noted that this (m_{eXi}) partial mass is different from the (total) effective mass m_e uniformly apportioned to the same internal radius, and stated by the expression:

$$m_{eXi-apportioned} = m_e \frac{R_{Xi}^3}{R^3} \neq m_{eXi} \quad (378)$$

whereby m_{eXi} is an actual effective mass by an actual internal absorption process, whereas $m_{eXi-apportioned}$ is a deemed effective mass from the outer (total) effective mass mathematically allocated; this distinction is needed during later derivations. The above notation is temporary and may later be replaced by a more consistent and more meaningful one after we take stock of the needs of this continually evolving theory.

For this and other parameters it will help our theoretical development to normalize them over their characteristic value at the outer surface. Thus, the normalized internal effective mass is:

$$m_{eXinorm} = \frac{m_{eXi}}{m_e} = \frac{S_{aXi}}{S_{aR}} \quad (379)$$

We apply the above definitions and derivations to obtain the effective mass inside a sphere for a set of fixed absorption coefficients k (and real density ρ): Thus, Fig. 59(a) shows the variation of factor S_{aXi} (being proportional to effective mass) and (b) the variation of the normalized factor over its maximum value

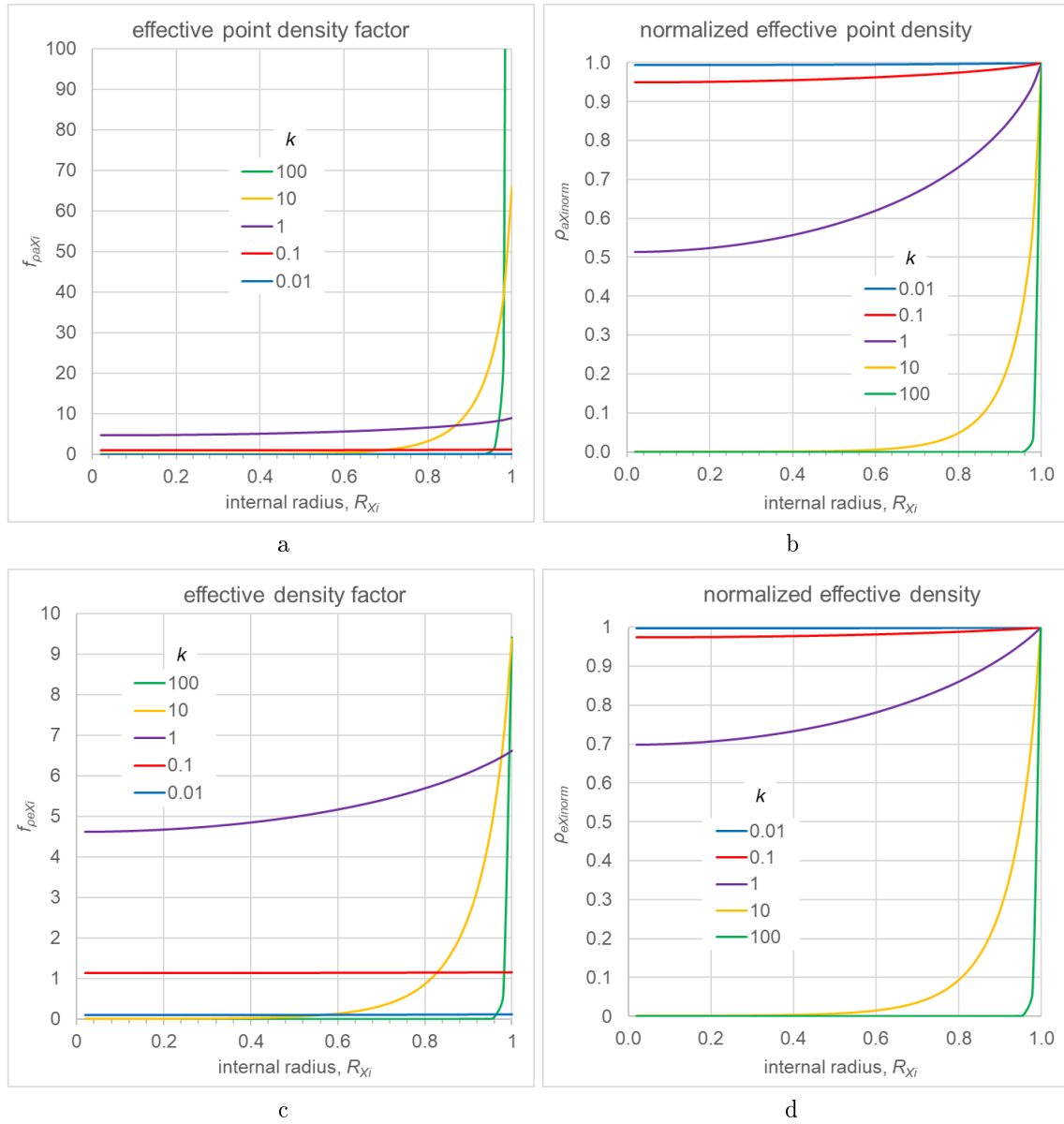


Figure 60: (a) Effective point density factor, (b) normalized effective point density, (c) effective density factor and (d) normalized effective density.

at $R_{X_i} = R$ (being equal to the normalized effective mass). For this and all other parameters, we choose five indicative values for $k = 0.01, 0.1, 1, 10, 100 \text{ m}^{-1}$. By setting the outer radius equal to unity ($R = 1 \text{ m}$), the internal radius R_{X_i} at any point X is normalized over the outer sphere radius. At the lowest of values of k the variation is very small becoming negligible as we approach the Newtonian condition, whereas at the highest values the internal effective mass is concentrated very close to the outer radius with close to zero value elsewhere.

Unlike m_{eX_i} , the real mass m_{X_i} at any internal radius is governed simply by a geometrical factor that uniformly apportions the total real mass:

$$m_{X_i} = m_{X_i\text{-apportioned}} = \frac{R_{X_i}^3}{R^3}m$$

and the normalized internal real mass is:

$$m_{X_i\text{norm}} = \frac{m_{X_i}}{m} = \frac{R_{X_i}^3}{R^3} \quad (380)$$

Now, with reference to Fig. 58 again, the extracted sphere (ii) has a different effective mass in the vacuum medium according to Eq. 376 as shown in Fig. 59c. The difference is more obvious by plotting the ratio S_{aX}/S_{aX_i} in (d) of this figure. The acquisition of mass is negligible in the Newtonian regime, but it becomes increasingly significant to at high values for the higher and highest density spheres.

The real density ρ (and associated absorption factor k) used in the derivations herewith is (are) unknown in the first place. We obtain this from the well known equation:

$$g_0 A_R - g_R = 0$$

with the known (best if measured) acceleration g_R at the surface establishing the equation:

$$g_0 \left(1 - \frac{1}{2k^2 R^2} + \frac{\exp(-2kR) \cdot (2kR + 1)}{2k^2 R^2} \right) - \frac{4\pi G R \rho_e}{3} = 0$$

that is solved for the unknown k provided that we have establish the actual value of g_0 . In conventional physics, we assume that the measured density ρ_e is invariant with radius. However, we have shown that the effective density measured should vary with radius while it is the real density that is invariant. A variable measured density with radius may be thought to be contrary with experience, but we allege that this is due only to our inability to measure extremely small density variations with sufficient accuracy for Newtonian bodies. If we could know the true effective density of a given spherical material with different radii, then the above equation would yield a constant absorption factor k and a constant real density for the given material. In all this, we also assume that there is no phase transformation (transition) and that the given material nature is invariant with radius. The latter assumption would be true over a certain radius range. In other words, we need only one good (sufficient) measurement of the density at a given radius with which we find the real density (and k) of a material, after which we can calculate the effective density with any other radius at constant k according to Fig. 60. All this necessitates that we have previously established the actual prevailing value for g_0 by some independent means once and for all. We should use a special notation for the actual g_0 to distinguish it from all its hypothetical values in a certain range that we often used throughout this report only because it is as yet unknown. The latter practice could easily lead to some confusion between assumed (variable) g_0 and an actual g_0 when it enters in our equations. Here, we use a bold faced g_0 for the actual one as typed in the last equation above (as often stated, we need to rationalize a new set of terminology and notations for PG theory as soon as we obtain sufficient data for its requirements). For experiments with ordinary falling bodies (like in Figs. 53 and 54), the possible effect of variable density with radius is by far much smaller than the other issues first needed to be addressed in Section 23.2.3. In any case, the fact there remains that the falling speed depends on the absorptivity per Eq. 365 so that care must be ultimately taken to include all possible effects with correct formulations.

Density A corresponding derivation is provided in Appendix D.2.2, where the effective density at an internal point X is found from Eq. 498 to be:

$$\rho_{e\text{-point}} = k M_{aO} \cdot \frac{1}{4\pi\Lambda} \quad (381)$$

It must be noted again that $\rho_e \neq \rho_{e\text{-point}}$, since the effective density ρ_e was introduced as an average density of an effective mass m_e , in lieu of the Newtonian mass, uniformly distributed inside a spherical body. We should have denoted it by the usual average symbolism $\bar{\rho}_e$ and should have reserved ρ_e for the effective point density; this can be done during a later re-write of this report, but for practical (convenience) interim

purposes, we now introduce the temporary symbol $\rho_a \equiv \rho_{e-point}$; it should be appreciated that this work is an exploratory project yielding new physics with variables not anticipated from the outset. The subscript (a) here denotes an activated density at a point resulting from the absorption of gravions at that point, whilst ρ continues to denote the "real density" at the same point and ρ_e the effective density throughout the entire sphere with radius R .

Then for internal point Xi we rewrite the above as:

$$\rho_{aXi} = kM_{aO} \cdot \frac{1}{4\pi\Lambda} \equiv f_{\rho aXi} \cdot \frac{1}{4\pi\Lambda} = \frac{M_{aO}}{4\pi} \rho \quad (382)$$

The point density at the surface is given by setting $R_O = R$ (or $R_{Xi} = R$) in Eq. 498 to yield the value of the surface M_a factor as

$$M_a = \int_0^{\pi/2} \exp\left(-kR\sqrt{1 - (\sin\varphi)^2}\right) [\exp(+kR\cos\varphi) + \exp(-kR\cos\varphi)] \cdot 2\pi \sin\varphi d\varphi \quad (383)$$

by which we obtain the normalized point density $\rho_{aXi\text{norm}}$ as:

$$\rho_{aXi\text{norm}} = \frac{\rho_{aXi}}{\rho_a} = \frac{M_{aO}}{M_a} \quad (384)$$

We can see the variation of the effective point density in Fig. 60(a) by plotting the proportional factor kM_{aO} ($f_{\rho aXi}$) and the normalized effective point density in (b) for the same set of fixed values of k . The trend is similar to the variation of effective mass, but we can now display a quantitative representation for each parameter. We thus reproduce the general picture of what we already found for a specific numerical example in Section 14.6.1 with Fig. 16 and schematically shown with Fig. 30. This was our conception and description of what happens in very dense bodies, like white dwarfs, neutron stars and black holes, for which we established an effect resembling to the conventionally described as an "event horizon".

We can further distinguish the corresponding derivations for the effective density: From effective mass, we obtain the effective density ρ_{eXi} and normalized effective density $\rho_{eXi\text{norm}}$ by:

$$\rho_{eXi} = \frac{S_{aXi}}{V_{Xi}} \cdot \frac{1}{4\pi\Lambda} = \frac{3S_{aXi}}{4\pi R_{Xi}^3} \cdot \frac{1}{4\pi\Lambda} \equiv f_{\rho eXi} \cdot \frac{1}{4\pi\Lambda} \quad (385)$$

$$\rho_{eXi\text{norm}} = \frac{\rho_{eXi}}{\rho_e} = \frac{S_{aXi}R^3}{S_{aR}R_{Xi}^3} \quad (386)$$

We plot the effective density factor $f_{\rho eXi}$ and the normalized effective density $\rho_{eXi\text{norm}}$ in Fig. 60c&d. The difference between point effective density and effective density is readily seen.

The above outcomes are inline with what we have already found previously, namely, that the effective mass is concentrated towards the outer surface, a negligible effect for Newtonian masses but becoming increasingly significant and important for heavy (dense) bodies.

Acceleration and contraction factor By our new notation, the internal PG acceleration g_{Xi} given by Eq. 91 is now written as:

$$g_{XiPG} \equiv g_{Xi} = \frac{g_0}{\pi} f_{gXi} \quad (387)$$

while the acceleration at the surface is:

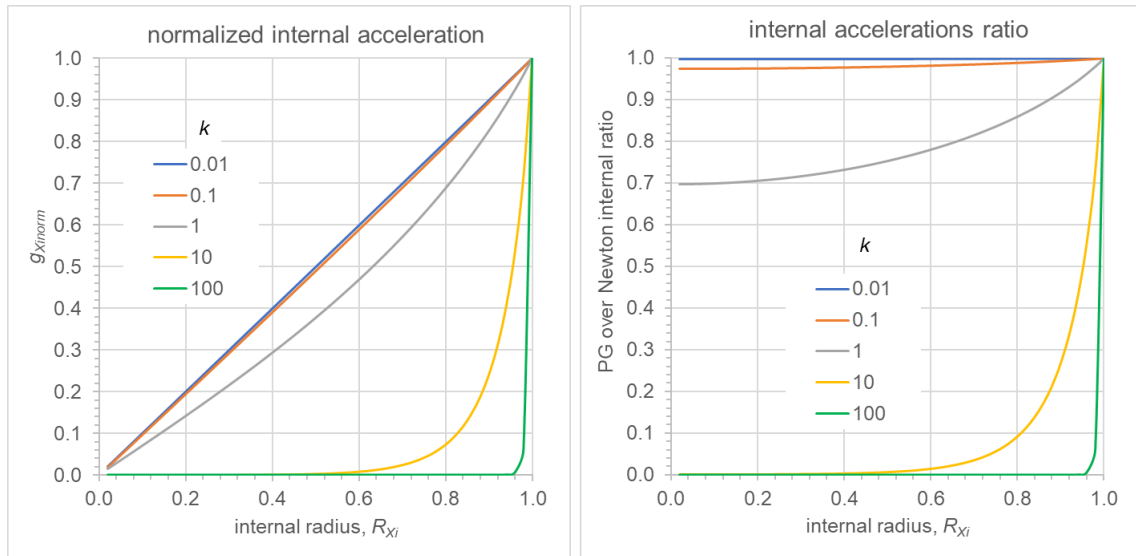
$$g_R = g_0 A_R \quad (388)$$

whereby we can normalize the internal acceleration by:

$$g_{Xi\text{norm}} = \frac{g_{Xi}}{g_R} = \frac{f_{gXi}}{\pi A_R} \quad (389)$$

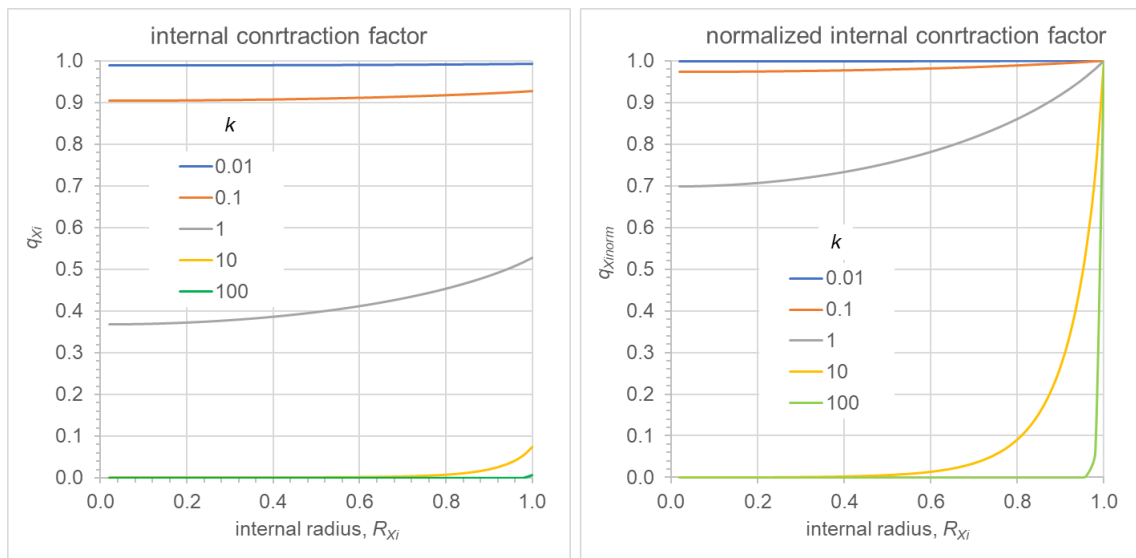
This is plotted in Fig. 61a. Close to Newtonian regime, we have a linear relationship against radius, as expected, but greatly diverging for denser bodies.

The contraction factor q was first introduced as the ratio of PG-acceleration over Newton-acceleration, whereby the first (PG) yields the actual force by an effective mass and the second the force that would be exerted by the real mass acting under Newton's gravitational law (as if effective). It was then found that the same factor is produced by the ratio of effective over real mass like also for a series of other variables. We



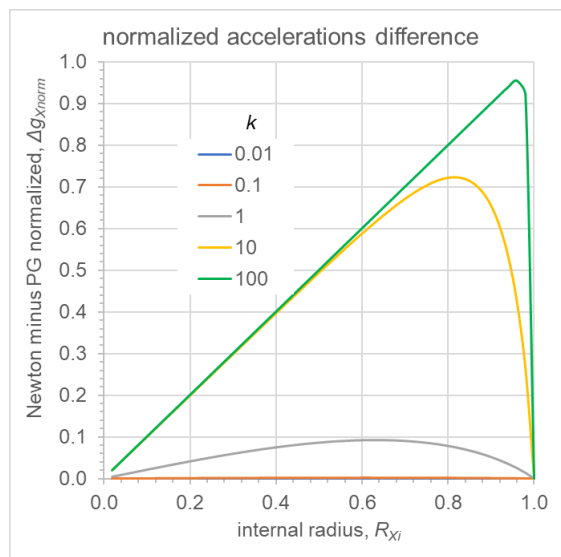
a

b



c

d



e

Figure 61: Internal acceleration and contraction parameters.

want here to investigate how the contraction factor behaves as an internal parameter. We may start with the internal contraction factor as the ratio of the internal masses by:

$$q_{Xi} = \frac{m_{eXi}}{m_{Xi}} = \frac{S_{aXi}}{4\pi\Lambda} \frac{3\Lambda}{4\pi R_{Xi}^3 k} = \frac{3S_{aXi}}{16\pi^2 R_{Xi}^3 k} \quad (390)$$

We can normalize the internal contraction factor over its value q at the outer surface (i.e. at $R_{Xi} = R$):

$$q_{Xinorm} = \frac{q_{R_{Xi}}}{q} = \frac{\frac{m_{eXi}}{m_{Xi}}}{\frac{m_e}{m}} = \frac{m_{eXi}}{m_{Xi}} \frac{m}{m_e} = \frac{m_{eXinorm}}{m_{Xinorm}} = \frac{S_{aXi}}{S_{aR}} \frac{R^3}{R_{Xi}^3} \quad (391)$$

Let us now return to the original formulation of contraction factor from accelerations:

$$q_{Xi} = \frac{g_{XiPG}}{g_{XiN}} = \frac{\frac{g_0}{\pi} f_{gXi}}{\frac{Gm_{Xi}}{R_{Xi}^2}} = \frac{\frac{g_0}{\pi} f_{gXi}}{G \frac{4}{3} \pi \rho R_{Xi}} \quad (392)$$

where we treated the real mass acting under Newton to yield an acceleration g_{XiN} .

However, in Section 8 we used Eqs. 91 and 93 in the ratio, namely:

$$\frac{PG-g_{Xi}}{Newton-g_{Xi}} = \frac{\frac{g_0}{\pi} f_{gXi}}{\frac{Gm_{eXi-apportioned}}{R_{Xi}^2}} = \frac{\frac{g_0}{\pi} f_{gXi}}{\frac{4}{3} \pi G \rho_e R_X} \quad (393)$$

where for good reason we used the apportioned effective mass $m_{eXi-apportioned}$ per Eq. 378. The purpose was then to find the difference between expected Newton-acceleration and PG-acceleration at various depths for prospective measurements on Earth. As a result, we have corresponding Eqs. 392 and 393 differing only in the densities ρ and ρ_e . As we now attempt to formalize the relationships for the internal and external regimes, we need to see the needed adjustment in the terminology used in preceding Section 8. The significance of this adjustment is found by taking the ratio of the two derivations in Eqs. 392 and 393 above:

$$\frac{\frac{q_{Xi}}{PG-g_{Xi}}}{Newton-g_{Xi}} = \frac{m_{eXi-apportioned}}{m_{Xi}} = \frac{m_{eXi-apportioned}}{m_{Xi-apportioned}} = \frac{m_e}{m} = q \quad (394)$$

Therefore,

$$\frac{PG-g_{Xi}}{Newton-g_{Xi}} = \frac{q_{Xi}}{q} = q_{Xinorm} \quad (395)$$

In other words, the ratio of accelerations provided in Section 8 with Fig. 8 must be understood to be the normalized contraction factor according to the generalized definitions in the present Section; the contraction factor continues to comply with its original formulation. The same observation applies also to Fig. 16 using the same ratio of Eq. 393, where we have now changed prior q_X to q_{Xinorm} ; that was plotted specifically close to the outer surface of a very dense sphere (as example) to demonstrate the extreme concentration of effective mass very close to the surface. We have now elucidated the exact meaning of internal versus external properties for these cases. The variation of internal contraction factor and the normalized one are plotted in Fig. 61c&d. The internal accelerations ratio per Eq. 393 is also plotted in Fig. 61b yielding identical graphs with (d) as expected above.

The numerical difference of accelerations with depth presented in Table 1 remains correct, while we further investigate again the same difference for the current set of k coefficients here. The internal Newtonian acceleration as given above is proportional to the internal radius, whilst at the surface is given by $g_0 A_R$; this is linearly distributed with radius expressed also as:

$$Newton-g_{Xi} = g_0 A_R \frac{R_{Xi}}{R}$$

from which we subtract the $PG-g_{Xi}$ to obtain the difference as a function of radius (and depth):

$$\Delta g_{Xi} = Newton-g_{Xi} - PG-g_{Xi} = g_0 A_R \frac{R_{Xi}}{R} - \frac{g_0}{\pi} f_{gXi} \quad (396)$$

We used the above equation to plot the said difference in Fig. 8 and Table 1 for Earth with $g_0 = 1000 \text{ ms}^{-2}$. It is useful to generalize this function by dividing by g_0 , as a special (only here) normalization for this particular quantity, namely, by:

$$\Delta g_{Xi\text{norm}} = \frac{\Delta g_{Xi}}{g_0} = A_R \frac{R_{Xi}}{R} - \frac{f_{gXi}}{\pi} \quad (397)$$

which we plot in Fig. 61e. From this, we can readily reproduce the graph in Fig. 8 for the values of k , R and g_0 applied in the example there.

Finally, we can complement the formulas of effective density at Xi by:

$$\rho_{eXi} = q_{Xi}\rho$$

and the normalized effective density:

$$\rho_{eXi\text{norm}} = \frac{\rho_{eXi}}{\rho_e} = \frac{q_{Xi}\rho}{q\rho} = q_{Xi\text{norm}}$$

which is also confirmed by the provided graphs for these parameters.

Absorptivity and absorption coefficient For a given g_0 , the absorptivity A_R of the outer sphere (i) in Fig. 58 is known in connection with absorption coefficient k and radius R and by:

$$A_R = 1 - \frac{1}{2k^2 R^2} + \frac{\exp(-2kR) \cdot (2kR + 1)}{2k^2 R^2}$$

so that for the sphere (ii) it is

$$A_{R_X} = 1 - \frac{1}{2k^2 R_X^2} + \frac{\exp(-2kR_X) \cdot (2kR_X + 1)}{2k^2 R_X^2}$$

because k is the same for the same real density ρ . For consistency, the internal sphere in (i) having radius R_{Xi} must be characterized by an internal absorptivity $A_{R_{Xi}}$ in connection with an internal g_{0Xi} and internal absorption coefficient k_{Xi} by:

$$A_{R_{Xi}} = 1 - \frac{1}{2k_{Xi}^2 R_{Xi}^2} + \frac{\exp(-2k_{Xi}R_{Xi}) \cdot (2k_{Xi}R_{Xi} + 1)}{2k_{Xi}^2 R_{Xi}^2}$$

The outer material shell depicted by (iii) in the above figure reduces the outermost flux intensity from J_o to J_{oXi} and the maximum acceleration from g_0 to g_{0Xi} . We can derive $A_{R_{Xi}}$ and k_{Xi} by solving the equation

$$q_{Xi} = \frac{3A_{R_{Xi}}}{4k_{Xi}R_{Xi}} \quad (398)$$

first for the product $k_{Xi}R_{Xi}$ and then deduce $A_{R_{Xi}}$ and k_{Xi} from the given radius R_{Xi} .

Again, we can normalize these internal quantities over their values at the surface by:

$$A_{R_{Xi}\text{norm}} = \frac{A_{R_{Xi}}}{A_R} \quad (399)$$

$$k_{Xi\text{norm}} = \frac{k_{Xi}}{k} \quad (400)$$

with which the contraction factor relates by

$$q_{Xi\text{norm}} = \frac{A_{R_{Xi}\text{norm}}}{k_{Xi\text{norm}}R_{Xi\text{norm}}} \quad (401)$$

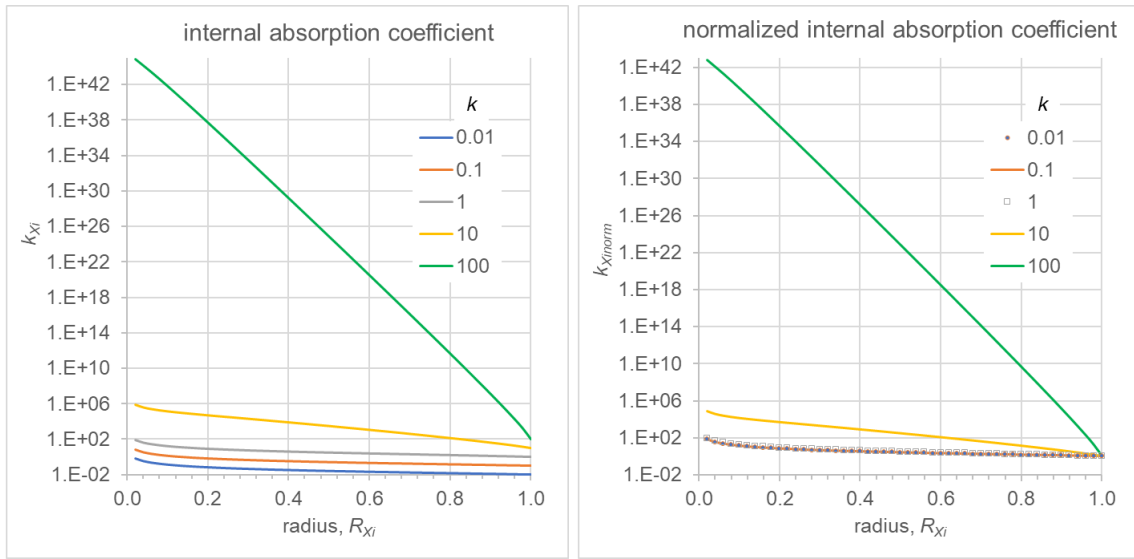
as can also be readily confirmed from Eq. 398. We show the above internal absorption coefficients and absorptivities in graphical form in Fig. 62a,b,c&d. For comparison, in Fig. 62e&f we also show the absorptivity of external partial sphere (ii) of Fig. 58 as well as the ratio of absorptivities of internal-over-external partial spheres. Interestingly, we note that the normalized absorptivity in (d) is greater than unity within a limited range of values; also the ratio in (f) is also within a particular range. We should later examine what the significance of those limiting values might be.

There are subtle differences in some expressions that we need to spell out if to avoid errors easily taking place. The internal acceleration factor can be written by alternative equations as:

$$f_{gXi} = g_{Xi\text{norm}}\pi A_R = g_{0Xi\text{norm}}\pi A_{R_{Xi}} \quad (402)$$

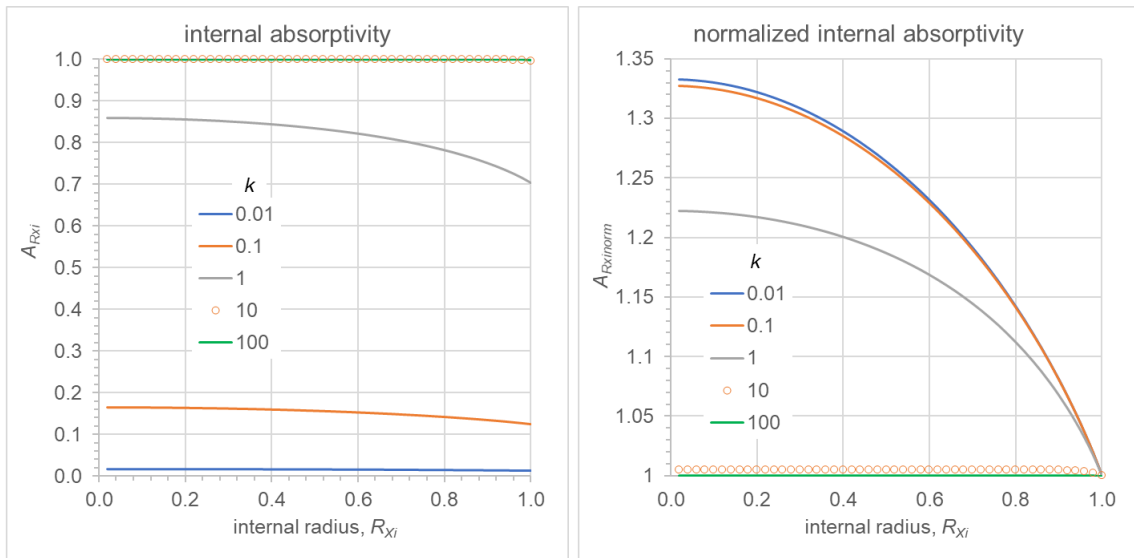
based on Eqs. 91 and 389.

It is worth noting that if the absorptivity of the external partial sphere shown in Fig. 62e is re-plotted against the product kR_X (reduced radius), we obtain the familiar sigmoid shape for external absorptivity as seen in Fig. 63a, but not the same for the internal absorptivity as seen in (b) of the same figure.



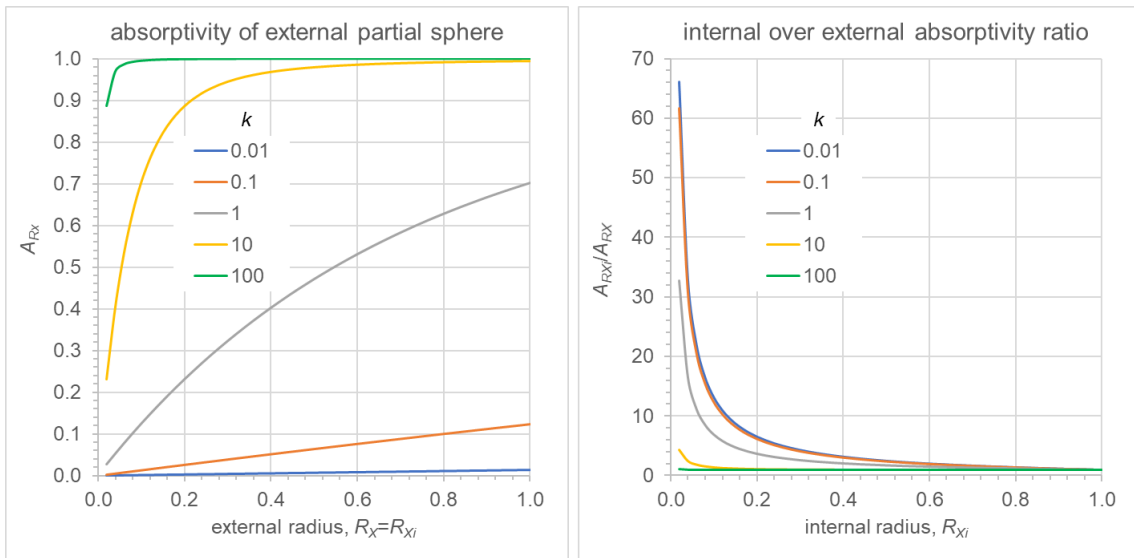
a

b



c

d



e

f

Figure 62: Absorptivity and absorption coefficients.

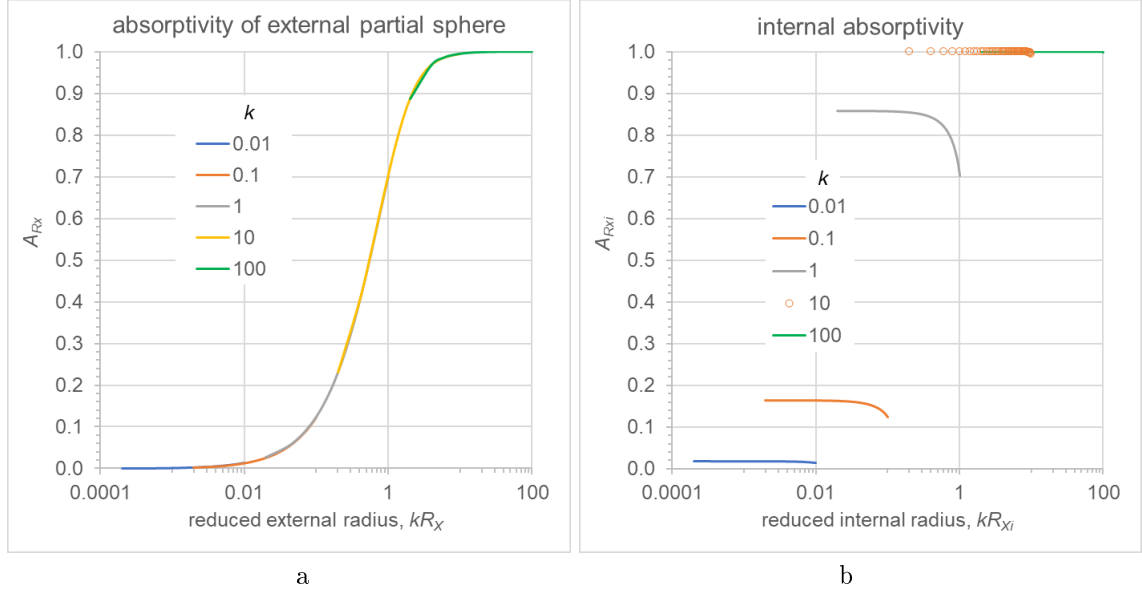


Figure 63: Absorptivities against reduced radius.

g_0, Λ_{Xi}, J_0 and G We have already established the connection between external g_0 and internal g_{0Xi} (see Eqs. 91 and 92), so that the normalized $g_{0Xinorm}$ is:

$$g_{0Xinorm} = \frac{g_{0Xi}}{g_0} = \frac{g_{Xi}}{g_0 A_{R_{Xi}}} = \frac{f_{gXi}}{\pi A_{R_{Xi}}} \quad (403)$$

[Note: The $g_{0Xi} = g_{0Xinorm}g_0$ has now been corrected in the preceding Fig. 8 for $g_0 = 1000 \text{ ms}^2$, whereby we inadvertently used the ratio given by Eq. 389 in previous versions of this report, i.e. we used A_R instead of $A_{R_{Xi}}$]. We can now see the variation of this generalized parameter in Fig. 64a.

For consistency in the formulation for the internal acceleration g_{Xi} , we replace the external universal constant G by G_{Xi} in

$$g_{Xi} = \frac{G_{Xi} m_{eXi}}{R_{Xi}^2} \quad (404)$$

The external Λ constant becomes internally Λ_{Xi} , so that from the corresponding Eqs. 73 like:

$$\Lambda = \frac{\pi G}{g_0} \text{ and } \Lambda_{Xi} = \frac{\pi G_{Xi}}{g_{0Xi}}$$

we deduce the normalized constant Λ_{Xinorm} :

$$\Lambda_{Xinorm} = \frac{\Lambda_{Xi}}{\Lambda} = \frac{\frac{\pi G_{Xi}}{g_{0Xi}}}{\frac{\pi G}{g_0}} = \frac{G_{Xinorm}}{g_{0Xinorm}} \quad (405)$$

where we have also introduced the normalized universal constant G_{Xinorm} by:

$$G_{Xinorm} = \frac{G_{Xi}}{G} \quad (406)$$

We can further process this per Eq. 404 as:

$$G_{Xinorm} = \frac{g_{0Xi} A_{R_{Xi}} R_{Xi}^2 m_e}{g_0 A_R R^2 m_e} = \frac{g_{0Xi} \Lambda_{Xi}}{g_0 \Lambda} = \frac{g_{0Xi} k_{Xi}}{g_0 k} = g_{0Xinorm} \Lambda_{Xinorm} = g_{0Xinorm} k_{Xinorm} \quad (407)$$

We connect the internal flux intensity J_{0Xi} via the known Eqs. 33 below:

$$G = \frac{J_0}{c} \Lambda^2 \text{ and } G_{Xi} = \frac{J_{0Xi}}{c} \Lambda_{Xi}^2$$

$$J_0 = \frac{cg_0^2}{\pi^2 G}$$

$$J_{0Xi} = \frac{cg_{0Xi}^2}{\pi^2 G_{Xi}}$$

The normalized internal flux intensity then is:

$$J_{0norm} = \frac{g_{0Xi}^2 G}{g_0^2 G_{Xi}} = g_{0Xinorm}^2 G_{Xinorm}$$

From Eq. 407 we deduce:

$$k_{Xinorm} = \Lambda_{Xinorm} \quad (408)$$

Also:

$$g_{Xi} = \frac{g_0 f_{gXi}}{\pi} = \frac{G_{Xi} m_{eXi}}{R_{Xi}^2} = \frac{G_{Xi} S_{aXi}}{4\pi \Lambda R_{Xi}^2} = \frac{G_{Xi} g_0 S_{aXi}}{4\pi^2 G R_{Xi}^2}$$

$$f_{gXi} = \frac{S_{aXi}}{4\pi R_{Xi}^2} \frac{G_{Xi}}{G} \quad (409)$$

which relates the integrals in the factors f_{gXi} and S_{aXi} .

For convenience in further processing the above formulas, we transfer some useful equations below:

$$\Lambda = \frac{\pi A}{m_e} = \frac{\pi R^2 A_R}{m_e} = \frac{\pi G}{g_0} = \frac{k}{\rho} = \frac{cg_0}{\pi J_0} \quad (410)$$

and together with Eqs. 375 and 403 we transform the normalized universal constant as:

$$G_{Xinorm} = \frac{g_{0Xi} k_{Xi}}{g_0 k} = \frac{g_{Xi}}{g_0 A_{R_{Xi}}} \frac{k_{Xi}}{k} = \frac{g_{Xi}}{\pi G A_{R_{Xi}}} \frac{k_{Xi}}{\rho} = \frac{g_{Xi}}{\pi G A_{R_{Xi}}} \Lambda_{Xi} = \frac{g_{Xi} \pi R_{Xi}}{\pi G m_{eXi}} = \frac{g_{Xi}}{G} \frac{m_{eXi}}{R_{Xi}^2} = \frac{g_{Xi}}{g_{Xi}} = 1 \quad (411)$$

which we highlight below:

$$G_{Xinorm} = 1 \quad \text{or} \quad G_{Xi} = G \quad (412)$$

As a result we can also simplify other parameters as:

$$\Lambda_{Xinorm} = \frac{1}{g_{0Xinorm}} \quad (413)$$

$$J_{0norm} = g_{0Xinorm}^2 \quad (414)$$

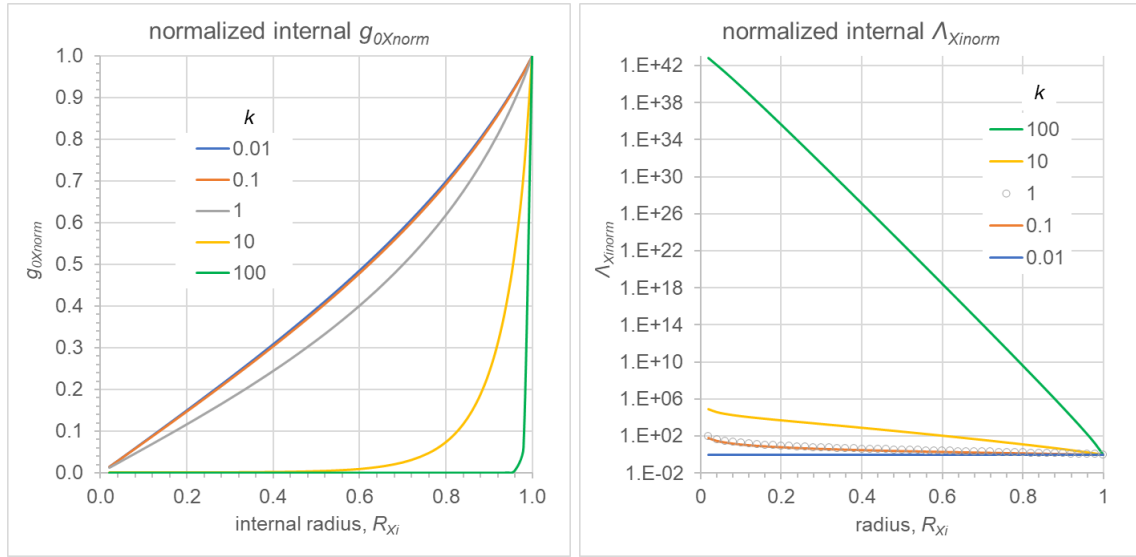
$$f_{gXi} = \frac{S_{aXi}}{4\pi R_{Xi}^2} \quad (415)$$

We can see the variation of the generalized internal parameters Λ_{Xinorm} and J_{Xinorm} in Fig. 64b&c.

The constancy of the internal universal gravitational constant per Eq. 412 has also been verified computationally via Eq 407 to always give:

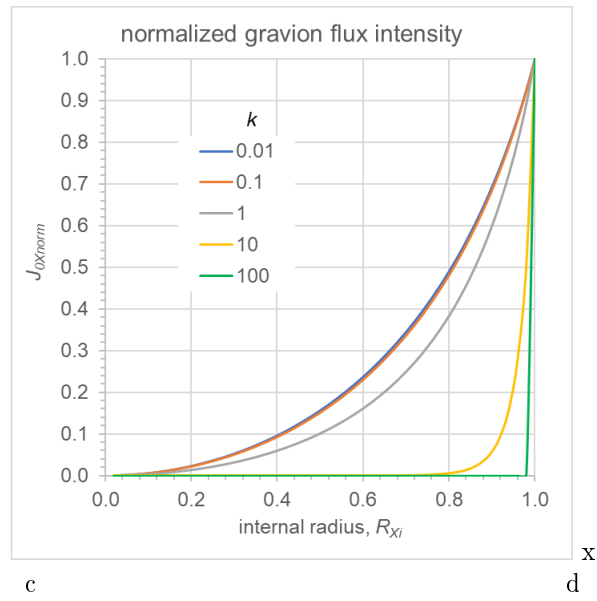
$$g_{0Xinorm} \Lambda_{Xinorm} = 1 \quad (416)$$

which we show by the graph in Fig. 64e. There is an oscillation for $k = 100 \text{ m}^{-1}$ of extremely small magnitude around unity. This arises from ‘‘round off’’ errors produced by the integration routine in the python program used. We can set an arbitrary precision for all other computations except for the integration routine that is governed by its own precision limits: As soon as we exceed some set level of precision, an error warning is issued. We purposefully present this limitation to warn potential users that high precision algorithms are often required to avoid misleading results. It may be that a devoted integrator must be developed to take on special requirements of PG theory.



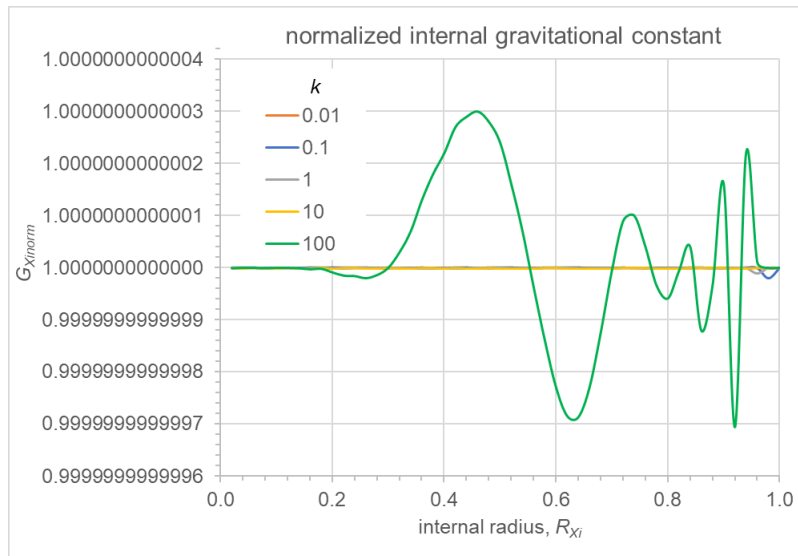
a

b



c

d



e

Figure 64: Internal parameters of g_{0X_i} , Λ_{X_i} , J_{0X_i} , G_{X_i} .

Miscellaneous discussion. The penultimate step of:

$$g_{Xi} = G \frac{m_{eXi}}{R_{Xi}^2}$$

in Eq. 411 is justified by the fact that m_{eXi} is the actual effective mass inside the sphere with radius R_{Xi} and not the apportioned Newtonian effective mass per Eq. 378; this m_{eXi} must produce the same acceleration whether it is derived from the action of the external g_0 (or J_0) as above or the action of the internal g_{0Xi} (or J_{0Xi}) as below:

$$g_{Xi} = G_{Xi} \frac{m_{eXi}}{R_{Xi}^2}$$

which can only happen if and only if $G_{Xi} = G$.

This outcome was not directly obvious at the outset of our formulations, while we had to introduce the general possibility of an unknown G_{Xi} in the equation above. In fact, having regard to the dependence of G via Eq. 34, we have already contemplated that the universal gravitational is a different “constant” at various remote locations in the cosmos. That understanding still remains valid whilst the new finding of $G_{Xi} = G$ concerns, so far, only the internal gravitational field inside a material body. We only need to adjust our speculated variation of G inside the heliosphere in Section 13 or elsewhere as regards internal situations. However, we still have a deviation from Newton’s gravitational law inside matter now not on account of a variable G but rather on account of variable m_{eXi} over and above the variation of mass on account of the two sphere interaction, in vacuum), established in Section 16. The two-sphere mass variation is ultimately consistent with Newton’s law, but we now have an extra variation of mass due to the internal field in the heliosphere presumed to consist of a very dilute matter that allows the motion of planets. Presumably, the density of heliosphere increases significantly as we approach the Sun, so that planet Mercury experiences the most of a variable mass arising from the variation of internal properties. Similarly, among various solutions for the Pioneer anomaly (a slowing slightly more than expected) offered so far, we can also propose that it is due to a slight continuous increase of effective mass as it approaches the outer reaches of the heliosphere; this should result in a deceleration of the spacecraft. The nature and physics of the presumed very dilute matter in the heliosphere is a separate issue to focus on later.

The above finding is most important for a deeper understanding of the universe. We have now learned that the big_ G must remain constant throughout an extended region comprising the heliosphere and beyond. How far beyond is a matter of conjecture and speculation. Since $G = \frac{J_0}{c} \Lambda^2$ and considering that Λ remains constant as an external (vacuum) parameter at constant J_0 (or Φ_0), then G will change only when J_0 changes. If gravions behave like a gas, then it is their mean free path (mfp) that could determine the size of the region beyond which the intensity of J_0 may change. It may remain constant for a much wider region well far greater than the mean free path of gravions, i.e. for a far too expansive region, until and unless there are events that can generate the said intensity variation. The suggestion of a mfp for gravions may appear incompatible with our understanding of the behavior of photons, but we have proposed that gravions and photons are different entities. This idea is further elaborated in Section 25.

We initially restricted Fig. 58 to “ordinary” bodies, not necessarily Newtonian, but we could include very dense systems, in which case we should involve the corresponding parameters of other fields, like the electric field in Section 21; this would involve a change of G to $G_{2-electric}$. We can extend a similar analysis for the electric field in later developments aiming to unify the two fields.

The process of normalization of various internal quantities (parameters) over their value at the surface has simplified their equations like 413 and 414. The finding that the normalized universal constant $G_{Xi norm}$ is unity raises the question whether this constant might be redundant after all and that the use of big G in conventional equations is the result of the way that the problem of gravitation was formulated. It is a constant of proportionality in an equation obtained by experiment and observation. Actually, big G is already absent in our Eq. 86. Furthermore, there are no masses involved but only absorptivities, Λ and g_0 . We replace Newton’s gravitational law by another equation (law) that involves no mass and no big G . Any godly attributes to these parameters may not be well deserved after all, while our reverence can now be directed to gravion flux and hyle (see next Section). It is now PG parameters that we need to consider and understand. We may have more to say on this in later development of PG.

Furthermore, the internal properties seem to be dependent on their value at the surface. The surface appears to be a reference boundary. Depending on the density of mass, variation of internal properties may be very small in the Newtonian regime, but variation increases with depth (distance from the surface) faster with increasing density (see “*total absorption layer (TAL)*” in Section 18.2). The sharpest variation occurs in neutron stars and finally in black holes whereby the “surface” has a finite thickness with spatially fastest transition from an external to internal regime having lost total communication from the outside. We may

generalize this description by saying that the surface of any material sphere is a boundary through which “information” is transferred from the outside to the inside, or that the inside properties start with those from the outside at the surface and then are modified in conjunction with the density of the material sphere. We might like to call this surface an “event horizon” under a new generalized meaning as opposed to the conventional meaning of the event horizon of black holes. Our difference then is a matter of quantity, i.e. our event-horizon may be very extended (in thickness) well beyond the size of the material sphere itself, or shorter than the radius of the sphere. Black holes create the shortest possible transition of the event horizon, which is real and tangible, in distinction from a mysterious mathematical surface, beyond which numerous claims and hypotheses have been made on what actually happens.

The above qualitative description has by now been quantitatively expressed via equations among various parameters. In particular, the acceleration factor f_g by Eq. 38 for an external point O at distance r from the center of a sphere is $f_g = \pi A/r^2$ all the way to the surface where it becomes a characteristic $f_{gR} = \pi A_R$, after which it becomes $f_{gX_i} = g_{0Xinorm} \pi A_{R_{X_i}}$ per Eq. 403; the latter contains (expresses) a transition from external (vacuum) g_0 regime to an internal g_{0X_i} regime of matter.

Throughout the above derivations we attempted to introduce notations in a way that would prevent confusion. When this is not fully achieved, we should make appropriate amends. Specifically, we need to do so for the factors S_{aX_i} and f_{gX_i} as already applied, We note that they are both “internal” parameters, however, both involving the external k in the integrals; they are internal factors “seen” or created from the outside. For good measure, we re-state them below:

$$S_{aX_i} = \int_0^{R_{X_i}} M_{aO} \cdot 4\pi k R_O^2 dR_O$$

which in the limiting case at the outer surface of the sphere yields:

$$S_{aR} = \int_0^R M_{aO} \cdot 4\pi k R_O^2 dR_O = 4\pi^2 R^2 A_R$$

Looking from the inside, we might feel inclined to use the internal absorption coefficient k_{X_i} in an analogous formulation by:

$$S_{aX_i-internal} = \int_0^{R_{X_i}} M_{aO} \cdot 4\pi k_{X_i} R_O^2 dR_O = 4\pi^2 R_{X_i}^2 A_{R_{X_i}}$$

which is numerically different from the prior S_{aX_i} on account of $k \neq k_{X_i}$, i.e. these two absorption area factor are:

$$S_{aX_i} \neq S_{aX_i-internal} \quad (417)$$

In any case both of the above parameters should yield an identical internal effective mass m_{eX_i} when multiplied by the corresponding factors like:

$$S_{aX_i} \cdot \frac{1}{4\pi A} = m_{eX_i}$$

$$S_{aX_i-internal} \cdot \frac{1}{4\pi \Lambda_{X_i}} = \frac{4\pi^2 R_{X_i}^2 A_{R_{X_i}}}{4\pi \Lambda_{X_i}} = \frac{\pi R_{X_i}^2 A_{R_{X_i}}}{\Lambda_{X_i}} = m_{eX_i}$$

with the last member of the second equation obtained by use Eq. 410 internally. The two factors relate via the equations:

$$\frac{S_{aX_i}}{A} = \frac{S_{aX_i-internal}}{\Lambda_{X_i}}$$

$$S_{aX_i} = \frac{S_{aX_i-internal}}{\Lambda_{Xinorm}} = g_{0Xinorm} S_{aX_i-internal} \quad (418)$$

Similarly, the internal acceleration factor f_{gX_i} is computed based on the external k , but if we feel inclined to use the internal k_{X_i} , then we would obtain a numerically different factor:

$$f_{gX_i-internal} = \pi A_{R_{X_i}}$$

which is not the same as that obtained by Eq. 90, namely:

$$f_{gX_i} \neq f_{gX_i\text{-internal}}$$

In any case both of the above parameters should yield an identical internal acceleration g_{X_i} when multiplied by the corresponding factors like:

$$f_{gX_i} \cdot \frac{g_0}{\pi} = g_{X_i}$$

$$f_{gX_i\text{-internal}} \cdot \frac{g_{0X_i}}{\pi} = \pi A_{R_{X_i}} \frac{g_{0X_i}}{\pi} = g_{X_i}$$

where the product $g_{0X_i} A_{R_{X_i}}$ (internally) corresponds to the product $g_0 A_R$ (externally). The two factors relate via the equations:

$$f_{gX_i} g_0 = f_{gX_i\text{-internal}} g_{0X_i}$$

$$f_{gX_i} = g_{0X_i} \text{norm} f_{gX_i\text{-internal}} = g_{0X_i} \text{norm} \pi A_{R_{X_i}} \quad (419)$$

The above subtle details, if unnoticed, can result in significant errors. This helps us also understand the different effect between k and k_{X_i} . In setting up computation equations, we use a constant k for all and through all bodies having the same real density, but it can vary when the density varies according to the constant ratio $\Lambda = k/\rho$. We do all this from an external point of view. Nonetheless, we can obtain equivalent outcomes also from an internal point of view according to the experience of graviton flux at an inside point of a material; the latter depends on the internal distribution of density, which attenuates the external graviton flux. In that case we can use the k_{X_i} at that point. The latter is variable with variable radial position in a spherical body. Therefore, this clarification should dispel possible misconceptions about the constancy or not of the absorption coefficient. Our computations have been set up correctly so far.

In this Section we have initiated an understanding of internal versus external parameters (properties) that can be appended to Part 1 of this report later. More investigation and formulations may continue in future work, its current form of which remains incomplete for the time being. Many important topics remain open. Furthermore, many details need to be worked out as, for example, the limiting values on the graphs in Fig 62d may (or may not) be important. Also, we have often established mathematical derivations based on the physics (physical considerations) but the same derivations should result from pure mathematical manipulations as well. PG has ushered a bonanza for mathematicians to make important contributions and help further expand the new physics. Archimedes is reported to be the first to have used physics to prove mathematical theorems in his codex Netz (2007).

24.2 Mass and hyle

We have demonstrated once more that mass is not a sacrosanct entity by being invariant and conserved. It is rather a property of a substrate along with other properties (parameters) entering inter-relationships that describe a mode of existence of the substrate. This substrate has been also described as “stuff” or matter that is generally something vague or unknown. It may be that the word mass has been subliminally implied to mean matter (stuff) with an attached force or acceleration that we can experience and measure. In fact, mass in English means a body of matter, which must have been the initial intention of the meaning of this word in early physics too. However, the word means a constant of proportionality between force and acceleration in established physics. The ordinary meaning of the word mass is divorced from its meaning in physics. It remains a question if and what relationship exists between the ordinary meaning of mass (as matter) and its meaning in physics. If they are separate entities, we must say so or introduce another word for mass. Even the word “matter” is divorced from “ant-matter”, so that we have no word for the possibility of describing the “stuff” that may underlie both matter and anti-matter. We are prejudiced to accept that the cosmos exists in the form of matter or anti-matter. If we want to break away from this prejudice, then we need to clearly define mass, matter, anti-matter and the possible underlying substrate (or stuff) of everything. The easiest or practical way is to introduce a new term for this (so far hypothetical) substrate and continue investigating the true physical meaning of the existing terms of mass, matter and anti-matter.

We propose that an underlying entity exists universally and it is measurable. For this, we need an unambiguous word (term). The words mass and matter seem too worn out and confusing. Short of adopting the word stuff for this purpose as being too colloquial in the English language, we might want to resurrect the ancient Greek term of “*hyle*” per Wikipedia contributors (2022). Historically, the term *hyle* ($\nu\lambda\eta$) fits in perfectly well with our purposes. Let its symbol then be the letter upsilon \mathcal{Y} .

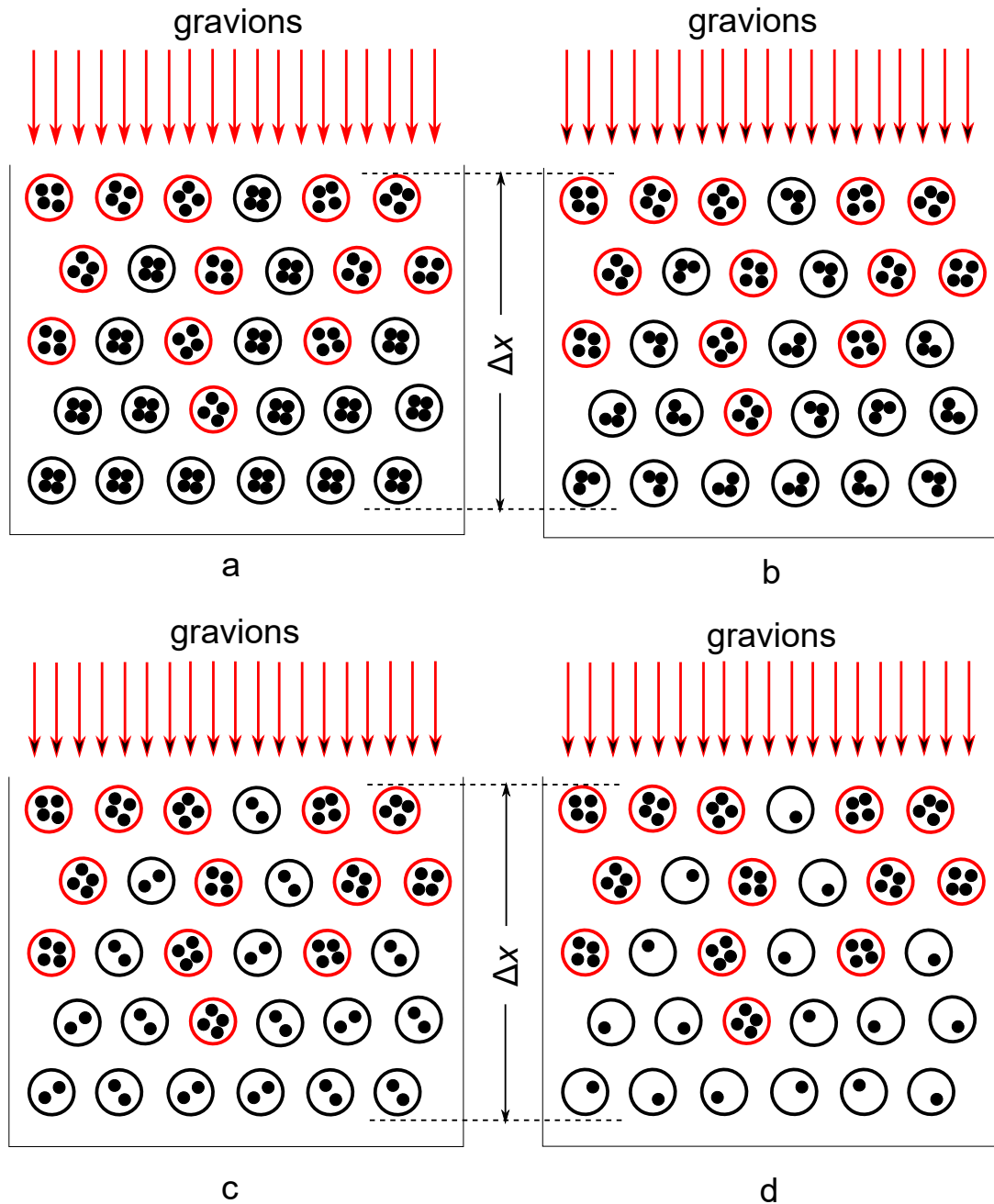


Figure 65: Macroscopic body: Effective mass as red circles, black mass as black circles and hyle (or matter) as black grains; arriving gravions combine their hyle with black hyle to create effective mass in various proportions per (b), (c) and (d) but have no hyle in (a).

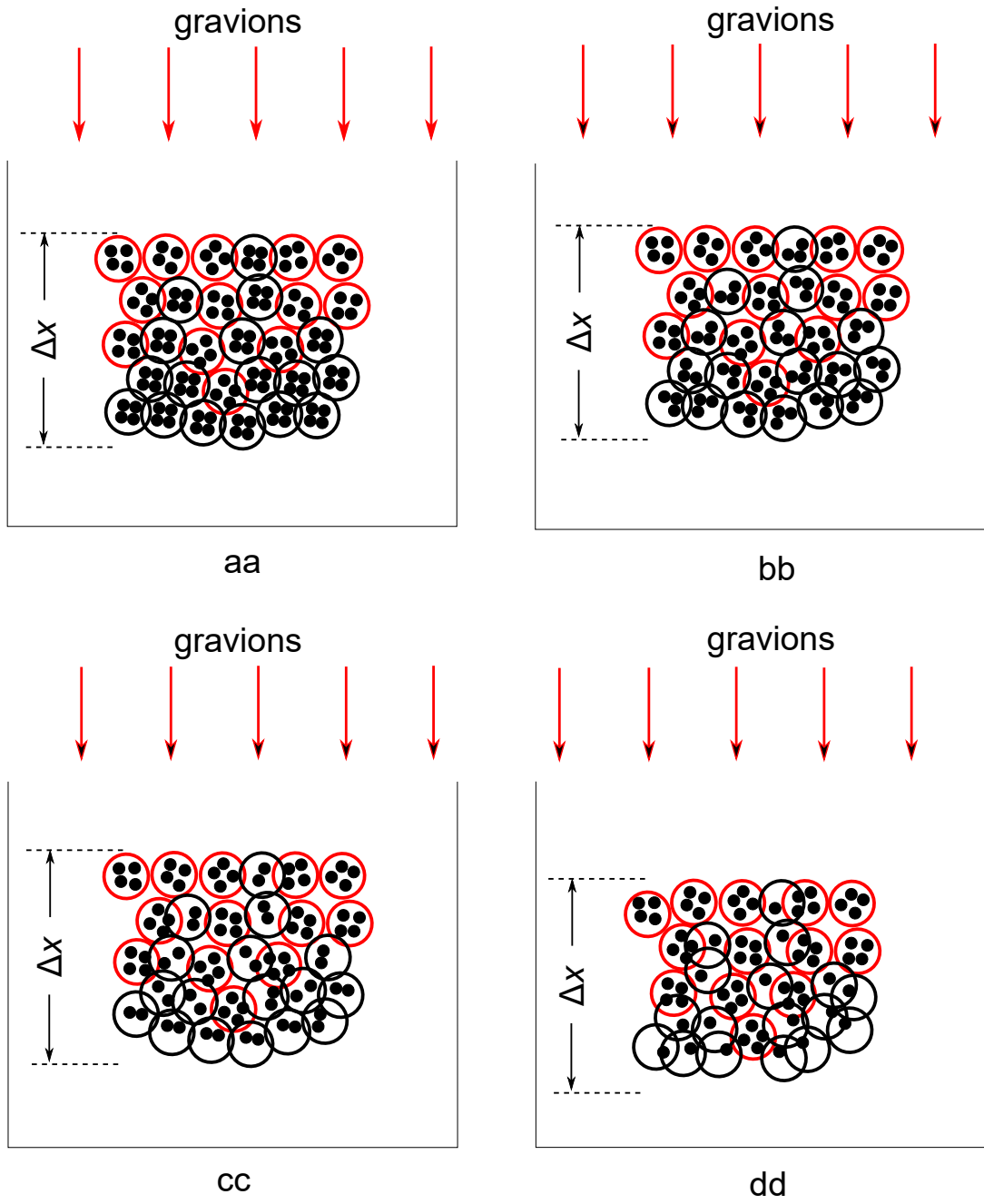


Figure 66: Fundamental body: Effective mass as red circles, black mass as black circles and hyle (or matter) as black grains; arriving gravions combine their hyle with black hyle to create effective mass in various proportions per (b), (c) and (d) but have no hyle in (a).

Whether we can identify the entity of hyle with one of the known quantities like energy, or the radiant flux of gravions Φ_0 , or some other remains to be seen. We don't aim to solve this fundamental question here, other than make an attempt to conceptualize a connection or relationship with mass as used in physics and in PG theory in particular. This is needed especially because we have often stated that *real-mass* is the substrate upon which gravions act (or being absorbed and released). It might be questionable that we allowed the word “mass” to be included in our terminology in the first place. This took place at the outset of our inquiry whereby we needed an absorbing substrate that lay dormant until it was activated by gravions to produce an effective-mass. It was clear that we referred to or implied a dormant mass waiting to be activated, so that it had to be a “mass-in-waiting” and we coined the term “real-mass”. Afterwards, we saw that it was the effective mass that had inertia, not the real-mass by itself. With that background and followup developments, we are in a better position now to make appropriate adjustments, which can maintain consistency with all our preceding PG findings.

To ease possible objections to our approach, we can say that the concept of hyle is not inconsistent with current theories. For example, one can continue stating that photons do not have a rest mass but at the same time we can also state that photons contain or are made of hyle. Photons is a mode of existence of hyle, like electrons are and so on and so forth. Energy is also a form of (or mode of existence) of hyle but we do not predispose ourselves on how to understand the connection between form and hyle yet. We have found that mass is proportional to the rate of absorption of energy or better, for a spherical body, according to Eqs. 196, 204 and 206

$$M_e = \frac{W}{4cg_0} = \frac{S_a}{4\pi\Lambda} \quad (420)$$

it is the rate of energy absorption/desorption per unit gravion-speed per unit of maximum-acceleration. This remotely resembles the original intention of the meaning of mass as matter, it is only a process riding on the back of hyle. We feel more certain to consider hyle as the underlying medium of that process and all other processes. This then may be the only way to strive towards a theory of everything. Hylism (= materialism) is set apart from dualism and idealism. If a theory of everything strives also to unify the cosmos, this can be conceivably achieved on the basis of monism as provided by a dynamic materialism. We consider this to be a sound basis of physics science.

We attempt to conceptualize and quantify the above approach via a series of diagrams. We assume that hyle can be quantified and quantized. In Fig. 65, we depict hyle with small black spheres (grains) each representing a single quantum or fixed multiples of quanta of hyle. The circles surrounding them depict the corresponding property of mass, which is either effective mass drawn in red color or black mass drawn in black color. Mass and hyle are thus separate entities but are interconnected via some process. This process for black mass is a deemed one, it does not exist yet, it is a potential or latent process in waiting until gravions are absorbed. The hyle with its red circle may be the minimum absorption (emission) center (MAC or MEC). For ordinary macroscopic bodies, these centers are distributed throughout and kept apart via the chemical structure of the body; hence they are shown at fixed separations uniformly. The MACs/MECs exist at subatomic level withing “elementary” particles. By “elementary”, we do not mean structure-less particles, in fact, we have proposed that conventional elementary particles are more likely to have structure (e.g. see our further electron modeling). We only wish to ensure that in this figure MACs do not migrate around the macroscopic body but kept apart via a given phase of hyle. They may migrate and redistribute themselves within each elementary particle. The effective mass is more concentrated toward the surface of the macroscopic body in the direction of incoming gravions; the representation is grossly exaggerated where black mass appears to be the only population after a certain depth. This is not the case with ordinary matter before some phase transition is triggered, say, to plasma phase. In ordinary matter the relative concentration of effective and black mass is not great enough as to induce a phase transition. This is a question to be taken up for what happens in stars and their cores, in white dwarfs and so on. We consider that the depiction of hyle in Fig. 65 is consistent with experience of ordinary matter up to the size of planets. At subatomic level, the situation is different as we will discuss in the next Fig. 66, with which we need to intermittently alternate to be able to convey our thinking.

Gravions travel in all directions but we have singled out only a net amount of them in a particular direction over an elementary depth Δx ; this fraction of gravions is responsible for the force exerted on the layer of hyle. If we wanted to calculate the total gravion absorption over the same layer, then we should have shown all gravions absorbed by the layer (energy is in the sum but force is in the net difference of gravions).

Referring specifically to the first diagram of Fig. 65a, we associate the same proportional amount of hyle to both effective and black mass, e.g four (arbitrarily) quanta (or multiples thereof) per MEC (in effective mass) or latent MEC (in black mass). The real-mass density is uniform throughout the body and corresponds also to a uniform hyle density. The real-mass is composed of the two fractions of effective and

black mass, each having their own specific distributions across Δx , for example, as they were determined in the preceding analysis for a sphere. For this case, the gravions absorbed do not alter the content of hyle but they somehow manage to activate the hyle hidden in black mass to hyle presenting as effective mass. In this case, the constancy (invariance) of hyle necessitates that the absorbed gravions have no hyle themselves. One might rush to suggest that they are “only energy without mass”, but such a statement is inconsistent with our initiated approach above. With our approach, we should state that gravions, in this case, must be of an entirely different entity of an entirely different nature without hyle; it is inconceivable (to us) that such an entirely different entity can interact with hyle, unless gravions and hyle have a common denominator via which they can interact. The situation of Fig. 65a is tantamount to dualism, which we have rejected. Further debate on this is left for general philosophy, or to other physicists who may like to take it up too.

As a result, the following three diagrams in Fig. 65b,c&d are the accepted classes of possibilities for our purposes. They all show accrual of hyle by the incoming gravions in different proportions, like 1:3, 2:2 and 3:1, i.e. all fractions greater than zero. The relative numbers of effective and black masses are all exactly the same as in (a) under the same uniform real-mass density. Each gravion conveys one quantum of hyle, which may combine with a certain number of body-hyle quanta, or one body-hyle quantum may combine with a certain number of gravion-hyle quanta to produce an activated center of mass; note that the arrowheads contain black color to indicate the conveyance of hyle, unlike the arrowheads in full red for case (a). It is unknown in what proportions of gravion-hyle to body-hyle the interaction forms activated mass. It is the task of particle physics to reconcile these proportions with existing data. We only propound the basis on which to proceed with PG when considering gravion absorption.

By the above scheme, we have the possibility (a mechanism) of maintaining the real-density ρ of a macroscopic body constant along with variable effective mass as that when we vary the distance between two material spheres per Section 16. The computations there were conducted under a constant k (hence ρ) and radius R for macroscopic spheres. We did not have re-arrangement of the fixed atoms, but we had a decrease of effective mass with a decrease of distance by way of radiation (or absorption) of hyle from within subatomic structures; by “radiation” we mean desorption of hyle and not necessarily radiation of electromagnetic waves. This variation of hyle might be experienced as radiation of mass or energy if our instruments were made to detect such signals and if they were sensitive enough. In any case, during this process, the real-mass remains constant but not the total hyle contained in the moving bodies. This understanding provides a great relief on possible physical processes involving the notion of constancy or variability of mass and hyle; real-mass enters as a parameter in our measurements during processes riding on hyle.

The situation is different at the subatomic (“fundamental” or elementary) particle level, as we try to depict in Fig. 66. MACs/MECs are created and redistributed inside a given particle with concomitant variation of the radius of the particle. We have used the same proportions of gravion-hyle combining with body-hyle in four cases corresponding to the four cases in the diagram for the macroscopic body. Case (aa) does not accrue hyle from gravions, it represents dualism and is not considered further. The remaining three cases (bb), (cc) and (dd) are possibilities to be taken into account. However, now both hyle-density and mass-densities are variable as they are free to re-arrange and re-distribute themselves within a variable radius particle while they are squashed close together as much as possible. This was the case when we attempted to build a proton from an electron in a series of exercises in Section 19.3.

We need to clarify that black mass (and its hyle) is not a “dead” entity. Only because it is shielded from gravions we call it “black” or inert relative to gravions. For example, see proposed modeling of electron in preceding and following sections. Black mass exists in its own world, it is just another mode of existence of hyle. The latter is necessary for the above modeling of mass and hyle. Black mass must be structured in self contained units and not in an amorphous agglomeration of hyle grains. In an amorphous black mass, gravions could be added or subtracted arbitrarily without any sensible outcome. To illustrate this point, black mass may consist of self contained vortices initially randomly oriented in a sphere. While they happen to absorb gravions, they could be oriented in the direction of incoming gravions, which makes them activated. As all the activated vortices are directed towards the center of a sphere, they exert a pressure keeping the sphere as a unified (integral) body. A vortex reverts back to the inactive state (black mass) as soon as it emits the extra absorbed gravions. That is why we have included “one” black mass circle at the surface in Fig. 65 to indicate the statistical nature of MACs and MECs and the dynamics of effective vs black mass throughout the entire body. We discuss in more detail the possible presence of vortices in the following section, but we need to move back-and-forth in our presentation to be able to convey our thinking. The hypothesis of vortex structures is not binding or limiting the PG theory, as other, more suitable, structures may be proposed later. However, the presence of some structure at the fundamental level seems inevitable for a consistent theory of PG. The conjecture of speed-mass relationship is thought of on the basis of a connection between speed and structure. It would be best if we could derive this relationship from first principles, from a synthesis

of acceptable relationships; the failure or success of our conjecture is only an initial tentative attempt and should not bear on the overall theory of PG (see also clarification at the outset of Part 2).

A distinction between macroscopic and microscopic (fundamental) level of hyle is critical in the development of PG. Failing to do this has led prior attempts on PG to failure or criticism and rejection. An initial step in connecting the two levels was made in Section 19.2 followed by various ensuing developments. Certain changes at the fundamental level leave the macroscopic body apparently “intact”, in the sense, for example, that its chemistry is conserved. It is analogous (not the same) with isotopes. The very high “thermal” energy absorption in PG that is feared to “melt” the planet instantly takes place within particles that are decoupled from the macroscopic observable properties. They do not melt. As explained in Section 15.8, the second thermodynamics law need not be violated either. The absorption takes place at the MAC level passing through “all” states over a very short time during which there is a favorable state capable of emitting the absorbed energy via another non-gravitational particle. This is allowed (or expected) by the fluctuation theorem. The second thermodynamics law is complemented by the fluctuation theorem law. This consideration is not more untenable than similar prevailing theories of “vacuum fluctuations”, etc. These are steady-state processes at the microscopic level of a stable macroscopic body. The above description explains the main possible process, which may not be the only (100%) one. There may be a statistical smaller amount of emissions that couples with the macroscopic body and result to a certain degree of heating, which may be exactly the internal heating of planets (in part also of stars, etc.). An analogy may be seen with electromagnetic radiation of a given wavelength being reflected by a body at a different wavelength with some remnant amount of heating. With gravions, the analogy differs by way of quantity (intensity) and quality (type), i.e. by way of one field converting to another as described in preceding sections.

The distinction between macroscopic and microscopic levels applies not only to ordinary bodies (planets, etc.) but also to stars, white dwarfs, neutron stars, etc. Only at the stage (phase) of black holes macroscopic and microscopic levels may coalesce, but can only vaguely be described at present. We need firmly develop a sound and consistent PG theory for most of the other phases before we venture into the ultimate structure of fundamental particles and black holes (likely to be similar). We cannot do this here.

The above convey only a minor part of the big picture, because the electrical mass (charge) is not sacrosanct either. We should draw similar diagrams for the electric field and electrions. Therefore, based on the materialist approach, we should associate hyle to the electrical mass too. This should be many orders of magnitude more than the amount of hyle associated with gravitational mass. We say the same for other types of mass (if any) corresponding to other force fields. On this basis, we now better understand that the decrease of effective mass towards the center of a macroscopic sphere is accompanied (or complemented) with an adjustment of electrical mass in the fashion envisaged by prior Fig. 41. The variations due to gravion flux may be negligible in comparison with the levels of electrion flux. In other words, the variation of gravitational mass is negligible relative to the absolute levels of electrical mass on which the said particle or body is structured. That is, we should not be misled by the exaggeration depicted by the provided qualitative diagrams. We need to combine both gravitational and electrical masses to convey the full picture of hyle, which is impractical to perform by gross diagrams. We need a rigorous mathematical description of both electric and gravitational fields individually and in combination as the best way to unify them. Clearly, this can be done in future work, while we only attempt here to lay the basis for further developments.

In unity, all types of mass ride on the substrate of the entire (total) hyle. In working out various relationships for the gravitational field, we may have, at some point, to consider concurrently also the presence of electric field while we introduce and quantify the total hyle involved. It is often said that “only about 5% of objects is stuff while the rest is energy”. However, the issue of stuff is sidelined, or muted, nothing is said about it, it is left to subliminal conceptions of the reader. This may be because the theory is based on mathematical deductions with no substance ever coming into play. Physics has been reduced to subjective mathematical idealism. It is well overdue to restore physics to its objective basis. PG provides this opportunity. In any closed system, the total hyle is conserved. Hyle must be the first and foremost entity that is conserved in the universe. Hyle exists in motion. The conservation of momentum and energy are different expressions in the form of measurable parameters (quantities) of the conservation of hyle. Hyle is the common quantifiable thread unifying our mathematical descriptions of the universe. This is how we envisage the possibility of arriving at a theory of everything.

We may establish a relationship between real mass and hyle following an analogous approach to the exercises for building a proton from an electron in Section 19.3.3. We always have the equation $m = m_e + m_b$. With the help of the diagrams in Figs. 65 and 66, we note that the number of the total circles (red and black) represent the total (real) mass. The total of the contents of these circles represents the total amount of hyle \mathcal{Y} , which depends on the mixing parts of gravion-hyle x and parts of black-mass-hyle y producing $x + y$ parts of effective-mass-hyle. The ratio $(x + y)/y$ is the factor by which the effective mass apportions hyle over and above the hyle apportioned by the black mass. If we denote by $C_{\mathcal{Y}}$ the amount of hyle per

unit of black-mass, then the black-hyle $\Upsilon_b = C_\Upsilon m_b$, the effective-hyle $\Upsilon_e = C_\Upsilon m_e(x + y)/y$ and the total hyle Υ is:

$$\Upsilon = \Upsilon_e + \Upsilon_b = C_\Upsilon \frac{x + y}{y} m_e + C_\Upsilon m_b \quad (421)$$

Referring to Figs. 65 and 66, cases (a) and (aa) have $x = 0, y = 4$; cases (b) and (bb) have $x = 1, y = 3$; cases (c) and (cc) have $2, y = 2$; and cases (d) and (dd) have $x = 3, y = 1$. For cases (a) and (aa), the above equation reduces to:

$$\Upsilon = C_\Upsilon (m_e + m_b) = C_\Upsilon m \quad (422)$$

stating that hyle is simply proportional to the real mass. At the outset we suggested that real mass may be the substrate or matter by which gravions are absorbed to create the effective mass portion of the total real mass. It was implied (intuitively) that $C_\Upsilon = 1$. All our hitherto equations involving the various types of mass are valid. We now extend the meaning of mass as corresponding to a certain proportion of hyle being the actual substrate upon which the gravions act. That is, we now shift the substrate to be a separate entity, of which mass is one property. That is, if we want to accept and adopt the materialist basis of cosmos, then we need to introduce hyle and liaise it to real mass in accordance with the Eq. 421, where the fraction $(x + y)/y$ remains to be found; it must comply with experimental data from various fields of physics.

The meaning of mass has been deciphered by the "Novel quantitative push gravity/electricity theory poised for verification". The gravitational constant G is redundant. Thus, "stuff" and mass are not the same thing, nor are they proportional to each other. This theory seems consistent with Higgs's ideas in some respects. We can establish some correspondence between the two: Stuff (now termed "hyle") by itself has no inertia or mass until it is activated by gravions, the underlying (creator of) field stuff (hyle); compare this idea with the contemporary idea that "the field gives mass" (we now say that the gravions give mass to hyle). We now have a tangible understanding of mass, field, and hyle.

In the light of these developments, it would be necessary, when we will re-write the PG theory, to take care to maintain consistency of terminology both within the theory and as much as possible with established terms in physics. For example, to avoid a re-write of the term "mass" in established literature, we can identify it with "effective mass" in PG, and so on, namely,

mass \equiv *effective mass*

real mass \equiv *hyle*

hyle minus mass \equiv *inert mass* \equiv *black mass*.

24.3 Continuation from Section 23.4

Equipped with the lessons above, we can now supplement the discussion in Section 23.4. In the case of acceleration during free fall (i.e. not involving an electric field as in rocket acceleration), we have computed the variation of effective mass m_{er} with distance r between two spheres. As one sphere is shielded by the other, it is like being an internal sphere but only in part; there is only a partial directional shielding of the gravion flux, not a complete shielding around a full 4π solid angle as in Fig. 58a&c. The computation of static m_{er} was correctly performed under a fixed external k for a fixed real density ρ . Static m_{er} decreases according to the finding for a two sphere system with concomitant increase of black mass so that their sum $m_r = m_{er} + m_{br} = m$ remains constant in the static situation. However, the corresponding (static) total hyle varies in accordance with Eq. 421. As the falling sphere acquires a speed, kinetic effective mass is added according to a conjectured relationship per Eq. 311, by which we have to make further assumptions about how this happens. If the kinetic effective mass is created by absorption of extra gravions from the direction of fall activating black mass, then the total (composite) real mass must remain also constant:

$$m_{rc} = m_{erc} + m_{brc} = m \quad (423)$$

It remains to be found about how hyle varies during fall. In contrast, during rocket acceleration, the accrued kinetic effective mass could originate from absorption of electrions, which themselves may be agglomerations of organized gravions, such as vortices (see next section); then we may have a net accrual of real mass via the electrion absorption and an absolute accrual of hyle during rocket acceleration.

Returning to the case of falling acceleration per above equation, an adjustment of the variation of masses is required in related figures, e.g. Fig. 46 and others. Still, a difficulty (or question) arises from the use of a kinetic mass formula per Eq. 372 pertaining to spherical symmetry of absorption, which seems not to be the case for a falling sphere. It may be that our conjectured mass-speed relationship should be based on the absorptivity of a material-line per Eq. 184 or a thin-rod aligned in the direction of velocity. This would require a repetition of computations to establish all related parameters for a thin-rod in lieu of a sphere

in future work. Until then, we draw attention to certain deficiencies of some of the preceding results. The variation of real mass was intriguing for some time leading to the current valuable investigation of internal parameters and the introduction of hyle. The variation of m_{er} as plotted is correct and a variation of m_{erc} is subject to a re-appraisal of the mass-speed relationship. From these variations there exists an emission of hyle instead of real mass, which yields an equivalent outcome to what we subliminally perceived via a loss of mass. The distinction between mass and hyle is a key issue. Pending proper rectification, we leave those graphs unchanged as they may also help a discussion and a deeper understanding of all the issues involving mass and now hyle.

24.4 Internal vs. external parameters (variable real density)

Work to formulate the problem of external acceleration from two concentric spheres with different densities was presented in Section 10. We should examine the variation of internal properties for that case too, as well as for the general case of a sphere with spherically variable density (i.e. as a function of radius). We need to establish a set of theorems governing all parameters involved. This investigation is left for later work due to other work constraints by this author. Other workers are welcome to make a contribution in this or related area too.

The heliosphere would be a practical application of that study. We have speculated on the influence on elliptical orbits of planets and Mercury above based on the finding for a uniform density of the sphere. With some reservation (until rigorously proven), we might qualitatively accept the same consideration for a variable density heliosphere. We might consider that the hyle above the aphelion and below the perihelion would have some equivalent effect of some equivalent uniform distribution, so that only the variation in the layer between aphelion-perihelion would make a quantitative difference; the latter is thought to be very small, but it could become conclusive when this is computed rigorously.

25 Further electron/positron modeling

In view of the preceding sections and analysis, we can discuss various possibilities and draw some important corollaries below. The accrual or diminution of real mass during acceleration and deceleration may not be properly explained without a concomitant understanding of the structure of material particles. The latter can be achieved by progressive modeling in continuation from the general proposal in Fig. 40.

First, we outline the general background on which all such modeling may be constructed. If accrued real mass (effective plus black mass) is a function of speed and vice-versa, then we can have a tangible interpretation of the kinetic mass concept. We have learned that effective mass is proportional to the energy rate of absorption that is proportional to the rate of gravion absorption. Furthermore, if gravions are thought of as particles of a gas (or aether), then we have two distinct possibilities regarding the distribution of gravion speeds:

(a) They all have the same constant speed as opposed to a Maxwell–Boltzmann distribution of molecular speeds in a ideal (classical) gas. That is, we consider gravions belonging to a “monochromatic” gas, for which we may derive corresponding relationships between the gravion speed and the propagation of a disturbance (or excitation) speed (like sound speed or light speed). In that case, we expect the (individual) gravion speed to be greater than the propagation speed (presumably c) by some factor to be worked out later. For example, this factor is $5/3$ for monatomic gases using classical mechanics but relativistic effects, if applicable, may also be taken into account. The important idea here is that each gravion has a dual nature of “body” and “speed”. The body-and-speed are integrated in a single entity to what makes a gravion. That is body-and-speed are objectively inseparable.

(b) They have some characteristic distribution of speeds (not necessarily Maxwell–Boltzmann). Such a possibility means that gravions are entities capable of exchanging and/or transferring speeds during interaction between them. If the “body” is invariable, then the speed must be variable. The variable speed might be continuous or discontinuous (quantized). The speed is some sort of a separate entity that can be exchanged and/or transferred from gravion to gravion. Hence, we have to accept a dual nature of matter but with separable entities of speed and body, each having its own “nature”.

The combination of having a variable body with invariable speed refers back to the first possibility by “sticking” the two gravions together (somehow) or getting them to move parallel and very close to each other. Otherwise, we would have fractional gravion bodies sticking together, a combination that we will not be dealing with here. The combination of having both a variable body and a variable speed refers back to the second possibility, because if the two gravions stick together to vary the mass but have a different speed, it means that the speed is a separable entity. We think that we could adopt either (a) or (b) of the above possibilities among other combinations that might also be proposed.

Those two possibilities lead to the dilemma about the deeper meaning of “body” and “speed”. We prefer to adopt initially the first case (a) and investigate the consequences. If not satisfied, we can always return to case (b) accordingly. The reason for opting to examine the (a) case first is because it offers a common denominator of the smallest quantum of matter, namely, the moving-gravion with an overall (integrated) invariable identity. A moving gravion then represents a quantum of momentum (impulse). In other words, momentum is quantized and the minimum amount is that of the moving gravion. The duality of its nature is inherent in the gravion from the outset of the theory. Then, we are left with the task of modeling the gravions in building other push particles, conventional particles and material bodies (forms of matter) in general and ultimately the cosmos. This is the subject/task of subsequent developments in PG. We only initiate some preliminary ideas.

Based on the above choice, we can arrive at a better understanding of the nature of effective and black mass. We have said that effective mass is the activated part of real mass and black mass is the inactive (inertia-less) part with “true” zero classical inertia and zero energy. This might seem to demand that we choose the second possibility (b) rather than the first (a) per above, because only then could we achieve gravions with zero speed (at rest), presumably packed with maximum density inside a black hole. In contrast, (a) demands that we would have highly packed gravions incessantly moving/colliding with each other at an extremely high density. The latter density could never reach the theoretically limiting density of gravions at rest. Essentially, we would have a medium of moving gravions with an extremely high density flux J_{black} of black matter. In the case of a black hole, this would be enveloped by an effective mass layer (the event horizon) separating it from the surrounding field created by push particles of type-x, with a density flux J_{0x} . To maintain the black mass core stable, it would require that $J_{0x} > J_{black}$, which is overall inconsistent with black mass having the highest possible density. However, the latter inconsistency can be resolved as follows:

Two gravions may be considered at rest relative to each other if they happen to move in parallel with the same velocity, the presumed fixed gravion velocity. Similarly, we may consider a swarm of gravions moving parallel with each other in a stream inside the surrounding chaotically moving gravions of a generally static, on average, gas. In this situation, we can invoke the classical gas dynamics laws. A static gas is characterized by a static pressure, whereas a gaseous stream is characterized generally by both a static and a dynamic pressure. For example, a gas flowing through an aperture from a region of high pressure to region of low pressure generates a jet (stream) whereby the chaotic molecular movement is converted to orderly stream movement. The static pressure converts to dynamic pressure during expansion. If the low pressure region is a vacuum, the gaseous stream passes from subsonic to supersonic velocity and finally to hypersonic and beyond velocity when all static pressure is converted to dynamic pressure. This is how a molecular beam is formed. Linear streams of gravions inside a surrounding static gas of gravions must be enveloped by a layered transition zone of gravions flowing with increasing order (uniformity of velocity) towards the axis of the stream.

Linear particle beams having a finite length would be rare and cannot contribute to building stable structures. However, with certain conditions present, it is possible to form circular streams of particles in the form of a vortex. Thereby, gravions in such a vortex are drawn from the periphery towards the axis and flow out along the axis in two opposite directions, like a double cyclone, back-to-back, in space. This provides a good scheme of a structure acting both as absorber and emitter, with which to simulate our MAC and MEC concepts. By such means, we can also describe the behavior of a rotating black hole in the shape of a disk, ellipsoid, sphere or shaft. In principle, we can have gravions at uniform (constant) velocity with increasing angular velocity inversely proportional to the radius from the axis of rotation. That would be the state of black mass, namely, a fluid with nearly all (or mostly) dynamic pressure and only a vanishing static pressure towards the axis. This is then the black mass that is enveloped with a layer characterized by a fast transition between dynamic and static pressure. This layer constitutes the event horizon that should be amenable to quantitative analysis to fit the best observations available by astrophysics. In such a model, the interior of black holes may then look like laminar flow but with vanishing low friction towards the axis. Because it is completely isolated from the outside push particles of various types, it presents no inertia to the outside world but maintains a huge amount of dynamic (latent) energy stored until it can be released during a black hole disintegration (explosion). In other words, black mass is still thought to be classically inertia-less but with “zero-point-energy” being the zero static energy (pressure) coexisting with latent dynamic energy due to the dynamic pressure of the rotating gravions. The latter description may bring PG close to current understanding of super-fluidity based on QED theory. Questions about the shape of a black hole, like spherical, ellipsoid or disk, should also fit available data. This in principle description of a black hole may also explain the accrual of real mass from equatorial periphery and emission via the polar regions in the form of hydrodynamic jets.

By similar means we may be able to describe also the structure of some elementary particles like electrons

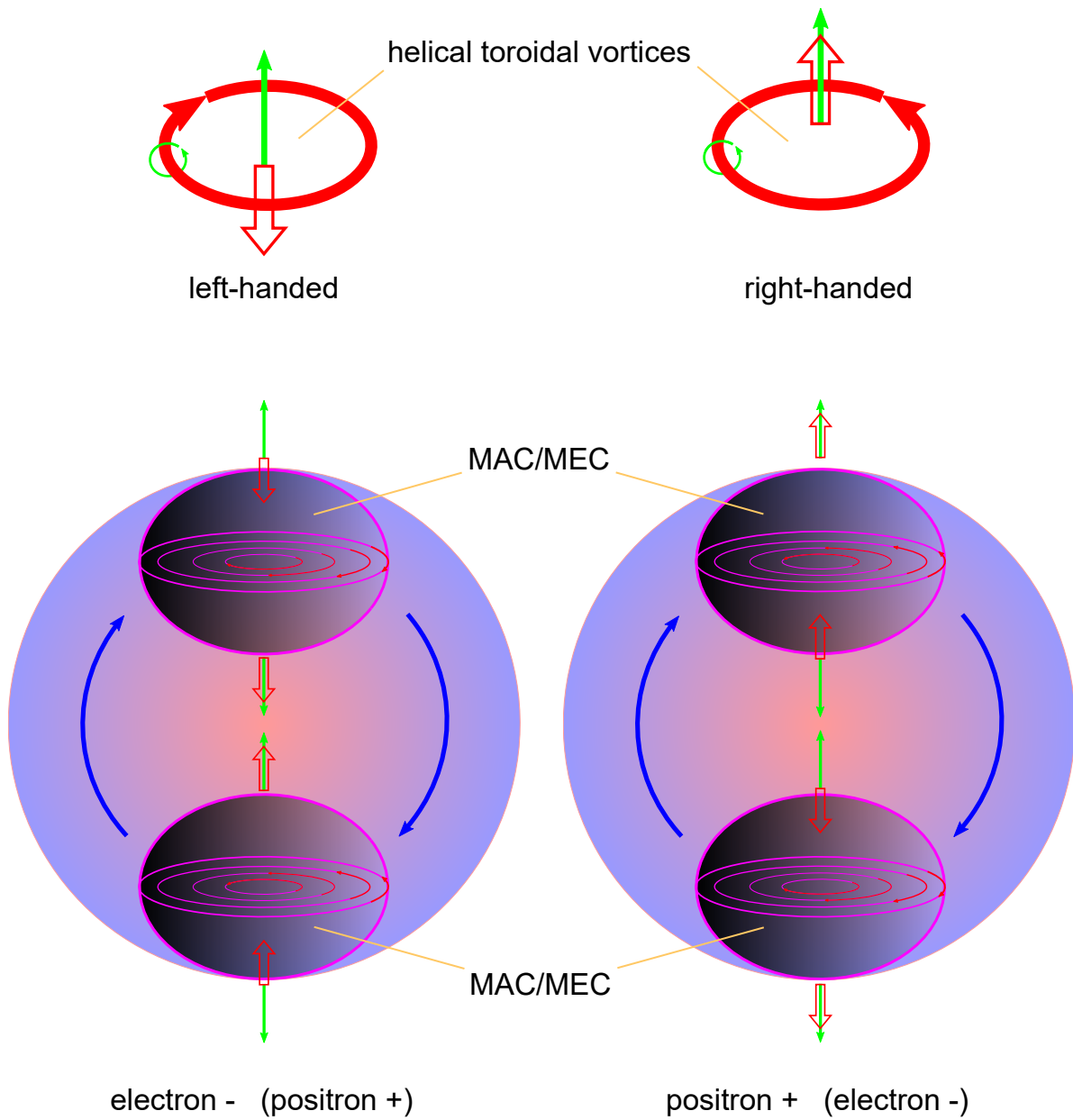


Figure 67: Pairs of MEC (MAC) at fixed distance and spinning in opposite directions emit outwardly either left-handed or right-handed helical toroidal vortices as negative or positive electrons; minimal structure for the electron and positron.

and positrons. They do not necessarily have to be exactly like the above hypothetical structure of a black hole. What we need is the application of Bernoulli law in analogous situations of gas and liquid flows of ordinary matter. In fact, there is a variety of forms of flows, from which we may use those that yield structures and properties consistent with particle physics data. Lord Kelvin (1867) already attempted to describe the structure of atoms with toroidal vortices. In fact, this trend continued for decades culminating to a description of chemistry (atoms and molecules) based on vortices until 1915 (Parson, 1915) before modern ideas prevailed to date. We do not propose to revert back to Parson's chemistry, but we can attempt to follow a similar path for the modeling of elementary particles, which are considered to be structure-less by prevailing theory. Such an approach is particularly promising under our platform of PG theory. Key to those old theories was a conceived stability of toroidal vortices to the extent that they could form permanent structures of matter, like atoms and molecules. On these principles, Papathanasiou & Papathanasiou (2020) have proposed a theory of everything based exclusively on "*stable ring-shaped cyclones within the pressure field of a universal ideal gas*".

For our purposes, we need not restrict ourselves to the use only of Kelvin's vortices, but also consider a great many variations of similar structures based on dynamic flows. For example, Consa (2018) has proposed a new semi-classical model of the electron charge with helical solenoid geometry. In lieu of such a charge distribution, we may assume real matter distributions of the same or similar form. Thus, in PG we may consider the "ring electron model" and the "helical solenoid model" combining toroidal and poloidal currents of gravions or other push particles in fractal layers. The number of fractal layers will be determined by the needs of a PG model replacing the Standard Model but consistent with existing data.

Our general proposal here is a combination of (a) uniform forms of flow of particles with (b) chaotic push particle flow inducing gravity and/or electricity. That is, specialized flows of push particles constitute the fundamental structures of matter and material fields, all immersed inside superstructures of matter propelled by pushing fields of various types.

We attempt to use these ideas in further modeling the positron and electron shown in Fig. 40. If Kelvin's vortex atoms did not prevail in the understanding of structure of atoms and molecules, or for being the panacea for "everything", similar structures seem plausible and appealing for substructures of elementary particles on the platform of PG. In particular, they could be the key for subatomic structures and more so for the structure of the electron and positron, in particular. That is what we propose now in more detail by Fig. 67. This is an early attempt to take advantage of a helical-toroidal-vortex flow, which could embody the presumed positive and negative attributes of electrions. We are not aware of extensive research on such flows, but it seems that they can form stable entities behaving like particles. Plain toroidal vortices may bounce off each other or merge, and various observations have been made with smoke ring guns. The helical toroidal vortices are rotating vortex rings around the axis of the ring. All vortices propagate along the ring axis in the direction of the central flow of the torus. A helical toroidal vortex can be formed by a rotating "smoke ring gun". In our case, we could postulate a spinning body (like a neutron star, black hole or electron) pumping out material in the form of rotating toroidal vortices from its poles. Discrete vortices would be emitted by a pulsating spinning body. Now, the material coming out of an electron could be rotating vortices of gravions. Such hypothetical entities would fit the requirements of electrions. They can be right-handed (or positive +) when the vector of velocity points in the same direction as the vector of rotation, and left-handed (negative -) when these vectors point in opposite directions with each other. Also, we may posit the existence of at least two MACs acting also as MECs. Somions are absorbed by each spinning MAC while concurrently acting as MEC emits positive electrions from one pole and negative electrions from the opposite pole. The pair of MECs (MAC) shown in the figure are disposed in opposition along their axes, so that they always emit the same type of electrion outwards from the electron or positron. Now, what happens to the same type of electrions emitted in-between the oppositely spinning pair of MECs is a matter of conjecture for now: We suppose that they repel each other if they happen to collide or are reflected if they happen to strike the other MEC across. We have said that the mean free path of electrions should be very long relative to atomic scale, but if the pair of opposing MECs are practically aligned along their common axis, then the question is reduced to the statistics of this alignment. We can safely assume that there is a wobble between these axis so that the probability of collisions between electrions in this confined region between MECs may allow a degree (rate) of collisions. Leaving quantification of this question aside for now, we may qualitatively say that there can be a net repulsion between the pair of MECs due to net statistical bouncing of electrions imparting a net momentum in an outward sense. However, this outward force is counter acted by the surrounding somions imparting a gravity-like force in the opposite direction. We have said that somions may act like the nuclear force in atoms, so that they may also act in a similar manner in keeping the two MECs together inside an electron or positron. This situation then poses the question of stability. Do they move like in a binary system or do they require a stabilizing third body or more bodies to be present? We cannot address this question, until we earnestly attempt to quantify all these

and other processes that may be present. For example, we may not exclude the presence of other particles contributing to the overall structure and stability of the electron (positron). We may be able to compose a minimum structure of particles acted upon by somions and gravions, and rotating in conformity according to classical laws or other laws as needed. By such methodology, we may be able to explain also the proton, which could be composed like a positron but with additional matter (real mass) of other stabilizing particles. Likewise we could build the neutron.

25.1 Discussion

The possibility of existence of the above structures for electrons and positrons may be questioned, since we have not considered detailed mathematical or experimental evidence to support such claims yet. However, the main purpose now is to initiate thinking in this direction for possible working structures. We have already discussed some questions above, but others may be equally or more important. ~~For example, it important to explain why the electron is stable but not the positron on account of their equivalent structures. The stability of proton might give us a clue.~~ For now, gas and fluid dynamics with emphasis on the above special flows seem to constitute important tools for the development of a complete PG theory. Recent work has applied these tools to quantized superfluid vortex rings in a Fermi gas (Bulgac *et al.*, 2011), and to planetary atmospheres and vortex movements in the vicinity of active galactic nuclei (Bannikova *et al.*, 2016). Also, a recent overview has been provided by Falconer (2019). Furthermore, computational simulations of gas flows like that by Bird (1995) could become indispensable tools in the study of force fields.

The possibility of making material structures and particles by way of various forms of circular motion from the chaotic random motion of particles opens a new way to study and understand cosmology. Early glimpses of this can be gathered by some direct quotations from Bulgac *et al.* (2011): ...*“A notable property of superfluids is their ability to sustain quantized vortex lines (3, 4), which, unlike classical hydro-dynamical vortices, have a quantized velocity circulation.... Abrikosov predicted that many quantized vortices self-organize into a triangular lattice (6)... In excited superfluids, vortices have a complicated time evolution; they cross and reconnect, a process extensively studied in Bose superfluids, which leads to quantum turbulence (9) and which, unlike turbulence in classical hydrodynamics, is realized basically in the absence of dissipation.”... A spherical projectile flying along the symmetry axis leaves in its wake two vortex rings.... Moreover, the system organizes itself in an almost perfect vortex lattice after the stirring is turned off. Even more surprising is that the system remains a superfluid, even when stirred at supercritical speeds“...*

It seems that we can have a better understanding, or more options in the behavior of an electron. This particle can easily appear in different modes of existence when free and when it is bound in a atom or molecule. Consa’s deterministic description of the orbital electron is helpful to conceive an upgraded structure: Whereas he describes the electron as helical toroidal vortex comprising toroidal and poloidal currents of charge distributed around the nucleus of an atom, we think that this may be the locus of trajectories of a single electron moving around the nucleus. This would resolve the huge discrepancy in the size of an electron between the two models, namely, Consa’s electron having the size of an atom (i.e. its orbital), while we may have a much smaller size between $10^{-22} - 10^{-23}$ m (per preceding findings) moving along Consa’s trajectories. Alternatively, we can go along with the quantum mechanical description of the electron orbital but again as being the probability of locating our PG electron inside such an orbital. In both cases, we maintain that the electron is a very small particle in motion around the nucleus in one way or other, but neither a QM continuum (wave cloud) nor a helical solenoid continuum of electrical current. We do not need to invoke the electrical charge as a distinct entity. Fractalization may also be taken into account to devise structures at various levels, like “*heavy solitons*” shown to be vortex rings Bulgac *et al.* (2014).

The notion of quarks may be compatible particles per above: Quarks may be combinations of MECs (MACs) in such a way that we may bridge experimental data with our theory. For this purpose, the electron model proposed may be a model for each quark existing in stable triplets. or having three pairs of MECs in some alternative stable configuration. Furthermore, the display of *zitterbewegung* at the Compton scale may also be exhibited by modeling around the proposed scheme in Fig. 67, which may also be consistent with certain QED aspects.

The proposed electron/positron model may help understand also the connection of accrued mass with the speed of a moving body. It is challenging to attempt to understand the mass-speed relationships proposed and to attempt to conceptualize the situations depicted in Figs. 41, 42 and 67. A moving body with constant speed relative to the gravion frame of reference is acted upon by a null total force, which can take place only if the rate of gravion flux from the advancing is the same as from the receding direction of motion in order to avoid drag. The effective mass of the moving body is greater that the effective mass at rest, whereby the extra effective mass is accrued during acceleration by the action of the rocket in Fig. 42. This is obtained by the excess rate of electrions absorbed from the receding direction via a process yielding an increment

of both effective and black mass in the accelerated body. As soon as the rocket action ceases, there is a new steady state equilibrium of gravion absorption with the surrounding flux density J_0 . An observer inside the famous “accelerated elevator” would report a real mass injection apportioned between the effective and black fractions, if the observer could detect push particles and monitor the building grains of matter. The elevator is integrated with the rocket body-with-fuel (elevator system) while the ejected propellant causes the excess electrons to accelerate the elevator system. A stationary observer (outside the elevator) with similar capabilities of detection would observe both the accrual of mass and the displacement of the elevator system. During deceleration via a rocket system again, the ejected propellant travels in the advancing direction with additional mass imparted from the stored excess mass in the rocket system. The accreted mass is preserved at constant speed without affecting its chemical constitution but the atoms become more massive in the form of extra effective and black mass.

The above description might spare us from the “twin paradox” and other effects now not necessary to address. However, there may come a point at sufficiently high speed when matter has to transform to another phase: Atoms may become plasma, then neutrons, then black matter and whatever transpires in all possible transitions. Our traveler inside the gedanken elevator would see those transformations provided consciousness survives beyond matter transformation. Such may be the fate of a falling body into a black hole.

Prior to any presumed phase transition of matter, the moving body must acquire some fundamental variation of structure at sub-elementary level that distinguishes it from its stationary state structure. If the chemistry is preserved, then some attribute may vary at the subatomic level over and above a plain quantitative accumulation of matter, and in a way that is reversible during deceleration. This may involve, for example, an alignment of the spin of MACs and MECs, in a fashion similar to nuclear magnetic resonance (NMR). The pushing particles in a particular direction of motion might provide the mechanism of alignment for a fraction of the total composite mass. The so “aligned” fraction of mass may coincide with the kinetic mass. By such or similar means, a moving body would be distinguishable from a stationary one by all observers, i.e. stationary or traveling with the body. Kinetic mass may be the distinguishing feature of a moving body. Therefore, further examination of the definitions in Table 27 may contribute in the modeling of matter at the fundamental level.

The circular movement of matter at the smallest and higher fractal scales is compatible with black mass, effective mass and push particles of gas-like media, such as gravions, electrons and somions. These is a continuous interchange of matter between its various forms. It seems that the classical “flux” of fields is an actual physical event of push particle flow: The magnetic flux in a solenoid, the electric flux from positive and negative charges and the gravitational flux are all representing a flow of material particles, all of which we think can be finally reduced to gravions.

The equation $E = mc^2$ holds quite well in transforming potential energy to mass, or (better) potential mass to kinematic mass when applied to very high density mass. Furthermore, PG reveals a wider range of mass types, the conversion of which via that equation yields outcomes that we may not experience directly in conventional physics, like the heat-pump effect (principle) applied between force fields, like electrical and gravitational fields. We can now close the energy-mass balance sheet properly. The “invisible” black mass is part of the total real mass equation that is absent in prior theories and practice.

The connection of motion to structure may be a way to make progress in understanding space-time, the dynamics of PG and the connection between speed and mass. The vortex structure may be at the basis of this hypothesis. A minimal effective mass may be that of a MAC/MEC. By way of illustration, we might simulate a moving vortex to a jet engine. In a stationary sphere, the effective mass is spherically distributed with the statistical average of the vortex vectors all pointing towards the center of the sphere with zero net sum. When the sphere moves, we may have a partial alignment of the vortices along the direction of velocity. A one-to-one correspondence exists between velocity and kinetic mass, which is composed of aligned vortices. This is one example of connecting speed to structure. We might find alternative and better structures for this purpose. This approach opens new vistas for experimentation and/or theoretical work. For a deeper appreciation of this proposal, we may quote from Feyerabend (2010) again: “*The consistency condition which demands that new hypotheses agree with accepted theories is unreasonable because it preserves the older theory, and not the better theory. Hypotheses contradicting well-confirmed theories give us evidence that cannot be obtained in any other way. Proliferation of theories is beneficial for science, while uniformity impairs its critical power. Uniformity also endangers the free development of the individual*”.

25.1.1 Lord Kelvin’s vortex atom

While the proposed model for electrons and positrons is admittedly speculative, its adoption entails a similar description for related particles like protons, neutrons and photons. This might trigger further ideas with regard to important unsolved issues in physics. The vortex modeling of electrons composing electrons, if

also used for other particles, may usher a novel perspective for understanding and explaining phenomena like the slit experiment and quantum entanglement.

Vortex in lieu of “wave packet” is our proposal herewith. It is the constituent building block of “particles” such as electrons, protons and photons. The particles (excitations) of quantum field theory are now thought to be composed of other real entities. The vortex exists in 3D space and can yield the wave-forms we experience upon its interaction with (or incidence upon) surfaces. This may also seen as “collapse” of the vortex upon a “surface”. The latter may correspond to the “collapse” of the wave function of quantum mechanics upon measurement (detection) of the particle. Lord Kelvin described the atom by way of a vortex as shown in Fig. 68. This is a copy-paste from his original paper, where we have added an arrow to indicate the direction of propagation. It is a traveling entity at high speed c , not a stationary atom envisaged by Kelvin; this is similar to the rings of air shot out of [vortex cannons](#). Atoms and molecules have been described very well by modern quantum theory, which is by no means challenged and its successes are not disputed. We only shift the Kelvin model to describe entities many orders of magnitude smaller than the level of quantum mechanics.

We have (tentatively) identified the electrion to be a single traveling Kelvin vortex. We have further used a combination of vortices to describe the electron and positron. Appropriate combinations may be devised to describe the structure of protons, neutrons and photons, some more complex, some rather simpler. We are only taking one step towards attributing some structure, about which [Dehmelt \(1989\)](#) felt compelled to surmise.

Kelvin’s schematic complements our visualization of a possible reality. The “particle” of an electron or a photon is not one homogeneous individual “particle” in the customary sense of the word. It is the sum-total of the synergy of sub-processes involving a huge number of other much smaller entities, like electrions, which are further made up by even smaller entities (perhaps, the gravions). Vortices form over a relatively extended space (albeit extremely minute to us). This possibility can readily explain the phenomenon of duality, i.e. of “particle” and “wave” exhibited by the same “particle”. By such means, we may better envisage the possibility of an electron or photon going through a double slit “simultaneously”. That is, it is not a single “particle paradoxically” passing through both slits, but parts of what appears to us to be a single particle. It remains to explain how these parts of the particle simultaneously “excite” or trigger the slit surfaces to reproduce the “particle” on the other side of the slits. The waves, in general, that we experience are inherent in or part of vortices. The wave interference of light that we record on a screen behind the slits are the outcome of the incidence of more complex entities, such as vortices. We now need to encompass these phenomena in a wider vortex theory. Vortices are not everyday customary (obvious) experiences, while they possess some extraordinary properties. Workers in this field are called upon to consider research along the lines envisaged herewith for push gravity.

Quantum entanglement (the ability of separated objects to share a condition or state), may then be given another perspective in terms of the vortex theory. Vortices provide the spatial expanse of particles (otherwise apparent points) and hence it may also explain the connection (entanglement) of opposite spin vortices, i.e. particles at a distance (spooky action at a distance). What is unclear now is whether the said vortices are traveling objects like in [vortex cannons](#) or moving formations like water waves without moving (transferring) of water at a distance. In addition, we have to ascribe a minimum set of attributes to the gravion enabling us to construct the vortex. Such attributes, for example, could be a quantum (minimum) vector of space-time-momentum with a collision (interaction) rule between gravions. This could be the starting entity by which the universe is made and all out theories must comply with.

In Fig. 68, we have included the schematic of the Kelvin vortex to indicate its relative position in a multilevel universe. It is placed at scales much smaller than the atom, i.e. much smaller than the range of validity of quantum mechanics. Quantum electron dynamics may then have to undertake the appropriate adjustments in describing superstructures above gravion and vortex levels. The current field theories encompass a number of levels, below and above which forces can be explained by alternative means. At galactic and super-galactic levels, we have proposed that cosmic weather determines what appear to be problematic phenomena for prevailing gravitational theories. The concept of mean free paths and the distribution of hyle over these paths becomes a key concept in our theory. The universe is self assembling at various levels separated by many orders of magnitude under an auto-sorting process of particles and bodies over a range of mean free paths. A universal medium (hyle) is distributed in a way that may explain our observations over a wide range of orders of magnitude (see more in Section 28.4).

By no means do we claim veracity of the above proposals and ideas. We only wish to indicate that we may need to start with a radical new approach to explain our accumulated large amount of data. This includes certain principles like the speed of light being the ultimate speed of the universe. If our hypothesis that photons are themselves a superstructure of other much finer processes, then speed of light is only the speed observed for this superstructure making it arbitrary to assume the same speed for its components.

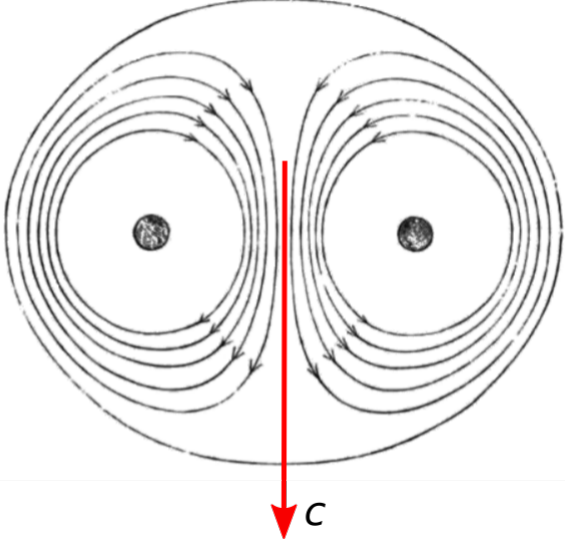
Multi-level universe		
	entities	forces
	galaxies	cosmic weather, gravitational, electromagnetic, nuclear fields
	white dwarfs, neutron stars, black holes	gravitational, electromagnetic, nuclear fields
	planets, stars	gravitational fields
	atoms, molecules	electromagnetic fields
<p style="text-align: center;">Kelvin vortex</p> 	particles, electrons, protons, photons	electromagnetic, nuclear fields
	electrons, somions	electromagnetic, nuclear fields
	gravions	gravitational fields

Figure 68: Schematic of the vortex atom published by Lord Kelvin (1867) now proposed as building unit (element) for particles like electrons, protons and photons, with corresponding forces (fields).

The above ideas of “mean free paths” and “collisions” (or interactions) at the levels of gravions and electrions may provide us with novel means to formulate a novel concept of the universe.

In fact, it seems that we are arriving at some important conclusions that are consistent with contemporary findings elsewhere in physics, albeit not everywhere. For example, we have learned that gravions create or “give” mass to hyle. This is consistent with the notion “that bosons give mass to all matter”. By the same token, we have further learned here that electrions create, or “give” charge to electrons (charged particles, another form of hyle). Is this a coincidence, or have we arrived at some fundamental truths about cosmology via another simpler and perhaps more precise way? This may be answered by those best learned experts of quantum field theory and the Higgs field. It may be about time to put aside certain “principles” that have locked physics in an impasse. It maybe about time to adopt the principle of similitude and fractals as the basis for understanding the multi-leveled cosmos. It may be that the gravion defines the quantum of space-time-momentum, whilst the rest of the universe is being built by gravions at different configurations and concentrations. The concept of atom proposed by Democritus has gone through a round about trip via our established chemistry/atomic/nuclear/quantum theories, all of which will finally come to rest on the ultimate “atom” being none other than the gravion.

26 Particle physics

26.1 Moving particles

In view of the new definitions and findings about speeding material bodies, we need to review the meaning of various masses previously derived for the proton, electron and positron in Sections 19.3 and 21, and similarly for other particles to be considered later.

The notion of intrinsic speed for a macroscopic body is connected with the intrinsic mass of a lone-and-stationary body with respect to the gravion gas (medium). However, this body consists of internally moving atoms and molecules (moving particles). These particles then have a composite mass each, the sum-total of which constitutes the intrinsic mass(es) of the macroscopic body. If we could bring all the particles to rest at the absolute zero temperature, then each particle would be left with an intrinsic mass of its own, the sum-total of which would constitute a new intrinsic mass for the macroscopic body. The intrinsic mass of the “frozen” body would clearly be less than the intrinsic mass of the body at “room” (elevated) temperature.

We can apply the same logic to sub-atomic particles even though we may not have the technical means to “freeze” them. All our measurements and experimental data on those sub-atomic particles refer to moving particles. We previously used the known masses for the proton, electron and positron under a static PG theory. However, those masses were actually the composite masses for each of those particles according to our latest understanding. Thus, the effective mass of an electron previously designated as $m_{e-electron} \equiv m_{e-e}$ actually represents the composite effective mass of a moving electron and should be reassigned as $m_{ec-electron} \equiv m_{ec-e}$. Similarly, the proton should be shown as $m_{ec-proton} \equiv m_{ec-p}$. Having said that these moving particles have a “composite” mass, leaves an open question if they also have an intrinsic mass of their own too. We need not answer this question here, other than point out this possibility. The latter depends on their possible internal structure, which we attempted to conceptualize in the previous section. For consistency, it is reasonable to assume that they do have an intrinsic mass, at least a theoretical one that would be had if the particle could be captured stationary inside the gravion medium.

The above considerations are important in view of Eqs. 368 and 371 on speed range and speed addition. The electron was found to be a very dense particle meaning that its absorptivity is very close to unity. If that absorptivity corresponded to its intrinsic mass, then its intrinsic speed would already be very high leaving minimal room for additional speed. In other words, we would have great difficulty to speed up the electron from its rest position, which is contrary to experience. We understand now that this contradiction does not occur because the masses we used are composite masses at already great speeds. To achieve the latter situation (already fast moving particle), should they have an intrinsic mass, it must be very small that allows all the known possible range of speed for the electron.

The above understanding is the counterpart of similar understanding of current theories, whereby material bodies are said to be composed of about 95% “energy” and 5% “mass”. We may arrive at similar descriptions but in terms of various forms (types) of mass, all of which are part of real mass. It seems that PG may “encompass” existing theories, which have missed out on black mass and internal structure of “fundamental” or “elementary” particles. Therefore, we need to return to these issues after, or better in conjunction with modeling of the structure of moving particles.

The above are only opening remarks for what may become a chapter of particle physics in later developments.

26.2 WIMP, WISP and dark matter

It is said that about 85% of the universe consists of dark matter. If this must be the case because of prevailing theories, then it can be consistent also under the PG platform. The only qualification is to say that the dark matter must also correspond to effective mass under PG, which, in turn, is further accompanied by an appropriate amount of black mass. In short, dark matter and black mass are different notions, not mutually exclusive and can coexist. The quantitative relationship between effective and black mass depends on the size of dark matter particles.

It is said that the weakly interacting massive particles (WIMPs) are hypothetical particles among various candidates for dark matter. They are broadly thought to be new “elementary” particles interacting via gravity and other force(s) as weak or weaker than the weak nuclear force; they are beyond the Standard Model. Since they do not interact with electromagnetic force, they may have a simpler structure than the one outlined for electrons/positrons in our preceding model. They may be more “elementary” having a kind of “amorphous” structure, but still have some structure in the arrangement between effective and black mass. Being more massive than neutrinos, they move slower under our PG relationships between absorptivity and mass outlined above. They are relatively large spheres (still particles) interacting via push gravity via graviton absorption. Experts on dark matter research may continue to study various candidates of particles like neutralino (WIMP) and axion (WISP) under the PG platform. The fundamental issue, however, remains if the search for dark matter is justified by being based on existing theories, should those theories need revision. Dark matter is necessitated to explain why rotating galaxies don’t tear themselves apart. However, this is not necessary to be the case under PG, but PG does not exclude dark matter for whatever other purpose. We have already accounted for black mass expelled in the form of jets from black holes and other dense bodies. This mass may be “sprayed” in the form of particles being activated by gravitons to form WIMPS, which consist of a black mass core enveloped by activated effective mass. They are minute black holes as particles, like electrons/positrons might be, but without the internal organization of the latter; i.e. they lack emission of vortex structures and they are “electrically” neutral. If WIMPs exist, their properties may be unlike those originally predicted. In the latter case, we have to re-appraise the entire background of our research efforts.

In the above context, a successful detection of dark matter does not solve the outstanding problems in physics. Detection of some rare WIMPs in the laboratory does not prove that we found the 85% missing matter “needed to prevent the galaxies from falling apart”. It does not disprove PG theory either, which can explain the integrity of galaxies even without dark matter. However, PG can easily accommodate dark matter, which is likely to exist simply as another component of the cosmos not yet detected.

Therefore, the world scientific endeavor should diversify its search of new frontiers. [We have added reasons and possibilities \(like the speed-mass relationships, spacecraft trajectory engineering, explanations for known anomalies and testing of the push-force principle for a fully fledged PG theory. This is poised for verification by a number of feasible experiments and potential data available within the reach of many laboratories and organizations around the world. Particle physics is a major source of already existing experimental data that may fit in and be readily explainable by PG. Only experiment will determine, which of the canvassed ideas in this report is the best suitable for a correct PG theory. Theoretical expansion of the theory is also promising with a hope to attract commensurable interest.](#)

Therefore, PG must be incorporated in the body of official and mainstream science and must remain on the table as an active candidate for possible explanations of existing data and theories for sufficient time before it may ever be abandoned again.

27 Literature survey

As stated at the outset of this report, the special circumstances of the author have not allowed extensive referencing to all and various diverse fields of science having a direct connection with this development. This work is mostly self-reliant, but it is natural and welcome that our findings overlap and agree in most respects with prior literature. After all, we should all converge in agreement with experimental data. We seek an understanding for many omissions in literature references. We intend to study prior literature that comes to our attention, as also we prefer to make proper and meaningful attributions instead of a mere reference listing. Historically, works on push gravity are rare and practically non-existent in the “mainstream” scientific literature. Worse than that, PG has been considered a “finished” or “discredited” theory by several authors including well known celebrities in physics. Under these circumstances, it requires a lot of courage by someone to come forward in an attempt to revive, develop and promote this theory. At any rate, we feel that a substantial body of work has been presented by now warranting due attention; the majority of the theory, especially its methodology and many important conclusions, is unique.

For a while, we will continue to provide our findings as long as this is possible and work on the literature will be mentioned intermittently under this new section, which for the moment is only a “stub”. We welcome suggestions to improve on all kinds of omissions.

Just briefly, it is important to mention that some recent works by Meis (2020) and Meis (2022) has come to our attention: It appears that quantum electron dynamics (QED) theory may independently predict the existence of push gravity, or push electric field. It may make it worthy to investigate the radiation pressure of the electromagnetic quantum vacuum field felt by bodies.

Likewise, Fedosin (2021) reporting “*on the structure of the force field in electro gravitational vacuum*” has clearly adopted the principle of push gravity. Furthermore, Simaciu (2006) has made a contribution to the development of the theory with absorption of gravitational interaction. We should examine if and to what extent those theories can interbreed with our approach to PG.

It seems that another perspective of the atomic structure outlined by Hunt (2019) may be compatible with our fledgling model for nuclear force in Section 21.3.1. Our *somion* medium may correspond to the description that “*nucleus of every atom is held together by energy in the form of a standing wave originating from the nucleus and surrounding it*” (Hunt, 2019). PG pressure and standing waves are compatible.

A “new perspective on Fatio’s flux” has been reported lately by Zinserling (2021).

It seems also that the ideas of “a superfluid theory of everything” reported by Fedi (2016) are compatible with our further modeling of the electron and the cosmos in Section 25. This work may deserve special attention for possible inclusion in the development of our PG theory.

The inclusion of certain works herewith does not imply endorsement or overall agreement with our theory.

28 General discussion

CAVEAT: Throughout this report, no claim is made or implied that PG theory will ultimately prevail, other than the assertive wish to be put to the test by objective means and not by means of another incomplete or erroneous theory. It never states that the theory of relativity is invalid other than it may be expanded and improved. The report is supplied as an open source publication with no financial or employment strings attached prior, during or after publication. It is motivated purely by a scientific urge of the author to overcome his ignorance on outstanding questions in physics during his free time outside life’s mundane tasks. By obtaining a new set of derivations for ostracized push gravity, it was felt compelling to share the novel findings publicly. It would be a great personal satisfaction, if the scientific community could engage in some way towards verification (i.e. testing) and further elaboration of PG. In particular, should the veracity of PG become proven, it would be to the greatest benefit of science, whilst, otherwise, the author will be content to feel that it was at least “*a good try with some novel work*”, but without the need for exorcisms.

By the same token, we expect a reciprocal caveat to apply from the scientific community with respect to our findings. What would happen if, in the course of this development, it is found or deduced that some fundamental tenets of mainstream science are broken? For example, we already found that the equivalence principle is an approximation in a certain realm of the universe and generally invalid elsewhere. We found that it is invalid with very dense bodies both at macroscopic and elementary particle levels; Kajari *et al.* (2010) have reported on this possibility on the inertial and gravitational mass in quantum mechanics. Likewise, we have proposed that we be free from the uncertainty principle at sub-quantum mechanical level, as the only way to progress with our push particle theory. We think that we have gained good ground there. We fully accept, endorse and adopt the great achievements of QM but only in its specific range of applicability. In fact, we have recently come across a report on possible violation of the uncertainty principle with experimentally direct observation of deterministic macroscopic entanglement (Kotler *et al.*, 2021).

Therefore, we anticipate reciprocal respect and attention from those who may have built a professional career on the validity of the above principles. We welcome constructive criticism of our findings from an objective and independent point of view, not based on authority alone.

Subject to the above caveats, it is now decided to release some discussion in relation to important topics such as the gravitational law, expanding universe, galaxies, perpetual motion universe and philosophy, which were omitted from the first version. They could constitute topics for further advances in PG later, but are provided only briefly on a tentative basis at present. This may at least help avoid unwarranted criticism based on some issues not yet addressed, even briefly, with the understanding that the following discussion does not reflect on the validity of a working PG per se. Even so, it is with some trepidation that the ideas are presented below. Some specific technical proposals may prove to be totally incorrect, whilst existing or new controversies can be dealt with by the relevant experts.

An interesting exposition of push gravity is presented by Thomas (2014). This provides a good philosophical basis of the concept of push/shadow gravity and a motive for further investigation. However, the

positive aspects of PG should not be diminished by possible failure of certain specific interpretations of important issues. For example, the referenced gravitons are thought to be a kind of strings as proposed therein, which may or may not be proven correct, so that PG should not be bound by such specific technical claims. The Allais effect is attributed to some sort of “lensing” mechanism of the gravitons around the Moon, but we have showed that the effect can be readily interpreted and even measured by the PG derivations in Part 1. These and other speculative technical interpretations, if found incorrect, should by no means reflect on PG in general. We have now tried to create an alternative paradigm of PG by building the mathematics on a set of postulates in order to arrive at the established laws of physics and beyond. One fundamental difference from all prior PG theories is that the gravion absorption need not be weak and linear, but must be exponential in accordance with established laws of absorption theory.

The present author’s main expertise lies outside the fields directly pertaining to this report. As a result, Part 2, in particular, may not be as authoritative as it should be, whilst Part 1 could be seen as an attempt to produce and report new data and evidence in support of a long standing hypothesis to explain gravity. It is hoped that others may use and apply the latter findings in a better way, or as they see fit. In this context, the primary aim would have been achieved, namely, to place PG within the mainstream of physics. For the latter, it would be an even greater achievement, if work is undertaken to test the veracity of the present findings within the programs of various institutions and organizations. Should an affirmative finding be achieved, then PG could immediately find its rightful place in science. At any rate, the present author should be excused for possible “collateral” errors, whilst attention to the novel disclosures may not diminish. It is in this context that we discuss some ideas necessitated for expanding the general PG theory.

28.1 Expanding universe

We already canvassed the various possibilities of mean free path (m.f.p) of gravions in Part 1. The case of an infinite m.f.p would result in a universal “attractive” force regardless of distance, pretty much the same as would be expected by Newton’s gravitational law. However, such a system would beg to explain how gravions interact with matter but never between themselves, i.e. how they have an affinity with matter but not with each other. As a result, it is more plausible to accept and consider a finite m.f.p., which also implies that gravions would behave like a gas in the vast universe.

The idea of push gravity occurred to this author during work on gas flows in an environmental scanning electron microscope (ESEM) (Danilatos, 1997) using the direct simulation Monte Carlo (DSMC) method (Bird, 1995). The latter method made possible the study of gaseous flows under specific conditions (e.g. novel differential pumping stages by Danilatos (2012)). It was tested and confirmed the idea of two spherical bodies being “attracted” to each other, when the mean free path of gaseous molecules was much greater than the diameter of the spheres, while absorption to any degree was also present. It was then thought that the same might happen, if planets and stars are immersed in a medium with particles having mean free paths much greater than the size of the celestial bodies. That would then be the cause of gravitational acceleration and force to start with. For distances much greater than the mean free path, no “attraction” force is generated, while the celestial bodies will float around.

The implication of this would go much further, if we can consider the analogy between a real (familiar) gas and the universe gas (gravion gas): Dust particles in a real gas under the above condition of mean free path would appear to attract each other (at close range), while also, if the overall gas is set free to expand, the dust particles would also expand in unison with the surrounding gas. Likewise, the stars, planets and celestial bodies are like dust particles attracting each other at relatively short distances but move apart from each other as a whole, when the distances become far greater than the mean free path of the gravions behaving like an expanding gas. We may then say that PG is consistent with an expanding universe and consistent with the conclusions of the theory of a big bounce or bang, but not with the theory itself (based on different premises). The visual picture of a starry night through a high resolution telescope conveys the impression of a dusty space, which might be more than a coincidence to treat it like an expanding dusty gas. In proposing such a model, the observed accelerated expansion rate of the universe might correspond to the initial accelerated rate of expansion of a gas, which, however, eventually reaches supersonic and hypersonic speeds, after which it expands at a constant rate. Therefore, if this model is correct, our universe exists still at an initial expanding rate state. Finally, if this model were to be accepted, dark energy (repulsion) of current theories might have a tangible explanation too via PG. Terminology is again important to avoid confusion. If the expanding gravion gas is responsible for pushing stars and galaxies apart (not “attracting” them), then we might as well call this type of field “negative push gravity” (NPG), consistent with “dark energy”.

Prior to all this, we take for granted that redshift can only be explained by an expanding universe and that we understand the nature of light and its propagation: We take for granted also that the Michelson-Morley experiment can only be interpreted by the exclusion of aether, while we are unclear about the wave-particle

duality principle and the double slit paradox. It seems that we may have to revisit all these experiments and phenomena anew under PG.

None of the above should be less plausible than various other hypotheses already on record to explain the observed expanding rate of the universe, like: A dark energy inherent in the fabric of space itself, or the quintessence field that expands space at changing rates, or a phantom energy and so and so forth. In any event, the said applications of PG in this area are only on a tentative basis, which should be adjusted as new data and information are compiled on any of these controversial topics.

28.2 Galaxies

Let us next consider the case where the mean free path is, say, several times the size of our heliosphere. The gravitational law derived in Part One will gradually degenerate and cease to apply at longer distances. The generated field will continue to generate a push for a significant transition region, after which stars will float around as previously described. Thus, there is a transition region corresponding to the transition region from free molecule flow to continuum flow in gas dynamics.

The galactic spiral shapes resemble closely to the spirals of weather storm clouds on Earth seen from space. This might be more than a coincidence, as it might provide a classically intuitive explanation for galaxies. The spiral storm formations are caused by pressure gradients in the Earth's atmosphere in conjunction with Coriolis forces. They belong to an atmospheric barometric low (bad weather), but a similar weather pattern is formed with a barometric high (good weather) circling in the opposite direction. We should then examine the possibility of galactic formations created by the gravion pressure gradients (barometric high) in conjunction with an as yet unknown cause for circular motion. The gravion gas beyond the galaxy in the greater universe may have its own "weather" patterns. The stars in galaxies may correspond to the condensed water droplets in clouds. They are stormy regions of a more general cosmic weather system. Galaxies have high concentrations of gravions at their center creating gravion pressure gradients toward the periphery. Macroscopic gravion pressure may play a major part in galaxy formation. This suggestion could be consistent with a "mock-gravity"-like of the creation not only of the chemical elements but also of the condensation of matter into galaxies (Gamow, 1949; Hogan, 1989; Wang & Field, 1989; Field, 1971). Gamow proposed that such a "mock gravity" could have played a role in galaxy formation after the Big Bang. Although there has been much controversy over such theories, it is envisaged now that the new PG could help re-appraise all these theories by incorporating them under a bigger framework for a new understanding of cosmic motion beyond the "local" gravitational fields.

PG then might provide a good explanation why galaxies rotate faster than the existing laws of physics predict, and the motion of vast clusters of galaxies in the universe. We are presented with an opportunity to consider ideas that are still possible and rule out others completely. Thus, one more anomaly may be readily accounted for by PG.

Furthermore, PG very nicely removes the singularities (infinities) of current theories, as the maximum force that can be generated is limited by the upper boundary of push gravion flux density. There is an asymptotic approach to this limit by an increase in mass or density of mass. The forces transmit at the speed of gravions, which can be the speed of light.

Galaxies are generally considered to date to be gravitationally bound systems of stars and not weather-like systems, as we propose now, so that the above ideas are totally out of established beliefs. Dark matter has been used to explain the galaxy rotational anomaly. However, if dark matter and dark energy have been invented to fill the shortcomings of other theories, PG may also be entitled for expansion (development) at long distances as well. For it might be ultimately easier to comprehend and apply weather-like systems in the cosmos than imaginary forces acting at vast distances.

Modified Newtonian dynamics (MOND) has been promoted to account for observed properties of galaxies. It is an alternative to the hypothesis of dark matter, but it still seems insufficient to account for all observable data. All of these theories are based on the idea that gravity is inherently generated by mass, whereas PG is a theory of an [emerging gravity](#) by an external source surrounding massive bodies (i.e. the gravions), like [mass is also an emerging property of hyle but not the source of gravity](#).

These and other anomalies reported, like by extra massive hydrogen clouds and extra energetic photons, should be also re-examined in the light of a general PG theory for possible explanations.

28.3 Perpetual motion of universe

The biggest challenge of PG is to understand and explain the recycling of the gravions in the universe overall. Our proposed model suggests that they are transformed successively to various types of push particles with a correspondingly smaller mean free path until they diffuse out back into space without an obvious direct trace to us yet, but somehow finding their way by accretion back into exploding massive stars, dwarfs, neutron

stars and black holes. By such means, the universe must be regenerated and overall frictionless in contrast to a forecast thermodynamic thermal death of the cosmos. The idea of a static universe recycling itself has been advocated before among others by Edwards (2007), who adopts yet another approach to PG. His model seems much more complex in an attempt to base it on (or use) existing theories, whereas our model of PG is being built from simple principles in the simplest possible terms. Then we try to see if it is consistent with existing data and theories. However, his central thesis might apply at least in some aspect. The central thesis of his model is an inter-conversion of photon and graviton energy, whereby the gravitons cumulatively establish a quantum lattice connecting all masses. “*Photons incident on the filaments of this lattice impart energy to the gravitons, while at the same time losing a portion of their original energy. This loss of energy corresponds in the model to the cosmological redshift in a static universe*”. Whilst the perpetual motion machine is readily rejected by thermodynamics, we may not say the same for the universe overall or parts thereof. Otherwise, the universe would come to a grinding halt, from which we would still require an exit without resorting to god; the Big Bang is only shifting the perpetual motion to a more distant past. Nothing should prevent the existence of frictionless regions in the universe, albeit extremely small and “invisible” to our instruments as yet.

If the entire universe existed in the form of a gravion gas only, we might say that the second law of thermodynamics has had its sway (has prevailed), i.e. to which everything has succumbed. However, the fluctuation theorem is also universally applicable and operates by way of another **law** for undoing the second law in no uncertain terms. This fact is often, or mostly overlooked in science. Fluctuation results in order and creation, whilst the second law results in disorder and destruction. It may be that quantitatively the amount of gravions constitutes an overwhelming majority of mass over and above the visible mass of the universe. Nevertheless, both laws coexist intent on undoing each other’s work. This is exactly a manifestation of another overriding universal law, namely, that of the coexistence of opposites. A one-sided view of things can lead to error and impasse, whereupon we should be spurred on to find the missing (overlooked) side of things.

The above is consistent with the thinking of the universe as continuously and continually recycling itself and appearing in different forms of matter and energy, all of which is spun from a common entity that pervades all that we can experience.

28.4 Philosophy of physics and theory of everything

To say that the human mind cannot conceive the most intricate workings of nature (when a particular theory becomes complex and unintelligible), may also be a cowardice preventing us from moving forward. Skepticism inevitably leads to religion and to the end of science. This author subscribes to the school of thought that humans can and will ultimately comprehend nature and in the simplest of terms.

There is now an opportunity and a need to disassemble certain ideas about rest mass, gravitational mass, inertial mass and relativistic mass under existing theories and re-assemble them under the platform of PG and the newly found concepts of effective and real mass.

Could the limiting speed of light for all material bodies be explained and not postulated? Could it be that, by matter organization from gravion level up, nothing can be pushed faster than gravions?

If there is a unifying theory of everything, would there be a unifying common denominator? What is it that would unify them? A common particle? Some common entity and what is its nature? If mass and energy are equivalent, and if energy can appear in different forms but always conserved, we should be able to reduce all those forms to a common denominator. That common denominator may be the gravions at different levels of organization.

Overall, nothing is invariable in the cosmos, but universal constants appear under “local” provisos and conditions, which are only recurring over the entire cosmos.

The universe consists of particles distributed over a wide range of mean free paths that allow auto-sorting of particles and bodies with the end result of a self-assembling universe like a DNA. Self-assembly and self-organization are general prevailing processes triggered by random fluctuations. In support of the above exposition, Nobel Prize winner Prigogine (1977) has described a theory of self-organization in non-equilibrium systems from dissipative structures to order through fluctuations. Furthermore, “*it has been argued by some that all emergent order in the universe from galaxies, solar systems, planets, weather, complex chemistry, evolutionary biology to even consciousness, technology and civilizations are themselves examples of thermodynamic dissipative systems; nature having naturally selected these structures to accelerate entropy flow within the universe to an ever-increasing degree*” (Gleick, 1998; Wikipedia contributors, 2021) . Allahverdyan & Nieuwenhuizen (2000) showed the feasibility of extracting zero-point energy for useful work from a single bath, without contradicting the laws of thermodynamics. Even before quantum theory, Nikola Tesla claimed that useful energy could be obtained from an all-pervasive aether. Last, we have also proposed an explanation of the fly-by acceleration, which can now be seen also as extraction of energy from the surrounding

gravions (see Section 14.3).

Ordinary matter is the decomposition of black holes and re-assembly to form elementary and/or other particles, which may still incorporate tiny black matter (holes) with their layered TALs. Conversely, black holes may also be the decomposition and “precipitation” or “distillation” of ordinary matter to corresponding massive bodies with black mass.

We now put forward the hypothesis that all particles are held together by the pressure of push particles. Different particles may be formed by different types or fractions of push particles, a topic to be taken up later in PG.

In attempting to conceptualize the deeper meaning and application of the second law of thermodynamics together with the re-emission of gravion energy, we may have come to a better understanding of quantum mechanics too. In quantum mechanics, anything that is possible to happen can happen governed by the probabilities of that situation. The latter provides a probabilistic relational description of the states of particles but not the origin or an explanation why quantum particles move about incessantly in certain patterns (e.g. electron orbitals). By analogy, general relativity provides an accurate relational explanation of various parameters but it does not provide a hint about how and why gravity exists, or why the spacetime around a mass is bent and warped. PG via an incessant gravion flow may provide the basis for understanding both quantum mechanics and relativity at the same time. The ever flowing gravions pass through various levels of material organizations via quantitative accumulations leading to qualitative transformations from level to level. The universal relationship between quantity and quality can be seen at all levels of organization of matter, starting from the smallest quantum mechanical states, to chemical and mechanical systems of ordinary sizes, and all the way up to white dwarfs, neutron stars and black holes. Actually, the smallest of entities may not even be subject to quantum mechanical rules, if quantum mechanics has so far described an “intermediate” level of the universe. Quantum mechanics may be simply a macroscopic description of other underlying processes, like pressure and temperature are macroscopic statistical properties of a gas. Likewise, those other underlying of quantum mechanics processes may be ultimately the simplest ones waiting for us to discover.

A perpetual motion of matter/energy can rightfully belong to the universe as a whole, a principle which has been attributed to Heraclitus (Wikipedia contributors, 2019a). All these ideas eventually lead to the need to understand the nature of gravions and its interactions with matter and with themselves.

29 Conclusion

An attempt has been made to modify and advance the old principle of push gravity theory to a stage where gravity may be seen from a totally novel perspective. It constitutes a daring step, because it challenges and potentially provokes a re-consideration of long standing ideas and principles. This has already required a daunting determination especially as it comes from a non-established expert in the field of gravity.

The basic new element is the use of a gravity particle absorption coefficient that is not limited only to very low values as in prior PG theories. The consequences of that can be dramatic.

The theory of PG has now been brought to a stage ready for verification with several proposed tests and methods. Should these tests yield a positive outcome, they could provide explanation to many outstanding issues in science. Otherwise, the test may prove insufficient pending further instrument refinements. Alternatively, if one produces sufficient evidence to reject PG once and for all, that would compel science to concentrate on other pathways, as it does, even more. At any rate, it should be appreciated that the proposed tests are inexpensive at least in relative terms for many organization to engage.

In summary, new work provides sufficient evidence for a genuine re-appraisal of push gravity. A novel quantitative theory has been advanced on the basis of a set of primary principles (postulates), from which the derivation of classical acceleration and force by stationary massive bodies in the steady state is possible. In contrast to prior conceptions, it is shown that the absorption of gravity particles by matter need not be extremely weak and linear, in order to derive and explain the observed classical laws of gravity. Any value of the absorption coefficient by a uniform spherical mass produces a gravitational field obeying the inverse square of distance law. The gravitational constant (big G), is itself a function of the ratio of the absorption coefficient over the density of matter. The latter ratio now becomes the new universal constant of the cosmos, whilst G can vary in different locations of the universe. The measured mass of planets and stars is only an effective or apparent mass actually smaller than the real mass due to a self-shadowing or shielding effect of the absorption of gravitational particles. Any given mass appears quantitatively different depending on its spatial distribution including orientation. We now find that Newton’s gravitational law uses only the apparent (or effective) masses with a potentially variable G, but the inverse square distance relationship is preserved in the cosmos. The radiant flux of energetic particles being uniform over a region of space creates a maximum acceleration of gravity for all material bodies in that region, so that any further mass accretion

over a certain upper limit does not create additional acceleration; this limit is reached when practically all gravitational particles are absorbed (saturation state) by the massive body above a saturation mass. The latter limit should be measurable, for which some tentative situations and experiments are proposed for prospective experiments and tests. The internal field of a spherical mass and the external field of a two layered sphere have been derived. The superposition principle of gravity fields has been reformulated and the Allais effect explained. The equivalence principle can now be properly understood and explained in a way that the principle per se becomes redundant. We can now better understand the meaning of matter, inertia and mass. For moving bodies, the established relationships from special and general relativity may continue to operate within the gravitational fields created by push particles, but may need to be adapted and re-aligned within the greater framework of push gravity principles operating at any distance.

An attempt is made to overcome the main remaining objection of presumed catastrophic thermal accretion of absorbed particles. A further attempt is made also for the push-gravity principles to explain the vastly higher intensity gravitational fields of white dwarfs, neutron stars and black holes. It is proposed that the field of white dwarf stars is created also by push particles but of a different kind, namely, by those responsible for mediating the electric field. In the same way, the field of neutron stars is created by yet a third kind of push particles, namely, those responsible for mediating the nuclear field. In general, push particles may exist with different energy (or mass) having different mean free paths as they traverse different concentrations of masses (black holes, neutron stars, dwarfs, stars, planets, ordinary masses, atoms, nuclei, protons and all the known or unknown sub-nuclear particles). The invariable principle of momentum transfer (push) by particles directly relating to their absorption rate by the various concentrations (density) of masses could be the basis and the starting principle for a prospective unification theory of everything. The first part of this report, if verified, should create the basis for new physics across many fields of physical science. Pending such a verification, we may also work towards the development of a general PG including a theory of the dynamics of the observed motion of celestial bodies.

If there is a “theory of everything”, then gravions could provide an underlying mechanism not only in gravity but also in quantum mechanics. Gravions may be responsible for both the gravitational fields and the associated masses being nothing else than effective masses. It may be that we can make one step closer to a better philosophical understanding of the cosmos, if we can grasp the nature of the gravion, perhaps, as being the embodiment of the coexistence of opposites in a perpetual flow of the universe.

REVIEW

This report has not been submitted to a regular journal for review. This is not to avoid the review process. The author himself has acted as reviewer in scores of official scientific journal publications in the field of his professional career. It has not been submitted to a journal for the following reasons: It is not in a form suitable for publication in a journal. It is incomplete and would result in many questions not yet addressed, because the author intends to continue the work, or he is not ready to answer. There is a need for re-write and re-arrangements of the extended material and topics. It covers a wide variety of fields in physics stretching from particle physics, astrophysics, theoretical physics and many more, so that no single journal is deemed suitable for publication of this type of work. It is not of a regular size paper. It is becoming more of a book publication. Whilst review and moderation definitely make better scientific standards for specialist journals, it could also be a hindrance, if working on the present paper depended on a few only specialist opinions, or a single endorser.

Zenodo should be gratefully acknowledged for providing an excellent platform to disseminate this special science report encompassing many different disciplines in physics. The possibility of successive versions is helpful, whilst the allocation of a unique DOI per version backed by CERN’s reputation and strength are good enough for our purposes.

It can provide a platform for a joint project with collaborating participants from diverse fields. This may take place, if other authors may like to write a critique or contribution along the lines of this theory. We welcome such contributions by eponymous authors that may be included in the form of Addenda. Optionally, such contributions may first appear elsewhere in Zenodo to secure the authorship of contributed ideas, and may be followed by a request for inclusion in our report herewith. The final decision will be left to this author only to ensure that the content can be easily read and integrated with our terminology while it falls within the scope of the work. There are many incomplete topics to contribute. Volume may also reach a limit. The invitation is open for a trial [in following versions](#).

APPENDIX

A Gravitoids

Let us be reminded that a prolate spheroid is a surface of revolution obtained by rotating an ellipse about its major axis, whereas an oblate spheroid is obtained by rotating about its minor axis. It is well known that spheroids acting as gravitational bodies would produce precession or regression of the elliptical orbit of a planet around it. This arises by the gravitational force being slightly greater or lesser than the inverse of the square of the distance. In other words, it is the distance (not the mass) responsible for these phenomena (here, we are not referring to the relativistic cause of the extra Mercurial precession). It is interesting to examine and clarify what happens with PG theory in this connection via the following observations.

Now, by virtue of Eq. 38, the self-shadowing effect produces a gravitational force (acceleration) less than the value expected from simple Newtonian attraction by a sphere. By increasing k with all else constant, the force increases in proportion to it (or the density) by Newtonian mechanics, but to a lesser degree by PG theory, on account of the exponential decrease along a chord (straight line) of the sphere in Fig. 2. That is, the Newtonian length that would produce an attractive force effectively contracts (shrinks) to produce the correct force. Each elemental component is then equivalent to having a lesser length at a given density, whilst in reality there is additional mass for the remainder of the length of the chord. This becomes, in effect, a virtual mass distributed inside a spheroid-like shape. It may initially look like an oblate spheroid, but it has a peculiar shape dependent on the distance OP and k . For a sufficiently long distance OP (i.e. r), the lines u are nearly parallel (very small angles φ), whilst as we approach the surface at point C, the same lines radiate at large angles φ , and the shape becomes more like a compressed egg along its axis while being inflated at right angles. We can see these and other effects by plotting the corresponding lengths and shapes quantitatively for two positions of the point O, namely, at the surface of the sphere and at a relatively long distance of $n_R = 100$.

On the surface of the sphere, we show pairs of the chord lengths and body shapes between Newtonian and virtual PG cases for three different values of k , in Fig. 69. To clarify, because point O lies on the surface of the sphere, any distance from the fixed point O to any other point on the surface defines the chord length, via which we also plot the sphere. Thus, these graphs show simultaneously both the chords and volumes of revolution corresponding to the real sphere and virtual shape yielded by PG. As expected, for $k < 0.01$, PG shapes become gradually indistinguishable from Newton. Otherwise, the difference increases significantly.

Next, we plot the virtual chord lengths for a sphere with unity radius from a distance $r = 100$ units. Planet Mercury approximately has this distance from the Sun at its aphelion. We consider again three values for $k = 0.01$, $k = 0.1$ and $k = 1$ in Fig. 70 together with the same **real** chord lengths of the same sphere (in black). We have used the same Eqs. 12 and 47.

Finally, we can visualize the corresponding virtual shapes of the sphere (here, like the Sun) from the same distance of 100 sphere radii (as from Mercury) with the same corresponding values of k in Fig. 71. This is obtained by adding the PG chord length by 47 to the corresponding u_1 provided by Eq. 16, i.e. we use the virtual end points of u_{e2} in PG given by Eq. 48.

The above spheroid-like shapes are bounded by the red lines together with overlapping black lines on the left. We note that a shallow dimple appears on the far side, the depth of which increases as we further increase k , effectively producing a *dimpled spheroid-like* shape.

As previously noted, the real shapes (and sizes) of a sphere effectively act as some peculiar virtual shapes, fictitious and invisible, for which we may collectively use (coin) the new term *gravitoids*. Their mass may be used with linear absorption as in Newton's law to yield the force as predicted by PG.

Below, we also present the analytical expressions already used to plot these gravitoids in Fig. 6 and discussed in Section 6.4. We follow the steps in finding the volume of a sphere to illustrate the point of deviation (departure) between the two approaches:

$$\begin{aligned}
 V_{sphere} &= \int_0^{\varphi_0} \int_{u_1}^{u_2} 2\pi \sin \varphi d\varphi \cdot u^2 du = \frac{2\pi}{3} \int_0^{\varphi_0} [\sin \varphi d\varphi \cdot u^3]_{u_1}^{u_2} \\
 &= \frac{2\pi r^3}{3} \int_0^{\varphi_0} \sin \varphi d\varphi \left[\left(\cos \varphi + \sqrt{a^2 - \sin^2 \varphi} \right)^3 - \left(\cos \varphi - \sqrt{a^2 - \sin^2 \varphi} \right)^3 \right] \quad (424)
 \end{aligned}$$

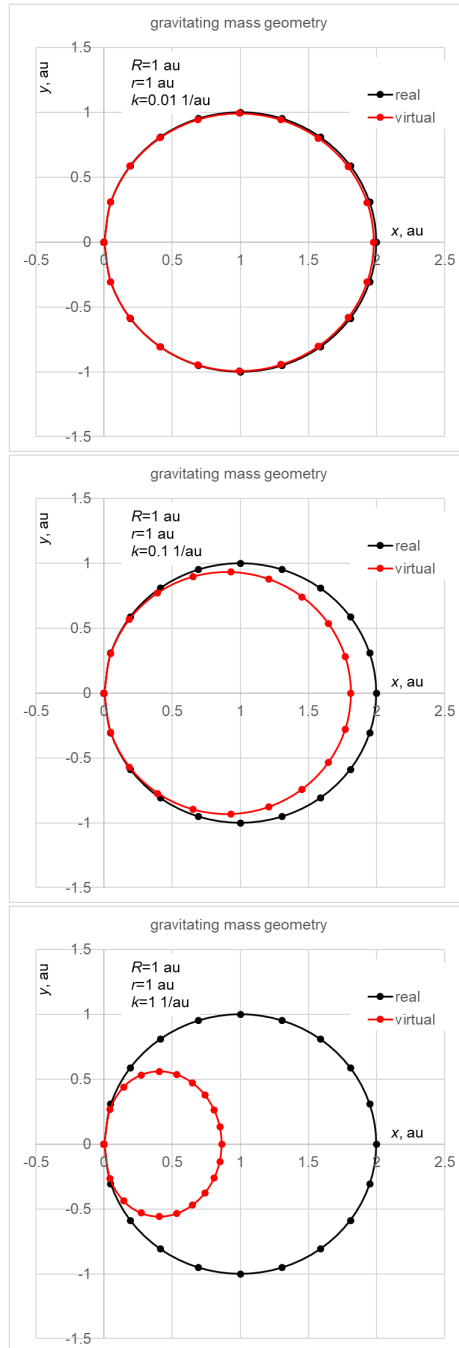


Figure 69: Real sphere in black, gravitoid (virtual) shape in red for three values of k and $r = R = 1$.

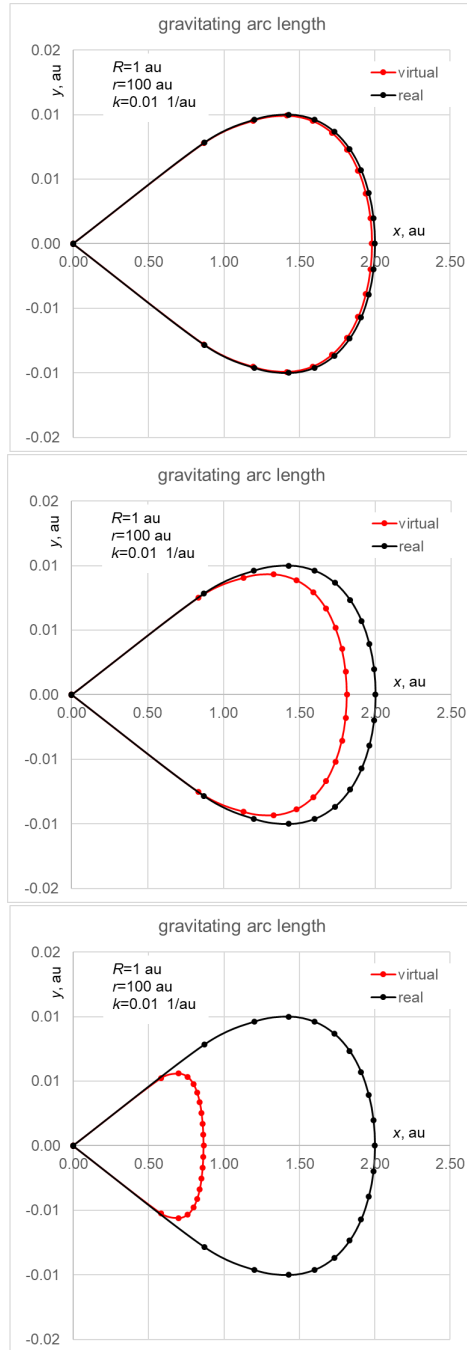


Figure 70: Arc length for real sphere in black and gravitoid (virtual) in red for three values of k at $n_R = 100$.

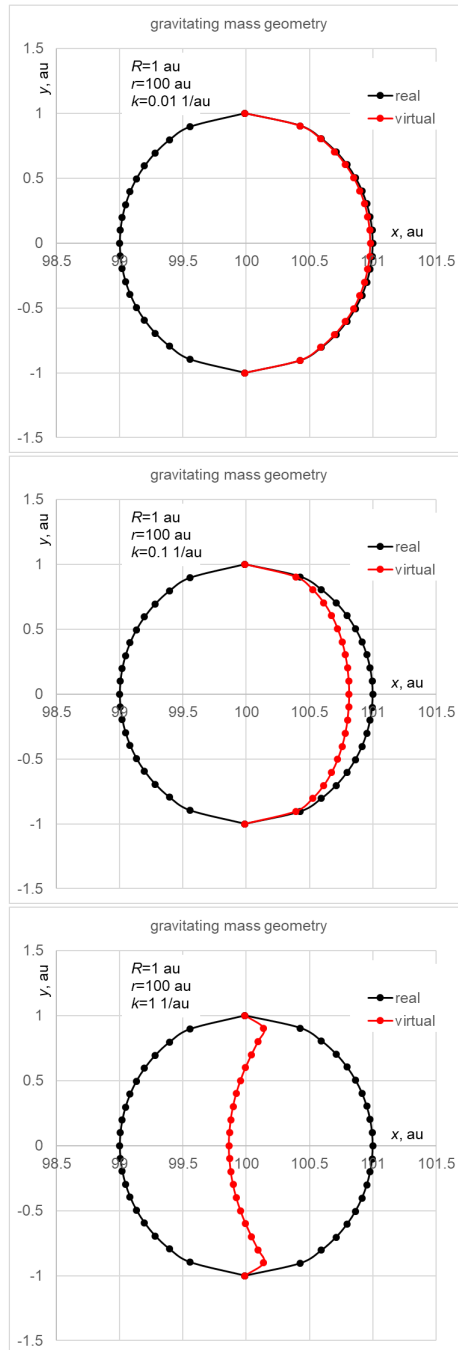


Figure 71: Real sphere in black, gravitoids (virtual) shape in red (together with black left of red line) for three values of k and $n_R = 100$.

and by using the limits in Eqs. 16 and 17, it finally yields the expected result:

$$V_{sphere} = \frac{2\pi r^3}{3} \left[-2 \cos \varphi (\cos^2 \varphi + a^2 - 1)^{3/2} \right]_0^{\varphi_0} = \frac{4\pi R^3}{3} \quad (425)$$

Similarly, starting from the same elementary volume equation

$$V_{gravitoid} = \int_0^{\varphi_0} \int_{u_1}^{u_2} 2\pi \sin \varphi d\varphi \cdot u^2 du = \frac{2\pi}{3} \int_0^{\varphi_0} [\sin \varphi d\varphi \cdot u^3]_{u_1}^{u_2} \quad (426)$$

but using the limits in Eqs. 16 and 48 we obtain:

$$V_{gravitoid} = \frac{2\pi}{3} \int_0^{\varphi_0} \sin \varphi d\varphi \cdot \left[\left(r \left(\cos \varphi - \sqrt{a^2 - \sin^2 \varphi} \right) + \frac{1}{k} - \frac{1}{k} \exp \left(-2kr \sqrt{a^2 - \sin^2 \varphi} \right) \right)^3 - \left(r \left(\cos \varphi - \sqrt{a^2 - \sin^2 \varphi} \right) \right)^3 \right] \quad (427)$$

by which we finish up with a different curve shape for the volume of the gravitoid. This shape filled with the actual (real) density may be used with Newton's law to reproduce the same force yielded by PG. The above examples simply illustrate that the initial common integration for a volume diverges on account of the different integration limits in the corresponding theories of Newton and PG. They illustrate the formal relationships between the two theories. The above integration has been performed numerically and plotted against k in Fig. 6 after it is normalized by dividing by the sphere in Eq. 425, as was done for the effective spherical volume defined by Eq. 52.

We note that the effective volume generally lies above the gravitoid, as it should, because it is further away from the gravitoid relative to the reference point O. If they both contain the same real density matter, then both yield the correct value of acceleration by applying Newton's equation. We further note that the gravitoid volume (effective mass) increases, as we move away from the gravitating mass (e.g. compare the obvious corresponding sizes provided by Figs. 69 and 71). However, this does not affect the inverse of r^2 dependency, because this effective mass increase is compensated by the integration to a lower upper limit of angle (i.e. over a smaller angle range). For a possible precession to be generated, we need to consider the time effects also in PG as in the corresponding GR theory.

B Field formulations around a single sphere

We have initially derived the absorption fraction of gravions at a point outside a sphere based on its axial symmetry around the line joining the point with the center of the sphere. However, we can also generally derive the same fraction by considering a Cartesian reference frame of x, y, z axes for later use in non-axially symmetric systems. We integrate the gravion absorption by revolving an elementary solid angle around each of the x, y, z axes to yield three components of absorption corresponding to the classical vector of acceleration. For simplicity, here we consider only a sphere intersecting one coordinate plane of symmetry along its diameter, but the derivation can be expanded for any location of the test point located outside the sphere; points inside the sphere are considered during the two sphere "bulk" formulation.

With reference to Fig. 72, the plane of symmetry intersecting the sphere is the yOz and we define and use the following notations of constants and parameters:

$$y_0 = OY = ZP.$$

$$z_0 = OZ = YP.$$

$$r = OP.$$

$$\varphi_z = \angle ZOB \text{ is the zenith angle of rotation around axis } z.$$

$$\theta_z = \text{is the azimuth angle of rotation around axis } z.$$

$$\varphi = \angle ZOP, \text{ the angle of axis of rotation with } OP.$$

$$a = \frac{R}{r} \equiv \sin \varphi_0 \text{ with } \varphi_0 \text{ (subtended angle by the sphere) used in the limit of integration.}$$

$$u_A = OA.$$

$$u_B = OB.$$

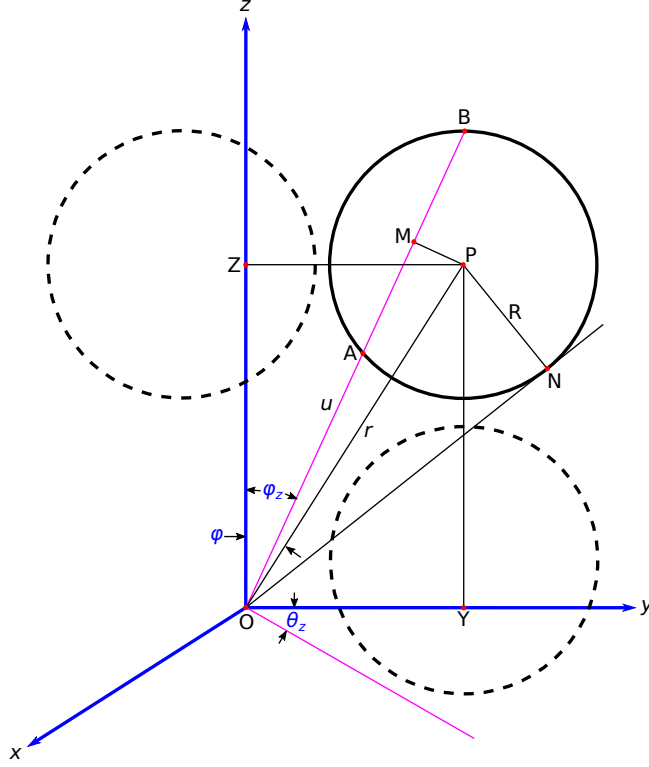


Figure 72: General derivation of acceleration for single sphere

$\psi = \angle POB = \psi(\varphi_z, \theta_z)$ varies with θ_z during rotation.

The length (chord) AB is obtained by the intersection of the straight line u with the surface of the sphere, for which we need to solve the analytical equations for u :

$$x^2 + (y - y_0)^2 + (z - z_0)^2 = R^2 \quad (428)$$

$$y = u \sin \varphi_z \cos \theta_z \quad x = u \sin \varphi_z \sin \theta_z \quad z = u \cos \varphi_z \quad (429)$$

yielding:

$$u_A = y_0 \sin \varphi_z \cos \theta_z + z_0 \cos \varphi_z - \sqrt{(y_0 \sin \varphi_z \cos \theta_z + z_0 \cos \varphi_z)^2 - (r^2 - R^2)} \quad (430)$$

$$u_B = y_0 \sin \varphi_z \cos \theta_z + z_0 \cos \varphi_z + \sqrt{(y_0 \sin \varphi_z \cos \theta_z + z_0 \cos \varphi_z)^2 - (r^2 - R^2)} \quad (431)$$

$$(AB)_z = 2\sqrt{(y_0 \sin \varphi_z \cos \theta_z + z_0 \cos \varphi_z)^2 - (r^2 - R^2)} \quad (432)$$

$$(AB)_z = 2\sqrt{OM(\varphi_z, \theta_z)^2 - (r^2 - R^2)} \quad (433)$$

$$(AB)_z = 2r\sqrt{a^2 - \sin^2 \psi} \quad (434)$$

Now, the operand under the square root must be positive, which sets the limits of azimuth angle as a function of zenith angle by solving the equation:

$$(y_0 \sin \varphi_z \cos \theta_z + z_0 \cos \varphi_z)^2 - (r^2 - R^2) = 0 \quad (435)$$

$$y_0 \sin \varphi_z \cos \theta_z + z_0 \cos \varphi_z = \pm \sqrt{(r^2 - R^2)} \quad (436)$$

$$\theta_z = \text{acos} \left(\frac{-z_0 \cos \varphi_z + \sqrt{(r^2 - R^2)}}{y_0 \sin \varphi_z} \right) \quad (437)$$

where we use the positive root sign because $OM = y_0 \sin \varphi_z \cos \theta_z + z_0 \cos \varphi_z$ must be positive and, when $OM=ON$, it becomes tangent at the limits:

$$\theta_{z1} = -\text{acos} \left(\frac{-z_0 \cos \varphi_z + \sqrt{(r^2 - R^2)}}{y_0 \sin \varphi_z} \right)$$

$$\theta_{z2} = \text{acos} \left(\frac{-z_0 \cos \varphi_z + \sqrt{(r^2 - R^2)}}{y_0 \sin \varphi_z} \right)$$

$$\varphi_{z1} = \varphi - \text{asin}(a)$$

$$\varphi_{z2} = \varphi + \text{asin}(a)$$

With the chord length AB found, the absorption fraction for the z-axis is given by the double integral:

$$f_{gz} = \int_{\varphi_{z1}}^{\varphi_{z2}} \int_{\theta_{z1}}^{\theta_{z2}} (1 - \exp(-k(AB)_z)) \sin \varphi_z \cos \varphi_z d\varphi_z \quad (438)$$

Similarly, we follow the same steps for the y axis by interchanging the corresponding parameters and notations and adding $\pi/2$ to φ_z as follows:

$$(AB)_y = 2\sqrt{(z_0 \sin \varphi_y \cos \theta_y + y_0 \cos \varphi_y)^2 - (r^2 - R^2)} \quad (439)$$

with limits:

$$\theta_{y1} = -\text{acos} \left(\frac{-y_0 \cos \varphi_y + \sqrt{(r^2 - R^2)}}{z_0 \sin \varphi_y} \right)$$

$$\theta_{y2} = \text{acos} \left(\frac{-y_0 \cos \varphi_y + \sqrt{(r^2 - R^2)}}{z_0 \sin \varphi_y} \right)$$

$$\varphi_{y1} = \varphi - \text{asin}(a)$$

$$\varphi_{y2} = \varphi + \text{asin}(a)$$

with which we obtain the integration around y axis for the absorption component f_{gy} , so that the total absorption fraction is $f_g = \sqrt{f_{gz}^2 + f_{gy}^2}$. Noted $(AB)_z = (AB)_y = AB$. The above equations are valid while the sphere does not cross any axis. In the case when it crosses one axis (let's say the z axis), there are two consecutive sub-ranges of the angles with limits:

First:

$$\theta_{z11} = -\pi$$

$$\theta_{z21} = \pi$$

$$\varphi_{z11} = 0$$

$$\varphi_{z21} = \varphi - \text{asin}(a)$$

Second:

$$\theta_{z12} = -\text{acos} \left(\frac{-y_0 \cos \varphi_y + \sqrt{(r^2 - R^2)}}{z_0 \sin \varphi_y} \right)$$

$$\theta_{z22} = \text{acos} \left(\frac{-y_0 \cos \varphi_y + \sqrt{(r^2 - R^2)}}{z_0 \sin \varphi_y} \right)$$

$$\varphi_{z22} = \varphi - a \sin(a)$$

$$\varphi_{z22} = \varphi + a \sin(a)$$

with which we obtain two sub-components for this axis to be added as $f_{gz} = f_{gz1} + f_{gz2}$

We repeat the same when the sphere crosses the other axis. Likewise, when the sphere crosses both axes. For negative values of $-\varphi$, we replace with positive φ , whilst for $\varphi > \pi/2$ we replace φ with $\pi - \varphi$.

B.1 Alternative formulation for the normal component

Beyond the general formulations above, the normal component of acceleration can be deduced with an alternative simpler way: The component of absorption around the normal axis y can be found concurrently during rotation around z axis inside the same solid angle used for axis z . As we rotate around the fixed z axis, we can project and find the component of the chord AB on the fixed y -axis by multiplying with azimuth $\cos \theta_z$ times zenith $\sin \varphi_z$, so the normal component is:

$$f_{gy} = \int_{\varphi_{z1}}^{\varphi_{z2}} \int_{\theta_{z1}}^{\theta_{z2}} (1 - \exp(-kAB)) \cos \theta_z \sin^2 \varphi_z d\varphi_z \quad (440)$$

The two components f_{gz} and f_{gy} must subsequently themselves be projected on the line OP to obtain the required total absorption fraction, namely:

$$f_g = f_{gz} \cos \varphi + f_{gy} \sin \varphi$$

We can re-write all above in a combined expression as:

$$f_g = \int_{\varphi_{z1}}^{\varphi_{z2}} \int_{\theta_{z1}}^{\theta_{z2}} (1 - \exp(-kAB)) (\sin \varphi_z \cos \varphi_z \cos \varphi + \cos \theta_z \sin^2 \varphi_z \sin \varphi) d\varphi_z \quad (441)$$

Although we have already described the field around the axis of symmetry at the outset of PG theory with the simplest equations, the above formulations are more than a theoretical exercise, because they are needed in more complex mass distributions like the two-sphere problem examined later.

Further theoretical processing and analysis of the above derivations can be done separately, but the above can be used immediately as “raw” material for numerical integration to obtain some early results without further ado.

C Force between two spherical masses - bulk method

For the formulation of the problem of force between two material spheres, we have used two different methods. One method involves the points (elements) inside the bulk of one sphere followed by integration over the entire bulk of the sphere. The other method involves the points (elements) on the surface of one sphere and integration over the entire surface of the sphere. The outcomes are equivalent (equal) since traces of gravions passing through any point inside the bulk of a sphere must also cross the surface of the sphere and vice-versa. The bulk method involves four integrals and takes far longer integration times with numerical methods. The second method has its own complexity, but it involves three integrals requiring much shorter integration times.

With reference to Fig. 73, we define and use the following notations of constants and parameters: We have sphere_1 (*sphere*₁) and sphere_2 (*sphere*₂) with corresponding radii $R_1 = P_1N$ and $R_2 = P_2M$, and with uniform material densities and hence uniform absorption coefficients k_1 and k_2 ; the distance between the centers of the spheres is $P_1P_2 = r$. We choose a random point O inside sphere_2 forming an angle $\angle OP_1P_2 = \varphi_2$ with corresponding differential semi-angle $d\varphi_2$ and maximum subtended angle $\angle P_2P_1S = \varphi_{20}$. From point O, we define the direction u along OP_1 , around which we draw a random solid angle Ω_1 with semi-angle $\angle P_1OB_1 = \varphi_1$ with corresponding differential angle $d\varphi_1$ and maximum subtended angle $\angle P_1ON = \varphi_{10}$. The solid angle Ω_1 is enveloped by line u' , which crosses sphere_1 at points A₁ and B₁, and sphere_2 at points A₂ and B₂; we will also need the points A and B, at which the axis u crosses the sphere_2. Normal to the axis u is the axis ν with a third axis y (not shown) normal to the plane of $u\nu$, thus defining the coordinate system (νuy). Another coordinate system (xzy') is rotated around y' by the angle φ_2 with the axis z aligned with the two centers P₁ and P₂ and y' normal to the plane xz , i.e. parallel to y .

Point O is at a distance u from the center P_1 , i.e. $OP_1 = u$, and the usual parameters are:

$$a_1(u) = R_1/u = \sin \varphi_{10} \quad (442)$$

$$a_2 = R_2/r = \sin \varphi_{20} \quad (443)$$

$$P_1B = u_1(\varphi_2) = r \cos \varphi_2 - r \sqrt{(a^2 - \sin^2 \varphi_2)} \quad (444)$$

$$P_1A = u_2(\varphi_2) = r \cos \varphi_2 + r \sqrt{(a^2 - \sin^2 \varphi_2)} \quad (445)$$

The normal from P_2 to u crosses AB at mid point M, so that we obtain for the segments:

$$OM(u, \varphi_2) = u - r \cos \varphi_2 \quad (446)$$

$$MP_2(\varphi_2) = r \sin \varphi_2 \quad (447)$$

The length A_1B_1 is derived per Eq. 12 again as:

$$A_1B_1(\theta, \varphi_1, u) = 2u \sqrt{a_1^2 - \sin^2 \varphi_1} \quad (448)$$

which is independent of (being constant with) the azimuth angle of rotation around axis u ; we introduce the azimuth because we further require to know the chord lengths OB_2 and OA_2 , which vary by rotating the line u' around the axis u at constant angle φ_1 ; the azimuth angle of rotation θ is not shown for simplicity of drawing. We derive the latter chords by solving the equations of sphere_2 and line u' per analytical geometry as follows:

$$y^2 + (\nu - MP_2)^2 + (u - OM)^2 = R_2^2 \quad (449)$$

$$\nu = (OB_2) \sin \varphi_1 \cos \theta \quad y = (OB_2) \sin \varphi_1 \sin \theta \quad u = (OB_2) \cos \varphi_1 \quad (450)$$

The simultaneous solution of above equations gives the required lengths

$$OA_2(\theta, \varphi_1, u, \varphi_2) = MP_2 \sin \varphi_1 \cos \theta + OM \cos \varphi_1 - \sqrt{(MP_2 \sin \varphi_1 \cos \theta + OM \cos \varphi_1)^2 + R_2^2 - OM^2 - MP_2^2} \quad (451)$$

$$OB_2(\theta, \varphi_1, u, \varphi_2) = MP_2 \sin \varphi_1 \cos \theta + OM \cos \varphi_1 + \sqrt{(MP_2 \sin \varphi_1 \cos \theta + OM \cos \varphi_1)^2 + R_2^2 - OM^2 - MP_2^2} \quad (452)$$

where it is important to take the absolute value of the above lengths (when they are negative) in the exponent of the exponential factor used to derive the graviton absorption below.

The general strategy is briefly as follows: We consider all graviton flows in all possible directions at every given point and vectorially sum the flows (forces) over all points inside the sphere. The components of flow in the direction P_1P_2 are responsible for the force, whilst those perpendicular (normal) to that direction contribute no force between the spheres. We first group all the components of flow in the direction of axis u and all the components in the normal direction of axis v , and then project the two outcomes in the direction of z defined by the centers of the two spheres, whilst all components in the normal direction x vanish. In the latter stage, the useful absorption fraction $f_g(O)$ at point O is the absorption $f_g(O)_z$ in direction (projection) z derived from the absorption $f_g(O)_u$ in direction u plus the absorption $f_g(O)_v$ in direction v as follows:

$$f_g(O) \equiv f_g(O)_z = f_g(O)_u \cos \varphi_2 + f_g(O)_v \sin \varphi_2 \quad (453)$$

This will be used in a final integration to find the force F by:

$$F = 2\pi \frac{J}{c} \int_0^{\varphi_{20}} \left(\int_B^A f_g(O) u^2 k_2 du \right) \sin \varphi_2 \cos \varphi_2 d\varphi_2 \quad (454)$$

The above provides only a general idea of what we better explain and clarify with detailed steps next.

C.1 u -axis

There are two components of gravion absorption by integration around this axis, namely, those crossing both spheres by joint traces and those crossing only sphere_2.

C.1.1 Joint crossing (*variable_{uj}*)

Gravions passing through point O and crossing both spheres (“jointly”) along the line B₁A₁B₂O A₂ undergo exponential absorption before they arrive at point O, the difference of which multiplied by the usual product $\sin \varphi_1 \cos \varphi_1$ yields the absorption component along the u axis:

$$f_{g-uj}(\theta, \varphi_1, u, \varphi_2) = [\exp(-|k_2 OA_2|) - \exp(-k_1 A_1 B_1 - k_2 OB_2)] \sin \varphi_1 \cos \varphi_1 \quad (455)$$

which we integrate around the axis over the full azimuth angle θ and over the zenith angle φ_1 within the subtended solid angle by sphere_1 at the given angle φ_2 of the axis with P₁P₂ and the given distance u of O from P₁:

$$F_{uj}(u, \varphi_2) = \int_0^{\text{asin}(a_1(u))} \int_{-\pi}^{\pi} f_{g-uj}(\theta, \varphi_1, u, \varphi_2) d\theta d\varphi_1 \quad (456)$$

The subscripts uj stand for u axis (direction) and “joint” traces. The above integrated gravion component exerts a pressure J_0/c on an elementary thin material segment disposed normal to the axis of rotation (u), so that the product of the pressure with the area of the element times the absorption coefficient k_2 of material sphere_2 over the elementary thickness du produces an elementary force at point O. We may omit the constant factor J_0/c from the interim formulations until we obtain the end result for the absorption factor. Now, we need to multiply by the area $u^2 d\Omega_2$, where $d\Omega_2$ is the elementary solid angle subtended by the surface element at the center P₁ times $k_2 du$ to allow for the absorption along du generating an elementary force:

$$d^2 S_{uj}(u, \varphi_2) = F_{uj}(u, \varphi_2) u^2 k_2 du d\Omega_2 \quad (457)$$

It is noteworthy at this point that the above factor has acquired the dimensions of an area being an elementary surface (S) after initially being a pure number. From the above, we find the total absorption along the length of chord A₂B₂

$$dS_{uj}(\varphi_2) = \left[\int_{u_1(\varphi_2)}^{u_2(\varphi_2)} F_{uj}(u, \varphi_2) u^2 k_2 du \right] d\Omega_2 \quad (458)$$

Here and in following derivations, when we use an elementary solid angle $d\Omega$, we replace it either with $d\Omega = \sin \varphi d\varphi$ in an asymmetrical rotation by involving the azimuth angle, or with the elementary annular solid angle $d\Omega = 2\pi \sin \varphi$ being the integral around a rotational symmetry without use of the azimuth angle. We do this without explicitly stating it. Thus, and by projecting the above force on P₁P₂ by $\cos \varphi_2$, we finally integrate over the entire bulk of sphere 2 by

$$S_{uj} = \int_0^{\text{asin}(a_2)} dS_{uj}(\varphi_2) \cdot 2\pi \sin \varphi_2 \cos \varphi_2 d\varphi_2 \quad (459)$$

C.1.2 Single crossing (*variable_{us}*)

For traces of gravions crossing only sphere_2, to which we refer with the term “single” or “lone” (with subscript s), the corresponding integrand of the innermost integral is a little simpler by:

$$f_{g-us}(\theta, \varphi_1, u, \varphi_2) = [\exp(-|k_2 OA_2|) - \exp(-k_2 OB_2)] \sin \varphi_1 \cos \varphi_1 \quad (460)$$

We repeat the same steps except that we integrate with respect to zenith angle from φ_{10} (i.e. $\text{asin}(a_1(u))$) to $\pi/2$, so that by changing the notation of “ j ” to “ s ”, we get:

$$F_{us}(u, \varphi_2) = \int_{\text{asin}(a_1(u))}^{\pi/2} \int_{-\pi}^{\pi} f_{g-us}(\theta, \varphi_1, u, \varphi_2) d\theta d\varphi_1 \quad (461)$$

and finally

$$S_{us} = \int_0^{\text{asin}(a_2)} dS_{us}(\varphi_2) \cdot 2\pi \sin \varphi_2 \cos \varphi_2 d\varphi_2 \quad (462)$$

We find that the terms for “single” absorption are not needed for the final force derivation, because they cancel out exerting a null force. However, we consider the steps involved not only for completeness, but also because we need to follow the corresponding steps during derivation of mass or energy in subsequent sections.

C.2 ν -axis

Again, there are two kinds of components of graviton absorption by integration around this axis, namely, those crossing both spheres by joint traces and those crossing only sphere_2. The latter “single” crossings contain two subgroups, namely, those in the complementary angle to the joint zenith angle (i.e. outside the joint zenith angle up to $\pi/2$) and those in the supplementary joint azimuth angle within the joint zenith angle (i.e. outside the joint azimuth angle $2\pi - \text{joint_azimuth}$ angle). We explain this in the following three steps.

C.2.1 joint crossing (*variable $_{\nu j}$*)

The notation of angles (θ, φ_1) could have been designated as (θ_u, φ_{1u}) for the u -axis and as $(\theta_\nu, \varphi_{1\nu})$ for the ν -axis, because the angles with reference to the normal axis ν are different, but there is no ambiguity to retain the same notation with both axes noting that the range of integration angles are different, for which special care is required to avoid possible errors; by use of the correct integration limits, we do not need to change notation of azimuth and zenith angles.

Now, A_1B_1 is found by a different expression:

If *operand* = $(u \sin \varphi_1 \cos \theta)^2 + R_1^2 - u^2 > 0$ then

$$A_1B_1 \equiv A_1B_{1\nu j}(\theta, \varphi_1, u) = 2\sqrt{\text{operand}} \quad (463)$$

From the condition of a positive operand above, we obtain the range of angles:

$$\begin{aligned} \theta_1 &= -\text{acos} \left(\sqrt{u^2 - R_1^2} / (u \sin \varphi_1) \right) \\ \theta_2 &= +\text{acos} \left(\sqrt{u^2 - R_1^2} / (u \sin \varphi_1) \right) \\ \varphi_{11} &= \pi/2 - \text{asin}(a_1(u)) \\ \varphi_{12} &= \pi/2 + \text{asin}(a_1(u)) \end{aligned}$$

The above limits ensure that the integration contains only joint traces. Note that φ_1 must cover the range on either side from $\pi/2$. The lengths OA_2 and OB_2 are given by the same Eqs. 451 and 452 provided we apply the above (correct) range of angles. Then, we follow the same steps changing the notation of u with ν accordingly:

$$f_{\nu j}(\theta, \varphi_1, u, \varphi_2) = [\exp(-|k_2OA_2|) - \exp(-k_1A_1B_1 - k_2OB_2)] \sin \varphi_1 \cos \varphi_1 \quad (464)$$

finally obtaining:

$$S_{\nu j} = \int_0^{\text{asin}(a_2)} dS_{\nu j}(\varphi_2) \cdot 2\pi \sin \varphi_2 \cos \varphi_2 d\varphi_2 \quad (465)$$

C.2.2 Single (or lone) crossing

There are two terms for “single” (lone) crossing traces to derive in ν -direction:

(i) ν -axis single complementary - (*variable $_{\nu s-c}$*) This term arises in the zenith angle range $0 \rightarrow \pi/2 - \text{asin}(a_1(u))$ (being the complement of the joint zenith angle), with corresponding full azimuth angle range $-\pi \rightarrow +\pi$. We follow the same steps leading to the final integral:

$$S_{\nu s-c} = \int_0^{\text{asin}(a_2)} dS_{\nu s-c}(\varphi_2) \cdot 2\pi \sin \varphi_2 \cos \varphi_2 d\varphi_2 \quad (466)$$

(ii) ν -axis single supplement (*variable* $_{\nu s-s}$) This term arises in half of the joint zenith angle range $\varphi_{11} \rightarrow \varphi_{12}$ (below) with corresponding partial (i.e. supplementary) azimuth angle range $\theta_1 \rightarrow \theta_2$ (i.e. outside the “joint” crossings), where

$$\begin{aligned}\theta_1 &= \text{acos}\left(\sqrt{u^2 - R_1^2}/(u \sin \varphi_1)\right) \\ \theta_2 &= 2\pi - \text{acos}\left(\sqrt{u^2 - R_1^2}/(u \sin \varphi_1)\right) \\ \varphi_{11} &= \pi/2 - \text{asin}(a_1(u)) \\ \varphi_{12} &= \pi/2\end{aligned}$$

It should be noted that, while the zenith range is actually between $\pi/2 - \text{asin}(a_1(u)) \rightarrow \pi/2 + \text{asin}(a_1(u))$, we use only half of this range to avoid a second pass of the same single crossing in the second semi-range $\pi/2 + \text{asin}(a_1(u))$ of the zenith angle.

The above limits ensure that the integration contains only “single” chords in the function of absorption along the given line u' . We follow again the same steps yielding the other additional component now indexed with “ $_{\nu s-s}$ ”

$$S_{\nu s-s} = \int_0^{\text{asin}(a_2)} dS_{\nu s-s}(\varphi_2) \cdot 2\pi \sin \varphi_2 \cos \varphi_2 d\varphi_2 \quad (467)$$

C.3 Summation of terms

In the general case above, we have formulated five terms initially to be summed for the total force between the two spheres. These terms are all components projected along the line joining the spheres, so that we must take their algebraic sum. Each derivation provides a positive number for each component. However, the configuration of Fig. 73 is such that all terms of the ν -axis are pointing in the negative direction and hence they must enter with a negative sign in the sum for the total S_F :

$$S_F = S_{uj} + S_{us} - S_{\nu j} - S_{\nu s-c} - S_{\nu s-s} \quad (468)$$

As already mentioned, the sum of all “single” terms vanishes, because $S_{us} = S_{\nu s-c} + S_{\nu s-s}$, leaving only the joint components:

$$S_F = S_{uj} - S_{\nu j} \quad (469)$$

The latter is to be finally multiplied by J_o/c to yield the force.

C.4 Alternative joint ν -axis component along with joint u -axis (combination) (*variable* $_{uvj}$)

Similar to the alternative derivation by Eq. B.1, it is possible also to account for the joint component arising from the ν -axis. This is facilitated first because all “single” components of force contribute a null effect. Therefore, if only the “joint” components are important for the force derivation, then we need to find the ν -axis joint component in the same range of limits of integration along (concurrently) with u -axis joint component. With this approach, the equations for the lengths A_1B_1 , OA_2 and OB_2 are all the same in both cases. To account for the ν -component while revolving around the u -axis, we use the factors $\cos \theta \sin^2 \varphi_1$ (corresponding to $\cos \theta_z \sin^2 \varphi_z$ in Eq. 440) in the first double integral followed by the same steps, namely:

$$f_{uvj}(\theta, \varphi_1, u, \varphi_2) = [\exp(-|k_2 OA_2|) - \exp(-k_1 A_1 B_1 - k_2 OB_2)] \cos \theta \sin^2 \varphi_1 \quad (470)$$

$$F_{uvj}(u, \varphi_2) = \int_0^{\text{asin}(a_1(u))} \int_{-\pi}^{\pi} f_{uvj}(\theta, \varphi_1, u, \varphi_2) d\theta d\varphi_1 \quad (471)$$

then we form the third integral in the usual way by

$$d^2 S_{uvj}(u, \varphi_2) = F_{uvj}(u, \varphi_2) u^2 k_2 du d\Omega_2 \quad (472)$$

$$dS_{uvj}(\varphi_2) = \left[\int_{u_1(\varphi_2)}^{u_2(\varphi_2)} F_{uvj}(u, \varphi_2) u^2 k_2 du \right] d\Omega_2 \quad (473)$$

Since $d\Omega_2 = 2\pi \sin \varphi_2$ and projecting on P_1P_2 , however, now by $\sin \varphi_2$, we finally integrate over the entire bulk of sphere 2 by

$$S_{uvj} = \int_0^{\text{asin}(a_2)} dS_{uvj}(\varphi_2) \cdot 2\pi \sin^2 \varphi_2 d\varphi_2 \quad (474)$$

Thus, we can write as an alternative formulation of the total force factor:

$$S_F = S_{uj} - S_{uvj} \quad (475)$$

which again multiplied by the pressure J_0/c yields the total force between the two spheres.

C.5 Quadruple integral

We have conducted numerical integration of all of the above formulations and have confirmed the expected equivalent results with all cases within the set integration tolerance. The starting formulations may be thought of as the ‘‘raw’’ constituting equations of PG theory. They can be further worked out. They are amenable to further theoretical analysis and processing, which can be done separately. For now, we can summarize with a general quadruple integration of all the above by taking advantage of the common integration limits when using the alternative ν -axis joint component as follows:

$$S_F = 2\pi k_2 \int_0^{\varphi_{20}} \left\{ \sin \varphi_2 \cos \varphi_2 \int_{u_1}^{u_2} \left[\left(\int_0^{\varphi_{10}} \int_{-\pi}^{\pi} f_u() d\theta d\varphi_1 \right) u^2 \right] du \right. \\ \left. - \sin^2 \varphi_2 \int_{u_1}^{u_2} \left[\left(\int_0^{\varphi_{10}} \int_{-\pi}^{\pi} f_v() dx dy \right) u^2 \right] du \right\} d\varphi_2 \quad (476)$$

where

$$f_u() = [\exp(-|k_2 O A_2|) - \exp(-k_1 A_1 B_1 - k_2 O B_2)] \sin \varphi_1 \cos \varphi_1 \quad (477)$$

$$f_v() = [\exp(-|k_2 O A_2|) - \exp(-k_1 A_1 B_1 - k_2 O B_2)] \cos \theta \sin^2 \varphi_1 \quad (478)$$

By re-writing we get

$$S_F = 2\pi k_2 \int_0^{\varphi_{20}} \int_{u_1}^{u_2} \int_0^{\varphi_{10}} \int_{-\pi}^{\pi} [f_u() \sin \varphi_2 \cos \varphi_2 - f_v() \sin^2 \varphi_2] u^2 \cdot d\theta d\varphi_1 du d\varphi_2 \quad (479)$$

or

$$S_F = 2\pi k_2 \int_0^{\varphi_{20}} \int_{u_1}^{u_2} \int_0^{\varphi_{10}} \int_{-\pi}^{\pi} f() [\sin \varphi_1 \cos \varphi_1 \sin \varphi_2 \cos \varphi_2 - \cos \theta \sin^2 \varphi_1 \sin^2 \varphi_2] u^2 \cdot d\theta d\varphi_1 du d\varphi_2 \quad (480)$$

where

$$f() = \exp(-|k_2 O A_2|) - \exp(-k_1 A_1 B_1 - k_2 O B_2) \quad (481)$$

with integration limits and chord lengths or segments as provided during the preceding detailed derivations.

We have also performed a numerical integration of the above and found consistency with all other other part term computations. With every computation, we have normalized by the factor $(\pi^2 A_1 A_2)/r^2$ where

$$A_1 = \left[R_1^2 - \frac{1}{2k_1^2} + \frac{\exp(-2k_1 R_1)(2k_1 R_1 + 1)}{2k_1^2} \right] \quad (482)$$

$$A_2 = \left[R_2^2 - \frac{1}{2k_2^2} + \frac{\exp(-2k_2 R_2)(2k_2 R_2 + 1)}{2k_2^2} \right] \quad (483)$$

as used with the original “reverse engineering” derivation by Eq. 85. The normalization has invariably resulted in unity within the prescribed tolerance of the integrals. Having said that, the original (“raw”) derivations of the various terms of absorption (like “single” and “joint”) are also needed to study the physics and underlying mechanisms of force and mass or energy not otherwise directly obvious from the end Eq. 85. This is done in the theory of the main body of this report in Section 16.

D Effective Mass or Energy for one and two spherical masses - bulk method

In this section, we formulate the problem of finding the gravion absorption rate by one (single) or two interacting spheres. Since we have also established that we can deduce the corresponding effective mass or energy from the gravion absorption rate per Sections 15.7 and 16, we can compare the expressions of mass or energy with the expressions of force.

D.1 General case for two spheres

The mass or energy, being a scalar, can be derived from summing (integrating) the absorption rate of gravions by the elementary volume around points O inside the bulk of the sphere. This is done first by summing, instead of subtracting, the two terms of Eq. 455 corresponding to the absorption lengths along the direction u' on either side of point O, so that the absorption factor f_{a-} is:

$$f_{a-uj}(\theta, \varphi_1, u, \varphi_2) = [\exp(-|k_2OA_2|) + \exp(-k_1A_1B_1 - k_2OB_2)] \sin \varphi_1 \quad (484)$$

without the factor $\cos \varphi_1$, which was necessary to obtain the projection of gravion flow along the direction u . We conduct the double integration by setting:

$$M_{uj}(u, \varphi_2) = \int_0^{\text{asin}(a_1(u))} \int_{-\pi}^{\pi} f_{a-uj}(\theta, \varphi_1, u, \varphi_2) d\theta d\varphi_1 \quad (485)$$

Then, we come to the third integral and account for the gravions absorbed by the elementary material slice facing in the direction u . The gravions absorbed by the elementary thickness $du = OU$ (see inset in Fig. 73) is actually proportional to the elementary length $OU' = du/\cos \varphi_1$, which must also be multiplied by the same $\cos \varphi_1$ to account for the cosine law reduction (oblique incidence) of the arriving gravions; the net result is that the absorption is proportional to the elementary thickness du times k_2 times the elementary area $u^2 d\Omega_2$, as with the force:

$$d^2S_{a-uj}(u, \varphi_2) = M_{uj}(u, \varphi_2) u^2 k_2 du d\Omega_2 \quad (486)$$

from which we correspondingly obtain the absorption along the length of chord A_2B_2

$$dS_{a-uj}(\varphi_2) = \left[\int_{u_1(\varphi_2)}^{u_2(\varphi_2)} M_{uj}(u, \varphi_2) u^2 k_2 du \right] d\Omega_2 \quad (487)$$

Now, we again have $d\Omega_2 = 2\pi \sin \varphi_2$, but there is no reason to project the scalar quantity of absorbed gravions on P_1P_2 to obtain the last integration over the entire bulk of sphere_2, so that we finally obtain

$$S_{a-uj} = \int_0^{\text{asin}(a_2)} dS_{a-uj}(\varphi_2) \cdot 2\pi \sin \varphi_2 d\varphi_2 \quad (488)$$

We must further add the absorption by the “single” sphere term in the remaining zenith angle from $\text{asin}(a_1(u))$ to $\pi/2$. Here, the absorption factor f_{a-} is a simpler expression:

$$f_{a-us}(x, y, u, \varphi_2) = [\exp(-|k_2OA_2|) + \exp(-k_2OB_2)] \sin \varphi_1 \quad (489)$$

as the gravions trace only the chord A_2B_2 of sphere_2, and

$$M_{us}(u, \varphi_2) = \int_{\text{asin}(a_1(u))}^{\pi/2} \int_{-\pi}^{\pi} f_{a-us}(\theta, \varphi_1, u, \varphi_2) d\theta d\varphi_1 \quad (490)$$

We do the third and fourth integral in the same way by replacing “j” with “s”, so that finally we have

$$S_{a-us} = \int_0^{\text{asin}(a_2)} dS_{a-us}(\varphi_2) \cdot 2\pi \sin \varphi_2 d\varphi_2 \quad (491)$$

The total graviton absorption rate is then the sum of the above two terms:

$$S_a = S_{a-uj} + S_{a-us} \quad (492)$$

The latter is again a characteristic area, the product of which with J_0 , i.e. $S_a J_0$, yields the total graviton rate of absorption by sphere_2. Equivalently, we also obtain the effective mass by $\frac{S_a}{4\pi\Lambda}$.

D.2 Single sphere

We have used and confirmed the following two alternative bulk method formulations for graviton absorption rate by a single sphere over and above the method already provided in Section 15.7.

D.2.1 Single sphere general

For a single sphere, say sphere_2, we can apply the preceding Eq. 491 by setting $\text{asin}(a_1(u)) = 0$, i.e. by initially integrating over the entire zenith angle ($0 < \varphi_1 < \pi/2$), i.e. by vanishing sphere_1 with $R_1 = 0$ at any arbitrary distance r :

$$M_{us-full}(u, \varphi_2) = \int_0^{\pi/2} \int_{-\pi}^{\pi} f_{a-us}(\theta, \varphi_1, u, \varphi_2) d\theta d\varphi_1 \quad (493)$$

Then, we follow with the same third and fourth integrals. The final integral is similar to Eq. 491 but for the full zenith angle (in the above integral):

$$S_{a-us-full} = \int_0^{\text{asin}(a_2)} dS_{a-us}(\varphi_2) \cdot 2\pi \sin \varphi_2 d\varphi_2 \quad (494)$$

D.2.2 Single sphere bulk alternative

With reference to Fig. 7 used to find the internal acceleration, we can derive a simple formulation for the graviton absorption rate as follows:

We now add the scalar terms of absorption to obtain the absorption factor at point O (prior $R_X = R_O$ here):

$$f_{aO} = 2\pi \sin \varphi d\varphi \cdot \left[\exp \left(-k\sqrt{R^2 - (R_O \sin \varphi)^2} + kR_O \cos \varphi \right) + \exp \left(-k\sqrt{R^2 - (R_O \sin \varphi)^2} - kR_O \cos \varphi \right) \right] \quad (495)$$

We integrate to find the absorption from all the traces radiating out from this point:

$$M_{aO} = \int_0^{\pi/2} 2\pi \sin \varphi d\varphi \cdot \left[\exp \left(-k\sqrt{R^2 - (R_O \sin \varphi)^2} + kR_O \cos \varphi \right) + \exp \left(-k\sqrt{R^2 - (R_O \sin \varphi)^2} - kR_O \cos \varphi \right) \right] \quad (496)$$

This is the same for all points on the internal spherical surface with radius R_O , so that the spherical shell with thickness dR_O absorbs $M_{aO} \cdot 4\pi R_O^2 \cdot kdR_O$, from which we sum (integrate) for the total bulk of the sphere by:

$$S_a = \int_0^R M_{aO} \cdot 4\pi k R_O^2 dR_O = 4\pi^2 R^2 A_R \quad (497)$$

Since

$$\frac{dS_a}{dR_O} = M_{aO} \cdot 4\pi k R_O^2$$

$$kM_{aO} = \frac{dS_a}{dR_O} \frac{1}{4\pi R_O^2} \quad (498)$$

we can readily recognize that the product kM_{aO} is a per unit volume characteristic area at point O, the product of which by $\frac{1}{4\pi\Lambda}$ yields the effective mass per unit volume at that point, i.e. the point effective density $\rho_{e-point}$.

D.3 Net loss of absorption rate between two spheres - bulk method

There is an important quantity arising by the difference of the absorption rate of one sphere in the presence of another from the absorption rate it has, when it is alone (without the absence of other bodies in the neighborhood). In this difference, there is a common term $f_{a-us}(x, y, u, \varphi_2)$ in the interval from $\text{asin}(a_1(u))$ to $\pi/2$ of the zenith angle, leaving only the difference between the “single” and “joint” terms in the common zenith interval from 0 to $\text{asin}(a_1(u))$:

$$f_{a-netloss}() = f_{a-us}() - f_{a-uj}() = [\exp(-|k_2OA_2|) - \exp(-k_1A_1B_1 - k_2OB_2)] \sin \varphi_1 \quad (499)$$

which is identical to the force term in Eq. 455 except for the $\cos \varphi_1$ that was necessitated to project the gravion flow on the axis joining the centers of the two spheres. We use the term “net” loss to distinguish it from the generally present (current) steady-state absorption in any or both spheres. The net loss is not “current”, i.e. it represents a loss of gravions that is not present absorption in any of the spheres, but which was present prior to the interaction between the two spheres and now has gone “missing”. We will return to this net loss and the common mathematical factor again, when we consider the “surface” derivations of gravion absorption.

E Effective Mass or Energy for one and two spherical masses - surface method

The “bulk” method for the force and effective mass appeared to be the logical or standard way to start with. It provides good insight on the various fractions of gravion absorption and their possible inter-relationships, whilst it forms a basis for further elaboration. However, it presents a practical disadvantage by the long computation times, if we opt to follow this method. Fortunately, there is also an alternative method by expanding the approach used in Section 15.7 for a single sphere. We have thus developed the “surface” method with one less integration and much faster computation time, but subject to considerable complexity in defining the integration ranges as we move around the surface of one sphere relative to the other. We explain this method in detail below.

E.1 General case for two spheres

With reference to Fig. 74, we have sphere_1 and sphere_2, for which we designate certain variables and relationships needed for the intended formulations. The three tangents from the sphere centers, namely, P_2D and P_2W and P_1L together with the two mutual tangents IS and KT cross the surface of sphere_2 at points G , S , L , T , E and F signaling a transition of the angle $\omega = \angle qP_2z$ from $0 \rightarrow \omega_G \rightarrow \omega_S \rightarrow \omega_L \rightarrow \omega_T \rightarrow \omega_E \rightarrow \pi$. Concomitant with these lines and points, we need the following lengths and relationships:

$$r = P_1P_2, \quad r_1 = P_1N, \quad r_2 = P_2N, \quad r_3 = P_2M$$

$$R_1 = P_1K, \quad R_2 = P_2T, \quad \frac{R_2}{r_2} = \frac{R_1}{r_1}$$

$$r_1 + r_2 = r, \quad r_1 = \frac{R_1}{R_1 + R_2}r, \quad r_2 = \frac{R_2}{R_1 + R_2}r, \quad r_3 = \frac{R_2}{R_2 - R_1}r$$

$$\omega_G = \angle P_1P_2D = \text{asin}\varphi_{01}$$

$$\omega_S = \text{acos}\left(\frac{R_2}{r_2}\right) = \text{acos}\left(\frac{R_1 + R_2}{r}\right)$$

$$\omega_L = \text{acos}\left(\frac{R_2}{r}\right)$$

$$\omega_T = \text{acos}\left(\frac{R_2}{r_3}\right) = \text{acos}\left(\frac{R_2 - R_1}{r}\right)$$

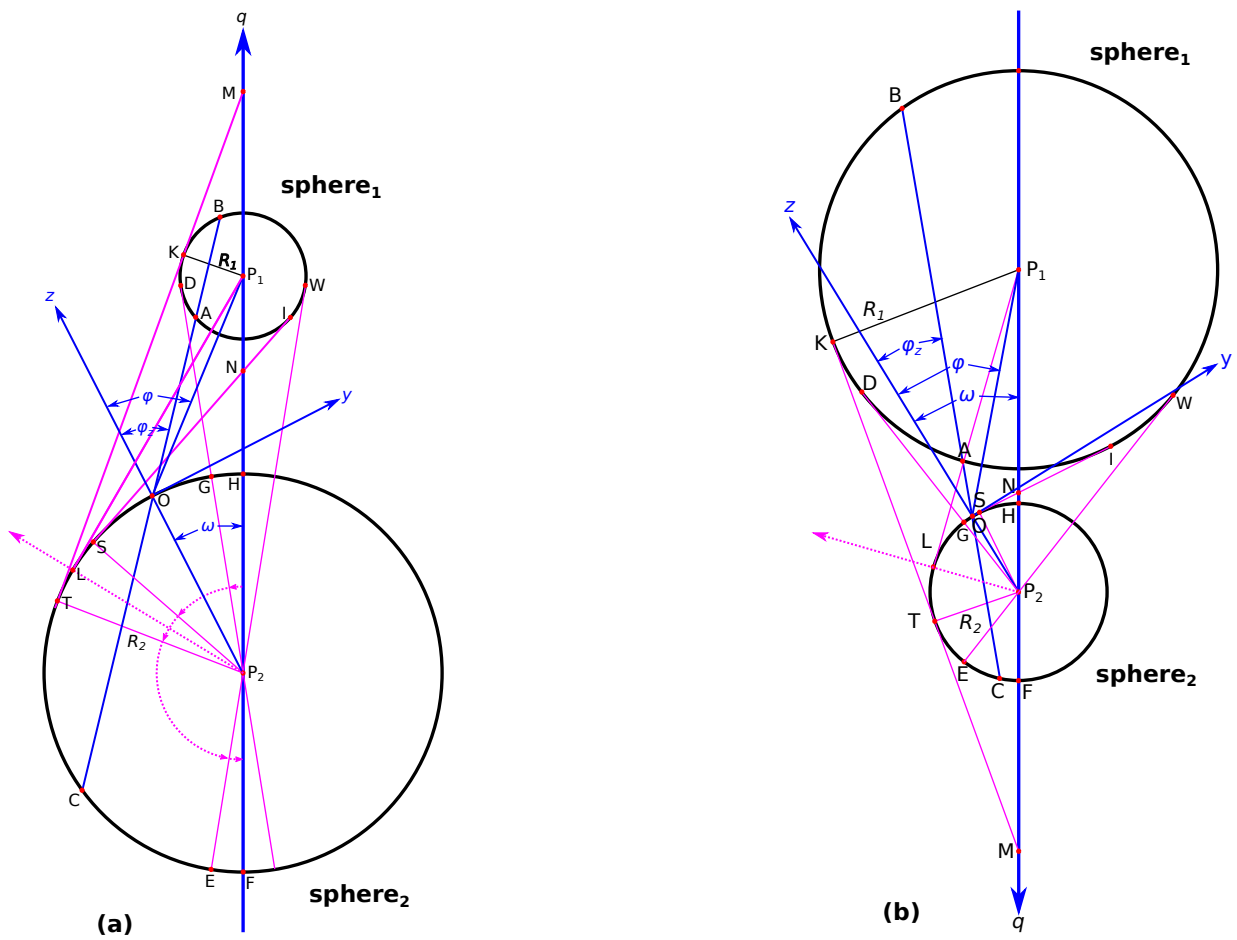


Figure 74: Surface method for the formulation of the energy absorption rate.

We consider all points O on the surface of this sphere and all the traces of gravions through this point crossing this sphere alone or both spheres. The line from the center of sphere_2 to point O on the surface constitutes the axis z of revolution, around which we calculate the first two integrals with respect to azimuth angle θ and zenith angle $\varphi_z = \angle zOB$. For this moving coordinate system with origin O, we further require the distance d of center P_1 and angle φ of OP_1 with axis z , which are easily found to be:

$$d = OP_1 = \sqrt{r^2 + R_2^2 - 2rR_2 \cos \omega}.$$

$$\varphi = \angle P_1Oz = \omega + \text{asin} \left(\frac{R_2}{d} \sin \omega \right).$$

We further require the usual limiting angles subtended by each sphere as:

$$a = \frac{R_1}{d}, \quad a_{01} = \frac{R_1}{r} = \sin \varphi_{01}, \quad a_{02} = \frac{R_2}{r} = \sin \varphi_{02}$$

Now, with such a configuration, there is always (at all zenith angles) a chord OC of sphere_2 with every trace through this point (even with one vanishing length), whilst only within the subtended solid angle by sphere_1 there are traces crossing sphere_1 along the chords AB. The length of these corresponding chords are:

$OC = 2R_2 |\cos \varphi_z|$, which always enters as a positive number in the exponential factor of absorption and

$$(AB)_z = 2\sqrt{(y_0 \sin \varphi_z \cos \theta_z + z_0 \cos \varphi_z)^2 - (d^2 - R_1^2)},$$

where $z_0 = d \cos \varphi$ and $y_0 = d \sin \varphi$, as we have found in Appendix B.

Next, we proceed to find the two fractions of absorption (“single” or “joint”) by this sphere by first establishing the integrand for absorption around axis P_2z . Since there is an axis of symmetry defined by the centers of the two spheres (P_1P_2), the situation must be the same for all points on the surface annulus around this axis at angle ω . Thus, we can find the absorption rate for the elementary surface annulus and then integrate with respect to ω in the interval $0 < \omega < \pi$. For the surface element at point O, we note that sphere_2 is always located entirely on one side of the plane of the element. However, sphere_1 changes location relative to the said surface element plane in ways that it can be (i) entirely on one side of the plane, or the other, i.e. on the same side as, or the alternate side from sphere_2, or (ii) the plane crosses sphere_1. In the latter case, sphere_1 can be crossed either above or below its “equator”, i.e. sphere_1 lies more than half above the horizon or more than half below the horizon of sphere_2, or (iii) the axis of rotation P_2z crosses sphere_1. The latter is also important to bear in mind, when we obtain the double integral of gravion absorption with respect to zenith and azimuth angles. During integration, we must either avoid doubling up the same absorption traces, or we must consistently do so and then divide by 2 (necessary to avoid dubious errors). Depending on how we decide to formulate the problem, we can finish up with 4, 5 or 6 absorption terms, the situation also depending on the relative size, configuration and distance of the spheres. Thus, for the “joint” absorption we require 4 terms, or 5 terms when the distance is very short, whilst 6 terms are used for the “single” absorption. The details of this are better explained inside the Python code used during numerical integration, which is planned for uploading in the near future. For consistency and to avoid confusion, let us consider sphere_2 the one, for which we wish to find its absorption as affected by the other sphere_1.

It is helpful to clarify again that ω_G is the semi-angle subtended by sphere_1 with $\omega_G = \text{asin}(a_{01})$, when the z -axis becomes tangent to sphere_1; ω_S is at the point where the normal axis y (i.e. the horizon plane of sphere 2) first becomes tangent to sphere_1, ω_L is at the point where the horizon plane crosses the center of sphere_1, ω_T is at the point where the horizon plane becomes again tangent with sphere_1, ω_E is where the z -axis becomes again tangent with sphere_1 and $\omega_F = \pi$. This subdivision is necessitated in order to apply the rules and limits of integration for a single sphere (sphere_1) as described in Appendix B regarding the various positions of sphere_1 relative to the frame of reference with origin at O. However, sphere_2 always being on one side of (“below” or “above”) the tangent plane, the rule is straightforward with absorption chords OC always radiating from point O. The need to distinguish the six intervals of angle ω arises from the changing integration limits of the first double integral. Thus, we integrate separately in each of these intervals and then sum all the results. In summing all the latter integrals, we should note that each chord is traced twice (once from each of its ends), so that we must divide the final result by a factor 2. Alternatively, we can take care to include only those terms (four or five terms), which exhaust all chords once, namely, by avoiding to integrate over the zenith angle below the horizon of sphere 2; then we should not divide by the factor 2, whilst it saves us dealing with unnecessary terms and speeds up the computation work. In the latter case, again care should be taken for the “single” traces not to cross the other sphere either above or below the horizon.

Further, it is important to note that, while the integration ranges of ω are for the most of distance r as depicted by Fig. 74(a), the situation is different at close enough distance depending on the given set of radii R_1 and R_2 and their relative location with regard to which sphere is under examination. For example, in the first diagram 74(a), point G lies between H and S, whilst in the second diagram Fig. 74(b), point S

lies between points G and H. This cross-over of points S and G occurs as we decrease the distance so that $\omega_G = \omega_S = \varphi_{01}$. Then $\text{acos}\left(\frac{R_1 + R_2}{r}\right) = \text{asin}\left(\frac{R_1}{r}\right)$, $\frac{R_1 + R_2}{r} = \sqrt{1 - \left(\frac{R_1}{r}\right)^2}$ and:

$$r_S = \sqrt{(R_1 + R_2)^2 + R_1^2} \quad (500)$$

It is also possible sometimes to have a cross-over of the corresponding points T and E, when $\omega_T = \omega_E = \pi - \varphi_{01}$. Then $\text{acos}\left(\frac{|R_1 - R_2|}{r}\right) = \text{asin}\frac{R_1}{r}$, $\frac{R_2 - R_1}{r} < \sqrt{1 - \left(\frac{R_1}{r}\right)^2}$ and:

$$r_T = \sqrt{(R_1 - R_2)^2 + R_1^2} \quad (501)$$

No diagram is shown for the latter condition here, but it can be easily envisaged. The latter characteristic situation can arise only when one of the spheres is sufficiently smaller than the other, whilst the two spheres do not merge (overlap). In summary, care should be taken to establish when and if the distance r is in the ranges:

$$r \leq r_T \leq r \leq r_S \leq r \quad (502)$$

in order to correctly define the corresponding ranges of ω with correct integration limits of the double integral.

As with the bulk method, we consider the two fractions of absorbed gravions, i.e. (a) along lines jointly crossing both spheres and (b) along lines singly crossing the sphere under investigation (let's say sphere_2).

For the joint absorption, in all traces of gravions through point O in the figure, we have $1 - \exp(-k_2 OC)$ absorbed from the side (direction) of sphere_2 and $\exp(-k_1 AB) - \exp(-k_1 AB)\exp(-k_2 OC)$ from the side (direction) of sphere_1. Their sum yields the integrand as a function of the azimuth and zenith angle by

$$f_{a-zj}(\theta_z, \varphi_z, \omega) = (1 - \exp(-k_2 OC)) (1 + \exp(-k_1 AB)) \sin \varphi_z \cos \varphi_z \quad (503)$$

where the factor $\cos \varphi_z$ is again introduced to allow for the oblique incidence of gravions relative to the sphere surface element. However, it is not canceled out now as it was for the gravions absorbed by the elementary material slice $du = OU$ (see inset in Fig. 73), because we use the integrated absorption through the entire chord length OC already containing the same factor in its exponential (not like the elementary length $OU' = du/\cos \varphi_1$). The distinction is subtle, but underlies an important mechanism: Both involve an elementary surface attached to an elementary mass slice in the bulk method but to the entire massive chord in the surface method. This saves us from the integration along this chord, which is a significant advantage of the "surface" method. Since the above integrand is not rotationally symmetric around the variable axis z , we must integrate with respect to the interdependent azimuth and the zenith angle to obtain the intermediate factor

$$M_{a-zj}(\omega) = \int_{\varphi_1}^{\varphi_2} \int_{\theta_1}^{\theta_2} f_{a-zj}(\theta_z, \varphi_z, \omega) d\theta_z d\varphi_z \quad (504)$$

It is important to obtain the limits of integration such that all traces fall inside the subtended solid angle by sphere_1 (see Appendix B). The above result is rotationally symmetric about the line joining the centers of the spheres and hence we multiply times the elementary annular surface $2\pi \sin \omega R_2^2 d\omega$ and integrate within each of the above defined ω intervals between points H, G, S, L, T and E, the limits denoted by ω_1 and ω_2 in the final integration for each term:

$$S_{a-j} = \int_{\omega_1}^{\omega_2} M_{a-zj}(\omega) \cdot 2\pi \sin \omega R_2^2 d\omega \quad (505)$$

It should be noted that the absorption factor given by Eq. 503 remains the same in all intervals of ω , because the absorption along chord OC is the same from whichever end we look at (as can be easily verified).

For single absorption, we follow the same steps: The absorption in each direction of the trace through point O is $(1 - \exp(-k_2 OC))$, and the starting integrand is the simplest by

$$f_{a-zs}(\theta_z, \varphi_z, \omega) = 2(1 - \exp(-k_2 OC)) \sin \varphi_z \cos \varphi_z \quad (506)$$

so that the first double integral gives:

$$M_{a-zs}(\omega) = \int_{\varphi_1}^{\varphi_2} \int_{\theta_1}^{\theta_2} f_{a-zs}(\theta_z, \varphi_z, \omega) d\theta_z d\varphi_z \quad (507)$$

Here, the limits of integration are the supplementary angle of the limits used for the azimuth (i.e. $2\pi - \theta_{joint}$) in joint absorption and the complementary angles used for the zenith ($0 \rightarrow \varphi_1$) and/or ($\varphi \rightarrow \pi/2$) of the joint absorption (in one or two parts). Extra care should be taken that the graviton trace does not cross sphere_1 in either direction as we rotate the trace. The final integral is similar by:

$$S_{a-s} = \int_{\omega_1}^{\omega_2} M_{a-zs}(\omega) \cdot 2\pi \sin \omega R_2^2 d\omega \quad (508)$$

While the distance r between the two spheres is fixed and not explicitly seen in the inegrands above, it is clear that the two absorption fractions are a function of distance, and we could also use the subscript r as we do in Section 16. The characteristic total surface factor S_a is the sum of the above:

$$S_a = S_{a-j} + S_{a-s} \quad (509)$$

The graviton absorption rate is the product $S_a J_0$ and the corresponding effective mass $\frac{S_a}{4\pi\Lambda}$

E.2 Net loss of absorption rate between two spheres - surface method

Like in Appendix D.3, we can derive the same net loss of absorption rate $f_{a-netloss}$ using the surface method. Again, we find the difference of the absorption rate of one sphere in the presence of another from the absorption rate it has when it is alone (in the absence of other bodies in the neighborhood). This is obtained from the difference of Eqs. 506 and 503 :

$$f_{a-netloss} = f_{a-zs}(\theta_z, \varphi_z, \omega) - f_{a-zj}(\theta_z, \varphi_z, \omega) = (1 - \exp(-k_2 OC)) (1 - \exp(-k_1 AB)) \sin \varphi_z \cos \varphi_z \quad (510)$$

in the common integration solid angle subtended by sphere_1, outside of which the terms of single absorption cancel out. Thus, we form the double integral:

$$M_{a-netloss}(\omega) = \int_{\varphi_1}^{\varphi_2} \int_{\theta_1}^{\theta_2} f_{a-netloss} d\theta_z d\varphi_z \quad (511)$$

The final integral yields a characteristic net-loss-surface-quantity $S_{a-netloss}$

$$S_{a-netloss} = \int_{\omega_1}^{\omega_2} M_{a-netloss}(\omega) \cdot 2\pi \sin \omega R_2^2 d\omega \quad (512)$$

We repeat the clarification as previously: We use the term “net” loss to distinguish it from the generally current (present) absorption in any or both spheres. This loss is not a “current” absorption loss, i.e. it represents a loss of gravions that is not present in any of the spheres at the given distance, but which was present prior to the interaction (at very long distance) between the two spheres but now gone “missing”.

F Force between two spherical masses - surface method

We can derive the total force exerted on sphere_2 by summing (integrating) all the forces exerted along all the chords traced by gravions in all possible directions through the point O on the surface. The “lone” or “single” crossings cancel out leaving only the “joint” ones. For any given chord OC, there is a force component from the direction that is free from (out of the way of) sphere_1 and caused by the absorption fraction $1 - \exp(-k_2 OC)$. The other component in the opposite direction arises from the arriving diminished intensity of absorption by a factor $\exp(-k_1 AB)$ after passing through sphere_1, while it traverses chord OC; The graviton absorption by this second beam of gravions is then $\exp(-k_1 AB) - \exp(-k_1 AB)\exp(-k_2 OC)$. The net force is the difference of the second from the first with a net force factor $(1 - \exp(-k_2 OC)) (1 - \exp(-k_1 AB))$. To prepare the integrand for integration around axis z , we should multiply by the usual product of $\sin \varphi_z$ (to account for the

elementary solid angle around the chord) and by $\cos \varphi_z$ to account for the per unit area oblique incidence with regard to absorption per se at that point. However, this is incomplete until we multiply again by $\cos \varphi_z$ to project that absorption flow on the axis z . Thus, the integrand for this component of force around this axis is given by:

$$f_{g-z}(\theta_z, \varphi_z, \omega) = (1 - \exp(-k_2 OC)) (1 - \exp(-k_1 AB)) \sin \varphi_z \cos^2 \varphi_z \quad (513)$$

with first double integration around this axis taken inside the solid angle subtended by sphere_1:

$$F_z(\omega) = \int_{\varphi_1}^{\varphi_2} \int_{\theta_1}^{\theta_2} f_{g-z}(\theta_z, \varphi_z, \omega) d\theta_z d\varphi_z \quad (514)$$

yielding the intermediate force factor per unit area on the surface at this point O. We multiply times the elementary annular surface at angle ω by $2\pi \sin \omega R_2^2$ as preciously, but we must also multiply by $\cos \omega$ to project this component of force on the line joining the centers of the two spheres. The above yields a characteristic surface area, which finally integrated is S_F :

$$S_{Fz} = \int_{\omega_1}^{\omega_2} F_z(\omega) \cdot 2\pi \sin \omega \cos \omega R_2^2 d\omega \quad (515)$$

Last, we must repeat the same steps for the normal component of force around y axis. It is easier (less complicated) to use the alternative method as per Appendix C.4. That is, we deduce the y component concurrently with the revolution used for integrating around z axis by using the same (common) limits of integration (see also Eq. 440). We again need to multiply Eq. 510 by the azimuth and zenith product $\cos \theta_z \sin \varphi_z$ as in:

$$f_{g-y}(\theta_z, \varphi_z, \omega) = (1 - \exp(-k_2 OC)) (1 - \exp(-k_1 AB)) \cos \theta_z \sin^2 \varphi_z \cos \varphi_z \quad (516)$$

and follow by the next two steps:

$$F_y(\omega) = \int_{\varphi_1}^{\varphi_2} \int_{\theta_1}^{\theta_2} f_{g-y}(\theta_z, \varphi_z, \omega) d\theta_z d\varphi_z \quad (517)$$

$$S_{Fy} = \int_{\omega_1}^{\omega_2} F_y(\omega) \cdot 2\pi \sin^2 \omega R_2^2 d\omega \quad (518)$$

noting that we used $\sin \omega$ to project this component on the line joining the centers, and the usual $2\pi \sin \omega$ for the elementary annular angle.

The algebraic sum $S_{Fz} + S_{Fy}$ yields a component of the total force for each interval $\omega_1 \rightarrow \omega_2$ prescribed for the angle ω , so that the final grand total S_F is the sum from all these intervals. Again, the total force acted upon sphere_2 by sphere_1 is given by the product $\frac{J_0}{c} S_F$. In the steady state considered by this report, this force is the same for both spheres (see also the symmetry of the force factor above).

Attention is drawn again (like with the bulk method) to the common factor presenting itself in the corresponding Eqs. 510, 513 and 516 between net loss and net force, which are discussed in the main body of the report in Section 16.

Whilst further theoretical processing and analysis of all of the above derivations can be done separately, we have used them to obtain some immediate results with numerical integration with simple Python codes and a good laptop computer. Computation time can be a practical problem with the “bulk” method, but this depends on each case. The “surface” method is the fastest that has allowed us to accumulate a significant amount of results. Computation time has been greatly reduced also by parallel running of codes in a multi-core CPU computer, i.e. separate codes are executed concurrently for the various terms involved in the mass and force derivations. Key cases have been run with both “bulk” and “surface” formulations yielding identical results within the integration tolerances set, which has provided further reassurance that no errors are involved with the derivation of equations or the computer codes. [The “personal” codes used are now available in the public domain separately. They have been edited with sufficient commentary and symbols consistent with \(matching\) the presented theory; this is necessary to make it readily understood and applicable by the general user. This task can also be better undertaken by expert computer programmers, who may prefer to develop a dedicated integrator for the fundamental needs of PG.](#) As a reference example,

the computer specifications used at present are: x64based PC, MS Windows 7 Home Premium, Processor: Intel(R) Core(TM) 3612QM CPU @2.10 GHz up to 3.0 GHz with turbo boost, 4-Core, 8-Logical Processors, 8 GB RAM. The codes can be found in <https://doi.org/10.5281/zenodo.7951860> with file named PYTHON CODES for PUSH GRAVITY.

References

- Adâmuți, I. A. (1982) The screen effect of the earth in the TETG. *Il Nuovo Cimento C* **5**(2), 189–208. doi:10.1007/BF02509010.
- Allahverdyan, A. E. & Nieuwenhuizen, Th. M.. (2000) Extraction of work from a single thermal bath in the quantum regime. *Physical Review Letters* **85**(9), 1799–1802.
- Bannikova, E. Yu., Kontorovich, V. M. & Poslavsky, S. A. (2016) Helicity of a toroidal vortex with swirl. *Journal of Experimental and Theoretical Physics* **122**(4), 769–775. doi:10.1134/s1063776116040026.
- Bialy, S. & Loeb, A. (2018) Could solar radiation pressure explain Oumuamua’s peculiar acceleration? *The Astrophysical Journal Letters* **868:L1**, 1–5. doi:<https://doi.org/10.3847/2041-8213/aaeda8>.
- Bird, G.A. (1995) *Molecular Gas Dynamics and the Direct Simulation of Gas Flows*. Oxford University Press, New York.
- Bulgac, A., Luo, Y.-L., Magierski, P., Roche, K. J. & Yu, Y. (2011) Real-time dynamics of quantized vortices in a unitary fermi superfluid. *Science* **332**(6035), 1288–1291. doi:10.1126/science.1201968.
- Bulgac, Aurel, Forbes, Michael McNeil, Kelley, Michelle M., Roche, Kenneth J. & Wlazłowski, Gabriel (2014) Quantized superfluid vortex rings in the unitary fermi gas. *Physical Review Letters* **112**(2). doi:10.1103/physrevlett.112.025301.
- Chappel, J.M., Iqbal, A. & Abbott, D. (2012) The gravitational field of a cube. *arXiv:1206.3857v1 [physics.class-ph]* .
- Consa, O (2018) Helical solenoid model of the electron. *Progress in Physics* **14**, 80–89.
- Danilatos, G.D. (1997) *In-Situ Microscopy in Materials Research*, chap. 2. Environmental Scanning Electron Microscopy, pp. 14–44. Kluwer Academic Publishers, Boston/Dordrecht/London.
- Danilatos, G.D. (2012) Velocity and ejector-jet assisted differential pumping: Novel design stages for environmental SEM. *Micron* **43**, 600–611.
- de Duillier, Nicolas Fatio (1929) *De la cause de la pesanteur*. Drei Untersuchungen zur Geschichte der Mathematik, in: Schriften der Strassburger Wissenschaftlichen Gesellschaft in Heidelberg, 10:(19-66). URL https://fr.wikisource.org/wiki/De_la_cause_de_la_pesanteur#.
- Dehmelt, HG (1989) Experiments with an isolated subatomic particle at rest URL <https://www.nobelprize.org/uploads/2018/06/dehmelt-lecture.pdf>.
- Dibrov, A. (2011) Unified model of shadow-gravity and the exploding electron. *Apeiron* **18**, 43–83.
- Edwards, R. M. (2007) Photon-graviton recycling as cause of gravitation. *Apeiron* **14**(3), 214–233.
- Falconer, Isobel (2019) Vortices and atoms in the maxwellian era. *Philosophical Transactions of the Royal Society A: Mathematical, Physical and Engineering Sciences* **377**(2158), 20180451. doi:10.1098/rsta.2018.0451.
- Fedi, Marco (2016) A superfluid Theory of Everything? URL <https://hal.archives-ouvertes.fr/hal-01312579>. Working paper or preprint.
- Fedosin, Sergey G. (2021) On the structure of the force field in electro gravitational vacuum doi:10.5281/zenodo.4515206.
- Feyerabend, Paul (2010) *Against Method*. Verso Books. ISBN 1844674428. URL https://www.ebook.de/de/product/9026002/paul_feyerabend_against_method.html.
- Field, G.B. (1971) Instability and waves driven by radiation in interstellar space and in cosmological models. *The Astrophysical Journal* **165**, 29–40. doi:10.1086/150873.

- Gagnebin, B (1949) De la cause de la pesanteur. Mémoire de Nicolas Fatio de Duillier présente à la Royal Society le 26 février 1690. *The Royal Society* **6(2)**, 125–160. doi:<https://doi.org/10.1098/rsnr.1949.0017>.
- Gamow, G. (1949) On relativistic cosmology. *Reviews of Modern Physics* **21(3)**, 367–373. doi:10.1103/RevModPhys.21.367.
- Giacintucci, S., Markevitch, M., Johnston-Hollitt, M., Wik, J. Q. D. R., Wang, H. S. & Clarke, T. E. (2020) Discovery of a giant radio fossil in the ophiuchus galaxy cluster. *arXiv:2002.01291 [astro-ph.GA]* .
- Gleick, J. (1998) *Chaos: Making a New Science*. Vintage. ISBN 9780749386061. URL https://www.ebook.de/de/product/3307050/james_gleick_chaos.html.
- Hogan, C.J. (1989) Mock gravity and cosmic structure. *The Astrophysical Journal* **340(1-10)**. doi:10.1086/167371.
- Hunt, A.J. (2019) New atomic model from the spectra of hydrogen, helium, beryllium, boron, carbon, and deuterium and their ions. *American Based Research Journal* ISSN 2304-7151. doi:10.5281/ZENODO.3456955.
- Kajari, E., Harshman, N.L., Rasel, E.M., Stenholm, S., Sussmann, G. & Schleich, W.P. (2010) Inertial and gravitational mass in quantum mechanics. *arXiv* doi:10.1007/s00340-010-4085-8. URL <https://arxiv.org/abs/1006.1988>.
- Kelvin, Lord (1867) On vortex atoms. *Proc. Royal Society of Edinburgh* **VI**, 94–105.
- Kotler, Shlomi, Peterson, Gabriel A., Shojaee, Ezad, Lecocq, Florent, Cacak, Katarina, Kwiatkowski, Alex, Geller, Shawn, Glancy, Scott, Knill, Emanuel, Simmonds, Raymond W., Aumentado, José & Teufel, John D. (2021) Direct observation of deterministic macroscopic entanglement. *Science* **372(6542)**, 622–625. doi:10.1126/science.abf2998.
- Llanes-Estrada, Felipe J. & Navardo, Gaspar Moreno (2012) CUBIC NEUTRONS. *Modern Physics Letters A* **27(06)**, 1250033. doi:10.1142/S0217732312500332.
- Lomas, Robert (1999) *The Man Who Invented the Twentieth Century*. Headline Book Publishing. ISBN 0747275882.
- Lorenzen, B. (2017) The cause of the allais effect solved. *International Journal of Astronomy and Astrophysics* **7**, 69–90.
- Loureiro, A, Cuceu, A, Abdalla, FiB., Moraes, B, Whiteway, L, McLeod, M, Balan, ST., Lahav, O, Benoit-Lévy, A, Manera, M & et al. (2019) Upper bound of neutrino masses from combined cosmological observations and particle physics experiments. *Physical Review Letters* **123(8)**. ISSN 1079-7114. doi:10.1103/physrevlett.123.081301. URL <http://dx.doi.org/10.1103/PhysRevLett.123.081301>.
- Meis, Constantin (2020) Quantum vacuum gravitation and cosmology. the electromagnetic nature of gravitation and matter-antimatter antigravity. doi:10.5281/ZENODO.4393542.
- Meis, Constantin (2022) The electromagnetic nature of gravitation and matter-antimatter antigravity. surmise on quantum vacuum gravitation and cosmology. *Journal of Modern Physics* **13(06)**, 949–968. doi:10.4236/jmp.2022.136054.
- Netz, Reviel (2007) *The Archimedes codex : revealing the secrets of the world's greatest palimpsest*. Weidenfeld & Nicolson, London. ISBN 9780297645474.
- Okun, R.F. (2006) The concept of mass in the einstein year. *arXiv* doi:10.1142/9789812772657_0001. URL <https://arxiv.org/abs/hep-ph/0602037v1>.
- Papathanasiou, KS & Papathanasiou, MK (2020) *Proton and Electron as Cyclones Formulation of a Theory of Everything*. ISBN 978-960-8257-77-1.
- Parson, A.L (1915) A magneton theory of the structure of the atom. *Smithsonian Miscellaneous Collections* **65(11)**, 1–86.
- Poincaré, H. (1908) La dynamique de l' électron. *Revue Gen. Sci. Pures Appl.* **19**, 386–402.
- Prigogine, N.G. (1977) *Self-organization in Nonequilibrium Systems: From Dissipative Structures to Order Through Fluctuations*. Wiley-Blackwell. ISBN ISBN 978-0471024019.

- Rankine, William John Macquorn (1855) LVII. on the hypothesis of molecular vortices, or centrifugal theory of elasticity, and its connexion with the theory of heat. *The London, Edinburgh, and Dublin Philosophical Magazine and Journal of Science* **10(68)**, 411–420. doi:10.1080/14786445508642001.
- Simaciu, I. (2006) Contribution to the development of the theory with absorption of gravitational interaction. *BULETINUL Universitatii Petrol - Gaze din Ploiesti* **Vol. LVIII(1)**, 73–80.
- Stein, Robert, van Velzen, Sjoert, Kowalski, Marek, Franckowiak, Anna, Gezari, Suvi, Miller-Jones, James C. A., Frederick, Sara, Sfaradi, Itai, Bietenholz, Michael F., Horesh, Assaf, Fender, Rob, Garrappa, Simone, Ahumada, Tomás, Andreoni, Igor, Belicki, Justin, Bellm, Eric C., Böttcher, Markus, Brinnet, Valery, Burruss, Rick, Cenko, S. Bradley, Coughlin, Michael W., Cunningham, Virginia, Drake, Andrew, Farrar, Glennys R., Feeney, Michael, Foley, Ryan J., Gal-Yam, Avishay, Golkhou, V. Zach, Goobar, Ariel, Graham, Matthew J., Hammerstein, Erica, Helou, George, Hung, Tiara, Kasliwal, Mansi M., Kilpatrick, Charles D., Kong, Albert K. H., Kupfer, Thomas, Laher, Russ R., Mahabal, Ashish A., Masci, Frank J., Necker, Jannis, Nordin, Jakob, Perley, Daniel A., Rigault, Mickael, Reusch, Simeon, Rodriguez, Hector, Rojas-Bravo, César, Rusholme, Ben, Shupe, David L., Singer, Leo P., Sollerman, Jesper, Soumagnac, Maayane T., Stern, Daniel, Taggart, Kirsty, van Santen, Jakob, Ward, Charlotte, Woudt, Patrick & Yao, Yuhan (2021) A tidal disruption event coincident with a high-energy neutrino. *Nature Astronomy* doi:10.1038/s41550-020-01295-8.
- Sukhorukov, NV (2017-2020) Electron radius in the macroneutrino model of the electron using the orbital conception of elementary particles URL <https://sites.google.com/site/snvspace22/science/electronradius>.
- Thomas, C.M. (2014) Graviton theory of everything. <http://astronomy-links.net/GToE.html>.
- Touboul, Pierre, Métris, Gilles, Rodrigues, Manuel, André, Yves, Baghi, Quentin, Bergé, Joel, Boulanger, Damien, Bremer, Stefanie, Chhun, Ratana, Christophe, Bruno, Cipolla, Valerio, Damour, Thibault, Danto, Pascale, Dittus, Hansjoerg, Fayet, Pierre, Foulon, Bernard, Guidotti, Pierre-Yves, Hardy, Emilie, Huynh, Phuong-Anh, Lämmerzahl, Claus, Lebat, Vincent, Liorzou, Françoise, List, Meike, Panet, Isabelle, Pires, Sandrine, Pouilloux, Benjamin, Prieur, Pascal, Reynaud, Serge, Rievers, Benny, Robert, Alain, Selig, Hanns, Serron, Laura, Sumner, Timothy & Visser, Pieter (2019) Space test of the equivalence principle: first results of the MICROSCOPE mission **36(22)**, 225006. doi:10.1088/1361-6382/ab4707.
- Vayenas, CG & Grigoriou, D (2020) Mass generation via gravitational confinement of relativistic neutrinos. *arXiv:2001.09760 [physics.gen-ph]* URL <https://arxiv.org/abs/2001.09760>.
- Vayenas, CG, Tsousis, D & Grigoriou, D (2020) Computation of the masses, energies and internal pressures of hadrons, mesons and bosons via the rotating lepton model. *Physica A: Statistical Mechanics and its Applications* **545**, 123679. ISSN 0378-4371. doi:<https://doi.org/10.1016/j.physa.2019.123679>. URL <http://www.sciencedirect.com/science/article/pii/S0378437119320515>.
- Wang, B. & Field, G.B. (1989) Galaxy formation by mock gravity with dust. *The Astrophysical Journal* **346**, 2–11. doi:10.1086/167981.
- Watkins, T (2020a) Estimates of the mass densities of up and down quarks and estimates of the outer radii of the small, medium and large up and down quarks URL <https://www.sjsu.edu/faculty/watkins/quarkmasses.htm>.
- Watkins, T (2020b) A sensible model for the confinement and asymptotic freedom of quarks URL <https://www.sjsu.edu/faculty/watkins/quarkconfine2.htm>.
- Wikipedia contributors (2018a) Le sage's theory of gravitation — Wikipedia, the free encyclopedia. URL https://en.wikipedia.org/w/index.php?title=Le_Sage%27s_theory_of_gravitation&oldid=867302622. [Online; accessed 14-December-2018].
- Wikipedia contributors (2018b) Nicolas fatio de duillier — Wikipedia, the free encyclopedia. URL https://en.wikipedia.org/w/index.php?title=Nicolas_Fatio_de_Duillier&oldid=859255512. [Online; accessed 14-December-2018].
- Wikipedia contributors (2019a) Heraclitus — Wikipedia, the free encyclopedia. URL <https://en.wikipedia.org/w/index.php?title=Heraclitus&oldid=918062946>. [Online; accessed 30-September-2019].

- Wikipedia contributors (2019b) Neutron star — Wikipedia, the free encyclopedia. URL https://en.wikipedia.org/w/index.php?title=Neutron_star&oldid=914385779. [Online; accessed 9-September-2019].
- Wikipedia contributors (2019c) Quantum fluctuation — Wikipedia, the free encyclopedia. URL https://en.wikipedia.org/w/index.php?title=Quantum_fluctuation&oldid=908783886. [Online; accessed 6-September-2019].
- Wikipedia contributors (2019d) Radioactive decay — Wikipedia, the free encyclopedia. URL https://en.wikipedia.org/w/index.php?title=Radioactive_decay&oldid=912368878. [Online; accessed 6-September-2019].
- Wikipedia contributors (2019e) Urca process — Wikipedia, the free encyclopedia. URL https://en.wikipedia.org/w/index.php?title=Urca_process&oldid=913174313. [Online; accessed 9-September-2019].
- Wikipedia contributors (2019f) White dwarf — Wikipedia, the free encyclopedia. URL https://en.wikipedia.org/w/index.php?title=White_dwarf&oldid=913789261. [Online; accessed 9-September-2019].
- Wikipedia contributors (2021) Zero-point energy — Wikipedia, the free encyclopedia URL https://en.wikipedia.org/w/index.php?title=Zero-point_energy&oldid=1004926536. [Online; accessed 5-February-2021].
- Wikipedia contributors (2022) Hyle — Wikipedia, the free encyclopedia. URL <https://en.wikipedia.org/w/index.php?title=Hyle&oldid=1078144578>. [Online; accessed 22-March-2022].
- Zinserling, Francois (2021) A new perspective on Fatio's Flux. doi:10.5281/zenodo.5773482. URL <https://doi.org/10.5281/zenodo.5773482>.
- Zumberge, Mark A., Ander, Mark E., Lautzenhiser, Ted V., Parker, Robert L., Aiken, Carlos L. V., Gorman, Michael R., Nieto, Michael Martin, Cooper, A. Paul R., Ferguson, John F., Fisher, Elizabeth, Greer, James, Hammer, Phil, Hansen, B. Lyle, McMechan, George A., Sasagawa, Glenn S., Sidles, Cyndi, Stevenson, J. Mark & Wirtz, Jim (1990) The greenland gravitational constant experiment. *Journal of Geophysical Research* **95(B10)**, 15483. doi:10.1029/jb095ib10p15483.